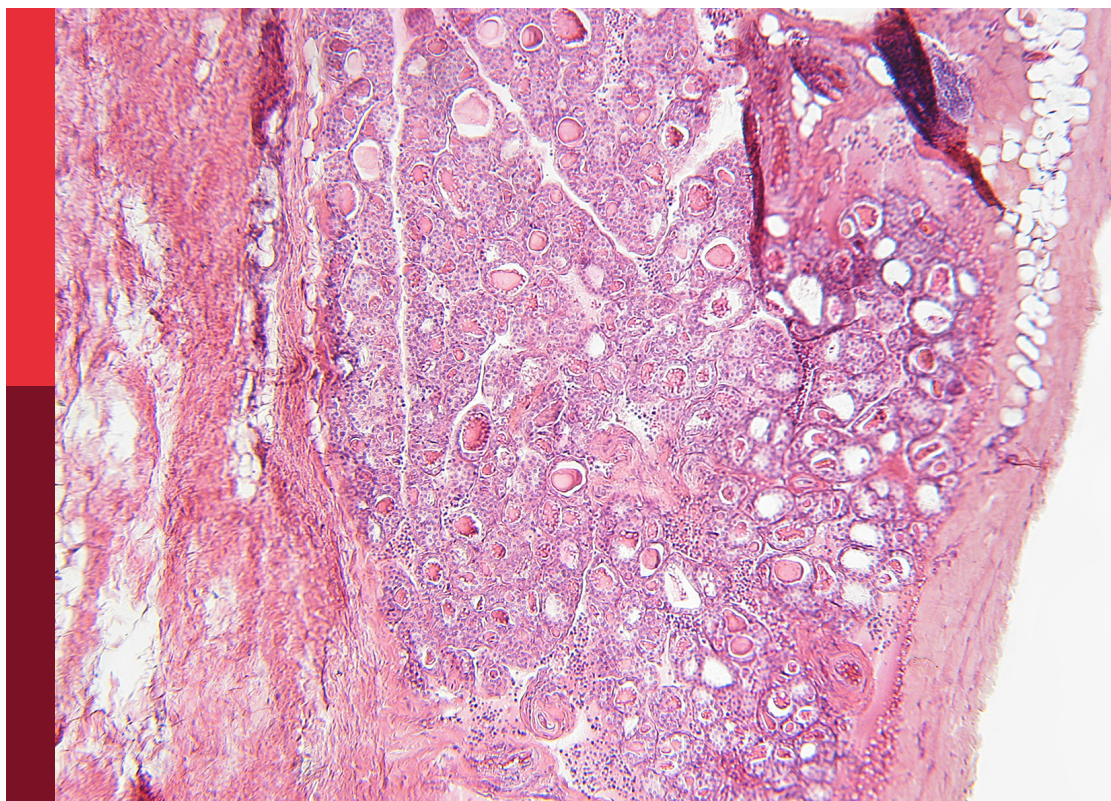


Biomolecular modifications in endocrine-related cancers

Edited by
Xianquan Zhan

Published in
Frontiers in Endocrinology



FRONTIERS EBOOK COPYRIGHT STATEMENT

The copyright in the text of individual articles in this ebook is the property of their respective authors or their respective institutions or funders. The copyright in graphics and images within each article may be subject to copyright of other parties. In both cases this is subject to a license granted to Frontiers.

The compilation of articles constituting this ebook is the property of Frontiers.

Each article within this ebook, and the ebook itself, are published under the most recent version of the Creative Commons CC-BY licence. The version current at the date of publication of this ebook is CC-BY 4.0. If the CC-BY licence is updated, the licence granted by Frontiers is automatically updated to the new version.

When exercising any right under the CC-BY licence, Frontiers must be attributed as the original publisher of the article or ebook, as applicable.

Authors have the responsibility of ensuring that any graphics or other materials which are the property of others may be included in the CC-BY licence, but this should be checked before relying on the CC-BY licence to reproduce those materials. Any copyright notices relating to those materials must be complied with.

Copyright and source acknowledgement notices may not be removed and must be displayed in any copy, derivative work or partial copy which includes the elements in question.

All copyright, and all rights therein, are protected by national and international copyright laws. The above represents a summary only. For further information please read Frontiers' Conditions for Website Use and Copyright Statement, and the applicable CC-BY licence.

ISSN 1664-8714
ISBN 978-2-83251-482-5
DOI 10.3389/978-2-83251-482-5

About Frontiers

Frontiers is more than just an open access publisher of scholarly articles: it is a pioneering approach to the world of academia, radically improving the way scholarly research is managed. The grand vision of Frontiers is a world where all people have an equal opportunity to seek, share and generate knowledge. Frontiers provides immediate and permanent online open access to all its publications, but this alone is not enough to realize our grand goals.

Frontiers journal series

The Frontiers journal series is a multi-tier and interdisciplinary set of open-access, online journals, promising a paradigm shift from the current review, selection and dissemination processes in academic publishing. All Frontiers journals are driven by researchers for researchers; therefore, they constitute a service to the scholarly community. At the same time, the *Frontiers journal series* operates on a revolutionary invention, the tiered publishing system, initially addressing specific communities of scholars, and gradually climbing up to broader public understanding, thus serving the interests of the lay society, too.

Dedication to quality

Each Frontiers article is a landmark of the highest quality, thanks to genuinely collaborative interactions between authors and review editors, who include some of the world's best academicians. Research must be certified by peers before entering a stream of knowledge that may eventually reach the public - and shape society; therefore, Frontiers only applies the most rigorous and unbiased reviews. Frontiers revolutionizes research publishing by freely delivering the most outstanding research, evaluated with no bias from both the academic and social point of view. By applying the most advanced information technologies, Frontiers is catapulting scholarly publishing into a new generation.

What are Frontiers Research Topics?

Frontiers Research Topics are very popular trademarks of the *Frontiers journals series*: they are collections of at least ten articles, all centered on a particular subject. With their unique mix of varied contributions from Original Research to Review Articles, Frontiers Research Topics unify the most influential researchers, the latest key findings and historical advances in a hot research area.

Find out more on how to host your own Frontiers Research Topic or contribute to one as an author by contacting the Frontiers editorial office: frontiersin.org/about/contact

Biomolecular modifications in endocrine-related cancers

Topic editor

Xianquan Zhan — Shandong First Medical University, China

Citation

Zhan, X., ed. (2023). *Biomolecular modifications in endocrine-related cancers*. Lausanne: Frontiers Media SA.
doi: 10.3389/978-2-83251-482-5

Table of contents

- 05 **Editorial: Biomolecular modifications in endocrine-related cancers**
Xianquan Zhan, Junwen Su and Lamei Yang
- 09 **Quantitative Acetylomics Revealed Acetylation-Mediated Molecular Pathway Network Changes in Human Nonfunctional Pituitary Neuroendocrine Tumors**
Siqi Wen, Jiajia Li, Jingru Yang, Biao Li, Na Li and Xianquan Zhan
- 33 **Impact of RSUME Actions on Biomolecular Modifications in Physio-Pathological Processes**
Mariana Fuertes, Belén Elguero, David Gonilski-Pacin, Florencia Herbstein, Josefina Rosmino, Nicolas Ciancio del Giudice, Manuel Fiz, Lara Falcucci and Eduardo Arzt
- 40 **Identifying Pupylation Proteins and Sites by Incorporating Multiple Methods**
Wang-Ren Qiu, Meng-Yue Guan, Qian-Kun Wang, Li-Liang Lou and Xuan Xiao
- 51 **The Emerging Roles and Therapeutic Implications of Epigenetic Modifications in Ovarian Cancer**
Yu Wang, Zhao Huang, Bowen Li, Lin Liu and Canhua Huang
- 69 **Quantitative Ubiquitinomics Revealed Abnormal Ubiquitinated ATP7A Involved in Down-Regulation of ACTH in Silent Corticotroph Adenomas**
Sida Zhao, Yue He, Hongyun Wang, Dan Li, Lei Gong, Yazhuo Zhang and Chuzhong Li
- 80 **Cancer glycomics offers potential biomarkers and therapeutic targets in the framework of 3P medicine**
Yuna Guo, Wenshuang Jia, Jingru Yang and Xianquan Zhan
- 102 **Towards an era of precise diagnosis and treatment: Role of novel molecular modification-based imaging and therapy for dedifferentiated thyroid cancer**
Jing Li, Yingjie Zhang, Fenghao Sun, Ligang Xing and Xiaorong Sun
- 120 **The role of protein acetylation in carcinogenesis and targeted drug discovery**
Jingru Yang, Cong Song and Xianquan Zhan
- 146 **Ubiquitination-mediated molecular pathway alterations in human lung squamous cell carcinomas identified by quantitative ubiquitinomics**
Xianquan Zhan, Miaolong Lu, Lamei Yang, Jingru Yang, Xiaohan Zhan, Shu Zheng, Yuna Guo, Biao Li, Siqi Wen, Jiajia Li and Na Li

- 168 **PKC-mediated phosphorylation and activation of the MEK/ERK pathway as a mechanism of acquired trastuzumab resistance in HER2-positive breast cancer**
Jeanesse Scerri, Christian Scerri, Felix Schäfer-Ruoff, Simon Fink, Markus Templin and Godfrey Grech
- 180 **Ovarian cancer subtypes based on the regulatory genes of RNA modifications: Novel prediction model of prognosis**
Peixian Zheng, Na Li and Xianquan Zhan



OPEN ACCESS

EDITED AND REVIEWED BY
Claire Perks,
University of Bristol, United Kingdom

*CORRESPONDENCE
Xianquan Zhan
✉ yjzhan2011@gmail.com

SPECIALTY SECTION
This article was submitted to
Cancer Endocrinology,
a section of the journal
Frontiers in Endocrinology

RECEIVED 29 December 2022
ACCEPTED 04 January 2023
PUBLISHED 13 January 2023

CITATION
Zhan X, Su J and Yang L (2023) Editorial:
Biomolecular modifications in endocrine-
related cancers.
Front. Endocrinol. 14:1133629.
doi: 10.3389/fendo.2023.1133629

COPYRIGHT
© 2023 Zhan, Su and Yang. This is an open-
access article distributed under the terms of
the [Creative Commons Attribution License
\(CC BY\)](https://creativecommons.org/licenses/by/4.0/). The use, distribution or
reproduction in other forums is permitted,
provided the original author(s) and the
copyright owner(s) are credited and that
the original publication in this journal is
cited, in accordance with accepted
academic practice. No use, distribution or
reproduction is permitted which does not
comply with these terms.

Editorial: Biomolecular modifications in endocrine-related cancers

Xianquan Zhan*, Junwen Su and Lamei Yang

Medical Science and Technology Innovation Center, Shandong Key Laboratory of Radiation Oncology, Shandong Cancer Hospital and Institute, Shandong First Medical University & Shandong Academy of Medical Sciences, Jinan, Shandong, China

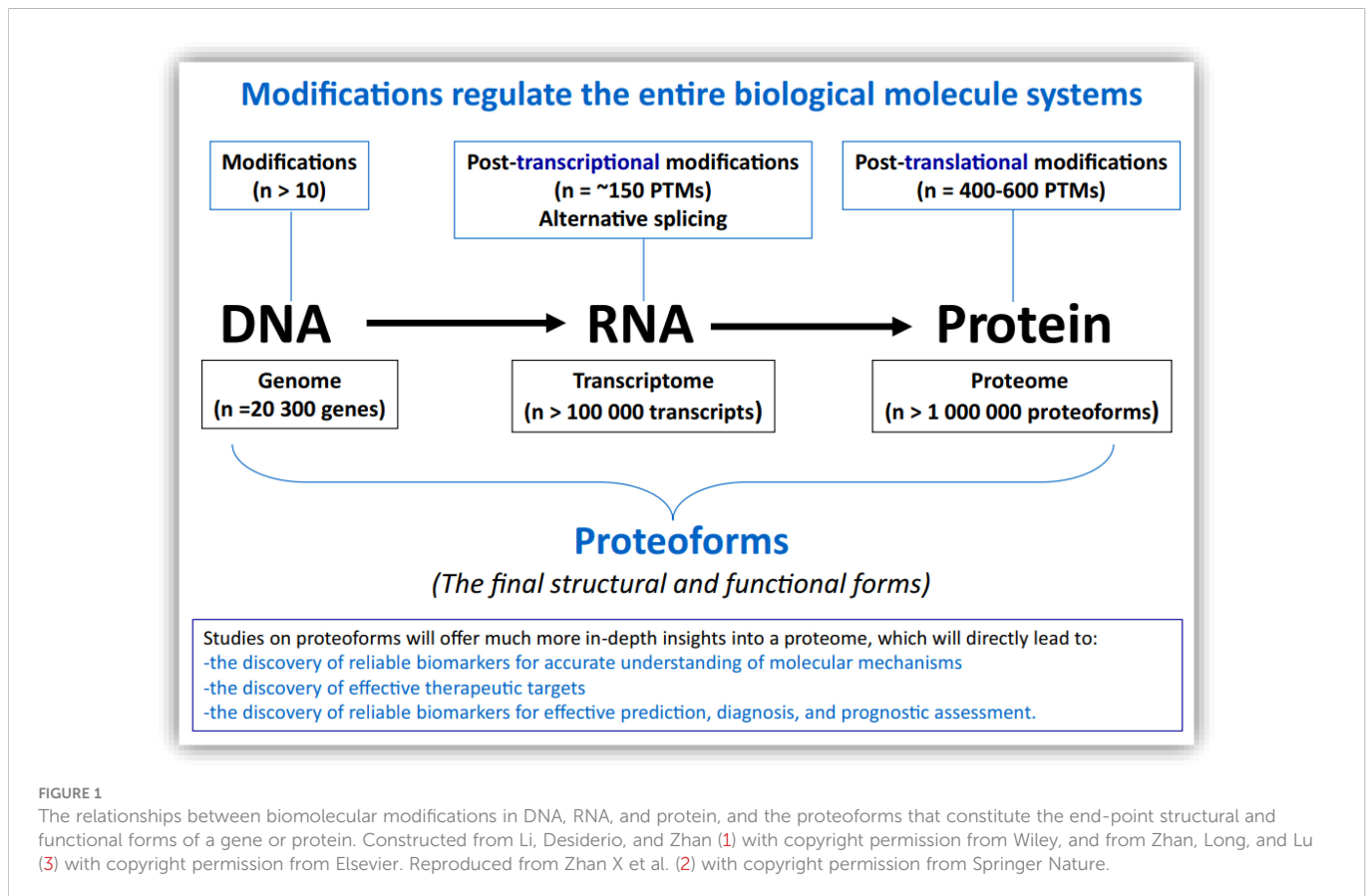
KEYWORDS

endocrine-related cancers, DNA modifications, post-transcriptional modifications, post-translational modifications, genomics, transcriptomics, proteomics, proteoformics

Editorial on the Research Topic:

Biomolecular modifications in endocrine-related cancers

The central dogma of genetics explains the sequence of information flow among three levels of biomolecules: from DNA, to RNA, to proteins (1). Modifications occurring in these biomolecules are key molecular events that regulate their structures and functions, and even the entire biological processes and systems in which they are involved (2). Biomolecular modifications are recognized as playing extensive roles in various pathophysiological conditions, including diabetics, metabolic disease, neurodegenerative disease, inflammatory disease, and cancer. Biomolecular modification is also a highly important factor in biomolecule diversity (3). It is estimated that at least 10 types of modifications, such as hydroxymethylation and cytosine methylation, occur in DNA, while at least 20 post-translational modifications (PTMs), such as acetylation, ubiquitination, and phosphorylation, occur in DNA-binding protein histones, which regulate the structures and functions of DNA; at least 170 post-transcriptional modifications, such as N1- and N6-methyladenosines (m1A, m6A, m6Am), 5-hydroxymethylcytosine (hm5C), 2'-O-methylation (Nm), 3- and 5-methylcytosines (m3C, m5C), and pseudouridine (Ψ), occur in RNA and thereby regulate the structures and functions of RNA; and 400-600 PTMs, such as glycosylation, acetylation, methylation, phosphorylation, ubiquitylation, SUMOylation, nitration, sulfation, hydroxylation, deamidation, prenylation, nitrosylation, succinylation, palmitoylation, and myristoylation, occur in proteins and thereby regulate the structures and functions of proteins (Figure 1) (1-3). Each biomolecular modification has its own characteristics and associated research methodologies. The development of various omics, including genomics, transcriptomics, proteomics, proteoformics, and bioinformatics, has been a significant driver of the large-scale analysis of biomolecular modifications to determine the modified sites and levels of modification, and to further elucidate the molecular mechanisms and biofunctions mediated by biomolecular modifications (3). Moreover, synergistic and antagonistic interactions between different biomolecular modifications can complicate the biological effects of a biomolecule to a remarkable extent. Up to this point, the number of biomolecular modification studies undertaken in the area of medical and life sciences has been far from adequate (3). It is time to put further effort into the broad and deep study of biomolecular modifications.



Endocrine-related cancers, such as ovarian cancer, pituitary adenoma, thyroid cancer, lung cancer, and breast cancer, are important endocrine system disorders and each involves a series of biomolecular modifications at the levels of DNA, RNA, and proteins. These biomolecular modifications are crucial factors contributing to the formation and development of endocrine-related cancers, in that they precisely regulate the molecular mechanisms underlying tumor-related pathophysiological processes, which in turn are a source of effective therapeutic targets and drugs, and reliable biomarkers of endocrine-related cancers (1–3). The present Research Topic includes articles discussing the presentation, functional roles, and mechanisms of various biomolecular modifications in endocrine-related cancers; this will pave the way for the systematic study of biomolecular modifications at the levels of DNA, RNA, and proteins in endocrine-related cancers.

A total of 11 articles are presented in this issue. (i) The first article addresses quantitative acetylomic alterations and the signaling pathway changes mediated by these alterations in human nonfunctional pituitary adenomas (Wen et al.). The authors identify 296 acetylated proteins with 517 acetylation sites, observing that most of these exhibit decreased acetylation levels in pituitary adenomas and play a role in multiple biological processes, including oxidative stress, cell adhesion, translation, and metabolism. Additionally, this study indicates that acetylation-mediated metabolic reprogramming contributes to invasive behaviors of the pituitary adenoma. (ii) The second article addresses protein pupylation; the authors construct the first pupylation prediction model for accurate prediction of pupylation sites and pupylated

proteins, which is of great significance for the study of basic biological processes and the development of pupylation-related drugs (Qiu et al.). (iii) The third article addresses the use of quantitative ubiquitinomics to reveal abnormal ubiquitinated ATP7A involved in down-regulation of ACTH secretion in silent corticotroph adenomas (Zhao et al.), and clearly demonstrates the effect of ubiquitylation on ACTH secretion in silent corticotroph adenomas. (iv) The fourth article addresses the roles and potential mechanisms of RSUME proteoforms, which are a set of small RWD domain-containing proteins that play a role in enhancing SUMO conjugation in tumorigenesis (Fuentes et al.). (v) The fifth article addresses the roles and therapeutic implications of epigenetic modifications, such as histone modifications, DNA methylation, and non-coding RNA regulation, in ovarian cancer; the authors also discuss the relationships of epigenetic modifications with multidrug resistance, the tumor microenvironment, and the immune response in tumorigenesis (Wang et al.). (vi) The sixth article addresses the concept of glycomics and associated methodologies, reviewing glycomics-derived biomarkers and therapeutic targets in cancers within the framework of 3P medicine (Guo et al.). (vii) The seventh article addresses ubiquitination-mediated signaling pathway changes in human lung squamous cell carcinomas (LSCC). The authors identify 627 ubiquitinated proteins (UPs) with 1209 ubiquitination sites, thereby providing an initial view of the landscape of UPs and molecular networks for human LSCC tissue (Zhan et al.). (viii) The eighth article addresses concepts and methodologies relating to protein acetylation, which is dynamically regulated by histone deacetylases (HDACs) and histone

acetyltransferases (HATs) in homeostasis; the authors review insights into acetylation-based mechanisms in carcinogenesis and targeted drug discovery in cancers (Yang et al.). (ix) The ninth article addresses eight types of RNA modification (m3C, ac4C, m7G, m5C, m6A, m1A, m6Am, and Ψ) and the corresponding RNA-modification regulatory genes (RRGs; n = 59). The authors analyze the variation in expression and the clinical relevance of these 59 RRGs in ovarian cancers, thereby constructing a differentially expressed RRG signature model for ovarian cancer consisting of four RRGs (ALYREF, ZC3H13, WTAP, and METTL1), which can be used as an independent prognostic model to classify ovarian cancer patients into high- and low-risk groups (Zheng et al.). (x) The tenth article addresses the biomolecular modifications occurring in dedifferentiated thyroid cancer, such as ubiquitination, phosphorylation, acetylation, glycosylation, and DNA methylation, and identifies new targets for radiological imaging and therapy, promising an era of precise diagnosis of and treatment for dedifferentiated thyroid cancer (Li et al.). (xi) Finally, the eleventh article presents clear evidence that PKC-mediated phosphorylation and activation of the MEK/ERK pathway is the mechanism underlying acquired trastuzumab resistance in HER2-positive breast cancer. This represents a typical application of targeted phosphorylation profiling in a given signaling pathway in the study of HER2-positive breast cancer (Scerri et al.).

As the above summary clearly demonstrates, the present issue covers the spectrum of biomolecular modifications at three different levels (those of DNA, RNA, and proteins), including histone modification, DNA methylation, and non-coding RNA regulation at the DNA level for ovarian cancer (Wang et al.) or dedifferentiated thyroid cancer (Li et al.); post-transcriptional modifications, such as m1A, m6A, m6Am, m5C, m7G, ac4C, m3C, and Ψ, at the RNA level for ovarian cancer (Zheng et al.); and post-translational modifications, such as acetylation (Wen et al.; Yang et al.), pupylation (Qiu et al.), ubiquitination (Zhao et al.; Zhan et al.), glycosylation (Guo et al.), phosphorylation (Scerri et al.), and RSUME proteoforms (Fuentes et al.), at the protein level for different forms of carcinogenesis. The aforementioned studies examining these molecular modifications contribute to the development of in-depth insight into the molecular mechanisms of cancers, such as the mediation of signaling pathway alterations by biomolecular alterations (Wen et al.; Zhan et al.; Scerri et al.), the identification of effective cancer biomarkers (Yang et al.; Guo et al.; Wen et al.; Zhan et al.), and the discovery of effective therapeutic targets and drugs in cancer treatment (Yang et al.; Guo et al.). Omics represent effective approaches in the study of biomolecular modification for the large-scale identification of modification sites and quantification of modification levels (Wen et al.; Zhan et al.; Zhao et al.). Moreover, data on biomolecular modifications, in combination with other types of omics data, have the potential for clinical applications. For example, an understanding of RNA modifications can be usefully combined with transcriptomics data (Zheng et al.); acetylation can be exploited in combination with transcriptomics to resolve invasive behaviors in pituitary adenomas (Wen et al.); and protein post-translational modifications can be used in combination with radiomics (Li et al.). For these reasons, biomolecular modifications are of crucial importance, but have not been sufficiently investigated in the field of cancers, where they are involved in every aspect of predictive, preventive, and personalized medicine (3P medicine). Biomolecular modifications are an important factor in diversity in proteoforms, each of which is defined

by its amino acid sequence + PTMs + spatial conformation + cofactors + binding partners + localization + a function (4, 6–8). Proteoforms are the basic units of a proteome, and represent the final structural and functional forms of a gene or a protein. We recommend that the study of “proteoforms” be strengthened in order to clarify the precise structural and functional alterations of a given molecule; this will enable the discovery of effective biomarkers for an accurate understanding of molecular mechanisms in cancer, the identification of reliable therapeutic targets and drugs, and the precise prediction, diagnosis, and assessment of prognosis in any given cancer (9–12).

In summary, significant advances have been achieved through biomolecular modification studies in the domain of endocrine-related cancers. The present issue collects various important articles on the topics of biomolecular modifications in DNA, DNA-binding protein histones, RNA, and proteins in endocrine-related cancers, and on the combination of various biomolecular modifications with other omics-related data in the identification of cancer biomarkers. However, it must be acknowledged that this special issue tackles only a very small fraction of the biomolecular modifications that are relevant in endocrine-related cancers. This Research Topic serves as a catalyst to stimulate and encourage researchers to conduct further biomolecular modification studies, which will result in important scientific developments in research and clinical practice in the domain of endocrine-related cancers. Future special issues will collect further multiomics-based studies of biomolecular modifications involving the large-scale use of clinical information in basic, translational, and clinical practice research in endocrine-related cancers. We will emphasize studies examining synergistic and antagonistic interactions among biomolecular modifications in a given biomolecule and their biological roles in various endocrine-related cancers. We strongly believe that biomolecular modification-based proteoformics studies represent a brighter future for the treatment of endocrine-related cancers within the framework of predictive, preventive, and personalized medicine (PPPM; 3P medicine) and precision medicine.

Author contributions

XZ conceived the concept; collated and analyzed the literature; planned, wrote, and critically revised the manuscript; and was responsible for financial support for this and related work. JS and LY participated in the collation of the literature and in part of the writing. All authors approved the final manuscript.

Funding

This work was supported by the Shandong First Medical University Talent Introduction Funds (awarded to XZ), Shandong First Medical University High-level Scientific Research Achievement Cultivation Funding Program (awarded to XZ), Shandong Provincial Taishan Scholar Engineering Project Special Funds (awarded to XZ), the Shandong Provincial Natural Science Foundation (ZR2021MH156 to XZ), Shandong First Medical University Undergraduate Innovation Research Program (Project No.:

2022104391511), and the National Natural Science Foundation of China (82203592).

Conflict of interest

The authors declare that the research was conducted in the absence of any commercial or financial relationships that could be construed as a potential conflict of interest.

References

- Li N, Desiderio DM, Zhan X. The use of mass spectrometry in a proteome-centered multiomics study of human pituitary adenomas. *Mass Spectrom Rev* (2022) 41:964–1013. doi: 10.1002/mas.21710
- Zhan X, Li J, Guo Y, Golubnitschaja O. Mass spectrometry analysis of human tear fluid biomarkers specific for ocular and systemic diseases in the context of 3P medicine. *EPMA J* (2021) 12:449–75. doi: 10.1007/s13167-021-00265-y
- Zhan X, Long Y, Lu M. Exploration of variations in proteome and metabolome for predictive diagnostics and personalized treatment algorithms: innovative approach and examples for potential clinical application. *J Proteomics* (2018) 188:30–40. doi: 10.1016/j.jprot.2017.08.020
- Zhan X, Li B, Zhan X, Schlüter H, Jungblut PR, Coorsen JR. Innovating the concept and practice of two-dimensional gel electrophoresis in the analysis of proteomes at the proteoform level. *Proteomes* (2019) 7(4):36. doi: 10.3390/proteomes7040036
- Zhan X, Li N, Zhan X, Qian S. Revival of 2DE-LC/MS in proteomics and its potential for large-scale study of human proteoforms. *Med One* (2018) 3:e180008. doi: 10.20900/mo.20180008
- Li J, Zhan X. Mass spectrometry-based proteomics analyses of post-translational modifications and proteoforms in human pituitary adenomas. *Biochim Biophys Acta Proteins Proteom* (2021) 1869(3):140584. doi: 10.1016/j.bbapap.2020.140584
- Li B, Wang X, Yang C, Wen S, Li J, Li N, et al. Human growth hormone proteoform pattern changes in pituitary adenomas: Potential biomarkers for 3P medical approaches. *EPMA J* (2021) 12(1):67–89. doi: 10.1007/s13167-021-00232-7
- Zhan X, Yang H, Peng F, Li J, Mu Y, Long Y, et al. How many proteins can be identified in a 2DE gel spot within an analysis of a complex human cancer tissue proteome? *Electrophoresis* (2018) 39(7):965–80. doi: 10.1002/elps.201700330
- Zhan X, Desiderio DM. The use of variations in proteomes to predict, prevent, and personalize treatment for clinically nonfunctional pituitary adenomas. *EPMA J* (2010) 1(3):439–59. doi: 10.1007/s13167-010-0028-z
- Hu R, Wang X, Zhan X. Multi-parameter systematic strategies for predictive, preventive and personalised medicine in cancer. *EPMA J* (2013) 4(1):2. doi: 10.1186/1878-5085-4-2
- Cheng T, Zhan X. Pattern recognition for predictive, preventive, and personalized medicine in cancer. *EPMA J* (2017) 8(1):51–60. doi: 10.1007/s13167-017-0083-9
- Lu M, Zhan X. The crucial role of multiomic approach in cancer research and clinically relevant outcomes. *EPMA J* (2018) 9(1):77–102. doi: 10.1007/s13167-018-0128-8

Publisher's note

All claims expressed in this article are solely those of the authors and do not necessarily represent those of their affiliated organizations, or those of the publisher, the editors and the reviewers. Any product that may be evaluated in this article, or claim that may be made by its manufacturer, is not guaranteed or endorsed by the publisher.



Quantitative Acetylomics Revealed Acetylation-Mediated Molecular Pathway Network Changes in Human Nonfunctional Pituitary Neuroendocrine Tumors

Siqi Wen^{1,2}, Jiajia Li^{1,2}, Jingru Yang², Biao Li^{1,2}, Na Li^{2,3} and Xianquan Zhan^{2,3,4*}

OPEN ACCESS

Edited by:

Peyuan Yin,
Dalian Medical University, China

Reviewed by:

Sumana Venkat,
University of Texas Southwestern
Medical Center, United States
Farida Tripodi,
University of Milano-Bicocca, Italy

*Correspondence:

Xianquan Zhan
yzhan2011@gmail.com

Specialty section:

This article was submitted to
Cancer Endocrinology,
a section of the journal
Frontiers in Endocrinology

Received: 05 August 2021

Accepted: 27 September 2021

Published: 12 October 2021

Citation:

Wen S, Li J, Yang J, Li B, Li N and
Zhan X (2021) Quantitative
Acetylomics Revealed Acetylation-
Mediated Molecular Pathway Network
Changes in Human Nonfunctional
Pituitary Neuroendocrine Tumors.
Front. Endocrinol. 12:753606.
doi: 10.3389/fendo.2021.753606

¹ Key Laboratory of Cancer Proteomics of Chinese Ministry of Health, Central South University, Changsha, China, ² Medical Science and Technology Innovation Center, Shandong First Medical University, Jinan, China, ³ Shandong Key Laboratory of Radiation Oncology, Shandong Cancer Hospital and Institute, Shandong First Medical University, Jinan, China, ⁴ Gastroenterology Research Institute and Clinical Center, Shandong First Medical University, Jinan, China

Acetylation at lysine residue in a protein mediates multiple cellular biological processes, including tumorigenesis. This study aimed to investigate the acetylated protein profile alterations and acetylation-mediated molecular pathway changes in human nonfunctional pituitary neuroendocrine tumors (NF-PitNETs). The anti-acetyl antibody-based label-free quantitative proteomics was used to analyze the acetylomes between NF-PitNETs (n = 4) and control pituitaries (n = 4). A total of 296 acetylated proteins with 517 acetylation sites was identified, and the majority of which were significantly down-acetylated in NF-PitNETs (p < 0.05 or only be quantified in NF-PitNETs/controls). These acetylated proteins widely functioned in cellular biological processes and signaling pathways, including metabolism, translation, cell adhesion, and oxidative stress. The randomly selected acetylated phosphoglycerate kinase 1 (PGK1), which is involved in glycolysis and amino acid biosynthesis, was further confirmed with immunoprecipitation and western blot in NF-PitNETs and control pituitaries. Among these acetylated proteins, 15 lysine residues within 14 proteins were down-acetylated and simultaneously up-ubiquitinated in NF-PitNETs to demonstrate a direct competition relationship between acetylation and ubiquitination. Moreover, the potential effect of protein acetylation alterations on NF-PitNETs invasiveness was investigated. Overlapping analysis between acetylomics data in NF-PitNETs and transcriptomics data in invasive NF-PitNETs identified 26 overlapped molecules. These overlapped molecules were mainly involved in metabolism-associated pathways, which means that acetylation-mediated metabolic reprogramming might be

the molecular mechanism to affect NF-PitNET invasiveness. This study provided the first acetylomics profiling and acetylation-mediated molecular pathways in human NF-PitNETs, and offered new clues to elucidate the biological functions of protein acetylation in NF-PitNETs and discover novel biomarkers for early diagnosis and targeted therapy of NF-PitNETs.

Keywords: acetylomics, label-free quantitative proteomics, gene ontology (GO), signaling pathway, biomarker, pituitary neuroendocrine tumor (PitNET)

INTRODUCTION

Pituitary neuroendocrine tumors (PitNETs) are the second most common primary central nervous system tumors in adults (1, 2). Based on serum hormone level, PitNETs are divided into clinically functional and nonfunctional PitNETs (F-PitNETs and NF-PitNETs). NF-PitNETs account for 15% to 54% of diagnosed PitNETs (3). F-PitNETs patients are generally diagnosed at early stage because of their hormonal hypersecretory syndrome and some of them are obtained efficient medical therapies to inhibit pituitary hormone secretion. Whereas, NF-PitNETs are not easily diagnosed at early stage because of no hormonal hypersecretory syndrome and lack effective medicine for noninvasive therapy (4). Currently, the only way to control NF-PitNET tumor mass effect (hypophysis dysfunction, visual field defect, and headache) is surgical resection. However, some NF-PitNETs seem to be more invasive and have higher postoperative recurrence rates, which severely decrease the quality of life of patients (5, 6). NF-PitNETs are becoming a challenging clinical problem. It is necessary to clarify molecular mechanisms of the occurrence and development of NF-PitNETs, and discover effective biomarkers for early diagnosis and treatment of NF-PitNETs to improve their quality of life.

Acetylation is a reversible post-translational modification (PTM), and is co-regulated by lysine acetyltransferases (KATs) and lysine deacetylases (KDACs). KATs catalyze lysine residue to be acetylated with acetyl-coenzyme A (acetyl-CoA) as a cofactor, and KDACs reverse this process. Acetylation modulates biological functions of many proteins related to tumorigenesis. Histone acetylation facilitates chromatin decondensation to regulate transcriptional activation (7). When DNA suffers from damage, particular sites of p53 protein are acetylated to modulate its functions in damage repair or cell apoptosis (8). The level of c-MYC oncoprotein tightly relates to cell cycle progression, its acetylation dramatically increases its protein stability (9). Study

found that many cancers existed aberrant expression, mutation, and translocation of one of specific lysine acetylation regulators (KATs, KDACs, and acetyl-lysine readers) or a group of them (10). These abnormalities might impact stabilities and expressions of many oncoproteins, tumor suppressor proteins, chaperones, and other functional proteins by altering their acetylation levels to initiate some of cancer-related signaling pathways and affect tumor growth, invasion, and metastasis (8, 9, 11–16). Thereby, it emphasizes that the altered acetylation levels of proteins have potential to affect tumorigenesis and development of NF-PitNETs.

However, acetylomics analysis in NF-PitNETs has not been reported. Previous studies on the effect of acetylation on pituitary tumorigenesis only focused on some specific molecules (17–19). Thus, elucidation of acetylome in NF-PitNETs might offer new insights into the role of lysine acetylation played in the pathophysiology of NF-PitNETs and lead to the discovery of novel biomarkers for its early diagnosis and efficacious therapeutic targets.

Anti-acetyl antibody-based label-free quantitative proteomics is widely used to detect, identify, and quantify acetylome in a given condition, such as substrates of acetyltransferases and deacetylases, and tumors vs. controls (16, 20, 21). This study selected a rigorous anti-acetyl antibody-based label-free quantitative mass spectrometry (MS) to identify and quantify acetylated proteins between NF-PitNET and control pituitary tissues. Subsequently, functional and pathway network analyses were performed to investigate the functional characteristics of differentially acetylated proteins (DAPs) and molecular network alterations that protein acetylation was involved in. The randomly selected acetylation status of phosphoglycerate kinase 1 (PGK1) that was identified with acetylomics in NF-PitNETs relative to normal pituitaries was confirmed with immunoprecipitation and western blot analyses.

In addition, approximately one-third of acetylation sites are also subjected to ubiquitination in human cells, which presents a competition and synergy relationship between acetylation and ubiquitination (22). Some proteins involved in important biological processes might affect tumor formation and progression through the regulatory crosstalk between acetylation and ubiquitination, such as p53, histone H3, and splicing factor SRSF5 (23–25). Thereby, an overlapping analysis between acetylated proteins data and ubiquitinated proteins data identified from the same NF-PitNET and control pituitary samples was performed to investigate the potential competition and synergy effects of protein acetylation and ubiquitination on NF-PitNETs.

Abbreviations: BPs, biological processes; CCs, cellular components; DAPs, differentially acetylated proteins; DEGs, differentially expressed proteins; DTT, dithiothreitol; F-PitNET, functional pituitary neuroendocrine tumor; GEO, Gene Expression Omnibus; GO, gene ontology; HEPEs, 2-hydroxyethyl; HPLC, high performance liquid chromatography; IAP, immunoaffinity purification; IP, immunoprecipitation; KATs, lysine acetyltransferases; KDACs, lysine deacetylases; LC, liquid chromatography; MFs, molecular functions; MS, mass spectrometry; MS/MS, tandem mass spectrometry; NF-PitNET, nonfunctional pituitary neuroendocrine tumor; PitNETs, pituitary neuroendocrine tumors; PGK1, phosphoglycerate kinase 1; PTM, post-translational modification; S/N, signal-to-noise; TFA, trifluoroacetic acid.

Moreover, invasiveness is a challenging clinical problem. This study further investigated the relationship of protein acetylation and invasive characteristics in NF-PitNETs. Differentially expressed genes (DEGs) were obtained between invasive NF-PitNETs and control tissues from Gene Expression Omnibus (GEO) database. The overlapping analysis between acetylated protein data and invasive DEG data was performed to identify acetylation-mediated molecular events for invasiveness of NF-PitNETs.

This study will provide promising scientific data for insights into molecular mechanisms of NF-PitNETs, and discover potential biomarkers for early diagnosis and therapy of NF-PitNET patients.

MATERIALS AND METHODS

Tissue Samples

Quantitative acetylomics was performed between the mixed NF-PitNET samples ($n = 4$) and mixed control samples ($n = 4$) (**Supplementary Table 1**). NF-PitNET samples were obtained from Department of Neurosurgery, Xiangya Hospital, China, with approval of the Xiangya Hospital Medical Ethics Committee of Central South University. Control pituitary tissues were obtained from the Memphis Regional Medical Center, with approval of the University of Tennessee Health Science Center Internal Review Board. Each sample was collected after obtaining written informed consent from each patient or the family of each control pituitary subject (autopsy tissues). The detailed information on samples was described previously (26), and collected (**Supplementary Table 1**).

Protein Extraction and Quality Assessment of Protein Sample

Each tissue sample was dealt with 1 mL urea pyrolysis solution [9 M urea (U5378, Merck), 20 mM 2-hydroxyethyl (HEPES; H3375, Merck), 1 mM sodium orthovanadate (S6508, Merck), 2.5 mM sodium pyrophosphate (P8010, Merck), and 1 mM β -glycerophosphate (G9422, Merck), pH 8.0] and ice bath ultrasonic treatment. The solution was centrifuged (18000 \times g, 30 min, and 4°C), and the supernatant of each sample was equally divided into three parts. The protein content of each part was measured with a Bradford Protein Quantification Kit (YEASEN, Cat# 20202ES76). An amount (20 μ g) of each extracted protein sample (NF-PitNETs; Controls) was mixed with 6X loading buffer (P0015F, Boyetime) in a ratio of 6:1(v/v), boiled (5 min), and centrifuged (14000 \times g, and 10 min). The supernatant was loaded onto 12.5% SDS-PAGE gel (P0012A, Boyetime) for electrophoretic separation (constant current 15 mA, and 60 min), followed by staining with Coomassie brilliant blue (P0017A, Boyetime).

Enzymatic Hydrolysis of Proteins

Dithiothreitol (DTT; D9760, Merck) was added to each extracted protein sample (NF-PitNETs; Controls), and achieved a final concentration of 10 mM DTT; and the mixture was incubated

(2.5h, and 37°C), and cooled to room temperature. Then indole-3-acetic acid (IAA; I3750, Merck) was added into each mixture, and achieved a final concentration of 50 mM IAA; and the mixture was kept (dark, 30 min). The water that was 5 times the volume of the mixture was added to make the concentration of urea to 1.5 M, followed by addition of trypsin into the mixture in a ratio of 1:50 to digest proteins for 18 h at 37 °C. The SPE C18 column (Waters WAT051910, Waters Corporation, Milford, CT, USA) was used to desalt and lyophilize tryptic peptides.

Enrichment of Acetylated Peptides

A volume (1.4 mL) of pre-cooled immunoaffinity purification (IAP) buffer was used to resuspend each lyophilized peptide sample (3x). The pre-processed anti-Ac-K antibody beads [PTMScan Acetyl-Lysine Motif (Ac-K) Kit, Cell Signal Technology] were added in each tryptic peptide sample, and incubated (1.5h, 4°C). Afterwards, anti-Ac-K antibody beads with acetylated peptides were washed with 1 mL pre-cooled IAP (3x), and with 1 mL pre-cooled water (3x). A volume (40 μ l) of 0.15% trifluoroacetic acid (TFA; 302031, Merck) was added to the washed anti-Ac-K antibody beads, and incubated (room temperature, 10 min), and then the same volume of TFA was added once again. The mixture was centrifuged (2000 \times g, 30s). The supernatant was desalted with C18 STAGE Tips (27). The desalted supernatant was the enriched acetylated peptide sample.

LC-MS/MS Analysis of Enriched Acetylated Peptides

LC-MS/MS was used to analyze the enriched acetylated peptides (NF-PitNETs; controls). Each enriched acetylated peptide sample was separated by high performance liquid chromatography (HPLC) system EASY-nLC1000 at nanoliter flow velocity. Chromatography column was balanced with 100% buffer A (0.1% acetonitrile formate aqueous solution that contained 2% acetonitrile). The enriched acetylated peptides were loaded onto the sample spindle, Thermo scientific EASY column (2 cm \times 100 μ m 5 μ m-C18), with an autosampler in buffer A, and then were separated when the sample flowed through analytical column (75 μ m \times 250 mm 3 μ m-C18) at a flow rate of 250 nL/min in buffer B (0.1% acetonitrile formate aqueous solution that contained 84% acetonitrile). The liquid-phase gradient was buffer B linear gradient from 0 to 55% for 220 min, buffer B linear gradient from 55 to 100% for 8 min, and then maintained 100% buffer B for 12 min. The Q-Exactive mass spectrometer (Thermo Finnigan) was used to perform MS/MS analysis when the enriched acetylated peptides were separated with capillary HPLC. The parameter of mass spectrometer was set as time 240 min, positive ion detection mode, and scan range of precursor ion m/z 350-1800. The top 20 intensive ions in MS scan (MS1) were selected for ion fragmentation with higher-energy collision dissociation (HCD) to generate MS/MS spectra (MS2). The MS1 resolution was 70,000 at m/z 200, and the MS2 resolution was 17,500 at m/z 200.

Label-Free Quantification With MaxQuant

The Maxquant software (version 1.3.0.5) was used for database searching and data analysis of 6 original LC-MS/MS datasets

(NF-PitNETs: $n = 3$; Controls: $n = 3$). The database was uniprot_human_154578_20160815.fasta (154,578 entries, downloaded on 15 August 2016). Its primary parameters were set as main search ppm = 6, missed cleavage = 4, MS/MS tolerance ppm = 20, de-isotopic = TRUE, enzyme = trypsin, database = uniprot_human_154578_20160815.fasta, fixed modification = carbamidomethyl (C), variable modification = oxidation (M), acetyl (protein N-term), and acetyl (K), decoy database pattern = reverse, iBAQ = TRUE, match between runs = 2 min, peptide false discovery rate (FDR) = 0.01, and protein FDR = 0.01. The MS/MS data were used to determine the amino acid sequence and acetylation sites, label-free quantification was used to determine the acetylation level.

Immunoaffinity Experiments Confirmed DAPs

Immunoprecipitation (IP) and western blot were used to semi-quantify PGK1 acetylation level in NF-PitNETs compared to controls. Three NF-PitNET tissue samples were equally mixed as the NF-PitNET sample, and five control protein samples were equally mixed as the control sample (Supplemental Table 1), which were used to extract protein samples, respectively. An amount (1 mg) of each protein sample (NF-PitNETs; controls) was incubated with the specific antibody against PGK1 (6 μ g; sc-130335, Santa Cruz Technology) to immunoprecipitate PGK1 from total proteins. The negative control IP experiment was performed with the use of the normal mouse IgG antibody (6 μ g; B900620, Proteintech) to replace the anti-PGK1 antibody, which tested the specificity of anti-PGK1 antibody. The IP products (PGK1 product; IgG product), anti-PGK1 antibody (2 μ g), and total protein samples (NF-PitNETs: 60 μ g; Controls: 60 μ g) were simultaneously immunoblotted with anti-acetyl-lysine antibody (1:1000; A2391, ABclonal).

Bioinformatics Analysis of DAPs

DAPs were used for KEGG pathway analysis and gene ontology (GO) analysis through David database. GO analysis included three categories - biological processes (BPs), cellular components (CCs), and molecular functions (MFs). The results of KEGG, BP, CC, and MF data were further clustered into different functional categories. Moreover, acetylation motif analysis was carried out by analysis of the sequences from -13 to +13 amino acid residues at those 517 acetylation sites within 296 acetylated proteins with Motif-X software to identify any motifs that were prone to be acetylated in NF-PitNETs.

Overlapping Analysis of Acetylated Protein Data and Ubiquitinated Protein Data

The acetylated protein data identified in this study were compared to the ubiquitinated protein data in our previous study (26), which found that acetylation and ubiquitination occurred at the same site in proteins. This overlapping analysis was based on the fact that quantitative acetylomics and quantitative ubiquitinomics were performed in the same samples (NF-PitNETs; controls).

Overlapping Analysis of Acetylated Protein Data and Invasive DEG Data

In total, 2751 statistically significant DEGs in invasive NF-PitNETs vs. controls were mined from the GEO database (Supplementary Table 2). The overlapped molecules between 166 DAP data in NF-PitNETs relative to controls and 2751 DEG data in invasive NF-PitNETs relative to controls were obtained, and further analyzed with GO and KEGG pathway enrichments to obtain functional characteristics and signaling pathways mediated by these overlapped molecules.

RESULT

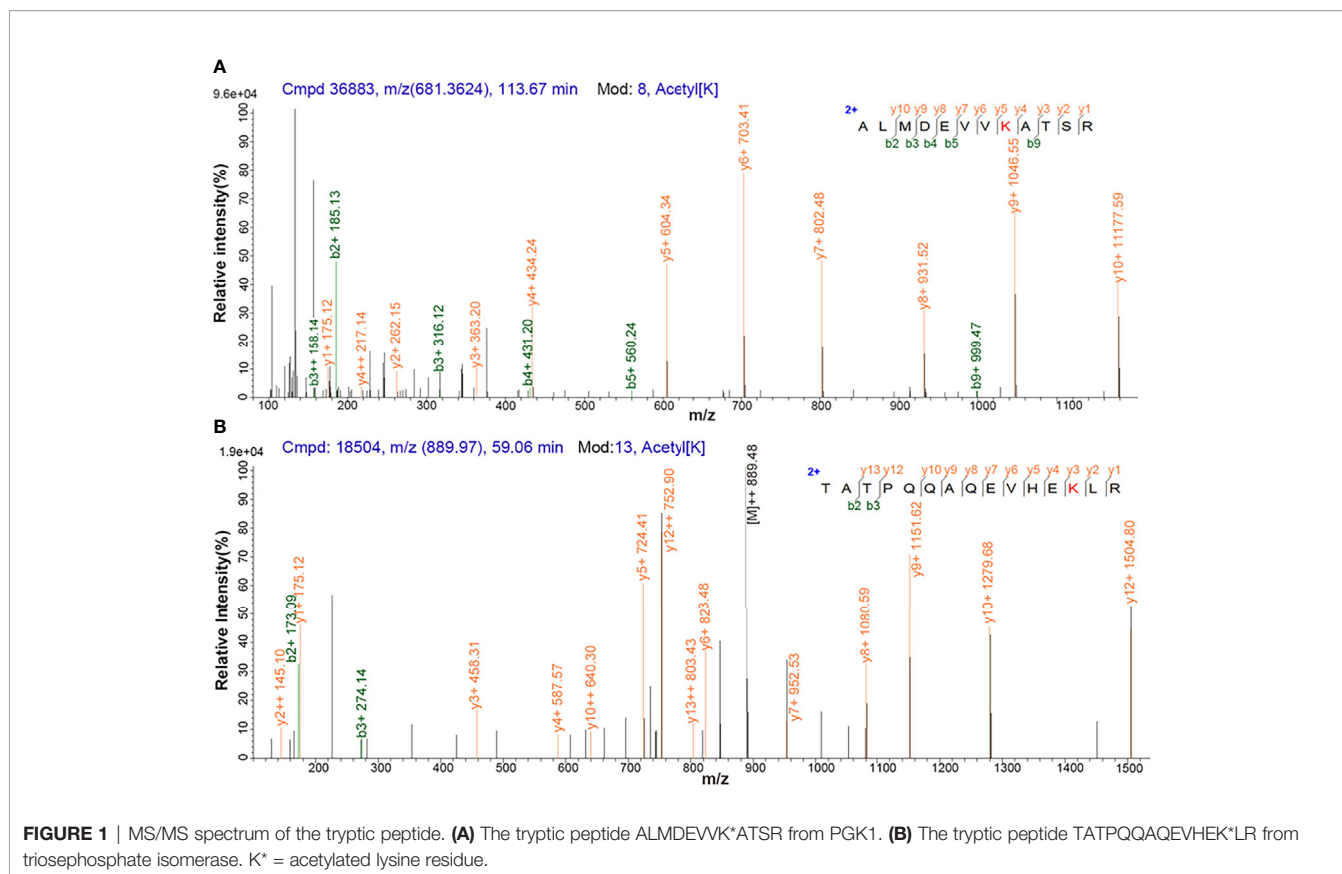
Protein Acetylation Profiling in NF-PitNETs

Antibody enrichment-based label-free quantitative acetylomics identified 517 acetylation sites within 296 proteins in NF-PitNETs and control pituitaries (Supplementary Table 3). A representative MS/MS spectrum was from acetylated peptide ALMDEVVK*ATSR $[(M + 2H)]^{2+}$, $m/z = 681.4$, K^* = acetylated lysine residue) derived from PGK1 (Swiss-Prot No.: P00558) (Figure 1A), with a high-quality MS/MS spectrum, excellent signal-to-noise (S/N) ratio, and extensive product ions b-ion and y-ion series ($b_2, b_3, b_4, b_5, b_9, Y_1, Y_2, Y_3, Y_4, Y_5, Y_6, Y_7, Y_8, Y_9$, and Y_{10}). Its acetylation site was localized at residue K^*361 , which was only acetylated in controls (N) but not in NF-PitNETs (T) (Supplementary Table 3). Another representative MS/MS spectrum was from acetylated peptide TATPQQAQEVHEK*LR $[(M + 2H)]^{2+}$, $m/z = 889.5$, K^* = acetylated lysine residue) of triosephosphate isomerase (Swiss-Prot No.: P60174) (Figure 1B), with a high-quality MS/MS spectrum, excellent S/N ratio, and extensive product ions b-ion and y-ion series ($b_2, b_3, Y_1, Y_2, Y_3, Y_4, Y_5, Y_6, Y_7, Y_8, Y_9, Y_{10}, Y_{12}$, and Y_{13}). Its acetylation site was localized at residue K^*225 , and its acetylation level was significantly decreased in NF-PitNETs compared to controls (ratio of T/N = 0.44; $P = 3.28E-04$) (Supplementary Table 3).

Among these 517 acetylation sites (Figure 2), (i) 341 sites were identified and quantified, including 58 sites only quantified in NF-PitNETs, 158 only quantified in controls, and 125 sites quantified in both NF-PitNET and control tissues, and 76 of these 125 sites had statistically significant difference at the acetylation level ($p < 0.05$) in NF-PitNETs compared to controls (53 decreased acetylation levels, and 23 increased acetylation levels); and (ii) 176 sites were only identified but not quantified in neither NF-PitNETs or controls. The acetylation level change of 292 (76 + 58 + 158) quantified lysine residues with statistically significant difference were visualized by heatmap based on their acetylation intensities in NF-PitNETs and control tissues (Figure 3), which revealed that the majority of quantified lysine residues were down-acetylated in NF-PitNETs relative to controls.

Amino Acid Motifs That Are Prone to Be Acetylated in NF-PitNETs

Two significantly distinguished motifs EK^* and K^*R (K^* = the acetylated lysine residue) were identified (Figure 4A), which



referred to 83 and 70 acetylated peptides, respectively. These two types of acetylation motifs had different abundances, which together accounted for 30.5% [(83 + 70)/501] of the identified acetylated peptides (**Figures 4B, C**). It indicates that the residue K within motifs EK and KR is prone to be acetylated in NF-PitNETs.

Functional Characteristics of DAPs in NF-PitNETs

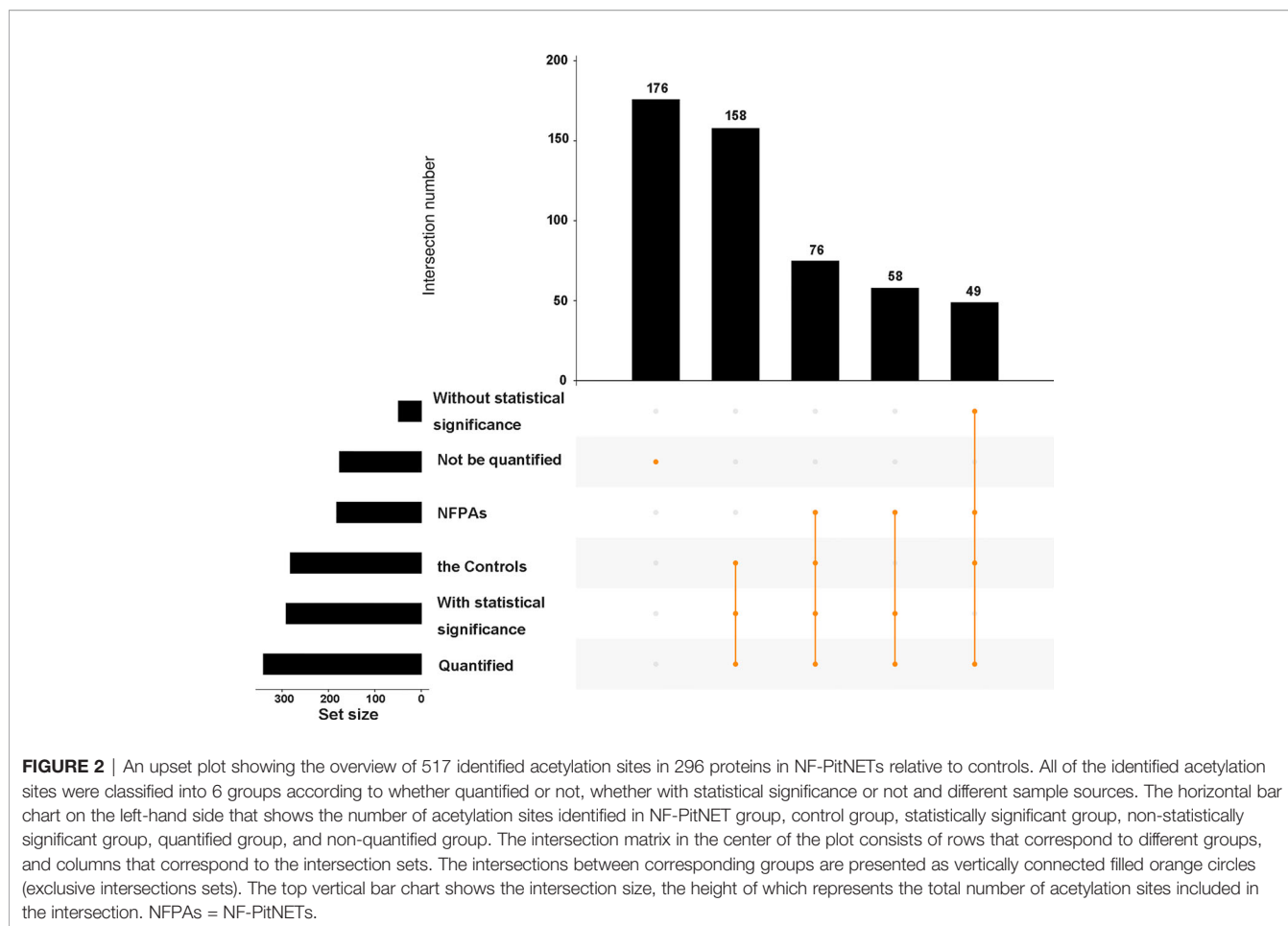
The functional characteristics of DAPs in NF-PitNETs were analyzed with GO enrichment analysis, including BPs, MFs, and CCs. (i) For BPs, a total of 97 BPs was identified, covering almost all cellular biological processes, including gene expression, metabolism, cell-cell (matrix) adhesion, apoptosis, and immune system regulation (**Supplementary Table 4**). In the aspect of gene expression, those DAPs participated in nucleosome assembly, adenine transport, translation, epigenetics, and post-translational processing and secretion of proteins. In the aspect of metabolism, those DAPs mainly participated in the metabolism of glucose and amino acid, and oxidative phosphorylation to yield ATPs. In the aspect of immune system regulation, those DAPs participated in B cell activation, macrophage phagocytosis, and response to interleukin-4. In addition, DAPs participated in the response to reactive oxygen species, catabolism of superoxide, and affect cellular detoxification process. (ii) For MFs, those DAPs also had extensive MFs (**Supplementary Table 5**). Those DAPs were able to bind mRNA, ADP, NADP, oxygen, cell adhesion molecule, kinds of

proteins, enzymes, and receptors, and exert their functions in translation, energy yield, oxygen transport, cell adhesion, proteins processing, cell signal transduction, immune regulation, and catalyzing many kinds of enzyme activities such as oxidoreductase and ubiquitin protein ligase. (iii) For CCs, those DAPs played their roles in different positions. Those DAPs located in almost everywhere in cell, including nucleus, cytoplasm, plasma membrane, and organelles such as mitochondrion, endoplasmic reticulum, and peroxisome. They were also distributed in extracellular region such as cell-cell adherens junction (**Supplementary Table 6**).

Cluster analysis grouped BPs, MFs, CCs, and KEGG pathways enriched from DAPs into 14 functional clusters (**Figure 5, Supplementary Table 7**), including 3 clusters related to biosynthesis, metabolism, and energy yield (Clusters 2-4), 4 clusters related to gene expression (Clusters 6, 8, 11, and 12), 2 clusters related to oxygen transport, and oxidant detoxification in cell (Clusters 5, 9), 1 cluster related to protein location and apoptosis (Cluster 14), 1 cluster related to cell adhesion (Cluster 1), 1 cluster related to immune system regulation (cluster 13), and clusters 7 and 10 related to blood coagulation and movement of cells or muscle, respectively (**Figure 6**).

Acetylation-Mediated Signaling Pathways in NF-PitNETs

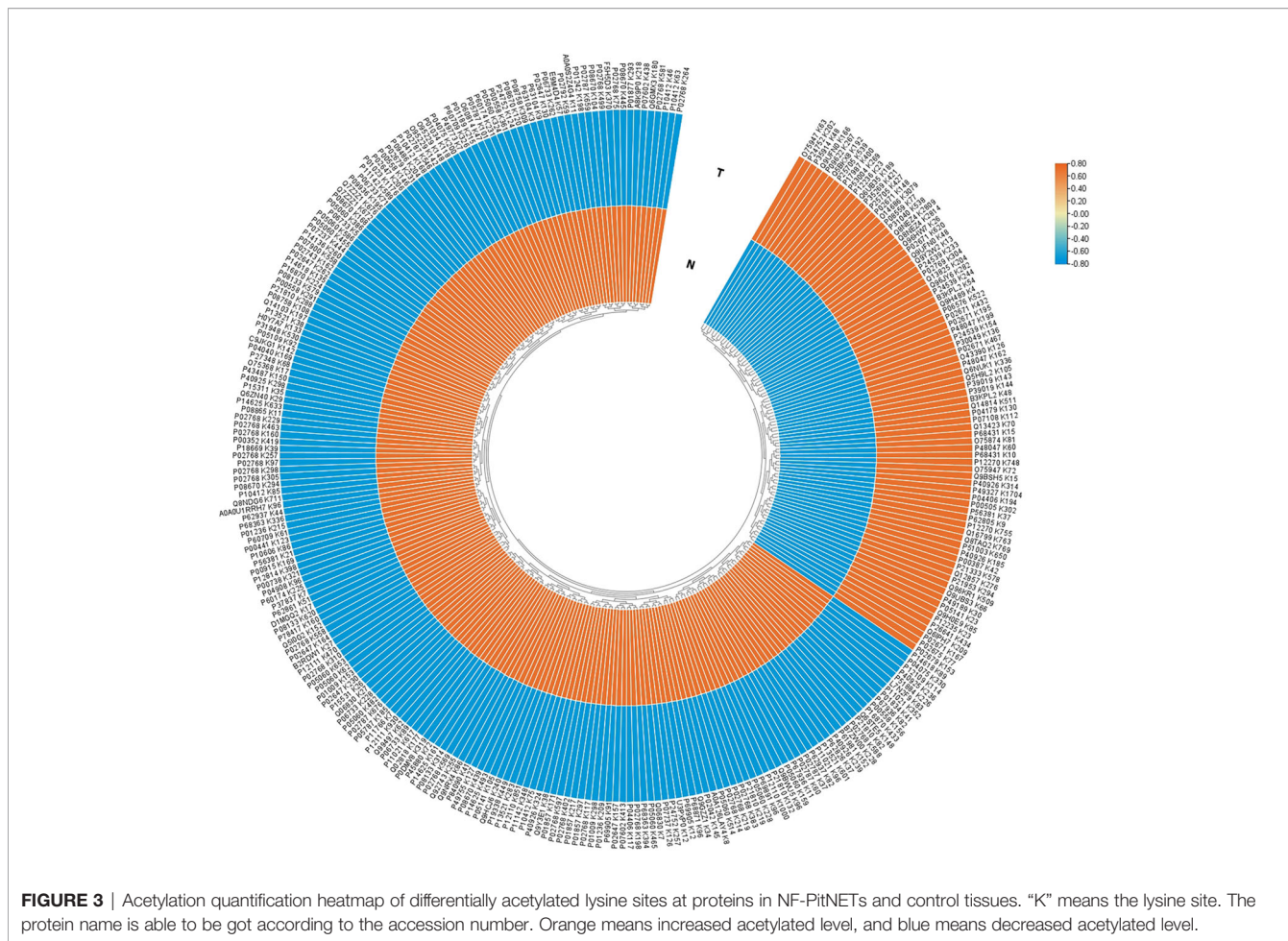
A total 18 statistically significant signaling pathways was identified to involve DAPs with KEGG pathway enrichment



analysis (**Figure 7, Supplementary Table 8**). Of them, 9 pathways were associated with metabolism and energy yield, 3 associated with nervous system diseases, 3 associated with infectious diseases, 1 was about anti-infection, 1 was about cellular oxidant detoxification, and 1 was about complement and coagulation.

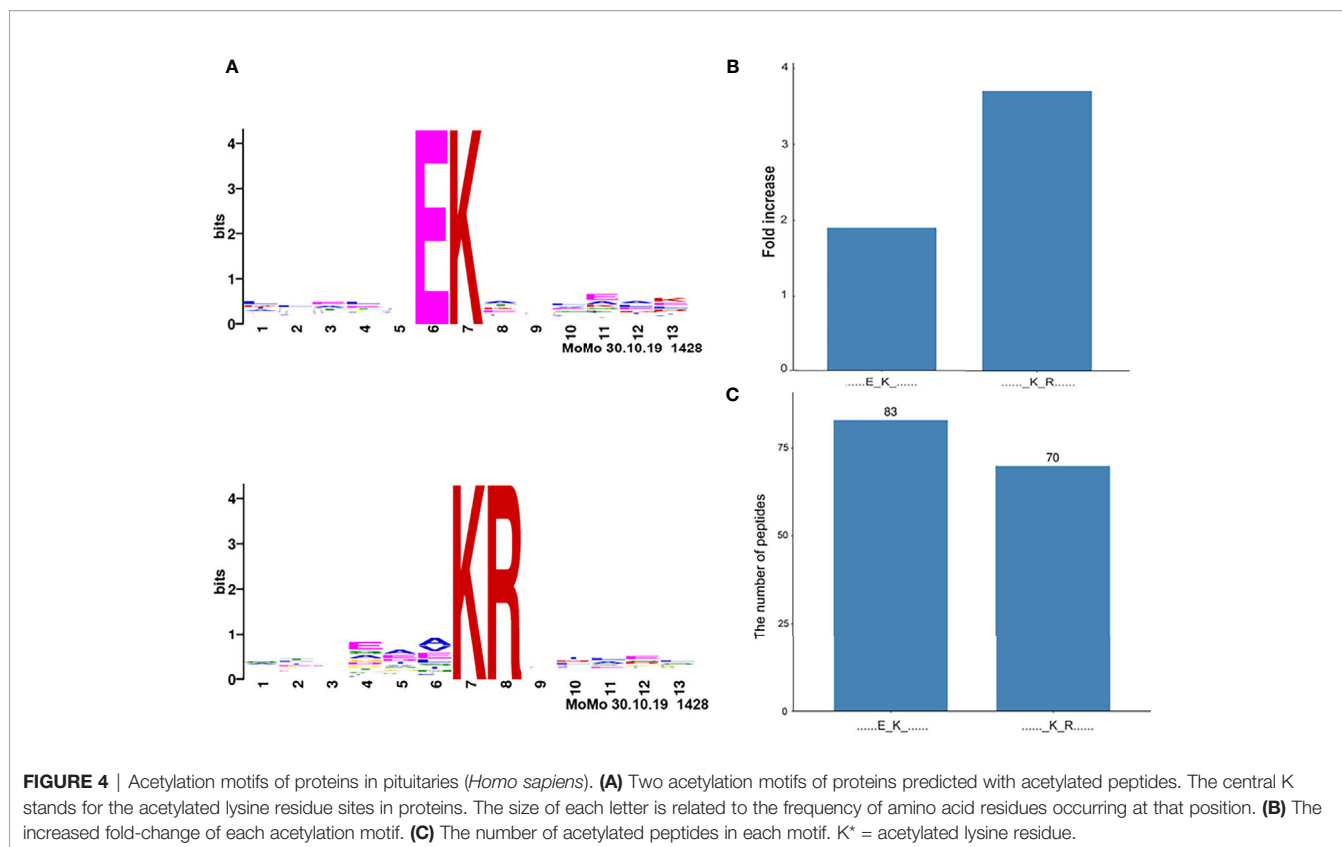
The pathways about metabolism and energy yield included carbon metabolism, glycolysis/gluconeogenesis, pyruvate metabolism, citrate cycle (TCA cycle), glyoxylate and dicarboxylate metabolism, metabolic pathways, biosynthesis of amino acids, oxidative phosphorylation, and valine, leucine and isoleucine degradation. (i) Carbon metabolism consisted of one-carbon metabolism and central carbon metabolism (**Supplementary Figure S1.1**). One-carbon metabolism integrates carbon units from amino acids to generate proteins, nucleotides, and lipids, maintain redox status, and provide substrates for methylation reactions (28). Central carbon metabolism, including glycolysis, TCA cycle, and pentose phosphate pathway, is essential to gain energy from carbohydrate, and provide precursors for many biosynthetic pathways (29). This study found that acetylation mainly occurred at the enzymes that were enriched on the central carbon metabolism, including acetylation at residues K89, K5, K228, K71, and K262 (only acetylated in controls) in alpha-enolase (ID: P06733), K77

(only acetylated in NF-PitNETs) in mitochondrial pyruvate dehydrogenase E1 component subunit alpha (somatic form) (ID: P08559), K135, and K89 (only acetylated in controls) in pyruvate kinase PKM (ID: P14618), K7 (ratio of T/N = 0.58, $p = 1.52E-02$) in transaldolase (ID: P37837), K194 (ratio of T/N = 1.74, $p = 4.24E-03$), and K117 (ratio of T/N = 0.25, $p = 2.50E-02$) in glyceraldehyde-3-phosphate dehydrogenase (ID: P04406), K81 (ratio of T/N = 5.38, $p = 3.75E-03$) in cytoplasmic isocitrate dehydrogenase [NADP] (ID: O75874), K314 (ratio of T/N = 2.71, $p = 2.20E-02$), K185 (only acetylated in NF-PitNETs), K324 and K239 (only acetylated in controls) in mitochondrial malate dehydrogenase (ID: P40926), K298, and K236 (only acetylated in controls) in cytoplasmic malate dehydrogenase (ID: P40925), K7 (only acetylated in controls) in alcohol dehydrogenase class-3 (ID: P11766), K39 (ratio of T/N = 0.06, $p = 7.09E-04$) in phosphoglycerate mutase 1 (ID: P18669), K302 (ratio of T/N = 1.71, $p = 8.69E-03$) in mitochondrial aspartate aminotransferase (ID: P00505), K291, K146, K156 and K361 (only acetylated in controls) in phosphoglycerate kinase 1 (ID: P00558), K538 (only acetylated in NF-PitNETs) mitochondrial succinate dehydrogenase [ubiquinone] flavoprotein subunit (ID: P31040), K231 (only acetylated in controls), and K225 (ratio of T/N = 0.44, $p = 3.28E-04$) in triosephosphate isomerase (ID: P60174), K169 (only acetylated in controls) in catalase (ID: P04040), K330 and K200 (only acetylated in controls) in fructose-bisphosphate aldolase



A (ID: P04075), K202 (ratio of T/N=4.13, $p=3.34E-02$), K257 (ratio of T/N=0.35, $p=1.13E-02$), and K124 (only acetylated in controls) in mitochondrial acetyl-CoA acetyltransferase (ID: P24752), and K267 (ratio of T/N =1.95, $p =1.42E-04$) in mitochondrial dihydrolipoylde hydrogenase (ID: P09622). The acetylation level of most lysine residues at these enzymes decreased in NF-PitNETs. (ii) Most microbe and mammalian cells depend on glycolysis to convert glucose into lactate, and produce energy in the absence of oxygen. However, most tumor cells uptake more glucose, and produce more lactate even in the presence of oxygen even though mitochondria function well, which is noted as aerobic glycolysis, or Warburg effect (30). Gluconeogenesis converts lactate or amino acids to glucose, which is the reverse pathway of glycolysis in essence (31) (**Supplementary Figure S1.2**). This study found that acetylation occurred at glycolysis/gluconeogenesis-related enzymes, including acetylation at residues K30 (only acetylated in NF-PitNETs) in 4-trimethylaminobutyraldehyde dehydrogenase (ID: P49189), K89, K5, K228, K71, and K262 (only acetylated in controls) in alpha-enolase (ID: P06733), K77 (only acetylated in NF-PitNETs) in mitochondrial pyruvate dehydrogenase E1 component subunit alpha (somatic form) (ID: P08559), K135, and K89 (only acetylated in controls) in pyruvate kinase PKM (ID: P14618),

K194 (ratio of T/N =1.74, $p = 4.24E-03$), and K117 (ratio of T/N=0.25, $p=2.50E-02$) in glyceraldehyde-3-phosphate dehydrogenase (ID: P04406), K7 (only acetylated in controls) in alcohol dehydrogenase class-3 (ID: P11766), K39 (ratio of T/N=0.06, $p=7.09E-04$) in phosphoglycerate mutase 1 (ID: P18669), K291, K146, K156, and K361 (only acetylated in controls) in phosphoglycerate kinase 1 (ID: P00558), K231 (only acetylated in controls), and K225 (ratio of T/N=0.44, $p=3.28E-04$) in triosephosphate isomerase (ID: P60174) and K330 and K200 (only acetylated in controls) in fructose-bisphosphate aldolase A (ID: P04075), and K267 (ratio of T/N =1.95, $p =1.42E-04$) in mitochondrial dihydrolipoylde hydrogenase (ID: P09622). The acetylation levels at more than 4/5 lysine residues in these enzymes enriched in glycolysis/gluconeogenesis pathways were decreased in NF-PitNETs, which might result in the convert of glycolysis to the aerobic glycolysis in NF-PitNETs, and further affect tumor progression. (iii) Pyruvate, the end product of glycolysis, is reduced to lactate in cytoplasm or transport into mitochondria to enter TCA cycle for full oxidation for ATP production, and sit at the switch point between these two important carbohydrate metabolism pathways (**Supplementary Figure S1.3**) (32, 33). Pyruvate kinase (ID: P14618) is the rate-limiting enzyme at the last step of glycolysis to catalyze phosphoenolpyruvate to pyruvate.



Its acetylation levels at residues K135 and K89 were decreased in NF-PitNETs (only acetylated in controls) in this study. Mitochondrial dihydrolipoyl dehydrogenase (ID: P09622) and mitochondrial pyruvate dehydrogenase E1 component subunit alpha (somatic form) (ID: P08559) are two components to form pyruvate dehydrogenase complex, which is able to catalyze pyruvate to acetyl-CoA for entering TCA cycle. Their acetylation levels at corresponding residues K267 (ratio of T/N=1.95, $p=1.42E-04$) and K77 (only acetylated in NF-PitNETs) were increased in NF-PitNETs in this study. In addition, this study found acetylation occurred at other enzymes enriched on pyruvate metabolism pathway, including acetylation at residues K30 (only acetylated in NF-PitNETs) in 4-trimethylaminobutyraldehyde dehydrogenase (ID: P49189), K314 (ratio of T/N =2.71, $p=2.20E-02$), K185 (only acetylated in NF-PitNETs), K324 and K239 (only acetylated in controls) in mitochondrial malate dehydrogenase (ID: P40926), K298, and K236 (only acetylated in controls) in cytoplasmic malate dehydrogenase (ID: P40925), and K202 (ratio of T/N=4.13, $p=3.34E-02$), K257 (ratio of T/N=0.35, $p=1.13E-02$) and K124 (only acetylated in controls) in mitochondrial acetyl-CoA acetyltransferase (ID: P24752). (iv) TCA cycle is the final metabolic pathway of carbohydrates, lipids, and amino acids, which is the central route for cellular oxidative phosphorylation and provides precursors for many anabolic pathways (34) (**Supplementary Figure S1.4**). TCA cycle occurs in mitochondria. This study found that acetylation occurred at the four enzymes residing in mitochondria, including acetylation at residues K77

(only acetylated in NF-PitNETs) in mitochondrial pyruvate dehydrogenase E1 component subunit alpha (somatic form) (ID: P08559), K314 (ratio of T/N =2.71, $p=2.20E-02$), K185 (only acetylated in NF-PitNETs), K324 and K239 (only acetylated in controls) in mitochondrial malate dehydrogenase (ID: P40926), K267 (ratio of T/N=1.95, $p=1.42E-04$) in mitochondrial dihydrolipoyl dehydrogenase (ID: P09622), and K538 (only acetylated in NF-PitNETs) in mitochondrial succinate dehydrogenase [ubiquinone] flavoprotein subunit (ID: P31040). The acetylation levels at most lysine residues in these enzymes were increased in NF-PitNETs. In addition, this study found acetylation occurred at other cytoplasmic enzymes enriched on TCA cycle, including acetylation at residues at K81 (ratio of T/N =5.38, $p=3.75E-03$) in cytoplasmic isocitrate dehydrogenase [NADP] (ID: O75874), and K298, and K236 (only acetylated in controls) in cytoplasmic malate dehydrogenase (ID: P40925). (v) Glyoxylate is a highly toxic substance because it is able to be rapidly oxidized to oxalate that forms insoluble crystals with calcium, which precipitates in various organs, especially the kidneys to cause renal failure. Therefore, glyoxylate metabolism in human mainly referred to glyoxylate detoxification (35). Dicarboxylate, also called dicarboxylic acids, included oxaloacetic acid, malic acid, and aspartic acid, which participated in many metabolism pathway such as ω -oxidation of fatty acids, TCA cycle, etc. (36) (**Supplementary Figure S1.5**). This study found that acetylation occurred at glyoxylate and dicarboxylate metabolism-related molecules, including acetylation at residues K314 (ratio of T/N =

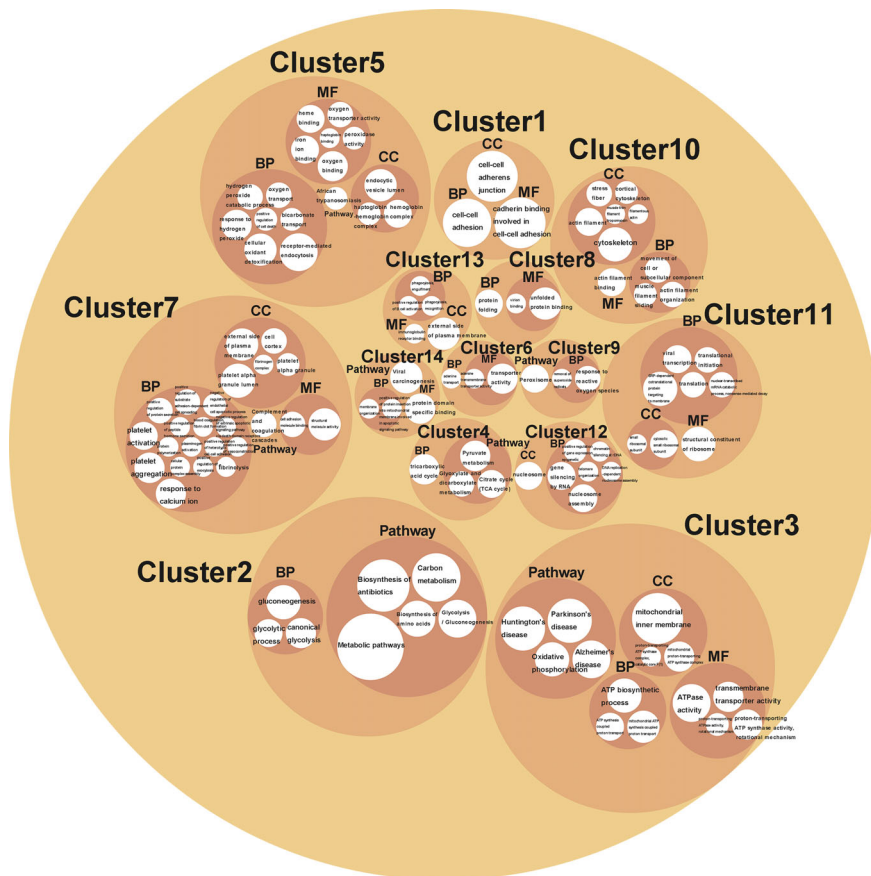


FIGURE 5 | A circle packing chart showing the cluster analysis results. The white circle size is associated to the count of genes enriched on each BP, MF, CC, or pathway. The meaning that each circle represented is annotated in or nearby the circle.

2.71, $p=2.20E-02$), K185 (only acetylated in NF-PitNETs), K324 and K239 (only acetylated in controls) in mitochondrial malate dehydrogenase (ID: P40926), K298, and K236 (only acetylated in controls) in cytoplasmic malate dehydrogenase (ID: P40925), K169 (only acetylated in controls) in catalase (ID: P04040), K202 (ratio of T/N =4.13, $p=3.34E-02$), K257 (ratio of T/N=0.35, $p=1.13E-02$), and K124 (only acetylated in controls) in mitochondrial acetyl-CoA acetyltransferase (ID: P24752), and K267 (ratio of T/N =1.95, $p=1.42E-04$) in mitochondrial dihydrolipoylde hydrogenase (ID: P09622). (vi) Valine, leucine and isoleucine, also known as branched-chain amino acids, are essential amino acids that have to be derived from diet, which can be oxidized in skeletal muscle for energy supply when exercise, and are also preferentially used by many tumor cells for protein synthesis and energy purposes. It is reported that many enzymes that catalyzed the degradation of valine, leucine and isoleucine were overexpressed in many cancers (37–40) (**Supplementary Figure S1.6**). This study found acetylation occurred at valine, leucine and isoleucine degradation-related molecules, including acetylation at residues K48 (ratio of T/N=2.97, $p=6.90E-03$) in mitochondrial hydroxymethylglutaryl-CoA lyase (ID: P35914), K294 (only acetylated in NF-PitNETs)

in mitochondrial 2-oxoisovalerate dehydrogenase subunit beta (ID: P21953), K30 (only acetylated in NF-PitNETs) in 4-trimethylaminobutyraldehyde dehydrogenase (ID: P49189), K204 (only acetylated in NF-PitNETs) in mitochondrial methylglutaconyl-CoA hydratase (ID: Q13825), K202 (ratio of T/N=4.13, $p=3.34E-02$), K257 (ratio of T/N=0.35, $p=1.13E-02$), and K124 (only acetylated in controls) in mitochondrial acetyl-CoA acetyltransferase (ID: P24752), and K267 (ratio of T/N=1.95, $p=1.42E-04$) in mitochondrial dihydrolipoylde hydrogenase (ID: P09622). The acetylation levels of most lysine residues at enzymes enriched in the valine, leucine and isoleucine degradation pathway increased in NF-PitNETs. (vii) Oxidative phosphorylation is the primary pathway for ATP synthesis and responsible for setting and maintaining metabolic homeostasis (41). It is reported that oxidative phosphorylation levels were abnormally altered in many cancers (42, 43) (**Supplementary Figure S1.7**). Except the decreased acetylation levels of residues K86 (ratio of T/N=0.36, $p=7.61E-04$) in mitochondrial cytochrome c oxidase subunit 5B (ID: P10606) and K21 (ratio of T/N=0.38, $P=2.11E-03$) in mitochondrial ATP synthase subunit epsilon (ID: P56381), the acetylation levels of all other lysine residues in enzymes enriched in

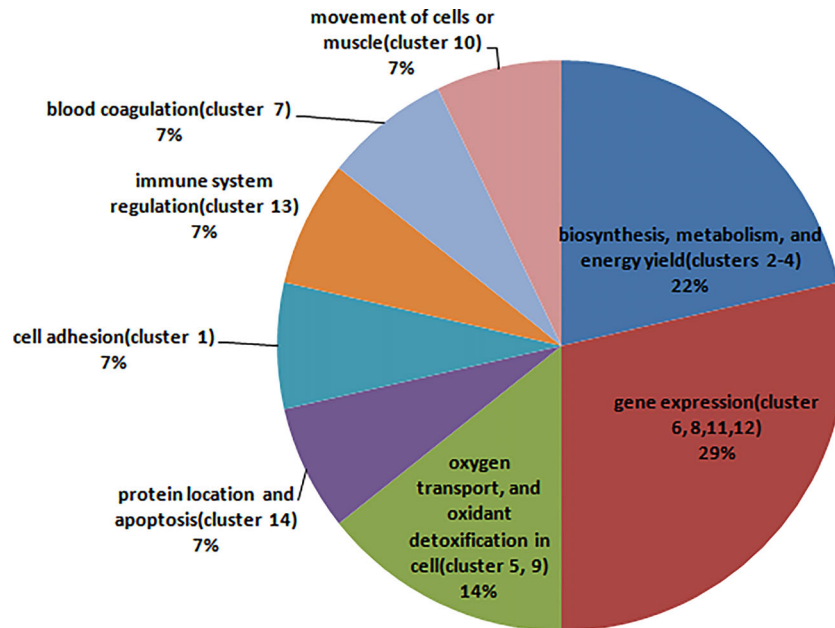


FIGURE 6 | The pie chart shows the main biological function that each cluster involved in, and the percentage that the count of the clusters involved in this biological function accounted for all clusters.

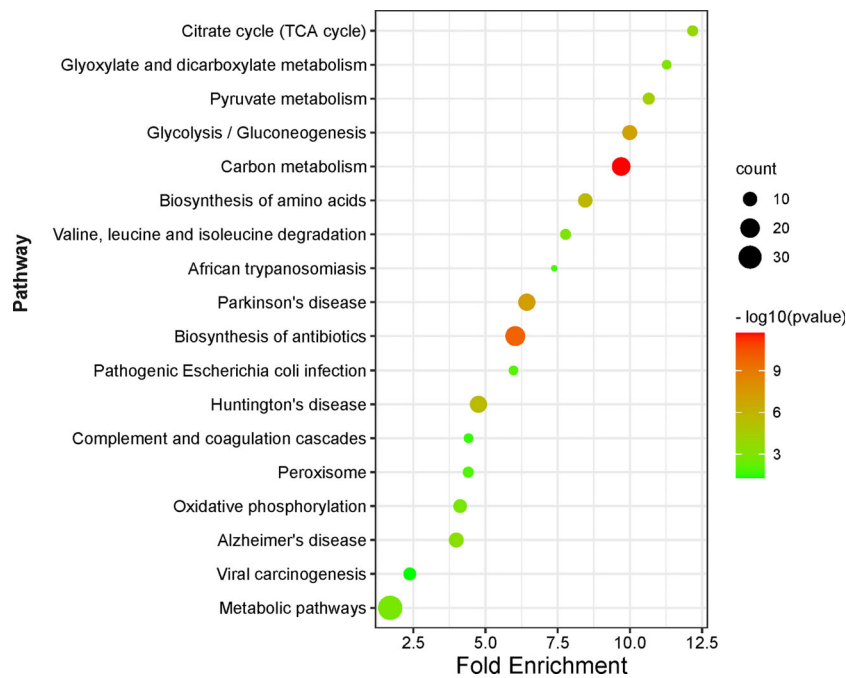


FIGURE 7 | KEGG pathway enrichment analysis of DAPs between NF-PitNETs and the controls. The Y axis shows different pathway terms, the X axis shows fold enrichment. Fold enrichment is calculated as followed: $\frac{Genehits}{Hitstotal} / \frac{Genepathway}{Genetotal}$. *Genehits* represents the number of hits in the selected pathway; *Genepathway* represents the number of genes in the selected pathway of KEGG background; *Hitstotal* is the number of total hits in all pathways; *Genetotal* means the number of total genes in all pathways of KEGG background. The circle size represents the count of genes enriched on the pathway. The circle color shows the $-\log_{10}(p\text{value})$ of the pathway.

oxidative phosphorylation pathway were increased in NF-PitNETs, including residues K538 (only acetylated in NF-PitNETs) in mitochondrial succinate dehydrogenase [ubiquinone] flavoprotein subunit (ID: P31040), K233, K154, and K244 (only acetylated in NF-PitNETs) in mitochondrial ATP synthase F(0) complex subunit B1 (ID: P24539), K522 (only acetylated in NF-PitNETs) in mitochondrial ATP synthase subunit beta (ID: P06576), K60 (ratio of T/N=3.79, $p=4.00E-02$), K199 and K162 (only acetylated in NF-PitNETs) in mitochondrial ATP synthase subunit O (ID: P48047), K136 (only acetylated in NF-PitNETs) in mitochondrial ATP synthase subunit delta (ID: P30049), K539 (ratio of T/N=1.77, $p=4.68E-02$), and K427 (only acetylated in NF-PitNETs) in mitochondrial ATP synthase subunit alpha (ID: P25705), K63 (ratio of T/N=5.48, $p=9.47E-05$), and K72 (ratio of T/N= 2.94, $p=2.02E-03$) in mitochondrial ATP synthase subunit d (ID: O75947), and K37 (ratio of T/N=1.61, $p=1.19E-02$) in mitochondrial ATP synthase subunit epsilon (ID: P56381). (viii) Metabolic pathway involves many interconnected cellular pathways that ultimately provide cells with energy required to execute their function (44). In cancer, oncogene activation and tumor suppressor loss promote metabolic reprogramming, and cause enhanced nutrient uptake to supply malignant cell energetic and biosynthetic pathways (45). Therefore, metabolic pathway alteration, in another word, metabolic reprogramming, might also be key for NF-PitNETs tumorigenesis and progression (**Supplementary Figure S1.8**). This study found that metabolic pathway enriched the largest number of DAPs ($n = 34$), and acetylation occurred at the metabolic pathway-related molecules, including acetylation at residues K89, K5, K228, K71, and K262 (only acetylated in controls) in alpha-enolase (ID: P06733), K77 (only acetylated in NF-PitNETs) in mitochondrial pyruvate dehydrogenase E1 component subunit alpha (somatic form) (ID: P08559), K135, and K89 (only acetylated in controls) in pyruvate kinase PKM (ID: P14618), K7 (ratio of T/N=0.58, $p=1.52E-02$) in transaldolase (ID: P37837), K194 (ratio of T/N=1.74, $p=4.24E-03$), and K117 (ratio of T/N=0.25, $p=2.50E-02$) in glyceraldehyde-3-phosphate dehydrogenase (ID: P04406), K81 (ratio of T/N=5.38, $p=3.75E-03$) in cytoplasmic isocitrate dehydrogenase [NADP] (ID: O75874), K314 (ratio of T/N =2.71, $p=2.20E-02$), K185 (only acetylated in NF-PitNETs), K324 and K239 (only acetylated in controls) in mitochondrial malate dehydrogenase (ID: P40926), K298, and K236 (only acetylated in controls) in cytoplasmic malate dehydrogenase (ID: P40925), K7 (only acetylated in controls) in alcohol dehydrogenase class-3 (ID: P11766), K39 (ratio of T/N=0.06, $p=7.09E-04$) in phosphoglycerate mutase 1 (ID: P18669), K302 (ratio of T/N=1.71, $p=8.69E-03$) in mitochondrial aspartate aminotransferase (ID: P00505), K291, K146, K156 and K361 (only acetylated in controls) in phosphoglycerate kinase 1 (ID: P00558), K538 (only acetylated in NF-PitNETs) in mitochondrial succinate dehydrogenase [ubiquinone] flavoprotein subunit (ID: P31040), K231(only acetylated in controls), and K225 (ratio of T/N=0.44, $p=3.28E-04$) in triosephosphate isomerase (ID: P60174), and K330 and K200 (only acetylated in controls) in fructose-bisphosphate aldolase A (ID: P04075), K202 (ratio of T/N =4.13, $p=3.34E-02$), K257 (ratio of T/N=0.35, $p=1.13E-02$), and K124 (only acetylated in controls) in mitochondrial acetyl-CoA acetyltransferase (ID:

P24752), K267 (ratio of T/N=1.95, $p=1.42E-04$) in mitochondrial dihydrolipoylde hydrogenase (ID: P09622), K63 (ratio of T/N= 5.48, $p=9.47E-05$), and K72 (ratio of T/N= 2.94, $p=2.02E-03$) in mitochondrial ATP synthase subunit d (ID: O75947), K30 (only acetylated in NF-PitNETs) in 4-trimethylaminobutyraldehyde dehydrogenase (ID: P49189), K539 (ratio of T/N=1.77, $p=4.68E-02$), and K427 (only acetylated in NF-PitNETs) in mitochondrial ATP synthase subunit alpha (ID: P25705), K233, K154, and K244 (only acetylated in NF-PitNETs) in mitochondrial ATP synthase F(0) complex subunit B1 (ID: P24539), K522 (only acetylated in NF-PitNETs) in mitochondrial ATP synthase subunit beta (ID: P06576), K60 (ratio of T/N = 3.79, $p= 4.00E-02$), K199 and K162 (only acetylated in NF-PitNETs) in mitochondrial ATP synthase subunit O (ID: P48047), K86 (ratio of T/N=0.36, $p=7.61E-04$) in mitochondrial cytochrome c oxidase subunit 5B (ID: P10606), K37 (ratio of T/N=1.61, $p=1.19E-02$), and K21 (ratio of T/N=0.38, $p=2.11E-03$) in mitochondrial ATP synthase subunit epsilon (ID: P56381), K294 (only acetylated in NF-PitNETs) in mitochondrial 2-oxoisovalerate dehydrogenase subunit beta (ID: P21953), K26 (only acetylated in controls) in nucleoside diphosphate kinase A (ID: P15531), K70 (ratio of T/N=13.46, $p = 1.97E-03$) in mitochondrial NAD(P) transhydrogenase (ID: Q13423), K1704 (ratio of T/N = 2.28, $p = 6.37E-03$) in fatty acid synthase (ID: P49327), K189 (only acetylated in NF-PitNETs) in mitochondrial monofunctional C1-tetrahydrofolate synthase (ID: Q6UB35), K419 (ratio of T/N=13.46, $p=5.17E-03$) in retinal dehydrogenase 1 (ID: P00352), K48 (ratio of T/N=2.97, $p=6.90E-03$) in mitochondrial hydroxymethylglutaryl-CoA lyase (ID: P35914), K204 (only acetylated in NF-PitNETs) in mitochondrial methylglutaconyl-CoA hydratase (ID: Q13825), and K136 (only acetylated in NF-PitNETs) in mitochondrial ATP synthase subunit delta (ID: P30049). These acetylated proteins and acetylation sites involved in the metabolic pathway would expand the research data for the study of NF-PitNETs pathogenesis. (ix) Biosynthesis of amino acids is a crucial process constructing the precursor of proteins to participate in vital movement. The deregulated catabolism/anabolism of amino acids, especially serine, glutamine and glycine, were reported to function as metabolic regulators in promoting cancer cell growth (46) (**Supplementary Figure S1.9**). The acetylated proteins enriched in this pathway mainly consisted of enzymes involved in glycolysis, which were able to catalyze syntheses of 3-hosphoglycerate, phosphoenolpyruvate, and pyruvic acid, and provided carbon skeleton for serine, tyrosine and alanine, etc. This study found acetylation occurred at the enzymes involved in biosynthesis of amino acids, including acetylation at residues K89, K5, K228, K71, and K262 (only acetylated in controls) in alpha-enolase (ID: P06733), K135, and K89 (only acetylated in controls) in pyruvate kinase PKM (ID: P14618), K7 (ratio of T/N=0.58, $p=1.52E-02$) in transaldolase (ID: P37837), K194 (ratio of T/N=1.74, $p=4.24E-03$), and K117 (ratio of T/N=0.25, $p=2.50E-02$) in glyceraldehyde-3-phosphate dehydrogenase (ID: P04406), K81 (ratio of T/N=5.38, $p=3.75E-03$) in cytoplasmic isocitrate dehydrogenase [NADP] (ID: O75874), K39 (ratio of T/N =0.06, $p=7.09E-04$) in phosphoglycerate mutase 1 (ID: P18669), K302 (ratio of T/N=1.71, $p=8.69E-03$) in mitochondrial aspartate aminotransferase (ID: P00505), K291, K146, K156 and K361

(only acetylated in controls) in phosphoglycerate kinase 1 (ID: P00558), K231 (only acetylated in controls), and K225 (ratio of T/N=0.44, $p=3.28E-04$) in triosephosphate isomerase (ID: P60174), and K330 and K200 (only acetylated in controls) in fructose-bisphosphate aldolase A (ID: P04075).

Three pathways associated with nervous system diseases were Parkinson's disease pathway, Huntington's disease pathway, and Alzheimer's disease pathway. The acetylated proteins enriched in these three pathways were mainly enzymes involved in metabolism and energy yield, which indicated that the acetylation mainly occurred at enzymes, and their alterations might result in extensive influence in metabolism by various pathway. (i) This study found acetylation occurred at the Parkinson's disease pathway-related molecules (**Supplementary Figure S1.10**), including acetylation at residues K538 (only acetylated in NF-PitNETs) in mitochondrial succinate dehydrogenase [ubiquinone] flavoprotein subunit (ID: P31040), K63 (ratio of T/N=5.48, $p=9.47E-05$), and K72 (ratio of T/N=2.94, $p=2.02E-03$) in mitochondrial ATP synthase subunit d (ID: O75947), K539 (ratio of T/N=1.77, $p=4.68E-02$), and K427 (only acetylated in NF-PitNETs) in mitochondrial ATP synthase subunit alpha (ID: P25705), K233, K154, and K244 (only acetylated in NF-PitNETs) in mitochondrial ATP synthase F(0) complex subunit B1 (ID: P24539), K522 (only acetylated in NF-PitNETs) in mitochondrial ATP synthase subunit beta (ID: P06576), K60 (ratio of T/N=3.79, $p=4.00E-02$), K199 and K162 (only acetylated in NF-PitNETs) in mitochondrial ATP synthase subunit O (ID: P48047), K86 (ratio of T/N=0.36, $p=7.61E-04$) in mitochondrial cytochrome c oxidase subunit 5B (ID: P10606), K37 (ratio of T/N=1.61, $p=1.19E-02$), and K21 (ratio of T/N=0.38, $p=2.11E-03$) in mitochondrial ATP synthase subunit epsilon (ID: P56381), and K136 (only acetylated in NF-PitNETs) in mitochondrial ATP synthase subunit delta (ID: P30049), K195 (only acetylated in controls) in ubiquitin carboxyl-terminal hydrolase isozyme L1 (ID: P09936), K72 (only acetylated in controls), and K427 (only acetylated in NF-PitNETs) in voltage-dependent anion-selective channel protein 2 (ID: P45880), K23 (only acetylated in NF-PitNETs) in ADP/ATP translocase 3 (ID: P12236), K23 (only acetylated in NF-PitNETs) in ADP/ATP translocase 1 (ID: P12235), K62 (only acetylated in controls) in protein deglycase DJ-1 (ID: Q99497), and K23 (only acetylated in NF-PitNETs) ADP/ATP translocase 2 (ID: P05141). (ii) This study found acetylation occurred at the Huntington's disease pathway-related molecules (**Supplementary Figure S1.11**), including acetylation at residues K538 (only acetylated in NF-PitNETs) in mitochondrial succinate dehydrogenase [ubiquinone] flavoprotein subunit (ID: P31040), K63 (ratio of T/N=5.48, $p=9.47E-05$), and K72 (ratio of T/N= 2.94, $p=2.02E-03$) in mitochondrial ATP synthase subunit d (ID: O75947), K539 (ratio of T/N=1.77, $p=4.68E-02$), and K427 (only acetylated in NF-PitNETs) in mitochondrial ATP synthase subunit alpha (ID: P25705), K233, K154, and K244 (only acetylated in NF-PitNETs) in mitochondrial ATP synthase F(0) complex subunit B1 (ID: P24539), K522 (only acetylated in NF-PitNETs) in mitochondrial ATP synthase subunit beta (ID: P06576), K60

(ratio of T/N=3.79, $p=4.00E-02$), K199 and K162 (only acetylated in NF-PitNETs) in mitochondrial ATP synthase subunit O (ID: P48047), K86 (ratio of T/N=0.36, $p=7.61E-04$) in mitochondrial cytochrome c oxidase subunit 5B (ID: P10606), K37 (ratio of T/N=1.61, $p=1.19E-02$), and K21 (ratio of T/N=0.38, $p=2.11E-03$) in mitochondrial ATP synthase subunit epsilon (ID: P56381), and K136 (only acetylated in NF-PitNETs) in mitochondrial ATP synthase subunit delta (ID: P30049), K72 (only acetylated in controls), and K427 (only acetylated in NF-PitNETs) in voltage-dependent anion-selective channel protein 2 (ID: P45880), K23 (only acetylated in NF-PitNETs) in ADP/ATP translocase 3 (ID: P12236), K23 (only acetylated in NF-PitNETs) in ADP/ATP translocase 1 (ID: P12235), K23 (only acetylated in NF-PitNETs) ADP/ATP translocase 2 (ID: P05141), K123 (ratio of T/N=0.30, $p=1.38E-03$) in superoxide dismutase [Cu-Zn] (ID: P00441), and K130 (only acetylated in NF-PitNETs) in mitochondrial superoxide dismutase [Mn] (ID: P04179). (iii) This study found acetylation occurred at the Alzheimer's disease pathway-related molecules (**Supplementary Figure S1.12**), including acetylation at residues K538 (only acetylated in NF-PitNETs) in mitochondrial succinate dehydrogenase [ubiquinone] flavoprotein subunit (ID: P31040), K63 (ratio of T/N=5.48, $p=9.47E-05$), and K72 (ratio of T/N= 2.94, $p=2.02E-03$) in mitochondrial ATP synthase subunit d (ID: O75947), K539 (ratio of T/N=1.77, $p=4.68E-02$), and K427 (only acetylated in NF-PitNETs) in mitochondrial ATP synthase subunit alpha (ID: P25705), K233, K154, and K244 (only acetylated in NF-PitNETs) in mitochondrial ATP synthase F(0) complex subunit B1 (ID: P24539), K522 (only acetylated in NF-PitNETs) in mitochondrial ATP synthase subunit beta (ID: P06576), K60 (ratio of T/N=3.79, $p=4.00E-02$), K199 and K162 (only acetylated in NF-PitNETs) in mitochondrial ATP synthase subunit O (ID: P48047), K86 (ratio of T/N=0.36, $p=7.61E-04$) in mitochondrial cytochrome c oxidase subunit 5B (ID: P10606), K37 (ratio of T/N=1.61, $p=1.19E-02$), and K21 (ratio of T/N=0.38, $p=2.11E-03$) in mitochondrial ATP synthase subunit epsilon (ID: P56381), and K136 (only acetylated in NF-PitNETs) in mitochondrial ATP synthase subunit delta (ID: P30049), K194 (ratio of T/N=1.74, $p=4.24E-03$), and K117 (ratio of T/N=0.25, $p=2.50E-02$) in glyceraldehyde-3-phosphate dehydrogenase (ID: P04406), and K133 (only acetylated in controls) in calmodulin (Fragment) (ID: H0Y7A7).

Three pathways pathogenic *Escherichia Coli* infection pathway, viral carcinogenesis, and African trypanosomiasis were associated with infectious diseases. (i) The acetylated proteins enriched in pathogenic *Escherichia Coli* infection pathway extensively existed in cytoplasm and nucleus. Tubulin, actin, and ezrin constituted cytoskeleton, maintained cell morphology and motility, and regulated cell cycle or cell-cell adhesion. Nucleolin participated in the cleavage of rRNA precursors, DNA replication, and cell cycle regulation (47) (**Supplementary Figure S1.13**). This study found that acetylation occurred at the pathogenic *Escherichia Coli* infection-related molecules, including acetylation at residues K449 (only acetylated in controls) in nucleolin (ID: P19338), K440 (only acetylated in controls) in tubulin alpha-1C chain (ID:

F5H5D3), K61 (ratio of T/N=0.22, $p=2.59E-04$) and K326 (only acetylated in controls) in actin cytoplasmic 1 (ID: P60709), K394 (ratio of T/N=0.29, $p=2.08E-02$) and K336 (ratio of T/N=0.21, $p=1.77E-04$) in tubulin alpha-1B chain (ID: P68363), and K35 (only acetylated in controls) in ezrin (ID: P15311). (ii) One of proteins enriched in viral carcinogenesis pathway is 14-3-3 protein. 14-3-3 protein has many subtypes, including 14-3-3 protein gamma, theta, and epsilon, and many of them have carcinogenic potential (48–50) (**Supplementary Figure S1.14**). This study found that acetylation occurred at the viral carcinogenesis-related molecules, including acetylation at residues K135 and K89 (only acetylated in controls) in pyruvate kinase (ID: P14618), K152 (only acetylated in controls) in 14-3-3 protein gamma (ID: P61981), K9 (ratio of T/N=1.60, $p=2.36E-02$) in histone H4 (ID: P62805), K398 (ratio of T/N=0.40, $p=4.72E-02$) in alpha-actinin-1 (ID: P12814), K47 (only acetylated in controls) in histone H2B type 1-K (ID: O60814), K68 (only acetylated in controls) in 14-3-3 protein theta (ID: P27348), K150 (only acetylated in controls) in ran-specific GTPase-activating protein (ID: P43487), and K3 and K9 (only acetylated in controls) in 14-3-3 protein zeta/delta (ID: P63104). The acetylation level decreased in 14-3-3 protein in NF-PitNETs, the alteration of which might support NF-PitNETs tumorigenesis. (iii) Human African trypanosomiasis is a potentially fatal disease caused by the *Trypanosoma Brucei* sp (a kind of parasite) (51) (**Supplementary Figure S1.15**). This study found that acetylation occurred at the African trypanosomiasis-related molecules, including acetylation at residues K12 (ratio of T/N=0.37, $p=4.29E-02$) and K91 (ratio of T/N=0.13, $p=1.13E-02$) in hemoglobin subunit alpha (ID: P69905), K96 (only acetylated in controls) in mutant hemoglobin beta chain (Fragment) (ID: Q9BWU5), K57 (only acetylated in controls) in hemoglobin alpha-1 globin chain (Fragment) (ID: E9M4D4), K12 (ratio of T/N=0.37, $p=4.29E-02$) in alpha globin chain (Fragment) (ID: U3XPX0), K96 (ratio of T/N=0.54, $p=2.14E-02$) in hemoglobin subunit beta (ID: P68871), K157 (ratio of T/N=0.18, $p=3.58E-03$), K262, K230, and K206 (only acetylated in controls) in apolipoprotein A-I (ID: P02647), and K17 (ratio of T/N=0.62, $p=2.01E-02$) in alpha-2 globin chain (ID: D1MGQ2).

In recent years, mammalian immune cells were found to synthesize antibiotics, itaconic acid, from citric acid cycle intermediate, to prevent bacteria from surviving in cells (52) (**Supplementary Figure S1.16**). All proteins enriched in biosynthesis of antibiotic pathway were also enriched in the nine metabolism and energy yield pathways. This study found that acetylation occurred at the biosynthesis of antibiotics-related molecules, including acetylation at residues K89, K5, K228, K71, and K262 (only acetylated in controls) in alpha-enolase (ID: P06733), K77 (only acetylated in NF-PitNETs) in mitochondrial pyruvate dehydrogenase E1 component subunit alpha (somatic form) (ID: P08559), K26 (only acetylated in controls) in nucleoside diphosphate kinase A (ID: P15531), K135, and K89 (only acetylated in controls) in pyruvate kinase PKM (ID: P14618), K7 (ratio of T/N=0.58, $p=1.52E-02$) in transaldolase (ID: P37837), K194 (ratio of T/N=1.74, $p=4.24E-$

03), and K117 (ratio of T/N=0.25, $p=2.50E-02$) in glyceraldehyde-3-phosphate dehydrogenase (ID: P04406), K294 (only acetylated in NF-PitNETs) in mitochondrial 2-oxoisovalerate dehydrogenase subunit beta (ID: P21953), K81 (ratio of T/N=5.38, $p=3.75E-03$) in isocitrate dehydrogenase [NADP] cytoplasmic (ID: O75874), K314 (ratio of T/N=2.71, $p=2.20E-02$), K185 (only acetylated in NF-PitNETs), K324 and K239 (only acetylated in controls) in mitochondrial malate dehydrogenase (ID: P40926), K298, and K236 (only acetylated in controls) in cytoplasmic malate dehydrogenase (ID: P40925), K7 (only acetylated in controls) in alcohol dehydrogenase class-3 (ID: P11766), K39 (ratio of T/N=0.06, $p=7.09E-04$) in phosphoglycerate mutase 1 (ID: P18669), K302 (ratio of T/N=1.71, $p=8.69E-03$) in mitochondrial aspartate aminotransferase (ID: P00505), K291, K146, K156 and K361 (only acetylated in controls) in phosphoglycerate kinase 1 (ID: P00558), K538 (only acetylated in NF-PitNETs) in mitochondrial succinate dehydrogenase [ubiquinone] flavoprotein subunit (ID: P31040), K231 (only acetylated in controls), and K225 (ratio of T/N=0.44, $p=3.28E-04$) in triosephosphate isomerase (ID: P60174), K330 and K200 (only acetylated in controls) in fructose-bisphosphate aldolase A (ID: P04075), K202 (ratio of T/N=4.13, $p=3.34E-02$), K257 (ratio of T/N=0.35, $p=1.13E-02$), and K124 (only acetylated in controls) in mitochondrial acetyl-CoA acetyltransferase (ID: P24752), and K267 (ratio of T/N=1.95, $p=1.42E-04$) in mitochondrial dihydrolipoyl dehydrogenase (ID: P09622), K30 (only acetylated in NF-PitNETs) in 4-trimethylaminobutyraldehyde dehydrogenase (ID: P49189), and K169 (only acetylated in controls) in catalase (ID: P04040). The acetylation levels of most of these proteins were decreased in NF-PitNETs.

Peroxisome is consisted of many kinds of oxidases, and contributes to cellular lipid metabolism and redox balance. Peroxisome has ability of detoxification, including removal of superoxide radicals originated from respiratory chain (53). The dysfunction of peroxisome is associated with the development of many cancers (54–56) (**Supplementary Figure S1.17**). This study found that acetylation occurred at the peroxisome complex, including acetylation at residues K48 (ratio of T/N=2.97, $p=6.90E-03$) in mitochondrial hydroxymethylglutaryl-CoA lyase (ID: P35914), K81 (ratio of T/N=5.38, $p=3.75E-03$) in isocitrate dehydrogenase [NADP] cytoplasmic (ID: O75874), K130 (ratio of T/N=0.31, $p=3.31E-03$), and K169 (only acetylated in controls) in peroxiredoxin-1 (ID: Q06830), K169 (only acetylated in controls) in catalase (ID: P04040), K123 (ratio of T/N=0.30, $p=1.38E-03$) in superoxide dismutase [Cu-Zn] (ID: P00441), and K130 (only acetylated in NF-PitNETs) in mitochondrial superoxide dismutase [Mn] (ID: P04179).

The last pathway was complement and coagulation cascade pathway, and all these DAPs enriched in this pathway were from blood. In the blood circulation, the coagulation system, platelets, complement system, and fibrinolysis system constructed a close and complex network. They activated and regulated each other, and mutually mediated tissue homeostasis and immune monitoring. The deregulation of each cascade system caused clinical manifestations and the progression of different diseases,

such as C3 glomerulonephritis, sepsis, and systemic lupus erythematosus (57) (**Supplementary Figure S1.18**). This study found that acetylation occurred at the complement and coagulation cascade-related molecules, including acetylation at residues K148, K620, K167, and K195 (only acetylated in NF-PitNETs) in fibrinogen alpha chain (ID: P02671), K153 (only acetylated in NF-PitNETs) and K231 (only acetylated in controls) in fibrinogen gamma chain (ID: P02679), K77 (only acetylated in NF-PitNETs) in fibrinogen beta chain (ID: P02675), K298 (ratio of T/N=0.07, $p=2.05E-03$) and K153 (only acetylated in controls) in alpha-1-antitrypsin (ID: P01009), and K1176 (only acetylated in controls) in alpha-2-macroglobulin (ID: P01023).

Integration of Acetylomics and Ubiquitinomics Data in NF-PitNETs Versus Controls

A total of 15 lysine sites within 14 proteins was modified by both acetyl group and ubiquitin (**Table 1**). Of them, histone H2A type 1 (P04908), histone H2A (A0A0U1RRH7), and histone H2B (B4DR52) were histone to constitute nucleosome, whose main molecular functions were DNA binding and protein heterodimerization. histone H2A type 1 (P04908) and histone H2A (A0A0U1RRH7) maintained the structure of chromatin and their silence repressed transcription (58). Histone H2A type 1 (P04908) negatively regulated cell proliferation. Epididymis luminal protein 112 (B2RDW1) had two lysine sites that were both acetylated and ubiquitinated, which contributed to form the complex structure of ribosome and participated in translation - a cellular metabolic process to form proteins. Vimentin (P08670) attached to the nucleus, mitochondria, and endoplasmic reticulum was found in various cells, especially mesenchymal cells. Vimentin (P08670) had extensive molecular functions; for example, vimentin (P08670) bound scaffold proteins to activate and localize signaling components to specific areas of cell (59, 60), also participated in SMAD protein signal transduction that was the key step of TGF- β pathway regulating cell proliferation, differentiation, migration, and death (61). Ubiquitin carboxyl-terminal hydrolase (D6R956) facilitated protein deubiquitination to affect protein catabolism (62). Vesicle-associated membrane protein 2 (L7N2F9) mediated membrane fusion, which was a basic step of many biological processes, such as neurotransmitter transmission and antigen presenting. Growth hormone A1 (Q5I0G2) was coded by PRL gene, and regulated the hormone activity. Actin cytoplasmic 1 (P60709) localized in the cytoplasm and nucleus, and participated in cytoskeleton formation, cell motility, gene transcription, and repair of damaged DNA (63, 64). Tubulin alpha-1C chain 1 (F5H5D3) was a member of tubulin superfamily, and played functions in cytoskeleton maintaining and spindle fiber constitution in mitosis. Alpha-2 globin chain (D1MGQ2), hemoglobin subunit beta (P68871), hemoglobin subunit alpha (P69905), and hemoglobin subunit delta (P02042) were the parts of hemoglobin, and played roles in oxygen transport, hemoglobin formation, and cellular oxidant

detoxification. Thereby, these proteins that were both acetylated and ubiquitinated at the same site in NF-PitNETs were involved in multiple biological processes, including gene expression, protein metabolic process, cell motility, oxygen transport, and hemostatic process. Furthermore, comparative analysis of these proteins (D1MGQ2, P6887, P04908, P60709, L7N2F9, F5H5D3, B2RDW1, and Q5I0G2), which were quantified with statistically significant ratio of T/N in both acetylomics and ubiquitinomics data, found that their acetylation levels were decreased but their ubiquitination levels were increased in NF-PitNETs, which showed the competitive characteristics of acetylation and ubiquitination at the lysine site in a protein in NF-PitNETs.

Integration of Acetylomics Data and Invasive Transcriptomics Data in NF-PitNETs Versus Controls

A total of 26 overlapped molecules was identified between DAP data and invasive DEG data to investigate the effect of acetylation on the invasive behavior of NF-PitNETs (**Figure 8; Table 2**). These overlapped molecules (DAPs; Invasive DEGs) were enriched in eight statistically significant KEGG signaling pathways, including glycolysis/gluconeogenesis, carbon metabolism, oxidative phosphorylation, fructose and mannose metabolism, biosynthesis of amino acids, Parkinson's disease, Alzheimer's disease, and Huntington's disease (**Supplementary Table 9**). GO analysis revealed that these overlapped molecules were significantly enriched in multiple MFs (**Supplementary Table 10**), CCs (**Supplementary Table 11**), and BPs (**Supplementary Table 12**). For example, TPI1 (triosephosphate isomerase) was located in extracellular space, extracellular exosome, and cytosol, performed protein binding molecular function, and participated in canonical glycolysis, glycolytic process, and gluconeogenesis. Clustering analysis of these KEGG pathways, MFs, CCs, and BPs showed that most overlapped molecules were related to metabolism and energy production (**Table 3**). Metabolic reprogramming, such as "Warburg effect", had been recognized as a promotion mechanism for tumorigenesis and malignant activity (30, 65), and acetylation regulated the physiological functions of most metabolic enzymes (66). Thereby, the invasiveness of NF-PitNETs might be associated with acetylation-mediated metabolic reprogramming.

Confirmation of DAPs in NF-PitNETs

A randomly selected DAP - PGK1 was used for further analysis with IP and western blot experiments (**Figure 9**). PGK1 was a down-acetylated protein in NF-PitNETs relative to controls identified with acetylomics. Acetylation at different lysine residues in PGK1 was able to positively or negatively regulate its enzymatic activities, which initiated or altered some signaling pathways, such as metabolism or autophagy, leading to tumor formation or progression (67–69). Acetylated PGK1 functioned in signaling pathways such as glycometabolism, carbon metabolism, and biosynthesis of amino acids. The decreased

TABLE 1 | The proteins that were simultaneously acetylated and ubiquitinated at the same sites in NF-PitNETs and controls.

Acetylated peptides											
Accession No.	Gene name	Protein name	Modified peptide	Modified positions	Modified probabilities	Average (N)	Average (T)	Ratio (T/N)	P-value (t-test)	Accession No.	Gene name
D1MGQ2	HEA2	Alpha-2 globin chain	AAWGKVGAAHGEYGAELER	17	1	41878000	26586667	0.62	2.01E-02	D1MGQ2	HEA2
P6871	HEB	Hemoglobin subunit beta	GTFTLSELHCDKLVHPENFR	96	1	351830000	189023333	0.54	2.14E-02	P6871	HEB
P04908	HISTH2AB	Histone H2A type 1-BE	NDEELNKLGR	96	1	18918933	7585433	0.40	1.28E-03	P04908	HISTH2AB
P60709	ACTB	Actin, cytoskeletal 1	DSYVDEAGSKR	61	1	107031000	23652333	0.22	2.98E-04	P60709	ACTB
AAOUJRRH7	HEA1	Histone H2A	NDEELNKLGR	96	1	17806333	3620733	0.20	3.38E-05	AAOUJRRH7	HEA1
P68905	HEA1	Hemoglobin subunit alpha	TYFPHDLHSGSAQK*	57	1	319430000	425226667	1.33	9.01E-02	P68905	HEA1
D6R936	UCHL1	Ubiquitin carboxyl-terminal hydrolase delta	CFEKNEAQAADAVAGEGQR	135	1	10472100	7052300	0.67	1.84E-01	D6R936	UCHL1
PQ2042	HEB	Hemoglobin subunit delta	GTFSQLSELHCDKLVHPENFR	96	1	264988667	864430000	0.36	5.18E-01	PQ2042	HEB
P06870	VM	Vimentin	OVQDLTNKAVR	168	1	7992500	P06870			P06870	VM
L7N2F9	TUBA1C	Uncharacterized protein Tubulin alpha-1C chain1	ADALGASQFETSAAKLK	83	1	10451000	L7N2F9			L7N2F9	TUBA1C
F5HED3	RFS30A	Epididymis luminal protein 112	VGNYPPTVPGDLAKVQR	370	1	21804500	F5HED3			F5HED3	RFS30A
B2RDW1	RFS30A	Epididymis luminal protein 112	TITLEVPSDTENKAVK	27	1	51187500	B2RDW1			B2RDW1	RFS30A
Q5I032	PRL	Prolactin	AVBEEOIKR	152	1	103715667	Q5I032			Q5I032	PRL
B4DR52	RFS30A	Histone H2B	HAVSEGTAVTK	117	1		B4DR52			B4DR52	RFS30A
B2RDW1	RFS30A	Epididymis luminal protein 112	LDKTEGPPDOQR	33	1		B2RDW1			B2RDW1	RFS30A

Ubiquitinated peptides											
Accession No.	Gene name	Protein name	Modified peptide	Modified positions	Modified probabilities	Average (N)	Average (T)	Ratio (T/N)	P-value (t-test)	Accession No.	Gene name
		Alpha-2 globin chain	AAWGKVGAAHGEYGAELER	17	1	7090000					
		Hemoglobin subunit beta	GTFTLSELHCDKLVHPENFR	96	1	91800000					
		Histone H2A type 1-BE	NDEELNKLGR	96	1	3450000					
		Actin, cytoskeletal 1	DSYVDEAGSKR	61	1	2050000					
		Histone H2A	NDEELNKLGR	96	0.996						
		Hemoglobin subunit alpha	TYFPHDLHSGSAQK*	57	1	203000000					
		Ubiquitin carboxyl-terminal hydrolase delta	CFEKNEAQAADAVAGEGQR	135	1	5960000					
		Hemoglobin subunit delta	GTFSQLSELHCDKLVHPENFR	96	1	20100000					
		Vimentin	OVQDLTNKAVR	168	1	2970000					
		Uncharacterized protein Tubulin alpha-1C chain1	ADALGASQFETSAAKLK	83	0.876	20100000					
		Epididymis luminal protein 112	VGNYPPTVPGDLAKVQR	370	1	37800000					
		Epididymis luminal protein 112	TITLEVPSDTENKAVK	27	0.956	19800000					
		Growth hormone A1	AVBEEOIKR	153	1	5210000					
		Histone H2B	HAVSEGTAVTK	117	1	47000000					
		Epididymis luminal protein 112	LDKTEGPPDOQR	33	1	36800000					

DISCUSSION

This present study provided the first quantitative profiling of protein acetylation in NF-PitNET tissues. A total of 296 proteins with 517 acetylated sites was identified in NF-PitNETs compared to control pituitaries. The KEGG pathways, MFs, CCs, and BPs enriched with DAPs were clustered into 14 functional categories, which demonstrated that DAPs were widely involved in cellular biological processes and signaling pathways associated with metabolism, gene expression, cell adhesion, and immune system. Among 18 statistically significant KEGG signaling pathways enriched with DAPs, twelve pathways were metabolism-related pathways. Immunoprecipitation and western blotting analysis semi-quantitatively validated that acetyl-PGK1, a protein widely involved in glycometabolism, was decreased in NF-PitNETs. Furthermore, overlapping analysis of acetylomics and ubiquitinomics, and of DAP data and invasive DEGs data, found: (i) proteins that were modified by both acetyl and ubiquitin in NF-PitNETs were involved in nucleosome or ribosome, hemoglobin, prolactin, ubiquitin hydrolase, membrane proteins, and proteins constituting cytoskeleton; and acetylation levels of these proteins were decreased, whereas their ubiquitination levels were increased in NF-PitNETs. (ii) The invasiveness-related acetylated proteins were mainly involved in biological processes and signaling pathways about metabolism and energy yield, which suggested that NF-PitNET invasive behaviors might be acetylation-mediated metabolic reprogramming process.

Many tumor cells prefer to provide bioenergetics and growth requirements through glycolysis, rather than oxidative phosphorylation, during tumor growth progression, even with sufficient oxygen and normal mitochondria. Because glycolysis is able to provide sufficient cellular ATPs, and additional important metabolites to support the biosynthetic demands of consecutive cell proliferation (70). It is recognized that PitNETs also displayed very low levels of oxygen consumption, which was similar with other malignant tumors (71). A recent study found that PitNETs presented lactate progressive accumulation in cells, which suggests a bioenergetic metabolic shift from aerobic oxidation towards glycolysis metabolism to make tumor cells adapt to different energy requirements and enhance their survival chances (72). In NF-PitNETs, the vast majority of acetylation levels of lysine residues in proteins were decreased in glycolysis pathway, but increased in aerobic oxidation-related pathways, including TCA cycle and oxidative phosphorylation. This opposite acetylation status presented between glycolysis pathway and aerobic oxidation-related pathways indicated that the altered protein acetylation levels might involve in NF-PitNET metabolic

Differentially acetylated protein data **Invasive DEG data**

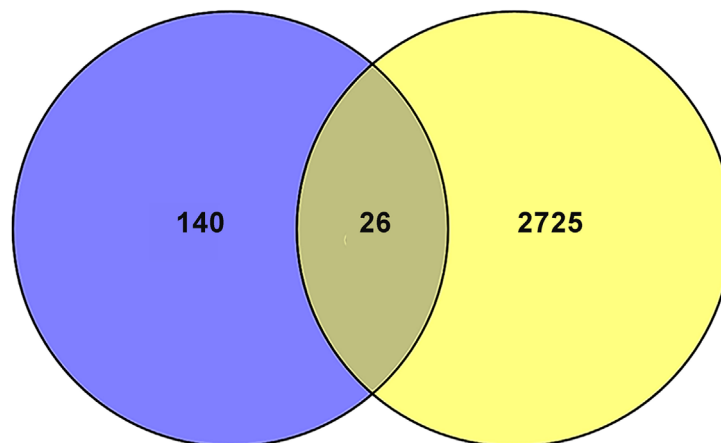


FIGURE 8 | The overlapping analysis between DAP data in NF-PitNETs vs. controls and DEG data in invasive NF-PitNETs vs. controls. The invasive DEG data were mined from the GEO database.

reprogram through changing enzyme activity, stability, or other potential ways to affect NF-PitNET progression. This study found that PGK1 acetylation status was decreased in NF-PitNETs with LC/MS analysis, which was further semi-quantitatively validated with IP in combination with an acetyl-lysine immunoblot. PGK1 functions in glycolysis metabolism, which reversibly catalyzes 1,3-diphosphoglycerate to 3-phosphoglycerate, and subsequently transfers a phosphoryl group to ADP, and yields a molecule of ATP. Study found that PGK1 acetylation affected brain tumorigenesis through mediating autophagy and the increased acetylation level of PGK1, which was correlated with the poor prognosis in glioblastoma (73). The PGK1 acetylation was also found to promote its enzymatic activity and liver cancer cell metabolism, and significantly associate with poor prognosis of liver cancer patients (68). Thus, the decreased acetylation level of PGK1 in NF-PitNETs might also affect NF-PitNET tumorigenesis and progression through metabolic reprogramming, autophagy or other underlying mechanisms, but of which detail is needed to be further studied.

The invasive characteristics of NF-PitNETs have been a hot pot for a long time. Invasive PitNETs tend to suffer tumor postoperative residual and re-growth because of cavernous sinus invasion or the internal carotid artery encircling, which is able to cause poor prognosis. However, their underlying invasive mechanism remains unclear (74). This study found 26 molecules were differentially acetylated, and were invasiveness-related DEGs, which were obtained through comparative analysis of DAP data and invasive DEG data. Most of these overlapped molecules (DAPs; Invasive DEGs) mainly functioned in metabolism-associated biological processes and pathways. Thus, it seems reasonable to propose that acetylation-mediated

metabolic reprogramming is associated with NF-PitNET invasive characteristics. Previous study found that metabolic stress, such as oxidative stress or hypoxia, was able to enhance invasiveness, angiogenesis, stemness, and metastatic potential of tumor cells (75). According to previous study, aerobic glycolysis was considered as one metabolic reprogram paradigm that might occur in NF-PitNETs (71, 72). It acidified extracellular matrix (ECM), and subsequently activated matrix metalloproteinase and cathepsin to increase ECM degradation, which paved the way for many basic cell behaviors, including cell migration (76). Some overlapped molecules, such as HSPA8 and GAPDH, were found to be regulated by acetylation and deacetylation and associated with invasiveness of cancers (77–81). The interesting mechanisms that how protein acetylation affects NF-PitNETs metabolic reprogram to enhance its invasiveness are worthy further investigating, which is promised to provide a novel therapeutic target for NF-PitNET radical treatment.

The co-regulation of acetylation and ubiquitination at specific lysine sites in some proteins might affect tumor development, such as Lys382 of p53 and Lys125 of SRSF5 (23, 25). One of mechanisms of acetylation and ubiquitination co-regulation is the direct competition between acetyl and ubiquitin at the same lysine sites to control protein stability. Under the complex of histone deacetylases and E3 (a factor transferring ubiquitin to proteins) actions, the substrate protein lysine sites relieve acetyl and are subsequently ubiquitinated to be degraded by the proteasome. The complex of histone acetyltransferases and ubiquitin-specific proteases in contrast would be free these ubiquitinated lysine residues and acetylated lysine residues, which protected the target proteins from proteasome-mediated protein degradation and maintained their stability (82). This

TABLE 2 | The overlapped molecules between differentially acetylated protein (DAP) data and invasive DEG data in NF-PitNETs. LogFC = log2(Fold change).

DAP data in NF-PitNETs											DEG data in invasive NF-PitNETs						
Accession No.	Gene name	Protein name	Modified positions	Modified probabilities	Charge	m/z	Average (N)	Average (T)	Ratio (T/N)	P-value (t-test)	DEG name	logFC	AveExpr	t	p-value	Adjusted p-value	B
P60174	TPH1	Triosephosphate isomerase	225	1	2	889.5	28466667	12484667	0.44	3.28E-04	TPH1	1.7746	10.1649	6.8527	5.53E-05	2.64E-03	2.2279
Q9HCJ6	VAT1L	Synaptic vesicle membrane protein VAT-1 homolog-like	240	1	2	632.3	3193300				VAT1L	-2.8646	8.1336	-4.2145	1.97E-03	1.87E-02	-1.4591
P02787	TF	Serotransferrin	676	1	2	826.9	7204767				TF	-3.9417	8.8827	-3.5149	5.98E-03	3.63E-02	-2.5952
			546	1	2	703.9	11366000										
			37	1	3	680.0	18033333										
			60	1	2	793.4	19133000										
			659	1	3	495.6	20861333										
P11142	HSPA8	Heat shock cognate 71 kDa protein	348	1	2	746.9	2893050				HSPA8	1.3891	11.6235	4.6920	9.61E-04	1.24E-02	-0.7175
P00738	HP	Haptoglobin	589	1	2	894.4	9957600				HP	-4.7051	9.9317	-5.5917	2.71E-04	6.08E-03	0.5913
P05060	CHGB	Secretogranin-1	321	1	2	658.8	6138650	2443767	0.40	1.66E-02	CHGB	-1.3288	14.5253	-3.2997	8.51E-03	4.53E-02	-2.9533
			465	1	3	512.3	12902000	3935700	0.31	2.52E-02							
			455	1	2	630.8	7019633										
			586	1	2	898.9	7349667										
			482	1	3	927.8	7493900										
			386	1	3	667.6	7725600										
			324	1	3	787.0	15918667										
			159	1	4	631.3	28833333										
			62	1	2	437.3	39083500										
			653	1	2	709.9	41254000										
			228	1	2	902.9	57414333										
			514	1	4	347.2	171960000										
P25705	ATP5A1	ATP synthase subunit alpha, mitochondrial	539	1	2	580.8	30030333	53227000	1.77	4.68E-02	ATP5A1	1.1189	14.7620	5.8239	1.99E-04	5.20E-03	0.9097
P12235	SLC25A4	ADP/ATP translocase 1	427	1	2	553.8		2483867			SLC25A4	1.1105	13.4174	3.9198	3.12E-03	2.44E-02	-1.9315
Q6UB35	MTHFD1L	Monofunctional C1-tetrahydrofolate synthase, mitochondrial	23	1	3	695.7		5633800			MTHFD1L	-1.9847	6.1122	-4.1324	2.24E-03	2.01E-02	-1.5898
O60814	HIST1H2BK	Histone H2B type 1-K	189	1	2	828.5		1644450			HIST1H2BK	1.2059	11.2191	3.8511	3.48E-03	2.60E-02	-2.0430

(Continued)

TABLE 2 | Continued

DAP data in NF-PitNETs											DEG data in invasive NF-PitNETs						
Accession No.	Gene name	Protein name	Modified positions	Modified probabilities	Charge	m/z	Average (N)	Average (T)	Ratio (T/N)	P-value (t-test)	DEG name	logFC	AveExpr	t	p-value	Adjusted p-value	B
P01189	POMC	Pro-opiomelanocortin	215	1	3	992.5	14740667				POMC	-7.4874	13.4887	-3.8110	3.71E-03	2.70E-02	-2.1083
P02768	ALB	Serum albumin	198	1	2	1084.0	21382667	6127633	0.29	3.96E-03	ALB	1.9536	6.1289	4.5055	1.27E-03	1.45E-02	-1.0035
			305	1	2	794.9	212540000	27026667	0.13	1.96E-03							
			298	1	2	863.9	216883333	26548667	0.12	1.44E-04							
			97	1	2	987.5	135626333	13136433	0.10	7.11E-03							
			257	1	2	847.0	87783000	6540100	0.07	1.14E-03							
			117	1	4	793.8	59130667	3887750	0.07	6.50E-03							
			160	1	3	940.8	575220000	28546333	0.05	1.68E-03							
			463	1	2	536.2	69895000	2682550	0.04	1.92E-02							
			402	1	3	696.4	148740000	5320100	0.04	1.20E-02							
			597	1	2	620.8	163196667	5693467	0.03	2.67E-03							
			229	1	2	619.3	284810000	9082167	0.03	8.56E-05							
			569	1	3	628.3	4536400										
			588	1	2	771.3	13804000										
			499	1	2	754.9	21198333										
			75	1	3	891.1	22158667										
			581	1	2	916.9	26848667										
			264	1	3	967.1	34013000										
310	0.5	4	1080.5	42471667													
558	1	2	654.4	68081667													
383	1	3	854.0	68391333													
219	1	2	630.8	104322667													
214	1	3	520.9	166796667													
P04406	GAPDH	Glyceraldehyde-3-phosphate dehydrogenase	194	1	2	629.3	57157667	99222000	1.74	4.24E-03	GAPDH	1.0920	14.8930	6.9715	4.82E-05	2.43E-03	2.3707
			117	1	2	554.3	29715667	7332267	0.25	2.50E-02							
P01236	PRL	Prolactin	215	1	2	581.3	60229667	13244000	0.22	6.75E-05	PRL	-11.8908	12.9988	-7.0186	4.56E-05	2.37E-03	2.4268
			209	1	3	425.6	62347667	6615500	0.11	4.54E-03							

(Continued)

TABLE 2 | Continued

DAP data in NF-PitNETs											DEG data in invasive NF-PitNETs						
Accession No.	Gene name	Protein name	Modified positions	Modified probabilities	Charge	m/z	Average (N)	Average (T)	Ratio (T/N)	P-value (t-test)	DEG name	logFC	AveExpr	t	p-value	Adjusted p-value	B
P06576	ATP5B	ATP synthase subunit beta, mitochondrial	522	1	2	564.8		40025000			ATP5B	1.7318	13.8762	7.3689	3.06E-05	1.99E-03	2.8353
P08865	RPSA	40S ribosomal protein SA	11	1	2	930.0	2031750				RPSA	-1.1474	12.2183	-5.7994	2.06E-04	5.28E-03	0.8765
P01242	GH2	Growth hormone variant	198	1	2	648.3	20045333				GH2	-11.4395	7.8750	-30.7801	6.85E-11	5.16E-07	13.8468
Q6ZN40	TPM1	Tropomyosin 1 (Alpha)	29	1	2	516.3	2542500				TPM1	2.2713	10.5676	7.2960	3.32E-05	2.05E-03	2.7515
P0DMV8	HSPA1A	Heat shock 70 kDa protein 1A	319	1	2	642.9	5140100				HSPA1A	-1.7989	11.7926	-4.7067	9.40E-04	1.22E-02	-0.6952
P05109	S100A8	Protein S100-A8	92	1	2	512.7	3562033				S100A8	4.4654	9.6276	4.6025	1.10E-03	1.33E-02	-0.8542
P04075	ALDOA	Fructose-bisphosphate aldolase A	330	1	2	568.3	9008850				ALDOA	1.2343	14.3796	5.4707	3.19E-04	6.64E-03	0.4222
P07602	PSAP	Prosaposin	200 413	1 1	3 2	1073.5 621.3	12204667 13188333	2534867	0.19	5.37E-03	PSAP	1.1000	11.9910	3.5359	5.78E-03	3.56E-02	-2.5605
P67936	TPM4	Tropomyosin alpha-4 chain	438 82	1 1	3 2	783.7 759.8	23948333 11726800				TPM4	-2.4119	9.3950	-3.9310	3.07E-03	2.42E-02	-1.9133
P14136	GFAP	Glial fibrillary acidic protein	11 260	1 1	2 2	621.3 654.3	20472333 6595600				GFAP	-4.2956	8.0496	-4.7014	9.48E-04	1.23E-02	-0.7033
P02647	APOA1	Apolipoprotein A-I	157	1	2	597.8	6918400	1258900	0.18	3.58E-03	APOA1	-1.8597	5.1153	-8.3617	1.06E-05	1.14E-03	3.9117
			262	1	2	778.9	6098750										
			230	1	2	728.9	8688850										
			206	1	2	600.3	10627500										
			130	1	2	711.9	18472967										
P56381	ATP5E		164 37	1 1	3 2	656.3 624.3	59276000 1963150	3165967	1.61	1.19E-02	ATP5E	1.8347	8.0226	4.8737	7.37E-04	1.06E-02	-0.4437
			21	1	2	619.3	7391700	2780333	0.38	2.11E-03							

LogFC >= 1: upregulated DEG. LogFC <= -1: downregulated DEGs.

TABLE 3 | Cluster analysis of KEGG pathways, MFs, CCs, and BPs enriched with overlapped molecules (DAPs; invasive DEGs) in NF-PitNETs.

Cluster	Category	ID	Term	Count	%	P Value	Overlapped molecules (DAPs; invasive DEGs)
Cluster 1	Cellular components	GO:0043209	myelin sheath	6	23.08	1.41E-06	HSPA8, ATP5B, ATP5A1, ALB, SLC25A4, GFAP
	Biological process	GO:0006754	ATP biosynthetic process	4	15.38	9.15E-06	ATP5B, ATP5E, ATP5A1, ALDOA
	Molecular functions	GO:0016887	ATPase activity	5	19.23	1.41E-04	HSPA8, ATP5B, ATP5E, ATP5A1, HSPA1A
	Molecular functions	GO:0046933	proton-transporting ATP synthase activity, rotational mechanism	3	11.54	2.82E-04	ATP5B, ATP5E, ATP5A1
	Cellular components	GO:0005753	mitochondrial proton-transporting ATP synthase complex	3	11.54	3.44E-04	ATP5B, ATP5E, ATP5A1
	Biological process	GO:0042776	mitochondrial ATP synthesis coupled proton transport	3	11.54	4.04E-04	ATP5B, ATP5E, ATP5A1
	Molecular functions	GO:0046961	proton-transporting ATPase activity, rotational mechanism	3	11.54	6.70E-04	ATP5B, ATP5E, ATP5A1
	Molecular functions	GO:0022857	transmembrane transporter activity	3	11.54	2.37E-03	ATP5B, ATP5E, ATP5A1
	Pathway	hsa05012	Parkinson's disease	4	15.38	6.55E-03	ATP5B, ATP5E, ATP5A1, SLC25A4
	Cellular components	GO:0005759	mitochondrial matrix	4	15.38	8.76E-03	ATP5B, MTHFD1L, ATP5E, ATP5A1
	Pathway	hsa05010	Alzheimer's disease	4	15.38	1.04E-02	ATP5B, ATP5E, ATP5A1, GAPDH
	Pathway	hsa05016	Huntington's disease	4	15.38	1.49E-02	ATP5B, ATP5E, ATP5A1, SLC25A4
	Cellular components	GO:0005739	mitochondrion	6	23.08	2.73E-02	ATP5B, MTHFD1L, ATP5A1, PSAP, SLC25A4, HSPA1A
	Pathway	hsa00190	Oxidative phosphorylation	3	11.54	5.12E-02	ATP5B, ATP5E, ATP5A1
Cluster 2	Molecular functions	GO:0016887	ATPase activity	5	19.23	1.41E-04	HSPA8, ATP5B, ATP5E, ATP5A1, HSPA1A
	Biological process	GO:0046034	ATP metabolic process	3	11.54	9.46E-04	HSPA8, ATP5B, HSPA1A
Cluster 3	Biological process	GO:0061621	canonical glycolysis	3	11.54	6.23E-04	TPI1, ALDOA, GAPDH
	Biological process	GO:0006096	glycolytic process	3	11.54	1.07E-03	TPI1, ALDOA, GAPDH
	Biological process	GO:0006094	gluconeogenesis	3	11.54	1.79E-03	TPI1, ALDOA, GAPDH
	Pathway	hsa00010	Glycolysis/Gluconeogenesis	3	11.54	1.44E-02	TPI1, ALDOA, GAPDH
	Pathway	hsa01230	Biosynthesis of amino acids	3	11.54	1.65E-02	TPI1, ALDOA, GAPDH
	Pathway	hsa01200	Carbon metabolism	3	11.54	3.81E-02	TPI1, ALDOA, GAPDH
Cluster 4	Cellular components	GO:0031012	extracellular matrix	4	15.38	6.67E-03	HSPA8, ATP5B, ATP5A1, GAPDH
	Cellular components	GO:0016020	membrane	8	30.77	2.00E-02	HSPA8, ATP5B, TPM4, MTHFD1L, ATP5A1, RPSA, ALDOA, GAPDH

study found that lysines co-regulated by acetylation and ubiquitination were down-acetylated but up-ubiquitinated in NF-PitNETs, which indicated that acetyl and ubiquitin directly competed for the same lysine, which might result in proteasome-mediated degradation of these proteins, and affect NF-PitNET development.

Moreover, NF-PitNET and control tissue samples were very limited and precious, only very limited amount of proteins were obtained for subsequent quantitative acetylomics analysis. More acetylated sites and acetylated proteins are promised to be

identified when the increased NF-PitNET protein samples available in future acetylomics analysis. This acetylome map of human NF-PitNETs described in this study is one component in the long-term program to find out NF-PitNET-specific acetylated proteins to clarify molecular mechanisms of NF-PitNETs. To achieve this goal, quantitative acetylomics needs to be further developed in the future.

In summary, the current study provided the first human acetylomics data in NF-PitNETs, offered a valuable resource for further study in NF-PitNET tumorigenesis and progression,

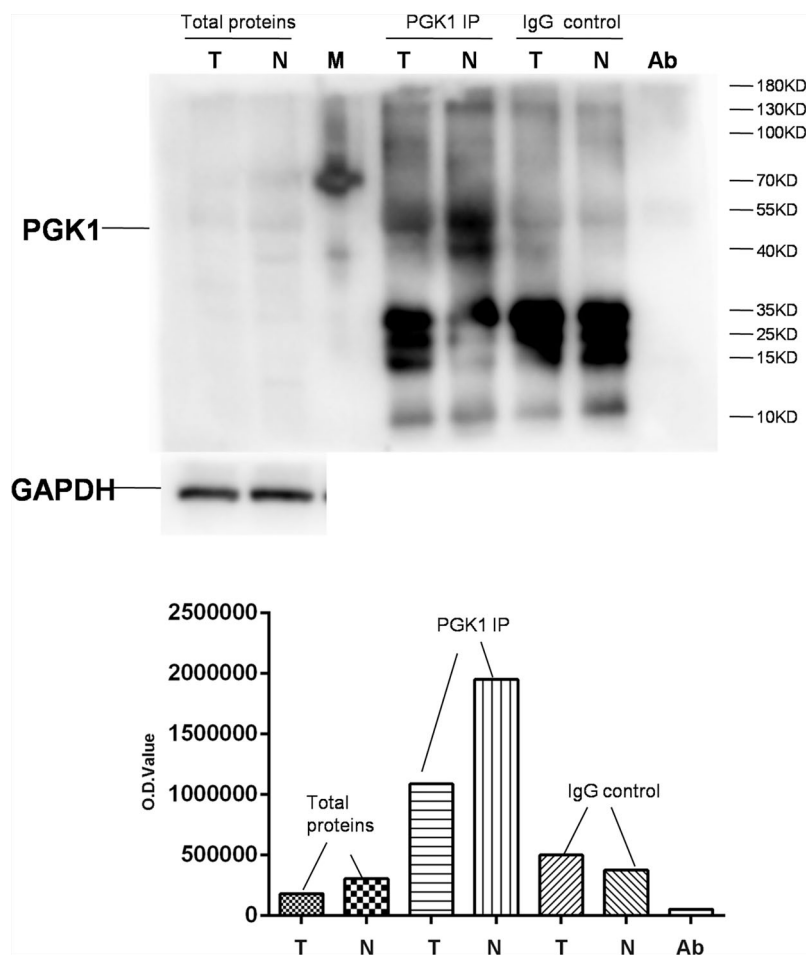


FIGURE 9 | Semi-quantitative analysis of acetylated PGK1 between NF-PitNETs and controls. PGK1 in protein samples extracted from NF-PitNET and control tissues was immunoprecipitated (IP) with anti-PGK1 antibody. A negative control immunoprecipitation experiment was performed with the normal mouse IgG antibody but not anti-PGK1 antibody to test the specificity of anti-PGK1 antibody. The IP products (PGK1 and IgG), anti-PGK1 antibodies (Ab), and total protein samples (tumor; control) were simultaneously immunoblotted with anti-acetyl-lysine antibody. T = NF-PitNETs. N = controls. M = markers.

which contributed to the discovery of effective biomarkers for early diagnosis and therapy of NF-PitNETs.

CONCLUSION

This study provided a comprehensive approach that integrated anti-acetyl antibody-based enrichment, LC-MS/MS, and literature-based bioinformatics to discover *in vivo* acetylated proteins and their acetylation sites, and to rationalize the functions of DAPs. A total of 296 acetylated proteins with 517 acetylated lysine sites provided a quantitative status of lysine acetylation in NF-PitNETs, and their bioinformatics analysis provided a new insight into the roles of protein lysine acetylation in formation and development of NF-PitNETs. The acetylation levels of more than half acetylated proteins were decreased in NF-PitNETs. Acetylation-mediated metabolic reprogramming might be considered as one of the underlying mechanisms in tumorigenesis and invasiveness of NF-

PitNETs. Further investigation is needed to ascertain the biological significance of these lysine acetylation events and their relevance to NF-PitNET pathogenesis.

DATA AVAILABILITY STATEMENT

The datasets presented in this study can be found in online repositories. The names of the repository/repositories and accession number(s) can be found in the article/**Supplementary Material**.

ETHICS STATEMENT

The studies involving human participants were reviewed and approved by the Xiangya Hospital Medical Ethics Committee of Central South University; the University of Tennessee Health

Science Center Internal Review Board. The patients/participants provided their written informed consent to participate in this study.

AUTHOR CONTRIBUTIONS

SW analyzed data, carried out western blot experiment and immunoprecipitation experiment, prepared figures and tables, designed and wrote the manuscript. JL, JY, BL, and NL participated in partial data analysis and experiments. XZ conceived the concept, designed experiments and manuscript, instructed experiments, analyzed data, obtained the acetylomics data, supervised results, coordinated, wrote and critically revised manuscript, and was responsible for its financial supports and the corresponding works. All authors contributed to the article and approved the submitted version.

FUNDING

This work was supported by the Shandong First Medical University Talent Introduction Funds (to XZ), the Hunan

Provincial Hundred Talent Plan (to XZ), Shandong Provincial Natural Science Foundation (ZR202103020356 to XZ), the National Natural Science Foundation of China (82172866), and the Academic Promotion Program of Shandong First Medical University (2019ZL002).

ACKNOWLEDGMENTS

The authors acknowledged the assistance of Professor Dominic M. Desiderio from University of Tennessee Health Science Center in obtaining the control pituitary tissue samples, and the assistance of Professor Xuejun Li and Qing Liu from Xiangya Hospital of Central South University in obtaining the pituitary neuroendocrine tumor tissue samples.

SUPPLEMENTARY MATERIAL

The Supplementary Material for this article can be found online at: <https://www.frontiersin.org/articles/10.3389/fendo.2021.753606/full#supplementary-material>

REFERENCES

- Bi WL, Greenwald NF, Ramkissoon SH, Abedalthagafi M, Coy SM, Ligon KL, et al. Clinical Identification of Oncogenic Drivers and Copy-Number Alterations in Pituitary Tumors. *Endocrinology* (2017) 158:2284–91. doi: 10.1210/en.2016-1967
- Ostrom QT, Gittleman H, Fulop J, Liu M, Blanda R, Kromer C, et al. CBTRUS Statistical Report: Primary Brain and Central Nervous System Tumors Diagnosed in the United States in 2008–2012. *Neuro Oncol* (2015) 17 (Suppl 4):iv1–iv62. doi: 10.1093/neuonc/nov189
- Molitch ME. Diagnosis and Treatment of Pituitary Adenomas: A Review. *JAMA* (2017) 317:516–24. doi: 10.1001/jama.2016.19699
- Mehta GU, Lonser RR. Management of Hormone-Secreting Pituitary Adenomas. *Neuro Oncol* (2017) 19:762–73. doi: 10.1093/neuonc/now130
- Mete O, Lopes MB. Overview of the 2017 WHO Classification of Pituitary Tumors. *Endocr Pathol* (2017) 28:228–43. doi: 10.1007/s12022-017-9498-z
- Yu C, Li J, Sun F, Cui J, Fang H, Sui G. Expression and Clinical Significance of miR-26a and Pleomorphic Adenoma Gene 1 (PLAG1) in Invasive Pituitary Adenoma. *Med Sci Monit* (2016) 22:5101–8. doi: 10.12659/msm.898908
- Jenuwein T, Allis CD. Translating the Histone Code. *Science* (2001) 293:1074–80. doi: 10.1126/science.1063127
- Liu L, Scolnick DM, Trievel RC, Zhang HB, Marmorstein R, Halazonetis TD, et al. P53 Sites Acetylated *In Vitro* by PCAF and P300 Are Acetylated *In Vivo* in Response to DNA Damage. *Mol Cell Biol* (1999) 19:1202–9. doi: 10.1128/mcb.19.2.1202
- Patel JH, Du Y, Ard PG, Phillips C, Carella B, Chen CJ, et al. The C-MYC Oncoprotein Is a Substrate of the Acetyltransferases Hgc5/PCAF and TIP60. *Mol Cell Biol* (2004) 24:10826–34. doi: 10.1128/mcb.24.24.10826-10834.2004
- Gil J, Ramirez-Torres A, Encarnación-Guevara S. Lysine Acetylation and Cancer: A Proteomics Perspective. *J Proteomics* (2017) 150:297–309. doi: 10.1016/j.jprot.2016.10.003
- Sharma M, Molehin D, Castro-Piedras I, Martinez EG, Pruitt K. Acetylation of Conserved DVL-1 Lysines Regulates its Nuclear Translocation and Binding to Gene Promoters in Triple-Negative Breast Cancer. *Sci Rep* (2019) 9:16257. doi: 10.1038/s41598-019-52723-3
- Chen L, Wei T, Si X, Wang Q, Li Y, Leng Y, et al. Lysine Acetyltransferase GCN5 Potentiates the Growth of Non-Small Cell Lung Cancer via Promotion of E2F1, Cyclin D1, and Cyclin E1 Expression. *J Biol Chem* (2013) 288:14510–21. doi: 10.1074/jbc.M113.458737
- Valenzuela-Fernández A, Cabrero JR, Serrador JM, Sánchez-Madrid F. HDAC6: A Key Regulator of Cytoskeleton, Cell Migration and Cell-Cell Interactions. *Trends Cell Biol* (2008) 18:291–7. doi: 10.1016/j.tcb.2008.04.003
- Gao L, Alumkal J. Epigenetic Regulation of Androgen Receptor Signaling in Prostate Cancer. *Epigenetics* (2010) 5:100–4. doi: 10.4161/epi.5.2.10778
- Bradbury CA, Khanim FL, Hayden R, Bunce CM, White DA, Drayson MT, et al. Histone Deacetylases in Acute Myeloid Leukaemia Show a Distinctive Pattern of Expression That Changes Selectively in Response to Deacetylase Inhibitors. *Leukemia* (2005) 19:1751–9. doi: 10.1038/sj.leu.2403910
- Zhang L, Wang W, Zhang S, Wang Y, Guo W, Liu Y, et al. Identification of Lysine Acetylome in Cervical Cancer by Label-Free Quantitative Proteomics. *Cancer Cell Int* (2020) 20:182. doi: 10.1186/s12935-020-01266-z
- Ebrahimi A, Schittenhelm J, Honegger J, Schluessener HJ. Histone Acetylation Patterns of Typical and Atypical Pituitary Adenomas Indicate Epigenetic Shift of These Tumours. *J Neuroendocrinol* (2011) 23:525–30. doi: 10.1111/j.1365-2826.2011.02129.x
- Ezzat S, Yu S, Asa SL. Ikaros Isoforms in Human Pituitary Tumors: Distinct Localization, Histone Acetylation, and Activation of the 5' Fibroblast Growth Factor Receptor-4 Promoter. *Am J Pathol* (2003) 163:1177–84. doi: 10.1016/s0002-9440(10)63477-3
- Fedele M, Visone R, De Martino I, Troncone G, Palmieri D, Battista S, et al. HMGA2 Induces Pituitary Tumorigenesis by Enhancing E2F1 Activity. *Cancer Cell* (2006) 9:459–71. doi: 10.1016/j.ccr.2006.04.024
- Rardin MJ, Newman JC, Held JM, Cusack MP, Sorensen DJ, Li B, et al. Label-Free Quantitative Proteomics of the Lysine Acetylome in Mitochondria Identifies Substrates of SIRT3 in Metabolic Pathways. *Proc Natl Acad Sci USA* (2013) 110:6601–6. doi: 10.1073/pnas.1302961110
- Liang M, Zhang S, Dong L, Kou Y, Lin C, Dai W, et al. Label-Free Quantitative Proteomics of Lysine Acetylome Identifies Substrates of Gcn5 in Magnaporthe Oryzae Autophagy and Epigenetic Regulation. *mSystems* (2018) 3(6):e00270–18. doi: 10.1128/mSystems.00270-18
- Wagner SA, Beli P, Weinert BT, Nielsen ML, Cox J, Mann M, et al. A Proteome-Wide, Quantitative Survey of *In Vivo* Ubiquitylation Sites Reveals Widespread Regulatory Roles. *Mol Cell Proteomics* (2011) 10:M111.013284. doi: 10.1074/mcp.M111.013284
- Ito A, Kawaguchi Y, Lai CH, Kovacs JJ, Higashimoto Y, Appella E, et al. MDM2-HDAC1-Mediated Deacetylation of P53 Is Required for Its Degradation. *EMBO J* (2002) 21:6236–45. doi: 10.1093/emboj/cdf616

24. Zhang X, Li B, Rezaeian AH, Xu X, Chou PC, Jin G, et al. H3 Ubiquitination by NEDD4 Regulates H3 Acetylation and Tumorigenesis. *Nat Commun* (2017) 8:14799. doi: 10.1038/ncomms14799
25. Chen Y, Huang Q, Liu W, Zhu Q, Cui CP, Xu L, et al. Mutually Exclusive Acetylation and Ubiquitylation of the Splicing Factor SRSF5 Control Tumor Growth. *Nat Commun* (2018) 9(1):2464. doi: 10.1038/s41467-018-04815-3
26. Qian S, Zhan X, Lu M, Li N, Long Y, Li X, et al. Quantitative Analysis of Ubiquitinated Proteins in Human Pituitary and Pituitary Adenoma Tissues. *Front Endocrinol* (2019) 10:328. doi: 10.3389/fendo.2019.00328
27. Rappsilber J, Mann M, Ishihama Y. Protocol for Micro-Purification, Enrichment, Pre-Fractionation and Storage of Peptides for Proteomics Using StageTips. *Nat Protoc* (2007) 2:1896–906. doi: 10.1038/nprot.2007.261
28. Locasale JW. Serine, Glycine and One-Carbon Units: Cancer Metabolism in Full Circle. *Nat Rev Cancer* (2013) 13:572–83. doi: 10.1038/nrc3557
29. Noor E, Eden E, Milo R, Alon U. Central Carbon Metabolism as a Minimal Biochemical Walk Between Precursors for Biomass and Energy. *Mol Cell* (2010) 39:809–20. doi: 10.1016/j.molcel.2010.08.031
30. Warburg O. On the Origin of Cancer Cells. *Science* (1956) 123:309–14. doi: 10.1126/science.123.3191.309
31. Grasmann G, Smolle E, Olschewski H, Leithner K. Gluconeogenesis in Cancer Cells - Repurposing of a Starvation-Induced Metabolic Pathway? *Biochim Biophys Acta Rev Cancer* (2019) 1872:24–36. doi: 10.1016/j.bbcan.2019.05.006
32. Gray LR, Tompkins SC, Taylor EB. Regulation of Pyruvate Metabolism and Human Disease. *Cell Mol Life Sci* (2014) 71:2577–604. doi: 10.1007/s00018-013-1539-2
33. Olson KA, Schell JC, Rutter J. Pyruvate and Metabolic Flexibility: Illuminating a Path Toward Selective Cancer Therapies. *Trends Biochem Sci* (2016) 41:219–30. doi: 10.1016/j.tibs.2016.01.002
34. Desideri E, Vegliante R, Ciriolo MR. Mitochondrial Dysfunctions in Cancer: Genetic Defects and Oncogenic Signaling Impinging on TCA Cycle Activity. *Cancer Lett* (2015) 356:217–23. doi: 10.1016/j.canlet.2014.02.023
35. Wanders RJA, Waterham HR, Ferdinandusse S. Peroxisomes and Their Central Role in Metabolic Interaction Networks in Humans. *Subcell Biochem* (2018) 89:345–65. doi: 10.1007/978-981-13-2233-4_15
36. Miura Y. The Biological Significance of ω -Oxidation of Fatty Acids. *Proc Jpn Acad Ser B Phys Biol Sci* (2013) 89:370–82. doi: 10.2183/pjab.89.370
37. Ananieva E. Targeting Amino Acid Metabolism in Cancer Growth and Anti-Tumor Immune Response. *World J Biol Chem* (2015) 6:281–9. doi: 10.4331/wjbc.v6.i4.281
38. Tönjes M, Barbus S, Park YJ, Wang W, Schlotter M, Lindroth AM, et al. BCAT1 Promotes Cell Proliferation Through Amino Acid Catabolism in Gliomas Carrying Wild-Type IDH1. *Nat Med* (2013) 19:901–8. doi: 10.1038/nm.3217
39. Dey P, Baddour J, Muller F, Wu CC, Wang H, Liao WT, et al. Genomic Deletion of Malic Enzyme 2 Confers Collateral Lethality in Pancreatic Cancer. *Nature* (2017) 542:119–23. doi: 10.1038/nature21052
40. Mayers JR, Torrence ME, Danai LV, Papagiannakopoulos T, Davidson SM, Bauer MR, et al. Tissue of Origin Dictates Branched-Chain Amino Acid Metabolism in Mutant Kras-Driven Cancers. *Science* (2016) 353:1161–5. doi: 10.1126/science.aaf5171
41. Wilson DF. Oxidative Phosphorylation: Regulation and Role in Cellular and Tissue Metabolism. *J Physiol* (2017) 595:7023–38. doi: 10.1113/jp273839
42. Weinberg SE, Chandel NS. Targeting Mitochondria Metabolism for Cancer Therapy. *Nat Chem Biol* (2015) 11:9–15. doi: 10.1038/nchembio.1712
43. Moreno-Sánchez R, Rodríguez-Enríquez S, Marín-Hernández A, Saavedra E. Energy Metabolism in Tumor Cells. *FEBS J* (2007) 274:1393–418. doi: 10.1111/j.1742-4658.2007.05686.x
44. Judge A, Dodd MS. Metabolism. *Essays Biochem* (2020) 64:607–47. doi: 10.1042/ebc20190041
45. Boroughs LK, DeBerardinis RJ. Metabolic Pathways Promoting Cancer Cell Survival and Growth. *Nat Cell Biol* (2015) 17:351–9. doi: 10.1038/ncb3124
46. Li Z, Zhang H. Reprogramming of Glucose, Fatty Acid and Amino Acid Metabolism for Cancer Progression. *Cell Mol Life Sci* (2016) 73:377–92. doi: 10.1007/s00018-015-2070-4
47. Parada CA, Roeder RG. A Novel RNA Polymerase II-Containing Complex Potentiates Tat-Enhanced HIV-1 Transcription. *EMBO J* (1999) 18:3688–701. doi: 10.1093/emboj/18.13.3688
48. Tzivion G, Gupta VS, Kaplun L, Balan V. 14-3-3 Proteins as Potential Oncogenes. *Semin Cancer Biol* (2006) 16:203–13. doi: 10.1016/j.semcancer.2006.03.004
49. Raungrut P, Wongkotsila A, Champoochana N, Lirdprapamongkol K, Svasti J, Thongsuksai P. Knockdown of 14-3-3 γ Suppresses Epithelial-Mesenchymal Transition and Reduces Metastatic Potential of Human Non-Small Cell Lung Cancer Cells. *Anticancer Res* (2018) 38:3507–14. doi: 10.21873/anticancer.12622
50. Xiao Y, Lin VY, Ke S, Lin GE, Lin FT, Lin WC. 14-3-3 τ Promotes Breast Cancer Invasion and Metastasis by Inhibiting Rhogdia. *Mol Cell Biol* (2014) 34:2635–49. doi: 10.1128/mcb.00076-14
51. Sekhar GN, Watson CP, Fidanboyu M, Sanderson L, Thomas SA. Delivery of Antihuman African Trypanosomiasis Drugs Across the Blood-Brain and Blood-CSF Barriers. *Adv Pharmacol* (2014) 71:245–75. doi: 10.1016/bs.apha.2014.06.003
52. Cordes T, Michelucci A, Hiller K. Itaconic Acid: The Surprising Role of an Industrial Compound as a Mammalian Antimicrobial Metabolite. *Annu Rev Nutr* (2015) 35:451–73. doi: 10.1146/annurev-nutr-071714-034243
53. Islinger M, Voelkl A, Fahimi HD, Schrader M. The Peroxisome: An Update on Mysteries 2.0. *Histochem Cell Biol* (2018) 150:443–71. doi: 10.1007/s00418-018-1722-5
54. Cai M, Sun X, Wang W, Lian Z, Wu P, Han S, et al. Disruption of Peroxisome Function Leads to Metabolic Stress, mTOR Inhibition, and Lethality in Liver Cancer Cells. *Cancer Lett* (2018) 421:82–93. doi: 10.1016/j.canlet.2018.02.021
55. Frederiks WM, Bosch KS, Hoeben KA, van Marle J, Langbein S. Renal Cell Carcinoma and Oxidative Stress: The Lack of Peroxisomes. *Acta Histochem* (2010) 112:364–71. doi: 10.1016/j.acthis.2009.03.003
56. Jiang Z, Woda BA, Rock KL, Xu Y, Savas L, Khan A, et al. P504S: A New Molecular Marker for the Detection of Prostate Carcinoma. *Am J Surg Pathol* (2001) 25:1397–404. doi: 10.1097/0000478-200111000-00007
57. Luo S, Hu D, Wang M, Zipfel PF, Hu Y. Complement in Hemolysis- and Thrombosis-Related Diseases. *Front Immunol* (2020) 11:1212. doi: 10.3389/fimmu.2020.01212
58. Straight AF, Shou W, Dowd GJ, Turck CW, Deshaies RJ, Johnson AD, et al. Net1, a Sir2-Associated Nucleolar Protein Required for rDNA Silencing and Nucleolar Integrity. *Cell* (1999) 97:245–56. doi: 10.1016/s0092-8674(00)80734-5
59. Good M, Tang G, Singleton J, Reményi A, Lim WA. The Ste5 Scaffold Directs Mating Signaling by Catalytically Unlocking the Fus3 MAP Kinase for Activation. *Cell* (2009) 136:1085–97. doi: 10.1016/j.cell.2009.01.049
60. Wong W, Scott JD. AKAP Signalling Complexes: Focal Points in Space and Time. *Nat Rev Mol Cell Biol* (2004) 5:959–70. doi: 10.1038/nrm1527
61. Hata A, Chen YG. TGF- β Signaling From Receptors to Smads. *Cold Spring Harb Perspect Biol* (2016) 8(9):a022061. doi: 10.1101/cshperspect.a022061
62. Wilkinson KD, Lee KM, Deshpande S, Duerksen-Hughes P, Boss JM, Pohl J. The Neuron-Specific Protein PGP 9.5 Is a Ubiquitin Carboxyl-Terminal Hydrolase. *Science* (1989) 246:670–3. doi: 10.1126/science.2530630
63. Drazic A, Aksnes H, Marie M, Boczkowska M, Varland S, Timmerman E, et al. NAA80 Is Actin's N-Terminal Acetyltransferase and Regulates Cytoskeleton Assembly and Cell Motility. *Proc Natl Acad Sci USA* (2018) 115:4399–404. doi: 10.1073/pnas.1718336115
64. Schrank BR, Aparicio T, Li Y, Chang W, Chait BT, Gundersen GG, et al. Nuclear ARP2/3 Drives DNA Break Clustering for Homology-Directed Repair. *Nature* (2018) 559:61–6. doi: 10.1038/s41586-018-0237-5
65. Vander Heiden MG, Cantley LC, Thompson CB. Understanding the Warburg Effect: The Metabolic Requirements of Cell Proliferation. *Science* (2009) 324:1029–33. doi: 10.1126/science.1160809
66. Baeza J, Smallegan MJ, Denu JM. Mechanisms and Dynamics of Protein Acetylation in Mitochondria. *Trends Biochem Sci* (2016) 41:231–44. doi: 10.1016/j.tibs.2015.12.006
67. Qian X, Li X, Lu Z. Protein Kinase Activity of the Glycolytic Enzyme PGK1 Regulates Autophagy to Promote Tumorigenesis. *Autophagy* (2017) 13:1246–7. doi: 10.1080/15548627.2017.1313945
68. Hu H, Zhu W, Qin J, Chen M, Gong L, Li L, et al. Acetylation of PGK1 Promotes Liver Cancer Cell Proliferation and Tumorigenesis. *Hepatology* (2017) 65:515–28. doi: 10.1002/hep.28887
69. Wang S, Jiang B, Zhang T, Liu L, Wang Y, Wang Y, et al. Insulin and mTOR Pathway Regulate HDAC3-Mediated Deacetylation and Activation of PGK1. *PLoS Biol* (2015) 13:e1002243. doi: 10.1371/journal.pbio.1002243
70. Chen H, Chan DC. Mitochondrial Dynamics in Regulating the Unique Phenotypes of Cancer and Stem Cells. *Cell Metab* (2017) 26:39–48. doi: 10.1016/j.cmet.2017.05.016
71. Lichter T, Dohrmann GJ. Respiratory Patterns in Human Brain Tumors. *Neurosurgery* (1986) 19:896–9. doi: 10.1227/00006123-198612000-00002

72. Sabatino ME, Grondona E, Sosa LDV, Mongi Bragato B, Carreño L, Juárez V, et al. Oxidative Stress and Mitochondrial Adaptive Shift During Pituitary Tumoral Growth. *Free Radic Biol Med* (2018) 120:41–55. doi: 10.1016/j.freeradbiomed.2018.03.019
73. Qian X, Li X, Cai Q, Zhang C, Yu Q, Jiang Y, et al. Phosphoglycerate Kinase 1 Phosphorylates Beclin1 to Induce Autophagy. *Mol Cell* (2017) 65:917–31. doi: 10.1016/j.molcel.2017.01.027
74. Cheng S, Xie W, Miao Y, Guo J, Wang J, Li C, et al. Identification of Key Genes in Invasive Clinically Non-Functioning Pituitary Adenoma by Integrating Analysis of DNA Methylation and mRNA Expression Profiles. *J Transl Med* (2019) 17:407. doi: 10.1186/s12967-019-02148-3
75. Gentric G, Mieulet V, Mehta-Grigoriou F. Heterogeneity in Cancer Metabolism: New Concepts in an Old Field. *Antioxid Redox Signal* (2017) 26:462–85. doi: 10.1089/ars.2016.6750
76. Swietach P, Vaughan-Jones RD, Harris AL. Regulation of Tumor pH and the Role of Carbonic Anhydrase 9. *Cancer Metastasis Rev* (2007) 26:299–310. doi: 10.1007/s10555-007-9064-0
77. Luo L, Martin SC, Parkington J, Cadena SM, Zhu J, Ibebunjo C, et al. HDAC4 Controls Muscle Homeostasis Through Deacetylation of Myosin Heavy Chain, PGC-1 α , and Hsc70. *Cell Rep* (2019) 29:749–763.e712. doi: 10.1016/j.celrep.2019.09.023
78. Hou L, Chen M, Wang M, Cui X, Gao Y, Xing T, et al. Systematic Analyses of Key Genes and Pathways in the Development of Invasive Breast Cancer. *Gene* (2016) 593:1–12. doi: 10.1016/j.gene.2016.08.007
79. Khosla R, Hemati H, Rastogi A, Ramakrishna G. miR-26b-5p Helps in EpCAM+cancer Stem Cells Maintenance via HSC71/HSPA8 and Augments Malignant Features in HCC. *Liver Int* (2019) 39:1692–703. doi: 10.1111/liv.14188
80. Fang M, Jin A, Zhao Y, Liu X. Homocysteine Induces Glyceraldehyde-3-Phosphate Dehydrogenase Acetylation and Apoptosis in the Neuroblastoma Cell Line Neuro2a. *Braz J Med Biol Res* (2016) 49:e4543. doi: 10.1590/1414-431x20154543
81. Hao L, Zhou X, Liu S, Sun M, Song Y, Du S, et al. Elevated GAPDH Expression Is Associated With the Proliferation and Invasion of Lung and Esophageal Squamous Cell Carcinomas. *Proteomics* (2015) 15:3087–100. doi: 10.1002/pmic.201400577
82. Caron C, Boyault C, Khochbin S. Regulatory Cross-Talk Between Lysine Acetylation and Ubiquitination: Role in the Control of Protein Stability. *Bioessays* (2005) 27:408–15. doi: 10.1002/bies.20210

Conflict of Interest: The authors declare that the research was conducted in the absence of any commercial or financial relationships that could be construed as a potential conflict of interest.

Publisher's Note: All claims expressed in this article are solely those of the authors and do not necessarily represent those of their affiliated organizations, or those of the publisher, the editors and the reviewers. Any product that may be evaluated in this article, or claim that may be made by its manufacturer, is not guaranteed or endorsed by the publisher.

Copyright © 2021 Wen, Li, Yang, Li, Li and Zhan. This is an open-access article distributed under the terms of the Creative Commons Attribution License (CC BY). The use, distribution or reproduction in other forums is permitted, provided the original author(s) and the copyright owner(s) are credited and that the original publication in this journal is cited, in accordance with accepted academic practice. No use, distribution or reproduction is permitted which does not comply with these terms.



Impact of RSUME Actions on Biomolecular Modifications in Physio-Pathological Processes

Mariana Fuertes^{1†}, Belén Elguero^{1†}, David Gonilski-Pacin¹, Florencia Herbstein¹, Josefina Rosmino¹, Nicolas Ciancio del Giudice¹, Manuel Fiz¹, Lara Falcucci¹ and Eduardo Arzt^{1,2*}

¹ Instituto de Investigación en Biomedicina de Buenos Aires (IBiBA) - Consejo Nacional de Investigaciones Científicas y Técnicas (CONICET) - Partner Institute of the Max Planck Society, Buenos Aires, Argentina, ² Departamento de Fisiología y Biología Molecular y Celular, Facultad de Ciencias Exactas y Naturales, Universidad de Buenos Aires, Buenos Aires, Argentina

OPEN ACCESS

Edited by:

Xianquan Zhan,
Shandong First Medical University,
China

Reviewed by:

Hartmut Schlüter,
University Medical Center Hamburg-
Eppendorf, Germany
Na Li,
Shandong Cancer Hospital, China

*Correspondence:

Eduardo Arzt
earzt@ibioba-mpsp-conicet.gov.ar

[†]These authors have contributed
equally to this work and share
first authorship

Specialty section:

This article was submitted to
Cancer Endocrinology,
a section of the journal
Frontiers in Endocrinology

Received: 28 January 2022

Accepted: 11 March 2022

Published: 21 April 2022

Citation:

Fuertes M, Elguero B,
Gonilski-Pacin D, Herbstein F,
Rosmino J, Ciancio del Giudice N,
Fiz M, Falcucci L and Arzt E (2022)
Impact of RSUME Actions on
Biomolecular Modifications in
Physio-Pathological Processes.
Front. Endocrinol. 13:864780.
doi: 10.3389/fendo.2022.864780

The small RWD domain-containing protein called RSUME or RWDD3 was cloned from pituitary tumor cells with increasing tumorigenic and angiogenic proficiency. RSUME expression is induced under hypoxia or heat shock and is upregulated, at several pathophysiological stages, in tissues like pituitary, kidney, heart, pancreas, or adrenal gland. To date, several factors with essential roles in endocrine-related cancer appear to be modulated by RWDD3. RSUME regulates, through its post-translational (PTM) modification, pituitary tumor transforming gene (PTTG) protein stability in pituitary tumors. Interestingly, in these tumors, another PTM, the regulation of EGFR levels by USP8, plays a pathogenic role. Furthermore, RSUME suppresses ubiquitin conjugation to hypoxia-inducible factor (HIF) by blocking VHL E3-ubiquitin ligase activity, contributing to the development of von Hippel-Lindau disease. RSUME enhances protein SUMOylation of specific targets involved in inflammation such as I κ B and the glucocorticoid receptor. For many of its actions, RSUME associates with regulatory proteins of ubiquitin and SUMO cascades, such as the E2-SUMO conjugase Ubc9 or the E3 ubiquitin ligase VHL. New evidence about RSUME involvement in inflammatory and hypoxic conditions, such as cardiac tissue response to ischemia and neuropathic pain, and its role in several developmental processes, is discussed as well. Given the modulation of PTMs by RSUME in neuroendocrine tumors, we focus on its interactors and its mode of action. Insights into functional implications and molecular mechanisms of RSUME action on biomolecular modifications of key factors of pituitary adenomas and renal cell carcinoma provide renewed information about new targets to treat these pathologies.

Keywords: RSUME, RWDD3, SUMOylation, ubiquitin, pituitary, RCC, VHL, PTTG

INTRODUCTION

RSUME is a small protein containing an RWD domain that has a role in enhancing SUMO conjugation (1). The function of this domain is unknown and extends from amino acid 7 to 114 of the human protein. RSUME was first identified following a screen of GH3 pituitary tumor cells over-expressing gp130, which typically generate aggressive and highly vascularized tumors in nude mice (2).

In endocrine-related cancers, RSUME appears as responsible for regulatory actions over several factors with essential roles in tumorigenesis. For many of these effects, RSUME acts by modulating post-translational modification (PTM) of proteins. Given the strong connection between RSUME and PTMs, it is important to better understand how RSUME associates with regulatory proteins of ubiquitin and ubiquitin-like protein cascades and its pathophysiological consequences.

We briefly review the body of related work that is available on this field and discuss the mechanisms of action and regulatory impact of RSUME action. In none of the known actions and examples provided does the mechanism involve a modification on RSUME, but on the interacting protein, by modifying either its PTM or the interacting capability of this protein.

RSUME OVERVIEW

Human RSUME is codified by the *RWDD3* gene located on chromosome 1. This gene generates seven mRNA splice variants, five of which code for different RSUME proteoforms (between 185 and 267 amino acids) and the rest are non-coding RNAs that are degraded by non-sense-mediated RNA decay due to their premature termination codons (3) (**Figure 1A**). RSUME is highly conserved in vertebrates (1) and is distributed in both the cytoplasm and the nucleus (1). *Rwdd3* gene gives rise to two

mRNA splice variants in mouse and only one mRNA in rat, coding for two murine RSUME proteoforms (267 and 339 amino acids) and one rat RSUME protein (267 amino acids), respectively.

All RSUME proteoforms contain an RWD domain, a protein-protein interaction motif, which has been shown to share significant structural homology to the mammalian E2 SUMO-conjugating enzyme Ubc9 and the yeast E2 ubiquitin conjugase Mms2 (4). A comparative analysis showed that the core structure of RWD appears to be common among RWD-containing proteins, while the specificity of interaction and/or the function of each RWD-containing protein seems to be given by variations on the surface residues. This also suggests that each RWD domain interacts with different E2-conjugating enzymes in the same way (4).

Under stress conditions such as hypoxia, CoCl_2 (hypoxia-mimicking stimulus), and heat shock, RSUME amounts were induced (1, 5) with a marked localization in the necrotic inner zone of tumor explants (1). Phosphorylation site prediction with KinasePhos software indicated that the RSUME protein sequence contains at least two putative JAK-STAT-sensitive tyrosine phosphorylation sites at positions 123 and 169 (6), a signaling pathway whose activation, either through elevated cytokine signaling during inflammation, or during hypoxic conditions, could lead to increased RSUME expression or activity (6).

The RSUME proteoforms are equally induced by hypoxia and exert similar actions, which may be related to the fact that all of them contain the same RWD domain (3). Since studies

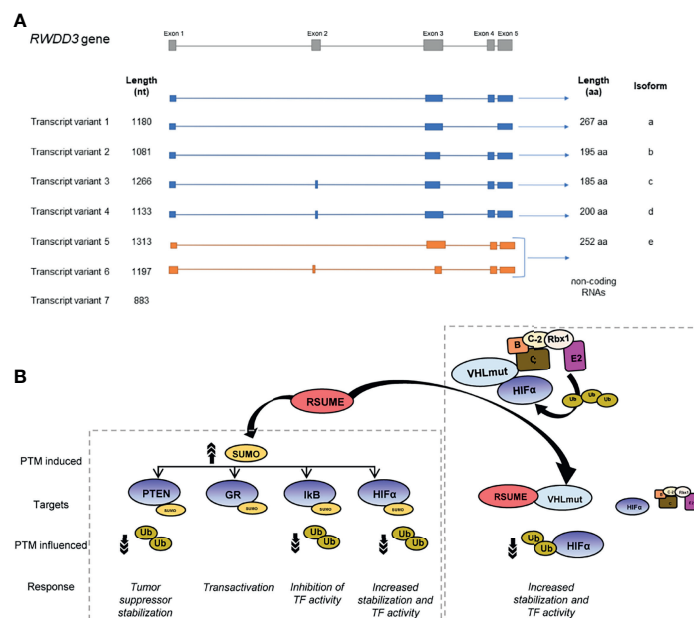


FIGURE 1 | Scheme of human *RWDD3* transcript variants and RSUME targeted proteins. **(A)** Seven transcript variants of *RWDD3* human gene, of which five are translated into protein and two of these proteins are the best characterized proteoforms, RSUME-195 and RSUME-267. **(B)** RSUME interacts and enhances SUMOylation of targeted proteins (PTEN, GR, IκB and HIFα), affecting other PTMs, occurring in the same protein. The reduction of ubiquitination enhances activity of transcription factors (TFs) such as HIFα or transcription factor regulators (IκB, PTEN). RSUME promotes HIFα accumulation and activity by another mechanism independent of SUMOylation: the interaction of RSUME with VHL (the HIFα ubiquitin E3 ligase that promotes its degradation in normoxia) decreases VHL-HIFα binding and consequently HIFα ubiquitination.

performed so far and revised here have been performed with the proteoform of 195 amino acids of length, the evaluation of others would be interesting in the future.

Tissue distribution of RSUME mRNA showed higher expression in cerebellum, pituitary, heart, kidney, liver, stomach, pancreas, adrenal gland, prostate, and spleen (1) (**Figure 2**). RSUME expression is upregulated in pituitary adenomas at mRNA (7) and protein levels (8,9).

In glioblastoma tumors, RSUME is overexpressed and correlates with shorter overall survival time of patients (10). Mechanistically, RSUME downregulation in glioblastoma cancer cells leads to diminished proliferative and invasive abilities by modulation of the PI3K/AKT signaling (10). It is important to note that the distribution of RSUME proteoforms differs between glioma samples, demonstrating that while the shorter RSUME proteoform is present in all gliomas studied, the longest RSUME proteoform is differentially expressed in those samples (3). These results suggest separate roles for RSUME proteoforms in this kind of tumor, which remains an open question to be studied.

The *RWDD3* gene, between a subset of 16 genes, has been associated with breast cancer recurrence, metastases, and mortality in survival analyses in patients (11). Furthermore, genome-wide association studies (GWAS) in breast cancer patients showed an allele dose dependent association of single-nucleotide polymorphisms (SNPs) residing in *RWDD3* gene with time to neuropathy (common toxicity criteria), in patients undergoing taxane therapy (12).

In pancreatic neuroendocrine tumors (PanNETs), the down-modulation of RSUME expression is associated to an increased tumoral size and metastatic capacity in a murine model. Accordingly, PanNET patient's tissues show reduced RSUME expression compared with normal pancreatic tissue. This action is mediated by its role in SUMOylation and stabilization of the tumor suppressor Phosphatase and Tensin Homolog deleted on Chromosome 10 (PTEN) (13) (**Figure 1B**).

RSUME CONTRIBUTES TO VHL SYNDROME THROUGH ITS INTERACTION WITH VHL AND HIF

RSUME emerges as a tumor-associated protein since it is expressed in many other tumors such as pheochromocytoma, hemangioblastoma and renal carcinoma (RCC) (**Figure 2**). This leads to link RSUME to the von Hippel–Lindau (VHL) tumor syndrome (14), being those neoplasms the most frequently associated with the disease. VHL tumor syndrome is caused by mutations in *VHL* tumor suppressor gene. VHL-related tumors are highly angiogenic, originated by hypoxia-inducible factor- α (HIF α) deregulation (15). The mechanism mediated by RSUME to promote angiogenesis by HIF α stabilization has been described in clear cell RCC (16) and is discussed in detail below.

A bioinformatic analysis revealed that RSUME expression is increased in RCC tumors bearing VHL mutated form and it rises from earlier to late tumor stages during RCC progression (16). In this kind of cancer, high RSUME expression correlates with worse overall survival compared with patients expressing low RSUME levels (16). Metabolomics analysis unveiled that RSUME is also involved in metabolic changes associated to RCC malignant phenotype, particularly linked to fatty acid metabolism and antioxidant response (17). Thus, RSUME participates in tumor progression through several pathways.

RSUME EXPRESSION IN PATHOLOGICAL TISSUE RESPONSES

Besides its role in tumor progression, recent studies reveal that RSUME is connected with cardiac tissue response to ischemia

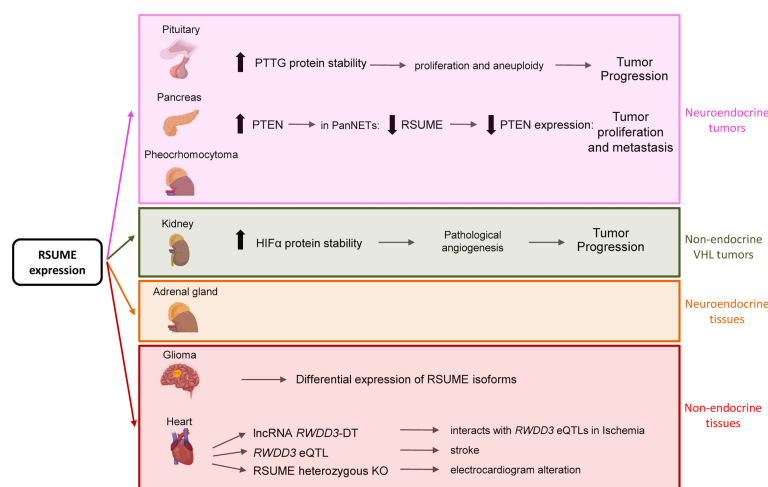


FIGURE 2 | Summary of RSUME actions in neuroendocrine or non-endocrine tissues and tumors. RSUME is expressed and acts in normal and tumoral tissues. Of particular interest are those tissues in which it is highly expressed, such as pituitary, pancreas, kidney, brain and heart, where it exerts different functions through the interaction with the indicated key factors. Interestingly it is also expressed at high levels in normal and tumoral (pheochromocytoma) adrenal gland, a VHL type of tumor, in which its functions remain to be studied.

and stroke (18, 19) (**Figure 2**). Enhanced SUMOylation has been proposed to protect from stroke and ischemia of the brain (20, 21). In line with this, RSUME has been associated with cardioembolic stroke in an Indian stroke patient's study (19). Interestingly, in this GWAS study, the authors discovered loci related to different stroke types and located close to certain genes, where *RWDD3* is one of them. Further analysis revealed that this locus is an expression quantitative trait locus (eQTL) for RSUME and also associated with platelet distribution width and lipid metabolism (19), suggesting that RSUME expression levels are tightly regulated in stroke. This finding points RSUME level as an important factor to the proper response of cardiac tissue.

Another pathological response involving differential modulation of RSUME levels is neuropathic pain. Rojewska et al. found thirty-nine genes modulated by this pathology, of which RSUME together with six other genes are differentially repressed under sciatic nerve injury in a rat model and rescued after treatment that alleviates pain (22). This treatment has a key effect in reduction of the microglia activation and neuroinflammation. In fact, RSUME is expressed in brain but it shows higher expression in glial cells (<https://www.proteinatlas.org/ENSG00000122481-RWDD3/single+cell+type>) from human tissues. Further studies will be needed to unveil the role of SUMOylation, described as a regulator of brain development (23), and RSUME in normal or activated glia and pain.

RSUME REGULATES PTMS AND IMPACTS IN DIFFERENT CELLULAR PROCESSES

Since its discovery, RSUME has been linked to several regulators of PTMs. Through its RWD domain, RSUME presents structural similarity to UEVs (ubiquitin E2 variant proteins) and to E2 conjugases (4) that allow its interplay with ubiquitin and ubiquitin-like protein machinery. RSUME interacts with the E2-conjugating enzyme of the SUMO pathway, Ubc9, increases its activity, and colocalizes with it (1). RSUME also interacts with SUMO-1 (1).

Additionally, RSUME interacts physically with VHL protein (14), an essential component of the E3 ubiquitin ligase ECV complex, which also includes Elongin B, Elongin C, Cullin-2, and Rbx-1 (24) (**Figure 1B**). The most known targets of ECV E3 ubiquitin ligase are HIF-1 and 2α (25). VHL-RSUME interaction is independent of VHL-substrate, HIF-1 α , as is demonstrated by *in vitro* interaction of these proteins. This observation is also confirmed by RSUME and VHL interaction in a cellular system with a mutant HIF unable to bind VHL (14). In spite of this, RSUME also interacts with VHL in the presence of the VHL-HIF α complex. Even more, increasing RSUME protein quantities displace HIF-VHL binding progressively (14), suggesting a competitive interaction between both proteins for VHL. This reduction in VHL-HIF binding suppresses HIF α ubiquitin conjugation by VHL promoting HIF stabilization. Additionally, RSUME interacts and downregulates the assembly of other components from the ECV complex (14, 16). Under

hypoxia, VHL is SUMOylated by SUMO-1 conjugation predominantly at 171 lysine residue (K171) promoted by Protein Inhibitor of Activated STAT γ (PIAS γ) SUMO ligase (26). This SUMO-1 modification of VHL blocks its ubiquitin E3 ligase action on HIF α proteolysis (26). RSUME also increases VHL K171 SUMOylation (14). SUMO conjugation to VHL as well as RSUME-VHL interaction can suppress HIF-2 α degradation, as demonstrated by HIF-2 α stabilization mediated by RSUME in cells bearing VHL K171R mutation (16). In fact, RSUME is able to promote SUMOylation of VHL mutated variants observed in VHL syndrome, but also abrogates HIF-2 α degradation by interacting with these VHL variants in a VHL-SUMOylation independent way (16). This HIF-2 α accumulation has a major consequence in the context of RCC tumors, where angiogenesis becomes relevant for tumor growth, mainly promoted through the HIF-2 α -VEGF pathway (27). In this cancer type, mutations in VHL gene are key drivers of carcinogenesis. As mentioned above, RSUME high expression is related to adverse prognosis in RCC patients. Mechanistically, RSUME promotes the wrong functioning of VHL mutated forms on HIF-2 α degradation (16). Consequently, reduced angiogenesis is observed in RCC models carrying VHL mutations when RSUME is silenced (16). This RSUME action on HIF-2 α ubiquitination mediated by VHL also occurs independent of VHL SUMOylation. It could be possible that both types of regulation, SUMOylation and protein interactions, act at different instances of VHL ubiquitin ligase activity.

RSUME also modulates two central players in inflammation. RSUME inhibits NF- κ B activity through the stabilization of I κ B (**Figure 1B**), which leads to the inhibition of two of its targets, interleukin-8 (IL-8) and cyclooxygenase-2 (Cox-2) (1). RSUME increases I κ B SUMOylation at lysines 21 and 22, and enhances I κ B protein stability in mammalian cells. RSUME also regulates the glucocorticoid receptor (GR) PTM (5) as detailed below. Further level of complexity appears because members of the PIAS family of SUMO E3 ligases also regulate GR-directed transcription (28) and HIF-1 α SUMOylation (29), just like RSUME.

BIOMOLECULAR MODIFICATIONS BY RSUME IN NEUROENDOCRINE CELLS

The hypothalamus-pituitary-adrenal axis (HPA axis) is a complex neuroendocrine system in which the GR plays a central role in regulating inflammation, glucose and lipid metabolism, stress response, and development, among other important processes. Some PTMs such as phosphorylation, ubiquitination, and SUMOylation modulate GR activity (30–33). RSUME is an important regulator of heat shock-induced GR SUMOylation, by interacting with the GR and increasing its SUMOylation (5) (**Figure 1B**). The lysine K721 of GR is critical for the RSUME effect, showing that this site has a positive action on GR transcriptional activity and the expression of its endogenous target genes, FKBP51 and S100P. In addition, both K721 mutation and RSUME knockdown compromise coactivator GRIP1-mediated GR activation. Thus, RSUME manages GR-mediated transcription, modulating the cellular outcome to glucocorticoid exposure.

RSUME is a novel and important player in pituitary tumor pathogenesis. RSUME also acts on the HPA axis at the pituitary stage, increasing pituitary tumor transforming gene (PTTG) protein stability (9) (**Figure 1B**). PTTG is the vertebrate securin (34, 35) whose overexpression correlates with tumor invasiveness and recurrence. RSUME and PTTG are both upregulated in human pituitary adenomas (9, 36), and this positive correlation of expressions involves not only an increment of PTTG protein in pituitary tumor cells, but also an improved half-life of PTTG protein and a co-regulation with estrogens of the PTTG induction. Accordingly, RSUME upturns PTTG transcription factor (over targets such as c-Myc or cyclin D3) and securin activities, allowing the appearance in the tumor of aneuploid cells or multinucleated as a consequence. RSUME knockdown reduces securin PTTG and its tumorigenic potential in xenografted mice. This explains the effect of RSUME modulating PTTG high protein levels that account for PTTG tumor abundance and demonstrates an important role of RSUME in tumor cells of the pituitary. Regarding the molecular mechanism, we have described that PTTG protein levels decrease when the SUMOylation pathway is inhibited by the viral Gam1 protein (37), and the consequent reversal of this effect when an inactive mutant is used (9), suggesting that SUMO signaling is involved in the stabilization of PTTG. For many proteins, SUMOylation could protect them from degradation by the ubiquitin/proteasome system, in addition to increasing their stability, changing their subcellular localization or distribution, and/or modifying their molecular interactions. Furthermore, PTTG is targeted by other PTMs such as ubiquitination (38) or phosphorylation (39), which could also be modulated by RSUME.

In addition, RSUME is involved in pituitary adenoma progression by means of initiating pituitary tumor neovascularization through regulating HIF-1 α levels and subsequent VEGF-A production under hypoxia in murine pituitary tumor cell lines and human pituitary adenoma cells (7, 8).

Regulation of protein stability by PTMs appears to be a key pathway in the control of these types of tumors. Almost half of ACTH-secreting pituitary tumors were reported to develop because of ubiquitin-specific peptidase 8 (USP8) somatic mutation (40), which leads to an increased USP8 deubiquitinating activity and triggers the release of adrenocorticotropic hormone (ACTH). Mutant USP8 inhibits EGFR ubiquitination and rescues it from proteasomal degradation, increasing the EGFR in the plasma membrane and returning to the cell surface by reversing the endocytosis and thus ultimately promoting ACTH secretion by activated EGFR signaling pathway (41). The overexpressed EGFR and E2F transcription factor 1 (E2F1) were implicated in the aggressiveness of pituitary tumors (42). E2F1 is also deubiquitinated and stabilized by a deubiquitinating enzyme named POH1 (43). Thus, the deubiquitinating enzyme USP8 could represent a great link within EGFR, E2F1, and ACTH in pituitary cancer.

RSUME AS A BIOMODULATOR IN DEVELOPMENT

In an extensive transcriptomic study in 12.5- to 16-day-old rat embryos, *Rwdd3* gene was identified as part of a large set of

upregulated genes of ganglionic eminence (GE), an embryonic structure that supplies the brain with diverse sets of GABAergic neurons (44). This pool of GE-enriched genes, including *Hod*, *Rwdd3*, *Nr2f2*, *Egr3*, *Cpta1*, *Cyp26b1*, and *Slit3*, may be important in telencephalic neural development. Taking into consideration the relevant role of SUMOylation in different regulatory mechanisms of brain development (23), future studies in *Rwdd3* KO mice will clarify its contribution in developmental processes in the brain.

RSUME has increasingly shown to be involved in cardiac pathologies. Ward et al. carried out a detailed study in which the comparison of ventricular tissue after and before ischemia in humans shows that several long non-coding RNAs (lncRNAs) are differentially expressed and related to fast response to ventricular ischemia (18). From the novel lncRNA group, a particular lncRNA targets five regulatory loci (expression quantitative trait loci, eQTL) for RSUME, and consequently, this lncRNA's expression correlates with RSUME expression in this study group (18).

Similarly, the previously described GWAS study that associates an SNP affecting an RSUME's QTL with cardioembolic stroke (19) provides a novel view for the hypoxia-mediated regulation of RSUME expression in cardiac tissue. Moreover, a different study found a suggestive locus near the RSUME gene that is involved in inter-individual levels of the Proprotein convertase subtilisin/kexin type 9 (PCSK9), which is a regulator of LDL receptor degradation and is associated with cardiovascular risk (45). Although the incidence of congenital heart defects is high, only a reduced number of them are caused by Mendelian inheritance (46). Noteworthy, defects in SUMOylation balance seem to play an important role in heart development as demonstrated by congenital heart defects observed in knockout mice for components of the SUMOylation system (46). Considering RSUME's role in SUMOylation, it is likely that RSUME may modulate cardiac development, a hypothesis supported by the cardiac phenotypic alteration in electrocardiogram of heterozygous *Rwdd3* KO mice developed under an international project to discover new functions of genes [International Mouse Phenotyping Consortium (IMPC), www.mousephenotype.org]. Subsequently, RSUME gene has been included between essential genes, since its KO mice displayed homozygous lethality (47), which opens new interesting avenues in the study of *Rwdd3*.

CONCLUSIONS AND FUTURE PERSPECTIVES

In the light of reported research at protein and mRNA levels, RSUME shows up as an important regulator of cellular function in various physiological and pathological processes, in which it appears as a promising biomarker and therapeutic target.

Although RSUME-mediated PTM regulation studies have been mainly performed in cancer, mainly neuroendocrine tumors, its participation in other processes including neuropathic pain and, more recently reported, stroke and ischemia has been described (**Figure 2**).

Since cancer must face an evolving environment, reversible modifications on proteins show additional regulation, more related to levels and cross-talk of PTMs in a specific moment. In this scenario, RSUME has an extensive participation by modulating key pathways such as VHL/HIF, PTTG, or NFκB.

Interestingly, two important mechanisms controlling pituitary growth, the regulation of PTTG protein stability and tumor abundance by RSUME, and the USP8/EGFR regulation, point to the involvement of the SUMO/ubiquitin pathways in pituitary pathogenesis.

VHL disease shows a non-predictable pattern of tumor development. The remaining questions about why some tissues are sensitive to tumor growth are still unanswered. In RCC, RSUME emerges as a modulator of VHL ubiquitin action on the HIF pathway, opening new perspectives on therapeutic strategies for this cancer type.

Considering the role of RSUME on regulatory mechanisms in several pathways, mostly described in pathology but relevant in physiology, research on RSUME KO will help to answer central questions about RSUME/RWDD3 modulatory actions, highlighting the relevance of coordinated PTMs.

AUTHOR CONTRIBUTIONS

MarF, BE, and EA conducted literature review, and conceptualized and wrote the manuscript. DG-P, FH, JR, NC-G,

ManF, and LF conducted literature review, designed the figures, and contributed to editing the manuscript. All authors contributed to the article and approved the submitted version.

FUNDING

This work was supported by the Max Planck Society from Germany (grant number 2012/2022); University of Buenos Aires (UBA) from Argentina (grant number N° 20020170100230BA); the Consejo Nacional de Investigaciones Científicas y Técnicas (CONICET) from Argentina (PUE-2016 N° 22920160100010CO); the Agencia Nacional de Promoción Científica y Tecnológica (ANPCyT) from Argentina (grant numbers PICT2014-3634, PICT2016-1620, and PICT-2018-03232); and Fondo para la Convergencia Estructural de Mercosur (FOCEM) (grant number COF 03/11).

ACKNOWLEDGMENTS

This work was supported by grants from the Max Planck Society, Germany; the University of Buenos Aires, Argentina; the Consejo Nacional de Investigaciones Científicas y Técnicas (CONICET), Argentina; the Agencia Nacional de Promoción Científica y Tecnológica (ANPCyT), Argentina; and Fondo para la Convergencia Estructural de Mercosur (FOCEM) (COF 03/11).

REFERENCES

- Carbia-Nagashima A, Gerez J, Perez-Castro C, Paez-Pereda M, Silberstein S, Stalla GK, et al. RSUME, a Small RWD-Containing Protein, Enhances SUMO Conjugation and Stabilizes HIF-1α During Hypoxia. *Cell* (2007) 131(2):309–23. doi: 10.1016/j.cell.2007.07.044
- Castro CP, Giacomini D, Nagashima AC, Onofri C, Graciarena M, Kobayashi K, et al. Reduced Expression of the Cytokine Transducer Gp130 Inhibits Hormone Secretion, Cell Growth, and Tumor Development of Pituitary Lactotomotropic GH3 Cells. *Endocrinology* (2003) 144(2):693–700. doi: 10.1210/en.2002-220891
- Gerez J, Fuertes M, Tedesco L, Silberstein S, Sevlever G, Paez-Pereda M, et al. In Silico Structural and Functional Characterization of the RSUME Splice Variants. *PLoS One* (2013) 8(2):e57795. doi: 10.1371/journal.pone.0057795
- Nameki N, Yoneyama M, Koshiba S, Tochio N, Inoue M, Seki E, et al. Solution Structure of the RWD Domain of the Mouse GCN2 Protein. *Protein Sci* (2004) 13(8):2089–100. doi: 10.1110/ps.04751804
- Druker J, Liberman AC, Antunica-Noguero M, Gerez J, Paez-Pereda M, Rein T, et al. RSUME Enhances Glucocorticoid Receptor SUMOylation and Transcriptional Activity. *Mol Cell Biol* (2013) 33(11):2116–27. doi: 10.1128/MCB.01470-12
- Fowkes RC, Vlotides G. Hypoxia-Induced VEGF Production 'Resumes' in Pituitary Adenomas. *Endocr Relat Cancer* (2012) 19(1):C1–5. doi: 10.1530/ERC-11-0297
- Shan B, Gerez J, Haedo M, Fuertes M, Theodoropoulou M, Buchfelder M, et al. RSUME is Implicated in HIF-1-Induced VEGF-A Production in Pituitary Tumour Cells. *Endocr Relat Cancer* (2012) 19(1):13–27. doi: 10.1530/ERC-11-0211
- He W, Huang L, Shen X, Yang Y, Wang D, Yang Y, et al. Relationship Between RSUME and HIF-1α/VEGF-A With Invasion of Pituitary Adenoma. *Gene* (2017) 603:54–60. doi: 10.1016/j.gene.2016.12.012
- Fuertes M, Sapochnik M, Tedesco L, Senin S, Attorresi A, Ajler P, et al. Protein Stabilization by RSUME Accounts for PTTG Pituitary Tumor Abundance and Oncogenicity. *Endocr Relat Cancer* (2018) 25(6):665–76. doi: 10.1530/ERC-18-0028
- Chen X, Kuang W, Huang H, Li B, Zhu Y, Zhou B, et al. Knockdown of RWD Domain Containing 3 Inhibits the Malignant Phenotypes of Glioblastoma Cells via Inhibition of Phosphoinositide 3-Kinase/Protein Kinase B Signaling. *Exp Ther Med* (2018) 16(1):384–93. doi: 10.3892/etm.2018.6135
- Huang CC, Tu SH, Lien HH, Jeng JY, Huang CS, Huang CJ, et al. Concurrent Gene Signatures for Han Chinese Breast Cancers. *PLoS One* (2013) 8(10):e76421. doi: 10.1371/journal.pone.0076421
- Schneider BP, Li L, Miller K, Flockhart D, Radovich M, Hancock BA, et al. Genetic Associations With Taxane-Induced Neuropathy by a Genome-Wide Association Study (GWAS) in E5103. *J Clin Oncol* (2011) 29(15_suppl):1000–. doi: 10.1200/jco.2011.29.15_suppl.1000
- Wu Y, Tedesco L, Lucia K, Schlitter AM, Garcia JM, Esposito I, et al. RSUME is Implicated in Tumorigenesis and Metastasis of Pancreatic Neuroendocrine Tumors. *Oncotarget* (2016) 7(36):57878–93. doi: 10.18632/oncotarget.11081
- Gerez J, Tedesco L, Bonfiglio JJ, Fuertes M, Barontini M, Silberstein S, et al. RSUME Inhibits VHL and Regulates its Tumor Suppressor Function. *Oncogene* (2015) 34(37):4855–66. doi: 10.1038/ncr.2014.407
- Bader HL, Hsu T. Systemic VHL Gene Functions and the VHL Disease. *FEBS Lett* (2012) 586(11):1562–9. doi: 10.1016/j.febslet.2012.04.032
- Tedesco L, Elguero B, Pacin DG, Senin S, Pollak C, Garcia Marchinena PA, et al. Von Hippel-Lindau Mutants in Renal Cell Carcinoma are Regulated by Increased Expression of RSUME. *Cell Death Dis* (2019) 10(4):266. doi: 10.1038/s41419-019-1507-3
- Martinefski MR, Elguero B, Knott ME, Gonilski D, Tedesco L, Gurevich Messina JM, et al. Mass Spectrometry-Based Metabolic Fingerprinting Contributes to Unveil the Role of RSUME in Renal Cell Carcinoma Cell Metabolism. *J Proteome Res* (2021) 20(1):786–803. doi: 10.1021/acs.jproteome.0c00655
- Ward Z, Schmeier S, Saddic L, Sigurdsson MI, Cameron VA, Pearson J, et al. Novel and Annotated Long Noncoding RNAs Associated With Ischemia in the Human Heart. *Int J Mol Sci* (2021) 22(21):11324. doi: 10.3390/ijms222111324

19. Kumar A, Chauhan G, Sharma S, Dabla S, Sylaja PN, Chaudhary N, et al. Association of SUMOylation Pathway Genes With Stroke in a Genome-Wide Association Study in India. *Neurology* (2021) 97(4):e345–e56. doi: 10.1212/WNL.00000000000012258
20. Guo C, Henley JM. Wrestling With Stress: Roles of Protein SUMOylation and Desumoylation in Cell Stress Response. *IUBMB Life* (2014) 66(2):71–7. doi: 10.1002/iub.1244
21. Lee YJ, Hallenbeck JM. SUMO and Ischemic Tolerance. *Neuromolecular Med* (2013) 15(4):771–81. doi: 10.1007/s12017-013-8239-9
22. Rojewska E, Korostynski M, Przewlocki R, Przewlocka B, Mika J. Expression Profiling of Genes Modulated by Minocycline in a Rat Model of Neuropathic Pain. *Mol Pain* (2014) 10:47. doi: 10.1186/1744-8069-10-47
23. Gwizdek C, Casse F, Martin S. Protein Sumoylation in Brain Development, Neuronal Morphology and Spineogenesis. *Neuromolecular Med* (2013) 15(4):677–91. doi: 10.1007/s12017-013-8252-z
24. Kamura T, Koepp DM, Conrad MN, Skowyra D, Moreland RJ, Iliopoulos O, et al. Rbx1, a Component of the VHL Tumor Suppressor Complex and SCF Ubiquitin Ligase. *Science* (1999) 284(5414):657–61. doi: 10.1126/science.284.5414.657
25. Kaelin WG Jr. The Von Hippel-Lindau Tumour Suppressor Protein: O2 Sensing and Cancer. *Nat Rev Cancer* (2008) 8(11):865–73. doi: 10.1038/nrc2502
26. Cai Q, Verma SC, Kumar P, Ma M, Robertson ES. Hypoxia Inactivates the VHL Tumor Suppressor Through PIASy-Mediated SUMO Modification. *PLoS One* (2010) 5(3):e9720. doi: 10.1371/journal.pone.0009720
27. Choueiri TK, Kaelin WG Jr. Targeting the HIF2-VEGF Axis in Renal Cell Carcinoma. *Nat Med* (2020) 26(10):1519–30. doi: 10.1038/s41591-020-1093-z
28. Tirard M, Jasbinsek J, Almeida OF, Michaelidis TM. The Manifold Actions of the Protein Inhibitor of Activated STAT Proteins on the Transcriptional Activity of Mineralocorticoid and Glucocorticoid Receptors in Neural Cells. *J Mol Endocrinol* (2004) 32(3):825–41. doi: 10.1677/jme.0.0320825
29. Kang X, Li J, Zou Y, Yi J, Zhang H, Cao M, et al. PIASy Stimulates HIF1alpha SUMOylation and Negatively Regulates HIF1alpha Activity in Response to Hypoxia. *Oncogene* (2010) 29(41):5568–78. doi: 10.1038/onc.2010.297
30. Ismaili N, Garabedian MJ. Modulation of Glucocorticoid Receptor Function via Phosphorylation. *Ann N Y Acad Sci* (2004) 1024:86–101. doi: 10.1196/annals.1321.007
31. Wallace AD, Cidlowski JA. Proteasome-Mediated Glucocorticoid Receptor Degradation Restricts Transcriptional Signaling by Glucocorticoids. *J Biol Chem* (2001) 276(46):42714–21. doi: 10.1074/jbc.M106033200
32. Tian S, Poukka H, Palvimo JJ, Janne OA. Small Ubiquitin-Related Modifier-1 (SUMO-1) Modification of the Glucocorticoid Receptor. *Biochem J* (2002) 367(Pt 3):907–11. doi: 10.1042/bj20021085
33. Paakinaho V, Kaikkonen S, Makkonen H, Benes V, Palvimo JJ. SUMOylation Regulates the Chromatin Occupancy and Anti-Proliferative Gene Programs of Glucocorticoid Receptor. *Nucleic Acids Res* (2014) 42(3):1575–92. doi: 10.1093/nar/gkt1033
34. Zou H, McGarry TJ, Bernal T, Kirschner MW. Identification of a Vertebrate Sister-Chromatid Separation Inhibitor Involved in Transformation and Tumorigenesis. *Science* (1999) 285(5426):418–22. doi: 10.1126/science.285.5426.418
35. Pei L, Melmed S. Isolation and Characterization of a Pituitary Tumor-Transforming Gene (PTTG). *Mol Endocrinol* (1997) 11(4):433–41. doi: 10.1210/mend.11.4.9911
36. Zhang X, Horwitz GA, Heaney AP, Nakashima M, Prezant TR, Bronstein MD, et al. Pituitary Tumor Transforming Gene (PTTG) Expression in Pituitary Adenomas. *J Clin Endocrinol Metab* (1999) 84(2):761–7. doi: 10.1210/jcem.84.2.5432
37. Boggio R, Colombo R, Hay RT, Draetta GF, Chiocca S. A Mechanism for Inhibiting the SUMO Pathway. *Mol Cell* (2004) 16(4):549–61. doi: 10.1016/j.molcel.2004.11.007
38. Stemmann O, Zou H, Gerber SA, Gygi SP, Kirschner MW. Dual Inhibition of Sister Chromatid Separation at Metaphase. *Cell* (2001) 107(6):715–26. doi: 10.1016/S0092-8674(01)00603-1
39. Ramos-Morales F, Dominguez A, Romero F, Luna R, Multon MC, Pintor-Toro JA, et al. Cell Cycle Regulated Expression and Phosphorylation of Hpttg Proto-Oncogene Product. *Oncogene* (2000) 19(3):403–9. doi: 10.1038/sj.onc.1203320
40. Reincke M, Sbiera S, Hayakawa A, Theodoropoulou M, Osswald A, Beuschlein F, et al. Mutations in the Deubiquitinase Gene USP8 Cause Cushing's Disease. *Nat Genet* (2015) 47(1):31–8. doi: 10.1038/ng.3166
41. Mizuno E, Iura T, Mukai A, Yoshimori T, Kitamura N, Komada M. Regulation of Epidermal Growth Factor Receptor Down-Regulation by UBPY-Mediated Deubiquitination at Endosomes. *Mol Biol Cell* (2005) 16(11):5163–74. doi: 10.1091/mbc.e05-06-0560
42. Araki T, Liu X, Kameda H, Tone Y, Fukuoka H, Tone M, et al. EGFR Induces E2F1-Mediated Corticotroph Tumorigenesis. *J Endocr Soc* (2017) 1(2):127–43. doi: 10.1210/js.2016-1053
43. Wang B, Ma A, Zhang L, Jin WL, Qian Y, Xu G, et al. POH1 Deubiquitylates and Stabilizes E2F1 to Promote Tumour Formation. *Nat Commun* (2015) 6:8704. doi: 10.1038/ncomms9704
44. Willi-Monnerat S, Migliavacca E, Surdez D, Delorenzi M, Luthi-Carter R, Terskikh AV. Comprehensive Spatiotemporal Transcriptomic Analyses of the Ganglionic Eminences Demonstrate the Uniqueness of its Caudal Subdivision. *Mol Cell Neurosci* (2008) 37(4):845–56. doi: 10.1016/j.mcn.2008.01.009
45. Bensenor I, Padilha K, Lima IR, Santos RD, Lambert G, Ramin-Mangata S, et al. Genome-Wide Association of Proprotein Convertase Subtilisin/Kexin Type 9 Plasma Levels in the ELSA-Brasil Study. *Front Genet* (2021) 12:728526. doi: 10.3389/fgene.2021.728526
46. Mendler L, Braun T, Muller S. The Ubiquitin-Like SUMO System and Heart Function: From Development to Disease. *Circ Res* (2016) 118(1):132–44. doi: 10.1161/CIRCRESAHA.115.307730
47. Dickinson ME, Flenniken AM, Ji X, Teboul L, Wong MD, White JK, et al. High-Throughput Discovery of Novel Developmental Phenotypes. *Nature* (2016) 537(7621):508–14. doi: 10.1038/nature19356

Conflict of Interest: The authors declare that the research was conducted in the absence of any commercial or financial relationships that could be construed as a potential conflict of interest.

Publisher's Note: All claims expressed in this article are solely those of the authors and do not necessarily represent those of their affiliated organizations, or those of the publisher, the editors and the reviewers. Any product that may be evaluated in this article, or claim that may be made by its manufacturer, is not guaranteed or endorsed by the publisher.

Copyright © 2022 Fuertes, Elguero, Gonilski-Pacin, Herbstein, Rosmino, Ciancio del Giudice, Fiz, Falcucci and Arzt. This is an open-access article distributed under the terms of the Creative Commons Attribution License (CC BY). The use, distribution or reproduction in other forums is permitted, provided the original author(s) and the copyright owner(s) are credited and that the original publication in this journal is cited, in accordance with accepted academic practice. No use, distribution or reproduction is permitted which does not comply with these terms.



Identifying Pupylation Proteins and Sites by Incorporating Multiple Methods

Wang-Ren Qiu*, Meng-Yue Guan, Qian-Kun Wang, Li-Liang Lou and Xuan Xiao*

School of Information Engineering, Jingdezhen Ceramic Institute, Jingdezhen, China

OPEN ACCESS

Edited by:

Xianquan Zhan,
Shandong First Medical University,
China

Reviewed by:

Na Li,
Central South University, China
Canhua Huang,
Sichuan University, China

*Correspondence:

Wang-Ren Qiu
qiuone@163.com
Xuan Xiao
jdzxiaoxuan@163.com

Specialty section:

This article was submitted to
Molecular and
Structural Endocrinology,
a section of the journal
Frontiers in Endocrinology

Received: 06 January 2022

Accepted: 07 March 2022

Published: 26 April 2022

Citation:

Qiu W-R, Guan M-Y, Wang Q-K,
Lou L-L and Xiao X (2022) Identifying
Pupylation Proteins and Sites by
Incorporating Multiple Methods.
Front. Endocrinol. 13:849549.
doi: 10.3389/fendo.2022.849549

Pupylation is an important posttranslational modification in proteins and plays a key role in the cell function of microorganisms; an accurate prediction of pupylation proteins and specified sites is of great significance for the study of basic biological processes and development of related drugs since it would greatly save experimental costs and improve work efficiency. In this work, we first constructed a model for identifying pupylation proteins. To improve the pupylation protein prediction model, the KNN scoring matrix model based on functional domain GO annotation and the Word Embedding model were used to extract the features and Random Under-sampling (RUS) and Synthetic Minority Over-sampling Technique (SMOTE) were applied to balance the dataset. Finally, the balanced data sets were input into Extreme Gradient Boosting (XGBoost). The performance of 10-fold cross-validation shows that accuracy (ACC), Matthew's correlation coefficient (MCC), and area under the ROC curve (AUC) are 95.23%, 0.8100, and 0.9864, respectively. For the pupylation site prediction model, six feature extraction codes (i.e., TPC, AAI, One-hot, PseAAC, CKSAAP, and Word Embedding) served to extract protein sequence features, and the chi-square test was employed for feature selection. Rigorous 10-fold cross-validations indicated that the accuracies are very high and outperformed its existing counterparts. Finally, for the convenience of researchers, PUP-PS-Fuse has been established at <https://bioinfo.jcu.edu.cn/PUP-PS-Fuse> and <http://121.36.221.79/PUP-PS-Fuse> as a backup.

Keywords: pupylation, multiple features, post-translational modification, chi-square test, word embedding

1 INTRODUCTION

Pupylation is a kind of prokaryotic ubiquitin-like protein (Pup), a posttranslational protein modification (PTM) that occurs in actinomycetes, and has made a great contribution to the life process of many cells (1, 2). Ubiquitylation is one of the most common PTM modifications (3). In eukaryotes, ubiquitylation modification plays an important role in DNA repair, transcription regulation, control signal transduction, endocytosis, and sorting (4); research has shown that ubiquitylation modification is closely related to human health, such as lung cancer, breast cancer, type II diabetes, and other complex diseases (5–8). Pupylation is similar to ubiquitin in that Pup is attached to specific lysine residues. Since the PTM small protein modification was originally

discovered in prokaryotes, the Pup in *Mycobacterium tuberculosis* (Mtb) plays an important role in the selection of protein degradation (5).

To better understand the biological mechanism of pupylation, the basic goal and fundamental task is to accurately and effectively predict the pupylation proteins and sites. For identifying PTM proteins, to the best of our knowledge, Qiu is the first one to have tried to identify phosphorylated (9) and acetylated (10) proteins, and nobody has done a similar work on pupylation protein until now. For a predictive analysis of pupylation sites, Liu proposed a GPS-PUP predictor for predicting pupylation sites with a group-based prediction system (GPS) method (11). Tung developed an iPUP predictor that implemented the support vector machine (SVM) algorithm with the composition of pairs of k-space amino acids (CKSAAP) (12). Chen designed a predictor called PupPred based on support vector machines (SVM), in which amino acid pairs were used to encode lysine-centered peptides (13). Hasan established a web server named pbPUP (14), which was a profile-based feature method to predict pupylation sites. Recently, FN Auliah developed PUP-Fuse web server for predicting pupylation sites (15); this algorithm was based on a variety of sequence features to predict pupylation sites. Although these algorithms could output higher specificity, their sensitivity scores are much lower.

In this work, a framework has been developed for predicting pupylation proteins and sites named as PUP-PS-Fuse, shown in **Figure 1**. In predicting the pupylation protein model, the KNN scoring matrix, the Word Embedding model (16–18), the Synthetic Minority Oversampling Technique (SMOTE) (19), and Random Under-sampling (RUS) (20) were applied to enhance the operation engine. Moreover, in the pupylation site prediction model, TPC (15, 21), AAI (22, 23), One-Hot (24), PseAAC (25, 26), CKSAAP (21, 27, 28), and Word Embedding (16–18) were used for feature extraction, and the chi-square test (15, 29, 30) was used to reduce the dimensionality of the feature space. Both these two models were verified with 10-fold cross-validation and compared with other existing predictors, the performance proved that this work is promising for the issue.

2 MATERIALS

2.1 Datasets for Predicting Pupylation Proteins

In this work, the negative samples were collected from UniProKB (2021_4), and the positive sample set was composed of 35 pupylation proteins collected from UniProKB and 233 pupylation proteins from PupDB (31). At least one pupylation

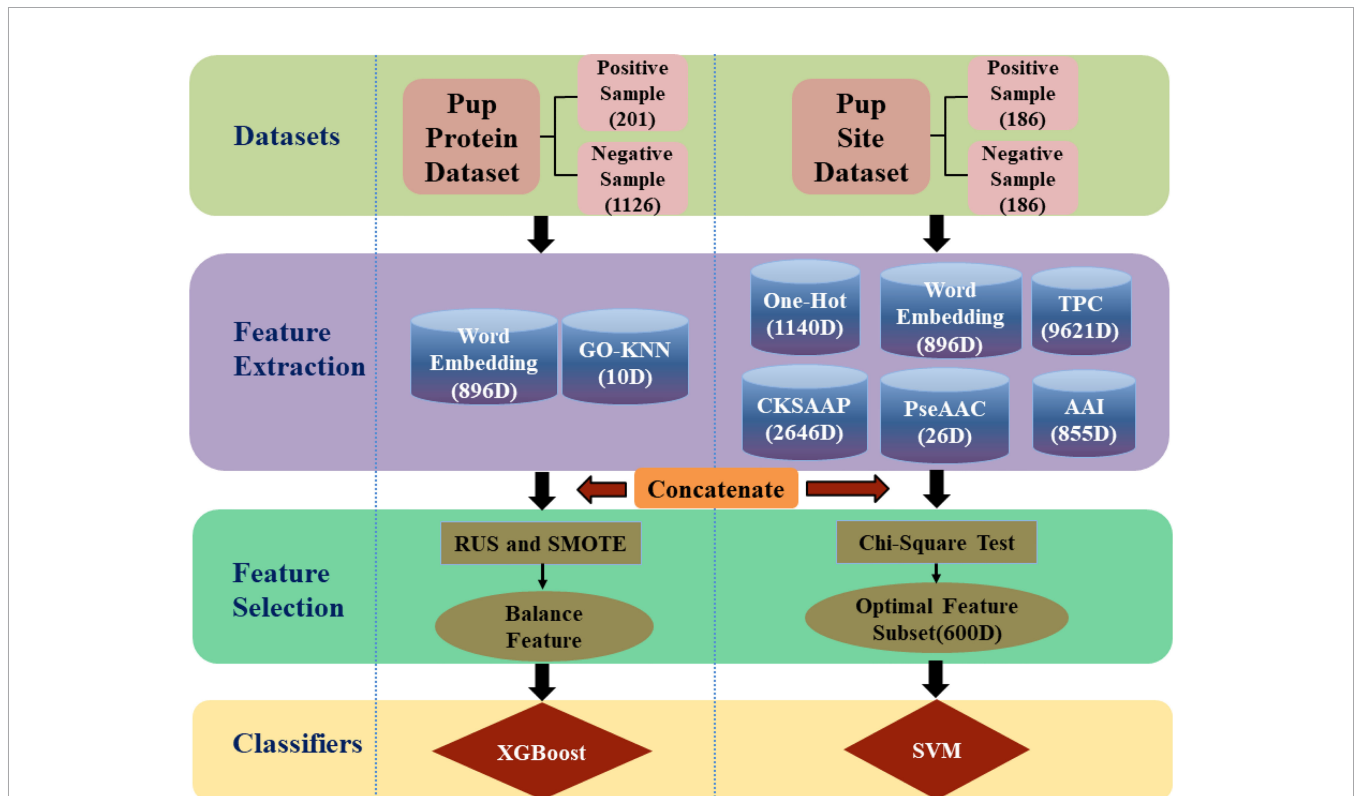


FIGURE 1 | The framework of PUP-PS-Fuse (rounded squares represent data sets, cylinders represent feature extraction methods, rectangles and ellipses represent feature selection methods, and diamonds represent classifiers. RUS is the abbreviation of Random Under-sampling and SMOTE is the abbreviation of Synthetic Minority Over-sampling).

site must exist in any positive protein sequence, and none of the pupylation sites must appear in the negative samples. A given protein sequence can be expressed as $P=R_1R_2R_3\dots R_i\dots R_L$; here, R_i represents the i th amino acid residue, and L represents the length of the protein sequence.

In order to make the results more rigorous, CD-HIT was used to remove 30% of the redundancy from 268 positive sampling as and 1,463 negative samples. Finally, 201 positive samples and 1,126 negative samples were collected for the proposed benchmark with a positive–negative ratio of 1:5.6.

2.2 Datasets for Predicting Pupylation Sites

This article used the same data set as that of Aulia (15). The data set was retrieved and obtained from the publications of PupDB (31) and contained 233 pupylation proteins which were subject to a cutting of redundancy treatment to remove those sequences that had $\geq 80\%$ pairwise sequence identity with any other. After strictly following the aforementioned procedures, the training set consists of 186 amino acid fragments with pupylation site as positive samples and 372 negative samples without any pupylation site. As a result, the positive–negative ratio is 1:2. Since the imbalance of the data will affect the prediction results of the model, we balanced the training set with a positive–negative ratio of 1:1 (186 positive samples and 186 negative samples) by randomly deleting negative samples. The test set is composed of 87 positive samples and 191 negative samples by randomly extracting from the benchmark data set. **Table 1** summarizes the data sets for predicting pupylation proteins and pupylation sites.

In order to formulate the pupylation site sequence in more detail and more comprehensively, the sequence fragment of the potential pupylation site can be expressed in the form of formula (1):

$$\theta_\delta(K) = R_1R_2 - R_{\delta-1}R_\delta KR_{\delta+1}R_{\delta+2} \dots R_{2\delta-1}R_{2\delta} \quad (1)$$

Where R_1 to R_δ represent the amino acid residues on the left of K , $R_{\delta+1}$ to $R_{2\delta}$ represent the amino acid residues on the right of K , δ is an integer, and the middle K means *Lysine* (32). In addition, the peptide sequence $\theta_\delta(K)$ can be divided into $\theta_\delta^+(K)$ and $\theta_\delta^-(K)$ (see formula (2)), where $\theta_\delta^+(K)$ represents a pupylation protein sequence fragment whose center point is K , and $\theta_\delta^-(K)$ denotes non-pupylation protein sequence fragments whose center point is K . The sliding window method was used to segment pupylation protein sequences with different window sizes. Judging from the analysis of the pupylation protein sequence preferred by FN Aulia et al. (15), it can be seen that the prediction is the best when the window size is 57 with $\delta = 28$.

TABLE 1 | Data set for prediction of pupylation protein and pupylation site.

Datasets	Positive	Negative	Ratio
Pupylation proteins	201	1126	1:5.6
Pupylation site training	186	186	1:1
Pupylation site test	87	191	1:2.2

Positive represents the number of positive samples, and Negative represents the number of negative samples.

When the sequence fragments were divided, in order to make the site sequence equal in length, the missing amino acids were filled in with X residues. As a result, the pupylation site data set adopts the form of formula (2):

$$\theta_\delta(K) = \theta_\delta^+(K) \cup \theta_\delta^-(K) \quad (2)$$

Among them, the subset of positive samples $\theta_\delta^+(K)$ represents a true pupylation site segment with K at its center, and the subset of negative samples $\theta_\delta^-(K)$ represents the false pupylation site fragment.

3 FEATURE EXTRACTION AND METHODS

3.1 Feature Extraction Methods for Predicting Pupylation Proteins

The basic step for predicting pupylation protein is to extract features of the protein sequence, and it is a key step that affects the effectiveness of the prediction model. When predicting pupylation protein, we chose GO-KNN (10) and Word Embedding coding schemes to extract protein sequence information.

3.1.1 GO-KNN

GO-KNN (10) is based on the KNN scoring matrix of functional domain GO annotations to extract features. In this study, we need to obtain the GO information of all proteins. For a protein without any GO information, we replace it with GO terms of its homologous protein and then calculate the distance between any two protein sequences. Taking protein R_1 and R_2 as example, their GO annotations can be expressed by $R_{GO}^1 = \{GO_1^1, GO_2^1, \dots, GO_M^1\}$ and $R_{GO}^2 = \{GO_1^2, GO_2^2, \dots, GO_N^2\}$, GO_i^1 and GO_i^2 represent the i th GO of the proteins R_1 and R_2 , respectively, and M and N are the numbers of their GO terms. The feature extraction steps are listed as follows:

(a). Calculating the distance between two proteins, as in formula (3).

$$Distance(R_1, R_2) = 1 - \frac{|R_{GO}^1 \cap R_{GO}^2|}{|R_{GO}^1 \cup R_{GO}^2|} \quad (3)$$

Where \cup and \cap represent the intersection and union of sets, and $| \cdot |$ represents the number of elements in the set.

(b) Sorting all the calculated distances from small to large.

(c) Calculating the percentage of positive samples in the Y neighbors.

In this study, the Y values were selected in order of 2, 4, 8, 16, 32, 64, 128, 256, and 1,024. Finally, a 10-dimensional feature vector was formed. Therefore, the digital feature vector of protein R_1 can be expressed as: $(x_1, x_2, \dots, x_{10})$.

3.1.2 Word Embedding

Word Embedding (16–18) is a method for converting words in text into digital vectors. The Word Embedding process was used to embed the high-dimensional space containing all the number of words into a low-dimensional continuous vector space, each word or phrase was mapped to a vector in the real number

domain, and the word vector was generated as a result of the Word Embedding. In this study, we quoted the word embedding method of Qiu (33, 34). This briefly introduces how word embedding was applied in this research as described below.

Step 1: Firstly, the pupylation protein sequence was split into fragments and a wordbook is created. In this study, we used three different word embedding models, and the pupylation protein sequence is cut into different fragment lengths. Their fragment lengths can be set to 2, 3, or 4, respectively, and the step size of the moving window is 1.

Step 2: The CBOW (Continuous Bag-of-Words) model was used to train the data. In order to speed up the training speed of word vectors, the negative sampling technique (35) and backpropagation algorithm (36) were adopted in the CBOW model. At this step, the dimension sizes of the word vectors were selected as 128, 256, and 512, respectively, and we then obtained three vectors W_{128} , W_{256} , and W_{512} for a given protein sequence.

Step 3: >A protein sequence was represented by combining CBOW vectors. At this step, we merge the features of each pupylation protein sequence of the three aforementioned words vector, as shown in formula (4), and finally get an 896-dimensional vector.

$$V = W_{128} \oplus W_{256} \oplus W_{512} \tag{4}$$

Among them, W_{128} , W_{256} , and W_{512} mean 128-, 256-, and 512-dimensional word vectors, and \oplus means to concatenate a two-word vector.

3.2 Feature Extraction Methods for Predicting Pupylation Sites

For predicting pupylation sites, TPC (15, 21), AAI (22, 23), One-Hot (21, 37), PseAAC (25, 26), CKSAAP (21, 27, 28), and Word Embedding (17, 18) coding schemes were involved in extracting protein fragment [for example, formula (2)] information and are briefly described as follows.

3.2.1 TPC

The first feature extraction algorithm applied for predicting pupylation sites in this paper is TPC (15, 21) which codes protein fragment information by calculating the frequency of occurrence of three consecutive amino acid pairs. Bian et al. (38) identified mitochondrial proteins of *Plasmodium*. In this method, we divide the number of occurrences of each of the three consecutive amino acid pairs in the fragment by the total number of all possible tripeptides [refer to formula (5)], and finally form a 9,261-dimensional digital feature vector.

$$p_i = \frac{N_i}{\sum_1^{9261} N_i} \tag{5}$$

where N_i represents the number of occurrences of the i th three consecutive amino acid pairs in the fragment.

3.2.2 AAI

The second algorithm, AAI code, is based on AAindex (22, 23), which is a database that collects more than 500 amino acid

indexes. After evaluating the different physicochemical and biological properties of amino acids, the top 15 useful and informative amino acid indexes selected by FN Auliah et al. (15) were used in this paper (fifteen types of AAI properties can be found at <https://www.mdpi.com/1422-0067/22/4/2120/s1>), with a window sequence length of 57. Therefore, AAI encoding produced 855 (57×15) dimensional feature vectors.

3.2.3 One-Hot

One-Hot coding (21, 37) is based on the 0–1 coding scheme. In this coding scheme, each amino acid is represented by a 20-dimensional binary vector. For example, alanine A is transformed into a vector (10000000000000000000), cysteine C is transformed into a vector (01000000000000000000), tyrosine Y is transformed into a vector (00000000000000000001), etc. In this study, a pseudo-amino acid code X was selected to represent it, which is represented by a (00000000000000000000) vector. The sequence length of the window is 57, so the total dimension of the proposed One-Hot feature vector is $20 \times (2\delta + 1)$, i.e., 1,140, dimensions.

3.2.4 PseAAC

PseAAC (25, 26) coding has been widely used in the study of protein and protein-related problems. It can be called a “pseudo-amino acid composition” model to represent protein samples. Here, six physical and chemical properties of amino acids, hydrophobicity, hydrophilicity, molecular side chain mass, PK1, PK2, and PI, were selected to convert the protein sequence into the feature vector. The parameters ω and λ were set to 0.05 and 5, respectively [the values of ω and λ are clearly explained by Chou (39) et al.]. Finally, a 25-dimensional digital feature vector is formed.

$$p_i = \begin{cases} \frac{f_i}{\sum_{i=1}^{20} f_i + \omega \sum_{j=1}^{\lambda} \theta_j} & (1 \leq i \leq 20) \\ \frac{\omega \theta_{i-20}}{\sum_{i=1}^{20} f_i + \omega \sum_{j=1}^{\lambda} \theta_j} & (20 + 1 \leq i \leq 20 + \lambda) \end{cases} \tag{6}$$

3.2.5 CKSAAP

CKSAAP (21, 27, 28) coding is a coding scheme based on K -spaced amino acid pairs. In the coding process, a protein sequence contains 441 (21×21) amino acid pairs (AA, AC, AD, ..., XX) and is expressed by formula (7).

$$\left(\frac{F_{AA}}{F_N}, \frac{F_{AC}}{F_N}, \frac{F_{AD}}{F_N}, \dots, \frac{F_{XX}}{F_N} \right) 441 \tag{7}$$

Where, F_{AA} , F_{AC} , F_{AD} , F_{XX} , represents the number of times the corresponding amino acid pair appears in the protein sequence, and L is used in this article to represent the length of the protein sequence, $F_N = L - k - 1$. For each k , 441 pairs of residues are formed, where k represents the space between two amino acids, the values of k are 0, 1, 2, 3, 4, 5, and the best k_{max} setting is 5. Therefore, each corresponding protein sequence can be represented with a 2,646 ($21 \times 21 \times (k_{max} + 1)$) dimensional feature vector.

3.3 Data Balancing and Feature Selection

In the model of pupylation protein prediction, the number of positive samples is 201 and the number of negative samples is 1126, and the ratio of positive to negative samples is approximately 1:5.6. Since it is an unbalanced data set, Random Under-sampling (RUS) (20) and Synthetic Minority Oversampling (SMOT) (19, 20) were used to process the sample data. Actually, the RUS is a very simple and popular under-sampling technique and the SMOT is one of the most popular methods in oversampling proposed by Chawla et al. (40).

In the model of pupylation site prediction, fusion of multiple features would generate a high-dimensional vector, and there may be some redundant or irrelevant features. Therefore, the chi-square test (15, 29, 30) was used to select the most beneficial feature. The chi-square test was first proposed by Karl Pearson (41), usually called the Pearson chi-square test, which is currently the most popular non-parametric (or no distribution) test based on the hypothesis of the chi-square χ^2 distribution test method (42). In the model, the first 600-dimensional features were selected to get a better prediction result.

4 MODEL EVALUATION METRICS AND OPERATION ENGINE

4.1 Model Evaluation Metrics

In this study, four indicators were used to evaluate the performance of the model. They are Accuracy (ACC) (43), Sensitivity (Sn), Specificity (Sp), and Matthews Correlation Coefficient (MCC) (44–47), which are defined as Eq. (8).

$$\begin{cases} Sn = \frac{TP}{TP+FN} \\ Sp = \frac{TN}{TN+FP} \\ ACC = \frac{TP+TN}{TP+FP+TN+FN} \\ MCC = \frac{TP \times TN - FP \times FN}{\sqrt{(TP+FP) \times (TP+FN) \times (TN+FP) \times (TN+FN)}} \end{cases} \quad (8)$$

In addition, the prediction accuracy can also be measured and analyzed using the ROC curve. For the prediction method, the ROC (48) curve plots the true positive rate (Sn) and false positive rate (Sp) of all possible thresholds as a function of the relationship. The calculation of AUC also provides a comprehensive understanding of the proposed prediction method. Generally, the closer the AUC (49) value is to 1, the better the prediction method.

4.2 Operation Engine

Most of the classification algorithms can handle the data with the digital vector; thus, this work tried diverse approaches include Random Forest (RF), Support Vector Machine (SVM), K nearest neighbor (KNN), eXtreme Gradient Boosting (XGBoost), and Ensemble Learning. Since they have been widely used in various fields such as marketing management (50), bioinformatics (51), and image retrieval (52), we would not repeat their principles in this manuscript in detail.

In fact, the Random Forest (RF) (51, 53) algorithm is based on the classification and regression tree (CART) (54) technology which is formed by integrating multiple decision trees through the idea of integrated learning. In the RF model, each decision tree is a classifier. For a given sample, each tree will get a classification result. All the voting results are integrated, and the final output is the category with the most votes. The SVM (55) is a supervised learning model whose main idea is to find the hyperplane that distinguishes the two types, to maximize the margin, some points in the sample that are closest to the hyperplane; these points are called support vectors. The KNN (56, 57) is a supervised learning model, and its main idea is to determine which category it belongs to when predicting a new value based on the category of the nearest K points. XGBoost (58) is an open-source machine learning project developed by Chen et al. It efficiently implements the GBDT (59) algorithm and has made many improvements to the algorithm and engineering.

Ensemble learning (60) is an important method for improving prediction accuracy in current data mining and machine learning. It is frequently used in the field of machine learning (5) due to its “fault tolerance.” It has better classification results than individual classifiers. The ensemble method is a meta-algorithm that combines several machine learning techniques into a predictive model. There are three commonly used frameworks for ensemble learning: Bagging (61) to reduce variance, Boosting (62) to reduce bias, and Stacking (63) to improve prediction results. In this research, we used the Stacking ensemble learning algorithm. The main idea of Stacking is as follows: we firstly train multiple different models, and then use the output of each model trained before as input to train a model to get a final output. For predicting Pupylation sites, we use three base classifiers, namely, RF, SVM, and KNN, and then use LogisticRegression (LR) to classify the results of the base classification to get the final classification results.

5 RESULTS AND DISCUSSION

5.1 Results and Discussion of Pupylation Proteins Prediction

5.1.1 Effect of the Different Features

In this study, the two single feature encoding methods are GO-KNN and Word Embedding, and 10 dimensions and 896 dimensions are obtained respectively. These two kinds of features have been fused into a 906-D feature vector PUP-P-Fuse. Through the 10-fold cross-folding verification, the prediction results of different features are shown in **Table 2**.

From **Table 2**, we can know that the prediction results after fusion are not as good as we expected; the best prediction performance is GO-KNN's with ACC of 94.36%, Sn of 77.08%, Sp of 97.45%, MCC of 0.7731, and AUC of 0.9530, which are slightly higher than those of CBOW and PUP-P-Fuse (see to the first 4 line of **Table 2**).

5.1.2 Effect of the RUS and SMOTE

Using Random Under-sampling (RUS) and Synthetic Minority Over-sampling (SMOTE) to balance the data, and then through

TABLE 2 | The prediction results of different feature extraction and balance methods for predicting pupylation proteins.

	Feature	ACC (%)	Sn (%)	Sp (%)	MCC	AUC
Unbalanced	GO-KNN	94.36	77.08	97.45	0.7731	0.9530
	CBOW	91.91	67.42	96.27	0.6700	0.9553
	PUP-P-Fuse	92.07	60.25	97.77	0.6615	0.9647
Balanced	PUP-P-Fuse	95.40	92.03	96.00	0.8327	0.9840

GO-KNN and CBOW represent two feature extraction methods for predicting pupylation proteins, and PUP-P-Fuse is a fusion of the above two methods. The bold values are means the best performance of the column with the same metric and are showed in following tables with the same meaning.

10-fold cross-folding verification, the prediction results of ACC, Sn, Sp, MCC, and AUC on balanced and unbalanced data sets were obtained and are shown in **Table 2**.

From the last line of **Table 2**, we can see that the PUP-P-Fuse’s ACC, Sn, MCC, and AUC predictive indicators have increased by 3%, 32%, 17%, and 2%, respectively, after the RUS and SMOTE technology balance. Therefore, the results show that multifeature fusion (PUP-P-Fuse) can improve the performance. In order to better analyze the influence of different features on pupylation protein prediction, the results obtained by two single coding and fusion features are as shown in **Figure 2**.

From **Figure 2**, we can see that the ACC, Sn, Sp, MCC, and AUC of GO-KNN are 93.37%, 82.64%, 95.36%, 0.7519, and 0.9509, respectively. Those of CBOW and PUP-P-Fuse are denoted with red and green bars, respectively. Compared with GO-KNN and CBOW’s ACC, Sn, Sp, MCC, and AUC predictive indicators, the PUP-P-Fuse increased by 2%–4%, 10%–11%, 0.6%–2%, 8%–13%, and 3%, respectively. In summary, all indicators of PUP-P-Fuse are higher than the other two models after data balancing. Therefore, it is proper to use RUS and SMOT in this issue.

5.1.3 Effect of Classifiers

Classifiers play an important role in prediction. In this work, we used the above five classifiers to identify pupylation proteins. After 10-fold cross-folding verification, the results of ACC, Sn, Sp, MCC, and AUC of each classifier are shown in **Table 3**. From **Table 3**, we can see that XGBoost gained the best performance on each evaluation index. In order to better compare the effects of different classifiers, the prediction results of the five classifiers are as shown in **Figure 3**.

The area under the ROC curve can evaluate the predictive performance of the model. It is seen in **Figure 3** that the XGBoost classifier, of which AUC is 0.9840, is the best choice for the proposed model.

5.1.4 Effect of Features on the Independent Dataset

To verify the effect of the PUP-P-Fuse model, we used 67 pupylation proteins and 134 negative samples for independent testing; PUP-P-Fuse has the highest performance, as shown in **Table 4**. It can be seen that the effect of the PUP-P-Fuse model is still very good. However, from **Table 4** we can see that the overall

TABLE 3 | The prediction results of different classifiers for predicting pupylation proteins.

Algorithms	Acc (%)	Sn (%)	Sp (%)	MCC	AUC
XGBoost	95.40	92.03	96.00	0.8327	0.9840
Ensemble Learning	93.87	90.61	94.48	0.7874	0.9788
SVM	91.36	93.65	90.96	0.7335	0.9689
RF	92.87	82.40	94.75	0.7355	0.9703
KNN	83.88	96.90	81.55	0.6104	0.9585

The bold values are means the best performance of the column with the same metric and are showed in following tables with the same meaning.

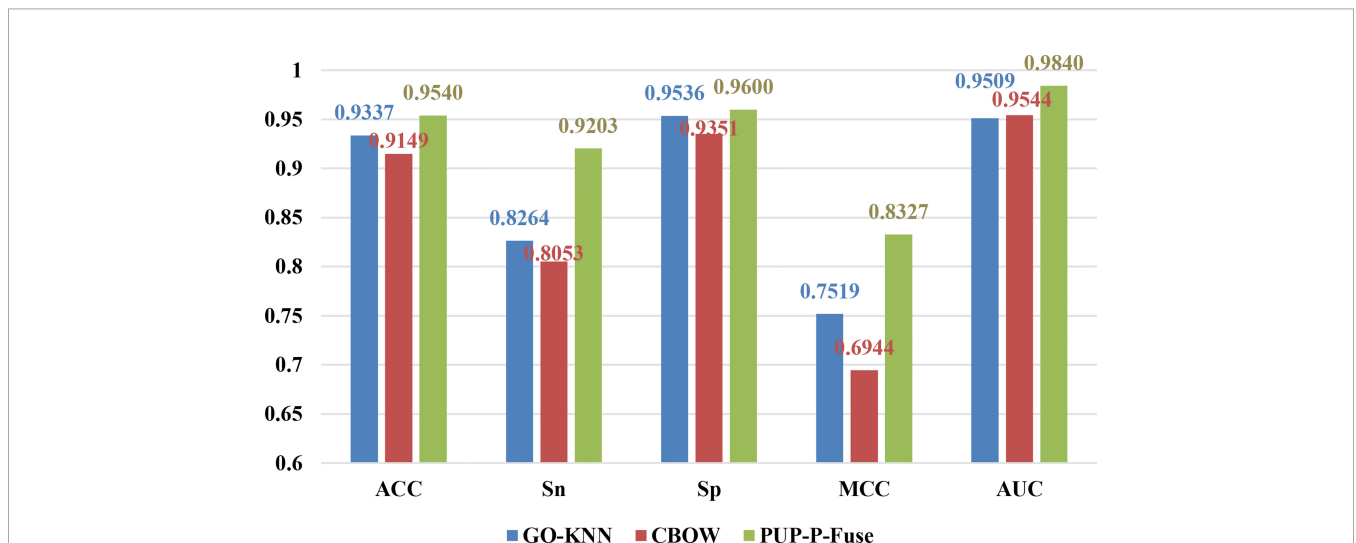


FIGURE 2 | The prediction results of different characteristics on balanced data for predicting pupylation proteins.

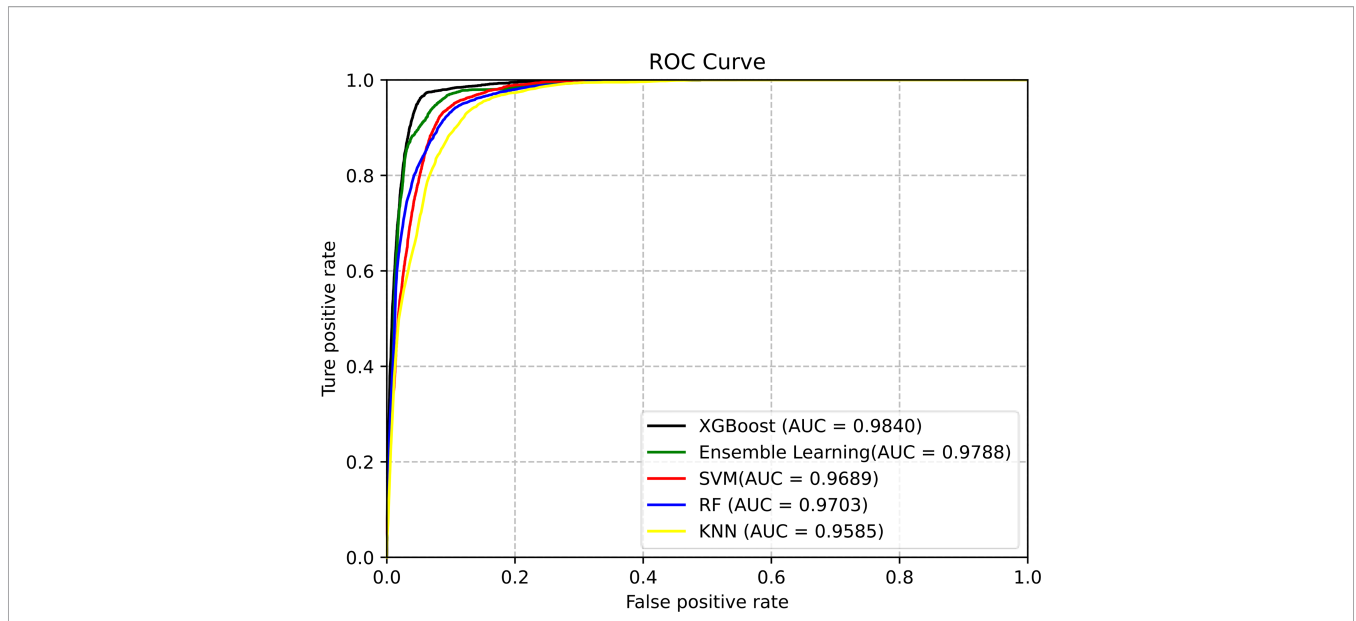


FIGURE 3 | ROC curves of different classifiers for predicting the pupylation protein.

TABLE 4 | The prediction results of different classifiers on the testing set of pupylation proteins.

Algorithms	Acc (%)	Sn (%)	Sp (%)	MCC	AUC
XGBoost	84.66	80.99	86.62	0.6630	0.9251
Ensemble Learning	85.34	80.96	87.41	0.6738	0.9376
SVM	85.48	88.78	83.85	0.6955	0.9317
RF	84.55	79.15	87.79	0.6571	0.9270
KNN	78.56	83.97	75.61	0.5653	0.8868

performance of the SVM classifier is better than those of other classifiers.

5.2 Results and Discussion of Pupylation Site Prediction

5.2.1 Effect of Features on the Training Dataset

In this study, six single-feature codes are AAI, One-Hot, PseAAC, Word Embedding, CKSAAP, and TPC, and the feature PUP-S-Fuse was obtained after fusion. The six features are coded separately and obtained 855, 1140, 26, 896, and 2,646 dimensions, respectively. Through 10-fold cross-folding

TABLE 5 | The effect of different feature extraction methods on the training set of pupylation sites.

Features	ACC (%)	Sn (%)	Sp (%)	MCC	AUC
AAI	56.71	56.21	57.52	0.1380	0.6148
One-Hot	57.49	59.49	55.95	0.1550	0.6296
PseAAC	61.56	62.00	61.64	0.2367	0.6597
Word Embedding	69.92	73.36	66.55	0.4001	0.7645
CKSAAP	68.84	68.92	69.20	0.3818	0.7596
TPC	70.36	70.69	70.65	0.4143	0.7697
PUP-S-Fuse	74.00	80.00	68.55	0.4883	0.7951

The bold values are means the best performance of the column with the same metric and are showed in following tables with the same meaning.

verification, we choose the SVM classifier for training. Without feature selection, we obtain the prediction results of different feature extractions with a ratio of positive samples to negative samples of 1:1, as shown in **Table 5**.

From **Table 5**, we can see that the ACC, Sp, MCC, and AUC indicators of TPC are all higher than other single codes, and the Sn indicators of Word Embedding are all higher than other single codes. The fusion feature code PUP-S-Fuse performs better than any single feature on ACC, Sn, Sp, MCC, and AUC indicators. Therefore, feature fusion is very necessary for this issue.

5.2.2 Effect of the Chi-Square Test on the Training Dataset

As regards the model for predicting the pupylation site, we selected different *K* values for the chi-square test and compared them and found that the prediction effect has been relatively greatly improved after the chi-square test was used to select features.

It is seen in **Table 6** that when the *K* value is selected as 600, the ACC, Sn, and MCC of the pupylation site are predicted to be higher than other *K* values. When the *K* value is selected as 1,000,

TABLE 6 | The effect of feature fusion Pup-S-Fuse by using the chi-square test for predicting pupylation sites.

Features	ACC (%)	Sn (%)	Sp (%)	MCC	AUC
<i>K</i> = 200	89.09	88.82	89.57	0.7830	0.9531
<i>K</i> = 400	91.21	92.89	89.52	0.8256	0.9565
<i>K</i> = 600	92.30	93.97	90.71	0.8477	0.9599
<i>K</i> = 800	91.99	93.31	90.55	0.8400	0.9634
<i>K</i> = 1,000	92.00	92.27	91.78	0.8394	0.9641
<i>K</i> = 1,200	90.70	91.77	89.70	0.8145	0.9604

The bold values are means the best performance of the column with the same metric and are showed in following tables with the same meaning.

TABLE 7 | The prediction results of different classifiers for predicting pupylation sites.

Algorithms	Acc (%)	Sn (%)	Sp (%)	MCC	AUC
EL	92.30	93.97	90.71	0.8477	0.9599
SVM	91.72	95.27	88.59	0.8377	0.9659
RF	86.72	87.50	86.24	0.7361	0.9347
KNN	81.34	90.37	75.63	0.6706	0.9388
XGBoost	78.49	79.02	77.94	0.5703	0.8622

EL, ensemble learning.

The bold values are means the best performance of the column with the same metric and are showed in following tables with the same meaning.

the Sp and AUC values of the pupylation site are higher than those of other K values. Therefore, from the overall effect, we finally selected 600 for predicting the pupylation site.

5.2.3 Effect of Classifiers on the Training Dataset

Choosing the right machine learning (ML) algorithm is also a crucial step for predicting results. When predicting pupylation sites, we used RF, SVM, KNN, Ensemble Learning (EL), and XGBoost algorithms. In order to verify the effectiveness and superiority of the EL algorithm used to predict pupylation sites, we compared these algorithms through 10-fold cross-validation on the same training set. The prediction results are shown in **Table 7**.

From **Table 7**, although we know that the prediction effect of the EL classifier and SVM classifier is better, the overall prediction effect of the EL is better than that of the SVM. The prediction results of RF, KNN, and XGBoost are relatively poor. In order to evaluate the performance of the classifier more comprehensively, the ROC curves of different classifiers are as shown in **Figure 4**.

From **Figure 4**, we can clearly see that the area under the ROC curve of EL and SVM is the largest, and the AUC of EL is

about 2%–10% higher than that of other ML models. Therefore, EL was selected as the best classifier for predicting pupylation sites.

5.2.4 Comparison With Other Methods on Independent Datasets

In order to compare PUP-S-Fuse with the existing five methods (GPS-PUP, iPUP, PUPS, PbPUP, and PUP-Fuse), tests were performed on the same independent set which contains 86 pupylation sites and 1,136 non-pupylation sites from 71 pupylation proteins. PUP-S-Fuse and PUP-Fuse were trained with the same training data set mentioned above, and the other four methods were quoted from the references. In the fairly compared performance, PUP-S-Fuse provided the highest performance, as shown in **Table 8**.

From **Table 8**, we know that the performance of PUP-S-Fuse on the test set is also better than that of PUP-Fuse. Acc, Sn, Sp, and MCC are increased by 9%, 19%, 6%, and 24%, respectively, which proves that PUP-S-Fuse is superior to existing predictors.

TABLE 8 | Comparison of methods on Independent Dataset for predicting pupylation sites.

Methods	Acc (%)	Sn (%)	Sp (%)	MCC	AUC
iPUP	73	40	88	0.32	
GPS-PUP	68	21	89	0.13	
PUPS	67	17	89	0.08	
PbPUP	79	48	82	0.45	
PUP-Fuse	82	59	91	0.55	
PUP-S-Fuse	91.35	78.26	97.38	0.7953	0.9550

The bold values are means the best performance of the column with the same metric and are showed in following tables with the same meaning.

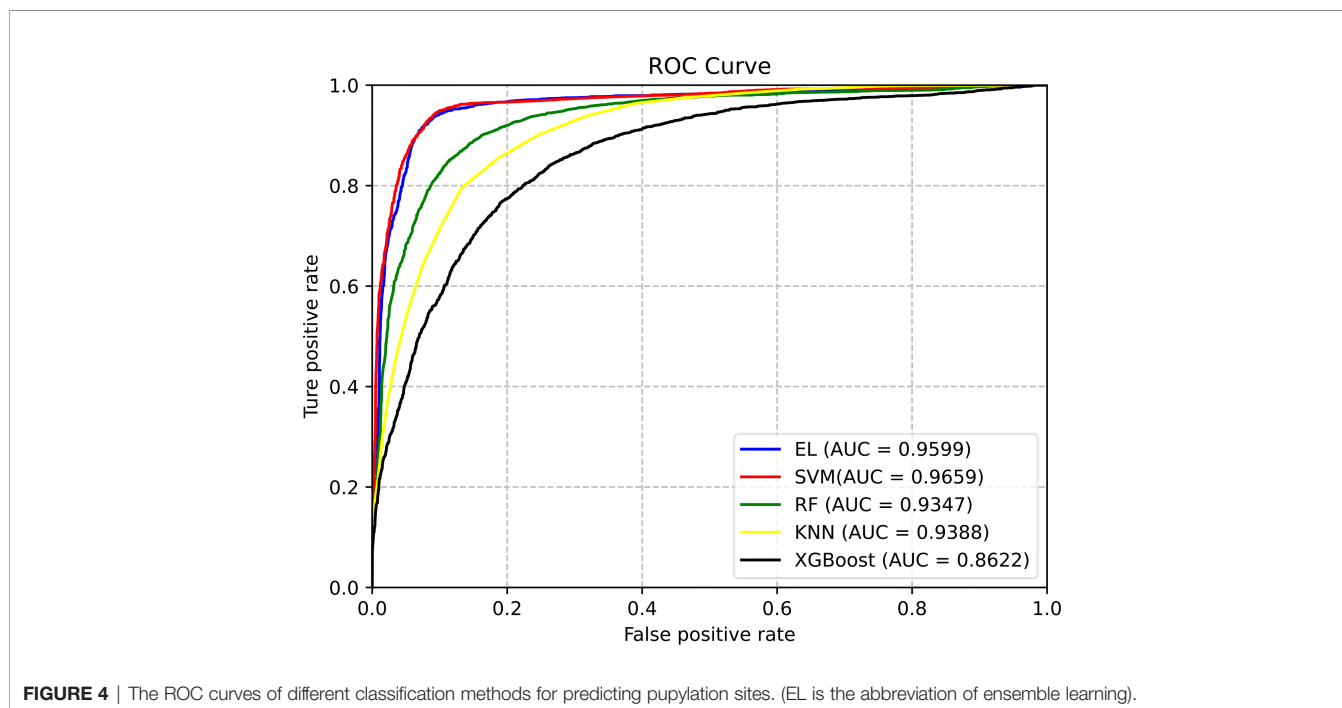


FIGURE 4 | The ROC curves of different classification methods for predicting pupylation sites. (EL is the abbreviation of ensemble learning).

6 WEB SERVER AND USER GUIDE

The actual application value of a prediction method can be significantly improved if it has a web server that can be viewed by the public; accordingly, the PUP-PS-Fuse web server has been established. To maximize the convenience of most experimental scientists, a guide for users is provided below.

Step 1. Opening the web server at “<https://bioinfo.jcu.edu.cn/PUP-PS-Fuse>,” the server consists of four main modules, namely, Pupylation Protein, Pupylation Site, Download (data download), and **Help** (website usage guide). You will see the top page of PUP-PS-Fuse on your computer screen.

Step 2. In the Pupylation Protein prediction module, you can enter the protein sequence in the input file box, but it must be in FASTA format. You can also click the example button where you will see that there are a correct example and an incorrect example as well as the text input format. Click the Close button, and you will return to the pupylation Protein prediction interface. Click the Submit button to get the prediction results. After 20 seconds or so since your submitting, you will see the following on the screen of your computer: “The Pupylation protein list includes ...” and “The non-Pupylation protein list includes ...”

Step 3. In the Pupylation Site prediction module, you can enter the protein sequence in FASTA format in the input file box. In the example_site submodule, you will see that there are a correct example and an incorrect example as well as the text input format. Click the Close button, and you will return to the pupylation Site prediction interface. Click the Submit button to get the predicted results. After 2 min or so since your submitting, you will see the following on the screen of your computer: “The number of “K” is X. Location M₁, M₂, M₃, ... is(are) predicted to be Pupylation Site(s).”

In the Download module, you can download the Pupylation protein dataset and Pupylation site dataset (also available in the **Supplementary Material**). By the way, you can click on the Help button to see a brief introduction about the predictors.

7 CONCLUSION

PUP-PS-Fuse was developed to predict pupylation proteins and sites. In order to predict pupylation proteins, GO-KNN and Word Embedding served as feature extraction methods. In the work, GO-KNN extracted features based on the KNN score matrix of functional domain GO annotations, and Word Embedding converted information of the amino acid sequence into digital feature vectors. In addition, RUS and SMOT technology were used to deal with the imbalance of the data set to reduce the negative impact of imbalance on the model. Finally, the XGBoost classifier was selected to make predictions. In order to predict pupylation sites, six feature extraction codes

and one fusion feature extraction code are used, named as TPC, AAI, One-Hot, PseAAC, CKSAAP, Word Embedding, and PUP-S-Fuse. In order to improve the computational efficiency and eliminate the redundancy and noise generated by the fusion feature, the chi-square test served to reduce the dimensionality of the fusion feature. The selected feature subset was input into the Ensemble Learning for classification, and then 10-fold cross-folding was used for verification. The performance of PUP-S-Fuse is evaluated based on an independent test data set, and compared with other existing methods, it is concluded that the predictive performance of PUP-S-Fuse is better than other existing methods. These processes only require calculation models and do not require any physical and chemical experiments, which saves experimental costs and improves work efficiency. We hope that this work will be helpful for dealing with some related biological problems with computational methods.

DATA AVAILABILITY STATEMENT

The original contributions presented in the study are included in the article/**Supplementary Material**. Further inquiries can be directed to the corresponding authors.

AUTHOR CONTRIBUTIONS

W-RQ conceived and designed the experiments. M-YG, Q-KW, and L-LL performed the extraction of features, model construction, model training, and evaluation. M-YG drafted the manuscript. XX and W-RQ supervised this project and revised the manuscript. All authors contributed to the article and approved the submitted version.

FUNDING

This work was supported by grants from the National Natural Science Foundation of China (Nos. 31760315, 62162032, 61761023) and Natural Science Foundation of Jiangxi Province, China (No. 20202BAB202007).

SUPPLEMENTARY MATERIAL

The Supplementary Material for this article can be found online at: <https://www.frontiersin.org/articles/10.3389/fendo.2022.849549/full#supplementary-material>

REFERENCES

- Li T, Chen Y, Li T, Jia C. Recognition of Protein Pupylation Sites by Adopting Resampling Approach. *Molecules* (2018) 23(12):3097–110. doi: 10.3390/molecules23123097

- Barandun J, Delley CL, Weber-Ban E. The Pupylation Pathway and Its Role in Mycobacteria. *BMC Biol* (2012) 10(1):95. doi: 10.1186/1741-7007-10-95
- Garcia BA, Hake SB, Diaz RL, Kauer M, Morris SA, Recht J, et al. Organismal Differences in Post-Translational Modifications in Histones H3 and H4. *J Biol Chem* (2007) 282(10):7641–55. doi: 10.1074/jbc.M607900200

4. Herrmann J, Lerman LO, Lerman A. Ubiquitin and Ubiquitin-Like Proteins in Protein Regulation. *Circ Res* (2007) 100(9):1276–91. doi: 10.1161/01.RES.0000264500.11888.f0
5. Afolabi LT, Saeed F, Hashim H, Petrinir OO. Ensemble Learning Method for the Prediction of New Bioactive Molecules. *PLoS One* (2018) 13(1):e0189538. doi: 10.1371/journal.pone.0189538
6. Faus H, Haendler B. Post-Translational Modifications of Steroid Receptors. *BioMed Pharmacother* (2006) 60(9):520–8. doi: 10.1016/j.biopha.2006.07.082
7. Poulsen C, Akhter Y, Jeon AH, Schmitt-Ulms G, Meyer HE, Stefanski A, et al. Proteome-Wide Identification of Mycobacterial Pupylation Targets. *Mol Syst Biol* (2010) 6(1):386. doi: 10.1038/msb.2010.39
8. Imkamp F, Rosenberger T, Striebel F, Keller PM, Amstutz B, Sander P, et al. Deletion of Dop in Mycobacterium Smegmatis Abolishes Pupylation of Protein Substrates *In Vivo*. *Mol Microbiol* (2010) 75(3):744–54. doi: 10.1111/j.1365-2958.2009.07013.x
9. Qiu WR, Sun BQ, Xiao X, Xu D, Chou KC. Iphos-PseEvo: Identifying Human Phosphorylated Proteins by Incorporating Evolutionary Information Into General PseAAC via Grey System Theory. *Mol Inform* (2017) 36(5-6):1600010. doi: 10.1002/minf.201600010
10. Qiu WR, Xu A, Xu ZC, Zhang CH, Xiao X. Identifying Acetylation Protein by Fusing Its PseAAC and Functional Domain Annotation. *Front Bioeng Biotechnol* (2019) 7:311. doi: 10.3389/fbioe.2019.00311
11. Liu Z, Ma Q, Cao J, Gao X, Ren J, Xue Y. GPS-PUP: Computational Prediction of Pupylation Sites in Prokaryotic Proteins. *Mol Biosyst* (2011) 7(10):2737–40. doi: 10.1039/c1mb05217a
12. Tung, Chun-Wei. Prediction of Pupylation Sites Using the Composition of K-Spaced Amino Acid Pairs. *J Theor Biol* (2013) 336(Complete):11–7. doi: 10.1016/j.jtbi.2013.07.009
13. Chen X, Qiu JD, Shi SP, Suo SB, Liang RP. Systematic Analysis and Prediction of Pupylation Sites in Prokaryotic Proteins. *PLoS One* (2013) 8(9):e74002. doi: 10.1371/journal.pone.0074002
14. Hasan MM, Zhou Y, Lu X, Li J, Song J, Zhang Z. Computational Identification of Protein Pupylation Sites by Using Profile-Based Composition of K-Spaced Amino Acid Pairs. *PLoS One* (2015) 10(6):e0129635. doi: 10.1371/journal.pone.0129635
15. Auliah FN, Nilamyani AN, Shoombuatong W, Alam MA, Hasan MM, Kurata H. PUP-Fuse: Prediction of Protein Pupylation Sites by Integrating Multiple Sequence Representations. *Int J Mol Sci* (2021) 22(4) 2120. doi: 10.3390/ijms22042120
16. Thapa N, Chaudhari M, McManus S, Roy K, Newman RH, Saigo H. DeepSuccinylSite: A Deep Learning Based Approach for Protein Succinylation Site Prediction. *BMC Bioinf* (2020) 21(3):1–10. doi: 10.1186/s12859-020-3342-z
17. Yang KK, Wu Z, Bedbrook CN, Arnold FH, Wren J. Learned Protein Embeddings for Machine Learning. *Bioinformatics* (2018) 34(15):2642–8. doi: 10.1093/bioinformatics/bty178
18. Wang H, Wang Z, Li Z, Lee TY. Incorporating Deep Learning With Word Embedding to Identify Plant Ubiquitylation Sites. *Front Cell Dev Biol* 8 (September 2020) 2020:572195. doi: 10.3389/fcell.2020.572195
19. Das S, Datta S, Chaudhuri BB. Handling Data Irregularities in Classification: Foundations, Trends, and Future Challenges. *Pattern Recognition* (2018) 81:674–93. doi: 10.1016/j.patcog.2018.03.008
20. Kim M-J, Kang D-K, Kim HB. Geometric Mean Based Boosting Algorithm With Over-Sampling to Resolve Data Imbalance Problem for Bankruptcy Prediction. *Expert Syst Appl* (2015) 42(3):1074–82. doi: 10.1016/j.eswa.2014.08.025
21. Chen YZ, Tang YR, Sheng ZY, Zhang Z. Prediction of Mucin-Type O-Glycosylation Sites in Mammalian Proteins Using the Composition of K-Spaced Amino Acid Pairs. *BMC Bioinf* (2008) 9:101. doi: 10.1186/1471-2105-9-101
22. Kawashima S, Pokarowski P, Pokarowska M, Kolinski A, Katayama T, Kanehisa M. AAindex: Amino Acid Index Database, Progress Report 2008. *Nucleic Acids Res* (2008) 36(Database issue):D202–205. doi: 10.1093/nar/gkm998
23. Kawashima S, Kanehisa M. AAindex: Amino Acid Index Database. *Nucleic Acids Res* (2000) 28(1):374. doi: 10.1093/nar/28.1.374
24. Charoenkwan P, Nantasenamat C, Hasan MM, Shoombuatong W. Meta-iPVP: A Sequence-Based Meta-Predictor for Improving the Prediction of Phage Virion Proteins Using Effective Feature Representation. *J Comput Aided Mol Des* (2020) 34(10):1105–16. doi: 10.1007/s10822-020-00323-z
25. Cheng X, Xiao X, Chou KC. Ploc_Bal-Mgneg: Predict Subcellular Localization of Gram-Negative Bacterial Proteins by Quasi-Balancing Training Dataset and General PseAAC. *J Theor Biol* (2018) 458:92–102. doi: 10.1016/j.jtbi.2018.09.005
26. Chou KC. Some Remarks on Protein Attribute Prediction and Pseudo Amino Acid Composition. *J Theor Biol* (2011) 273(1):236–47. doi: 10.1016/j.jtbi.2010.12.024
27. Hasan MM, Khatun MS, Kurata H. iLBE for Computational Identification of Linear B-Cell Epitopes by Integrating Sequence and Evolutionary Features. *Genomics Proteomics Bioinf* (2020) 18(5):593–600. doi: 10.1016/j.gpb.2019.04.004
28. Khatun MS, Hasan MM, Kurata H. PreAIP: Computational Prediction of Anti-Inflammatory Peptides by Integrating Multiple Complementary Features. *Front Genet* (2019) 10:129. doi: 10.3389/fgene.2019.00129
29. Koziol JA. On Maximally Selected Chi-Square Statistics. *Biometrics* (1991) 47(4):1557–61. doi: 10.2307/2532406
30. McHugh ML. The Chi-Square Test of Independence. *Biochem Med (Zagreb)* (2013) 23(2):143–9. doi: 10.11613/bm.2013.018
31. Tung CW. PupDB: A Database of Pupylated Proteins. *BMC Bioinf* (2012) 13(1):40. doi: 10.1186/1471-2105-13-40
32. Hasan MAM, Ahmad S. Mlypsptmpred: Multiple Lysine PTM Site Prediction Using Combination of SVM With Resolving Data Imbalance Issue. *Natural Sci* (2018) 10(09):370–84. doi: 10.4236/ns.2018.109035
33. Wang P, Huang X, Qiu W, Xiao X. Identifying GPCR-Drug Interaction Based on Wordbook Learning From Sequences. *BMC Bioinf* (2020) 21(1):150. doi: 10.1186/s12859-020-3488-8
34. Qiu W, Lv Z, Hong Y, Jia J, Xiao X. BOW-GBDT: A GBDT Classifier Combining With Artificial Neural Network for Identifying GPCR-Drug Interaction Based on Wordbook Learning From Sequences. *Front Cell Dev Biol* (2020) 8:623858(1789). doi: 10.3389/fcell.2020.623858
35. Mikolov T, Sutskever I, Chen K, Corrado GS, Dean J. Distributed Representations of Words and Phrases and Their Compositionality. *Adv Neural Inf Process Syst* (2013) 3111–9. doi: 10.48550/arXiv.1301.3781
36. Bottou L. "Large-Scale Machine Learning With Stochastic Gradient Descent,". In: *Proceedings of COMPSTAT'2010*. Springer (2010). p. 177–86.
37. Rodríguez P, Bautista MA, González J, Escalera S. Beyond One-Hot Encoding: Lower Dimensional Target Embedding. *Image Vision Computing* (2018) 75:21–31. doi: 10.1016/j.imavis.2018.04.004
38. Bian H, Guo M, Wang J. Recognition of Mitochondrial Proteins in Plasmodium Based on the Tripeptide Composition. *Front Cell Dev Biol* (2020) 8:578901(875). doi: 10.3389/fcell.2020.578901
39. Chou KC. Prediction of Protein Cellular Attributes Using Pseudo-Amino Acid Composition. *Proteins: Structure Function Genet* (2001) 44(1):60–0. doi: 10.1002/prot.1072
40. Chawla NV, Bowyer KW, Hall LO, Kegelmeyer WP. SMOTE: Synthetic Minority Over-Sampling Technique. *J Artif Intell Res* (2002) 16:321–57. doi: 10.1613/jair.953
41. Pandis N. The Chi-Square Test. *Am J Orthod Dentofacial Orthop* (2016) 150(5):898–9. doi: 10.1016/j.ajodo.2016.08.009
42. Sharpe D. Chi-Square Test Is Statistically Significant: Now What? *Pract Assessment Res Eval* (2015) 20(1):8. doi: 10.7275/tbfa-x148
43. Manavalan B, Shin TH, Kim MO, Lee G. PIP-EL: A New Ensemble Learning Method for Improved Proinflammatory Peptide Predictions. *Front Immunol* (2018) 9:1783. doi: 10.3389/fimmu.2018.01783
44. Su R, Hu J, Zou Q, Manavalan B, Wei L. Empirical Comparison and Analysis of Web-Based Cell-Penetrating Peptide Prediction Tools. *Brief Bioinform* (2020) 21(2):408–20. doi: 10.1093/bib/bby124
45. Shoombuatong W, Schaduagrang N, Pratiwi R, Nantasenamat C. THPep: A Machine Learning-Based Approach for Predicting Tumor Homing Peptides. *Comput Biol Chem* (2019) 80:441–51. doi: 10.1016/j.compbiolchem.2019.05.008
46. Schaduagrang N, Nantasenamat C, Prachayasittikul V, Shoombuatong W. Meta-iAVP: A Sequence-Based Meta-Predictor for Improving the Prediction of Antiviral Peptides Using Effective Feature Representation. *Int J Mol Sci* (2019) 20(22):5743–67. doi: 10.3390/ijms20225743
47. Win TS, Malik AA, Prachayasittikul V, JE SW, Nantasenamat C, Shoombuatong W. HemoPred: A Web Server for Predicting the Hemolytic

- Activity of Peptides. *Future Med Chem* (2017) 9(3):275–91. doi: 10.4155/fmc-2016-0188
48. Centor RM. Signal Detectability: The Use of ROC Curves and Their Analyses. *Med Decis Making* (1991) 11(2):102–6. doi: 10.1177/0272989X9101100205
 49. Jiménez-Valverde A. Insights Into the Area Under the Receiver Operating Characteristic Curve (AUC) as a Discrimination Measure in Species Distribution Modelling. *Global Ecol Biogeogr* (2012) 21(4):498–507. doi: 10.1111/j.1466-8238.2011.00683.x
 50. Cui D, Curry D. Prediction in Marketing Using the Support Vector Machine. *Marketing Sci* (2005) 24(4):595–615. doi: 10.1287/mksc.1050.0123
 51. Cai CZ, Han LY, Ji ZL, Chen X, Chen YZ. SVM-Prot: Web-Based Support Vector Machine Software for Functional Classification of a Protein From Its Primary Sequence. *Nucleic Acids Res* (2003) 31(13):3692–7. doi: 10.1093/nar/gkg600
 52. Tong S, Chang E. Support Vector Machine Active Learning for Image Retrieval. *Proc Ninth ACM Int Conf Multimed* (2001) 107–18. doi: 10.1145/500141.500159
 53. Zavaljevski N, Stevens FJ, Reifman J. Support Vector Machines With Selective Kernel Scaling for Protein Classification and Identification of Key Amino Acid Positions. *Bioinformatics* (2002) 18(5):689–96. doi: 10.1093/bioinformatics/18.5.689
 54. Gordon AD, Breiman L, Friedman JH, Olshen RA, Stone CJ. Classification and Regression Trees. *Biometrics* (1984) 40(3):358. doi: 10.2307/2530946
 55. Noble WS. What Is a Support Vector Machine? *Nat Biotechnol* (2006) 24(12):1565–7. doi: 10.1038/nbt1206-1565
 56. Gao J, Thelen JJ, Dunker AK, Xu D. Musite, a Tool for Global Prediction of General and Kinase-Specific Phosphorylation Sites. *Mol Cell Proteomics* (2010) 9(12):2586–600. doi: 10.1074/mcp.M110.001388
 57. Kowalski BR, Bender CF. K-Nearest Neighbor Classification Rule (Pattern Recognition) Applied to Nuclear Magnetic Resonance Spectral Interpretation. *Analytical Chem* (2002) 44(8):1405–11. doi: 10.1021/ac60316a008
 58. Chen T, He T, Benesty M, Khotilovich V, Tang Y, Cho H. Xgboost: Extreme Gradient Boosting. *R Package version 0.4-2* (2015) 1(4):1–4. doi: 10.1145/2939672.2939785
 59. Friedman JH. Greedy Function Approximation: A Gradient Boosting Machine. *Ann Stat* (2001) 29(5):1189–232. doi: 10.2307/2699986
 60. Simopoulos CMA, Weretilnyk EA, Golding GB. Prediction of Plant lncRNA by Ensemble Machine Learning Classifiers. *BMC Genomics* (2018) 19(1):316. doi: 10.1186/s12864-018-4665-2
 61. Galar M, Fernandez A, Barrenechea E, Bustince H, Herrera F. A Review on Ensembles for the Class Imbalance Problem: Bagging-, Boosting-, and Hybrid-Based Approaches. *IEEE Trans Syst Man Cybernetics Part C (Applications Reviews)* (2012) 42(4):463–84. doi: 10.1109/tsmcc.2011.2161285
 62. Svetnik V, Wang T, Tong C, Liaw A, Sheridan RP, Song Q. Boosting: An Ensemble Learning Tool for Compound Classification and QSAR Modeling. *J Chem Inf Model* (2005) 45(3):786–99. doi: 10.1021/ci0500379
 63. Agarwal S, Chowdary CR. A-Stacking and A-Bagging: Adaptive Versions of Ensemble Learning Algorithms for Spoof Fingerprint Detection. *Expert Syst Appl* (2020) 146:113160. doi: 10.1016/j.eswa.2019.113160

Conflict of Interest: The authors declare that the research was conducted in the absence of any commercial or financial relationships that could be construed as a potential conflict of interest.

Publisher's Note: All claims expressed in this article are solely those of the authors and do not necessarily represent those of their affiliated organizations, or those of the publisher, the editors and the reviewers. Any product that may be evaluated in this article, or claim that may be made by its manufacturer, is not guaranteed or endorsed by the publisher.

Copyright © 2022 Qiu, Guan, Wang, Lou and Xiao. This is an open-access article distributed under the terms of the Creative Commons Attribution License (CC BY). The use, distribution or reproduction in other forums is permitted, provided the original author(s) and the copyright owner(s) are credited and that the original publication in this journal is cited, in accordance with accepted academic practice. No use, distribution or reproduction is permitted which does not comply with these terms.



The Emerging Roles and Therapeutic Implications of Epigenetic Modifications in Ovarian Cancer

Yu Wang^{1†}, Zhao Huang^{1†}, Bowen Li¹, Lin Liu^{2*} and Canhua Huang^{1*}

¹ State Key Laboratory of Biotherapy and Cancer Center, West China Hospital, and West China School of Basic Medical Sciences & Forensic Medicine, Sichuan University, and Collaborative Innovation Center for Biotherapy, Chengdu, China,

² Department of Anesthesiology, The Affiliated Hospital of Medical School, Ningbo University, Ningbo, China

OPEN ACCESS

Edited by:

Xianquan Zhan,
Shandong First Medical University,
China

Reviewed by:

Na Li,
Shandong Cancer Hospital, China
Jianling Bi,
The University of Iowa, United States

*Correspondence:

Lin Liu
104797809@qq.com
Canhua Huang
hcanhua@scu.edu.cn

[†]These authors have contributed
equally to this work

Specialty section:

This article was submitted to
Cancer Endocrinology,
a section of the journal
Frontiers in Endocrinology

Received: 06 February 2022

Accepted: 30 March 2022

Published: 10 May 2022

Citation:

Wang Y, Huang Z, Li B, Liu L and
Huang C (2022) The Emerging Roles and
Therapeutic Implications of Epigenetic
Modifications in Ovarian Cancer.
Front. Endocrinol. 13:863541.
doi: 10.3389/fendo.2022.863541

Ovarian cancer (OC) is one of the most lethal gynecologic malignancies globally. In spite of positive responses to initial therapy, the overall survival rates of OC patients remain poor due to the development of drug resistance and consequent cancer recurrence. Indeed, intensive studies have been conducted to unravel the molecular mechanisms underlying OC therapeutic resistance. Besides, emerging evidence suggests a crucial role for epigenetic modifications, namely, DNA methylation, histone modifications, and non-coding RNA regulation, in the drug resistance of OC. These epigenetic modifications contribute to chemoresistance through various mechanisms, namely, upregulating the expression of multidrug resistance proteins (MRPs), remodeling of the tumor microenvironment, and deregulated immune response. Therefore, an in-depth understanding of the role of epigenetic mechanisms in clinical therapeutic resistance may improve the outcome of OC patients. In this review, we will discuss the epigenetic regulation of OC drug resistance and propose the potential clinical implications of epigenetic therapies to prevent or reverse OC drug resistance, which may inspire novel treatment options by targeting resistance mechanisms for drug-resistant OC patients.

Keywords: ovarian cancer, drug resistance, cancer epigenetics, DNA methylation, histone modifications, non-coding RNA, epigenetic therapy

1 INTRODUCTION

With around 239,000 new cases and 152,000 deaths each year, ovarian cancer (OC) is the seventh most prevalent cancer and the second leading cause of death from gynecologic cancer (1). Despite advances in surgical procedures, platinum-based chemotherapy, targeted medicines, and immunotherapy in recent decades, patients with OC still have a poor prognosis due to advanced and extensive disseminated tumors (2–4). The high death rate of OC is partly attributable to its extremely invasive growth pattern, which is hard to detect in early stages and frequently resistant to drugs (5, 6).

Drug resistance is a significant barrier to treating OC and leads to a poor prognosis. While 80% of individuals initially diagnosed with OC respond to conventional first-line therapy, such as platinum-based chemotherapy and surgical cytoreduction, roughly 75% of patients with advanced OC relapse within three years, which is usually fatal (2, 5). With notable therapeutic advantages, poly (ADP-ribose) polymerase (PARP) inhibitors have emerged as the first targeted medicines for patients with platinum-sensitive recurrent OC (7, 8). However, the effectiveness of PARP inhibitors is severely limited in OC due to the narrow spectrum of administration and various resistance mechanisms (9, 10). To improve the prognosis of patients with OC, it is vital to understand the underlying mechanisms of treatment resistance in OC and develop techniques to postpone or overcome drug resistance (**Figure 1**).

It is now generally accepted that drug resistance may arise from the diminished intracellular accumulation of drugs, alterations of drug targets, deregulation of immune response, and issues with the cell death executioner machinery, as well as the generation and maintenance of drug-resistant cells (11–15). Furthermore, a recent study suggested that epigenetic regulation (namely, DNA methylation, histone modifications, and non-coding RNA regulation) is one of the key mechanisms in OC that drives both intrinsic and acquired treatment resistance (16–19) (**Figure 2**). For instance, as one of the most effective

broad-spectrum anti-cancer drugs, cisplatin kills tumor cells *via* DNA damage. However, epigenetic alterations are frequently observed in this process and are associated with cisplatin resistance (20, 21). For example, DNA methylation plays an indispensable role in OC drug resistance. Early studies suggested that hypermethylation of the BRCA1 gene in OC cells confers susceptibility to platinum-based chemotherapy (22, 23). At least 20 post-translational modifications occur in histone to govern the structures and activities of DNA. Accumulating evidence demonstrates that histone modifications, namely, acetylation, methylation, and phosphorylation, are linked to OC development and treatment resistance (24–26). Moreover, non-coding RNAs (ncRNAs), such as long non-coding RNAs (lncRNAs) and microRNAs (miRNAs), are currently recognized to be involved in various biological processes, including drug resistance (27, 28). As discussed above, we have summarized the epigenetic regulation in OC drug resistance (**Table 1**). Importantly, epigenetic alterations are reversible, and emerging epigenome-targeted therapy strategies can overcome OC drug resistance by reversing histone modifications and DNA methylation or by targeting ncRNAs. In this review, we will discuss the detailed mechanisms of epigenetic regulation that contribute to drug resistance in OC and highlight the advantages and challenges of epigenome-targeted therapy strategies for treating OC.

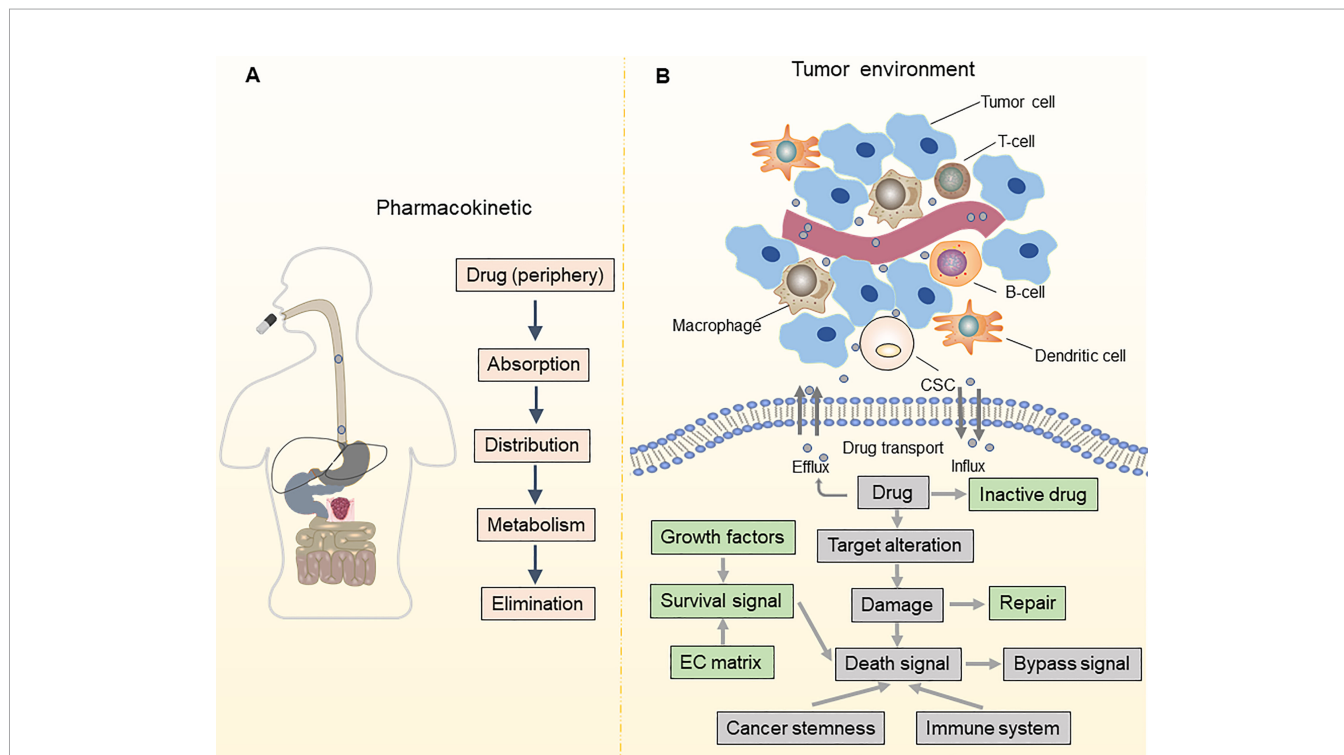


FIGURE 1 | Pharmacokinetic and TME-associated factors contribute to drug resistance. **(A)** Mechanisms of drug resistance can be due to pharmacokinetics, including drug absorption, distribution, metabolism, and elimination; **(B)** Alterations in drug influx and efflux system impact the intracellular accumulation of anti-cancer drugs in tumor cells. The leading determinants of drug resistance are altered in drug targets, bypass signaling pathways, DNA damage and repair, and cell death signaling. Besides, maintenance of cancer stemness and a tumor-promoting immune microenvironment also contribute to drug resistance.

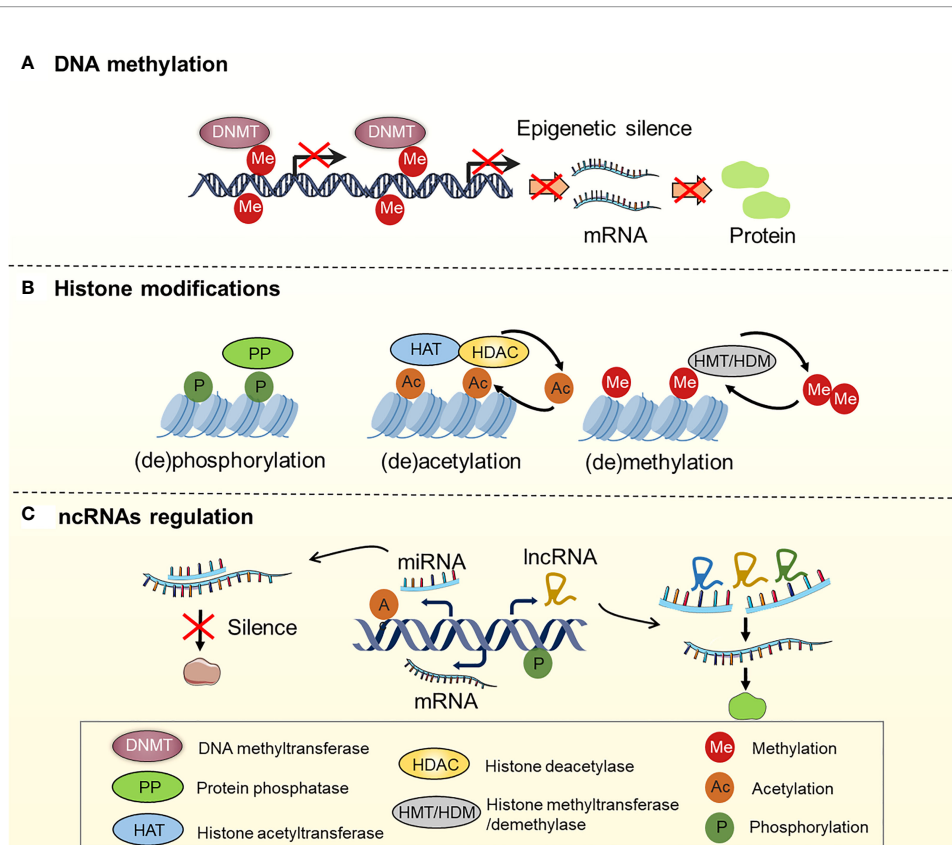


FIGURE 2 | Regulation of DNA methylation, histone modifications and ncRNAs in OC. **(A)** Genes are silenced by hypermethylation, which is catalyzed by DNA methyltransferases (DNMTs); **(B)** Histone modifications, including histone (de)phosphorylation, (de)acetylation, (de)methylation, etc. Histone (de)phosphorylation is catalyzed by protein phosphatase (PP). Histone (de)acetylation is catalyzed by histone acetyltransferase (HAT) and histone deacetylase (HDAC). Histone (de)methylation is catalyzed by histone methyltransferase (HMT) and histone demethylase (HDM); **(C)** ncRNAs regulation: miRNAs and lncRNAs regulate gene expression by interacting with mRNA.

TABLE 1 | Summary of epigenetic regulation in OC drug resistance.

Epigenetic regulation	Resistance against	Function	Target/pathway	References
MGMT	Paclitaxel Cisplatin	Chemoresistance	MGMT, DUB3, MCL1	(29)
DNMT1	Paclitaxel	Reverse paclitaxel resistance	DNMT1/CHFR/ Aurora A	(30)
DNMT3A	Cisplatin	Cisplatin resistance	miR-143	(31)
DNMT3B	Cisplatin	Autophagy, cisplatin resistance	RBP1	(32)
H3K14ac	Paclitaxel Cisplatin	Chemoresistance	RBP2/KDM5A/ Jarid1A	(33)
H3K27ac	Platinum	Platinum resistance	IL2/STAT5, TGF- β	(34)
miR-136	Paclitaxel	Inhibition of proliferation	Notch3	(35)
miR-98-5p	Cisplatin	Promotion of drug resistance	miR-98-5p/ Dicer1/miR-152	(36)
miR-142-5p	Cisplatin	Inhibition of drug resistance	XIAP, BIRC3, BCL2	(37)
miR-509-3p	Platinum	Enhance drug sensitivity	GOLPH3, WLS	(38)
miR-34a-5p	Cisplatin	Inhibition of proliferation	PD-L1	(39)
HOTAIR	Cisplatin	DNA damage response	NF- κ B, miR-200c	(40, 41)
UCA1	Paclitaxel Cisplatin	Drug effluent system	miR-143/FOSL2	(42)
BC200	Carboplatin	Tumor suppressor	Proliferation	(43)
GAS5	Platinum	Induction of apoptosis	Cyclin D1, p21, APAF1	(44)
LSINCT5	Paclitaxel	Promotion of proliferation, migration, invasion	CXCL12/CXCR4	(45)

2 EPIGENETIC MODIFICATIONS IN OC DRUG RESISTANCE

Since the discovery of methylation of DNA repair genes by O⁶-methylguanine-DNA methyltransferase (MGMT), the role of epigenetic modifications in the context of inherent or acquired drug resistance has been extensively explored (46). Multiple mechanisms, namely, altered drug targets and bypass signaling pathways, enhanced drug efflux and metabolism, downstream adaptive responses, and maintenance of cancer stemness, are the primary causes of decreased anti-cancer drug effectiveness (47–50). Furthermore, emerging evidence suggests that the tumor microenvironment (TME) is crucial to multidrug resistance (MDR) in cancer cells (51–53). The molecular mechanisms of epigenetic regulation-mediated OC drug resistance, namely, enhanced drug efflux and metabolism, alteration of drug targets and bypass signaling pathways, downstream adaptive responses, maintenance of cancer stemness, and TME, are discussed here.

2.1 Epigenetic Modifications Involved in Drug Transport and Metabolism

Effective cytotoxic drug treatment requires a sufficient intracellular drug concentration in tumor cells. Drug concentration is coordinated by transporters mediating the influx and efflux of drugs and enzymes mediating drug metabolism. The effectiveness of chemotherapeutic and targeted drug delivery into cancer cells is determined by drug inflow and efflux transporters. The most known such transporters are the ATP-binding cassette (ABC) transporter family members, namely, ABCB1 (MDR1), ABCC2 (MRP-2), and ABCG2 (BCRP/MXR1), which have been widely shown to be

associated with drug resistance (54, 55). The epigenetic control of ABC transporter-induced OC resistance has recently progressed significantly (**Figure 3**). ABCB1 is the first ABC transporter identified and plays a crucial role in determining drug sensitivity. The epigenetic regulation of ABCB1 is related to drug transportation in OC cells. For instance, paclitaxel therapy increased histone H3 acetylation and targeted the ABCB1 promoter in conjunction with the androgen receptor (AR), resulting in ABCB1 gene expression and the establishment of the paclitaxel resistance phenotype (56). Wu et al. found that overexpression of miR-873 improved the susceptibility of OC cells to paclitaxel and cisplatin by targeting ABCB1 (57). Besides, Tian et al. demonstrated that miR-490-3p enhances the sensitivity of OC cells to cisplatin by downregulating ABCC2 expression (58). Nevertheless, hnRNPA2B1 was shown to bind to the 5'UTR of ABCC2 mRNA and promote its translation, leading to cisplatin resistance in OC (59). Furthermore, ABCG2 is strongly expressed in cisplatin- or paclitaxel-resistant OC and OC stem cells, indicating the key role of ABCG2 in drug resistance and stemness acquisition in OC (60). Calcagno and colleagues discovered that elevated acetylation of histone H3 in the ABCG2 promoter is a cellular response to the treatment of doxorubicin, which underlies its doxorubicin resistance (61). Some lncRNAs and miRNAs found in extracellular vesicles (EVs) generated by drug-resistant cells control the expression of ABCG2, hence impacting tumor drug resistance (62–65). These investigations indicate that epigenetic regulation plays an essential role in OC drug resistance by modulating the ABC transporter family.

Drug metabolism regulates bioactivation, catabolism, conjugation, and excretion, determining drug clinical efficacy and toxicity (66). Drug metabolism enzymes can be affected by

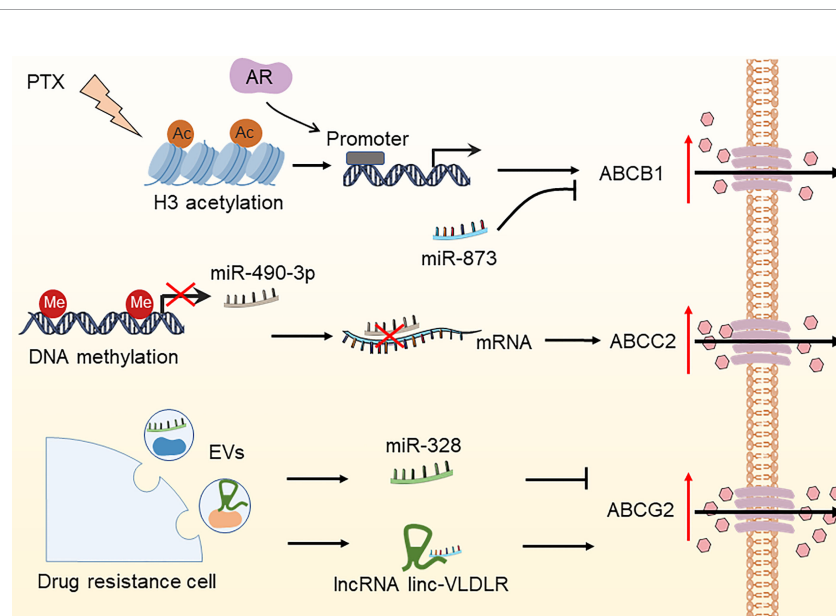


FIGURE 3 | Epigenetic modifications regulate the expression of ABC transporters in OC. The DNA methylation of miR-490-3p, increased histone H3 acetylation due to paclitaxel treatment, miR-328, and lncRNA linc-VLDLR in EVs have been reported to increase drug efflux by regulating the expression of ABCC2, ABCB1, and ABCG2, thereby leading to OC drug resistance. PTX, paclitaxel; AR, androgen receptor; EVs, extracellular vesicles.

alterations in the expression level of affect drug metabolism. For instance, epigenetic alterations regulate the expression of the cytochrome P450 (CYP) enzyme family, which is the most well-known drug-metabolizing enzyme, thus affecting the metabolism of several anti-cancer medications. A recent study showed that histone modification enzyme G9a regulates the expression of CYP450 by affecting histone 3 lysine 4 and histone 3 lysine 27 methylation, suggesting G9a alters drug sensitivity (67). Luo and colleagues emphasized an unconventional epigenetic regulation mechanism of CYP gene expression; that is, miR-148a stimulates CYP2B6 expression by binding to the 3'UTR region to improve mRNA stability (68). Furthermore, miR-543 overexpression increases the production of CYP3A4, which is involved in the metabolism of ruxolitinib (69). Other drug-metabolizing enzymes are controlled by epigenetic alterations, which must be investigated further.

2.2 Epigenetic Modifications Regulate Drug Targets and Bypass Signaling Pathways

Over the past decade, targeted agents have been steadily introduced into clinical trials for treating recurrent OC, namely, the anti-VEGFR agent bevacizumab, PARP inhibitors (olaparib, niraparib, and rucaparib), the anti-MEK inhibitor trametinib, and anti-HER2 pertuzumab. However, chemotherapy resistance resulting from epigenetic alterations limits the effectiveness of these targeted treatments. Resistance to targeted therapy arises primarily through reduced expression of drug targets and activated bypass signaling pathways during treatment with targeted drugs (70–72). Here, we summarize the epigenetic modification-mediated drug resistance in OC, caused by the deregulated expression of drug targets, mutation of drug targets, and the persistent activation of bypass signaling pathways.

Angiogenesis is critical in the etiology of OC, which is associated with the generation of vascular endothelial growth factor (VEGF), linked to the progression of malignant ascites and OC (73, 74). In clinical trials, bevacizumab, an anti-VEGF monoclonal antibody, has been proven to improve outcomes in OC patients in clinical trials (75, 76). However, epigenetic modifications may diminish VEGF expression. Vesna and colleagues found twenty significant CpG sites in promoter regions, suggesting that the concentration of VEGF-A can be regulated by DNA methylation (77). Based on The Cancer Genome Atlas (TCGA) databases, Zhou and colleagues discovered that overexpression of insulin-like growth factor 2 mRNA-binding protein 3 (IGF2BP3) was related to cancer progression and poor survival of patients. Mechanistically, IGF2BP3 can bind with the mRNA of VEGF, where IGF2BP3 serves as a reader to recognize the m6A modification on VEGF mRNA. This effect controls both the production and stability of VEGF mRNA, which may affect drug sensitivity (78). Besides, VEGFA is the direct target of miR-652-5p, and miR-652-5p is down-regulated by hypermethylation at the upstream CpG site. Increasing VEGF synthesis is linked to tumor progression and metastasis (79). Moreover, it has been shown that cells with methylated BRCA1 have defective homologous recombination

(HR) activity, thus being highly responsive to PARP inhibitors (olaparib, niraparib, and rucaparib), implying that BRCA1 inactivated by epigenetic mechanisms contributes to drug sensitivity (80–82).

In addition to alterations in drug targets, epigenetic modifications are implicated in the activation of bypass signaling pathways to regulate OC drug resistance. Although the Notch pathway is closely related to the growth of OC tumors, its clinical significance and molecular mechanisms remain unclear. Hu et al. found that alterations in the Notch pathway are prevalent and closely related to poor clinical outcomes in patients with OC (83, 84). For instance, epigenetic regulation of multiple Notch target genes (such as PPARG, CCND1, and RUNX1) can regulate the activation of the Notch pathway, which is associated with the prognosis of OC patients (85). Liu and colleagues found that Fas deficiency inhibits the release of miR-29b, thereby increasing intracellular miR-29b levels and subsequently downregulating DNA methyltransferase 1 (DNMT1) expression, which results in hypomethylation of the Notch1 promoter region and activation of Notch signaling (86). Hirsch et al. discovered that inhibition of histone deacetylase might alleviate abnormalities in the Notch and Eph axis in prion protein PrP deficient and prion-infected cells (87). Besides, studies have demonstrated that lncRNA HOTAIR induces OC drug resistance to cisplatin through activating the Wnt/ β -catenin pathway (88). Further studies of epigenetic modifications that regulate drug targets and bypass signaling pathways may increase our understanding of the development of potential strategies to reverse drug resistance.

2.3 Epigenetic Modifications Modulate DNA Damage and Repair

Most chemotherapeutic drugs induce cell death through apoptosis due to DNA damage (89, 90). After treatment with cytotoxic agents, eukaryotic cells usually undergo damage repair to avoid apoptosis, leading to drug resistance (91). Therefore, components of the DNA repair system, such as O6-methylguanine-DNA methyltransferase (MGMT), can promote chemotherapeutic resistance. MGMT mediates the direct removal of O6-methylguanine (O6-MEG), a mark of DNA damage induced by temozolomide (TMZ), thereby facilitating DNA repair in melanoma cells. Other TMZ-induced lesions are mostly repaired by base excision repair (BER) or direct removal mechanisms catalyzed by DNA demethylase ALKBH2/3 (91, 92). Poly-ADP-ribose polymerase inhibitors (PARPis) are the most effective therapies approved for treating OC, and poly-ADP-ribose polymerase (PAPR) inhibitors (olaparib, niraparib, and rucaparib) are already being investigated in OC clinical trials. Indeed, all PARPis exhibit radio- or chemo-potential effects *in vitro* and *in vivo*, which is consistent with their ability to inhibit DNA damage repair (93, 94). According to a recent study by Nephew and colleagues, platinum-induced DNA damage contributes to the activation of the NF- κ B pathway by the lncRNA HOTAIR and cellular senescence. Furthermore, DNA damage response activated NF- κ B, which in turn triggered HOTAIR and created a positive-feedback loop, resulting in

sustained NF- κ B activation and persistent DNA damage signaling (40). Mutations in p53 are observed in 42% of human tumors (95). The regulation of RNA m6A on TP53 has been proven to overcome drug resistance by controlling downstream pathways and DNA damage repair, suggesting that it is a viable therapeutic approach (96). Meng et al. discovered that AZD1775, not only carboplatin, can increase sensitivity to gemcitabine and olaparib in TP53-mutated gynecologic cancer cells (97). WEE1 is a tyrosine kinase that blocks the CDK1/cyclin B complex by inducing CDK1 phosphorylation at tyrosine 15 (Y15), inducing cell cycle arrest and allowing DNA repair (98, 99). AZD1775 is a first-in-class, powerful, and selective WEE1 inhibitor that has shown a considerable anti-tumor effect in OC patients with TP53 mutations when combined with carboplatin (100). In conclusion, uncovering the mechanisms that influence epigenetic modification function in DNA damage repair may develop new strategies for the sensitization of OC cells to DNA damage inducers.

2.4 Epigenetic Modifications Activate Downstream Adaptive Responses

The interaction of anti-cancer drugs with corresponding cellular targets can induce cell death. However, a variety of adaptive cellular responses governed by epigenetic modifications are engaged to support the survival of tumor cells, which is the major target of cancer therapy. These include inhibition of apoptosis, initiation of autophagy, ferroptosis, and activation of pro-survival signals (101–103).

2.4.1 Apoptosis

After medication therapy, cancer cells with enhanced DNA repair capacities can survive drug-induced DNA damage. The anti-apoptotic proteins (Bcl-2), inhibitor of apoptosis proteins (IAPs), and FLICE inhibitor proteins (FLIP) are upregulated in tumor cells, which contributes to their medication resistance (90). As an anti-apoptotic member of the Bcl-2 family, MCL1 plays an important role in the advanced chemotherapy resistance of OC. Wu et al. found that the deubiquitinating enzyme 3 (DUB3) in the cytoplasm of OC cells interacts with and deubiquitinates MCL1, thereby protecting MCL1 from degradation. Furthermore, they discovered that histone deacetylase inhibitors (HDACis) could increase the expression level of MGMT/DUB3, and HDACis combined with PaTrin-2 treatment has a significant effect on OC (29). Zhu et al. found that ALKBH5 is a potential target for OC therapy, which activates the EGFR-PIK3CA-AKT-mTOR signaling pathway, enhancing the stability of BCL-2 mRNA and promoting the interaction between Bcl-2 and Beclin1 (104). Abedini et al. discovered that p53 could promote the ubiquitination and subsequent proteasomal degradation of FLIP in response to cisplatin treatment, leading to the apoptosis of OC cells, potentially improving the therapeutic effects of cisplatin on OC.

2.4.2 Autophagy

Autophagy partly enables tumor cells to cope with external stress, leading to the survival of cancer cells treated with anti-

cancer drugs (105–107). Bi et al. have demonstrated that blocking autophagy can overcome resistance to HDAC inhibitors in gynecologic cancers (108). Autophagy can be activated by the upregulation of autophagy-related gene 14 (ATG14), and the abnormal expression of autophagy-related proteins contributes to drug resistance in OC. MiR-29c-3p inhibits autophagy and cisplatin resistance in part by downregulating the FOXP1/ATG14 pathway, suggesting that miR-29c-3p is a novel target for overcoming cisplatin resistance in OC (109). Bi et al. found that inhibition of methyltransferase-like 3 (METTL3) inhibits miR-126-5p's upregulation of PTEN by regulating m6A modification, thereby preventing the activation of the PI3K/Akt/mTOR pathway and inhibiting the occurrence of OC. This finding highlights the role of m6A modification as a potential target for future OC treatment (110). O-GlcNacylation is a post-translational modification in which the O-GlcNAc transferase (OGT) transfers glucosamine (GlcNAc) to serine or threonine residues. Zhou et al. found that the levels of O-GlcNAc and OGT in OC chemically sensitive tissues were significantly higher than those in chemoresistant OC tissues, which reduced apoptotic cell death, resulting in increased resistance of OC cells to cisplatin (107). Together, the epigenetic modifications play an orchestrated role in regulating autophagy, and the effects of the epigenetic modifications on autophagy are cancer context-dependent. Additional studies are needed to elucidate other determinants of autophagy regulation related to epigenetic modifications.

2.4.3 Ferroptosis

Using anti-cancer drugs to trigger apoptotic cell death is one of the principal ways to kill cancer cells. However, due to the acquired or intrinsic resistance of cancer cells to apoptosis, the effect of apoptosis inducers is limited (111, 112). Recently, a growing number of compounds and anti-cancer drugs kill tumor cells by ferroptosis (113–116). For instance, PARP inhibitors like olaparib kill BRCA mutant OC cells through ferroptosis (117). Ferroptosis is a newly discovered form of oxidative cell death caused by iron-dependent peroxidation of lipids. Thus, the redox balance controlled by various redox-active enzymes, which detoxify free radicals and lipid oxidation products, is critical for cells to avoid ferroptosis (118). Several regulatory molecules, such as GPX4, Nrf2, and members of the solute carrier (SLC) family of molecules, play essential roles in the aberrant iron metabolism and maladjustment of the antioxidant system. Studies have shown that epigenetic modification of these potent genes allows cancer cells to escape drug-induced ferroptosis, leading to drug resistance. Among them, ROS scavenger GPX4 is a key regulatory molecule of ferroptosis, which can convert lipid hydrogen peroxide into non-toxic lipid alcohols (119, 120). Due to upstream DNA hypomethylation and high levels of H3K27ac and H3K4me3, the expression level of GPX4 in OC tissues is higher than that in normal tissues, and it is negatively correlated with the prognosis of patients, indicating that aberrant GPX4 expression in cancer may result from epigenetic regulation (121). Additionally, they found that the GPX4 inhibitor RSL3 improves the anti-cancer effects of cisplatin by enhancing ferroptosis *in vitro* and *in vivo* (121, 122). Studies

have shown that the activity of GPX4 depends on glutathione produced by system Xc (also known as SLC7A11 or xCT) (123). Indeed, p53 or the histone deubiquitinating enzyme BAP1 inhibiting SLC7A11 expression promotes ferroptosis (124, 125).

In addition to the above, the epigenetic alterations of transcription factor nuclear factor erythroid 2-related factor 2 (NRF2), a vital regulator of cellular antioxidant response and ferroptosis by upregulating SLC7A11, can affect the treatment resistance of OC (126, 127). For instance, hypermethylation of the gene promoter in the KEAP1/NRF2 axis has been described in various tumor tissues and is closely related to tumor recurrence and drug resistance (128–130). Van Jaarsveld et al. demonstrated that miR-141-mediated regulation of the KEAP1/NRF2 axis plays a crucial role in the OC response to cisplatin (131). Taken together, these findings provide evidence that epigenetic modifications play a significant role in ferroptosis and drug resistance of OC cells.

2.4.4 Pro-Survival Signaling

Cell survival and death are determined by the epidermal growth factor receptor (EGFR) and AKT (protein kinase B) signaling pathways. Cell survival and death (132, 133) are regulated by HR and non-homologous terminal junctions (NHEJ). The activation of EGFR and AKT can be induced by epigenetic alterations, which may lead to chemotherapy resistance in OC treatment. Overexpression or gene amplification of EGFR and HER2 is frequent in multiple cancers, including OC (134). Cao et al. found that EGFR, phosphorylated EGFR (P-EGFR), and phosphorylated AKT (P-Akt) were up-regulated in miR-125A-5p- and TAZ-transfected OC cells through m(6)A modification (135). Lin et al. discovered that the RNA methyltransferase METTL3, which is involved in mRNA biosynthesis, degradation, and translation regulation, enhances the translation of EGFR and the TAZ in human cancer cells (136). Furthermore, Luo et al. have identified that the RNA polymerase II transcriptional mediator subunit 12 (MED12) down-regulates EGFR expression by binding to the EGFR promoter and mediates chemotherapy resistance in OC (137). Therefore, targeting epigenetic modifications might be an effective strategy to sensitize tumor cells to DNA-damaging agents.

2.5 Epigenetic Modifications Involved in the Maintenance of Cancer Stem Cells

Cancer stem cells (CSCs) are a sub-population of tumor cells that are responsible for driving tumor growth, metastasis, and therapy resistance (52, 138, 139). Emerging results indicate that CSCs contribute to chemoresistance and poor clinical outcomes in various malignancies, including OC (140). Accumulating evidence has shown that CSCs display an innate predisposition to be chemotherapy-resistant and result in tumor relapse (141–143). Furthermore, ovarian cancer stem cells (OCSCs) contribute to resistance to chemotherapy (144). Therefore, solving this thorny problem might lead to the development of new strategies to tackle drug-resistant OC. Because epigenetic regulation plays an integral role in the control of normal stem cell differentiation, strategies to target

cancer stem cells can be developed through epigenetics. Epigenetic modifications enable cancer cells to self-renew and generate CSCs, leading to drug resistance (140).

Wang and colleagues hypothesized that hypomethylation drugs might target resistant OCSCs to cure tumors along with chemotherapy drugs. In an orthotopic mouse model, they identified and analyzed ALDH (+) OCSC from OC cell lines and clinical samples, finding that ALDH (+) cells were more chemoresistant than ALDH (–) cells. Treatment with SGI-110, a second-generation DNA methyltransferase inhibitor (DNMTi), re-sensitizes OCSCs to platinum (140). Xu et al. demonstrated that STON2 could negatively regulate the stemness in OC cells by DNMT1-MUC1. STON2 plays a role in OCSC biology and could be used as a therapeutic target for OC treatment (145). Studies have shown that MYPT1 encoding myosin phosphatase target subunit 1 is down-regulated in OC, leading to resistance to platinum-based therapy (146). Similarly, miR-30b could target MYPT1 to lead to enhanced CSC-like properties in OC cells and activate the Hippo pathway. Moreover, inhibition of YAP sensitizes cells to platinum-based therapy (50). Taken together, these studies suggest that epigenetic modifications of these signaling pathways play an essential role in the development of drug resistance in OC.

2.6 Epigenetic Modifications and the Tumor Microenvironment

A tumor microenvironment (TME) refers to the ecological niche in which tumor cells interact with the host stroma, including various immune cells, endothelial cells, fibroblasts, tumor cells, and metabolites. It is now generally accepted that TME significantly influences the efficacy of anti-cancer drugs (51). TME reprogramming caused by epigenetic dysregulations has recently been recognized as an important factor in the progression and drug resistance of OC (2, 147). Here, we systematically generalize the epigenetic modifications of non-malignant OC-related microenvironment cells (namely, cancer-associated fibroblasts, mesenchymal stem cells, and tumor-associated macrophages), which is conducive to evaluating the therapeutic potential of epigenetic regulation of TME-associated cells (Figure 4).

2.6.1 Cancer-Associated Fibroblasts (CAFs)

Fibroblasts located in the TME, also termed CAFs, are the main components of host stromal cells and the main source of collagenous cells in solid tumors (148). They play an essential role in supporting tumors by reconstructing the extracellular matrix. Multiple studies have identified the important role of CAFs in tumor-stroma communication through the excretion of various growth factors and chemokines, contributing to tumor growth, immunosuppression, angiogenesis, cell stemness, and drug resistance (149, 150). Therefore, epigenetic modifications associated with CAFs may affect the resistance of OC.

Studies have reported that the DNA methylation state of genes in mesenchymal fibroblasts from various cancer tissues conforms to the methylation features identified in nearby malignant cells (151, 152). Furthermore, the expression of

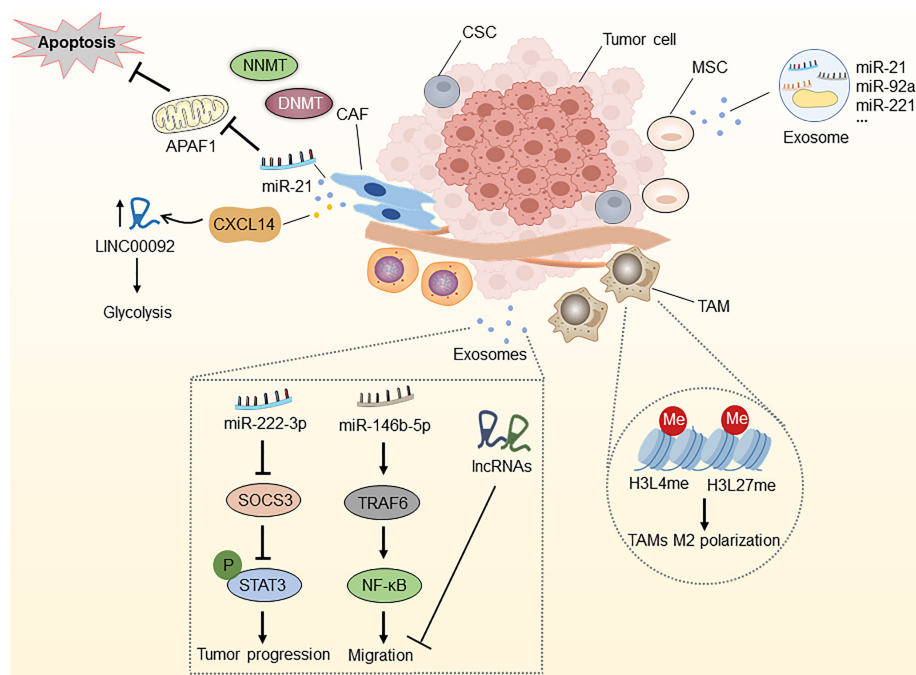


FIGURE 4 | Epigenetic modifications in the tumor microenvironment. NNMT can diminish histone methylation in CAFs, and CAFs secrete miR-21 and CXCL14, which enhance OC development, metastasis, and therapy resistance. MiR-21, miR-92a, and miR-221, which are abundant in MSC-derived exosomes, are associated with OC development. Epigenetic alterations in histone H3 lysine4 and histone H3 lysine27 methylation in TAMs can induce macrophage M2 polarization. Epithelial ovarian cancer (EOC)-released exosomal miRNAs and lncRNAs via the SOCS3/STAT3 pathway and miR-146b-5p/TRAF6/NF- κ B/MMP2 pathway regulate the progression, migration and drug resistance of OC. CAF, cancer-associated fibroblast; MSC, mesenchymal stem cell; TAM, tumor-associated macrophage; CSC, cancer stem cell; NNMT, nicotinamide N-methyltransferase; DNMT, DNA methyltransferase; APAF1, apoptosis protease activator-1; APAF6, TNF receptor associated factor 6.

stromal nicotinamide N-methyltransferase (NNMT) is essential for the functional aspects of the CAF phenotype and supports the growth and metastasis of OC. Stromal NNMT expression in CAFs depletes S-adenosyl methionine and histone methylation, which is related to the global alternations of gene expression in the tumor stroma (153). Additionally, CAFs secrete miR-21, which targets apoptosis protease activator-1 (APAF1), leading to paclitaxel resistance in metastatic or recurrent OC (154). New evidence suggests that OC cells reprogram fibroblasts into CAFs through the action of miRNAs in the TME, including miR-31, miR-214, and miR-155. Targeting these miRNAs in stromal cells might be of therapeutic value, suggesting these miRNAs as novel therapeutic targets for halting OC progression (155). Curtis and colleagues discovered that CAF-secreted CXCL14 promoted OC development and invasion by interacting with the major restriction enzyme, 6-Phosphofructo-2-Kinase/Fructo-2,6-Biphosphatase 2 (PFKFB2) and boosting LINC0009, a long non-coding RNA, to accelerate glycolysis (156, 157). These observations suggest that molecular insights into the abnormally expressed lncRNAs in CAFs are essential for the further diagnostic and therapeutic strategies of OC.

2.6.2 Mesenchymal Stem Cells (MSCs)

MSCs contain various pluripotent cell subpopulations, and MSCs have been reported in most organs and tissues, including the

ovaries (158). Because of their potential to develop into other active cancer-promoting stromal components (such as CAFs and cancer-associated adipocytes) and sustain cancer stem cell (CSC) populations, MSCs are strongly linked to cancer progression. In particular, OC-associated MSCs exhibit pluripotency and promote stem cell growth, increase resistance to platinum-based chemotherapy, and provide tumor matrix support and neovascularization (159–161). Although the great bulk of research has concentrated on understanding the impact of cellular signaling pathways, the epigenetic interactions between MSCs and OC remain largely unexplored.

Considering the function of epigenetic modifications in CSC reprogramming, MSCs can be efficiently transformed into CSCs by custom chromatin remodeling. Besides, MSCs can also differentiate into distinct stromal cells by epigenetic regulation (162–164). Through exosomal RNA sequencing, Reza et al. demonstrated numerous miRNAs that exhibit anti-cancer activity by targeting different molecules associated with OC survival (165). New evidence suggests that miR-21, miR-92a, and miR-221, abundant in MSC-derived extracellular vesicles, are associated with OC development (166). Taken together, the above findings revealed a direct or indirect epigenetic relationship between MSCs and OC cells, which should be investigated further and might lead to the identification of new therapeutic targets for OC.

2.6.3 Tumor-Associated Macrophages (TAMs)

TAMs are the most abundant myeloid cell type in the TME and are involved in cancer-related inflammation, matrix remodeling, angiogenesis, metastasis, cancer cell stemness, tumor immune escape, and drug resistance (167–170). The unique TME determines macrophage diversity and the ability to switch between M1 (pro-inflammatory with anti-tumor activity) and M2 (anti-inflammatory with pro-tumor activity) phenotypes (171, 172). Epigenetic regulation plays a significant role in TAM differentiation and activation, which is significantly associated with tumor drug resistance. For instance, studies have found that epithelial ovarian cancer (EOC)-released exosomal miR-222-3p activated M2 polarization and tumor-promoting capacities in ovarian TAMs by the SOCS3/STAT3 pathway. Similarly, exosomal miR-940 released from hypoxic epithelial ovarian tumors induces a shift in the macrophage M2 phenotype (173, 174). Furthermore, TAM-secreted exosomes prevented endothelial migration by targeting the miR-146b-5P/TRAF6/NF- κ B/MMP2 pathway, and the lncRNAs in OC-secreted exosomes effectively inhibit migration (175). Ishii et al. described M2 macrophage polarization through STAT6-mediated reciprocal epigenetic alterations in histone H3 lysine4 and histone H3 lysine27 methylation, which resulted in transcriptional activation of particular M2 manufacturing

genes (176). Together, these findings highlight the importance of TAM-regulated epigenetic alterations in OC, as they may reveal novel diagnostic and therapeutic approaches.

3 THERAPEUTIC TARGETING OF THE OC EPIGENOME

OC treatment prioritizes surgery and cytoreduction, followed by cytotoxic platinum and taxane chemotherapy. Although most OC patients respond effectively in the early phases of therapy, new therapeutic options are urgently needed to enhance outcomes for the most advanced patients (1). In the last decade, immunotherapy and targeted therapy have shown remarkable benefits for treating OC (177–179). Furthermore, due to the reversibility of epigenetic alterations, the prevention of treatment resistance through epigenetic drugs has become an attractive therapeutic concept, and the combination of epigenetic therapies with chemotherapy, immunotherapy, and molecularly targeted treatments holds a lot of promise for OC treatment. Based on this, epigenetic regulation, namely, DNA methylation, histone modifications, and ncRNA regulation, has emerged as a potential therapeutic target for OC (Figure 5).

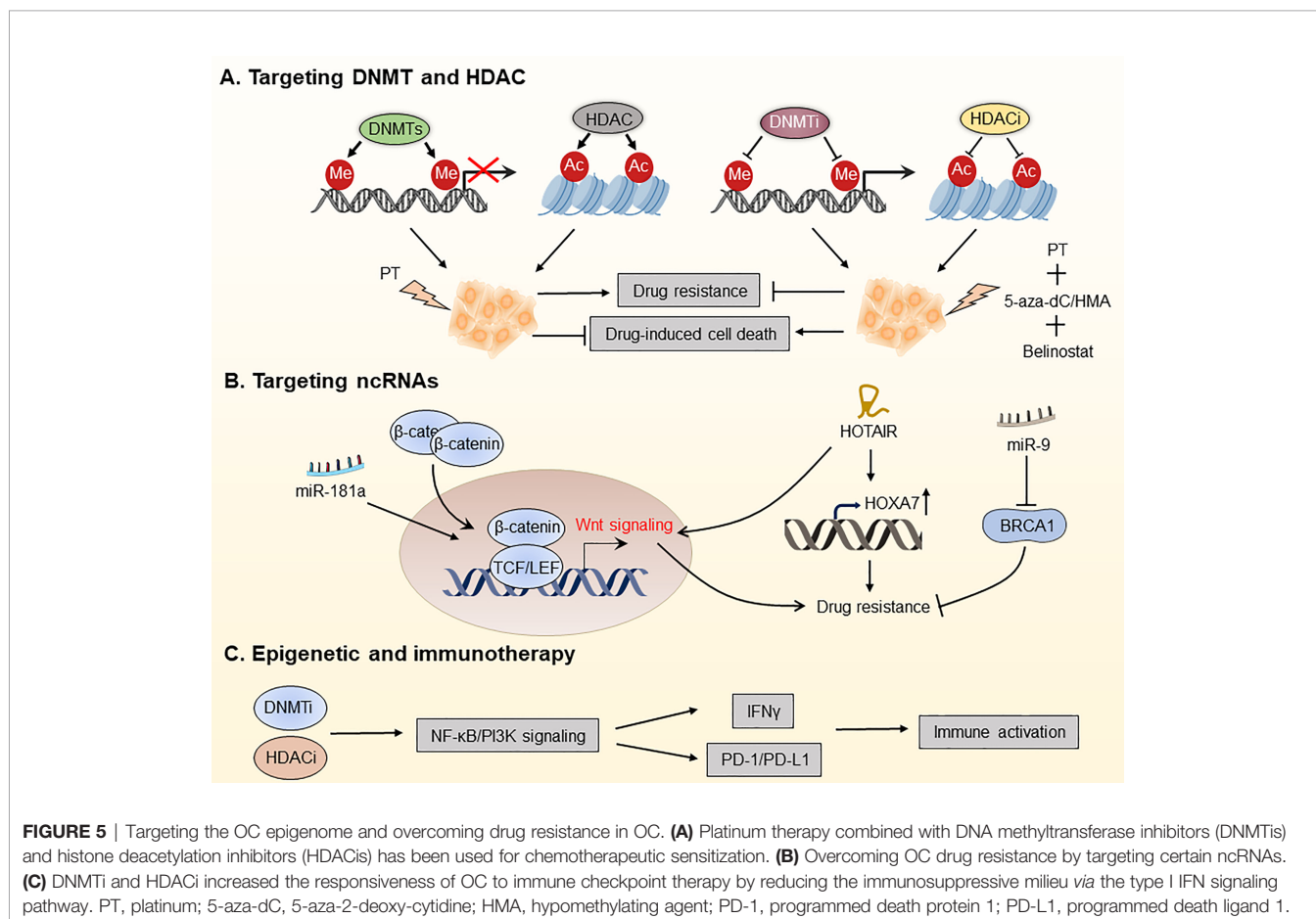


FIGURE 5 | Targeting the OC epigenome and overcoming drug resistance in OC. **(A)** Platinum therapy combined with DNA methyltransferase inhibitors (DNMTi) and histone deacetylase inhibitors (HDACi) has been used for chemotherapeutic sensitization. **(B)** Overcoming OC drug resistance by targeting certain ncRNAs. **(C)** DNMTi and HDACi increased the responsiveness of OC to immune checkpoint therapy by reducing the immunosuppressive milieu via the type I IFN signaling pathway. PT, platinum; 5-aza-dC, 5-aza-2-deoxy-cytidine; HMA, hypomethylating agent; PD-1, programmed death protein 1; PD-L1, programmed death ligand 1.

3.1 Targeting DNMT

As one of the most well-known epigenetic modifications, DNA methylation plays an essential role in DNA repair, apoptosis, angiogenesis, gene expression regulation, and drug resistance. To date, aberrant DNA hypermethylation has been found in drug-resistant cancer cells, and drug-induced DNA hypermethylation has been proposed as a potential mechanism and biomarker of drug resistance. DNA methylation is mediated by three DNA methyltransferases (DNMTs), primarily by DNMT1, which mediates maintenance (one strand) methylation, and by DNMT3A and DNMT3B, which catalyze *de novo* methylation (180). The activity of DNMTs can be blocked by DNMT inhibitors (DNMTis), which are analogs of deoxycytosine and effectively block methyl transfer (181). 5-aza-2-deoxy-cytidine (decitabine) and 5-azacytidine were first successfully studied in hematological malignancies and myelodysplastic syndrome (MDS) and were approved by the FDA in 2006 for treating MDS, where they exhibit anti-tumor activity through the inhibition of DNA methylation (182).

To date, DNMTis has been successfully used for treating chemotherapy-resistant OC, restoring platinum sensitivity in refractory to standard chemotherapy of patients. DNA hypomethylation caused by DNMTi decitabine renders OC patients more susceptible to platinum treatment and is associated with a better prognosis. Matei et al. found that platinum resistance is mostly induced by epigenetic abnormalities, including abnormal DNA methylation. The regimen consists of a modest dosage of decitabine 5 days before the administration of carboplatin, which decreases toxicity and boosts the demethylation effect of decitabine, leading to the recovery of carboplatin sensitivity in patients with advanced OC (183). Decitabine has been shown in studies to be more effective than 5-azacytidine for treating platinum-resistant OC. It is capable of regulating the methylation status of the tumor antigen NY-ESO-1 to improve immunotherapy efficacy (184). Furthermore, decitabine improves responses of OC patients to platinum therapy by influencing signaling pathways that promote tumor progression, such as the TGF- β signaling pathway (185). Taken together, DNMTis plays a promising role in reversing or preventing chemotherapeutic and molecular-targeted drug resistance in OC patients.

3.2 Targeting HDAC

Histone deacetylase (HDAC) enzymes, which remove acetyl groups from histone and non-histone proteins, downregulate the transcription of genes (186). In cancer cells, HDAC inhibitors (HDACis) can restore transcriptional inhibition of tumor suppressor genes and generate an anti-cancer environment. Meng et al. showed that a combination of proteasome and HDAC inhibitors can inhibit gynecologic cancer growth (187). Inhibitors of enzyme-catalyzed histone modifications, among which HDACis are the most rapidly developed, have been investigated in solid tumors (188).

Fukumoto et al. found that ARID1A mutations confer sensitivity to pan-HDAC inhibitors such as SAHA in OC, which is associated with more significant effects of growth

inhibition owing to suppression of HDAC2 activity (189). By suppressing HDAC6 with the small molecule ACY1215, Bitler et al. revealed that mice with ARID1A mutant tumors had dramatically increased survival. Mechanistically, HDAC6 deacetylates Lys120 on p53, thereby inactivating the pro-apoptotic function of p53 (190). However, not all HDAC subtypes are abnormally expressed in all malignancies, so pan-inhibition of HDAC is not an effective way to treat cancer (191). Besides, because of its poor activity as a single agent, HDACis have been investigated along with radiotherapy, chemotherapy, and other epigenetic drugs. For instance, belinostat re-sensitized drug-resistant OC cells to platinum, and the combination of decitabine and belinostat was more effective in re-sensitizing platinum than belinostat alone (192, 193). Furthermore, there is mounting evidence showing that HDACs-mediated deacetylation of non-histones is involved in many key cellular processes associated with drug resistance, such as apoptosis, suggesting that enhanced acetylation of non-histones using HDACis is promising for overcoming the drug resistance of OC. Taken together, targeting HDACs is an appealing strategy for OC treatment.

3.3 Targeting ncRNAs

Multiple ncRNAs, including miRNAs and lncRNAs, are increasingly implicated in the treatment resistance in OC (194, 195). Therefore, targeting tumor-specific miRNAs and lncRNAs is expected to overcome drug resistance of OC. Recently, miRNAs have received increasing attention as biomarkers and therapeutic targets for OC. For instance, Belur Nagaraj and colleagues found that miR-181a is an activator of Wnt/ β -catenin signaling, driving stemness and chemotherapy resistance in high-grade serous ovarian cancer (HGSOC), thus being a potential target for treating recurrent OC (194). Using next-generation sequencing (NGS) techniques, Au Yeung et al. identified miR-21 in exosomes and tissue lysates isolated from cancer-associated adipocytes and fibroblasts, which is significantly higher than OC cells. They discovered that miR21 is transferred from CAAs or CAFs to OC cells, suppresses apoptosis and confers chemotherapeutic resistance in OC cells by binding with APAF1 (154). Additionally, Vescarelli et al. have demonstrated that miR-200c significantly enhanced the anti-cancer effect of the PARP inhibitor olaparib in drug-resistant OC cells (196). This finding indicates that combining olaparib with miRNA-based therapy is a potential therapeutic option for drug-resistant OC. Sun et al. found that miR-9 increases the sensitivity of OC cells to DNA damage by down-regulating BRCA1, thus improving the efficacy of chemotherapy (197).

In addition to miRNAs, lncRNAs are considered promising therapeutic targets for OC. For instance, the non-coding RNA HOTAIR has been shown to be a potential target for overcoming carboplatin resistance in OC (195). Furthermore, it has been discovered that HOTAIR is overexpressed in cisplatin-resistant OC cells, and knocking down HOTAIR enhances apoptosis in cisplatin-resistant OC cells by down-regulating HOXA7, thereby restoring cisplatin sensitivity (198, 199). Additionally, HOTAIR-mediated platinum resistance in

OC can also be attributed to the upregulation of HOXA7 and activation of the Wnt/ β -catenin pathway (88). These findings point to it as a possible target for re-sensitizing OC cells to platinum therapy. Besides, Wu et al. demonstrated that the lncRNA WDFY3-AS2 modulates the hsa-miR-139-5p/SDC4 axis and may play an essential role in the platinum resistance of OC (200). Taken together, the above studies show that it is promising to prevent or overcome OC resistance by targeting ncRNAs.

3.4 Epigenetic Therapy in Combination With Immunotherapy in OC

Antibodies against inhibitory immune receptors, namely, cytotoxic T-lymphocyte-associated protein 4 (CTLA-4/CD152), programmed death protein 1 (PD-1/CD279), and programmed death ligand 1 (PD-L1/B7H1/CD274), have become effective standard immunotherapy for many advanced malignancies (177, 201). However, its effectiveness has yet to be successfully applied to the treatment of OC (202). Although a small fraction of OC patients respond well to immunotherapy, most patients fail to respond or develop secondary resistance to immunotherapy. Therefore, a combinatorial strategy is needed to enhance the efficacy of immunotherapy for OC, which can be achieved by drug repurposing or *de novo* drug development that stimulates the immune response.

Initial findings showed that epigenetic repressive processes were linked to a “cold” immunological environment in OC. Based on them, epigenetic modifiers were used in several of preclinical and clinical trials to explore immune targeting techniques (188). For instance, Stone and colleagues have demonstrated that DNMTi 5-azacytidine (AZA) activates the type I interferon signaling pathway, boosts IFN γ + T cells and natural killer (NK) cells, and reduces the percentage of macrophages in the TME. They also discovered that clinically relevant dosages of DNMTi and HDACi increased the responsiveness of OC to immune checkpoint therapy by reducing the immunosuppressive milieu *via* the type I IFN signaling pathway (203). The triple combination of DNMTi/HDACi with the immune checkpoint inhibitor α -PD-1 showed significantly better anti-tumor efficacy than DNMTi 5-azacytidine (AZA) alone or AZA along with HDACi, which may be a therapeutic option for treating OC. In a follow-up study, Travers et al. employed a hypomethylating agent (HMA) in conjunction with 2-difluoromethylornithine (DFMO) to rewire TME in OC, leading to a longer-lasting anti-tumor response. They found that AZA and DFMO, either alone or in combination, significantly recruited CD4⁺/CD8⁺ T and NK cells, decreased tumor burden, and improved the survival of OC patients (204). Another trial used decitabine in conjunction with paclitaxel and carboplatin to treat 55 patients with recurrent OC and found that the triple combination treatment group had a 58% overall response rate, which is superior to other groups (205). Therefore, combinational therapy with epigenetic modifiers may be able to avoid the loss of tumor antigens and expand the T cell pool by recognizing the initially targeted

antigens and epitopes, showing a new and intriguing promise for vaccine and cell transfer platforms.

4 CONCLUSIONS AND PERSPECTIVES

Although notable progress has been made in treating OC recently, most patients with advanced OC still relapse and eventually die from chemotherapy resistance, notably platinum. In fact, tumorigenesis, progression, and treatment resistance of OC are largely mediated by epigenetic regulation. These epigenetic alterations, such as DNA methylation and histone modifications, may occur before or during drug treatment and develop drug resistance by controlling several essential signaling pathways. Recently, with the improvement of our understanding of cancer-specific epigenetic alterations, targeting the epigenome to prevent or overcome OC drug resistance may be a viable therapeutic option.

In this article, we reviewed how epigenetic modifications play a key role in drug resistance in OC cells by affecting pivotal processes, namely, drug transport and metabolism, downstream signaling pathways, cancer stemness, and the immune microenvironment. Meanwhile, we also highlighted the biological functions of several key epigenetic modifiers, such as DNMT, HDAC, and ncRNAs. As the machinery embroidering epigenetic regulation continues to be deciphered, we conclude that the epigenome may emerge as a novel therapeutic target for OC. In fact, some small-molecule inhibitors targeting epigenetic alterations have entered the stage of clinical trials, which are expected to prevent or overcome OC resistance by changing the drug-responsive epigenome of OC. However, for complex reasons, the response rates of OC to monotherapy are typically modest. Although ongoing clinical trials have shown that epigenetic agents can significantly improve the drug sensitivity of OC when combined with targeted agents (e.g., PARP inhibitors) or immune drugs (e.g., anti-PD-1), leveraging the unique properties of epigenetics to obtain the optimal therapeutic advantage still requires considerable effort in the following research.

AUTHOR CONTRIBUTIONS

Conceptualization, CH and LL. Investigation, YW. Writing-original draft preparation, YW and ZH. Writing-review and editing, YW, ZH, and BL. Visualization, YW and BL. Supervision, CH and LL. All authors listed have made a substantial, direct, and intellectual contribution to the work and approved it for publication.

FUNDING

This work was supported by the National Natural Science Foundation of China (82003113, 82102738, 82103168).

REFERENCES

- Lheureux S, Braunstein M, Oza AM. Epithelial Ovarian Cancer: Evolution of Management in the Era of Precision Medicine. *CA: Cancer J Clin* (2019) 69(4):280–304. doi: 10.3322/caac.21559
- Jiang Y, Wang C, Zhou S. Targeting Tumor Microenvironment in Ovarian Cancer: Promise and Promise. *Biochim Biophys Acta Rev Cancer* (2020) 1873(2):188361. doi: 10.1016/j.bbcan.2020.188361
- Cummings M, Freer C, Orsi NM. Targeting the Tumour Microenvironment in Platinum-Resistant Ovarian Cancer. *Semin Cancer Biol* (2021) 77:3–28. doi: 10.1016/j.semcancer.2021.02.007
- Oza AM, Cook AD, Pfisterer J, Embleton A, Ledermann JA, Pujade-Lauraine E, et al. Standard Chemotherapy With or Without Bevacizumab for Women With Newly Diagnosed Ovarian Cancer (ICON7): Overall Survival Results of a Phase 3 Randomised Trial. *Lancet Oncol* (2015) 16(8):928–36. doi: 10.1016/S1470-2045(15)00086-8
- Christie EL, Bowtell DDL. Acquired Chemotherapy Resistance in Ovarian Cancer. *Ann Oncol* (2017) 28(suppl_8):viii13–5. doi: 10.1093/annonc/mdx446
- Moschetta M, George A, Kaye SB, Banerjee S. BRCA Somatic Mutations and Epigenetic BRCA Modifications in Serous Ovarian Cancer. *Ann Oncol* (2016) 27(8):1449–55. doi: 10.1093/annonc/mdw142
- Mirza MR, Monk BJ, Herrstedt J, Oza AM, Mahner S, Redondo A, et al. Niraparib Maintenance Therapy in Platinum-Sensitive, Recurrent Ovarian Cancer. *N Engl J Med* (2016) 375(22):2154–64. doi: 10.1056/NEJMoa1611310
- Mirza MR, Coleman RL, González-Martín A, Moore KN, Colombo N, Ray-Coquard I, et al. The Forefront of Ovarian Cancer Therapy: Update on PARP Inhibitors. *Ann Oncol Off J Eur Soc Med Oncol* (2020) 31(9):1148–59. doi: 10.1016/j.annonc.2020.06.004
- Kwon JS, Daniels MS, Sun CC, Lu KH. Preventing Future Cancers by Testing Women With Ovarian Cancer for BRCA Mutations. *J Clin Oncol Off J Am Soc Clin Oncol* (2010) 28(4):675–82. doi: 10.1200/JCO.2008.21.4684
- Slade D. PARP and PARG Inhibitors in Cancer Treatment. *Genes Dev* (2020) 34(5-6):360–94. doi: 10.1101/gad.334516.119
- Vasconcelos MH, Caires HR, Âbols A, Xavier CPR, Linē A. Extracellular Vesicles as a Novel Source of Biomarkers in Liquid Biopsies for Monitoring Cancer Progression and Drug Resistance. *Drug Resist Update* (2019) 47:100647. doi: 10.1016/j.drug.2019.100647
- Bar-Zeev M, Livney YD, Assaraf YG. Targeted Nanomedicine for Cancer Therapeutics: Towards Precision Medicine Overcoming Drug Resistance. *Drug Resist Update* (2017) 31:15–30. doi: 10.1016/j.drug.2017.05.002
- Assaraf YG, Brozovic A, Gonçalves AC, Jurkovicova D, Linē A, Machuqueiro M, et al. The Multi-Factorial Nature of Clinical Multidrug Resistance in Cancer. *Drug Resist Update* (2019) 46:100645. doi: 10.1016/j.drug.2019.100645
- Zhang Z, Qin S, Chen Y, Zhou L, Yang M, Tang Y, et al. Inhibition of NPC1L1 Disrupts Adaptive Responses of Drug-Tolerant Persister Cells to Chemotherapy. *EMBO Mol Med* (2022) 14(2):e14903. doi: 10.15252/emmm.202114903
- Galluzzi L, Senovilla L, Vitale I, Michels J, Martins I, Kepp O, et al. Molecular Mechanisms of Cisplatin Resistance. *Oncogene* (2012) 31(15):1869–83. doi: 10.1038/onc.2011.384
- Morel D, Jeffery D, Aspeslagh S, Almouzni G, Postel-Vinay S. Combining Epigenetic Drugs With Other Therapies for Solid Tumours - Past Lessons and Future Promise. *Nat Rev Clin Oncol* (2020) 17(2):91–107. doi: 10.1038/s41571-019-0267-4
- Wilting RH, Dannenberg JH. Epigenetic Mechanisms in Tumorigenesis, Tumor Cell Heterogeneity and Drug Resistance. *Drug Resist Update* (2012) 15(1-2):21–38. doi: 10.1016/j.drug.2012.01.008
- Li B, Jiang J, Assaraf YG, Xiao H, Chen ZS, Huang C, et al. Surmounting Cancer Drug Resistance: New Insights From the Perspective of N(6)-Methyladenosine RNA Modification. *Drug Resist Update* (2020) 53:100720. doi: 10.1016/j.drug.2020.100720
- Konstantinopoulos PA, Ceccaldi R, Shapiro GI, D'Andrea AD. Homologous Recombination Deficiency: Exploiting the Fundamental Vulnerability of Ovarian Cancer. *Cancer Discov* (2015) 5(11):1137–54. doi: 10.1158/2159-8290.CD-15-0714
- Shen DW, Pouliot LM, Hall MD, Gottesman MM. Cisplatin Resistance: A Cellular Self-Defense Mechanism Resulting From Multiple Epigenetic and Genetic Changes. *Pharmacol Rev* (2012) 64(3):706–21. doi: 10.1124/pr.111.005637
- Li H, Yu G, Shi R, Lang B, Chen X, Xia D, et al. Cisplatin-Induced Epigenetic Activation of miR-34a Sensitizes Bladder Cancer Cells to Chemotherapy. *Mol Cancer* (2014) 13:8. doi: 10.1186/1476-4598-13-8
- Bolton KL, Chenevix-Trench G, Goh C, Sadezki S, Ramus SJ, Karlan BY, et al. Association Between BRCA1 and BRCA2 Mutations and Survival in Women With Invasive Epithelial Ovarian Cancer. *JAMA* (2012) 307(4):382–90. doi: 10.1001/jama.2012.20
- Yang D, Khan S, Sun Y, Hess K, Shmulevich I, Sood AK, et al. Association of BRCA1 and BRCA2 Mutations With Survival, Chemotherapy Sensitivity, and Gene Mutator Phenotype in Patients With Ovarian Cancer. *JAMA* (2011) 306(14):1557–65. doi: 10.1001/jama.2011.1456
- Yang Q, Yang Y, Zhou N, Tang K, Lau WB, Lau B, et al. Epigenetics in Ovarian Cancer: Promise, Properties, and Perspectives. *Mol Cancer* (2018) 17(1):109. doi: 10.1186/s12943-018-0855-4
- Watson ZL, Yamamoto TM, McMellen A, Kim H, Hughes CJ, Wheeler LJ, et al. Histone Methyltransferases EHMT1 and EHMT2 (GLP/G9A) Maintain PARP Inhibitor Resistance in High-Grade Serous Ovarian Carcinoma. *Clin Epigenet* (2019) 11(1):165. doi: 10.1186/s13148-019-0758-2
- Abbosch PH, Montgomery JS, Starke JA, Novotny M, Zuhowski EG, Egorin MJ, et al. Dominant-Negative Histone H3 Lysine 27 Mutant Derepresses Silenced Tumor Suppressor Genes and Reverses the Drug-Resistant Phenotype in Cancer Cells. *Cancer Res* (2006) 66(11):5582–91. doi: 10.1158/0008-5472.CAN-05-3575
- Zhang X, Xie K, Zhou H, Wu Y, Li C, Liu Y, et al. Role of Non-Coding RNAs and RNA Modifiers in Cancer Therapy Resistance. *Mol Cancer* (2020) 19(1):47. doi: 10.1186/s12943-020-01171-z
- Wei L, Sun J, Zhang N, Zheng Y, Wang X, Lv L, et al. Noncoding RNAs in Gastric Cancer: Implications for Drug Resistance. *Mol Cancer* (2020) 19(1):62. doi: 10.1186/s12943-020-01185-7
- Wu X, Luo Q, Zhao P, Chang W, Wang Y, Shu T, et al. MGMT-Activated DUB3 Stabilizes MCL1 and Drives Chemoresistance in Ovarian Cancer. *Proc Natl Acad Sci USA* (2019) 116(8):2961–6. doi: 10.1073/pnas.1814742116
- Zhang X, et al. The Inhibition of UBC13 Expression and Blockage of the DNMT1-CHFR-Aurora A Pathway Contribute to Paclitaxel Resistance in Ovarian Cancer. *Cell Death Dis* (2018) 9(2):93. doi: 10.1038/s41419-017-0137-x
- Han X, Liu D, Zhou Y, Wang L, Hou H, Chen H, et al. The Negative Feedback Between miR-143 and DNMT3A Regulates Cisplatin Resistance in Ovarian Cancer. *Cell Biol Int* (2021) 45(1):227–37. doi: 10.1002/cbin.11486
- Li H, Lei Y, Li S, Li F, Lei J. MicroRNA-20a-5p Inhibits the Autophagy and Cisplatin Resistance in Ovarian Cancer via Regulating DNMT3B-Mediated DNA Methylation of RBP1. *Reprod Toxicol (Elmsford N.Y.)* (2022) 109:93–100. doi: 10.1016/j.reprotox.2021.12.011
- Sharma SV, Lee DY, Li B, Quinlan MP, Takahashi F, Maheswaran S, et al. A Chromatin-Mediated Reversible Drug-Tolerant State in Cancer Cell Subpopulations. *Cell* (2010) 141(1):69–80. doi: 10.1016/j.cell.2010.02.027
- Shang S, Yang J, Jazaeri AA, Duval AJ, Tufan T, Lopes Fischer N, et al. Chemotherapy-Induced Distal Enhancers Drive Transcriptional Programs to Maintain the Chemoresistant State in Ovarian Cancer. *Cancer Res* (2019) 79(18):4599–611. doi: 10.1158/0008-5472.CAN-19-0215
- Jeong JY, Kang H, Kim TH, Kim G, Heo JH, Kwon AY, et al. MicroRNA-136 Inhibits Cancer Stem Cell Activity and Enhances the Anti-Tumor Effect of Paclitaxel Against Chemoresistant Ovarian Cancer Cells by Targeting Notch3. *Cancer Lett* (2017) 386:168–78. doi: 10.1016/j.canlet.2016.11.017
- Wang Y, Bao W, Liu Y, Wang S, Xu S, Li X, et al. miR-98-5p Contributes to Cisplatin Resistance in Epithelial Ovarian Cancer by Suppressing miR-152 Biogenesis via Targeting Dicer1. *Cell Death Dis* (2018) 9(5):447. doi: 10.1038/s41419-018-0390-7
- Li X, Chen W, Jin Y, Xue R, Su J, Mu Z, et al. miR-142-5p Enhances Cisplatin-Induced Apoptosis in Ovarian Cancer Cells by Targeting Multiple Anti-Apoptotic Genes. *Biochem Pharmacol* (2019) 161:98–112. doi: 10.1016/j.bcp.2019.01.009
- Niu L, Ni H, Hou Y, Du Q, Li H. miR-509-3p Enhances Platinum Drug Sensitivity in Ovarian Cancer. *Gene* (2019) 686:63–7. doi: 10.1016/j.gene.2018.11.011

39. Zuo Y, Zheng W, Liu J, Tang Q, Wang SS, Yang XS, et al. MiR-34a-5p/PD-L1 Axis Regulates Cisplatin Chemoresistance of Ovarian Cancer Cells. *Neoplasma* (2020) 67(1):93–101. doi: 10.4149/neo_2019_190202N106
40. Özeş AR, Miller DF, Özeş ON, Fang F, Liu Y, Matei D, et al. NF-κB-HOTAIR Axis Links DNA Damage Response, Chemoresistance and Cellular Senescence in Ovarian Cancer. *Oncogene* (2016) 35(41):5350–61. doi: 10.1038/ncr.2016.75
41. Yang C, Li H, Zhang T, Chu Y, Chen D, Zuo J, et al. miR-200c Overexpression Inhibits the Invasion and Tumorigenicity of Epithelial Ovarian Cancer Cells by Suppressing lncRNA HOTAIR in Mice. *J Cell Biochem* (2020) 121(2):1514–23. doi: 10.1002/jcb.29387
42. Li Z, Niu H, Qin Q, Yang S, Wang Q, Yu C, et al. lncRNA UCA1 Mediates Resistance to Cisplatin by Regulating the miR-143/FOSL2-Signaling Pathway in Ovarian Cancer. *Mol Ther Nucleic Acids* (2019) 17:92–101. doi: 10.1016/j.omtn.2019.05.007
43. Wu DI, Wang T, Ren C, Liu L, Kong D, Jin X, et al. Downregulation of BC200 in Ovarian Cancer Contributes to Cancer Cell Proliferation and Chemoresistance to Carboplatin. *Oncol Lett* (2016) 11(2):1189–94. doi: 10.3892/ol.2015.3983
44. Li J, Huang H, Li Y, Li L, Hou W, You Z, et al. Decreased Expression of Long Non-Coding RNA GAS5 Promotes Cell Proliferation, Migration and Invasion, and Indicates a Poor Prognosis in Ovarian Cancer. *Oncol Rep* (2016) 36(6):3241–50. doi: 10.3892/or.2016.5200
45. Long X, Li L, Zhou Q, Wang H, Zou D, Wang D, et al. Long Non-Coding RNA LSINCT5 Promotes Ovarian Cancer Cell Proliferation, Migration and Invasion by Disrupting the CXCL12/CXCR4 Signalling Axis. *Oncol Lett* (2018) 15(5):7200–6. doi: 10.3892/ol.2018.8241
46. Berdasco M, Esteller M. Clinical Epigenetics: Seizing Opportunities for Translation. *Nat Rev Genet* (2019) 20(2):109–27. doi: 10.1038/s41576-018-0074-2
47. Bivona TG, Doebele RC. A Framework for Understanding and Targeting Residual Disease in Oncogene-Driven Solid Cancers. *Nat Med* (2016) 22(5):472–8. doi: 10.1038/nm.4091
48. Li B, Jiang J, Assaraf YG, Xiao H, Chen ZS, Huang C, et al. Surmounting Cancer Drug Resistance: New Insights From the Perspective of N-Methyladenosine RNA Modification. *Drug Resist Updates Rev Commentaries Antimicrob Anticancer Chemother* (2020) 53:100720. doi: 10.1016/j.drug.2020.100720
49. Chen Z, Shi T, Zhang L, Zhu P, Deng M, Huang C, et al. Mammalian Drug Efflux Transporters of the ATP Binding Cassette (ABC) Family in Multidrug Resistance: A Review of the Past Decade. *Cancer Lett* (2016) 370(1):153–64. doi: 10.1016/j.canlet.2015.10.010
50. Muñoz-Galván S, Felipe-Abrio B, Verdugo-Sivianes EM, Perez M, Jiménez-García MP, Suarez-Martinez E, et al. Downregulation of MYPT1 Increases Tumor Resistance in Ovarian Cancer by Targeting the Hippo Pathway and Increasing the Stemness. *Mol Cancer* (2020) 19(1):7. doi: 10.1186/s12943-020-1130-z
51. Erin N, Grahovac J, Brozovic A, Efferth T. Tumor Microenvironment and Epithelial Mesenchymal Transition as Targets to Overcome Tumor Multidrug Resistance. *Drug Resist Updates Rev Commentaries Antimicrob Anticancer Chemother* (2020) 53:100715. doi: 10.1016/j.drug.2020.100715
52. Ahmed N, Escalona R, Leung D, Chan E, Kannourakis G. Tumour Microenvironment and Metabolic Plasticity in Cancer and Cancer Stem Cells: Perspectives on Metabolic and Immune Regulatory Signatures in Chemoresistant Ovarian Cancer Stem Cells. *Semin Cancer Biol* (2018) 53:265–81. doi: 10.1016/j.semcancer.2018.10.002
53. Qu Y, Dou B, Tan H, Feng Y, Wang N, Wang D, et al. Tumor Microenvironment-Driven Non-Cell-Autonomous Resistance to Antineoplastic Treatment. *Mol Cancer* (2019) 18(1):69. doi: 10.1186/s12943-019-0992-4
54. Li W, Zhang H, Assaraf YG, Zhao K, Xu X, Xie J, et al. Overcoming ABC Transporter-Mediated Multidrug Resistance: Molecular Mechanisms and Novel Therapeutic Drug Strategies. *Drug Resist Update* (2016) 27:14–29. doi: 10.1016/j.drug.2016.05.001
55. Fletcher JL, Williams RT, Henderson MJ, Norris MD, Haber M. ABC Transporters as Mediators of Drug Resistance and Contributors to Cancer Cell Biology. *Drug Resist Update* (2016) 26:1–9. doi: 10.1016/j.drug.2016.03.001
56. Sun NK, Kohli A, Huang SL, Chang TC, Chao CC. Androgen Receptor Transcriptional Activity and Chromatin Modifications on the ABCB1/MDR Gene Are Critical for Taxol Resistance in Ovarian Cancer Cells. *J Cell Physiol* (2019) 234(6):8760–75. doi: 10.1002/jcp.27535
57. Wu DD, Li XS, Meng XN, Yan J, Zong ZH. MicroRNA-873 Mediates Multidrug Resistance in Ovarian Cancer Cells by Targeting ABCB1. *Tumour Biol* (2016) 37(8):10499–506. doi: 10.1007/s13277-016-4944-y
58. Tian J, Xu YY, Li L, Hao Q. MiR-490-3p Sensitizes Ovarian Cancer Cells to Cisplatin by Directly Targeting ABCC2. *Am J Transl Res* (2017) 9(3):1127–38.
59. Wang JM, Liu BQ, Zhang Q, Hao L, Li C, Yan J, et al. ISG15 Suppresses Translation of ABCC2 via ISGylation of Hnrnpa2b1 and Enhances Drug Sensitivity in Cisplatin Resistant Ovarian Cancer Cells. *Biochim Biophys Acta Mol Cell Res* (2020) 1867(4):118647. doi: 10.1016/j.bbamcr.2020.118647
60. Zhang S, Balch C, Chan MW, Lai HC, Matei D, Schilder JM, et al. Identification and Characterization of Ovarian Cancer-Initiating Cells From Primary Human Tumors. *Cancer Res* (2008) 68(11):4311–20. doi: 10.1158/0008-5472.CAN-08-0364
61. Calcagno AM, Fostel JM, To KK, Salcido CD, Martin SE, Chewing KJ, et al. Single-Step Doxorubicin-Selected Cancer Cells Overexpress the ABCG2 Drug Transporter Through Epigenetic Changes. *Br J Cancer* (2008) 98(9):1515–24. doi: 10.1038/sj.bjc.6604334
62. Chen Y. Effects of (Linc-VLDLR) Existing in Extracellular Vesicles on the Occurrence and Multidrug Resistance of Esophageal Cancer Cells. *Pathol Res Pract* (2019) 215(3):470–7. doi: 10.1016/j.prp.2018.12.033
63. Dong Y, Lin Y, Gao X, Zhao Y, Wan Z, Wang H, et al. Targeted Blocking of Mir328 Lysosomal Degradation With Alkylated Exosomes Sensitizes the Chronic Leukemia Cells to Imatinib. *Appl Microbiol Biotechnol* (2019) 103(23–24):9569–82. doi: 10.1007/s00253-019-10127-3
64. Liang G, Zhu Y, Ali DJ, Tian T, Xu H, Si K, et al. Engineered Exosomes for Targeted Co-Delivery of miR-21 Inhibitor and Chemotherapeutics to Reverse Drug Resistance in Colon Cancer. *J Nanobiotechnol* (2020) 18(1):10. doi: 10.1186/s12951-019-0563-2
65. Liu T, Zhang X, Du L, Wang Y, Liu X, Tian H, et al. Exosome-Transmitted miR-128-3p Increase Chemosensitivity of Oxaliplatin-Resistant Colorectal Cancer. *Mol Cancer* (2019) 18(1):43. doi: 10.1186/s12943-019-0981-7
66. Thakur C, Chen F. Connections Between Metabolism and Epigenetics in Cancers. *Semin Cancer Biol* (2019) 57:52–8. doi: 10.1016/j.semcancer.2019.06.006
67. Pande P, Zhong X-B, Ku WW. Histone Methyltransferase G9a Regulates Expression of Nuclear Receptors and Cytochrome P450 Enzymes in HepaRG Cells at Basal Level and in Fatty Acid Induced Steatosis. *Drug Metab Dispos: Biol Fate Chemicals* (2020) 48(12):1321–9. doi: 10.1124/dmd.120.000195
68. Luo J, Xie M, Hou Y, Ma W, Jin Y, Chen J, et al. A Novel Epigenetic Mechanism Unravels hsa-miR-148a-3p-Mediated CYP2B6 Downregulation in Alcoholic Hepatitis Disease. *Biochem Pharmacol* (2021) 188:114582. doi: 10.1016/j.bcp.2021.114582
69. Fuentes-Mattei E, Bayraktar R, Manshoury T, Silva AM, Ivan C, Gulei D, et al. miR-543 Regulates the Epigenetic Landscape of Myelofibrosis by Targeting TET1 and TET2. *JCI Insight* (2020) 5(1):e121781. doi: 10.1172/jci.insight.121781
70. Luo M, Yang X, Chen HN, Nice EC, Huang C. Drug Resistance in Colorectal Cancer: An Epigenetic Overview. *Biochim Biophys Acta Rev Cancer* (2021) 1876(2):188623. doi: 10.1016/j.bbcan.2021.188623
71. Minari R, Bordi P, La Monica S, Squadrilli A, Leonetti A, Bottarelli L, et al. Concurrent Acquired BRAF V600E Mutation and MET Amplification as Resistance Mechanism of First-Line Osimertinib Treatment in a Patient With EGFR-Mutated NSCLC. *J Thorac Oncol Off Publ Int Assoc Study Lung Cancer* (2018) 13(6):e89–91. doi: 10.1016/j.jtho.2018.03.013
72. Nayar U, Cohen O, Kapstad C, Cuoco MS, Waks AG, Wander SA, et al. Acquired HER2 Mutations in ER Metastatic Breast Cancer Confer Resistance to Estrogen Receptor-Directed Therapies. *Nat Genet* (2019) 51(2):207–16. doi: 10.1038/s41588-018-0287-5
73. Monk BJ, Pujade-Lauraine E, Burger RA. Integrating Bevacizumab Into the Management of Epithelial Ovarian Cancer: The Controversy of Front-Line Versus Recurrent Disease. *Ann Oncol Off J Eur Soc Med Oncol* (2013) 24 Suppl 10:x53–8. doi: 10.1093/annonc/mdt472

74. Monk BJ, Dalton H, Farley JH, Chase DM, Benjamin I. Antiangiogenic Agents as a Maintenance Strategy for Advanced Epithelial Ovarian Cancer. *Crit Rev Oncol Hematol* (2013) 86(2):161–75. doi: 10.1016/j.critrevonc.2012.09.012
75. Ray-Coquard I, Pautier P, Pignata S, Pérol D, González-Martín A, Berger R, et al. Olaparib Plus Bevacizumab as First-Line Maintenance in Ovarian Cancer. *N Engl J Med* (2019) 381(25):2416–28. doi: 10.1056/NEJMoa1911361
76. Burger RA, Brady MF, Bookman MA, Fleming GF, Monk BJ, Huang H, et al. Incorporation of Bevacizumab in the Primary Treatment of Ovarian Cancer. *N Engl J Med* (2011) 365(26):2473–83. doi: 10.1056/NEJMoa1104390
77. Gorenjak V, Vance DR, Dade S, Stathopoulou MG, Doherty L, Xie T, et al. Epigenome-Wide Association Study in Healthy Individuals Identifies Significant Associations With DNA Methylation and PBMc Extract VEGF-A Concentration. *Clin Epigenet* (2020) 12(1):79. doi: 10.1186/s13148-020-00874-w
78. Yang Z, Wang T, Wu D, Min Z, Tan J, Yu B, et al. RNA N6-Methyladenosine Reader IGF2BP3 Regulates Cell Cycle and Angiogenesis in Colon Cancer. *J Exp Clin Cancer Res CR* (2020) 39(1):203. doi: 10.1186/s13046-020-01714-8
79. Gao P, Wang D, Liu M, Chen S, Yang Z, Zhang J, et al. DNA Methylation-Mediated Repression of Exosomal miR-652-5p Expression Promotes Oesophageal Squamous Cell Carcinoma Aggressiveness by Targeting PARG and VEGF Pathways. *PLoS Genet* (2020) 16(4):e1008592. doi: 10.1371/journal.pgen.1008592
80. Integrated Genomic Analyses of Ovarian Carcinoma. *Nature* (2011) 474(7353):609–15. doi: 10.1038/nature10166
81. Fong PC, Yap TA, Boss DS, Carden CP, Mergui-Roelvink M, Gourley C, et al. Poly(ADP)-Ribose Polymerase Inhibition: Frequent Durable Responses in BRCA Carrier Ovarian Cancer Correlating With Platinum-Free Interval. *J Clin Oncol* (2010) 28(15):2512–9. doi: 10.1200/JCO.2009.26.9589
82. Audeh MW, Carmichael J, Penson RT, Friedlander M, Powell B, Bell-McGuinn KM, et al. Oral Poly(ADP-Ribose) Polymerase Inhibitor Olaparib in Patients With BRCA1 or BRCA2 Mutations and Recurrent Ovarian Cancer: A Proof-of-Concept Trial. *Lancet* (2010) 376(9737):245–51. doi: 10.1016/S0140-6736(10)60893-8
83. Hu W, Liu T, Ivan C, Sun Y, Huang J, Mangala LS, et al. Notch3 Pathway Alterations in Ovarian Cancer. *Cancer Res* (2014) 74(12):3282–93. doi: 10.1158/0008-5472.CAN-13-2066
84. McAuliffe SM, Morgan SL, Wyant GA, Tran LT, Muto KW, Chen YS, et al. Targeting Notch, a Key Pathway for Ovarian Cancer Stem Cells, Sensitizes Tumors to Platinum Therapy. *Proc Natl Acad Sci USA* (2012) 109(43):E2939–48. doi: 10.1073/pnas.1206400109
85. Ivan C, Hu W, Bottsford-Miller J, Zand B, Dalton HJ, Liu T, et al. Epigenetic Analysis of the Notch Superfamily in High-Grade Serous Ovarian Cancer. *Gynecologic Oncol* (2013) 128(3):506–11. doi: 10.1016/j.ygyno.2012.11.029
86. Liu S, Liu D, Chen C, Hamamura K, Moshaverinia A, Yang R, et al. MSC Transplantation Improves Osteopenia via Epigenetic Regulation of Notch Signaling in Lupus. *Cell Metab* (2015) 22(4):606–18. doi: 10.1016/j.cmet.2015.08.018
87. Hirsch TZ, Martin-Lannerée S, Reine F, Hernandez-Rapp J, Herzog L, Dron M, et al. Epigenetic Control of the Notch and Eph Signaling Pathways by the Prion Protein: Implications for Prion Diseases. *Mol Neurobiol* (2019) 56(3):2159–73. doi: 10.1007/s12035-018-1193-7
88. Li J, Yang S, Su N, Wang Y, Yu J, Qiu H, et al. Overexpression of Long non-Coding RNA HOTAIR Leads to Chemoresistance by Activating the Wnt/ β -Catenin Pathway in Human Ovarian Cancer. *Tumour Biol J Int Soc Oncodevelopmental Biol Med* (2016) 37(2):2057–65. doi: 10.1007/s13277-015-3998-6
89. Brinkman JA, Liu Y, Kron SJ. Small-Molecule Drug Repurposing to Target DNA Damage Repair and Response Pathways. *Semin Cancer Biol* (2021) 68:230–41. doi: 10.1016/j.semcancer.2020.02.013
90. Carneiro BA, El-Deiry WS. Targeting Apoptosis in Cancer Therapy. *Nat Rev Clin Oncol* (2020) 17(7):395–417. doi: 10.1038/s41571-020-0341-y
91. Gobin M, Nazarov PV, Warta R, Timmer M, Reifenberger G, Felsberg J, et al. A DNA Repair and Cell-Cycle Gene Expression Signature in Primary and Recurrent Glioblastoma: Prognostic Value and Clinical Implications. *Cancer Res* (2019) 79(6):1226–38. doi: 10.1158/0008-5472.CAN-18-2076
92. Wu S, Li X, Gao F, de Groot JF, Koul D, Yung WKA, et al. PARP-Mediated PARylation of MGMT Is Critical to Promote Repair of Temozolomide-Induced O6-Methylguanine DNA Damage in Glioblastoma. *Neuro Oncol* (2021) 23(6):920–31. doi: 10.1093/neuonc/noab003
93. Calabrese CR, Almassy R, Barton S, Batey MA, Calvert AH, Canan-Koch S, et al. Anticancer Chemosensitization and Radiosensitization by the Novel Poly(ADP-Ribose) Polymerase-1 Inhibitor AG14361. *J Natl Cancer Inst* (2004) 96(1):56–67. doi: 10.1093/jnci/djh005
94. Mateo J, Lord CJ, Serra V, Tutt A, Balmaña J, Castroviejo-Bermejo M, et al. A Decade of Clinical Development of PARP Inhibitors in Perspective. *Ann Oncol* (2019) 30(9):1437–47. doi: 10.1093/annonc/mdz192
95. Cao X, Hou J, An Q, Assaraf YG, Wang X. Towards the Overcoming of Anticancer Drug Resistance Mediated by P53 Mutations. *Drug Resist Updates Rev Commentaries Antimicrob Anticancer Chemother* (2020) 49:100671. doi: 10.1016/j.drug.2019.100671
96. Uddin MB, Roy KR, Hosain SB, Khiste SK, Hill RA, Jois SD, et al. An N-Methyladenosine at the Transited Codon 273 of P53 pre-mRNA Promotes the Expression of R273H Mutant Protein and Drug Resistance of Cancer Cells. *Biochem Pharmacol* (2019) 160:134–45. doi: 10.1016/j.bcp.2018.12.014
97. Meng X, Bi J, Li Y, Yang S, Zhang Y, Li M, et al. AZD1775 Increases Sensitivity to Olaparib and Gemcitabine in Cancer Cells With P53 Mutations. *Cancers* (2018) 10(5):149. doi: 10.3390/cancers10050149
98. Squire CJ, Dickson JM, Ivanovic I, Baker EN. Structure and Inhibition of the Human Cell Cycle Checkpoint Kinase, Wee1A Kinase: An Atypical Tyrosine Kinase With a Key Role in CDK1 Regulation. *Struct (London Engl 1993)* (2005) 13(4):541–50. doi: 10.1016/j.str.2004.12.017
99. McGowan CH, Russell P. Human Wee1 Kinase Inhibits Cell Division by Phosphorylating P34cdc2 Exclusively on Tyr15. *EMBO J* (1993) 12(1):75–85. doi: 10.1002/j.1460-2075.1993.tb05633.x
100. Leijen S, van Geel RM, Sonke GS, de Jong D, Rosenberg EH, Marchetti S, et al. Phase II Study of WEE1 Inhibitor AZD1775 Plus Carboplatin in Patients With TP53-Mutated Ovarian Cancer Refractory or Resistant to First-Line Therapy Within 3 Months. *J Clin Oncol Off J Am Soc Clin Oncol* (2016) 34(36):4354–61. doi: 10.1200/JCO.2016.67.5942
101. Roos WP, Thomas AD, Kaina B. DNA Damage and the Balance Between Survival and Death in Cancer Biology. *Nat Rev Cancer* (2016) 16(1):20–33. doi: 10.1038/nrc.2015.2
102. Sabnis AJ, Bivona TG. Principles of Resistance to Targeted Cancer Therapy: Lessons From Basic and Translational Cancer Biology. *Trends Mol Med* (2019) 25(3):185–97. doi: 10.1016/j.molmed.2018.12.009
103. Vera-Ramirez L. Cell-Intrinsic Survival Signals. The Role of Autophagy in Metastatic Dissemination and Tumor Cell Dormancy. *Semin Cancer Biol* (2020) 60:28–40. doi: 10.1016/j.semcancer.2019.07.027
104. Zhu H, Gan X, Jiang X, Diao S, Wu H, Hu J. ALKBH5 Inhibited Autophagy of Epithelial Ovarian Cancer Through miR-7 and BCL-2. *J Exp Clin Cancer Res CR* (2019) 38(1):163. doi: 10.1186/s13046-019-1159-2
105. Piya S, Andreeff M, Borthakur G. Targeting Autophagy to Overcome Chemoresistance in Acute Myelogenous Leukemia. *Autophagy* (2017) 13(1):214–5. doi: 10.1080/15548627.2016.1245263
106. Zhitomirsky B, Assaraf YG. Lysosomes as Mediators of Drug Resistance in Cancer. *Drug Resist Updates Rev Commentaries Antimicrob Anticancer Chemother* (2016) 24:23–33. doi: 10.1016/j.drug.2015.11.004
107. Zhou F, Yang X, Zhao H, Liu Y, Feng Y, An R, et al. Down-Regulation of OGT Promotes Cisplatin Resistance by Inducing Autophagy in Ovarian Cancer. *Theranostics* (2018) 8(19):5200–12. doi: 10.7150/thno.27806
108. Bi J, Zhang Y, Malmrose PK, Losh HA, Newton AM, Devor EJ, et al. Blocking Autophagy Overcomes Resistance to Dual Histone Deacetylase and Proteasome Inhibition in Gynecologic Cancer. *Cell Death Dis* (2022) 13(1):59. doi: 10.1038/s41419-022-04508-2
109. Hu Z, Cai M, Zhang Y, Tao L, Guo R. miR-29c-3p Inhibits Autophagy and Cisplatin Resistance in Ovarian Cancer by Regulating FOXPI1/ATG14 Pathway. *Cell Cycle (Georgetown Tex.)* (2020) 19(2):193–206. doi: 10.1080/15384101.2019.1704537
110. Bi X, Lv X, Liu D, Guo H, Yao G, Wang L, et al. METTL3-Mediated Maturation of miR-126-5p Promotes Ovarian Cancer Progression via PTEN-Mediated PI3K/Akt/mTOR Pathway. *Cancer Gene Ther* (2021) 28(3–4):335–49. doi: 10.1038/s41417-020-00222-3
111. Wong RS. Apoptosis in Cancer: From Pathogenesis to Treatment. *J Exp Clin Cancer Res* (2011) 30(1):87. doi: 10.1186/1756-9966-30-87
112. Hassannia B, Vandenabeele P, Vanden Berghe T. Targeting Ferroptosis to Iron Out Cancer. *Cancer Cell* (2019) 35(6):830–49. doi: 10.1016/j.jccell.2019.04.002

113. Chen P, Li X, Zhang R, Liu S, Xiang Y, Zhang M, et al. Combinative Treatment of β -Elemene and Cetuximab Is Sensitive to KRAS Mutant Colorectal Cancer Cells by Inducing Ferroptosis and Inhibiting Epithelial-Mesenchymal Transformation. *Theranostics* (2020) 10(11):5107–19. doi: 10.7150/thno.44705
114. Gao W, Huang Z, Duan J, Nice EC, Lin J, Huang C, et al. Elesclomol Induces Copper-Dependent Ferroptosis in Colorectal Cancer Cells via Degradation of ATP7A. *Mol Oncol* (2021) 15(12):3527–44. doi: 10.1002/1878-0261.13079
115. Conrad M, Angeli JP, Vandenamele P, Stockwell BR. Regulated Necrosis: Disease Relevance and Therapeutic Opportunities. *Nat Rev Drug Discov* (2016) 15(5):348–66. doi: 10.1038/nrd.2015.6
116. Badgley MA, Kremer DM, Maurer HC, DelGiorno KE, Lee HJ, Purohit V, et al. Cysteine Depletion Induces Pancreatic Tumor Ferroptosis in Mice. *Science* (2020) 368(6486):85–9. doi: 10.1126/science.aaw9872
117. Hong T, Lei G, Chen X, Li H, Zhang X, Wu N, et al. PARP Inhibition Promotes Ferroptosis via Repressing SLC7A11 and Synergizes With Ferroptosis Inducers in BRCA-Proficient Ovarian Cancer. *Redox Biol* (2021) 42:101928. doi: 10.1016/j.redox.2021.101928
118. Tang D, Chen X, Kang R, Kroemer G. Ferroptosis: Molecular Mechanisms and Health Implications. *Cell Res* (2021) 31(2):107–25. doi: 10.1038/s41422-020-00441-1
119. Yang WS, Stockwell BR. Ferroptosis: Death by Lipid Peroxidation. *Trends Cell Biol* (2016) 26(3):165–76. doi: 10.1016/j.tcb.2015.10.014
120. Ursini F, Maiorino M. Lipid Peroxidation and Ferroptosis: The Role of GSH and Gpx4. *Free Radic Biol Med* (2020) 152:175–85. doi: 10.1016/j.freeradbiomed.2020.02.027
121. Zhang X, Sui S, Wang L, Li H, Zhang L, Xu S, et al. Inhibition of Tumor Propellant Glutathione Peroxidase 4 Induces Ferroptosis in Cancer Cells and Enhances Anticancer Effect of Cisplatin. *J Cell Physiol* (2020) 235(4):3425–37. doi: 10.1002/jcp.29232
122. Sui X, Zhang R, Liu S, Duan T, Zhai L, Zhang M, et al. RSL3 Drives Ferroptosis Through GPX4 Inactivation and ROS Production in Colorectal Cancer. *Front Pharmacol* (2018) 9:1371. doi: 10.3389/fphar.2018.01371
123. Chen X, Li J, Kang R, Klionsky DJ, Tang D. Ferroptosis: Machinery and Regulation. *Autophagy* (2021) 17(9):2054–81. doi: 10.1080/15548627.2020.1810918
124. Jiang L, Kon N, Li T, Wang SJ, Su T, Hibshoosh H, et al. Ferroptosis as a P53-Mediated Activity During Tumour Suppression. *Nature* (2015) 520(7545):57–62. doi: 10.1038/nature14344
125. Zhang Y, Shi J, Liu X, Feng L, Gong Z, Koppula P, et al. BAP1 Links Metabolic Regulation of Ferroptosis to Tumour Suppression. *Nat Cell Biol* (2018) 20(10):1181–92. doi: 10.1038/s41556-018-0178-0
126. Dodson M, Castro-Portuguez R, Zhang DD. NRF2 Plays a Critical Role in Mitigating Lipid Peroxidation and Ferroptosis. *Redox Biol* (2019) 23:101107. doi: 10.1016/j.redox.2019.101107
127. Liu N, Lin X, Huang C. Activation of the Reverse Transsulfuration Pathway Through NRF2/CBS Confers Erastin-Induced Ferroptosis Resistance. *Br J Cancer* (2020) 122(2):279–92. doi: 10.1038/s41416-019-0660-x
128. Muscarella LA, Barbano R, D'Angelo V, Copetti M, Coco M, Balsamo T, et al. Regulation of KEAP1 Expression by Promoter Methylation in Malignant Gliomas and Association With Patient's Outcome. *Epigenetics* (2011) 6(3):317–25. doi: 10.4161/epi.6.3.14408
129. Yamamoto M, Kensler TW, Motohashi H. The KEAP1-NRF2 System: A Thiol-Based Sensor-Effector Apparatus for Maintaining Redox Homeostasis. *Physiol Rev* (2018) 98(3):1169–203. doi: 10.1152/physrev.00023.2017
130. Kansanen E, Kuosmanen SM, Leinonen H, Levonen AL. The Keap1-Nrf2 Pathway: Mechanisms of Activation and Dysregulation in Cancer. *Redox Biol* (2013) 1(1):45–9. doi: 10.1016/j.redox.2012.10.001
131. Fabrizio FP, Sparaneo A, Trombetta D, Muscarella LA. Epigenetic Versus Genetic Deregulation of the KEAP1/NRF2 Axis in Solid Tumors: Focus on Methylation and Noncoding RNAs. *Oxid Med Cell Longevity* (2018) 2018:2492063. doi: 10.1155/2018/2492063
132. Castejón-Griñán M, Herráiz C, Olivares C, Jiménez-Cervantes C, García-Borrón JC. cAMP-Independent Non-Pigmentary Actions of Variant Melanocortin 1 Receptor: AKT-Mediated Activation of Protective Responses to Oxidative DNA Damage. *Oncogene* (2018) 37(27):3631–46. doi: 10.1038/s41388-018-0216-1
133. Zhou Z, Lu H, Zhu S, Goma A, Chen Z, Yan J, et al. Activation of EGFR-DNA-PKcs Pathway by IGF2R Protects Esophageal Adenocarcinoma Cells From Acidic Bile Salts-Induced DNA Damage. *J Exp Clin Cancer Res CR* (2019) 38(1):13. doi: 10.1186/s13046-018-1021-y
134. Zanini E, Louis LS, Antony J, Karali E, Okon IS, McKie AB, et al. The Tumor-Suppressor Protein OPCML Potentiates Anti-EGFR- and Anti-HER2-Targeted Therapy in HER2-Positive Ovarian and Breast Cancer. *Mol Cancer Ther* (2017) 16(10):2246–56. doi: 10.1158/1535-7163.MCT-17-0081
135. Cao Y, Shen T, Zhang C, Zhang QH, Zhang ZQ. MiR-125a-5p Inhibits EMT of Ovarian Cancer Cells by Regulating TAZ/EGFR Signaling Pathway. *Eur Rev Med Pharmacol Sci* (2019) 23(19):8249–56. doi: 10.26355/eurrev_201910_19134
136. Lin S, Choe J, Du P, Triboulet R, Gregory RI. The M(6)A Methyltransferase METTL3 Promotes Translation in Human Cancer Cells. *Mol Cell* (2016) 62(3):335–45. doi: 10.1016/j.molcel.2016.03.021
137. Luo XL, Deng CC, Su XD, Wang F, Chen Z, Wu XP, et al. Loss of MED12 Induces Tumor Dormancy in Human Epithelial Ovarian Cancer via Downregulation of EGFR. *Cancer Res* (2018) 78(13):3532–43. doi: 10.1158/1538-7445.AM2018-5503
138. Ottevanger PB. Ovarian Cancer Stem Cells More Questions Than Answers. *Semin Cancer Biol* (2017) 44:67–71. doi: 10.1016/j.semcancer.2017.04.009
139. Li J, Condello S, Thomes-Pepin J, Ma X, Xia Y, Hurlley TD, et al. Lipid Desaturation Is a Metabolic Marker and Therapeutic Target of Ovarian Cancer Stem Cells. *Cell Stem Cell* (2017) 20(3):303–14.e5. doi: 10.1016/j.stem.2016.11.004
140. Wang Y, Cardenas H, Fang F, Condello S, Taverna P, Segar M, et al. Epigenetic Targeting of Ovarian Cancer Stem Cells. *Cancer Res* (2014) 74(17):4922–36. doi: 10.1158/0008-5472.CAN-14-1022
141. Steinbichler TB, Dudás J, Skvortsov S, Ganswindt U, Riechelmann H, Skvortsova II, et al. Therapy Resistance Mediated by Cancer Stem Cells. *Semin Cancer Biol* (2018) 53:156–67. doi: 10.1016/j.semcancer.2018.11.006
142. Pieterse Z, Amaya-Padilla MA, Singomat T, Binju M, Madjid BD, Yu Y, et al. Ovarian Cancer Stem Cells and Their Role in Drug Resistance. *Int J Biochem Cell Biol* (2019) 106:117–26. doi: 10.1016/j.biocel.2018.11.012
143. Keyvani V, Farshchian M, Esmaeili SA, Yari H, Moghbeli M, Nezhad SK, et al. Ovarian Cancer Stem Cells and Targeted Therapy. *J Ovarian Res* (2019) 12(1):120. doi: 10.1186/s13048-019-0588-z
144. Wen Y, Hou Y, Yi X, Sun S, Guo J, He X, et al. EZH2 Activates CHK1 Signaling to Promote Ovarian Cancer Chemoresistance by Maintaining the Properties of Cancer Stem Cells. *Theranostics* (2021) 11(4):1795–813. doi: 10.7150/thno.48101
145. Xu S, Yue Y, Zhang S, Zhou C, Cheng X, Xie X, et al. STON2 Negatively Modulates Stem-Like Properties in Ovarian Cancer Cells via DNMT1/MUC1 Pathway. *J Exp Clin Cancer Res CR* (2018) 37(1):305. doi: 10.1186/s13046-018-0977-y
146. Pinheiro AS, Marsh JA, Forman-Kay JD, Peti W. Structural Signature of the MYPT1-PP1 Interaction. *J Am Chem Soc* (2011) 133(1):73–80. doi: 10.1021/ja107810r
147. Hansen JM, Coleman RL, Sood AK. Targeting the Tumour Microenvironment in Ovarian Cancer. *Eur J Cancer* (2016) 56:131–43. doi: 10.1016/j.ejca.2015.12.016
148. Bhowmick NA, Neilson EG, Moses HL. Stromal Fibroblasts in Cancer Initiation and Progression. *Nature* (2004) 432(7015):332–7. doi: 10.1038/nature03096
149. Kalluri R. The Biology and Function of Fibroblasts in Cancer. *Nat Rev Cancer* (2016) 16(9):582–98. doi: 10.1038/nrc.2016.73
150. Lin H-J, Lin J. Seed-In-Soil: Pancreatic Cancer Influenced by Tumor Microenvironment. *Cancers* (2017) 9(7):93. doi: 10.3390/cancers9070093
151. Hanson JA, Gillespie JW, Grover A, Tangrea MA, Chuaqui RF, Emmert-Buck MR, et al. Gene Promoter Methylation in Prostate Tumor-Associated Stromal Cells. *J Natl Cancer Inst* (2006) 98(4):255–61. doi: 10.1093/jnci/dij051
152. Hu M, Yao J, Cai L, Bachman KE, van den Brûle F, Velculescu V, et al. Distinct Epigenetic Changes in the Stromal Cells of Breast Cancers. *Nat Genet* (2005) 37(8):899–905. doi: 10.1038/ng1596
153. Eckert MA, Coscia F, Chryplewicz A, Chang JW, Hernandez KM, Pan S, et al. Proteomics Reveals NNMT as a Master Metabolic Regulator of Cancer-Associated Fibroblasts. *Nature* (2019) 569(7758):723–8. doi: 10.1038/s41586-019-1173-8

154. Au Yeung CL, Co NN, Tsuruga T, Yeung TL, Kwan SY, Leung CS, et al. Exosomal Transfer of Stroma-Derived Mir21 Confers Paclitaxel Resistance in Ovarian Cancer Cells Through Targeting APAF1. *Nat Commun* (2016) 7:11150. doi: 10.1038/ncomms11150
155. Mitra AK, Zillhardt M, Hua Y, Tiwari P, Murmann AE, Peter ME, et al. MicroRNAs Reprogram Normal Fibroblasts Into Cancer-Associated Fibroblasts in Ovarian Cancer. *Cancer Discov* (2012) 2(12):1100–8. doi: 10.1158/2159-8290.CD-12-0206
156. Curtis M, Kenny HA, Ashcroft B, Mukherjee A, Johnson A, Zhang Y, et al. Fibroblasts Mobilize Tumor Cell Glycogen to Promote Proliferation and Metastasis. *Cell Metab* (2019) 29(1):141–55.e9. doi: 10.1016/j.cmet.2018.08.007
157. Zhao L, Ji G, Le X, Wang C, Xu L, Feng M, et al. Long Noncoding RNA LINC00092 Acts in Cancer-Associated Fibroblasts to Drive Glycolysis and Progression of Ovarian Cancer. *Cancer Res* (2017) 77(6):1369–82. doi: 10.1158/0008-5472.CAN-16-1615
158. da Silva Meirelles L, Chagastelles PC, Nardi NB. Mesenchymal Stem Cells Reside in Virtually All Post-Natal Organs and Tissues. *J Cell Sci* (2006) 119 (Pt 11):2204–13. doi: 10.1242/jcs.02932
159. McLean K, Gong Y, Choi Y, Deng N, Yang K, Bai S, et al. Human Ovarian Carcinoma-Associated Mesenchymal Stem Cells Regulate Cancer Stem Cells and Tumorigenesis via Altered BMP Production. *J Clin Invest* (2011) 121 (8):3206–19. doi: 10.1172/JCI45273
160. Lis R, Touboul C, Mirshahi P, Ali F, Mathew S, Nolan DJ, et al. Tumor Associated Mesenchymal Stem Cells Protects Ovarian Cancer Cells From Hyperthermia Through CXCL12. *Int J Cancer* (2011) 128(3):715–25. doi: 10.1002/ijc.25619
161. Cho JA, Park H, Lim EH, Kim KH, Choi JS, Lee JH, et al. Exosomes From Ovarian Cancer Cells Induce Adipose Tissue-Derived Mesenchymal Stem Cells to Acquire the Physical and Functional Characteristics of Tumor-Supporting Myofibroblasts. *Gynecologic Oncol* (2011) 123(2):379–86. doi: 10.1016/j.ygyno.2011.08.005
162. Muñoz P, Iliou MS, Esteller M. Epigenetic Alterations Involved in Cancer Stem Cell Reprogramming. *Mol Oncol* (2012) 6(6):620–36. doi: 10.1016/j.molonc.2012.10.006
163. Teven CM, Liu X, Hu N, Tang N, Kim SH, Huang E, et al. Epigenetic Regulation of Mesenchymal Stem Cells: A Focus on Osteogenic and Adipogenic Differentiation. *Stem Cells Int* (2011) 2011:201371. doi: 10.4061/2011/201371
164. Meyer MB, Benkusky NA, Sen B, Rubin J, Pike JW. Epigenetic Plasticity Drives Adipogenic and Osteogenic Differentiation of Marrow-Derived Mesenchymal Stem Cells. *J Biol Chem* (2016) 291(34):17829–47. doi: 10.1074/jbc.M116.736538
165. Reza AMMT, Choi YJ, Yasuda H, Kim JH. Human Adipose Mesenchymal Stem Cell-Derived Exosomal-miRNAs Are Critical Factors for Inducing Anti-Proliferation Signalling to A2780 and SKOV-3 Ovarian Cancer Cells. *Sci Rep* (2016) 6:38498. doi: 10.1038/srep38498
166. Lopatina T, Gai C, Deregius MC, Kholia S, Camussi G. Cross Talk Between Cancer and Mesenchymal Stem Cells Through Extracellular Vesicles Carrying Nucleic Acids. *Front Oncol* (2016) 6:125. doi: 10.3389/fonc.2016.00125
167. Shu Y, Cheng P. Targeting Tumor-Associated Macrophages for Cancer Immunotherapy. *Biochim Biophys Acta Rev Cancer* (2020) 1874(2):188434. doi: 10.1016/j.bbcan.2020.188434
168. Pan Y, Yu Y, Wang X, Zhang T. Tumor-Associated Macrophages in Tumor Immunity. *Front Immunol* (2020) 11:583084. doi: 10.3389/fimmu.2020.583084
169. Cortese N, Carriero R, Laghi L, Mantovani A, Marchesi F. Prognostic Significance of Tumor-Associated Macrophages: Past, Present and Future. *Semin Immunol* (2020) 48:101408. doi: 10.1016/j.smim.2020.101408
170. Li C, Xu X, Wei S, Jiang P, Xue L, Wang J, et al. Tumor-Associated Macrophages: Potential Therapeutic Strategies and Future Prospects in Cancer. *J Immunother Cancer* (2021) 9(1):e001341. doi: 10.1136/jitc-2020-001341
171. Lawrence T, Natoli G. Transcriptional Regulation of Macrophage Polarization: Enabling Diversity With Identity. *Nat Rev Immunol* (2011) 11(11):750–61. doi: 10.1038/nri3088
172. Xue J, Schmidt SV, Sander J, Draffehn A, Krebs W, Quester I, et al. Transcriptome-Based Network Analysis Reveals a Spectrum Model of Human Macrophage Activation. *Immunity* (2014) 40(2):274–88. doi: 10.1016/j.immuni.2014.01.006
173. Ying X, Wu Q, Wu X, Zhu Q, Wang X, Jiang L, et al. Epithelial Ovarian Cancer-Secreted Exosomal miR-222-3p Induces Polarization of Tumor-Associated Macrophages. *Oncotarget* (2016) 7(28):43076–87. doi: 10.18632/oncotarget.9246
174. Chen X, Ying X, Wang X, Wu X, Zhu Q, Wang X, et al. Exosomes Derived From Hypoxic Epithelial Ovarian Cancer Deliver microRNA-940 to Induce Macrophage M2 Polarization. *Oncol Rep* (2017) 38(1):522–8. doi: 10.3892/or.2017.5697
175. Wu Q, Wu X, Ying X, Zhu Q, Wang X, Jiang L, et al. Suppression of Endothelial Cell Migration by Tumor Associated Macrophage-Derived Exosomes Is Reversed by Epithelial Ovarian Cancer Exosomal lncRNA. *Cancer Cell Int* (2017) 17:62. doi: 10.1186/s12935-017-0430-x
176. Ishii M, Wen H, Corsa CA, Liu T, Coelho AL, Allen RM, et al. Epigenetic Regulation of the Alternatively Activated Macrophage Phenotype. *Blood* (2009) 114(15):3244–54. doi: 10.1182/blood-2009-04-217620
177. Odunsi K. Immunotherapy in Ovarian Cancer. *Ann Oncol Off J Eur Soc Med Oncol* (2017) 28(suppl_8):viii1–7. doi: 10.1093/annonc/mdx444
178. Pujade-Lauraine E. New Treatments in Ovarian Cancer. *Ann Oncol Off J Eur Soc Med Oncol* (2017) 28(suppl_8):viii57–60. doi: 10.1093/annonc/mdx442
179. Kuroki L, Guntupalli SR. Treatment of Epithelial Ovarian Cancer. *BMJ (Clin Res ed.)* (2020) 371:m3773. doi: 10.1136/bmj.m3773
180. Cai Y, Tsai HC, Yen RC, Zhang YW, Kong X, Wang W, et al. Critical Threshold Levels of DNA Methyltransferase 1 Are Required to Maintain DNA Methylation Across the Genome in Human Cancer Cells. *Genome Res* (2017) 27(4):533–44. doi: 10.1101/gr.208108.116
181. Lyko F, Brown R. DNA Methyltransferase Inhibitors and the Development of Epigenetic Cancer Therapies. *J Natl Cancer Inst* (2005) 97(20):1498–506. doi: 10.1093/jnci/dji311
182. Mahfouz RZ, Jankowska A, Ebrahim Q, Gu X, Visconte V, Tabarrok A, et al. Increased CDA Expression/Activity in Males Contributes to Decreased Cytidine Analog Half-Life and Likely Contributes to Worse Outcomes With 5-Azacytidine or Decitabine Therapy. *Clin Cancer Res an Off J Am Assoc Cancer Res* (2013) 19(4):938–48. doi: 10.1158/1078-0432.CCR-12-1722
183. Matei D, Fang F, Shen C, Schilder J, Arnold A, Zeng Y, et al. Epigenetic Resensitization to Platinum in Ovarian Cancer. *Cancer Res* (2012) 72 (9):2197–205. doi: 10.1158/0008-5472.CAN-11-3909
184. Griffiths EA, Srivastava P, Matsuzaki J, Brumberger Z, Wang ES, Kocent J, et al. NY-ESO-1 Vaccination in Combination With Decitabine Induces Antigen-Specific T-Lymphocyte Responses in Patients With Myelodysplastic Syndrome. *Clin Cancer Res an Off J Am Assoc Cancer Res* (2018) 24(5):1019–29. doi: 10.1158/1078-0432.CCR-17-1792
185. Cicek MS, Koestler DC, Fridley BL, Kalli KR, Armasu SM, Larson MC, et al. Epigenome-Wide Ovarian Cancer Analysis Identifies a Methylation Profile Differentiating Clear-Cell Histology With Epigenetic Silencing of the HERG K+ Channel. *Hum Mol Genet* (2013) 22(15):3038–47. doi: 10.1093/hmg/ddt160
186. Kim H-J, Bae S-C. Histone Deacetylase Inhibitors: Molecular Mechanisms of Action and Clinical Trials as Anti-Cancer Drugs. *Am J Trans Res* (2011) 3 (2):166–79. doi: 10.1007/978-1-4419-6612-4_66
187. Meng X, Yang S, Li Y, Li Y, Devor EJ, Bi J, et al. Combination of Proteasome and Histone Deacetylase Inhibitors Overcomes the Impact of Gain-Of-Function P53 Mutations. *Dis Markers* (2018) 2018:3810108. doi: 10.1155/2018/3810108
188. Matei D, Nephew KP. Epigenetic Attire in Ovarian Cancer: The Emperor's New Clothes. *Cancer Res* (2020) 80(18):3775–85. doi: 10.1158/0008-5472.CAN-19-3837
189. Fukumoto T, Park PH, Wu S, Fatkhutdinov N, Karakashev S, Nacarelli T, et al. Repurposing Pan-HDAC Inhibitors for ARID1A-Mutated Ovarian Cancer. *Cell Rep* (2018) 22(13):3393–400. doi: 10.1016/j.celrep.2018.03.019
190. Bitler BG, Wu S, Park PH, Hai Y, Aird KM, Wang Y, et al. ARID1A-Mutated Ovarian Cancers Depend on HDAC6 Activity. *Nat Cell Biol* (2017) 19 (8):962–73. doi: 10.1038/ncb3582
191. Shetty MG, Pai P, Deaver RE, Satyamoorthy K, Babitha KS. Histone Deacetylase 2 Selective Inhibitors: A Versatile Therapeutic Strategy as Next Generation Drug Target in Cancer Therapy. *Pharmacol Res* (2021) 170:105695. doi: 10.1016/j.phrs.2021.105695
192. Qian X, LaRochele WJ, Ara G, Wu F, Petersen KD, Thougaard A, et al. Activity of PXD101, a Histone Deacetylase Inhibitor, in Preclinical Ovarian

- Cancer Studies. *Mol Cancer Ther* (2006) 5(8):2086–95. doi: 10.1158/1535-7163.MCT-06-0111
193. Steele N, Finn P, Brown R, Plumb JA. Combined Inhibition of DNA Methylation and Histone Acetylation Enhances Gene Re-Expression and Drug Sensitivity *In Vivo*. *Br J Cancer* (2009) 100(5):758–63. doi: 10.1038/sj.bjc.6604932
 194. Belur Nagaraj A, Knarr M, Sekhar S, Connor RS, Joseph P, Kovalenko O, et al. The miR-181a-SFRP4 Axis Regulates Wnt Activation to Drive Stemness and Platinum Resistance in Ovarian Cancer. *Cancer Res* (2021) 81(8):2044–55. doi: 10.1158/0008-5472.CAN-20-2041
 195. Teschendorff AE, Lee SH, Jones A, Fiegl H, Kalwa M, Wagner W, et al. HOTAIR and Its Surrogate DNA Methylation Signature Indicate Carboplatin Resistance in Ovarian Cancer. *Genome Med* (2015) 7:108. doi: 10.1186/s13073-015-0233-4
 196. Vescarelli E, Gerini G, Megiorni F, Anastasiadou E, Pontecorvi P, Solito L, et al. MiR-200c Sensitizes Olaparib-Resistant Ovarian Cancer Cells by Targeting Neuropilin 1. *J Exp Clin Cancer Res CR* (2020) 39(1):3. doi: 10.1186/s13046-019-1490-7
 197. Sun C, Li N, Yang Z, Zhou B, He Y, Weng D, et al. miR-9 Regulation of BRCA1 and Ovarian Cancer Sensitivity to Cisplatin and PARP Inhibition. *J Natl Cancer Inst* (2013) 105(22):1750–8. doi: 10.1093/jnci/djt302
 198. Liu S, Lei H, Luo F, Li Y, Xie L. The Effect of lncRNA HOTAIR on Chemoresistance of Ovarian Cancer Through Regulation of HOXA7. *Biol Chem* (2018) 399(5):485–97. doi: 10.1515/hsz-2017-0274
 199. Wang Y, Wang H, Song T, Zou Y, Jiang J, Fang L, et al. HOTAIR is a Potential Target for the Treatment of Cisplatin-Resistant Ovarian Cancer. *Mol Med Rep* (2015) 12(2):2211–6. doi: 10.3892/mmr.2015.3562
 200. Wu Y, Wang T, Xia L, Zhang M. LncRNA WDFY3-AS2 Promotes Cisplatin Resistance and the Cancer Stem Cell in Ovarian Cancer by Regulating hsa-miR-139-5p/SDC4 Axis. *Cancer Cell Int* (2021) 21(1):284. doi: 10.1186/s12935-021-01993-x
 201. Olino K, Park T, Ahuja N. Exposing Hidden Targets: Combining Epigenetic and Immunotherapy to Overcome Cancer Resistance. *Semin Cancer Biol* (2020) 65:114–22. doi: 10.1016/j.semcancer.2020.01.001
 202. McCaw TR, Randall TD, Arend RC. Overcoming Immune Suppression With Epigenetic Modification in Ovarian Cancer. *Trans Res J Lab Clin Med* (2019) 204:31–8. doi: 10.1016/j.trsl.2018.06.003
 203. Stone ML, Chiappinelli KB, Li H, Murphy LM, Travers ME, Topper MJ, et al. Epigenetic Therapy Activates Type I Interferon Signaling in Murine Ovarian Cancer to Reduce Immunosuppression and Tumor Burden. *Proc Natl Acad Sci USA* (2017) 114(51):E10981–90. doi: 10.1073/pnas.1712514114
 204. Travers M, Brown SM, Dunworth M, Holbert CE, Wiehagen KR, Bachman KE, et al. DFMO and 5-Azacytidine Increase M1 Macrophages in the Tumor Microenvironment of Murine Ovarian Cancer. *Cancer Res* (2019) 79(13):3445–54. doi: 10.1158/0008-5472.CAN-18-4018
 205. Zhang Y, Mei Q, Liu Y, Li X, Brock MV, Chen M, et al. The Safety, Efficacy, and Treatment Outcomes of a Combination of Low-Dose Decitabine Treatment in Patients With Recurrent Ovarian Cancer. *Oncoimmunology* (2017) 6(9):e1323619. doi: 10.1080/2162402X.2017.1323619

Conflict of Interest: The authors declare that the research was conducted in the absence of any commercial or financial relationships that could be construed as a potential conflict of interest.

Publisher's Note: All claims expressed in this article are solely those of the authors and do not necessarily represent those of their affiliated organizations, or those of the publisher, the editors and the reviewers. Any product that may be evaluated in this article, or claim that may be made by its manufacturer, is not guaranteed or endorsed by the publisher.

Copyright © 2022 Wang, Huang, Li, Liu and Huang. This is an open-access article distributed under the terms of the Creative Commons Attribution License (CC BY). The use, distribution or reproduction in other forums is permitted, provided the original author(s) and the copyright owner(s) are credited and that the original publication in this journal is cited, in accordance with accepted academic practice. No use, distribution or reproduction is permitted which does not comply with these terms.

GLOSSARY

OC	ovarian cancer
PARP	poly (ADP-ribose) polymerase
lncRNA	long non-coding RNA
miRNA	microRNA
MGMT	O6-methylguanine-DNA methyltransferase
TME	tumor microenvironment
MDR	multidrug resistance
ABC	ATP-binding cassette
EVs	vesicles
CYP	cytochrome P450
VEGF	vascular endothelial growth factor
TCGA	The Cancer Genome Atlas
IGF2BP3	insulin-like growth factor 2 mRNA-binding protein 3
HR	homologous recombination
DNMT1	DNA methyltransferase 1
TMZ	temozolomide
PARPi	Poly-ADP-ribose polymerase inhibitors
FLIP	FLICE inhibitor proteins
DUB3	deubiquitinating enzyme 3
HDACis	histone deacetylase inhibitors
ATG14	autophagy-related gene 14
METTL3	methyltransferase-like 3
OGT	O-GlcNAc transferase
NRF2	nuclear factor erythroid 2-related factor 2
EGFR	epidermal growth factor receptor
NHEJ	non-homologous terminal junction
CSCs	Cancer stem cells
OCSCs	ovarian cancer stem cells
CAFs	Cancer-Associated Fibroblasts
NNMT	nicotinamide N-methyltransferase
APAF1	apoptosis protease activator-1
PFKFB2	Phosphofructo-2-Kinase/Fructo-2,6-Biphosphatase 2
MSCs	Mesenchymal Stem Cells
TAMs	tumor-Associated Macrophages
DNMTs	DNA methyltransferases
MDS	myelodysplastic syndrome
HDAC	histone deacetylase
HGSOC	high-grade serous ovarian cancer
NGS	next-generation sequencing
CTLA-4/CD152	cytotoxic T-lymphocyte-associated protein 4
PD-1/CD279	programmed death protein 1
PD-L1/B7H1/CD274	programmed death ligand 1
AZA	azacytidine
DFMO	2-difluoromethylornithine



Quantitative Ubiquitinomics Revealed Abnormal Ubiquitinated ATP7A Involved in Down-Regulation of ACTH in Silent Corticotroph Adenomas

Sida Zhao¹, Yue He¹, Hongyun Wang¹, Dan Li¹, Lei Gong¹, Yazhuo Zhang^{1,2*} and Chuzhong Li^{3*}

¹ Beijing Neurosurgical Institute, Capital Medical University, Beijing, China, ² Beijing Institute for Brain Disorders Brain Tumor Center, Capital Medical University, Beijing, China, ³ Beijing Tiantan Hospital, Capital Medical University, Beijing, China

OPEN ACCESS

Edited by:

Xianquan Zhan,
Shandong First Medical University,
China

Reviewed by:

Canhua Huang,
Sichuan University, China
Na Li,
Shandong Cancer Hospital, China

*Correspondence:

Yazhuo Zhang
zyz2004520@yeah.net
Chuzhong Li
lichuzhong@163.com

Specialty section:

This article was submitted to
Cancer Endocrinology,
a section of the journal
Frontiers in Endocrinology

Received: 26 January 2022

Accepted: 22 March 2022

Published: 11 May 2022

Citation:

Zhao S, He Y, Wang H, Li D, Gong L,
Zhang Y and Li C (2022) Quantitative
Ubiquitinomics Revealed Abnormal
Ubiquitinated ATP7A Involved in
Down-Regulation of ACTH in Silent
Corticotroph Adenomas.
Front. Endocrinol. 13:863017.
doi: 10.3389/fendo.2022.863017

Ubiquitination is reported to be a critical biological event on ACTH secretion in corticotroph adenomas. However, the effect of ubiquitylation on ACTH secretion in silent corticotroph adenomas (SCAs) remains unclear. The aim of our study was to explore the mechanism of decreased secretion of ACTH in SCAs with ubiquitinomics. The differently expressed ubiquitinated proteins between SCAs and functioning corticotroph adenomas (FCAs) were identified by 4D label-free mass spectrometer, followed by bioinformatics analysis. The function of the candidate ubiquitinated protein ATP7A (K333) was validated in AtT20 cells. A total of 111 ubiquitinated sites corresponding to 94 ubiquitinated proteins were typically different between SCAs and FCAs. Among all the ubiquitinated sites, 102 showed decreased ubiquitination in SCAs, which mapped to 85 ubiquitinated proteins. Pathway enrichment analysis revealed that ubiquitinated proteins were mainly enriched in vesicle pathway and protein secretion pathway. ATP7A (K333) was one of the proteins enriched in vesicle pathway and protein secretion pathway with decreased ubiquitination level in SCAs. *In vitro* assay indicated that both ATP7A siRNA and omeprazole (ATP7A protein inhibitor) increased the secretion of ACTH in AtT20 cell supernatant compared to control groups ($p < 0.05$). These results indicated that ATP7A might be related to the abnormal expression of ACTH in SCAs and potential for the treatment of SCAs.

Keywords: silent corticotroph adenomas, ATP7A, ubiquitination, mass spectrum, ACTH

INTRODUCTION

Silent Corticotroph Adenoma (SCA) is a kind of high-risk pituitary adenoma. It composed of 20% of all corticotroph adenomas (1). SCAs often exhibit characters of highly proliferative, and up to 43% of SCAs exhibit an aggressive growth into cavernous sinus (2) which lead to a more difficult surgery treatment. Additionally, SCAs patients showed a character of high recurrence rate (nearly

36%) (3) which makes surgery of SCAs difficult. Accordingly, an alternative method is required for a better treatment of SCAs. In the search to establish a reasonable treatment strategy, some scientists have struggled to enlighten the biological mechanism of abnormal blood ACTH level in SCA patients in the past few years.

Different from FCAs patients with Cushing's Diseases, SCAs patients have no clinical and biological features of Cushing's Diseases and they show lower blood ACTH level (4). The clinical and endocrinological appearances of SCAs are more like non-functioning pituitary adenomas (NFPAs). Several studies propose hypotheses about the silencing mechanism of SCAs. Kovacs et al. proposed that a large number of lysosomes fused with ACTH secretory granules and since contribute to the damage of secretory granules before release (5). Others suggest that SCAs mainly secrete biological inactive ACTH instead of normal ACTH (1–39) (6). Single cells in SCAs may secrete ACTH insufficiently or inactively (7).

Ubiquitination is a kind of reversible post-translational modification (PTMs) that deeply reported (8). Ubiquitination process is a cascade response regulated by ubiquitin activating (E1), conjugating (E2), and ligating (E3) enzymes, and the ubiquitin molecule (76 amino acids, 8.5Kd) was attached to the lysine residue of the substrate proteins (9). This process controls the dynamic balance of proteins synthesis and degradation. Ubiquitination leads to the degradation of proteins by ubiquitin-proteasome system (UPS) (10). Disfunctional ubiquitination of protein relates to many cell process, such as intracellular trafficking, enzymatic activity regulation and assembly of multiprotein complexes (11). Sesta A et. announced that inhibition of the ubiquitin-proteasome pathway increased ACTH secretion in corticotroph adenomas (12). However, there are no clear reports about the expression profiling of ubiquitination in SCAs and the potential mechanism of ubiquitination in ACTH secretion.

In this study, we clarified the ubiquitinomics in SCAs by 4D mass spectrometer and identified the ubiquitinated proteins which may play important roles in regulating the secretion of ACTH in SCAs. These findings may be meaningful and provide a target for the treatment of SCAs.

MATERIALS AND METHODS

Human Samples Collection

Tumor samples used in this study were obtained from Beijing Tiantan Hospital by transsphenoidal surgery. Fresh tumor samples were stored in liquid nitrogen. Five SCA tissue samples and five functioning corticotroph adenoma (FCA) were used for 4D leble free mass spectrometer. All tumor samples were classified according to the 2017 WHO classification.

This study was approved by the ethics committees of Beijing Tiantan Hospital (KY2018-053-02). Informed consent was obtained from all enrolled subjects, and the study was performed in full compliance with all principles of the Declaration of Helsinki.

Protein Extraction

The sample was grinded with liquid nitrogen into cell powder and then transferred to a 5-mL centrifuge tube. After that, four volumes of lysis buffer (8 M urea, 1% protease inhibitor cocktail) was added to the cell powder, followed by sonication three times on ice using a high intensity ultrasonic processor (Scientz). (Note: For PTM experiments, inhibitors were also added to the lysis buffer, e.g. 3 μ M TSA and 50 mM NAM for acetylation, 1% phosphatase inhibitor for phosphorylation). The remaining debris was removed by centrifugation at 12,000 g at 4°C for 10 min. Finally, the supernatant was collected and the protein concentration was determined with BCA kit according to the manufacturer's instructions.

Trypsin Digestion

For digestion, the protein solution was reduced with 5 mM dithiothreitol for 30 min at 56°C and alkylated with 11 mM iodoacetamide for 15 min at room temperature in darkness. The protein sample was then diluted by adding 100 mM TEAB to urea concentration less than 2 M. Finally, trypsin was added at 1:50 trypsin-to-protein mass ratio for the first digestion overnight and 1:100 trypsin-to-protein mass ratio for a second 4 h-digestion. Finally, the peptides were desalted by C18 SPE column.

Pan-Antibody-Based PTM Enrichment

To enrich modified peptides, tryptic peptides dissolved in NETN buffer (100 mM NaCl, 1 mM EDTA, 50 mM Tris-HCl, 0.5% NP-40, pH 8.0) were incubated with pre-washed antibody beads (Lot number xxx, PTM Bio) at 4°C overnight with gentle shaking. Then the beads were washed for four times with NETN buffer and twice with H₂O. The bound peptides were eluted from the beads with 0.1% trifluoroacetic acid. Finally, the eluted fractions were combined and vacuum-dried. For LC-MS/MS analysis, the resulting peptides were desalted with C18 ZipTips (Millipore) according to the manufacturer's instructions.

4D Mass Spectrometer

The tryptic peptides were dissolved in solvent A (0.1% formic acid, 2% acetonitrile/in water), directly loaded onto a home-made reversed-phase analytical column (25-cm length, 75/100 μ m i.d.). Peptides were separated with a gradient from 6% to 24% solvent B (0.1% formic acid in acetonitrile) over 70 min, 24% to 35% in 14 min and climbing to 80% in 3 min then holding at 80% for the last 3 min, all at a constant flow rate of 450 nL/min on a nanoElute UHPLC system (Bruker Daltonics).

The peptides were subjected to capillary source followed by the timsTOF Pro (Bruker Daltonics) mass spectrometry. The electrospray voltage applied was 1.60 kV. Precursors and fragments were analyzed at the TOF detector, with a MS/MS scan range from 100 to 1700 m/z. The timsTOF Pro was operated in parallel accumulation serial fragmentation (PASEF) mode. Precursors with charge states 0 to 5 were selected for fragmentation, and 10 PASEF-MS/MS scans were acquired per cycle. The dynamic exclusion was set to 30 s.

Database Search

The resulting MS/MS data were processed using MaxQuant search engine (v.1.6.15.0). Tandem mass spectra were searched against the human SwissProt database (20422 entries) concatenated with reverse decoy database. Trypsin/P was specified as cleavage enzyme allowing up to 2 missing cleavages. The mass tolerance for precursor ions was set as 20 ppm in first search and 5 ppm in main search, and the mass tolerance for fragment ions was set as 0.02 Da. Carbamidomethyl on Cys was specified as fixed modification, and acetylation on protein N-terminal and oxidation on Met were specified as variable modifications. FDR was adjusted to < 1%.

Cell Culture and Hormone Measurement

AtT20 cells were purchased from American Type Culture Collection (ATCC; Manassas, VA, USA) and were cultured in F12K medium (ATCC; Manassas, VA, USA) supplemented with 2.5% fetal bovine serum (FBS; Gibco) and 15% horse medium (Gibco).

Cells were plated into 24-well dishes with 200,000 cells and 1ml of medium per well and incubated for 72h. AtT20 cells treated with omeprazole (HY-B0113A, MedChemExpress) and the ACTH levels were assessed by an enzyme-linked immunosorbent assay (ELISA) (SBJ-M0483, SBJbio) according to the manufacture's protocol.

Transfection and RNA Interference

siRNA transfection was performed using Lipofectamine 3000 (L3000001, Thermo Fisher), according to the manufacturer's protocol. siRNA synthesis was performed by Beijing Syngentech and the siRNA sequences for mouse ATP7A is 5'GAACAUGAGUAAUGAAGAAT-T3'.

Bioinformatic and Statistical Analysis

UbiBrowser (13) was used to generate known and predicted human ubiquitin ligase (E3)-substrate interaction (<http://ubibrowser.ncpsb.org.cn>). Functional annotation databases

were utilized based on the biological process, molecular function, and cellular component classifications of differently expressed ubiquitinated proteins between SCAs and FCAs as determined by Gene Ontology (GO) (available online at <http://www.geneontology.org>). The enrichment pathway analysis of differently expressed ubiquitinated proteins between SCAs and FCAs was performed based on the Hallmark Gene Sets of Molecular Signatures database (Gene Set Enrichment Analysis, GSEA, <http://software.broadinstitute.org/gsea/msigdb/index.jsp>). STRING was used to build (protein-protein interactions) PPI networks with the ubiquitinated proteins.

All statistical analyses were conducted using the GraphPad Prism software package (GraphPad Software, San Diego, CA 92108). Unpaired Student's *t*-tests and chi-squared (Fisher's exact) tests were used for comparisons of quantitative and qualitative data, respectively. Differences with a $p < 0.05$ were considered significant.

RESULTS

Profiling of Ubiquitination Sites in SCA

In the profiling result, we identified 111 lysine-ubiquitinated sites totally between SCAs and FCAs (score>40, $p>0.05$ and fold change>1.5, **Supplementary Table 1**). The 111 lysine-ubiquitinated sites includes 102 down-regulated and 9 up-regulated sites in SCAs. 111 ubiquitinated sites were mapped to 94 proteins, which includes 85 down-regulated and 9 up-regulated proteins in SCAs (**Figure 1A**). The 111 ubiquitinated sites mapped to 110 unique peptides, and only 1 peptide had 2 ubiquitinated sites. The lengths of ubiquitinated peptides were obviously different (**Figure 1B**). For example, the identified ubiquitinated peptides with 11, 12 or 13 amino acid were separately 13.51% (15/111), 16.22%(18/111), and 11.71% (13/111). Meanwhile, most of the identified proteins had single ubiquitination site (88.30%, 83/94) and 8 proteins get 2

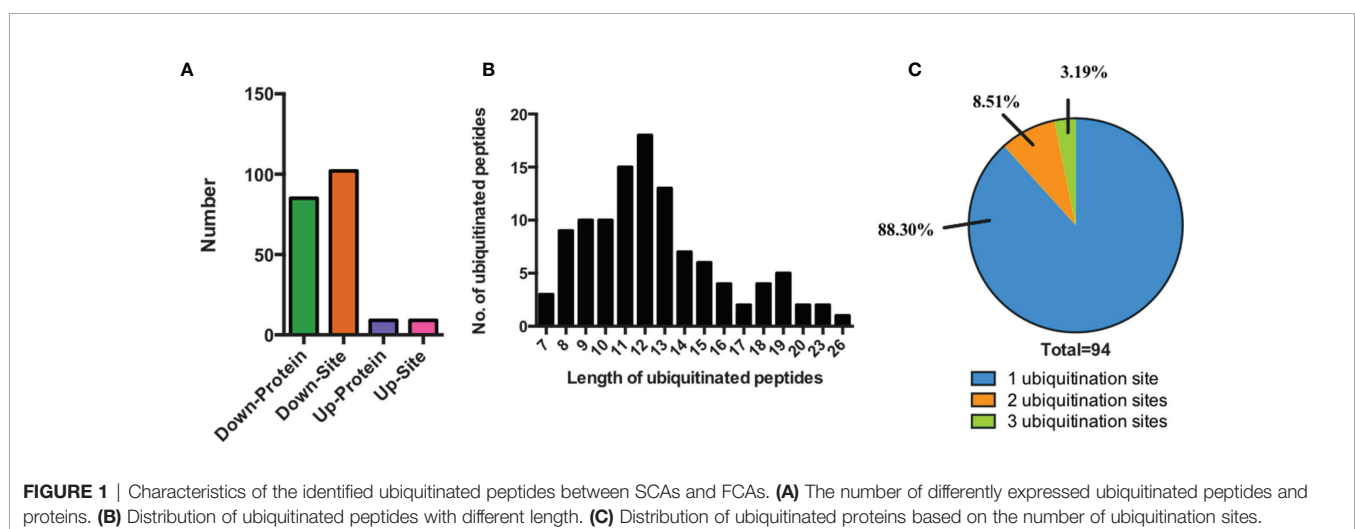


FIGURE 1 | Characteristics of the identified ubiquitinated peptides between SCAs and FCAs. **(A)** The number of differently expressed ubiquitinated peptides and proteins. **(B)** Distribution of ubiquitinated peptides with different length. **(C)** Distribution of ubiquitinated proteins based on the number of ubiquitination sites.

ubiquitination site (8.51%, 8/94) and 3 proteins had at least 3 ubiquitination sites (3.19%, 3/94, (**Figure 1C**).

A representative ubiquitinated peptide spectrum from ATP7A (Protein Session: Q04656) was shown: $^{333}\text{K}^*\text{AIEAVSPGLYR}^{344}$ ($m/z=709.39$), was a high-quality spectrum, with excellent b ion and y ion series (b2, b3, b4, b5, b6, b7, b10, b11, y5, y6, y7, y8, y9, y10, y11). The ubiquitination site of ATP7A was localized at K^{333} residue, and the ubiquitination level was significantly decreased in SCAs compared to FCAs (ratio of S/F=0.17, **Figure 2**).

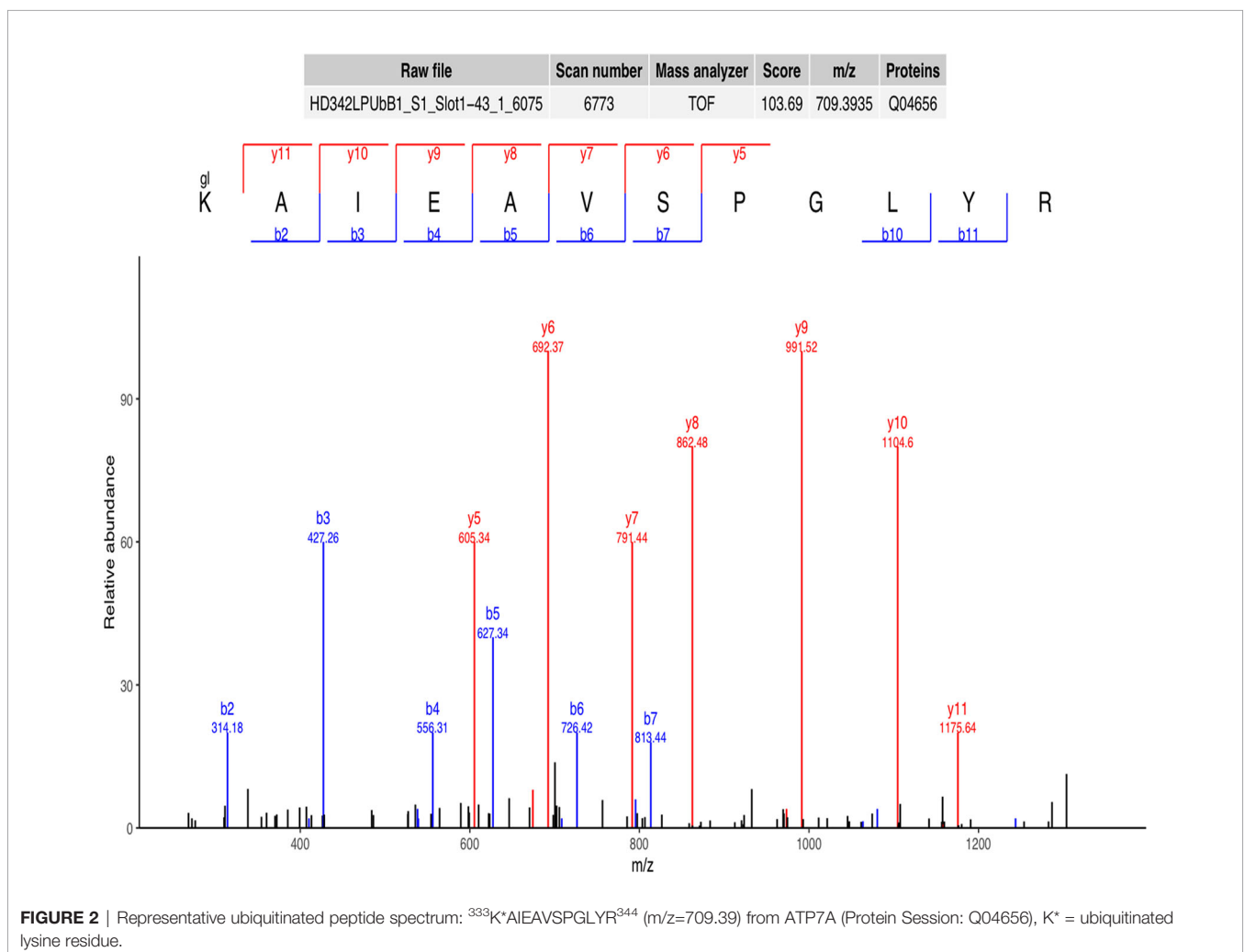
Ubiquitination Motifs Analysis in SCA

Motif-X was used for analysis of the significant ubiquitination motifs that were preferred to be ubiquitinated in SCAs. We identified 3 significant motifs that were prone to be ubiquitinated in the tumor, including $\text{K}^{\text{ub}}\text{-L}$, $\text{K}^{\text{ub}}\text{-E}$, and $\text{R-X-X-X-X-X-X-X-K}^{\text{ub}}$ (K^{ub} represent for the ubiquitinated lysine residue and X represents for the amino acid), with 13, 9 and 4 ubiquitinated sites respectively among all of the 111 differently expressed ubiquitinated sites (**Figure 3**). Of them, $\text{K}^{\text{ub}}\text{-L}$ was the most significant motif to be ubiquitinated and leucine residue (L) was a vital downstream ubiquitination site. Arginine residue (R) was a

representative upstream amino acid for the ubiquitination at K residue. The above 3 types of modification account for 23.42% of all the identified ubiquitinated site in SCAs and FCAs (26/111).

Functional Enrichment Analysis of the Identified Ubiquitinated Proteins

GO enrichment analysis was used to identify the functional clusters of 94 ubiquitinated proteins. Comprehensive analysis revealed that these proteins were obviously involved in many vesicle-related cellular component (**Figure 4A** and **Supplementary Table 2**), such as vesicle membrane ($p=6.46E-04$), vesicle ($p=1.14E-03$), cytoplasmic vesicle membrane ($p=1.77E-03$), cytoplasmic vesicle ($p=2.28E-03$), and intracellular vesicle ($p=2.30E-03$), which may indicate the ubiquitinated proteins were deeply involved in cell storage transport and secretion functions. Besides, ubiquitinated proteins were found to be enriched in multiple biological process (**Figure 4B**) including regulation of protein catabolic process ($p=8.19E-05$), developmental cell growth ($p=2.55E-04$), morphogenesis of an endothelium ($p=2.20E-03$), cell projection morphogenesis ($p=3.11E-03$), epithelial cell migration ($p=3.17E-03$), and cell



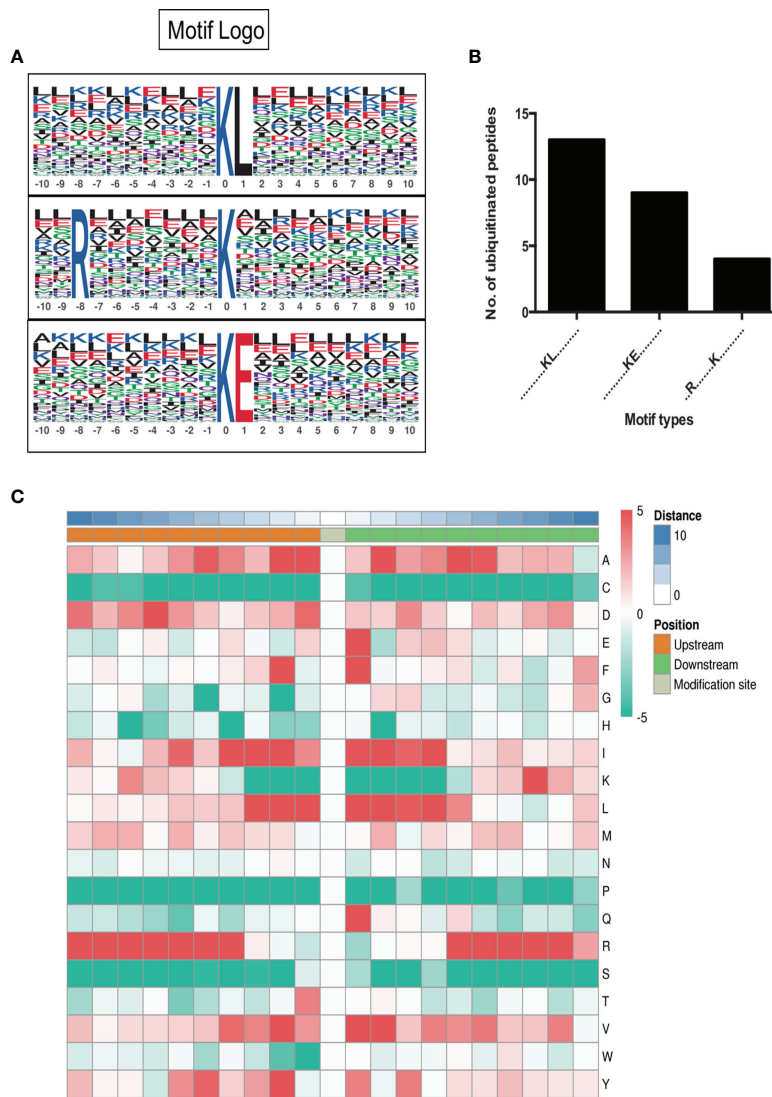


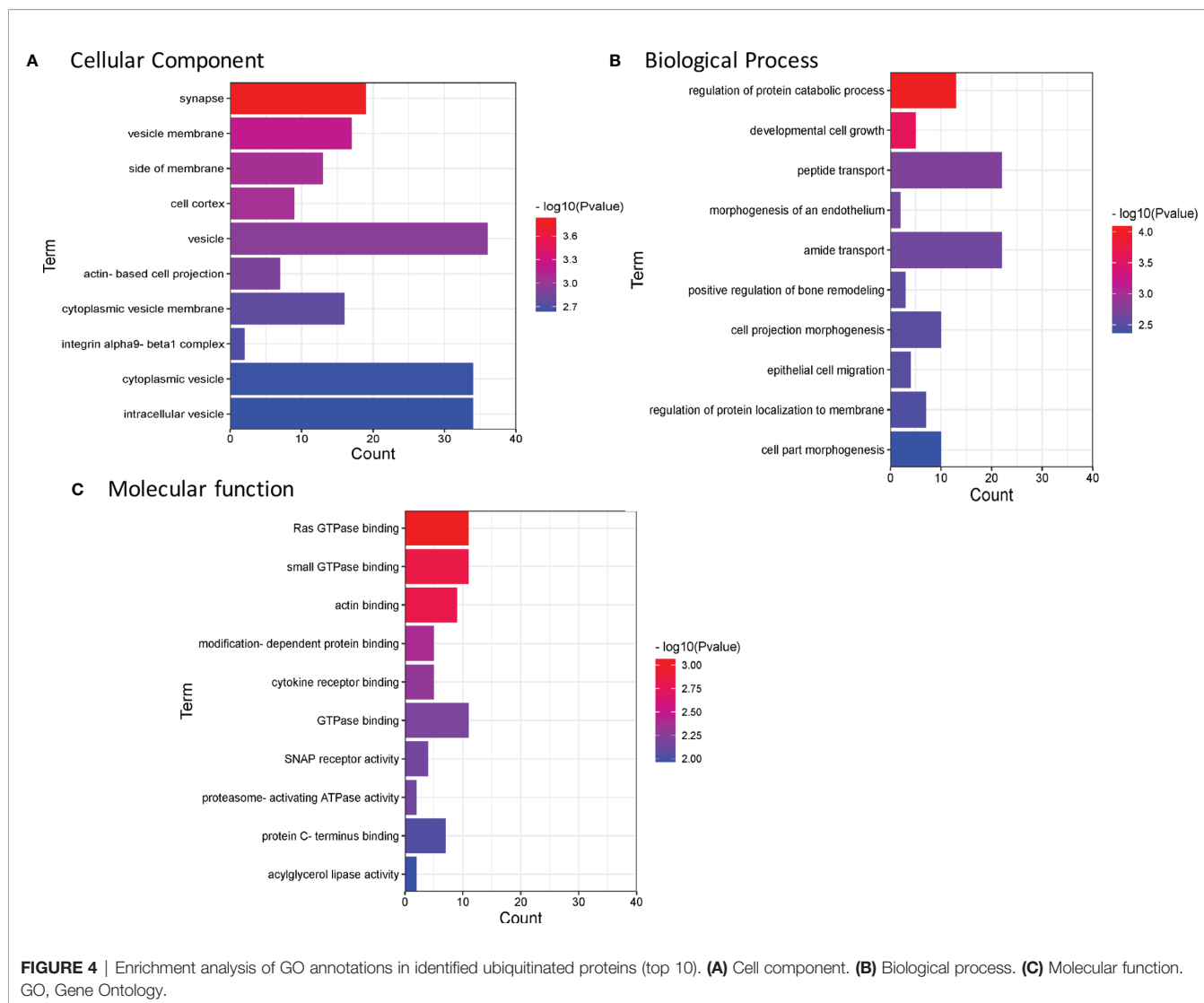
FIGURE 3 | Motif analysis of differently expressed ubiquitination sites. **(A)** Potential ubiquitin recognition motif logos. The height of each letter represents the frequency of the residue in that position. K in the middle represent for the ubiquitinated lysine. **(B)** The number of identified peptides among the three motifs. **(C)** The heatmap for the amino acid distribution flanking ubiquitination sites.

part morphogenesis ($p=4.28E-03$). The most important molecular functions (**Figure 4C**) were related to Ras GTPase binding ($p=8.64E-04$) and small GTPase binding ($p=1.42E-03$). Meanwhile, proteasome-activating ATPase activity pathway ($7.33E-03$) were enriched. Based on the above enrichment analysis result, we concluded that the identified ubiquitinated proteins participate in a variety of biological process and functions.

Meanwhile, Kyoto Encyclopedia of Genes and Genomes (KEGG) was used to analyze the pathway enrichment (**Figure 5A** and **Supplementary Table 3**). The result showed that Rap1 signaling pathway ($p=2.57E-03$), Focal adhesion ($p=1.39E-02$), Synaptic vesicle cycle ($p=3.04E-02$) and SNARE interactions in vesicular transport ($p=4.57E-02$). The above result indicated that ubiquitinated proteins in our profiling

involved in a series of fundamental biological process critical for the development of SCA.

Gene Set Enrichment Analysis (GSEA) was also used for the pathway enrichment of the ubiquitinated proteins (**Figure 5B** and **Supplementary Table 4**). The result showed that the most significant pathways were heme metabolism ($p=2.46E-08$) and protein secretion ($p=1.07E-07$) pathway. There were 6 proteins were enriched in the protein secretion pathway, including EGFR, CLTC, ATP7A, AP2S1, RER1, and ERGIC3, indicated that these ubiquitinated proteins were responsible for protein secretion process. The ubiquitinated levels of these proteins were all decreased (**Table 1**). As the table showed that EGFR had 6 ubiquitinated sites while other proteins had 1 ubiquitinated sites.



Molecular Network of Ubiquitinated Proteins in SCAs

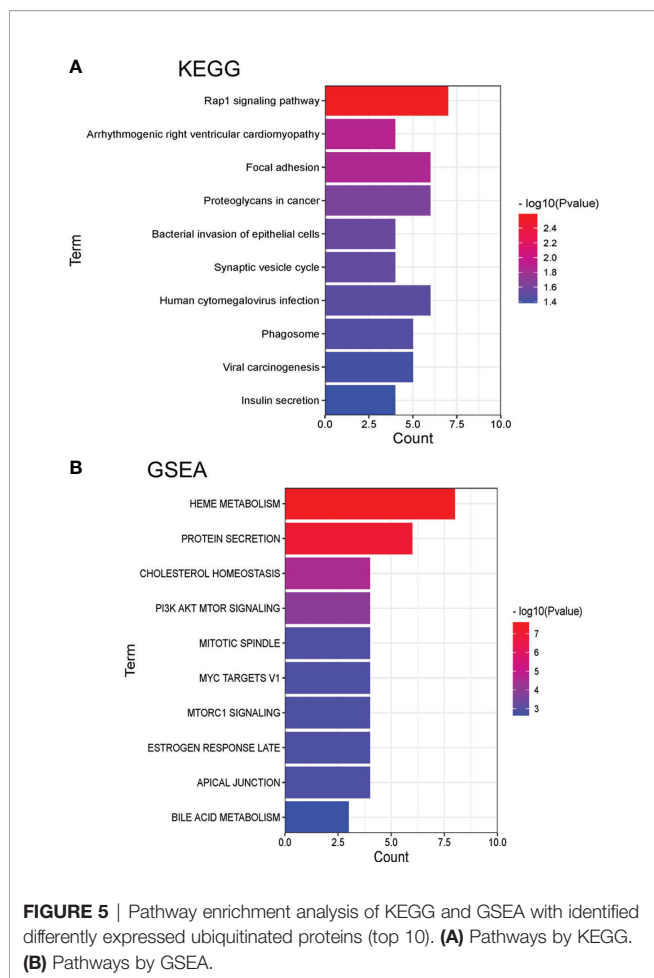
POMC was an important molecule in corticotroph adenomas and were closely related to the secretion of ACTH, so we explored relation between POMC and ubiquitinated proteins. All of the 94 differently ubiquitinated proteins and POMC were analyzed by STRING database to build PPI networks. There are 95 nodes (proteins) and 195 edges (protein-protein associations) in the network (**Figure 6**). The average node degree and average local clustering coefficient in the network were 4.11 and 0.436, respectively. The PPI enrichment p-value of the network was $4.59E-09$, indicating that ubiquitinated proteins in the network exhibit more interactions among themselves than would be expected for a random set of proteins of similar size obtained from the genome. The network indicated that POMC was interacted with ATP6AP1, ATP7A, CHGB, GNAO1, and PRKAR1A. The combined score of POMC and ATP7A was 0.726 (high confidence, interaction score >0.7 , **Table 2**), which was the highest among the 5 POMC related ubiquitinated proteins.

Function of ATP7A in SCAs

ATP7A was ubiquitinated at K333 residue. The ubiquitinated level of ATP7A in SCAs was clearly lower compared to FCAs (ratio of S/F=0.17, $p=0.049$, **Figure 7A**). To validate the function of ATP7A in SCAs, we construct ATP7A siRNA. ATP7A siRNA was transfected to AtT20 cells. ATP7A siRNA result in increased ACTH level in cell culture sodium compared to control groups (**Figure 7B**).

Omeprazole, proved to exert the function of inhibiting ATP7A (14). In our study, omeprazole was used to regulate the expression and detect the function of ATP7A. AtT20 cell was incubated with or without 20uM omeprazole for 72h, and the level of ACTH in culture medium was detected. The result proved that omeprazole increased the expression of ACTH (**Figure 7C**).

38 E3 ligases were predicted to promote the ubiquitination of ATP7A (**Supplemental Table 5**) with high confidence. The top 20 E3 ligases of ATP7A were shown in **Figure 7D**. The top 5 E3 ligases were PRKN, MARCHF7, MUL1, OSTM1, and RC3H1, with the confidence score from 0.85-0.87 and PRKN had the



highest confidence score of 0.87. It suggested that PRKN may be a E3 ligases for ATP7A.

DISCUSSION

Ubiquitination of proteins exhibit a critical role in approximately every biological process (15). This study systematically introduced the ubiquitinome profiling of SCAs. In the study, we identified 94 ubiquitinated proteins with 111 ubiquitinated

sites in SCAs compared to FCAs. The pathway enrichment analysis result showed that ubiquitinated proteins were involved in various of biological process, such as vesicle process and protein secretion process. ATP7A, a ubiquitinated protein enriched in vesicle process and protein secretion process, was proved to be able to regulate the expression of ACTH in AtT20 cells. Our findings may help explain the biological behaviors of SCAs and provide promising targets for advanced treatment for SCAs.

Some vesicles are present in neurons or especially endocrine cells including pituitary cells (16), and responsible for the secretion of pituitary hormones (17). Previous studies confirmed that the release of ACTH required vesicles dock with the cell membrane (18). In our study, we concluded that differently expressed ubiquitinated proteins were obviously involved in many vesicle-related pathways, such as vesicle, cytoplasmic vesicle, and intracellular vesicle. On the other hand, GSEA enrichment analysis showed that differently expressed ubiquitinated proteins were enriched in protein secretion pathway. ACTH is a kind of small molecule protein secreted from cells. Taken together, we speculated that these ubiquitinated proteins enriched in vesicle-related pathways and protein secretion pathway may be involved in ACTH release.

Corticotroph adenomas are immunopositive for ACTH and exhibit with increased circulating ACTH (19). The secretion of ACTH is a flexible process. POMC (Proopiomelanocortin) is a type of polypeptide precursor of neuropeptides and hormones (20). It is cleaved by pro-hormone convertase 1/3 (PC1/3) to yield pro-ACTH and β -LPH (18) in the anterior pituitary. Pro-ACTH was then cleaved by PC1/3 to produce functional ACTH. Meanwhile, ACTH can be cleaved by pro-hormone convertase 2 (PC2) to form α -MSH (21). Different from ACTH, α -MSH need to be amidated by PAM (Peptidylglycine Alpha-Amidating Monooxygenase) enzymes to be active (22). PAM is a kind of peptide-processing enzymes. It catalyzes the post-translational modification of inactive peptidylglycine precursors to the corresponding bioactive alpha-amidated peptides (23). α -MSH is a kind of peptides needs to be amidated and processed by PAM (18). Alpha-amidation involves two sequential reactions, both of which are catalyzed by separate catalytic domains of the enzyme (24). The first step, catalyzed by peptidyl alpha-hydroxylating monooxygenase (PHM) domain, is the copper-, ascorbate-, and O₂- dependent stereospecific hydroxylation (with S stereochemistry) at the alpha-carbon (C-

TABLE 1 | Ubiquitinated proteins enriched in protein secretion pathway by GSEA.

Gene name	S/F Ratio	S/F P value	Regulated Type
EGFR	0.32	0.03	Down
EGFR	0.38	0.01	Down
EGFR	0.13	0.00	Down
EGFR	0.30	0.02	Down
EGFR	0.24	0.03	Down
EGFR	0.23	0.01	Down
CLTC	0.39	0.02	Down
ATP7A	0.17	0.05	Down
AP2S1	0.20	0.01	Down
RER1	0.11	0.04	Down
ERGIC3	0.25	0.01	Down

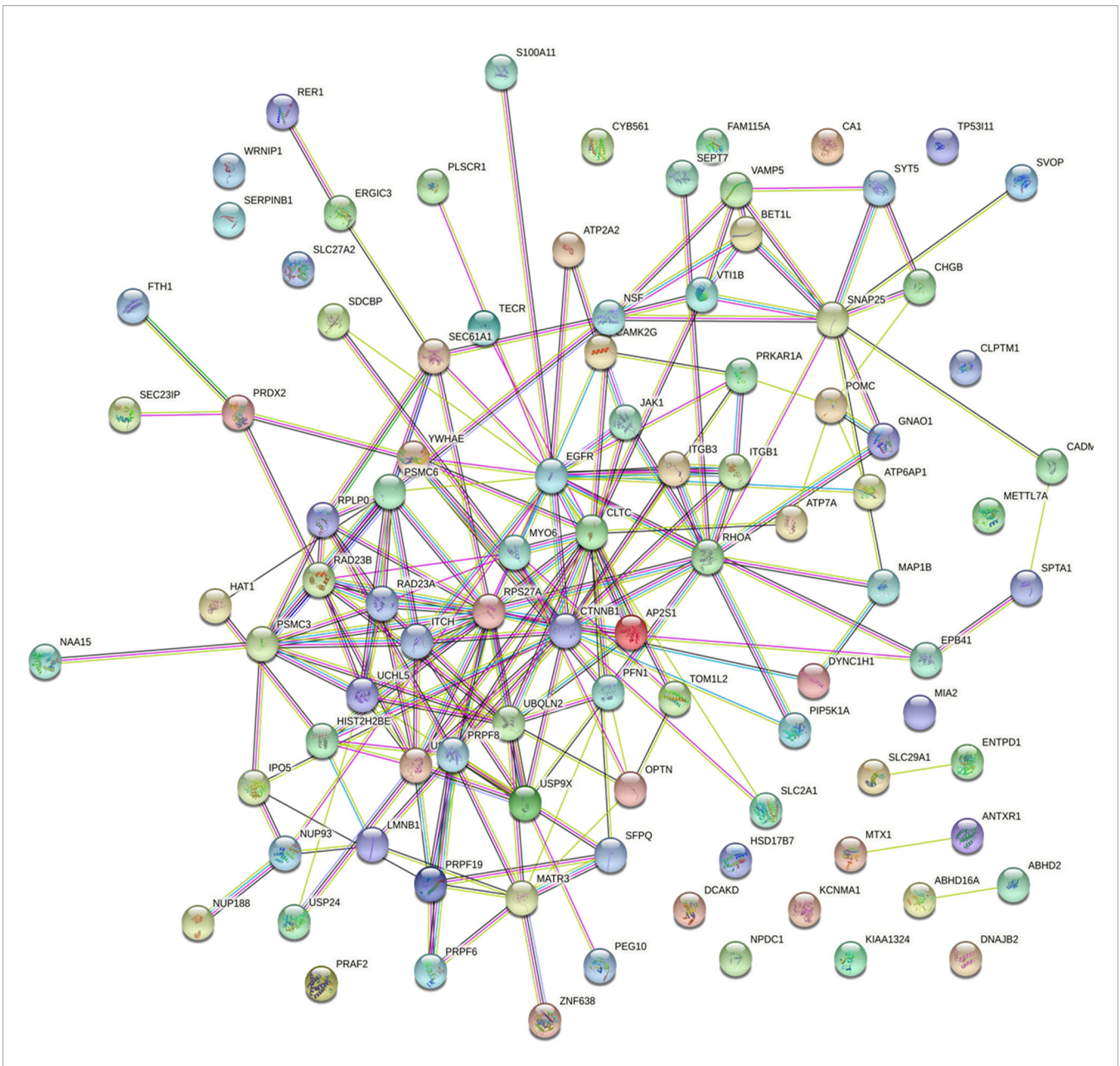


FIGURE 6 | Protein-protein interaction (PPI) network in SCAs.

alpha) of the C-terminal glycine of the peptidylglycine substrate (25). The second step, catalyzed by the peptidylglycine amidoglycolate lyase (PAL) domain, is the zinc-dependent cleavage of the N-C-alpha bond, producing the alpha-amidated

peptide and glyoxylate (26). Several metals are involved in the secretory granule formation of anterior pituitary (27). The accumulation and depot of growth hormone and prolactin in somatotrope and lactotrope secretory granules is separately

TABLE 2 | Proteins interacted with POMC.

#node1	node2	coexpression	database_annotated	automated_textmining	combined_score
POMC	GNAO1	0.062	0.6	0.175	0.663
POMC	ATP7A	0	0	0.726	0.726
POMC	ATP6AP1	0	0	0.508	0.508
POMC	CHGB	0	0	0.427	0.426
POMC	PRKAR1A	0	0	0.602	0.602

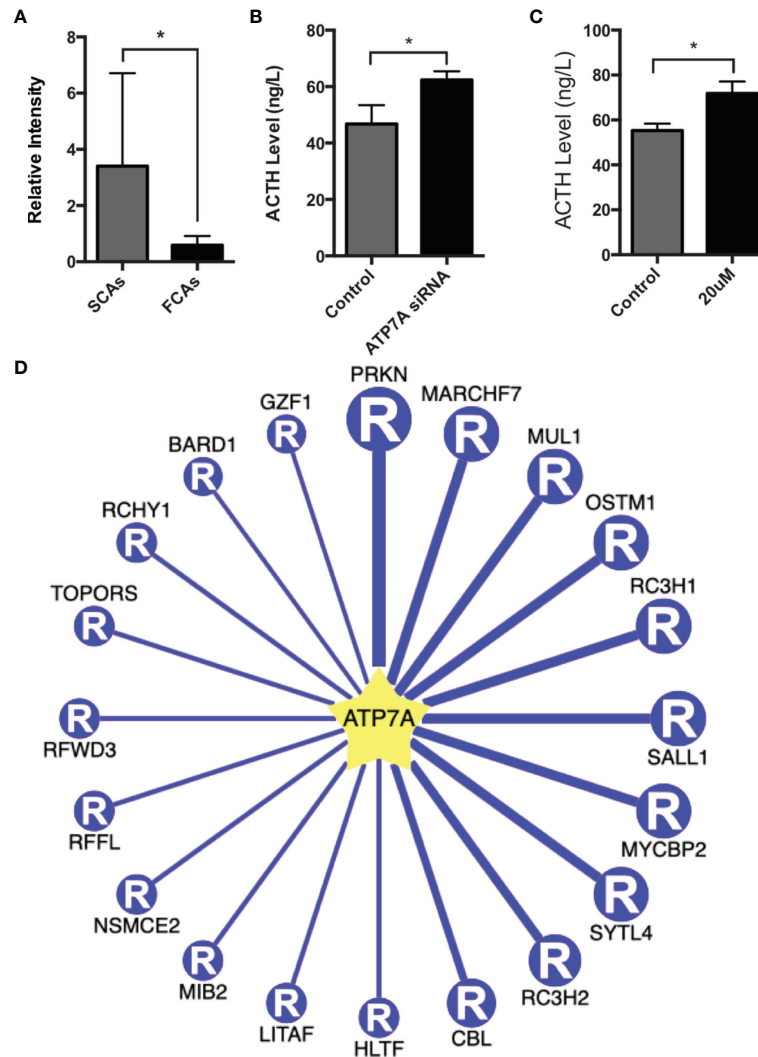


FIGURE 7 | Function of ATP7A in AtT20 cells. **(A)** The intensity of ubiquitinated peptides of ATP7A in SCAs and FCAs. **(B)** Up-regulation of the ACTH level in AtT20 cells with the knockdown of ATP7A by ATP7A siRNA. **(C)** Up-regulation of the ACTH level in AtT20 cells treated with 20uM omeprazole. All assays were performed in triplicate. **(D)** The top 20 potential E3 ligases of ATP7A. *Compared to control, $p < 0.05$.

promoted by zinc (28). ATP7A (ATPase Copper Transporting Alpha) is a copper transporter which plays a critical role in intracellular copper ion homeostasis (29). It may supply copper ion to enzyme PAM in the first step (29). In our study, we identified the decreased ubiquitination of ATP7A in SCAs compared to FCAs. Previous research reported that ubiquitinated proteins were degraded *via* the ubiquitin-proteasome system (UPS) (30). Thus, we speculated that the decreased ubiquitination of ATP7A in SCAs lead to the increased expression of ACTH compared to FCAs. Since ATP7A is crucial for α -MSH amidation by PAM, the high expression of ATP7A tend to produce more α -MSH and contribute to less production of ACTH. This may explain the decreased blood level of ACTH in SCAs.

Moreover, ATP7A was a crucial ubiquitinated protein enriched in both vesicle-related pathway and protein secretion

pathway. It may regulate the ACTH release by protein secretion pathway and vesicle process. There was a study revealed that omeprazole inhibits the function of ATP7A, since ATP7A is a P-type ATPase (14). So we choose omeprazole to block the expression of ATP7A in AtT20 cells. *In vitro* assay proved that omeprazole may up-regulate the level of ACTH. PRKN was predicted to be a E3 ligases for ATP7A with a high confidence score. It suggests that ATP7A and PRKN may be potential targets for the treatment of SCAs. ATP7A is a potential ubiquitinated protein which was speculated to be a molecule associated with the decreased expression of the ACTH secretion. Ubiquitination is a kind of post-translational modification that leads to the degradation of proteins (1). Hence, we speculated that the ubiquitination of ATP7A contribute to the decreased expression of ATP7A. So we used ATP7A siRNA and 20uM

omeprazole to change the expression of ATP7A to imitate the function of ubiquitination of ATP7A. However, besides of the function of degradation of proteins, ubiquitination exerts other function on proteins. Here is a limitation that we have not detect the function of ATP7A (K333) in cells. We are now doing this part of work and will report the result in the future study.

4D label-free mass spectrometer is an efficient method to identify differently ubiquitinated proteins and ubiquitination sites in SCAs. Totally 111 differently expressed ubiquitination sites were identified between SCAs and FCAs which mapped to 94 ubiquitinated proteins. Pathway enrichment analysis proved the ubiquitinated proteins were obviously contained in vesicles and involved in protein transport and release. We detected the function of ATP7A in AtT20 cells. Our ubiquitinome profiling result declared the differently expressed ubiquitination sites and proteins in SCAs and FCAs, and also classified the candidate proteins to investigate the hidden mechanism for the decreased expression of ATP7A in SCAs. These discoveries contribute to further researched about the adjustment of ubiquitination in SCAs.

DATA AVAILABILITY STATEMENT

The original contributions presented in the study are included in the article/**Supplementary Material**. Further inquiries can be directed to the corresponding authors.

REFERENCES

- Nishioka H, Inoshita N, Mete O, Asa SL, Hayashi K, Takeshita A, et al. The Complementary Role of Transcription Factors in the Accurate Diagnosis of Clinically Nonfunctioning Pituitary Adenomas. *Endocrine Pathol* (2015) 26:349–55. doi: 10.1007/s12022-015-9398-z
- Ben-Shlomo A, Cooper O. Silent Corticotroph Adenomas. *Pituitary* (2018) 21:183–93. doi: 10.1007/s11102-018-0864-8
- Langlois F, Lim DST, Yedinak CG, Cetas I, McCartney S, Cetas J, et al. Predictors of Silent Corticotroph Adenoma Recurrence; a Large Retrospective Single Center Study and Systematic Literature Review. *Pituitary* (2018) 21:32–40. doi: 10.1007/s11102-017-0844-4
- Jiang S, Chen X, Wu Y, Wang R, Bao X. An Update on Silent Corticotroph Adenomas: Diagnosis, Mechanisms, Clinical Features, and Management. *Cancers (Basel)* (2021) 13(23):6134. doi: 10.3390/cancers13236134
- Kovacs K, Horvath E, Bayley TA, Hassaram ST, Ezrin C. Silent Corticotroph Cell Adenoma With Lysosomal Accumulation and Crinophagy A Distinct Clinicopathologic Entity. *Am J Med* (1978) 64:492–9. doi: 10.1016/0002-9343(78)90236-X
- Matsuno A, Okazaki R, Oki Y, Nagashima T. Secretion of High-Molecular-Weight Adrenocorticotrophic Hormone From a Pituitary Adenoma in a Patient Without Cushing Stigmata. *Case Rep J Neurosurg* (2004) 101:874–7. doi: 10.3171/jns.2004.101.5.0874
- Kojima Y, Suzuki S, Yamamura K, Ohhashi G, Yamamoto I. Comparison of ACTH Secretion in Cushing's Adenoma and Clinically Silent Corticotroph Adenoma by Cell Immunoblot Assay. *Endocr J* (2002) 49:285–92. doi: 10.1507/endocrj.49.285
- Roberts JZ, Crawford N, Longley DB. The Role of Ubiquitination in Apoptosis and Necroptosis. *Cell Death Differ* (2022) 29(2):272–84. doi: 10.1038/s41418-021-00922-9
- Lu M, Chen W, Zhuang W, Zhan X. Label-Free Quantitative Identification of Abnormally Ubiquitinated Proteins as Useful Biomarkers for Human Lung

ETHICS STATEMENT

The studies involving human participants were reviewed and approved by Ethics committees of Beijing Tiantan Hospital (KY2018-053-02). The patients/participants provided their written informed consent to participate in this study.

AUTHOR CONTRIBUTIONS

SZ have drafted the work or substantively revised it. HW, DL, and YH collected tumor samples and analysis the data. LG interpret the data, YZ and CL contribute to the conception of the work. All authors contributed to the article and approved the submitted version.

FUNDING

This work is supported by the National Natural Science Foundation of China (82103048, 81771489, 82072804, 82071559).

SUPPLEMENTARY MATERIAL

The Supplementary Material for this article can be found online at: <https://www.frontiersin.org/articles/10.3389/fendo.2022.863017/full#supplementary-material>

- Squamous Cell Carcinomas. *EPMA J* (2020) 11:73–94. doi: 10.1007/s13167-019-00197-8
- Fulda S, Rajalingam K, Dikic I. Ubiquitylation in Immune Disorders and Cancer: From Molecular Mechanisms to Therapeutic Implications. *EMBO Mol Med* (2012) 4:545–56. doi: 10.1002/emmm.201100707
- Herhaus L, Dikic I. Expanding the Ubiquitin Code Through Post-Translational Modification. *EMBO Rep* (2015) 16:1071–83. doi: 10.15252/embr.201540891
- Sesta A, Cassarino MF, Terreni M, Ambrogio AG, Libera L, Bardelli D, et al. Ubiquitin-Specific Protease 8 Mutant Corticotrope Adenomas Present Unique Secretory and Molecular Features and Shed Light on the Role of Ubiquitylation on ACTH Processing. *Neuroendocrinology* (2020) 110:119–29. doi: 10.1159/000500688
- Li Y, Xie P, Lu L, Wang J, Diao LH, Liu ZY, et al. An Integrated Bioinformatics Platform for Investigating the Human E3 Ubiquitin Ligase-Substrate Interaction Network. *Nat Commun* (2017) 8(1):347. doi: 10.1038/s41467-017-00299-9
- Matsui MS, Petris MJ, Niki Y, Karaman-Jurukovska N, Muizzuddin N, Ichihashi M, et al. Omeprazole, a Gastric Proton Pump Inhibitor, Inhibits Melanogenesis by Blocking ATP7A Trafficking. *J Invest Dermatol* (2015) 135:834–41. doi: 10.1038/jid.2014.461
- Yu X, Zhu Y, Xie Y, Li L, Jin Z, Shi Y, et al. Ubiquitylomes and Proteomes Analyses Provide a New Interpretation of the Molecular Mechanisms of Rice Leaf Senescence. *Planta* (2022) 255:43. doi: 10.1007/s00425-021-03793-z
- Zorec R, Sikdar SK, Mason WT. Increased Cytosolic Calcium Stimulates Exocytosis in Bovine Lactotrophs Direct Evidence From Changes in Membrane Capacitance. *J Gen Physiol* (1991) 97:473–97. doi: 10.1085/jgp.97.3.473
- Kreft M, Jorgacevski J, Stenovec M, Zorec R. Angstrom-Size Exocytotic Fusion Pore: Implications for Pituitary Hormone Secretion. *Mol Cell Endocrinol* (2018) 463:65–71. doi: 10.1016/j.mce.2017.04.023

18. Harno E, Gali Ramamoorthy T, Coll AP, White A. POMC: The Physiological Power of Hormone Processing. *Physiol Rev* (2018) 98:2381–430. doi: 10.1152/physrev.00024.2017
19. Nieman LK, Biller BM, Findling JW, Newell-Price J, Savage MO, Stewart PM, et al. The Diagnosis of Cushing's Syndrome: An Endocrine Society Clinical Practice Guideline. *J Clin Endocrinol Metab* (2008) 93:1526–40. doi: 10.1210/jc.2008-0125
20. Toda C, Santoro A, Kim JD, Diano S. POMC Neurons: From Birth to Death. *Annu Rev Physiol* (2017) 79:209–36. doi: 10.1146/annurev-physiol-022516-034110
21. Benjannet S, Rondeau N, Day R, Chretien M, Seidah NG. PC1 and PC2 Are Proprotein Convertases Capable of Cleaving Proopiomelanocortin at Distinct Pairs of Basic Residues. *Proc Natl Acad Sci USA* (1991) 88:3564–8. doi: 10.1073/pnas.88.9.3564
22. Kumar D, Mains RE, Eipper BA. 60 YEARS OF POMC: From POMC and Alpha-MSH to PAM, Molecular Oxygen, Copper, and Vitamin C. *J Mol Endocrinol* (2016) 56:T63–76. doi: 10.1530/JME-15-0266
23. Satani M, Takahashi K, Sakamoto H, Harada S, Kaida Y, Noguchi M. Expression and Characterization of Human Bifunctional Peptidylglycine Alpha-Amidating Monooxygenase. *Protein Expr Purif* (2003) 28:293–302. doi: 10.1016/S1046-5928(02)00684-8
24. Bousquet-Moore D, Mains RE, Eipper BA. Peptidylglycine Alpha-Amidating Monooxygenase and Copper: A Gene-Nutrient Interaction Critical to Nervous System Function. *J Neurosci Res* (2010) 88:2535–45. doi: 10.1002/jnr.22404
25. Bell J, El Meskini R, D'Amato D, Mains RE, Eipper BA. Mechanistic Investigation of Peptidylglycine Alpha-Hydroxylating Monooxygenase via Intrinsic Tryptophan Fluorescence and Mutagenesis. *Biochemistry* (2003) 42:7133–42. doi: 10.1021/bi034247v
26. Prigge ST, Kolhekar AS, Eipper BA, Mains RE, Amzel LM. Amidation of Bioactive Peptides: The Structure of Peptidylglycine Alpha-Hydroxylating Monooxygenase. *Science* (1997) 278:1300–5. doi: 10.1126/science.278.5341.1300
27. Bonnemaïson ML, Duffy ME, Mains RE, Vogt S, Eipper BA, Ralle M. Copper, Zinc and Calcium: Imaging and Quantification in Anterior Pituitary Secretory Granules. *Metallomics* (2016) 8:1012–22. doi: 10.1039/C6MT00079G
28. Suckale J, Solimena M. The Insulin Secretory Granule as a Signaling Hub. *Trends Endocrinol Metab* (2010) 21:599–609. doi: 10.1016/j.tem.2010.06.003
29. Skjorringe T, Amstrup Pedersen P, Salling Thorborg S, Nissen P, Gourdon P, Birk Moller L. Characterization of ATP7A Missense Mutants Suggests a Correlation Between Intracellular Trafficking and Severity of Menkes Disease. *Sci Rep* (2017) 7:757. doi: 10.1038/s41598-017-00618-6
30. Nandi D, Tahiliani P, Kumar A, Chandu D. The Ubiquitin-Proteasome System. *J Biosci* (2006) 31:137–55. doi: 10.1007/BF02705243

Conflict of Interest: The authors declare that the research was conducted in the absence of any commercial or financial relationships that could be construed as a potential conflict of interest.

Publisher's Note: All claims expressed in this article are solely those of the authors and do not necessarily represent those of their affiliated organizations, or those of the publisher, the editors and the reviewers. Any product that may be evaluated in this article, or claim that may be made by its manufacturer, is not guaranteed or endorsed by the publisher.

Copyright © 2022 Zhao, He, Wang, Li, Gong, Zhang and Li. This is an open-access article distributed under the terms of the Creative Commons Attribution License (CC BY). The use, distribution or reproduction in other forums is permitted, provided the original author(s) and the copyright owner(s) are credited and that the original publication in this journal is cited, in accordance with accepted academic practice. No use, distribution or reproduction is permitted which does not comply with these terms.



OPEN ACCESS

EDITED BY
Dragana Nikitovic,
University of Crete, Greece

REVIEWED BY
Atit Silsirivanit,
Khon Kaen University, Thailand
David Mitchell Lubman,
University of Michigan, United States

*CORRESPONDENCE
Xianquan Zhan
yjzhan2011@gmail.com

SPECIALTY SECTION
This article was submitted to
Cancer Endocrinology,
a section of the journal
Frontiers in Endocrinology

RECEIVED 16 June 2022
ACCEPTED 02 August 2022
PUBLISHED 22 August 2022

CITATION
Guo Y, Jia W, Yang J and Zhan X
(2022) Cancer glycomics offers
potential biomarkers and
therapeutic targets in the
framework of 3P medicine.
Front. Endocrinol. 13:970489.
doi: 10.3389/fendo.2022.970489

COPYRIGHT
© 2022 Guo, Jia, Yang and Zhan. This is
an open-access article distributed under
the terms of the [Creative Commons
Attribution License \(CC BY\)](https://creativecommons.org/licenses/by/4.0/). The use,
distribution or reproduction in other
forums is permitted, provided the
original author(s) and the copyright
owner(s) are credited and that the
original publication in this journal is
cited, in accordance with accepted
academic practice. No use,
distribution or reproduction is
permitted which does not comply with
these terms.

Cancer glycomics offers potential biomarkers and therapeutic targets in the framework of 3P medicine

Yuna Guo^{1,2}, Wenshuang Jia^{1,2}, Jingru Yang^{1,2}
and Xianquan Zhan^{1,2*}

¹Shandong Key Laboratory of Radiation Oncology, Shandong Cancer Hospital and Institute, Shandong First Medical University, Jinan, China, ²Medical Science and Technology Innovation Center, Shandong First Medical University, Jinan, China

Glycosylation is one of the most important post-translational modifications (PTMs) in a protein, and is the most abundant and diverse biopolymer in nature. Glycans are involved in multiple biological processes of cancer initiation and progression, including cell-cell interactions, cell-extracellular matrix interactions, tumor invasion and metastasis, tumor angiogenesis, and immune regulation. As an important biomarker, tumor-associated glycosylation changes have been extensively studied. This article reviews recent advances in glycosylation-based biomarker research, which is useful for cancer diagnosis and prognostic assessment. Truncated O-glycans, sialylation, fucosylation, and complex branched structures have been found to be the most common structural patterns in malignant tumors. In recent years, immunochemical methods, lectin recognition-based methods, mass spectrometry (MS)-related methods, and fluorescence imaging-based *in situ* methods have greatly promoted the discovery and application potentials of glycomic and glycoprotein biomarkers in various cancers. In particular, MS-based proteomics has significantly facilitated the comprehensive research of extracellular glycoproteins, increasing our understanding of their critical roles in regulating cellular activities. Predictive, preventive and personalized medicine (PPPM; 3P medicine) is an effective approach of early prediction, prevention and personalized treatment for different patients, and it is known as the new direction of medical development in the 21st century and represents the ultimate goal and highest stage of medical development. Glycosylation has been revealed to have new diagnostic, prognostic, and even therapeutic potentials. The purpose of glycosylation analysis and utilization of biology is to make a fundamental change in health care and medical practice, so as to lead medical research and practice into a new era of 3P medicine.

KEYWORDS

glycosylation, cancer biomarker, immunochemical method, lectin recognition, mass spectrometry, fluorescence imaging, immunotherapy, 3P medicine

1 Introduction

Post-translational modifications (PTMs) are chemical modifications of proteins during or after translation (1, 2), which include phosphorylation (3), glycosylation (4), ubiquitination (5), acetylation (6), alkylation (7), nitration (8), etc., according to the functional groups modified (1–8). Of these, glycosylation is the most common type of PTMs, and approximately half of all proteins in the human body are glycosylated (9). Glycosylation is a basic enzymatic modification in which glycans are covalently linked to proteins or lipids under the action of enzymes to form glycoproteins and lipopolysaccharides, respectively (4). Glycoproteins are divided into *N*-linked and *O*-linked glycosylations according to the modification site. *N*-glycosylation covalently modifies *N*-acetylglucosamine (GlcNAc) to the nitrogen atom on the side chain of asparagine (Asn). *O*-glycosylation covalently modifies *N*-acetylgalactosamine (GalNAc) to the oxygen atom of a serine (Ser) or threonine (Thr) residue (4, 9). Glycosylation is the most complex PTM process. The diversity of monosaccharides and their combinations greatly increases the diversity of the glycoproteome (10). Glycosylation affects the spatial conformation, activity, and stability of a protein, which in turn affects its subcellular localization and protein-protein interactions (11). Glycosylation is involved in a series of cancer pathophysiological processes, which offers effective and reliable biomarkers for patient stratification, early diagnosis, and prognostic assessment of cancer patients, and effective therapeutic targets/drugs for targeted prevention, and personalized therapy of cancer, in the framework of predictive, preventive, and personalized medicine (PPPM; 3P medicine).

2 Structure and functions of glycosylation

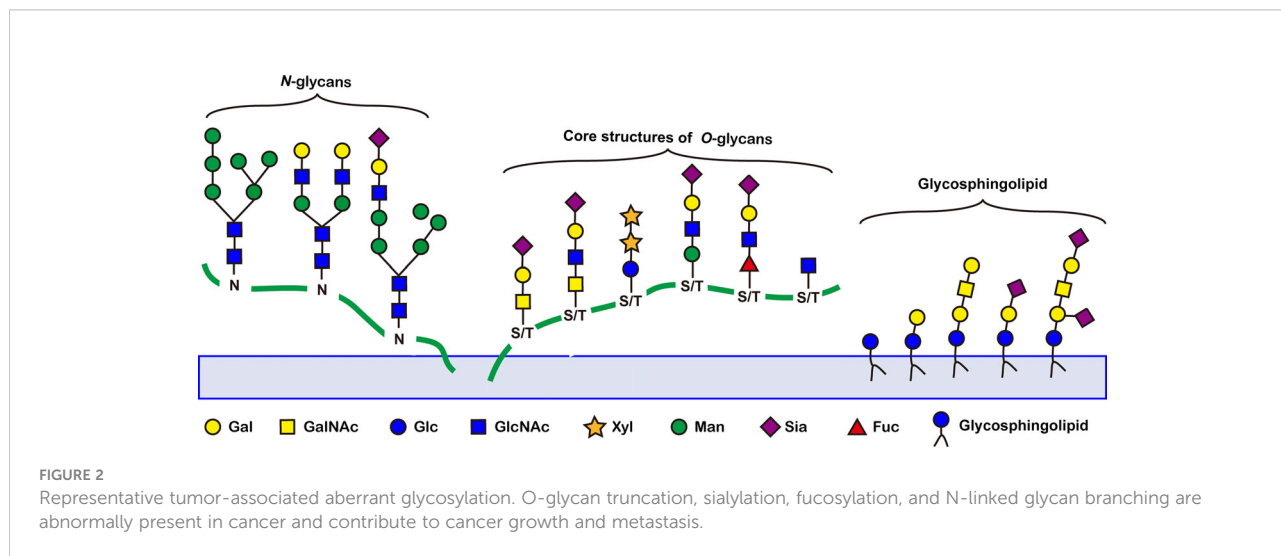
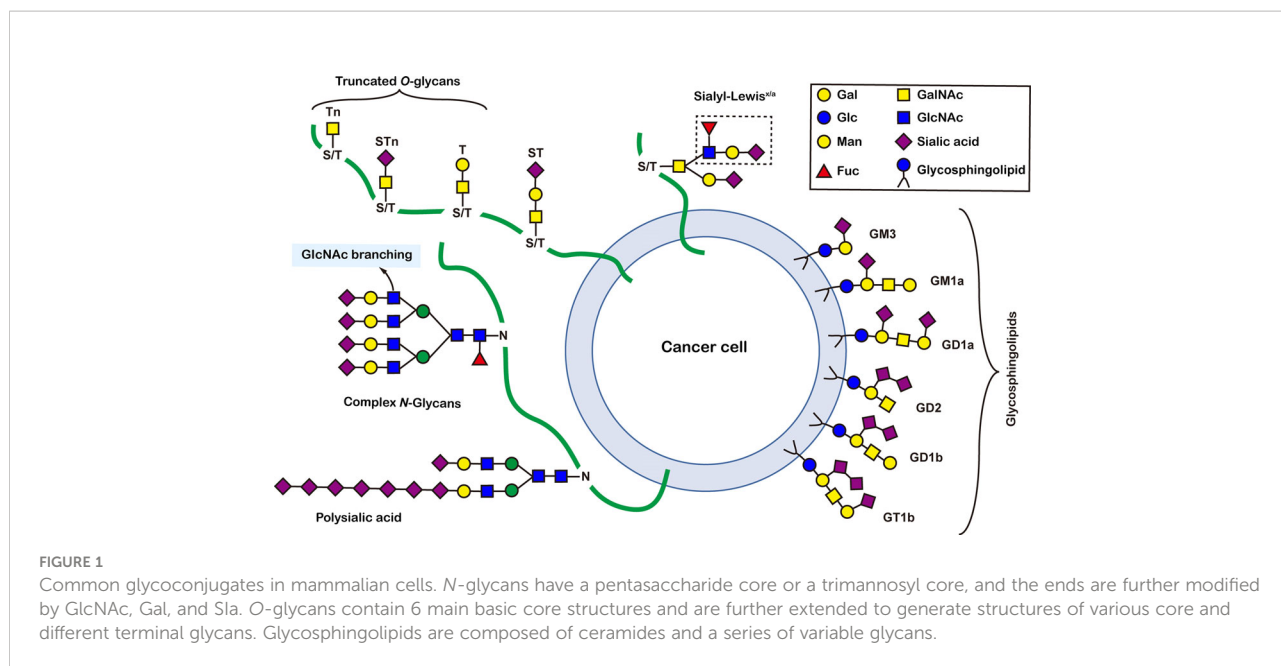
There are more than seven thousand configurations of glycan chains in mammals (9). Ten kinds of monosaccharides, namely glucose (Glc), galactose (Gal), mannose (Man), xylose (Xyl), fucose (Fuc), GlcNAc, GalNAc, glucuronic acid (GlcA), iduronic acid (IDOA), and sialic acid (Sia) are the main monomers for glycosylation (4, 9). Glycosylation is a non-templated and highly coordinated process that requires coordination between different glycosyltransferases, glycosidases, nucleotide sugar transporters, and appropriate substrates. Glycosylation changes rapidly with the changes of physiological and pathological conditions (4, 9). Unlike other general types of PTMs such as phosphorylation and ubiquitination that occur in the cytoplasm or nucleus, most glycosylation processes, with the exception of *O*-GlcNAcylation, occur in the endoplasmic reticulum (ER) and the lumen of the Golgi apparatus middle (10). *N*-glycosylations occur in a very large number of proteins and play key roles to regulate many intracellular and extracellular functions. The structural features of *N*-glycans are that they contain a GlcNAc₂(Man)₃ core, with the addition or

removal of other monosaccharides (Figure 1). These additives include Gal, GlcNAc, Sia, and Fuc. *N*-glycosylation in cells starts in ER, and is generally completed in Golgi apparatus. Many glycoproteins have both *N*- and *O*-linked sugar chains. *O*-glycans contain 6 major basic core structures that occur on amino acids with functional hydroxyl groups. *O*-glycosylation takes place in the Golgi apparatus, usually the first linked sugar unit is *N*-GalNAc, and then the sugars are sequentially transferred onto it to form oligosaccharide chains. Glycosylation changes the conformation of polypeptides and increases protein stability (11). Glycosphingolipids are composed of ceramides and oligosaccharide chains, and are common components of eukaryotic plasma membranes. Glycosphingolipids play an important role in cell recognition and communication, especially in the nervous system. In recent years, abnormal glycosylation has received more and more attention in cancer research, mainly in two aspects: (i) Aberrant glycosylation is a non-invasive tumor biomarker, and most FDA-approved tumor markers are glycoprotein or glycan antigens (12). (ii) Glycosylation plays an important role in the occurrence, development, and metastasis of cancer. Researches have shown that glycosylation is associated with cell proliferation, invasion, cell-cell interactions, and cell-matrix interactions (13). In addition, abnormal glycosylation also affects immune regulation (14) and promotes tumor metastasis (15). These have facilitated the development of efficient and innovative analytical methods for glycosylation.

3 Aberrant glycosylation in tumors

Abnormal glycosylation is a hallmark of cancer. A number of tumor-associated aberrant glycosylation (Figure 2), such as *O*-linked glycan (16–25), sialylation (26–42), fucosylation (43–48), *N*-linked glycan branching (13), are aberrantly present in cancer and contribute to cancer growth and metastasis (Table 1). The exploration of aberrant glycosylation that accompanies tumorigenesis and progression began in the 1960s (16, 17). Lectins were used to compare the glycosylation difference between breast cancer and normal cells, which found that tumor cells had stronger binding affinity for lectins, indicating that tumor cells have a higher abundance of specific mucopolysaccharides (17). Mucin is one of the earliest breast cancer serum biomarkers, and truncated *O*-glycans are found in 90% of breast cancers (18). Truncated *O*-glycans, also known as CA72-4 antigen, including Tn (GalNAc-Ser/Thr), T (gal-GalNAc-Ser/Thr), and Sia-Tn (STn, Sia-GalNAc -Ser/Thr) (19). Truncated *O*-glycans are one of the representatives of abnormal glycans in cancer, with increased expressions in gastric (20), pancreatic (21), ovarian (22), bladder (23), and colon cancers (24). STn that is associated with tumor recurrence is considered an important prognostic biomarker, and has been used as a target for antitumor vaccine design (25).

By the 1980s, researchers successively discovered that glycosyltransferase activity was differentially expressed between normal and tumor cells. Especially compared to normal cells,



tumor cell sialyltransferase and fucosyltransferase activities were significantly increased (26, 27). Abnormally high expressions of Sia and Fuc were quickly recognized as a tumor biomarker due to altered glycosyltransferase expressions. Sialylation is an important modification of cellular glycosylation, and sialylation plays an important role in cell-cell interactions and signal transduction (28). Lewis antigens, including sialyl-Lewis X (SLe_x, α1,3 fucosylation) and sialyl-Lewis A (SLe_a, α1,4 fucosylation), also known as CA19-9, are highly expressed in many malignancies (29–33), such as pancreatic (29), colonic (30), gastric (31), breast (32), and biliary tract (33) cancers, and high expression of CA19-9 is associated with poor survival in

cancer patients (34). Polysialic acid is an α-2,8-glycosidically linked polymer of Sia, usually expressed as *N*-glycans on neural cell adhesion molecule 1 (NCAM1) (35). The abnormal expression of polysialic acid is associated with the occurrence of lung cancer (35), breast cancer (36), and neuroblastoma (37), and is associated with poor prognosis (38). The increased level of sialylation also involves overexpression of gangliosides (39–42). Gangliosides refer to sialylated glycosphingolipids that are abnormally expressed in tumors such as neuroblastoma (39), lung cancer (40), cervical cancer (41), and breast cancer (42).

Fucosylation plays an important role in tumor pathology, including regulation of signaling pathways and tumor metastasis

TABLE 1 Representative glycosylated protein or glycan biomarkers in tumors.

Cancer	Biomarkers	Sample types	Methods	Effect	Reference
Breast cancer	LY6G6F, VWF, BSG, C1QA, ANGPT1, CDH6	Serum of human	LC-MS	Diagnosis	(12)
Breast cancer	Mucin	Cell of human	Lectin method	Diagnosis	(17)
Breast cancer	Tn	Tissue of mouse	Immunohistological	Functional reseach	(18)
Gastric cancer	Mucin	Tissue of mouse	ELISA	Functional reseach	(20)
Pancreatic cancer	Tn, T, sTn	Tissue of mouse	Immunohistological	Functional reseach	(21)
Ovarian cancer	Tn, T, sTn	Cell of human	Immunohistological	Functional reseach	(22)
Colorectal cancer	Tn	Tissue of human	WB	Diagnosis	(24)
Pancreatic cancer	CA19-9	Tissue of mouse	Immunohistological	Functional reseach	(29)
Colorectal Cancer	CEA, CA19-9	Tissue of human	Public DataBase	Statistics	(30)
Gastric cancer	CEA, CA19-9, CA72-4	Tissue of human	ELISA	Diagnosis	(31)
Metastatic breast cancer	CA15.3, CEA, CA-125, CA19.9	Serum of human	ELISA	Diagnosis	(32)
Gallbladder carcinoma	CA19-9 and CEA	Serum of human	ELISA	Diagnosis	(33)
Breast cancer	Polysialic acid	Tissue of human	HPLC	Diagnosis, functional reseach	(36)
Neuroblastoma	Polysialic acid	Cell of human	WB	Functional reseach	(37)
Cervical cancer	GM1	Serum of human	PCR	Functional reseach	(41)
Breast cancer	GM3	Serum of human	LC-MS	Diagnosis	(42)
Hepatocellular carcinoma	AFP-L3	Serum of human	ELISA	Diagnosis	(44)
Ovarian cancer	Integrins and haptoglobin	Tissue of human	Immunofluorescence	Functional reseach	(45)
Gastric cancer	Haptoglobin	Serum of human	TOF-MS	Diagnosis	(46)
Pancreatic cancer	Fucosylated haptoglobin	Serum of human	L-ELISA	Diagnosis	(47)
Lung cancer	Sialylation, fucosylation	Cell of human	MALDI-TOF MS	Functional reseach	
Lung cancer	Hsp90 α	Serum of human	ELISA	Diagnosis	(49)
Liver cancer	AFP	Serum of human	ELISA	Diagnosis	(50)
Breast cancer	AFP	Cell of huma	ELISA	Diagnosis	(51)
Pancreatic cancer	SLex	Tissue of human	Immunofluorescence	Diagnosis	(52)
Pancreatic cancer	MUC6, GlcNAc	Cell and tissue of human	WB	Functional reseach	(53)
Breast cancer	CD82	Tissue of human	Immunohistochemical	Diagnosis	(54)
Lung Cancer	EGFR	Cell	WB	Functional reseach	(55)
Prostate cancer	PSA	Serum and urine of human	L-ELISA	Functional reseach	(56)
Breast cancer	CA15-3	Serum of human	L-ELISA	Diagnosis	(57)
Breast Cancer	Alpha-1-acid glycoprotein (AGP)	Serum of human	ELISA	Diagnosis	(58)
Pancreatic cancer	Sialylation	Tissue of human	Lectin microarray	Functional reseach	(59)
Liver cancer	Tn, α -GalNAc, GlcNAc, Sia	Tissue of human	Lectin microarray	Functional reseach	(60)
Ovarian cancer	Complex N-glycans	Tissue of human	MS	Functional reseach	(61)
Colorectal cancer	Complex N-glycans		MS	Functional reseach	(62)
Triple-negative breast cancer	Polylectosamines	Tissue of human	MS	Functional reseach	(63)
Non-small Cell Lung	Sialylation, fucosylation	Cell of human	MS	Functional reseach	(64)
Colorectal cancer	Carcinoembryonic antigen (CEA)	Tissue of human	MS	Diagnosis	(65)
Liver cancer	GlcNAc, Sialylation, fucosylation	Serum of human	MS	Diagnosis	(66)

(43). Aberrant fucosylation has been reported in many cancer types, such as the Lewis antigen is typically associated with tumor progression and metastasis (29–33). The FDA-approved core fucosylated α -fetoprotein (AFP-L3) is widely used as an early diagnosis of hepatocellular carcinoma, and AFP-L3 is more specific than AFP (44). Blood samples from 2447 patients were

analyzed for both AFP and AFP-L3. The sensitivity, specificity, and diagnostic odds ratio of AFP and AFP-L3 for hepatocellular carcinoma were analyzed and compared, which found that AFP-L3 had high-specificity and low-sensitivity in diagnosing early hepatocellular carcinoma. It suggests that AFP-L3 could be used to exclude hepatocellular carcinoma in the presence of elevated

AFP. Haptoglobin is a protein normally present in the blood that promotes angiogenesis (43). Fucosylated haptoglobin is associated with a variety of diseases, including ovarian (45), gastric (46), and pancreatic (47) cancers. The sensitivity of fucosylated haptoglobin to pancreatic cancer exceeds CA19-9 and CEA (47). When Fuc is highly expressed in epidermal growth factor receptor (EGFR), EGFR dimerization and phosphorylation are increased, and EGFR-mediated tumor cell growth and malignancy-related signaling pathways are increased (48).

4 Recent advances in glycomics-based biomarker discovery

Since tumor-associated glycosylation alterations are a distinct feature of cancer diagnosis and prognosis, a great deal of effort has been devoted to identify, label, and characterize glycosylation in recent years. Four types of glycosylation research tools have been developed, including immunochemical methods, lectin recognition-based methods, mass spectrometry (MS)-related methods, and fluorescence imaging-based *in situ* analysis methods. These studies not only focus on the analysis of glycosylation, but also reveal the regulatory mechanism of glycosylation.

4.1 Immunochemical methods

Immunochemical methods mainly include enzyme-linked immunosorbent assay (ELISA) and western blotting (WB). ELISA uses specific antibodies to specifically recognize and quantify glycans/glycosylated proteins of interest (67). ELISA is widely used in clinical disease diagnosis and is the gold standard (68) for protein detection due to its simple sample pretreatment and quick results. Four main types of ELISAs, including direct, indirect, sandwich, and competition, are used (Figure 3) (49, 67, 68). (i) For the direct method (Figure 3A), the target is adhered to the well plate, the HRP-labeled antibody binds to the antigen (target), and the enzyme catalyzes the chromogenic substrate to produce a visible colorimetric output, which is measured by a UV-Vis spectrophotometer. The concentration of the analyte is proportional to the intensity of the color. (ii) For the indirect method (Figure 3B), the target is adhered to the well plate, the enzyme is bound to the secondary antibody that can recognize the primary antibody, and the signal recognized by the primary antibody is displayed by the secondary antibody. The enzyme catalyzes a chromogenic substrate, and the degree of color development is proportional to the concentration of the analyte. (iii) For the sandwich method (Figure 3C), the captured antibody is adhered to the well plate, the antigen in the analyte is bound to the captured antibody, and the HRP-labeled antibody binds to the antigen and catalyzes the coloration of the substrate. Sandwich methods

generally have higher sensitivity and specificity than direct and indirect methods. For the competition method (Figure 3D), both the target and competitor can bind the HRP-labeled antibody. The more antigens in the sample, the weaker the signal. The antigen concentration in the sample is therefore inversely proportional to the color intensity. A wide range of samples have been analyzed with ELISA, and new markers of tumor progression and prognosis have been discovered (49). Traditional ELISA relies on the chromogenic reaction of substrate and enzyme, which has low sensitivity, and cannot meet the needs of biomarker analysis in complex biological samples (67, 68). Moreover, the enzyme tag used by ELISA is a natural protein, and heat, pH, or chemical induction can make the enzyme lose its catalytic activity, which is not conducive to the stability of the method (Table 2). Researchers have developed several strategies to improve the performance of traditional ELISAs, which can be broadly classified into biotechnology-based (50, 69) and nanotechnology-based (51, 68, 70) methods. For biotechnology-based ELISA, blocking agents have been innovatively used to effectively reduce the background noise of ELISA and eliminate various false positive and false negative signals in serum assays (69). Peptides with binding affinity have been designed and utilized to develop recombinant proteins with higher affinity and thermostability to AFP than natural antibodies (50). For nanotechnology-based ELISA, metal-organic frameworks (MOF)@Hemin-Au composite (70) have been utilized to enhance the stability of AFP immunoassays with labeled antibodies. Nanocomplexes can accelerate electron transfer in electrochemical ELISA, and the research achieved high-sensitivity analysis of EGFR (51) and tumor antigen 125 (68) with nanocomplexes, in which the sensitivity of tumor antigen 125 was more than 6 times that of traditional ELISA (68). WB is a traditional protein analysis method to identify and quantify specific proteins in biological samples (48). Tumor biomarkers such as MUC1 (52), MUC6 (53), CD82 (54), EGFR (55), PSA (56), and other glycosylated proteins (71) have been extensively studied with WB. These methods are very sensitive, capable of detecting up to 0.1 nanograms of proteins in a sample (72). Despite its high sensitivity and specificity, WB can still produce incorrect results. For example, false negatives can occur when large proteins do not have enough time to transfer to the membrane. Moreover, processing samples at high temperature may destroy their PMTs (72), which is not conducive to revealing the true state of the samples. Therefore, we hold the view that WB can only be used as an aid in early diagnosis (Table 2).

4.2 Lectin-based method

Immunochemical methods require the use of well-validated antibodies to ensure diagnostic sensitivity and specificity (67, 72). However, the lack of glycan/glycosylated protein-specific

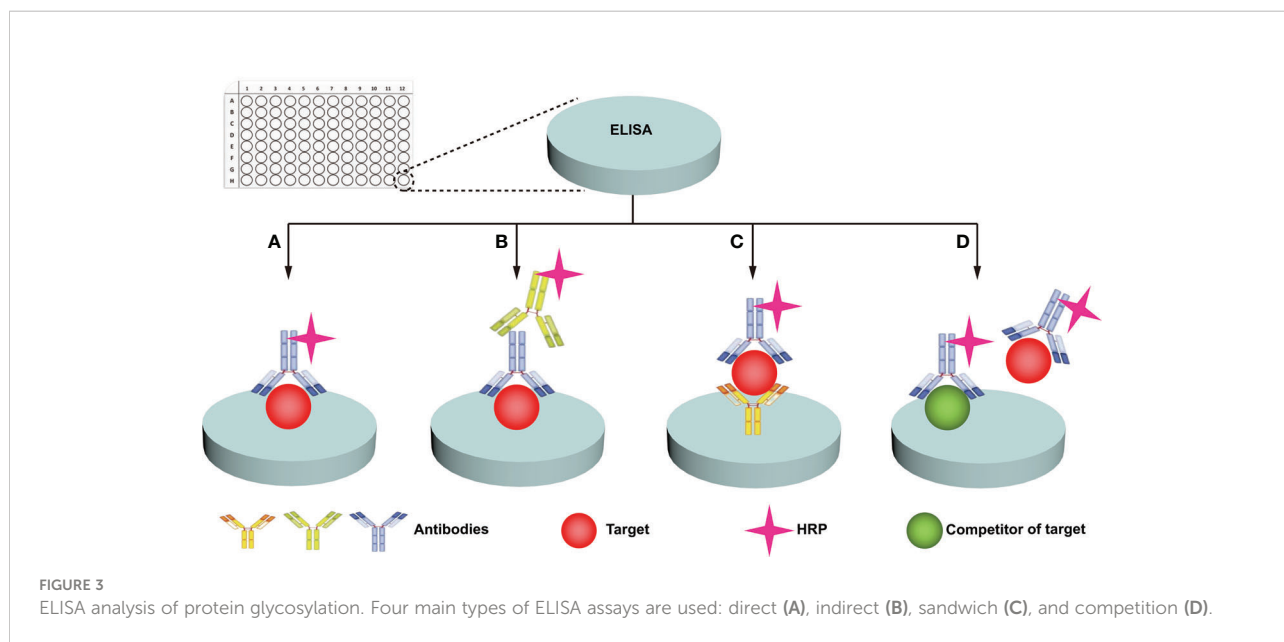


TABLE 2 Advantages and disadvantages of representative glycosylation analysis techniques.

Technical classification	Research methods	Advantages	Disadvantages	References
Immunochemical Methods	ELISA	Simple sample pretreatment; short analysis time; gold standard for clinical diagnosis	Low-Stability of the kit; lack of glycosylation antibodies; inability to obtain glycosylation site and structure information	(49–51, 67–70)
	WB	Ultrahigh sensitivity; high throughput; wide range of applications	Lack of glycosylation antibodies; False negatives may occur; inability to obtain glycosylation site and structure information	(52–56, 71, 72)
Lectin-based method	L-ELISA	Wide variety of lectins; simple sample preparation; short analysis time	Low-Stability of the kit; inability to obtain glycosylation site and structure information	(57, 58, 73, 74)
	lectin blotting	Ultrahigh sensitivity; high throughput; wide application	False negatives can occur; inability to obtain glycosylation site and structure information	(75)
	lectin cytochemistry	Ultrahigh sensitivity; <i>in-situ</i> information acquisition; dynamic tracking possible	Inability to obtain glycosylation site and structure information	(76)
	lectin microarray	High dynamic range; ultrahigh sensitivity; high throughput	Inability to obtain glycosylation site and structure information; no <i>in-situ</i> information available	(59, 60, 77–79)
MS	Top-down MS	Simple sample pretreatment; short analysis time; without any digestion; suitable for proteoform analysis Identify glycan structure information	Not suitable for analysis of hydrophobins; difficult to obtain glycosylation sites; low abundance protein signal suppressed; expensive	(80–85)
	Bottom-up MS	Antibody-free; Identify glycosylation site and structure information; wide range of application	Complex sample preprocessing; no <i>in-situ</i> information available; expensive	(61–66, 86–115)
Fluorescence imaging		High dynamic range; ultrahigh sensitivity; <i>in-situ</i> information acquisition; dynamic tracking possible	Inability to obtain glycosylation site and structure information; expensive	(116–128)

antibodies hinders the widespread application of immunochemical methods. Fortunately, lectins have broader specificities, and are considered to be very useful tools for glycan research, and the information on lectins specifically recognizing glycans is summarized (Table 3) (57–60, 73–78). Lectin-based methods include lectin-antibody sandwich ELSA (L-ELISA) (67), lectin blotting (67), lectin cytochemistry (67), and lectin microarray (67). L-ELISA and lectin blotting are the extension of ELISA and WB. The principle is the same as that of immunochemical methods, just lectin is used to replace antibody as the recognition molecule (74). L-ELISA has been designed and implemented for the analysis of two breast cancer biomarkers,

CA15-3 (57) and α -1-acid glycoprotein (AGP) (58), showing a higher sensitivity than ELISA, distinguishing breast cancer stages I, IIA, and IIB. Lectin blotting has been utilized to explore the link between the development of liver cancer and the intracellular action of GALNT glycosyltransferase (75). Lectins are widely used for *in situ* tracking of glycan signatures on surfaces; for example, Huang evaluated and compared the glycan structures among 64 cell lines, 37 tissues, and primary colon tumor tissues with 19 fluorescently conjugated lectins (76). Lectin microarray is a fast, sensitive, high-throughput glycan analysis technique suitable for studies with large sample numbers (77) (Table 2). Lectin microarrays were used to analyze and compare glycosylation

TABLE 3 Properties of representative lectins (57–60, 73–78).

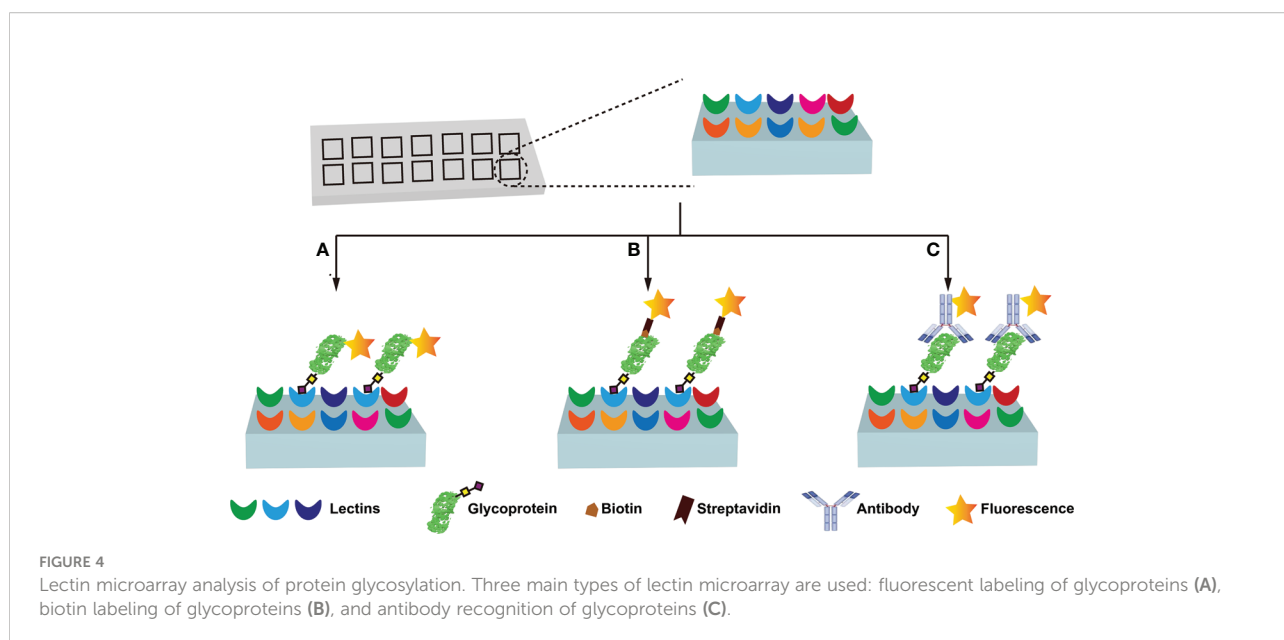
Lectin	Abbreviation	Glycoprotein	Metal Ions	Specificity
<i>Aleuria aurantia</i>	AAL	No	–	Fuc α 6GlcNAc
Concanavalin A	Con A	No	Ca ²⁺ , Mn ²⁺	α Man, α Glc
Succinylated Concanavalin A	Succinylated Con A	No	Ca ²⁺ , Mn ²⁺	α Man, α Glc
<i>Datura stramonium</i>	DSL	Yes	No	(GlcNAc) ₂₋₄
<i>Euonymus europaeus</i>	EEL	Yes	Ca ²⁺ , Zn ²⁺	Gal α 3Gal
<i>Galanthus nivalis</i>	GNL	No	No	α Man
<i>Griffonia (Bandeiraea) simplicifolia</i> I	GSL I, BSL I	Yes	Ca ²⁺ , Mn ²⁺	α Gal, α GalNAc
<i>Hippeastrum</i> hybrid	HHL, AL	No	No	α Man
Jacalin	Jacalin	Yes	No	Gal β 3GalNAc
<i>Lens culinaris</i>	LCA, LcH	No	Ca ²⁺ , Mn ²⁺	α Man, α Glc
<i>Lotus tetragonolobus</i>	LTL	Yes	Ca ²⁺ , Mn ²⁺	α Fuc
<i>Lycopersicon esculentum</i>	LEL, TL	Yes	–	(GlcNAc) ₂₋₄
<i>Maackia amurensis</i> I	MAL I, MAL	Yes	No	Gal β 4GlcNAc
<i>Maackia amurensis</i> II	MAL II, MAH	Yes	No	Neu5Ac α 3Gal β 4GalNAc
<i>Maclura pomifera</i>	MPL	No	No	Gal β 3GalNAc
<i>Narcissus pseudonarcissus</i>	NPL, NPA,	No	No	α Man
Peanut	PNA	No	Ca ²⁺ , Mg ²⁺	Gal β 3GalNAc
<i>Pisum sativum</i>	PSA	Trace	Ca ²⁺ , Mn ²⁺	α Man, α Glc
<i>Psophocarpus tetragonolobus</i> I	PTL I, WBA I	Yes	–	GalNAc, Gal
<i>Psophocarpus tetragonolobus</i> II	PTL II, WBA II	Yes	–	GalNAc, Gal
<i>Ricinus communis</i> I	RCA I, RCA120	Yes	No	Gal
<i>Ricin B Chain</i>	Ricin B Chain	Yes	No	Gal
<i>Sambucus nigra</i>	SNA, EBL	Yes	No	Neu5Ac α 6Gal/GalNAc
<i>Solanum tuberosum</i>	STL, PL	Yes	No	(GlcNAc) ₂₋₄
<i>Sophora japonica</i>	SJA	Yes	Ca ²⁺ , Mn ²⁺	β GalNAc
Soybean	SBA	Yes	Ca ²⁺ , Mn ²⁺	α - β GalNAc
<i>Ulex europaeus</i> I	UEA I	Yes	Ca ²⁺ , Mn ²⁺ , Zn ²⁺	α Fuc
<i>Vicia villosa</i>	VVL, VVA	Yes	Ca ²⁺ , Mn ²⁺	GalNAc
Wheat Germ	WGA	No	Ca ²⁺	GlcNAc
Succinylated Wheat Germ	Succinylated WGA	No	Ca ²⁺	GlcNAc
<i>Wisteria floribunda</i>	WFA, WFL	Yes	–	GalNAc

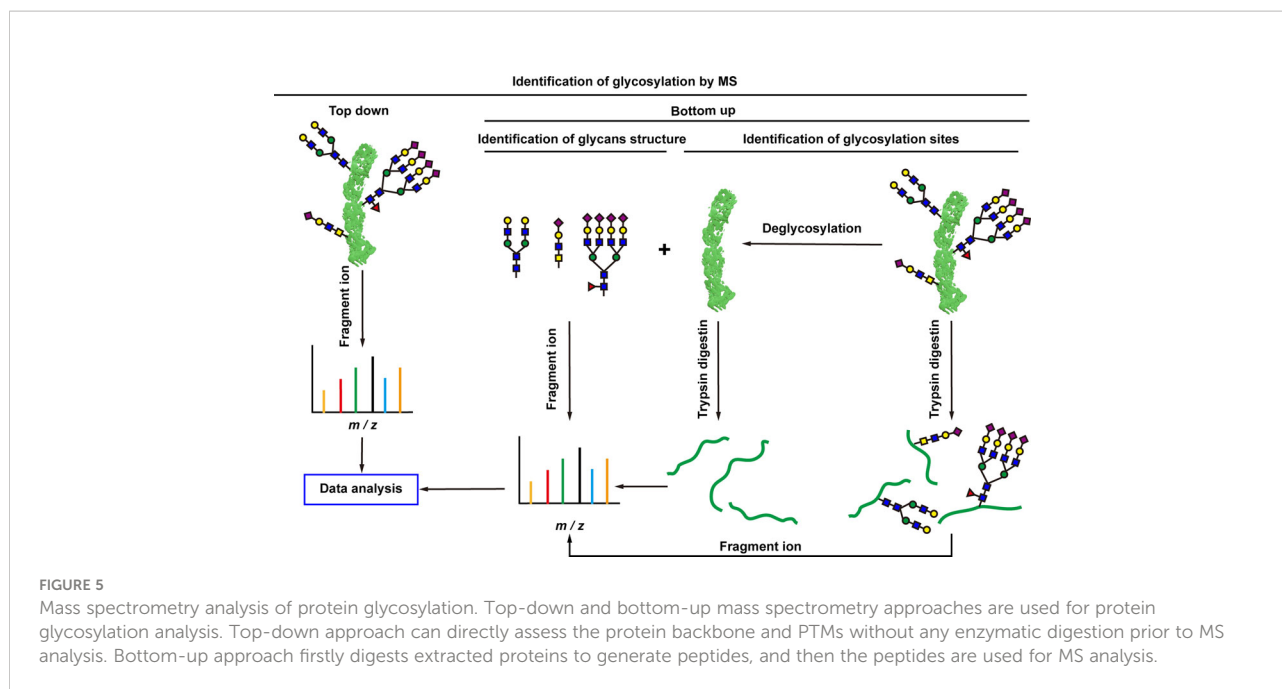
in non-tumor and tumor regions of pancreatic ductal adenocarcinoma (59). Lectin microarray requires less sample, simple pretreatment, and no glycan release or purification, enabling high-throughput, rapid and sensitive glycosylation analysis of different clinical samples. Its analytical methods usually include fluorescent labeling of glycoproteins (Figure 4A), biotin labeling of glycoproteins (Figure 4B), and antibody recognition of glycoproteins (Figure 4C) (59, 77). The most commonly used method is fluorescent labeling of proteins. Briefly, the protein is pre-labeled with a fluorescent dye, and after the glycoprotein is captured by the lectin, the amount of the corresponding glycoprotein is reflected by the fluorescence intensity. Fluorescent dyes such as Cyanine3 and tetramethylrhodamine were widely used (60). Biotin labeling of proteins can further increase the sensitivity of glycosylation assays with streptavidin. However, these two methods have an obvious disadvantage - in order to ensure the reproducibility of the analysis using the direct labeling strategy, a relatively large number of glycoproteins need to be labeled. One way to overcome this deficiency is to employ an antibody-covered lectin microarray strategy, which is more applicable. Increased abundances of sialylated glycans and *N*-GalNAc were found in tumor regions, and the mechanisms underlying these glycosylation-related abnormalities were explored (59). The protein glycosylation changes induced by the drug Sorafenib during tumor therapy have been explored with lectin arrays (78); the high-throughput advantages of lectin arrays were also exploited to systematically analyze the glycosylation of 56 lectins in 207 samples (79). Further, normal and cancerous breast cells were differentiated using lectin microarrays, which have also been used to study cell development and differentiation (60, 74). Another point worth mentioning is that the reversed lectin arrays modify carbohydrates on microarrays,

which can be used to analyze carbohydrate-binding proteins such as lectins, and can also be used to study different carbohydrate structures and various biological targets (RNA, virus and whole cell) interactions (60). These studies provided ideas for revealing the molecular mechanism related to glycosylation and designing new anticancer drugs.

4.3 MS-based method

Cells are complex living organisms, and subtle changes in glycosylation may transmit different signals and produce different biological effects (129). There is an increasing demand for detailed analysis of the structure and modification sites of glycans. The most significant advantage of MS is the ability to obtain detailed structural information of glycans, which makes MS the best tool for analyzing glycosylations. Matrix-assisted laser desorption/ionization MS (MALDI-MS) and electrospray ionization MS (ESI-MS) are two commonly used MS approaches (130, 131). MALDI is often combined with time-of-flight (TOF) MS, which has a theoretically infinite m/z range and fast scan speed, enabling extremely low detection lines. ESI is a form of soft ionization protonation that progressively desolvates the sample and forms analyte ions at lower temperatures. A major advantage of ESI is that it can be easily combined with high performance liquid chromatography (HPLC) to pre-separate complex mixtures of glycans (130, 131). Generally, two types of protein glycosylation MS analyses are used, including top-down and bottom-up (80) (Figure 5). Top-down glycoprotein analysis is the direct assessment of PTMs of the protein backbone without any digestion, which





has found some new proteoforms (81–84), and some of these proteoforms cannot be reliably identified by bottom-up method (83). It is significant to better understand the molecular mechanisms of a disease. The top-down method is more efficient and rapid for the analysis of glycosylation. The analysis of 38 glycoforms has been achieved in a few hours in combination with bioinformatics tools (82). However, despite the strong potential and technological advancement of the top-down approach, it has rarely seen its widespread and clinical application. Top-down MS study has its own limitations: (i) it is not suitable for the analysis of hydrophobic proteins such as membrane proteins; (ii) it inhibits low-abundance proteins such as glycoproteins, and lack of separation methods for glycosylated proteins; (iii) it is difficult to accurately locate unstable glycosylation modification site (85); and (iv) it requires additional bioinformatics tools to process the complex data generated by top-down approaches (86). These are the problems that need to be solved urgently in the development of top-down MS. Whereas, the bottom-up MS approach digests extracted proteins to generate peptides suitable for MS analysis (87). Glycopeptides are easier to be analyzed with MS than intact glycoproteins because they may exhibit higher ionization efficiencies and yield simpler tandem mass spectrometry (MS/MS) spectra, partially due to their smaller size than glycoproteins (87). Glycopeptides are often required to be enriched prior to MS/MS analysis, and glycopeptides have relatively low ionization efficiencies compared to non-glycosylated peptides. Analysis of glycan structure requires the release of glycans. *N*-glycans are released from glycopeptides by peptide-*N*-glycosidase F (PNGase F) digestion (61). *O*-glycans have many core structures, and no general release enzymes are used;

however, there are corresponding enzymes for specific core structures. Alternatively, any *O*-glycans can be released through the chemical process of β -elimination, with the potential for undesirable side effects (61). In recent years, bottom-up MS has been widely used to study glycosylation changes in tumorigenesis and development at different specificity levels including global, cell-specific, and local-specific.

4.3.1 MS analysis of global glycosylation

MS is widely used in cancer diagnosis and mechanism research. It has been found that *N*-glycan structure is closely related to tumor molecular subtypes, and fucosylation is differentially modified in different subtypes of ovarian cancers (62). MS has been used to characterize changes in glycosylation in sera and tissues from colon cancer patients with stages II and III. Oligosaccharides, hypogalactosylated, and tetra-antennary forms are up-regulated in tumor tissues (63). The structural distribution of specific types of glycans in the stroma, necrosis, and tumor areas of breast cancer has been studied, and high-Man, branched, and fucosylated glycans were predominantly present in the tumor region (64). More abundant fucosylated and sialylated glycopeptides are found in drug-resistant non-small cell lung cancer cells (65). Researchers also improved MS methods in many ways to obtain more sensitive and comprehensive information. For example, CEA samples purified from human colon cancer and its liver metastatic tissues were cleaved by specific enzymes such as trypsin, intracellular protease gluc, and nonspecific enzyme pronase, respectively; which identified 28 *N*-glycosylations of CEA. Of them, three more *N*-glycosylation sites were identified by gluc digestion than trypsin digestion. This research provides a better

understanding of the heterogeneity of CEA glycosylation pattern (88). Virtual multi-stage MS was utilized to simultaneously obtain glycan, peptide sequence, and glycosylation sites. The deglycosylated peptides and intact glycopeptides were mixed for MS analysis. MS² spectra of intact glycopeptides were used to determine glycosyl groups, while MS² spectra of deglycosylated peptides were used to identify peptide backbone sequences. Compared to the traditional multi-stage strategy, the MS² spectrum of deglycosylated peptide can directly recognize the peptide backbone with higher sensitivity (66). Researchers also improved the detection sensitivity and breadth of MS from the methods of glycan labeling (89) and data analysis (90).

4.3.2 MS analysis of membrane protein glycosylation

The cytoplasmic membrane provides a highly interactive platform for intracellular and extracellular information transfer. Proteins on the cell surface are extremely important for the development of tumors (13). Most membrane proteins are glycosylated to regulate life activities such as cell-cell interaction and signal transduction (14). About 70% of FDA-approved drugs target cell surface proteins (91). MS itself cannot distinguish cell surface glycoproteins from intracellular glycoproteins. Compared to the whole cell glycoproteins, cell membrane glycoproteins are less abundant, and are easily confused with intracellular proteins. The enrichment of surface glycoproteins is of great significance for comprehensive analysis by MS. To better investigate the glycosylation on the cell membrane, researchers use density-gradient centrifugation to separate the plasma membrane from the cell, especially sucrose-gradient centrifugation is the most widely used method, which is also a classic method for membrane protein separation (92, 93). However, ultracentrifugation does not separate membrane glycoproteins but all membrane proteins, and this method cannot completely eliminate cytoplasmic proteins (93). In recent years, with the development of chemical biology and MS-based proteomics, more precise analysis of cell surface glycoproteins has become possible.

A typical method for *in situ* labeling of membrane glycoproteins is to oxidize cell surface glycoproteins with sodium periodate, followed by hydrazine chemical capture to enrich the membrane proteins and identify them with MS. A method, cell-surface-capturing (CSC) technology, was first developed by Wollscheid et al. in 2009 for large-scale analysis of surface glycoproteins (94). It optimized the periodate concentration and reaction conditions to maintain cell viability and minimize side-effects. The aldehyde group oxidized by periodate can react orthogonally with biotin hydrazine (BH). After cell lysis, the biotinylated glycopeptides were enriched by streptavidin beads, and then glycopeptides were eluted by PNGase F treatment. CSC enables site-specific analysis of cell surface glycoproteins, which significantly reduces the false-positive rate of surface glycoprotein identification.

Characterization of the cell surface proteome of lymphoid malignancies is a first step toward improving personalized diagnosis and treatment of leukemias and lymphomas. The CSC technique was utilized to characterize the cell surface *N*-glycoproteome of four human malignant lymphocyte cell lines, and a total of 404 cell surface *N*-glycoproteins were identified. Of them, 82 *N*-glycoproteins had not been previously mentioned in the cell surface protein map. Cluster analysis of these MS data was used to reveal the most representative proteins of each cell type, which would facilitate mapping their stages of differentiation, and help identify associated malignancies (95). With the use of this CSC strategy, researchers constructed an extensive database of cell surface proteins. The Cell Surface Protein Atlas (CSPA; wlab.ethz.ch/cspa/) is a public resource containing experimental evidence for cell surface proteins identified in 41 human cell types (96). To improve the performance of CSC technology, researchers made some changes to it, mainly focusing on optimizing the conditions for labeling aldehyde groups, and optimizing peptide enrichment procedures. The bioorthogonal reaction rates of hydrazide and aldehyde groups used in the CSC strategy are slow and inefficient. Aniline was used as a catalyst to increase the labeling rate. Furthermore, biotinylated surface glycoproteins were enriched at the levels of protein rather than peptide. Biotinylated proteins were enriched with streptavidin-coated beads. Beads were rigorously washed, and bound proteins were trypsinized. The resulting peptide mixture was analyzed by liquid chromatography-MS/MS (LC-MS/MS). As a result, approximately 900 plasma membrane and secreted proteins were identified, including more than 300 transporters and ion channels (97). CSC method requires a large amount of starting material (10⁷ to 10⁸ cells per experiment), possibly due to the large number of sample processing steps resulting in severe loss of samples. Cell surface protein isolation protocols were also optimized to increase cell surface protein coverage. With a special pipette tip, the new workflow is suitable for very small numbers of cells, 10 times less than traditional CSC methods. A total of ~600 cell surface-associated proteins were identified from 1105 cells alone (98).

The oxidative properties of periodate often harm the active state of cells, and labeling conditions based on enzyme-catalyzed cell surface glycoproteins are milder, and the reaction is more efficient (99). Galactose oxidase can specifically oxidize the hydroxyl group at C₆ position on Gal/GalNAc to an aldehyde group. The reaction rate of galactose oxidase on the cell membrane surface was also improved by the researchers (99). Galactose oxidase releases H₂O₂ when it oxidizes glycoproteins. H₂O₂ inhibits the activity of galactose oxidase. The authors added HRP to consume H₂O₂ at the same time of oxidation, which promoted the completion of the oxidation reaction. The number of identified glycoproteins increased by ~25% after the addition of HRP, and 953 *N*-glycosylation sites within 393 surface glycoproteins were identified in MCF7 cells (99).

Combined with quantitative proteomics, ones performed a systematic quantitative analysis of the changes in the surface glycoproteome of breast cancer under drug treatment. The resulting data contribute to a better understanding of the functions of glycoproteins and molecular mechanisms of a disease (99). Moreover, GlcNAc and GalNAc are two common glycosylations, with the same molecular weights and glycosylation sites, which two are difficult to be distinguished with MS. This problem was solved by exploiting the specificity of galactose oxidase. GalNAc can be oxidized by galactose oxidase but GlcNAc cannot. Combined with MS analysis of glycoproteins, 96 Tn antigen-containing glycoproteins were identified in Jurkat cells (100). These data clearly show that this method can clearly distinguish the two glycoforms, mainly due to the specificity of galactose oxidase (100). We believe that this method can be widely used in the biomedical research of Tn antigen. Compared to periodate, galactose oxidase is promising for oxidizing glycans on the cell surface: (i) The reaction is mild, and the oxidation process does not affect cell viability and growth; (ii) With high specificity, the enzyme, a large molecular weight protein, cannot penetrate the cell membrane of living cells, and only extracellular glycans are labeled. This method is suitable for the analysis of surface glycoproteins.

The unnatural sugar metabolism-labeling technology was first proposed by Bertozzi's team (101). The basic principle is to use the original metabolic pathway of the organism to metabolize the unnatural sugar with bioorthogonal groups to the original position of the natural glycan, and then realize the labeling and research of the unnatural sugar through the bioorthogonal reaction. This method made outstanding contributions to the identification (101) and dynamic changes (101) of glycosylation. Metabolic labeling techniques were also utilized to explore the glycosylation of cell surface glycoproteins. Cell surface glycoproteins are metabolically labeled with functionalized sugars and then labeled with biotin by copper-free click chemistry. Biotin-containing surface glycopeptides were selectively enriched and analyzed with MS. On average, 683 glycosylation sites and 354 surface glycoproteins are identified per cell (102). Glycoproteins were quantified in combination with label-free quantification, distinguishing between cell-specific and cell-ubiquitous glycoproteins (102). This study led to a better understanding of cell surface glycoproteins, and provided important information for the discovery of new biomarkers and drug targets.

Metabolic labeling techniques were also used to visualize, identify, and quantify proteins. The labeling of three carbohydrate analogs (GalNAz, ManNAz and GlcNAz) was compared, and the results showed that GalNAz labelled more cell surface protein glycosylation sites than GlcNAz or ManNAz (102). Not only the metabolic ratios of different sugars on *N*-glycans are different, but also the incorporation efficiency of the same sugar among *N*-/*O*-glycans, glycosides and glycosphingolipids is significantly different (104). A comprehensive, site-specific analysis of changes in *N*-

glycosylation of surface proteins on statin-treated versus untreated cells was performed. Compared to untreated cells, many glycopeptides were downregulated in statin-treated HepG2 cells because statins prevented the synthesis of dolichol, which is essential to form dolichol-linked precursor oligosaccharides. *N*-glycosylation on surface proteins associated with Alzheimer's disease was found to be downregulated (103). Furthermore, with the use of stable isotope labeling of amino acids in cell culture (SILAC), time-dependent changes in cell surface glycoprotein abundance were localized and quantified for the first time (105). Briefly, after cells were subjected to full heavy isotope incorporation and full light isotope incorporation with SILAC method, cell collection was performed every two hours until the 48-hour time course was completed. Over time, heavy proteins are degraded, and newly synthesized proteins are theoretically light proteins, thus measured protein half-life (105, 106). However, a limitation of SILAC method is that proteins with very long half-lives may not be accurately determined because the protein may not be renewed over the course of the assay time. Also, SILAC strategy was used to explore the conversion rate of *O*-GlcNAcylated proteins (107). Glycoproteins on the cell surface are dynamic to adapt to the changing extracellular environment. Thus, the dynamic changes of these glycoproteins can guide disease states with important biomedical significance.

Currently, few unnatural carbohydrate metabolism precursors are widely used, which greatly limits the systematic research of glycosylation in a cell membrane protein (93). Unnatural sugar incorporation relies on competing cellular metabolic processes with natural sugars, which is inefficient and time-consuming. The use of glycosyltransferases and nucleotide-sugar analogs to directly label cell surface glycans was also pursued by researchers (93). Selective exo-enzymatic labeling (SEEL) method was developed to efficiently label cell surface glycans with recombinant sialyltransferases and nucleotide-Sia analogs. Two sialyltransferases, ST6Gal1 and ST3Gal1, were used to label the Sia of *N*- and *O*-glycans, respectively. SEEL in combination with MS identified 37% more sialylated proteins than metabolic labeling method. This SEEL study compared the levels of sialylated proteins in undifferentiated vs. differentiated human erythroleukemia cells (HEL), and found that differentiated cells had more *N*-linked sialylated proteins (108). Biotin-functionalized nucleotide-Sia analogs were synthesized to label cell surface Sia in one step, which labels nearly twice as many proteins as the two-step SEEL method. The protocol of this one-step strategy is technically simple, and the transport and turnover of glycoproteins can be easily explored (109), with higher sensitivity compared to typical two-step reporting strategy (110). The glycosyltransferase approach is also flawed and limited to study glycoproteins that can serve as enzyme substrates. However, due to the simple steps and high efficiency, it is especially suitable to detect low-abundance glycan epitopes on living cells.

4.3.3 MS analysis of regional membrane protein glycosylation

Glycoprotein interaction networks are important in many intracellular and extracellular events, and abnormal protein interactions are closely related to various diseases including cancers (14). A proteomic approach in combination with chemical cross-linking, enzymatic reaction, and MS identification was developed to systematically characterize proteins that interact with surface glycans. Bis(sulfosuccinimidyl)suberate (BS³), a membrane-impermeable crosslinker, was first used to covalently crosslink surface glycoproteins and their interacting proteins. For the extraction of glycoproteins, a strategy similar to the CSC technique was adopted. Galactose oxidase was used to oxidize glycans on surface glycoproteins, which were then enriched for surface glycoproteins and their interactors by hydrazine chemistry, followed by quantitative proteomics. As a result, it identified more than 300 proteins interacting with surface glycoproteins, and the glycoprotein interaction network was constructed (111). Combined with chemical cross-linking, the analysis of cell surface interaction networks, especially glycan-interacting proteins, became more precise. Azide-labeled Sia on the cell surface through the metabolic pathway, and the bifunctional linker was used to covalently couple Sia and Sia-interacting proteins. Cells were lysed and trypsinized, and the cross-linked glycan-peptides were purified with reversed-phase chromatography columns and strong cation exchange cartridges, and analyzed with reversed-phase liquid chromatography-high-resolution Orbitrap MS. The enriched glycan-peptides were identified by an improved proteomic approach with fragmentation using high-energy collision-induced dissociation. This study unequivocally provides direct information on the network of Sia-mediated protein action on the cell membrane (112). For glycan-protein interactions, covalent bonds created by cross-linking between interacting proteins cannot be cleaved by MS, which is difficult to make direct identification with search software. Proximity labeling-based methods are frequently used to analyze protein interactions; especially APEX2-based methods were widely used in proteomics because of its high catalytic activity, small size (28 kDa), and activity in different cellular compartments (113). APEX2 is fused to the N-terminus of Galectin-3 and mapped glycoproteins that interact with Galectin-3. Quantitative proteomics based on tandem mass tag (TMT) labeling identified these interacting glycoproteins with high sensitivity. At the same time, the glycoprotein interacting with galectin-3 was further verified by *in vitro* experiments such as WB (114). In addition to enzymes, chemical probes with catalytic activity are also developed to study lectin-interacting proteins. Iron (S)-1-(p-bromoacetamidobenzyl) EDTA (FeBABE) was used as a catalyst to coupling lectins. Free radicals are generated in the presence of H₂O₂ to oxidize lectin-interacting proteins, and lectin-interacting cell surface glycoproteins were identified with MS. This method was extended to study surface glycoproteins that interact with different types of lectins, such as SNA, MAL, AAL, and WGA (115). Similar methods are also developed to identify Sia-interacting

proteins (116). Such methods provide an unprecedented insight into the interaction of lectins with specific glycoproteins.

MS has made outstanding contributions to the comprehensive analysis of glycosylation studies of plasma, cell membrane proteins, and glycan-interacting proteins, and the widespread use of MS is mainly due to several key advantages: (i) MS analysis does not require antibodies that are expensive, cumbersome to obtain, and limited in types. Moreover, the performance of antibodies varies to affect the test results. (ii) MS does not require prior knowledge of the type of protein to be studied. WB, immunoprecipitation (IP), and other methods commonly used in traditional biology require pre-judgment of the proteins to be analyzed. MS is a common technique in analysis of proteins. Without prior knowledge of proteins, MS enables large-scale marker screening in complex biological samples. (iii) The advent of tagging methods, such as iTRAQ and TMT labeling, can efficiently perform deep quantification of biomarkers, which has an essential feature in comparison of multiple samples. (iv) Perhaps, the most significant advantage of MS-based methods is able to obtain the detailed structural information on glycan structures and to identify glycosylation sites, which might directly impact cell function. In recent years, the combination of chemical biology and MS has made an indelible contribution to the research of glycosylation at different specificity levels, which deepens one's understanding of the synergistic regulation of cellular protein activities. We believe that it is the focus and direction of future research (Table 2).

4.4 Fluorescence imaging-based *in situ* cellular glycan analysis

Although proteomics and glycomics have made great advances in the *in vitro* research of glycosylated structure and function, they cannot provide *in situ* real-time qualitative or quantitative information on glycosylated structures on cells, especially the spatial distribution information. Moreover, the complex cleavage and separation process prior to MS analysis might lead to unpredictable loss of glycan information (117). Some studies used lectin, metabolism and other methods to study the overall state of glycosylation of tumor cells (118). In order to achieve more precise analysis, more comprehensive surface accessibility, higher sensitivity, and wider applicability, cell-specific (119–123) and protein-specific (124–128, 132–134) glycan *in situ* analytical methods have been continuously developed in the past five years.

4.4.1 Cell-specific glycosylation analysis

A common method to image glycans of specific cells is to design the caged probes, and this probe can be activated by enzymes that are produced by target cells, such as cancer-associated proteases. A cathepsin B-specific cleavable substrate (KGRR) was conjugated to an azide-modified metabolic sugar precursor, where specific sites of the azide sugar are blocked from being taken up by cells (119). When cathepsin B was

present on the surface of tumor cells, it acted like “scissors”, chopping peptide fragments, releasing metabolic precursors, and causing tumor cells to generate unnatural glycans containing azide groups (119). For cell culture and tumor-bearing mice, unnatural glycans on the surface of tumor cells were conjugated to near-infrared fluorescent (NIRF) dye-labeled molecules *via* a bioorthogonal click reaction (119). However, this method is only applicable to a limited number of cells with extracellular protease expression. To overcome this limitation, a metabolic labeling method that target to specific cells was developed by encapsulating unnatural sugars in liposomes modified with the targeting integrin $\alpha v\beta 3$. Azide-labeled unnatural saccharides were selectively present in specific cells *via* receptor-mediated endocytosis, followed by coupling to fluorescent dyes *via* copper-free click chemistry (120). This strategy was also extended further to the *in vivo* level, where intravenously injected liposomal nanoparticles selectively bind to cancer cell-specific receptors to install azide into melanoma glycans in a tissue-specific manner (120). Such studies are promising for tumor-specific imaging or drug delivery. Some studies also directly act on the cells with enzymes modified with targeting ligands, and achieve cell selectivity by adjusting the concentration of probes (121). To avoid non-specific reactions caused by collisions, this method must use very low enzyme concentrations, and cell specificity is not optimistic. A strategy was developed to achieve cell-selective glycan remodeling by modulating enzymatically active center accessibility (SEA). Encapsulation of enzymes with MOFs prevents them from reacting with macromolecular enzyme substrates, and the encapsulated enzymes bind to target cells and degrade encapsulates to remodel the target cells. The SEA protocol adopts a modular design and is expected to be a general tool for cell-selective glycan analysis (122). Furthermore, the thermosensitive microgel was used to encapsulate sialidase, combined with the targeted recognition of aptamers, to achieve cell-specific desialylation, and for the first time, tumor-specific desialylation of complex tissue sections was achieved. This method enhances the killing ability of NK cells to target tumor cells through heat-triggered cell-specific desialylation, which provides a new idea for cancer therapeutic intervention targeting glycoimmune checkpoints (123).

4.4.2 Protein-specific glycosylation analysis

Glycans on specific proteins play an important role in regulating the structure and function of proteins to further affect the biological function and physiological state of cells. Therefore, protein-specific glycan analysis provides a powerful tool to reveal glycan-related biological processes. Fluorescence resonance energy transfer (FRET) is the main method to analyze protein-specific glycans (117, 124). Methods based on site-specific duplexed luminescence resonance energy transfer (D-LRET) (125), hierarchical coding (HieCo) (126), localized chemical remodeling (LCM) (127), and DNA enzymatic

reactions (128, 132) have also been developed in the past five years. A FRET strategy based on hybridization chain reaction (HCR) amplification was reported (124). Briefly, target cells were subjected to metabolic labeling of glycans to modify FRET donors. Aptamers that can trigger HCR and generate a large number of receptors were added, and the HCR nanoassembly induced the amplification and labeling of the target protein, which resulted in a high FRET signal for enhanced imaging of cell surface glycosylation. To achieve simultaneous imaging of two glycans on a specific protein, upconversion nanoparticles (UCNPs) with multicolor luminescence properties was used as a common donor to construct a D-LRET system on a specific protein on the cell surface (125). Aptamer-modified UCNPs were able to specifically bind to the target MUC1. Meanwhile, two different fluorescent receptors, AF555 and AF660, were labeled with metabolic techniques on two target monosaccharides, Sia and Fuc. Two glycan-labeled fluorescent acceptors on MUC1 were simultaneously excited by D-LRET under near-infrared excitation. This system enabled simultaneous imaging of Sia and Fuc on MUC1 on different cell surfaces. Relative quantification of Sia and Fuc on MUC1 was also achieved with *O*-GalNAc as an internal control (126).

The FRET strategy needs to use two different fluorophores that can undergo fluorescence resonance energy transfer when used for protein-specific glycoform imaging. It is very difficult to obtain two pairs of fluorescent donor-acceptor pairs that do not interfere with each other at the same time, so it is difficult for this strategy to simultaneously image multiple glycans in a specific protein. This problem was addressed by designing a hierarchical coding strategy. DNA sequences were used to encode proteins and different classes of glycans. Decoding process started with the addition of a “time code” that exposed the “protein code”. Exposed “protein code” was hybridized with a hairpin that was covalently modified on the sugar, opening the hairpin and exposing the “monosaccharide code”. The clever introduction of “time encoding” in this strategy strictly distinguishes the encoding and decoding process, and the decoding event can be started at any time (126). A similar method was developed to visualize signal amplification of glycans on specific proteins with metabolic labeling and proximity-induced hybridization chain reaction (133). The number of DNA sequences that could be used as markers was theoretically infinite, so this method, with its ability to image many different glycoforms simultaneously, is a scalable and versatile platform.

LCM strategy was proposed to remodel Gal/GalNAc-specific proteins. Galactose oxidase activity was inhibited in the presence of potassium ferrocyanide, and galactose oxidase activity was “on” when potassium ferricyanide was added. This switch enabled the specific oxidation of Gal/GalNAc at the end of MUC1 on the cell surface. Bioorthogonal labeling was then performed for the purpose of localized glycan analysis (127). DNA technology was used to design a hairpin structure with filter function for the imaging of specific protein glycoforms on

the cell surface. The platform relied on the nicking action of restriction endonuclease (NE), and the two ends of the designed hairpin molecular probe were modified with fluorophore and quencher, respectively (128). The site specifically recognized by NE was designed in the middle region of the hairpin. The probe was not cleaved by NE in the hairpin configuration, but could be cleaved by NE when the hairpin was opened by the protein probe. Fluorescent signal of the closed-loop structure was covalently retained at the end of the sugar chain, and the fluorescent signal of the open-loop structure was released into the solution. Based on this method, a multifunctional DNA localization nanomachine was further improved and developed to analyze multiple targeted modifications (MOIs) at the protein-specific level (132).

In summary, it clearly demonstrates that the current protein-specific glycoform imaging strategies need to use a “gating” guarantee mechanism. For example, the FRET strategy relies on distance as the “gating”, the LCM strategy uses ions as the “gating”, and the HieCo strategy designs DNA as the “gating”. These strategies are cleverly designed, but also suffer from disadvantages such as limited generalizability (LCM) and complex design (HieCo). Therefore, a fundamental shift in detection mode is also required in the future to achieve highly sensitive protein-specific glycoform imaging with a simplified “gated-free” design (Table 2).

5 Glycan-related tumor therapy

5.1 Glycan-related targeted therapy

As previously discussed, tumor-associated glycans/glycoproteins have been widely used as biomarkers for clinical diagnosis and prognostic assessment of patients (133). The abnormal changes in glycosylation on the surface of tumor cells relative to normal cells can also be extended to therapeutic targets (134). In the context of 3P medicine, abnormal glycosylation provides a clear label for tumor cell identification, and individualized diagnosis and treatment plans can be implemented according to the special situation of each patient (135). It can greatly improve the specificity of tumor treatment and has a huge impact on monitoring and treatment. Research on targeting glycosylation mainly covers two levels:

(i) tumor suppressive effects of glycan-binding molecules (136–138). Since cancer-specific glycan biomarkers are only highly present on the surface of tumor cells, glycan-binding molecules can be used to discriminate tumor cells from normal cells. The glycan-binding molecule contains lectins and anti-glycan antibodies. The addition of the glycan-binding molecule blocks the corresponding signaling pathway and triggers cancer cell death. For example, the ganglioside focusyl-GM1 is a tumor-associated antigen that is aberrantly expressed in human small cell lung cancer but not in most normal adult tissues, making it a

promising target in tumors (136). A new fully human anti-focusyl-GM1 antibody was discovered. In multiple mouse SCLC models, the focusyl-GM1 antibody showed good efficacy and was well tolerated. The focusyl-GM1 antibody was used in a preclinical model of small cell lung cancer and showed strong *in vitro* and *in vivo* antitumor activity. As a common tumor biomarker, GD2 antibody was also used in the treatment of neuroblastoma (137). It was found that interleukin 2 in combination with anti-GD2 antibody therapy improves outcomes of high-risk neuroblastoma patients who respond to standard induction and consolidation therapy. The GM3 (Neu5Gc) ganglioside, a tumor-specific antigen, was identified as a promising target for cancer immunotherapy (138). A humanized antibody against this ganglioside, 14F7hT, was developed and demonstrated to have significant antitumor effects. Studies have shown that 14F7hT has antibody-dependent cytotoxicity and anti-tumor effects *in vivo*.

(ii) Targeting function of glycan-binding molecules (139–149). Glycan-binding ligands can be used to increase the selectivity and efficiency of antineoplastic drugs against cancer cells and increase their concentration at tumor sites. For example, Tn antigens are highly specific to tumors, and Tn antibodies have been used in targeted drug delivery (139). With the use of the specificity of Tn monoclonal antibodies and the strong cytotoxicity of anticancer drugs, a new type of antibody-drug targeting Tn antigens was introduced. The specificity of monoclonal antibody *in vivo* was first explored, and the antibody-drug conjugate was further applied to Tn-positive tumor cells *in vitro*, showing effective cytotoxicity, and the cytotoxicity was positively correlated with the expression level of Tn in the tumor. Antibody-drug conjugates also showed potent antitumor activity *in vivo*. The study demonstrated for the first time the effectiveness of Tn antibodies as antibody-drug conjugates. Further, Tn antibody was used to provide targeting effect for the drug-encapsulated nanocapsules, the encapsulation efficiency of nanocapsules for antitumor drugs reached 99.9% and the biotin-avidin method was used to attach antibodies to nanocapsules (140). *In vitro* uptake studies and viability assays in the A549 human lung cancer cell line demonstrated that Tn antibodies enhanced nanoparticle internalization and decreased cell viability. MUC1 is aberrantly expressed in epithelial malignant cells, making it an interesting diagnostic and therapeutic target (141). NK cells express abundant Fc receptors, which promote the binding of NK cells and tumor cells, thereby enabling NK cells to precisely target and destroy cancer cells. A protein coupled with MUC1 antibody and Fc receptor was developed, which was highly specific to tumors, and applied to tumor immunotherapy. In addition to antibodies, aptamers are also widely used for targeted binding of proteins due to their small molecular weight and high specificity (142). A novel MUC1 aptamer-modified nanocomplex was developed for the targeted delivery of epirubicin (143). In addition to chemotherapeutic drug delivery, the study of MUC1 aptamer-

functionalized hybrid nanoparticles for targeted delivery of miRNA-29b to non-small cell lung cancer was proposed (144). The MUC1 aptamer was coupled to the nanoparticle surface and enhanced the selectivity of miRNA-29b for tumor cells and tissues. Sialic acid and fucose are typical tumor cell biomarkers that have been widely used in tumor-targeted therapy (145). Bispecific Janus agglutination can simultaneously bind sialic acid and fucosylated glycoconjugates, and Janus lectin-mediated targeted tumor therapy was developed (146). Janus lectins were used to modify giant unilamellar vesicles to induce lipid internalization, leading to precise drug uptake by human epithelial cancer cells. In addition to macromolecular proteins, small molecules such as phenylboronic acid can also specifically bind sialic acid (147). Boronic acid-targeting sialic acid nanocomposites were proposed for the combined delivery of etoposide and the herbal berberine for local treatment of lung cancer. Etoposide, as a potential lung cancer therapy, is limited in its application due to its poor solubility and overall side effects. This study shows that the inhalable nanocomposite has a good antitumor effect. SLea functionalization is a glycan known to mediate tumor metastasis (148). Monoclonal antibody-targeted nanoparticles targeted the controlled release of cytotoxic drugs for intravenous and oral support. The nanocapsules also reduced the initial toxicity of the drug to gastric cells. The study of CD19 antibody chimeric CAR T cells for targeted immunotherapy of tumors resulted in remission in most refractory and relapsed patients (149).

Altered glycosylation is a key change in tumors, and aberrant glycosylation is a component of tumor growth, survival, metastasis, and immune evasion (150). Targeting glycosylation has many advantages in tumor 3P medicine. Cancer-associated glycans represent a valuable opportunity for cancer diagnosis, prognosis, and treatment. Molecules exhibiting glycan recognition properties, as described herein, may represent a powerful strategy for stem cancer diagnosis and treatment (151, 152).

5.2 Glycan-related vaccine design and immunotherapy

Immune checkpoint inhibitors, such as anti-PD1 and anti-CTLA-4 blocking antibodies, were widely used in tumor therapy and improved long-term survival of patients (153, 154). However, not all patients benefit from checkpoint inhibitor therapy. The reason for these lack of benefit is often the absence of T-cell infiltration in the tumor microenvironment, a subset of patients who could benefit from tumor vaccination (154, 155). Antitumor vaccines can be divided into preventive tumor vaccines and therapeutic tumor vaccines. Preventive tumor vaccines are represented by the HPV (human papillomavirus) vaccine approved by the FDA in 2006 (136). The HPV vaccine was developed by Merck & Co., which is immunized to healthy people before the occurrence of tumors, and the human body obtains tumor immune responses in advance (156).

The HPV vaccine can effectively prevent the occurrence of cervical cancer in women, and has achieved great clinical success. Therapeutic tumor vaccines are injected after the occurrence of tumors. It is hoped that the vaccines can induce specific anti-tumor immune responses in tumor patients to achieve the purpose of tumor treatment. Therapeutic tumor vaccines developed with glycoconjugates are a research hotspot and are regarded as an innovative biologic that can be used in a variety of therapeutic settings. Glycoconjugate vaccines are divided into three categories: (i) glycolipid antigens, such as gangliosides Fuc-GM1 (157), GM3 (158, 159), GD2 (160), GD3 (161, 162), SLeA (163), SLeX (163), and Globo H (164). (ii) glycoproteins, such as mucin-associated epitopes Tn, TF, and STn (62, 165); (iii) proteoglycans, such as polysialic acid (147). Glycoconjugate vaccines have high efficiency, low toxicity and high specificity, and are a hot spot in tumor immunotherapy (Table 4).

6 Future perspective

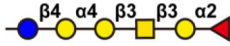



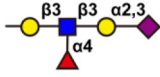
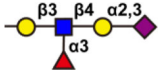
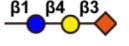

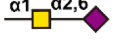

6.1 Glycosylation analysis and 3P medicine

Tumor-related glycosylation changes are a significant feature of cancer diagnosis and prognosis. In recent years, researchers have made great efforts to better analyze and utilize glycosylation. For glycosylation analysis, methods including immunochemical methods, lectin recognition-based methods, MS-related methods, and fluorescence imaging-based *in situ* analysis methods have been developed. Immunochemical methods have high sensitivity and specificity, but are overly antibody-dependent and prone to false positives. Lectin microarray is a fast, sensitive, high-throughput glycan analysis technique suitable for studies with large sample sizes. Immunochemical methods, lectin recognition-based methods, and fluorescence imaging-based *in situ* analysis methods all require prior knowledge of the protein being analyzed, which is disadvantageous for 3P medicine PPPM (166). MS is a versatile technique that enables large-scale marker screening in complex biological samples without prior knowledge of proteins, enabling detailed structural information about glycan structure, and identifying potential implications for cellular function. Traditional MS technology cannot perform *in situ* analysis at different specificity levels. The combination of chemical biology methods with MS technology makes up for this drawback. A thorough investigation of a patient's inability to undergo glycosylation at different levels of specificity can help map precise glycophenotypes (167).

6.2 Glycan-related immunotherapy and 3P medicine

Cell surface glycans are key cellular components that influence cell recognition behavior. Injecting glycan-related vaccines often

TABLE 4 Representative polysaccharide vaccine in tumor immunotherapy.

Tumor-associated polysaccharide vaccines	Structure	Cancer type	References	
Type	Glycan			
Ganglioside	Fuc-GM1		Liver cancer, lung cancer	(156)
	GM3		Lung cancer, brain cancer, breast cancer, and melanoma	(157, 158)
	GD2		Neuroblastoma, lymphoma, melanoma, and osteosarcoma	(159)
	GD3		Breast cancer, melanoma	(160, 161)
	SLeA		Colon, stomach, biliary, and pancreatic cancer	(162)
	SLeX			
	Globo H		Small cell lung, prostate, pancreatic, gastric, and ovarian cancers	(163)
Glycoproteins	Tn		Bladder, colorectal, ovarian, and breast cancer	(164, 165)
	STn			
	TF			
Proteoglycan	Polysialic acid		Lung cancer, breast cancer, and neuroblastoma	(62)

brings problems of poor specificity, which is not conducive to 3P medicine. Glycan editing on the cell surface to achieve glycoform remodeling and further modification of other biomolecules can modulate cellular recognition and communication functions. Using glycan editing to enhance anti-tumor immune responses by blocking glycan immune checkpoints has brought new breakthroughs in the field of cancer therapy (121, 168, 169). Sia residues send a healthy signal to the body, suppressing immune activation through multiple pathways. The high sialylation status of tumor cells/tissues plays an important role in the ability to evade immune recognition. Sia upregulation has been associated with poor tumor prognosis and decreased immunogenicity. Removal of cell surface Sia was found to enhance NK cell activation. An antibody-enzyme conjugate biotherapeutic molecule was designed (121). The antibody specifically recognizes tumor cells, guides sialyl cleavage enzymes to specifically desialylate tumor cells, and guides immune cells to kill desialylated cancer cells. The conjugate increased tumor cell killing compared to the antibody alone. This method was successfully used in breast cancer mice (168). However, this method lacks cell-specific controls, thermosensitive smart microgels were used to modulate the editing ability of glycan editing enzymes, and in combination with aptamers, an *in situ*, cell-specific glycan editing strategy was developed. Sia cleavage was limited to the surface of the target cell, thus enabling thermoresponsive cell-specific glycan editing. This method achieves the enhancement of innate anti-tumor immunity

and avoids the interference of glycan editing with the normality of other cells. Redirecting or boosting the immune response is an effective treatment (118). A key challenge of this immunotherapy is to selectively install molecules that recruit immune responses on the surface of relevant cells. By selectively delivering metabolic sugar precursors to folate receptor-overexpressing cells, an azide group was added to cell surface glycans. Rhamnose was efficiently introduced to the surface of expressing cells. Studies have demonstrated that rhamnose mounted on the target surface recruits anti-rhamnose antibodies and promotes apoptosis of folate receptor overexpressing cells through complementation-dependent cytotoxicity (CDC) and antibody-dependent phagocytosis (ADCP) (169, 170). In turn, customized treatment algorithms can be created to provide optimal clinical approaches for personalized, predictive and preventive medical services, which we believe will be the focus and direction of future research.

7 Conclusion and expert recommendation in framework of 3P medicine in cancer

Glycosylation modification is one of the most important post-modification modifications of proteins. Glycans greatly enrich the biological information of proteins, thereby

enhancing their role in cellular behavior. Glycosylation is a template-free process, and the expression of related genes is affected by transcription factors, epigenetic changes, microenvironment, etc. The complexity of carbohydrates and the limitations of research methods make the research of glycomics seriously lag behind the research of genomics and proteomics. In the past five years, driven by the latest technological advancements, analytical methods based on immunochemical methods, lectin recognition, MS, and fluorescence imaging have gained momentum in cancer research, in terms of providing new glycosyl-based markers, has considerable potential. Although immunochemical-based methods are limited by antibody species and affinity, assays for specific glycosylated target proteins are easier to standardize and reduce redundancy, making them suitable for clinical applications. The *in situ* analysis methods based on fluorescence imaging have made great efforts to study the dynamic changes and spatial distribution of glycans and functions; however, it cannot obtain specific glycan structures. A significant advantage of MS-based method is the ability to obtain detailed information about glycan structure and to identify glycosylation sites that may have direct effects on cellular function. However, they cannot provide real-time information about glycoproteins on intact cells, especially the spatial distribution. The organic combination of chemical biology and MS has made an indelible contribution to the research of glycosylation at different levels of specificity, deepening our understanding of the synergistic regulation of cellular activities by proteins. Combining biochemical, *in situ* analysis, and omics techniques to research glycosylation together provides interdisciplinary insights into deciphering diseases at multiple levels, which we believe is also the focus and direction of future research. In addition, glycans in organelles, such as mitochondria, Golgi and nucleus, need more attention. At the same time, recent research results have also highlighted the relationship between glycosylation and immunity, suggesting that the use of glycan editing can enhance anti-tumor immune responses, which has brought new breakthroughs in the field of cancer therapy. In the future, glycosylation will surely be revealed with new diagnostic, prognostic, and even therapeutic applications. After entering the new century, medicine has entered a new 3P era, which represents the ultimate goal and highest stage of medical development. Glycosylation-based

marker analysis and immunotherapy have achieved rapid development in the past decade. This new model of early warning, prevention and individualized treatment has also promoted the rapid development of oncology to certainly improve people's quality of life.

Author contributions

YG collected and analyzed literature, designed and wrote the manuscript. WJ and JY participated in the collection and analysis of literature. XZ conceived the concept, coordinated, critically revised manuscript, and was responsible for the corresponding works. All authors approved the final manuscript.

Funding

This work was supported by the Shandong First Medical University Talent Introduction Funds (to YG), the Shandong First Medical University Talent Introduction Funds (to XZ), Shandong First Medical University High-level Scientific Research Achievement Cultivation Funding Program (to XZ), the Shandong Provincial Natural Science Foundation (ZR202103020356 or ZR2021MH156 to XZ), and the Academic Promotion Program of Shandong First Medical University (2019ZL002).

Conflict of interest

The authors declare that the research was conducted in the absence of any commercial or financial relationships that could be construed as a potential conflict of interest.

Publisher's note

All claims expressed in this article are solely those of the authors and do not necessarily represent those of their affiliated organizations, or those of the publisher, the editors and the reviewers. Any product that may be evaluated in this article, or claim that may be made by its manufacturer, is not guaranteed or endorsed by the publisher.

References

1. Conibear AC. Deciphering protein post-translational modifications using chemical biology tools. *Nat Rev Chem* (2020) 4(12):674–95. doi: 10.1038/s41570-020-00223-8
2. Zhan X, Li B, Zhan X, Schluter H, Jungblut PR, Coorsen JR. Innovating the concept and practice of two-dimensional gel electrophoresis in the analysis of proteomes at the proteoform level. *Proteomes* (2019) 7(4):36–50. doi: 10.3390/proteomes7040036
3. Li J, Wen S, Li B, Li N, Zhan X. Phosphorylation-mediated molecular pathway changes in human pituitary neuroendocrine tumors identified by quantitative phosphoproteomics. *Cells* (2021) 10(9):2225. doi: 10.3390/cells10092225
4. Schjoldager KT, Narimatsu Y, Joshi HJ, Clausen H. Global view of human protein glycosylation pathways and functions. *Nat Rev Mol Cell Biol* (2020) 21(12):729–49. doi: 10.1038/s41580-020-00294-x

5. Lu M, Chen W, Zhuang W, Zhan X. Label-free quantitative identification of abnormally ubiquitinated proteins as useful biomarkers for human lung squamous cell carcinomas. *EPMA J* (2020) 11(1):73–94. doi: 10.1007/s13167-019-00197-8
6. Wen S, Li J, Yang J, Li B, Li N, Zhan X. Quantitative acetylomics revealed acetylation-mediated molecular pathway network changes in human nonfunctional pituitary neuroendocrine tumors. *Front Endocrinol (Lausanne)* (2021) 12:753606. doi: 10.3389/fendo.2021.753606
7. Hansen BK, Gupta R, Baldus L, Lyon D, Narita T, Lammers M, et al. Analysis of human acetylation stoichiometry defines mechanistic constraints on protein regulation. *Nat Commun* (2019) 10(1):1055. doi: 10.1038/s41467-019-09024-0
8. Zhan X, Huang Y, Qian S. Protein tyrosine nitration in lung cancer: Current research status and future perspectives. *Curr Med Chem* (2018) 25(29):3435–54. doi: 10.2174/0929867325666180221140745
9. Zhang X. Alterations of golgi structural proteins and glycosylation defects in cancer. *Front Cell Dev Biol* (2021) 9:665289. doi: 10.3389/fcell.2021.665289
10. Eichler J. Protein glycosylation. *Curr Biol* (2019) 29(7):R229–R31. doi: 10.1016/j.cub.2019.01.003
11. Jayaprakash NG, Surolia A. Role of glycosylation in nucleating protein folding and stability. *Biochem J* (2017) 474(14):2333–47. doi: 10.1042/BCJ20170111
12. Chen IH, Aguilar HA, Paez Paez JS, Wu X, Pan L, Wendt MK, et al. Analytical pipeline for discovery and verification of glycoproteins from plasma-derived extracellular vesicles as breast cancer biomarkers. *Anal Chem* (2018) 90(10):6307–13. doi: 10.1021/acs.analchem.8b01090
13. Pinho SS, Reis CA. Glycosylation in cancer: Mechanisms and clinical implications. *Nat Rev Cancer* (2015) 15(9):540–55. doi: 10.1038/nrc3982
14. Sun R, Kim AMJ, Lim SO. Glycosylation of immune receptors in cancer. *Cells* (2021) 10(5):1100. doi: 10.3390/cells10051100
15. Josic D, Martinovic T, Pavelic K. Glycosylation and metastases. *Electrophoresis* (2019) 40(1):140–50. doi: 10.1002/elps.201800238
16. Gillette MA, Satpathy S, Cao S, Dhanasekaran SM, Vasaiakar SV, Krug K, et al. Proteogenomic characterization reveals therapeutic vulnerabilities in lung adenocarcinoma. *Cell* (2020) 182(1):200–25. doi: 10.1016/j.cell.2020.06.013
17. Aub JC, Tieslau C, Lankester A. Reactions of normal and tumor cell surfaces to enzymes. i. wheat-germ lipase and associated mucopolysaccharides. *Proc Natl Acad Sci U.S.A.* (1963) 50(4):613. doi: 10.1073/pnas.50.4.613
18. Song K, Herzog BH, Fu J, Sheng M, Bergstrom K, McDaniel JM, et al. Loss of core 1-derived O-glycans decreases breast cancer development in mice. *J Biol Chem* (2015) 290(33):20159–66. doi: 10.1074/jbc.M115.654483
19. Silsirivanit A. Glycosylation markers in cancer. *Adv Clin Chem* (2019) 89:189–213. doi: 10.1016/bs.acc.2018.12.005
20. Liu F, Fu J, Bergstrom K, Shan X, McDaniel JM, McGee S, et al. Core 1-derived mucin-type O-glycosylation protects against spontaneous gastritis and gastric cancer. *J Exp Med* (2020) 217(1):1–17. doi: 10.1084/jem.20182325
21. Radhakrishnan P, Dabelsteen S, Madsen FB, Francavilla C, Kopp KL, Steentoft C, et al. Immature truncated O-glycophenotype of cancer directly induces oncogenic features. *Proc Natl Acad Sci U.S.A.* (2014) 111(39):E4066–75. doi: 10.1073/pnas.1406619111
22. Coelho R, Marcos-Silva L, Mendes N, Pereira D, Brito C, Jacob F, et al. Mucins and truncated O-glycans unveil phenotypic discrepancies between serous ovarian cancer cell lines and primary tumours. *Int J Mol Sci* (2018) 19(7):2045. doi: 10.3390/ijms19072045
23. Jian Y, Xu Z, Xu C, Zhang L, Sun X, Yang D, et al. The roles of glycans in bladder cancer. *Front Oncol* (2020) 10:957. doi: 10.3389/fonc.2020.00957
24. Jiang Y, Liu Z, Xu F, Dong X, Cheng Y, Hu Y, et al. Aberrant O-glycosylation contributes to tumorigenesis in human colorectal cancer. *J Cell Mol Med* (2018) 22(10):4875–85. doi: 10.1111/jcmm.13752
25. Chang TC, Manabe Y, Fujimoto Y, Ohshima S, Kametani Y, Kabayama K, et al. Syntheses and immunological evaluation of self-advanting clustered n-acetyl and n-propionyl sialyl-tn combined with a T-helper cell epitope as antitumor vaccine candidates. *Angew Chem Int Ed Engl* (2018) 57(27):8219–24. doi: 10.1002/anie.201804437
26. Feizi T. Demonstration by monoclonal antibodies that carbohydrate structures of glycoproteins and glycolipids are onco-developmental antigens. *Nature* (1985) 314(6006):53–7. doi: 10.1038/314053a0
27. Fernandez-Ponce C, Geribaldi-Doldan N, Sanchez-Gomar I, Quiroz RN, Ibarra LA, Escorcia LG, et al. The role of glycosyltransferases in colorectal cancer. *Int J Mol Sci* (2021) 22(11):5822. doi: 10.3390/ijms22115822
28. Gao Z, Xu M, Yue S, Shan H, Xia J, Jiang J, et al. Abnormal sialylation and fucosylation of saliva glycoproteins: Characteristics of lung cancer-specific biomarkers. *Curr Res Pharmacol Drug Discovery* (2022) 3:100079. doi: 10.1016/j.crphar.2021.100079
29. Engle DD, Tiriac H, Rivera KD, Keith D, Rivera KD, Pommier A, et al. The glycan CA19-9 promotes pancreatitis and pancreatic cancer in mice. *Science* (2019) 364(6446):1156–62. doi: 10.1126/science.aaw3145
30. Lakemeyer L, Sander S, Wittau M, Henne-Bruns D, Kornmann M, Lemke J. Diagnostic and prognostic value of CEA and CA19-9 in colorectal cancer. *Diseases* (2021) 9(1):21. doi: 10.3390/diseases9010021
31. Liang Y, Wang W, Fang C, Fang C, Raj SS, Hu WM, et al. Clinical significance and diagnostic value of serum CEA, CA19-9 and CA72-4 in patients with gastric cancer. *Oncotarget* (2016) 7(31):49565. doi: 10.18632/oncotarget.10391
32. Gaughran G, Aggarwal N, Shadbolt B, Harris RS. The utility of the tumor markers CA15. 3, CEA, CA-125 and CA19. 9 in metastatic breast cancer. *Breast Cancer Manage* (2020) 9(4):BMT50. doi: 10.2217/bmt-2020-0015
33. Sachan A, Saluja SS, Nekarakanti PK, Nimisha, Mahajan B, Nag HH, et al. Raised CA19-9 and CEA have prognostic relevance in gallbladder carcinoma. *BMC Cancer* (2020) 20(1):826. doi: 10.1186/s12885-020-07334-x
34. van Manen L, Groen JV, Putter H, Pichler M, Vahrmeijer AL, Bonsing BA, et al. Stage-specific value of carbohydrate antigen 19-9 and carcinoembryonic antigen serum levels on survival and recurrence in pancreatic cancer: A single center study and meta-analysis. *Cancers (Basel)* (2020) 12(10):2970. doi: 10.3390/cancers12102970
35. Lenman A, Liaci AM, Liu Y, Frangmyr L, Frank M, Blaum BS, et al. Polysialic acid is a cellular receptor for human adenovirus 52. *Proc Natl Acad Sci U.S.A.* (2018) 115(18):E4264–73. doi: 10.1073/pnas.1716900115
36. Wang X, Li X, Zeng YN, He F, Yang XM, Guan F. Enhanced expression of polysialic acid correlates with malignant phenotype in breast cancer cell lines and clinical tissue samples. *Int J Mol Med* (2016) 37(1):197–206. doi: 10.3892/ijmm.2015.2395
37. Scheer M, Bork K, Simon F, Nagasundaram M, Horstkorte R, Gnanapragassam VS. Glycation leads to increased polysialylation and promotes the metastatic potential of neuroblastoma cells. *Cells* (2020) 9(4):868. doi: 10.3390/cells9040868
38. Elkashef SM, Allison SJ, Sadiq M, Basheer HA, Ribeiro Morais G, Loadman PM, et al. Polysialic acid sustains cancer cell survival and migratory capacity in a hypoxic environment. *Sci Rep* (2016) 6:33026. doi: 10.1038/srep33026
39. Schengrund CL. Gangliosides and neuroblastomas. *Int J Mol Sci* (2020) 21(15):5313. doi: 10.3390/ijms21155313
40. Kanaji N, Kume K, Mizoguchi H, Inoue T, Watanabe N, Nishiyama N, et al. Subacute sensorimotor neuropathy accompanied by anti-ganglioside GM1 antibody in a patient with lung cancer. *Intern Med* (2018) 57(22):3289–92. doi: 10.2169/internalmedicine.0667-17
41. Danolic D, Heffer M, Wagner J, Skrclec I, Alvir I, Mamic I, et al. Role of ganglioside biosynthesis genetic polymorphism in cervical cancer development. *J Obstet Gynaecol* (2020) 40(8):1127–32. doi: 10.1080/01443615.2019.1692801
42. Li Q, Sun M, Yu M, Fu Q, Jiang H, Yu G, et al. Gangliosides profiling in serum of breast cancer patient: GM3 as a potential diagnostic biomarker. *Glycoconj J* (2019) 36(5):419–28. doi: 10.1007/s10719-019-09885-z
43. Jia L, Zhang J, Ma T, Guo Y, Yu Y, Cui J. The function of fucosylation in progression of lung cancer. *Front Oncol* (2018) 8:565. doi: 10.3389/fonc.2018.00565
44. Zhou JM, Wang T, Zhang KH. AFP-L3 for the diagnosis of early hepatocellular carcinoma: A meta-analysis. *Med (Baltimore)* (2021) 100(43):27673. doi: 10.1097/MD.00000000000027673
45. Villegas-Pineda JC, Garibay-Cerdenares OL, Hernandez-Ramirez VI, Gallardo-Rincon D, Cantu de Leon D, Perez-Montiel-Gomez MD, et al. Integrins and haptoglobin: Molecules overexpressed in ovarian cancer. *Pathol Res Pract* (2015) 211(12):973–81. doi: 10.1016/j.prp.2015.10.002
46. Lee J, Hua S, Lee SH, Oh MJ, Yun J, Kim JY, et al. Designation of fingerprint glycopeptides for targeted glycoproteomic analysis of serum haptoglobin: Insights into gastric cancer biomarker discovery. *Anal Bioanal Chem* (2018) 410(6):1617–29. doi: 10.1007/s00216-017-0811-y
47. Kuwatani M, Kawakami H, Kubota Y, Kawakubo K, Ito YM, Togo S, et al. Verification of the effectiveness of fucosylated haptoglobin as a pancreatic cancer marker in clinical diagnosis. *Pancreatol* (2019) 19(4):569–77. doi: 10.1016/j.pan.2019.04.007
48. Liu YC, Yen HY, Chen CY, Chen CH, Cheng PF, Juan YH, et al. Sialylation and fucosylation of epidermal growth factor receptor suppress its dimerization and activation in lung cancer cells. *Proc Natl Acad Sci U.S.A.* (2011) 108(28):11332–7. doi: 10.1073/pnas.1107385108
49. Liu W, Li J, Zhang P, Hou Q, Feng S, Liu L, et al. A novel pan-cancer biomarker plasma heat shock protein 90alpha and its diagnostic determinants in clinic. *Cancer Sci* (2019) 110(9):2941–59. doi: 10.1111/cas.14143
50. Liu J, Cui D, Jiang Y, Li Y, Liu Z, Tao L, et al. Selection and characterization of a novel affibody peptide and its application in a two-site ELISA for the detection of cancer biomarker alpha-fetoprotein. *Int J Biol Macromol* (2021) 166:884–92. doi: 10.1016/j.ijbiomac.2020.10.245
51. Billingsley MM, Riley RS, Day ES. Antibody-nanoparticle conjugates to enhance the sensitivity of ELISA-based detection methods. *PLoS One* (2017) 12(5):177592. doi: 10.1371/journal.pone.0177592

52. Balmana M, Duran A, Gomes C, Llop E, Lopez-Martos R, Ortiz MR, et al. Analysis of sialyl-Lewis x on MUC5AC and MUC1 mucins in pancreatic cancer tissues. *Int J Biol Macromol* (2018) 112:33–45. doi: 10.1016/j.ijbiomac.2018.01.148
53. Yuki A, Fujii C, Yamanoi K, Matoba H, Harumiya S, Kawakubo M, et al. Glycosylation of MUC6 by Alpha1,4-linked n-acetylglucosamine enhances suppression of pancreatic cancer malignancy. *Cancer Sci* (2022) 113(2):576–86. doi: 10.1111/cas.15209
54. Wang X, Zhong W, Bu J, Li Y, Li R, Nie R, et al. Exosomal protein CD82 as a diagnostic biomarker for precision medicine for breast cancer. *Mol Carcinog* (2019) 58(5):674–85. doi: 10.1002/mc.22960
55. Codony-Servat J, Codony-Servat C, Cardona AF, Gimenez-Capitan A, Drozdowskyj A, Berenguer J, et al. Cancer stem cell biomarkers in EGFR-Mutation-Positive non-Small-Cell lung cancer. *Clin Lung Cancer* (2019) 20(3):167–77. doi: 10.1016/j.clcc.2019.02.005
56. Barrabes S, Llop E, Ferrer-Batalle M, Ramirez M, Alexandre RN, Perry AS, et al. Analysis of urinary PSA glycosylation is not indicative of high-risk prostate cancer. *Clin Chim Acta* (2017) 470:97–102. doi: 10.1016/j.cca.2017.05.009
57. Choi JW, Moon BI, Lee JW, Kim HJ, Jin Y, Kim HJ. Use of CA153 for screening breast cancer: An antibodylectin sandwich assay for detecting glycosylation of CA153 in sera. *Oncol Rep* (2018) 40(1):145–54. doi: 10.3892/or.2018.6433
58. Choi JW, Jeong KH, You JW, Lee JW, Moon BI, Kim HJ, et al. Serum levels and glycosylation changes of alpha-1-Acid glycoprotein according to severity of breast cancer in Korean women. *J Microbiol Biotechnol* (2020) 30(9):1297–304. doi: 10.4014/jmb.2006.06007
59. Wagatsuma T, Nagai-Okatani C, Matsuda A, Masugi Y, Imaoka M, Yamazaki K, et al. Discovery of pancreatic ductal adenocarcinoma-related aberrant glycosylations: A multilateral approach of lectin microarray-based tissue glycomic profiling with public transcriptomic datasets. *Front Oncol* (2020) 10:338. doi: 10.3389/fonc.2020.00338
60. Patwa T, Li C, Simeone DM, Lubman DM. Glycoprotein analysis using protein microarrays and mass spectrometry. *Mass Spec Rev* (2010) 29(5):630–844. doi: 10.1002/mas.20269
61. Tabang DN, Ford M, Li L. Recent advances in mass spectrometry-based glycomic and glycoproteomic studies of pancreatic diseases. *Front Chem* (2021) 9:707387. doi: 10.3389/fchem.2021.707387
62. Guo M, Luo B, Pan M, Li M, Zhao F, Dou J. MUC1 plays an essential role in tumor immunity of colorectal cancer stem cell vaccine. *Int Immunopharmacol* (2020) 85:106631. doi: 10.1016/j.intimp.2020.106631
63. Coura MMA, Barbosa EA, Brand GD, Bloch CJr., de Sousa JB. Identification of differential n-glycan compositions in the serum and tissue of colon cancer patients by mass spectrometry. *Biol (Basel)* (2021) 10(4):343. doi: 10.3390/biology10040343
64. Scott DA, Casadonte R, Cardinali B, Spruill L, Mehta AS, Carli F, et al. Increases in tumor n-glycan polyactosamines associated with advanced HER2-positive and triple-negative breast cancer tissues. *Proteomics Clin Appl* (2019) 13(1):1800014. doi: 10.1002/prca.201800014
65. Waniwan JT, Chen YJ, Capangpangan R, Weng SH, Chen YJ. Glycoproteomic alterations in drug-resistant nonsmall cell lung cancer cells revealed by lectin magnetic nanoprobe-based mass spectrometry. *J Proteome Res* (2018) 17(11):3761–73. doi: 10.1021/acs.jproteome.8b00433
66. Qin H, Chen Y, Mao J, Cheng K, Sun D, Dong M, et al. Proteomics analysis of site-specific glycoforms by a virtual multistage mass spectrometry method. *Anal Chim Acta* (2019) 1070:60–8. doi: 10.1016/j.aca.2019.04.025
67. Gao Y, Zhou Y, Chandrawati R. Metal and metal oxide nanoparticles to enhance the performance of enzyme-linked immunosorbent assay (ELISA). *ACS Appl Nano Materials* (2019) 3(1):1–21. doi: 10.1021/acsanm.9b02003
68. Zhang D, Li W, Ma Z, Han H. Improved ELISA for tumor marker detection using electro-readout-mode based on label triggered degradation of methylene blue. *Biosens Bioelectron* (2019) 126:800–5. doi: 10.1016/j.bios.2018.11.038
69. Waritani T, Chang J, McKinney B, Terato K. An ELISA protocol to improve the accuracy and reliability of serological antibody assays. *MethodsX* (2017) 4:153–65. doi: 10.1016/j.mex.2017.03.002
70. Zhang L, Fan C, Liu M, Liu F, Bian S, Du S, et al. Biomimetic gold-Hemin@MOF composites with peroxidase-like and gold catalysis activities: A high-throughput colorimetric immunoassay for alpha-fetoprotein in blood by ELISA and gold-catalytic silver staining. *Sensors Actuators B: Chem* (2018) 266:543–52. doi: 10.1016/j.snb.2018.03.153
71. Hou Q, Bing ZT, Hu C, Li MY, Yang KH, Mo Z, et al. RankProd combined with genetic algorithm optimized artificial neural network establishes a diagnostic and prognostic prediction model that revealed CIQTNF3 as a biomarker for prostate cancer. *EBioMedicine* (2018) 32:234–44. doi: 10.1016/j.ebiom.2018.05.010
72. Perrone A, Giovino A, Benny J, Martinelli F. Advanced glycation end products (AGEs): Biochemistry, signaling, analytical methods, and epigenetic effects. *Oxid Med Cell Longev* (2020) 2020:3818196. doi: 10.1155/2020/3818196
73. Ruben LC, Laura MR, Almudena FB, Emilio GM. Glycan array analysis of pholiota squarrosa lectin and other fucose-oriented lectins. *Glycobiology* (2021) 31(4):459–76. doi: 10.1093/glycob/cwaa093
74. Zhu J, Warner E, Parikh ND, Lubman DM. Glycoproteomic markers of hepatocellular carcinoma-mass spectrometry based approaches. *Mass Spectrom Rev* (2019) 38(3):265–90. doi: 10.1002/mas.21583
75. Nguyen AT, Chia J, Ros M, Hui KM, Saltel F, Bard F. Organelle specific O-glycosylation drives MMP14 activation, tumor growth, and metastasis. *Cancer Cell* (2017) 32(5):639–53. doi: 10.1016/j.ccell.2017.10.001
76. Huang YF, Aoki K, Akase S, Ishihara M, Liu YS, Yang G, et al. Global mapping of glycosylation pathways in human-derived cells. *Dev Cell* (2021) 56(8):1195–209. doi: 10.1016/j.devcel.2021.02.023
77. Syed P, Gidwani K, Kekki H, Leivo J, Pettersson K, Lamminmaki U. Role of lectin microarrays in cancer diagnosis. *Proteomics* (2016) 16(8):1257–65. doi: 10.1002/pmic.201500404
78. Liu T, Liu R, Zhang S, Guo K, Zhang Q, Li W, et al. Sorafenib induced alteration of protein glycosylation in hepatocellular carcinoma cells. *Oncol Lett* (2017) 14(1):517–24. doi: 10.3892/ol.2017.6177
79. Zeng X, Li S, Tang S, Li X, Zhang G, Li M, et al. Changes of serum IgG glycosylation patterns in primary biliary cholangitis patients. *Front Immunol* (2021) 12:669137. doi: 10.3389/fimmu.2021.669137
80. Li N, Desiderio DM, Zhan X. The use of mass spectrometry in a proteome-centered multiomics study of human pituitary adenomas. *Mass Spectrom Rev* (2021), 1–50. doi: 10.1002/mas.21710
81. Kang T, Boland BB, Jensen P, Alarcon C, Nawrocki A, Grimsby JS, et al. Characterization of signaling pathways associated with pancreatic beta-cell adaptive flexibility in compensation of obesity-linked diabetes in db/db mice. *Mol Cell Proteomics* (2020) 19(6):971–93. doi: 10.1074/mcp.RA119.001882
82. O'Rourke MB, Town SEL, Dalla PV, Bicknell F, Koh Belic N, Viola JP, et al. What is normalization? the strategies employed in top-down and bottom-up proteome analysis workflows. *Proteomes* (2019) 7(3):29. doi: 10.3390/proteomes703029
83. Delcourt V, Franck J, Quanicco J, Gimeno JP, Wiszorski M, Raffo-Romero A, et al. Spatially-resolved top-down proteomics bridged to MALDI MS imaging reveals the molecular physiome of brain regions. *Mol Cell Proteomics* (2018) 17(2):357–72. doi: 10.1074/mcp.M116.065755
84. Wei L, Gregorich ZR, Lin Z, Cai W, Jin Y, McKiernan SH, et al. Novel sarcopenia-related alterations in sarcomeric protein post-translational modifications (PTMs) in skeletal muscles identified by top-down proteomics. *Mol Cell Proteomics* (2018) 17(1):134–45. doi: 10.1074/mcp.RA117.000124
85. Chen B, Brown KA, Lin Z, Ge Y. Top-down proteomics: Ready for prime time? *Anal Chem* (2018) 90(1):110–27. doi: 10.1021/acs.analchem.7b04747
86. Melby JA, Roberts DS, Larson EJ, Brown KA, Bayne EF, Jin S, et al. Novel strategies to address the challenges in top-down proteomics. *J Am Soc Mass Spectrom* (2021) 32(6):1278–94. doi: 10.1021/jasms.1c00099
87. Xu Y, Wang Y, Hoti N, Clark DJ, Chen SY, Zhang H. The next "sweet" spot for pancreatic ductal adenocarcinoma: Glycoprotein for early detection. *Mass Spectrom Rev* (2021), 21748. doi: 10.1002/mas.21748
88. Pont L, Kuzyk V, Benavente F, Sanz-Nebot V, Mayboroda OA, Wuhler M, et al. Site-specific n-linked glycosylation analysis of human carcinoembryonic antigen by sheathless capillary electrophoresis-tandem mass spectrometry. *J Proteome Res* (2021) 20(3):1666–75. doi: 10.1021/acs.jproteome.0c00875
89. Yang L, Du X, Peng Y, Cai Y, Wei L, Zhang Y, et al. Integrated pipeline of isotopic labeling and selective enriching for quantitative analysis of n-glycome by mass spectrometry. *Anal Chem* (2019) 91(2):1486–93. doi: 10.1021/acs.analchem.8b04525
90. Zhao X, Zheng S, Li Y, Huang J, Zhang W, Xie Y, et al. An integrated mass spectroscopy data processing strategy for fast identification, in-depth, and reproducible quantification of protein O-glycosylation in a large cohort of human urine samples. *Anal Chem* (2020) 92(1):690–8. doi: 10.1021/acs.analchem.9b02228
91. Xiao H, Suttapitugsakul S, Sun F, Wu R. Mass spectrometry-based chemical and enzymatic methods for global analysis of protein glycosylation. *Acc Chem Res* (2018) 51(8):1796–806. doi: 10.1021/acs.accounts.8b00200
92. Lund R, Leth-Larsen R, Jensen ON, Ditzel HJ. Efficient isolation and quantitative proteomic analysis of cancer cell plasma membrane proteins for identification of metastasis-associated cell surface markers. *J Proteome Res* (2009) 8(6):3078–90. doi: 10.1021/pr801091k
93. Sun F, Suttapitugsakul S, Wu R. Systematic characterization of extracellular glycoproteins using mass spectrometry. *Mass Spectrom Rev* (2021), 1–27. doi: 10.1002/mas.21708
94. Wollscheid B, Bausch-Fluck D, Henderson C, O'Brien R, Bibel N, Schiess R, et al. Mass-spectrometric identification and relative quantification of n-linked cell surface glycoproteins. *Nat Biotechnol* (2009) 27(4):378–86. doi: 10.1038/nbt.1532

95. Haverland NA, Waas M, Ntai I, Keppel T, Gundry RL, Kelleher NL. Cell surface proteomics of n-linked glycoproteins for typing of human lymphocytes. *Proteomics* (2017) 17(19):1700156. doi: 10.1002/pmic.201700156
96. Bausch-Fluck D, Goldmann U, Muller S, van Oostrum M, Muller M, Schubert OT, et al. The in silico human surfaceome. *Proc Natl Acad Sci U.S.A.* (2018) 115(46):E10988–97. doi: 10.1073/pnas.1808790115
97. Kalxdorf M, Gade S, Eberl HC, Bantscheff M. Monitoring cell-surface n-glycoproteome dynamics by quantitative proteomics reveals mechanistic insights into macrophage differentiation. *Mol Cell Proteomics* (2017) 16(5):770–85. doi: 10.1074/mcp.M116.063859
98. Li Y, Wang Y, Mao J, Yao Y, Wang K, Qiao Q, et al. Sensitive profiling of cell surface proteome by using an optimized biotinylation method. *J Proteomics* (2019) 196:33–41. doi: 10.1016/j.jprot.2019.01.015
99. Sun F, Suttapitugsakul S, Wu R. Enzymatic tagging of glycoproteins on the cell surface for their global and site-specific analysis with mass spectrometry. *Anal Chem* (2019) 91(6):4195–203. doi: 10.1021/acs.analchem.9b00441
100. Zheng J, Xiao H, Wu R. Specific identification of glycoproteins bearing the tn antigen in human cells. *Angew Chem Int Ed Engl* (2017) 56(25):7107–11. doi: 10.1002/anie.201702191
101. Saxon E, Bertozzi CR. Cell surface engineering by a modified staudinger reaction. *Science* (2000) 287(5460):2007–10. doi: 10.1126/science.287.5460.2007
102. Suttapitugsakul S, Ulmer LD, Jiang C, Sun F, Wu R. Surface glycoproteomic analysis reveals that both unique and differential expression of surface glycoproteins determine the cell type. *Anal Chem* (2019) 91(10):6934–42. doi: 10.1021/acs.analchem.9b01447
103. Xiao H, Tang GX, Wu R. Site-specific quantification of surface n-glycoproteins in statin-treated liver cells. *Anal Chem* (2016) 88(6):3324–32. doi: 10.1021/acs.analchem.5b04871
104. Park DD, Xu G, Wong M, Phoomak C, Liu M, Haigh NE, et al. Membrane glycomics reveal heterogeneity and quantitative distribution of cell surface sialylation. *Chem Sci* (2018) 9(29):6271–85. doi: 10.1039/c8sc01875h
105. Xiao H, Wu R. Quantitative investigation of human cell surface n-glycoprotein dynamics. *Chem Sci* (2017) 8(1):268–77. doi: 10.1039/c6sc01814a
106. Xiao H, Wu R. Simultaneous quantitation of glycoprotein degradation and synthesis rates by integrating isotope labeling, chemical enrichment, and multiplexed proteomics. *Anal Chem* (2017) 89(19):10361–7. doi: 10.1021/acs.analchem.7b02241
107. Qin W, Lv P, Fan X, Quan B, Zhu Y, Qin K, et al. Quantitative time-resolved chemoproteomics reveals that stable O-GlcNAc regulates box C/D SnoRNP biogenesis. *Proc Natl Acad Sci U.S.A.* (2017) 114(33):E6749–58. doi: 10.1073/pnas.1702688114
108. Yu SH, Zhao P, Sun T, Gao Z, Moremen KW, Boons GJ, et al. Selective exoenzymatic labeling detects increased cell surface sialoglycoprotein expression upon megakaryocytic differentiation. *J Biol Chem* (2016) 291(8):3982–9. doi: 10.1074/jbc.M115.700369
109. Sun T, Yu SH, Zhao P, Meng L, Moremen KW, Wells L, et al. One-step selective exoenzymatic labeling (SEEL) strategy for the biotinylation and identification of glycoproteins of living cells. *J Am Chem Soc* (2016) 138(36):11575–82. doi: 10.1021/jacs.6b04049
110. Wen L, Liu D, Zheng Y, Huang K, Cao X, Song J, et al. A one-step chemoenzymatic labeling strategy for probing sialylated thomsen-friedenreich antigen. *ACS Cent Sci* (2018) 4(4):451–7. doi: 10.1021/acscentsci.7b00573
111. Sun F, Suttapitugsakul S, Wu R. Unraveling the surface glycoprotein interaction network by integrating chemical crosslinking with MS-based proteomics. *Chem Sci* (2021) 12(6):2146–55. doi: 10.1039/d0sc06327d
112. Xie Y, Chen S, Li Q, Sheng Y, Alvarez MR, Reyes J, et al. Glycan-protein cross-linking mass spectrometry reveals sialic acid-mediated protein networks on cell surfaces. *Chem Sci* (2021) 12(25):8767–77. doi: 10.1039/d1sc00814e
113. Loh KH, Stawski PS, Draycott AS, Udeshi ND, Lehrman EK, Wilton DK, et al. Proteomic analysis of unbound cellular compartments: Synaptic clefts. *Cell* (2016) 166(5):1295–307. doi: 10.1016/j.cell.2016.07.041
114. Joeh E, O'Leary T, Li W, Hawkins R, Hung JR, Parker CG, et al. Mapping glycan-mediated galectin-3 interactions by live cell proximity labeling. *Proc Natl Acad Sci U.S.A.* (2020) 117(44):27329–38. doi: 10.1073/pnas.2009206117
115. Xie Y, Sheng Y, Li Q, Ju S, Reyes J, Lebrilla CB. Determination of the glycoprotein specificity of lectins on cell membranes through oxidative proteomics. *Chem Sci* (2020) 11(35):9501–12. doi: 10.1039/d0sc04199h
116. Li Q, Xie Y, Xu G, Lebrilla CB. Identification of potential sialic acid binding proteins on cell membranes by proximity chemical labeling. *Chem Sci* (2019) 10(24):6199–209. doi: 10.1039/c9sc01360a
117. Chen Y, Ding L, Ju H. *In situ* cellular glycan analysis. *Acc Chem Res* (2018) 51(4):890–9. doi: 10.1021/acs.accounts.7b00617
118. Feng Y, Guo Y, Li Y, Tao J, Ding L, Wu J, et al. Lectin-mediated in situ rolling circle amplification on exosomes for probing cancer-related glycan pattern. *Anal Chim Acta* (2018) 1039:108–15. doi: 10.1016/j.aca.2018.07.040
119. Shim MK, Yoon HY, Ryu JH, Koo H, Lee S, Park JH, et al. Cathepsin b-specific metabolic precursor for *In vivo* tumor-specific fluorescence imaging. *Angew Chem Int Ed Engl* (2016) 55(47):14698–703. doi: 10.1002/anie.201608504
120. Xie R, Dong L, Huang R, Hong S, Lei R, Chen X. Targeted imaging and proteomic analysis of tumor-associated glycans in living animals. *Angew Chem Int Ed Engl* (2014) 53(51):14082–6. doi: 10.1002/anie.201408442
121. Xiao H, Woods EC, Vukojicic P, Bertozzi CR. Precision glycolyx editing as a strategy for cancer immunotherapy. *Proc Natl Acad Sci U.S.A.* (2016) 113(37):10304–9. doi: 10.1073/pnas.1608069113
122. Zhang P, Li Y, Yu X, Ju H, Ding L. Switchable enzymatic accessibility for precision cell-selective surface glycan remodeling. *Chemistry* (2019) 25(44):10505–10. doi: 10.1002/chem.201902113
123. Yu X, Shi H, Li Y, Guo Y, Zhang P, Wang G, et al. Thermally triggered, cell-specific enzymatic glyco-editing: *In situ* regulation of lectin recognition and immune response on target cells. *ACS Appl Mater Inter* (2020) 12(49):54387–98. doi: 10.1021/acscami.0c15212
124. Yuan B, Chen Y, Sun Y, Guo Q, Huang J, Liu J, et al. Enhanced imaging of specific cell-surface glycosylation based on multi-FRET. *Anal Chem* (2018) 90(10):6131–7. doi: 10.1021/acs.analchem.8b00424
125. Wu N, Bao L, Ding L, Ju H. A single excitation-duplexed imaging strategy for profiling cell surface protein-specific glycoforms. *Angew Chem Int Ed Engl* (2016) 55(17):5220–4. doi: 10.1002/anie.2016101233
126. Li S, Liu Y, Liu L, Feng Y, Ding L, Ju H. A hierarchical coding strategy for live cell imaging of protein-specific glycoform. *Angew Chem Int Ed Engl* (2018) 57(37):12007–11. doi: 10.1002/anie.201807054
127. Hui J, Bao L, Li S, Zhang Y, Feng Y, Ding L, et al. Localized chemical remodeling for live cell imaging of protein-specific glycoform. *Angew Chem Int Ed Engl* (2017) 56(28):8139–43. doi: 10.1002/anie.201703406
128. Liu Y, Liu L, Li S, Wang G, Ju H, Ding L. Filter beacon: A gating-free architecture for protein-specific glycoform imaging on cell surface. *Anal Chem* (2019) 91(9):6027–34. doi: 10.1021/acs.analchem.9b00551
129. Dawson KA, Yan Y. Current understanding of biological identity at the nanoscale and future prospects. *Nat Nanotechnol* (2021) 16(3):229–42. doi: 10.1038/s41565-021-00860-0
130. Peng W, Gutierrez Reyes CD, Gautam S, Yu A, Cho BG, Goli M, et al. MS-based glycomics and glycoproteomics methods enabling isomeric characterization. *Mass Spectrom Rev* (2021), 1–40. doi: 10.1002/mas.21713
131. Chang D, Zaia J. Methods to improve quantitative glycoprotein coverage from bottom-up LC-MS data. *Mass Spectrom Rev* (2021), 1–16. doi: 10.1002/mas.21692
132. Liu L, Li S, Mao A, Wang G, Liu Y, Ju H, et al. A localized molecular automaton for in situ visualization of proteins with specific chemical modifications. *Chem Sci* (2020) 11(6):1665–71. doi: 10.1039/c9sc04161c
133. Yin Y, Hu B, Yuan X, Cai L, Gao H, Yang Q. Nanogel: A versatile nanodelivery system for biomedical applications. *Pharmaceutics* (2020) 12(3):290. doi: 10.3390/pharmaceutics12030290
134. Costa AF, Campos D, Reis CA, Gomes C. Targeting glycosylation: A new road for cancer drug discovery. *Trends Cancer* (2020) 6(9):757–66. doi: 10.1016/j.trecan.2020.04.002
135. Diniz F, Coelho P, Duarte HO, Sarmiento B, Reis CA, Gomes J. Glycans as targets for drug delivery in cancer. *Cancers (Basel)* (2022) 14(4):911. doi: 10.3390/cancers14040911
136. Ponath P, Menezes D, Pan C, Chen B, Oyasu M, Strachan D, et al. A novel, fully human anti-fucosyl-GM1 antibody demonstrates potent *In vitro* and *In vivo* antitumor activity in preclinical models of small cell lung cancer. *Clin Cancer Res* (2018) 24(20):5178–89. doi: 10.1158/1078-0432.CCR-18-0018
137. Ladenstein R, Pötschger U, Valteau-Couanet D, Luksch R, Castel V, Yaniv I, et al. Interleukin 2 with anti-GD2 antibody Ch14.18/CHO (Dinutuximab beta) in patients with high-risk neuroblastoma (HR-NBL1/SIOPEN): A multicentre, randomised, phase 3 trial. *Lancet Oncol* (2018) 19(12):1617–29. doi: 10.1016/s1470-2045(18)30578-3
138. Dorvignit D, Boligan KF, Relova-Hernandez E, Clavell M, Lopez A, Labrada M, et al. Antitumor effects of the GM3(Neu5Gc) ganglioside-specific humanized antibody 14F7hT against cmah-transfected cancer cells. *Sci Rep* (2019) 9(1):9921. doi: 10.1038/s41598-019-46148-1
139. Sedlik C, Heitzmann A, Viel S, Ait Sarkouh R, Batisse C, Schmidt F, et al. Effective antitumor therapy based on a novel antibody-drug conjugate targeting the tn carbohydrate antigen. *Oncoimmunology* (2016) 5(7):e1171434. doi: 10.1080/2162402X.2016.1171434
140. Castro A, Berois N, Malanga A, Ortega C, Oppezio P, Pristich O, et al. Docetaxel in chitosan-based nanocapsules conjugated with an anti-tn antigen Mouse/Human chimeric antibody as a promising targeting strategy of lung tumors. *Int J Biol Macromol* (2021) 182:806–14. doi: 10.1016/j.ijbiomac.2021.04.054
141. Maleki F, Rezazadeh F, Varmira K. MUC1-targeted radiopharmaceuticals in cancer imaging and therapy. *Mol Pharm* (2021) 18(5):1842–61. doi: 10.1021/acs.molpharmaceut.0c01249

142. Gong Y, Klein Wolterink RGJ, Gulaia V, Cloosen S, Ehlers FAI, Wieten L, et al. Defucosylation of tumor-specific humanized anti-MUC1 monoclonal antibody enhances NK cell-mediated anti-tumor cell cytotoxicity. *Cancers (Basel)* (2021) 13(11):2579. doi: 10.3390/cancers13112579
143. Perepelyuk M, Sacko K, Thangavel K, Shoyele SA. Evaluation of MUC1-aptamer functionalized hybrid nanoparticles for targeted delivery of miRNA-29b to non-small cell lung cancer. *Mol Pharm* (2018) 15(3):985–93. doi: 10.1021/acs.molpharmaceut.7b00900
144. Bahreyni A, Alibolandi M, Ramezani M, Sarafan Sadeghi A, Abnous K, Taghdisi SM. A novel MUC1 aptamer-modified PLGA-epirubicin-PbetaAE-antimir-21 nanocomplex platform for targeted Co-delivery of anticancer agents in vitro and *In vivo*. *Colloids Surf B Biointerfaces* (2019) 175:231–8. doi: 10.1016/j.colsurfb.2018.12.006
145. Torres-Perez SA, Torres-Perez CE, Pedraza-Escalona M, Perez-Tapia SM, Ramon-Gallegos E. Glycosylated nanoparticles for cancer-targeted drug delivery. *Front Oncol* (2020) 10:605037. doi: 10.3389/fonc.2020.605037
146. Siukstaite L, Rosato F, Mitrovic A, Muller PF, Kraus K, Notova S, et al. The two sweet sides of janus lectin drive crosslinking of liposomes to cancer cells and material uptake. *Toxins (Basel)* (2021) 13(11):792. doi: 10.3390/toxins13110792
147. Elgohary MM, Helmy MW, Abdelfattah EA, Ragab DM, Mortada SM, Fang JY, et al. Targeting sialic acid residues on lung cancer cells by inhalable boronic acid-decorated albumin nanocomposites for combined Chemo/Herbal therapy. *J Control Release* (2018) 285:230–43. doi: 10.1016/j.jconrel.2018.07.014
148. Fernandes E, Ferreira D, Peixoto A, Freitas R, Relvas-Santos M, Palmeira C, et al. Glycoengineered nanoparticles enhance the delivery of 5-fluorouracil and paclitaxel to gastric cancer cells of high metastatic potential. *Int J Pharm* (2019) 570:118646. doi: 10.1016/j.ijpharm.2019.118646
149. DeSelm C, Palomba ML, Yahalom J, Hamieh M, Eyquem J, Rajasekhar VK, et al. Low-dose radiation conditioning enables CAR T cells to mitigate antigen escape. *Mol Ther* (2018) 26(11):2542–52. doi: 10.1016/j.ymthe.2018.09.008
150. Cai L, Gu Z, Zhong J, Wen D, Chen G, He L, et al. Advances in glycosylation-mediated cancer-targeted drug delivery. *Drug Discovery Today* (2018) 23(5):1126–38. doi: 10.1016/j.drudis.2018.02.009
151. Thomas D, Rathinavel AK, Radhakrishnan P. Altered glycosylation in cancer: A promising target for biomarkers and therapeutics. *Biochim Biophys Acta Rev Cancer* (2021) 1875(1):188464. doi: 10.1016/j.bbcan.2020.188464
152. Mereiter S, Balmana M, Campos D, Gomes J, Reis CA. Glycosylation in the era of cancer-targeted therapy: Where are we heading? *Cancer Cell* (2019) 36(1):6–16. doi: 10.1016/j.ccell.2019.06.006
153. Li J, Liu S, Sun L, Li W, Zhang SY, Yang S, et al. Amplified visualization of protein-specific glycosylation in zebrafish *via* proximity-induced hybridization chain reaction. *J Am Chem Soc* (2018) 140(48):16589–95. doi: 10.1021/jacs.8b08442
154. Rotte A. Combination of CTLA-4 and PD-1 blockers for treatment of cancer. *J Exp Clin Cancer Res* (2019) 38(1):1–12. doi: 10.1186/s13046-019-1259-z
155. Brunner-Weinzler MC, Rudd CE. CTLA-4 and PD-1 control of T-cell motility and migration: Implications for tumor immunotherapy. *Front Immunol* (2018) 9:2737. doi: 10.3389/fimmu.2018.02737
156. Luisi MLR. From bad to worse: The representation of the HPV vaccine Facebook. *Vaccine* (2020) 38(29):4564–73. doi: 10.1016/j.vaccine.2020.05.016
157. Groux-Degroote S, Delannoy P. Cancer-associated glycosphingolipids as tumor markers and targets for cancer immunotherapy. *Int J Mol Sci* (2021) 22(11):6145. doi: 10.3390/ijms22116145
158. Lin H, Hong H, Feng L, Shi J, Zhou Z, Wu Z. Synthesis of DNP-modified GM3-based anticancer vaccine and evaluation of its immunological activities for cancer immunotherapy. *Chin Chem Lett* (2021) 32(12):4041–4. doi: 10.1016/j.ccl.2021.04.034
159. Yin XG, Lu J, Wang J, Zhang RY, Wang XF, Liao CM, et al. Synthesis and evaluation of liposomal anti-GM3 cancer vaccine candidates covalently and noncovalently adjuvanted by alphaGalCer. *J Med Chem* (2021) 64(4):1951–65. doi: 10.1021/acs.jmedchem.0c01186
160. Cheung IY, Cheung NKV, Modak S, Mauguen A, Feng Y, Basu E, et al. Survival impact of anti-GD2 antibody response in a phase II ganglioside vaccine trial among patients with high-risk neuroblastoma with prior disease progression. *J Clin Oncol* (2021) 39(3):215–26. doi: 10.1200/JCO.20.10.1200/JCO.20.01892
161. Hutchins LF, Makhoul I, Emanuel PD, Pennisi A, Siegel ER, Jousheghany F, et al. Targeting tumor-associated carbohydrate antigens: a phase I study of a carbohydrate mimetic-peptide vaccine in stage IV breast cancer subjects. *Oncotarget* (2017) 8(58):99161–78. doi: 10.18632/oncotarget.21959
162. Hutchison S, Sahay B, de Mello SC, Sayour EJ, Lejeune A, Szivek A, et al. Characterization of myeloid-derived suppressor cells and cytokines GM-CSF, IL-10 and MCP-1 in dogs with malignant melanoma receiving a GD3-based immunotherapy. *Vet Immunol Immunopathol* (2019) 216:109912. doi: 10.1016/j.vetimm.2019.109912
163. Thurin M. Tumor-associated glycans as targets for immunotherapy: The wistar institute Experience/Legacy. *Monoclon Antib Immunodiagn Immunother* (2021) 40(3):89–100. doi: 10.1089/mab.2021.0024
164. Ghosh S, Trabbic KR, Shi M, Nishat S, Eradi P, Kleski KA, et al. Chemical synthesis and immunological evaluation of entirely carbohydrate conjugate globo h-PS A1. *Chem Sci* (2020) 11(48):13052–9. doi: 10.1039/d0sc04595k
165. Freitas R, Relvas-Santos M, Azevedo R, Soares J, Fernandes E, Teixeira B, et al. Single-pot enzymatic synthesis of cancer-associated MUC16 O-glycopeptide libraries and multivalent protein glycoconjugates: a step towards cancer glycovaccines. *New J Chem* (2021) 45(20):9197–211. doi: 10.1039/d0nj06021f
166. Zhan X, Li J, Guo Y, Golubnitschaja O. Mass spectrometry analysis of human tear fluid biomarkers specific for ocular and systemic diseases in the context of 3P medicine. *EPMA J* (2021) 12(4):449–75. doi: 10.1007/s13167-021-00265-y
167. Wen S, Li C, Zhan X. Multi-omics integration analysis revealed molecular network alterations in human nonfunctional pituitary neuroendocrine tumors in the framework of 3P medicine. *EPMA J* (2022) 13(1):9–37. doi: 10.1007/s13167-022-00274-5
168. Gray MA, Stanczak MA, Mantuano NR, Xiao H, Pijnenborg JFA, Malaker SA, et al. Targeted glycan degradation potentiates the anticancer immune response in vivo. *Nat Chem Biol* (2020) 16(12):1376–84. doi: 10.1038/s41589-020-0622-x
169. Li S, Yu B, Wang J, Zheng Y, Zhang H, Walker MJ, et al. Biomarker-based metabolic labeling for redirected and enhanced immune response. *ACS Chem Biol* (2018) 13(6):1686–94. doi: 10.1021/acschembio.8b00350
170. Kou Y, Feng R, Chen J, Duan L, Wang S, Hu Y, et al. Development of a natto kinase-polysialic acid complex for advanced tumor treatment. *Eur J Pharm Sci* (2020) 145:105241. doi: 10.1016/j.ejps.2020.105241

Glossary

AAL	Aleuria aurantia lectin
ADCP	antibody-dependent phagocytosis
AFP-L3	fucosylated α -fetoprotein
AGP	α -1-acid glycoprotein
Asn	asparagine
BH	biotin hydrazine
CDC	complementation-dependent cytotoxicity
CSC	cell-surface-capturing
CSPA	Cell Surface Protein Atlas
D-LRET	duplexed luminescence resonance energy transfer
EGFR	epidermal growth factor receptor
ELISA	enzyme-linked immunosorbent assay
ER	endoplasmic reticulum
ESI	electrospray ionization
FRET	fluorescence resonance energy transfer
Fuc	fucose
Gal	galactose
GalNAc	N-acetylgalactosamine
Glc	glucose
GlcA	glucuronic acid
GlcNAc	N-acetylglucosamine
HCR	hybridization chain reaction
HEL	human erythroleukemia cells
HieCo	hierarchical coding
HPV	human papillomavirus
IDOA	iduronic acid
L-ELISA	lectin-antibody sandwich enzyme-linked immunosorbent assay
LCM	localized chemical remodeling
MAL	Maackia amurensis leucoagglutinin
MALDI	Matrix-assisted laser desorption/ionization
Man	mannose
MOF	metal-organic frameworks
MOIs	multiple targeted modifications
MS	mass spectrometry
NCAM1	neural cell adhesion molecule 1
NE	nicking action of restriction endonuclease
NIRF	near-infrared fluorescent
PNGase F	peptide-N-glycosidase F
PTMs	post-translational modifications
Ser	serine
Sia	sialic acid
SILAC	stable isotope labeling of amino acids in cell culture
SEEL	selective exo-enzymatic labeling
SLea	sialyl-Lewis A
SLex	sialyl-Lewis X
SNA	Sambucus nigra agglutinin
Thr	threonine
TMT	tandem mass tag

Continued

TOF	time-of-flight
UCNPs	Upconversion nanoparticles
WB	Western blotting
WGA	Wheat germ agglutinin
Xyl	xylose

(Continued)



OPEN ACCESS

EDITED BY

Xianquan Zhan,
Shandong First Medical
University, China

REVIEWED BY

Alessandro Prete,
University of Pisa, Italy
Xiao-Feng Li,
Jinan University, China

*CORRESPONDENCE

Xiaorong Sun
251400067@qq.com

[†]These authors have contributed
equally to this work and share
first authorship

SPECIALTY SECTION

This article was submitted to
Cancer Endocrinology,
a section of the journal
Frontiers in Endocrinology

RECEIVED 28 June 2022

ACCEPTED 04 August 2022

PUBLISHED 08 September 2022

CITATION

Li J, Zhang Y, Sun F, Xing L and Sun X
(2022) Towards an era of precise
diagnosis and treatment: Role of novel
molecular modification-based imaging
and therapy for dedifferentiated
thyroid cancer.

Front. Endocrinol. 13:980582.

doi: 10.3389/fendo.2022.980582

COPYRIGHT

© 2022 Li, Zhang, Sun, Xing and Sun.
This is an open-access article
distributed under the terms of the
[Creative Commons Attribution License
\(CC BY\)](#). The use, distribution or
reproduction in other forums is
permitted, provided the original
author(s) and the copyright owner(s)
are credited and that the original
publication in this journal is cited, in
accordance with accepted academic
practice. No use, distribution or
reproduction is permitted which does
not comply with these terms.

Towards an era of precise diagnosis and treatment: Role of novel molecular modification-based imaging and therapy for dedifferentiated thyroid cancer

Jing Li^{1,2†}, Yingjie Zhang^{2†}, Fenghao Sun², Ligang Xing³
and Xiaorong Sun^{2*}

¹Department of Graduate, Shandong First Medical University and Shandong Academy of Medical Sciences, Jinan, China, ²Department of Nuclear Medicine, Shandong Cancer Hospital and Institute, Shandong First Medical University and Shandong Academy of Medical Sciences, Jinan, China,

³Department of Radiation Oncology, Shandong Cancer Hospital and Institute, Shandong First Medical University and Shandong Academy of Medical Sciences, Jinan, China

Dedifferentiated thyroid cancer is the major cause of mortality in thyroid cancer and is difficult to treat. Hence, the essential molecular mechanisms involved in dedifferentiation should be thoroughly investigated. Several studies have explored the biomolecular modifications of dedifferentiated thyroid cancer such as DNA methylation, protein phosphorylation, acetylation, ubiquitination, and glycosylation and the new targets for radiological imaging and therapy in recent years. Novel radionuclide tracers and drugs have shown attractive potential in the early diagnosis and treatment of dedifferentiated thyroid cancer. We summarized the updated molecular mechanisms of dedifferentiation combined with early detection by molecular modification-based imaging to provide more accurate diagnosis and novel therapeutics in the management of dedifferentiated thyroid cancer.

KEYWORDS

dedifferentiated thyroid cancer, radioactive iodine resistance, biomolecular modifications, molecular imaging, targeted therapy

Introduction

Thyroid cancer (TC) is the most frequent type of cancer in the endocrine system, the incidence of which has been increasing globally in recent years (1). Although differentiated thyroid cancer (DTC) has a good prognosis, the dedifferentiated thyroid cancer, including DTC with gradual dedifferentiation, poorly differentiated thyroid cancer (PDTC) and anaplastic thyroid cancer (ATC), is the key to treatment dilemma, and leads to the death of patients.

Approximately 6-12% of DTC patients gradually lose iodine uptake ability due to dedifferentiation and eventually develop resistance to radioactive iodine (RAI) therapy, identified as RAI-refractory DTC (RAIR-DTC), demanding additional effective treatments (2, 3) The 10-year survival rate of RAIR-DTC patients with distant metastasis is only about 10% (4). PDTC and ATC account for nearly 6% and 2% of all thyroid malignancies, respectively, and usually have a poor prognosis and high mortality (5). Thus, the treatment of patients with dedifferentiated thyroid cancer remains a major clinical challenge.

In the past decade, several studies emerged and illuminated molecular mechanisms responsible for dedifferentiated thyroid cancer. The discovery of molecular modification targets has raised high hope for new potential avenues for the management of dedifferentiated thyroid cancer. In this review, there will be a focus on investigating the comprehensive and updated molecular modification-based management strategies in dedifferentiated thyroid cancer.

Molecular modifications of dedifferentiation

Dedifferentiated thyroid cancers lose their differentiation characteristics by various mechanisms, the most important of which is the decreased expression, localization, or abnormal function of sodium/iodide symporter (NIS) proteins (6, 7).

Biomolecular modifications such as DNA methylation, protein phosphorylation, acetylation, ubiquitination, and glycosylation are significant epigenetic factors in thyroid cancer. The potential molecular basis for RAIR is the silencing of expression of thyroid-specific genes NIS, thyroglobulin (Tg), TSH receptor (TSHR), thyroperoxidase, transcription factors paired box gene-8 (PAX-8), and thyroid transcription factor-1, which are involved in alterations in cell surface receptors, signaling pathways, and nuclear receptors and epigenetics, respectively (4, 8) (Figure 1). The following detailed description is based on the site of molecular modifications and the expression levels.

Cell surface receptors

Receptor tyrosine kinase (RTKs) is a transmembrane protein expressed in the cell membrane or adjacent to the plasm, which binds to specific ligands resulting in its autophosphorylation, and mutations in the gene could constitutively activate different downstream signaling pathways, ultimately leading to dysregulation of cell proliferation, dedifferentiation, and reduced apoptosis.

Neurotrophic tyrosine receptor kinase (NTRK)

NTRK genes include NTRK1, NTRK2, and NTRK3. The autophosphorylation of NTRK1 tyrosine residues in the tyrosine-kinase domain increase NTRK1 activity. NTRK gene

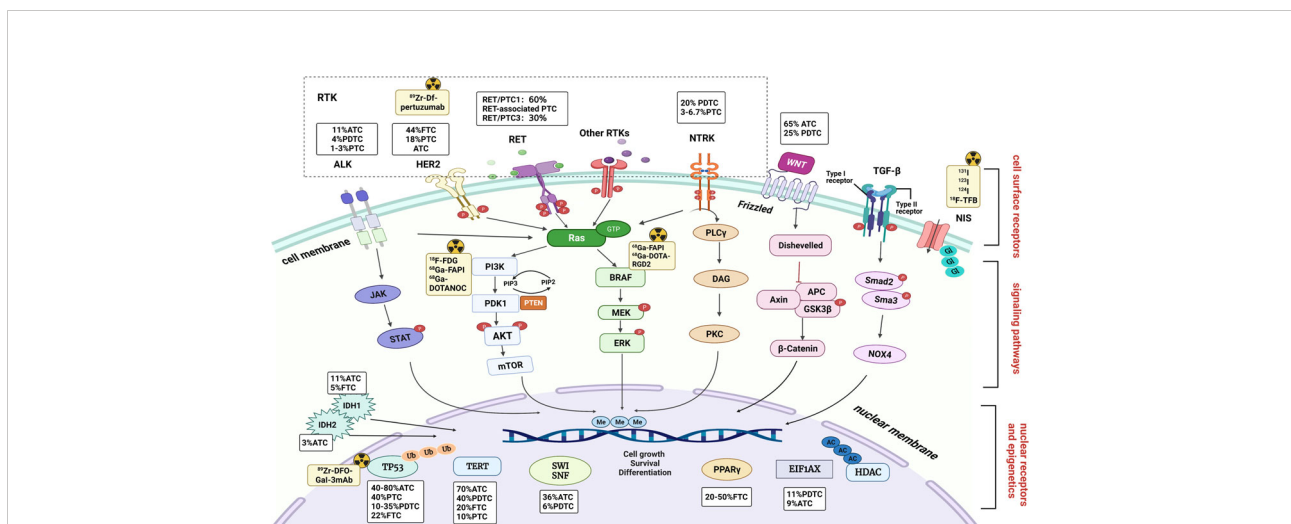


FIGURE 1 Mechanisms and molecular imaging involved in dedifferentiation of thyroid cancer. Molecular modifications and genetic mutations are described at the three levels of cell surface receptors, signaling pathways, nuclear receptors, and epigenetics. The incidence in different histologies are indicated in boxes. And the radioactive sign indicates the target for molecular imaging. RTK, receptor tyrosine kinase; ALK, anaplastic lymphoma kinase; HER2, human epidermal growth factor receptor 2; NTRK, neurotrophic tyrosine receptor kinase; NIS, sodium/iodide symporter; P, phosphorylation; JAK, Janus kinase; STAT, signal transducers and activators of transcription; ERK, extracellular signal-regulated kinase; PLCγ, phospholipase C-γ; DAG, diacylglycerol; PKC, protein kinase C; TGF-β, transforming growth factor-β; PI3K, phosphoinositide 3-kinase; APC, adenomatous polyposis coli; AXIN1, axis inhibition protein 1; GSK3β, glycogen synthase kinase 3β; NOX4, NADPH oxidase 4; PPAR-γ, peroxisome proliferator activated receptor gamma; HDAC, histone deacetylase; TERT, telomere reverse transcriptase; IDH, isocitrate dehydrogenase; EIF1AX, eukaryotic translation initiation factor 1A.

fusions are oncogenic drivers that lead to NTRK gene fusions due to intra- or inter-chromosomal rearrangements, and cytoplasmic Trk fusion proteins activate downstream signals through phosphoinositide 3-kinase (PI3K), mitogen-activated protein kinase (MAPK), and phospholipase C- γ (PLC γ) to drive tumor proliferation and spread. NTRK fusions have been found in 3-6.7% of papillary thyroid cancer (PTC) and 20% of PDTC (9).

Anaplastic lymphoma kinase (ALK)

The ALK is a transmembrane tyrosine kinase of the insulin receptor family that, when the ligand binds to its extracellular structural domain, promotes activation of multiple downstream signaling pathways, such as PI3K/AKT, MAPK, and Janus kinase (JAK)-signal transducer and activator of transcription (STAT). ALK mutations and rearrangements are most common in ATC (11.1%) and PDTC (4%), and they play a role in disease progression and aggressiveness (10).

RET

The RET gene is a proto-oncogene that encodes the RET protein of the tyrosine kinase receptor superfamily. RET protein is a receptor tyrosine kinase, undergoing phosphorylation at several tyrosine residues, that can activate various downstream signaling pathways, such as MARK and PI3K, to induce cell proliferation. Rearrangements of the RET and other genes are common (5% - 25%) in PTC (3). The expression of thyroid-specific genes, increasing the differentiation process was suppressed by conditional activation of RET/PTC1 or RET/PTC3 (6). RET/PTC1 accounts for about 60% of RET-associated PTC, with RET/PTC3 accounting for approximately 30%. Although uncommon, RET/PTC rearrangements have been discovered in ATC and PDTC, primarily in carcinomas with a differentiated component.

Other RTKs

Copy number increases have been found in different subtypes of thyroid cancer such as epidermal growth factor receptor (EGFR), platelet-derived growth factor receptor A/B (PDGFRA/B), vascular endothelial growth factor receptor 1,2 (VEGFR1,2), mast/stem cell growth factor receptor kit (c-Kit) and metabotropic proto-oncogene receptor tyrosine kinase (MET). Missense mutations such as fibroblast growth factor receptor 2 (FGFR2) and FMS-like tyrosine kinase 3 (FLT3) were found in 11% and 17% of PDTC, respectively (3). The human epidermal growth factor receptor 2 (HER2) gene (ERBB2) overexpression was discovered in follicular thyroid cancer (FTC) (44%), PTC (18%), and some ATC (11). HER2 and HER3 are essential actors upstream of the signal-regulated kinase Extracellular Signal-Regulated Kinase (ERK) and AKT signaling pathways. Overexpression of HER2 and HER3 may

provide a RAI-DTC tumor escape mechanism for BRAF mutant cells treated with the BRAF inhibitor vemurafenib (12).

Signaling pathway

PI3K pathway

RAS

The RAS proto-oncogene is one of the most common mutation targets in the PI3K/AKT cascade, and the G protein-like signaling protein it encodes is located on the inner surface of the cell membrane and is active when combined with GTP. Signaling pathways transmit signals from cell membrane RTKs and G protein-coupled receptors. The RasGRP3 mutation was shown to be more common in metastatic RAI-DTC, promoting cell proliferation, invasion, and migration. RAS mutations, harboring more DNA hypermethylations, show the preferential association with AKT phosphorylation and are more likely to activate the PI3K/AKT pathway, which can occur in 30%-50% of FTC, 15% of PTC, 30%-45% of follicular variant papillary thyroid cancer (FVPTC), and 20%-40% of PDTC and ATC (13).

PIK3CA

Activating mutations or increases in the copy number of PIK3CA can increase the protein's expression. Some studies have found that activation of PIK3CAE^{545K} plays a role in the progression of well-differentiated thyroid cancer to ATC. PIK3CA mutations are common in ATC (18%) but less common in PDTC (2%) and PTC (0.5%) (14).

AKT

The PI3K/AKT signaling pathway has long been recognized to regulate a variety of cellular and molecular processes, including cell growth, proliferation, and cell motility. AKT mutations represent a late event in thyroid cancer and, therefore, are more common in PDTC (19%) (15). In thyroid cancer cells, the phosphorylation of AKT reduced NIS and TSHR expression and RAI absorption. These findings imply that an activated AKT signaling pathway might be engaged in RAI-DTC through mediating RasGRP3 mutation. Furthermore, suppression of the PI3K/AKT signaling pathway has been shown to promote NIS expression and RAI absorption in thyroid cancer cells (6).

PTEN

PTEN is a tumor suppressor gene that is found on chromosome 10 and is altered or deleted in heritable and spontaneous malignancies. PTEN is one of the most important downstream regulators of PI3K signaling, and its dysregulation could have a significant impact on this pathway. PTEN

mutations, decreasing the conversion from PIP3 to PIP2 followed by increasing AKT phosphorylation, may prevent NIS from being glycosylated and inhibit it from reaching the plasma membrane. As a result, cytoplasmic NIS expression increases (16). PTEN mutations have been found in ATC (15%), FTC (14%), PDTC (4%), and PTC (2%) (3).

MAPK pathway

Many human cancer types exhibit activation of the MAPK signaling pathway, which is accomplished by activating mutations or overexpression of MAPK upstream activators such as RTKs, Ras, and Raf, leading to MEK phosphorylation followed by ERK phosphorylation. Changes in the MAPK pathway are prevalent in thyroid cancer, particularly in PTC (40–80%), ATC (10–50%), and PDTC (5–35%) (17). It mostly includes mutations in the BRAF gene, which result in cell differentiation loss and apoptosis inhibition. Furthermore, patients with BRAF mutations show hypermethylation of the TSHR gene promoter. The most frequent BRAF mutation is the V600E gene replacement, which boosts BRAF protein activity and keeps it active. It forms a monomer independent of the upstream RAS kinase, leading to persistent activation of MEK/ERK, cell differentiation loss, tumor development, and apoptosis inhibition. BRAF^{V600E} mutations are found in 45–50% of PTC and 36% of ATC (18).

WNT pathway

Molecular alterations in the Wnt/ β -catenin signaling pathway involved in adenomatous polyposis coli (APC), axis inhibition protein 1 (AXIN1), and catenin beta 1 (CTNNB1) contribute to thyroid tumorigenesis. Furthermore, the direct phosphorylation of glycogen synthase kinase 3 β (GSK3 β) activates the WNT/ β -catenin pathway and the association between β -direct catenin and PAX-8 boosts its gene transcription for NIS expression. These changes become more common in ATC (66%) and PDTC (25%) (19).

Transforming growth factor- β (TGF- β)/Smad signaling pathway

Several studies have found that TGF- β is essential for the proliferation and differentiation of thyroid cells (6). The TGF- β -type II receptor complex motivates the phosphorylation of Smad2 and Smad3. Some researchers demonstrated that a BRAF mutation could increase NADPH oxidase 4 (NOX4) expression in thyroid cancer cells by the TGF β /SMAD3 signaling pathway. NOX4-reactive oxygen species (ROS) generation suppresses NIS expression in follicular cells by interfering with the binding of the PAX8 to the NIS gene promoter. NOX4 might be used as a therapeutic target in conjunction with other MAPK-kinase inhibitors to enhance their efficacy on RAI-DTC redifferentiation (20).

Nuclear receptors and epigenetic alterations

TP53

TP53 gene is an oncogene that encodes a protein involved in a variety of cellular activities, which could cause cell cycle arrest, apoptosis, senescence, DNA repair, or metabolic alterations in response to cellular stress. TP53 inactivation, its degradation mediated by p53 poly-ubiquitination, has long been thought to be a final step in tumor growth. TP53 mutations were found in around 40–80% of ATC, 10–35% of PDTC, 40% of PTC, and 22% of oncogenic FTC (21).

Telomere reverse transcriptase (TERT)

TERT maintains the length and stability of chromosomes by adding telomeres to the ends of chromosomes, which is of great significance to the lifespan of the body and various cellular activities. Mutations of the TERT promoter are mostly late events in the development of thyroid cancer, the incidence of which is high, especially in ATC (70%), PDTC (40%), FTC (20%), and PTC (10%) (15). TERT promoter mutations have also been shown to be strongly associated with aggressive clinicopathological characteristics and the probability of recurrence or distant metastasis (22).

SWI/SNF

The SWI/SNF complexes gene mutations have been detected in ATC (36%) and PDTC (6%) (3). SWI/SNF complexes are critical for maintaining differentiated function in thyroid cancer, and their loss imparts radioiodine refractoriness as well as resistance to MAPK inhibitor-based redifferentiation therapy (23).

Eukaryotic translation initiation factor 1A (EIF1AX)

The EIF1AX gene encodes an essential eukaryotic translation initiation factor. EIF1AX mutations have been reported in PDTC (11%) and ATC (9%) associated with oncogenic RAS. In advanced disease, the dramatic interplay of EIF1AX and RAS mutations shows that they may work together to induce tumor progression (24). The mechanism of EIF1AX mutation in thyroid cancer tumorigenesis and dedifferentiation still needs to be further studied.

Isocitrate dehydrogenase (IDH1/IDH2)

The IDH1 mutations are frequently found in thyroid cancer, identified in ATC (11%), FTC (5%), and PDTC (1.25%). While IDH2 mutation was identified in 3% of ATC (25). However,

further research is needed to identify their functions in the pathogenesis of thyroid carcinomas.

Peroxisome proliferator activated receptor gamma (PPAR γ)

PAX8/PPAR γ rearrangement is the second most common genetic alteration in 20-50% of FTC besides RAS mutation, with an incidence of 30-35%, and it is also present in a minority of FVPTC (5%). It plays a role in the control of cell proliferation and redifferentiation. PPAR agonists have been proven to trigger redifferentiation in thyroid cancer in some studies (6).

Histone deacetylase (HDAC)

Notably, dysregulated histone acetyltransferase and HDAC activity are linked to cancer cell growth, proliferation, and differentiation. Some researchers have discovered that histone acetylation is altered in thyroid tumorigenesis and H3 histone is turned off in the progression from differentiated to undifferentiated thyroid cancer (26).

Molecular imaging in detection of dedifferentiated thyroid cancer

Nowadays, molecular imaging, which uses radionuclides or intentionally changed molecules to find biomarkers, prospective therapy targets, or define signaling networks, has grown in popularity. These targets are important in the diagnosis and

treatment of dedifferentiated thyroid cancer because they allow the molecular component of tumor tissue to be characterized and quantified. Molecular imaging has been demonstrated to help with thyroid cancer diagnosis, individualized treatment, and prognostic indicators prediction (27) (Figure 1). Furthermore, molecular imaging is required for multimodality-based thyroid cancer treatment options, which could drive the invention of novel therapeutic or diagnostic tracers (28). Recently, a growing number of clinical studies have explored molecular imaging in dedifferentiated thyroid cancer.

Sodium iodide symporter targeted molecular imaging (NIS)

Radioiodine

A widely used radioisotope, radioiodine, plays a critical role in the diagnosis and treatment of DTC, such as ^{123}I , ^{124}I , and ^{131}I . ^{131}I SPECT/CT has become a routine tool for visualizing the lesions and evaluating distant metastases in patients receiving radioactive iodine therapy (29). ^{124}I PET/CT could improve the sensitivity and spatial resolution of SPECT/CT, leading to superior diagnostic performance of post-therapy ^{131}I -WBS. However, it is expensive and has low accessibility (30) (Table 1).

Fluorine-18-tetrafluoroborate (^{18}F -TFB)

TFB is a sodium/iodide symporter substrate with similar NIS affinities to radioiodine. ^{18}F -TFB has recently been established as a flexible PET probe for imaging the activity of human sodium/

TABLE 1 The diagnostic efficacy of radiotracers in dedifferentiated thyroid cancer with negative post-therapy ^{131}I -WBS and elevated Tg

Radiotracers	Study Phase	Population	n	Sensitivity	Specificity	Accuracy	PPV	NPV
^{124}I	Prospective (2016) (30)	DTC	17	44%	100%	NA	100%	62%
^{18}F -TFB	Retrospective (2020) (32)	recurrent DTC	25	64%	NA	64%	100%	NA
^{18}F -FDG	Retrospective (2021) (34)	DTC	113	92%	94%	93%	87%	93%
^{68}Ga -DOTANOC	Prospective (2019) (36)	DTC	62	78.4%	100%	82.3%	100%	50%
^{68}Ga -DOTA-RGD ₂	Prospective (2020) (37)	RAIR-DTC	44	82.3%	100%	82.4%	NA	NA
^{68}Ga -PSMA	Retrospective (2020) (39)	RAIR-DTC	5	NA	NA	NA	NA	NA
^{68}Ga -FAPI	Prospective (2022) (40)	metastatic DTC	35	83% in neck lesions, 79% in distant metastases	NA	NA	NA	NA

RAIR, radioactive iodine-refractory; DTC, differentiated thyroid cancer; Tg, thyroglobulin; n, number; NA, not available; PPV, positive prognostic value; NPV, negative prognostic value; ^{18}F -TFB, fluorine-18-tetrafluoroborate; ^{18}F -FDG, fluorine-18-fluorodeoxyglucose; PSMA, prostate-specific membrane antigen; FAPI, fibroblast activation protein inhibitor.

iodide symporters. As a result, ^{18}F -TFB PET could be a valuable method for evaluating NIS expression in human diseases and be able to visualize DTC metastases in negative ^{124}I PET (31). Compared to conventional diagnostic WBS and SPECT-CT, ^{18}F -TFB PET could detect more local recurrence or metastases of DTC (32). The combination of ^{18}F -TFB PET and fluorine-18-fluorodeoxyglucose (^{18}F -FDG) PET appears to be a feasible technique for characterizing DTC tumor presentations in terms of differentiation and, as a result, individually planning and monitoring therapy. Prospective studies evaluating the potential of ^{18}F -TFB PET in recurrent DTC are needed in the future.

Glucose transporter targeted molecular imaging

^{18}F -FDG

^{18}F -FDG is well-known radiopharmaceutical glucose that is mostly carried by glucose-transporter family-1 (GLUT1), and its uptake has been reported to be influenced by the degree of tumor proliferation and differentiation. Additionally, the surface expression of GLUT is controlled by the PI3k/AKT pathway. Advanced TC with low radioiodine uptake usually had high ^{18}F -FDG uptake. Some researchers observed that ^{18}F -FDG showed positive uptake in 50 patients (17%) among 258 DTC patients, 39 (78%) of which did not show positive lesions on post-therapy WBS (33). ^{18}F -FDG PET/CT might allow RR-DTC patients to classify their prognosis by revealing tumor aggressiveness. ^{18}F -FDG PET/CT has shown good diagnostic performance in non-iodine avid DTC with a sensitivity, specificity, and accuracy of 92%, 94%, and 93%, respectively. Therefore, ^{18}F -FDG PET/CT could enable clinicians in identifying individuals with RAIR-DTC and developing a treatment strategy earlier (34).

Peptide-based molecular imaging

Somatostatin receptor (SSTR)

SSTRs are highly expressed in neuroendocrine tumors. But in recent studies, SSTRs have been found to be overexpressed in dedifferentiated thyroid cancer. Less differentiated carcinomas are more likely to express a wider range of SSTR subtypes, primarily subtypes 2, 3, and 5, bolstering the theories of peptide receptor-based nuclear diagnosis and treatment. SSTR1-5 activation suppresses PI3K/AKT signaling (35). Parveen et al. evaluate the value of ^{68}Ga -DOTANOC PET/CT in DTC with negative ^{131}I WBS and elevated serum Tg levels. The detection of recurrent disease in DTC with a sensitivity and specificity of 78.4%, and 100%, respectively. It may also assist in the selection of possible peptide receptor radionuclide treatment candidates (36).

$\alpha v \beta 3$ Integrin

The integrin $\alpha v \beta 3$ is overexpressed in the tumor vascular system. The tripeptide sequence arginine-glycine-aspartate (RGD) shows a high affinity and specificity for integrin $\alpha v \beta 3$. Recently, a prospective study has indicated that ^{68}Ga -DOTA-RGD₂ PET/CT showed a better diagnostic performance in RAIR-DTC with negative post-therapy ^{131}I -WBS with an accuracy, sensitivity, and specificity of 86.4%, 82.3%, and 100%, respectively, compared to ^{18}F -FDG PET/CT [75%, 82.3%, 50% (37)]. Moreover, the novel radiotracer could provide the potential for the selection of eligible RAIR-DTC candidates for treatment with ^{177}Lu -DOTA-RGD₂.

Prostate-specific membrane antigen (PSMA)

PSMA is a type II transmembrane glycoprotein receptor expressed in prostate cancer cells and the endothelium of tumor-associated neovasculature in several malignancies. Similarly, PSMA expression has been observed in 62% of persistent or recurrent DTC. Some studies have shown that PSMA expression was also related to poor prognosis and that very high PSMA expression was associated with poorer PFS (38). For patients with RAIR-DTC, ^{68}Ga -PSMA PET/CT can be useful for staging because it could identify different types of lesions and may discover lesions that ^{18}F -FDG PET/CT does not detect. Additionally, ^{68}Ga -PSMA might be utilized to screen patients for ^{177}Lu -PSMA targeted therapy in the future (39).

Other molecular imaging

^{68}Ga -labeled fibroblast activation protein inhibitor (FAPI)

In over 90% of epithelial carcinomas, FAP is significantly expressed in cancer-associated fibroblasts. Increased FAP expression is associated with dedifferentiation and aggressiveness outcome of thyroid cancer. In some cases, ^{68}Ga -FAPI PET/CT revealed high activity in the metastatic DTC with elevated Tg and negative iodine scan. ^{68}Ga -FAPI might perform better than ^{18}F -FDG in detecting metastatic DTC, particularly in pulmonary and lymph node metastases (40). Another research has also found that ^{68}Ga -DOTA-FAPI-04 PET/CT may have a good performance in the detection of lymph node metastasis and distant metastasis in 87.5% (21/24) of RAIR-DTC patients (41). More multicenter prospective studies with bigger sample sizes are needed to confirm these findings.

Lectin galactoside-binding soluble 3

Galactin-3 (Gal-3) is a β -galactoside binding protein of the lectin family that is absent in normal and benign thyroid tissues but overexpressed in the cytoplasm, cell membranes, and intercellular components of DTC and ATC (42). Meanwhile, Gal-3 is a physiological target of p53 transcriptional activity, and

its downregulation mediated by p53 is essential for p53-induced apoptosis. ^{89}Zr -DFO-Gal-3mAb detected specific and reliable uptake of human thyroid cancer xenograft *in vivo*. ^{89}Zr -DFO-F(ab')₂ anti-gal-3 exhibited specific uptake in tumor tissue, while the normal thyroid tissue had no uptake. Besides, in the absence of radioiodine uptake, specific and selective detection of thyroid tumors was achieved by targeting Gal-3 (43). Gal-3 immunoPET is still a new field of research, and these findings imply that diagnostic and clinical applications of Gal-3 targeted radiotracers for thyroid cancer need further investigation.

HER2

In a recent study, a HER2-specific PET imaging probe ^{89}Zr -Df-pertuzumab was developed to assess the diagnostic effectiveness in orthotopic ATC. These findings suggested that noninvasive HER2 molecular imaging offers a great potential for detecting HER2 status in ATC (11). With extensive clinical translation and use of ^{89}Zr -Df-pertuzumab PET, this imaging method may be able to identify the diverse levels of HER2 around the body. This suggests that this unique imaging method could identify ATC patients who may react to HER2-targeted therapy (such as pertuzumab and trastuzumab) and dynamically monitor therapeutic responses.

Landscape of treatment in dedifferentiated thyroid cancer

Tyrosine kinase inhibitors (TKIs)

In the past decade, the findings of signaling pathways and activating mutations have spurred the development of biomarker-driven targeted therapies. Most extensively investigated and clinically approved targeted therapies in thyroid cancer include the TKIs that target antiangiogenic markers, BRAF mutation, and MAPK pathway components. The initiation into systemic treatment is based on tumor burden and tumor growth rate. Watchful surveillance can be considered in patients with stable or slowly progressive thyroid cancer. Patients with rapidly progressive and/or symptomatic diseases are candidates for TKIs (44).

Multi-kinase inhibitors (MKIs)

MKIs inhibit the activity of multiple receptor tyrosine kinases such as VEGFR, PDGFR, FGFR, and various Raf kinases, thereby suppressing tumor cell proliferation and angiogenesis. Novel MKIs have been evaluated and approved by FDA for advanced RAI-DTC such as sorafenib, lenvatinib and cabozantinib (45–47). Other commercially available MKIs (such as anlotinib, donafenib, surufatinib, sunitinib, and pazopanib) can be considered if clinical trials are not available or appropriate (Tables 2, 3) (48–52). MKIs have demonstrated

clinical efficacy to prolong median progression-free survival (PFS), but in most cases, no significant benefit was observed in overall survival (OS), except in the SELECT study of lenvatinib, OS was significantly improved among patients aged > 65 years compared with placebo (53). Due to these multiple target effects, molecular testing does not predict clinical responses. And the off-target side effects are common and sometimes severe. The most common treatment-related adverse events (TRAEs) include diarrhoea, fatigue, hypertension, hand-foot skin reactions et al. Most adverse effects can be managed and are reversible with discontinuation. Below, we summarize the most important results of TKIs clinical trials in advanced or dedifferentiated thyroid cancer.

Sorafenib

Sorafenib is an orally active TKI that targets VEGFR, RET, RAF, and PDGFR et al. In the DECISION trial, sorafenib showed significantly longer PFS (10.8 months vs. 5.8 months in the placebo arm) and a 12% objective response rate (ORR) (45). Sorafenib was approved by U.S. Food and Drug Administration (FDA) in 2013 as the first TKI for RAI-DTC. In subsequent clinical practice, cases are reported and reveal tumor shrinkage efficacy of sorafenib as neoadjuvant treatment for unresectable thyroid carcinoma (54).

Lenvatinib

Lenvatinib, an orally active multi-targeted TKI, has been approved by both the FDA and the European Medicines Agency (EMA) for advanced and progressive RAI-DTC. The phase III SELECT trial demonstrated significant improvements in median PFS (18.3 months vs 3.6 months) and ORR (64.8% vs. 1.5%) compared lenvatinib to placebo in 392 RAI-DTC with or without previous TKI (46). Of note, OS was significantly improved among patients aged > 65 years (53). Lenvatinib may have a neoadjuvant role in selected cases of locally advanced DTC to reduce tumor volume and facilitate complete resection (55, 56). A real-world study demonstrated that treatment with first-line lenvatinib followed by another second-line therapy, including other TKI such as sorafenib or cabozantinib/chemotherapy/immunotherapy, may deliver a clinical benefit for RAI-DTC. This study added evidence to a sequential strategy for the treatment of RAI-DTC (57).

Cabozantinib

Cabozantinib is a selective inhibitor of MET, VEGFR-2, and RET et al. In the COSMIC-311 phase III trial for RAI-DTC patients who failed first-line therapy with sorafenib and/or lenvatinib, cabozantinib showed significant improvement in PFS over placebo (median PFS not reached vs. 1.9 months) and in ORR (15% vs. 0%). Based on the COSMIC-311 study, FDA approved cabozantinib for advanced thyroid cancer as second-line therapy in September 2021 (47).

TABLE 2 Published pivot clinical trials for RAIR DTC and ATC.

Agents	Targets	Phase	Clinical Trials	population	n	PFS (month)	OS (month)	ORR	Dosage	Common TRAEs
Sorafenib (2014) (45)	VEGFR1-3, PDGFR, RET, RAF, c-KIT	III	NCT00984282 (DECISION)	RAIR-DTC	417	10.8 vs. 5.8 of placebo arm	Not reached	12.2% vs. 0.5%	400 mg orally twice daily	hand-foot skin reaction, diarrhoea, alopecia
Sorafenib (2013) (87)	VEGFR1-3, PDGFR, RET, RAF, c-KIT	II	NCT00126568	ATC	20	1.9	3.9	10%	400 mg orally twice daily	fatigue, anemia, hypocalcemia
Lenvatinib (2015) (46)	VEGFR1-3, PDGFR, RET, FGFR I-4, c-KIT	III	NCT01321554 (SELECT)	RAIR-DTC	392	18.3 vs. 3.6 of placebo arm	Not reached	64.8% vs. 1.5%	24 mg orally once daily	hypertension, diarrhoea, fatigue
Lenvatinib (2017) (88)	VEGFR1-3, PDGFR, RET, FGFR I-4, c-KIT	II	NCT01728623	ATC	17	7.4	10.6	24%	24 mg orally once daily	decreased appetite, hypertension, fatigue, nausea, proteinuria
Lenvatinib (2021) (89)	VEGFR1-3, PDGFR, RET, FGFR I-4, c-KIT	II	NCT02657369	ATC	34	2.6	3.2	2.9%	24 mg orally once daily	hypertension, decreased appetite, fatigue, and stomatitis
Cabozantinib (2021) (47)	Tie-2, c-MET, KIT, VEGFR1, VEGFR2, RET	III	NCT03690388 (COSMIC-311)	RAIR-DTC	227	Not reached vs. 1.9 of placebo arm	Not reached	15% vs. 0	60 mg orally once daily	hand-foot syndrome, diarrhoea, nausea
Anlotinib (2020) (48)	VEGFR, PDGFR, FGFR, and c-Kit	II	NCT02586337	RAIR-DTC	113	40.5 vs. 8.4 of placebo arm	Not reached	59.2% vs. 0	12 mg orally once daily	hypertension, hypertriglyceridemia
Donafenib (2021) (49)	VEGF, PDGF, RAF	II	NCT02870569	RAIR-DTC	35	14.98 in 300 mg arm and 9.44 months in 200 mg arm	NA	13.3% in 300 mg arm and 12.5% in 200 mg arm	200 mg/300 mg orally twice daily	palmar-plantar erythrodysesthesia and hypertension
Surufatinib (2020) (50)	VEGFR, FGFR	II	NCT02588170	RAIR-DTC, MTC	59	11.1	NA	23.2%	300 mg orally once daily	hypertension, proteinuria, elevated blood pressure, hypertriglyceridemia, pulmonary inflammation
Sunitinib (2017) (51)	PDGFR, FLT3, c-KIT, VEGFR, RET	II	NCT00510640	RAIR-DTC/ ATC	41/4	13.1/NA	26.4/NA	22%/0%	50 mg orally once daily	asthenia/fatigue, mucosal cutaneous toxicities, hand-foot syndrome
Pazopanib (2010) (52)	VEGF, PDGFR, c-kit	II	NCT00625846	RAIR-DTC	37	NA	NA	49%	800 mg orally once daily	atigue, hair hypopigmentation, diarrhoea, nausea
Apatinib (2022) (59)	VEGFR-2	III	NCT03048877 (REALITY)	RAIR-DTC	92	22.2 vs. 4.5 of placebo arm	Not reached vs. 29.9	54.3% vs. 2.2%	500 mg orally once daily	hypertension, hand-foot syndrome, proteinuria
Axitinib (2014) (60)	VEGF, PDGFR, c-kit	II	NCT00094055	advanced thyroid cancer of any histology	60	15	35	38%	5 mg orally twice daily	hypertension, proteinuria, diarrhea, weight decrease

(Continued)

TABLE 2 Continued

Agents	Targets	Phase	Clinical Trials	population	n	PFS (month)	OS (month)	ORR	Dosage	Common TRAEs
Vemurafenib (2016) (62)	BRAF	II	NCT01286753	RAIR-DTC (BRAF ^{V600E+})	51	18.2 in TKI-naïve cohort; 8.9 in non-TKI-naïve cohort	Not reached	38.50% in TKI-naïve cohort; 27.3% in non-TKI-naïve cohort	960 mg orally twice daily	rash, fatigue, asthenia, alopecia
Dabrafenib + Trametinib (2018) (66)	BRAF ^{V600E} , MEK	II	NCT02034110	RAIR-DTC (BRAF ^{V600E+})	16	Not reached	Not reached	66%	Dabrafenib 150 mg orally twice daily + Trametinib 2mg orally once daily	fatigue, pyrexia, nausea
Selumetinib +RAI (2022) (68)	MEK 1/2	III	NCT01843062 (ASTRA)	DTC at high risk of primary treatment failure	233	NA	NA	CR rate for selumetinib+RAI (40%) vs. placebo+RAI (38%)	75 mg orally twice daily	rash, fatigue, diarrhea, peripheral edema
Larotrectinib (2018) (71)	NTRK1/2/3, ROS1, ALK	I/II	NCT02122913 NCT02637687 NCT02576431	TRK fusion (+) solid tumor	55 (5 thyroid cases)	Not reached	NA	75%	100 mg orally twice daily	increased ALT or AST leve, fatigue, vomiting
Entrectinib (2020) (73)	NTRK1/2/3, ROS1, ALK	I/II	NCT02650401 NCT02097810 NCT02568267	NTRK fusion (+) solid tumor including TC	54	NA	NA	57%	600 mg orally once daily	increased weight, anaemia
Everolimus (2018) (75)	mTOR	II	NA	RAIR-DTC/ATC	33/7	12.9/NA	Not reached/NA	3%/14.3%	10 mg orally once daily	mucositis, acneiform rash, fatigue, cough
Temsirolimus + Sorafenib (2017) (77)	mTOR + VEGFR, PDGFR, BRAF	II	NCT01025453	RAIR-DTC	36	NA	NA	22.0%	sorafenib 200 mg orally twice a day and temsirolimus 25 mg intravenous weekly	hyperglycemia, fatigue, anemia, and oral mucositis
Pralsetinib (2021) (79)	RET	I/II	NCT03037385 (ARROW)	RET fusion (+) thyoird caner	20	Not reached	Not reached	89%	400 mg orally once daily	hypertension, neutropenia, lymphopenia,

RAIR, radioactive iodine-refractory; DTC, differentiated thyroid cancer; ATC, anaplastic thyroid cancer; n, number; NA, not available; PFS, progression-free survival; OS, overall survival; ORR, objective response rate; TRAEs, treatment-related adverse events. VEGFR, vascular endothelial growth factor receptor; PDGFR, platelet-derived growth factor receptor; EGFR, epidermal growth factor receptor; FGFR, fibroblast growth factor receptor; c-kit, mast/stem cell growth factor receptor kit, NTRK, neurotrophic tyrosine receptor kinase; FLT3, FMS-like tyrosine kinase 3; ALK, anaplastic lymphoma kinase.

Anlotinib

Anlotinib is a novel multitarget tyrosine kinase inhibitor targeting VEGFR, PDGFR and FGFR et al. Outcome from a phase II trial of anlotinib vs. placebo for RAIR-DTC showed promising clinical efficacy with a prolonged median PFS (40.5 months vs. 8.3 months) and ORR of 59.2% (48). Notably, all of the enrolled patients were TKI-naïve, which may contribute partially to the extraordinary clinical efficacy. Phase III study of anlotinib for RAIR-DTC has been completed and the trial data will be published soon. Based on its promising efficacy, anlotinib is currently approved by the Chinese National Medical Products Administration (NMPA) for the indication of RAIR-DTC. A report in 2021 ASCO showed that 10 out of 13 (76.9%) locally advanced thyroid cancer patients achieved partial response (PR),

reflecting a significant prospect of anlotinib for neoadjuvant therapy in unresectable RAIR-DTC.

Donafenib

Donafenib, a modified form of sorafenib with a trideuterated N-methyl group, inhibits VEGFR, PDGFR, and various Raf kinases with improved molecular stability and pharmacokinetic profile (58). In the phase II dose exploratory study of donafenib for RAIR-DTC, the 300 mg arm showed clinical benefit in terms of PFS (14.98months) and ORR (13.3%) as well as tolerable safety profile (49). Phase III clinical trial to assess donafenib vs. placebo among patients with RAIR-DTC has been completed and is expected to unveil soon.

TABLE 3 Ongoing TKIs clinical trials for RAIR-DTC and ATC.

Drugs	Mechanism/Targets	Clinical Trials	Population	Phase	Status
Anlotinib	VEGFR, PDGFR, FGFR, and c-Kit	NCT02586337	DTC	III	Terminated
Donafenib	VEGF, PDGF, RAF	NCT03602495 (DIRECTION)	RAIR DTC	III	Terminated
Vandetanib	RET, VEGFR, EGFR	NCT01876784 (VERIFY)	locally advanced or metastatic DTC	III	Active, not recruiting
Lenvatinib, Denosumab	VEGFR1-3, PDGF β , RET, FGFR-I +RANKL(Bone metastases from RAI-R DTC)	NCT03732495 (LENVOS)	Bone Metastatic RAIR DTC	II	Recruiting
Dabrafenib, Trametinib	BRAF ^{V600E, K601E} + MEK	NCT03244956 (MERAIODE)	Metastatic RAIR TC	II	Active, not recruiting
Dabrafenib, Trametinib	BRAF ^{V600E, K601E} + MEK	NCT04940052	BRAF ^{V600E(+)} RAIR-DTC with previous treatment	III	Recruiting
Dabrafenib, Trametinib (Neoadjuvant)	BRAF ^{V600E, K601E} + MEK	NCT04739566 (ANAPLAST-NEO)	ATC	II	Recruiting
Dabrafenib, Lapatinib	BRAF ^{V600E, K601E} + EGFR, HER	NCT01947023	RAIR TC	I	Active, not recruiting
Selpercatinib (Neoadjuvant)	RET	NCT04759911	RET-altered thyroid cancer	II	Recruiting
Crizotinib	ALK, ROS1	NCT02465060	Solid cancer	II	Recruiting
Sorafenib, Everolimus	VEGFR, PDGFR, BRAF + mTOR	NCT02143726	Advanced, RAIR Hurthle Cell Thyroid Cancer	II	Active, not recruiting

RAIR, radioactive iodine refractory; DTC, differentiated thyroid cancer; TC, thyroid cancer; PTC, papillary thyroid cancer; ATC, anaplastic thyroid cancer; VEGFR, vascular endothelial growth factor receptor; PDGFR, platelet-derived growth factor receptor; EGFR, epidermal growth factor receptor; FGFR, fibroblast growth factor receptor; PD-L1, programmed death-ligand 1; c-kit, mast/stem cell growth factor receptor kit; HER, human epidermal growth factor receptor; RANKL, receptor activator for nuclear factor- κ B ligand.

Anti-angiogenic agents

Apatinib

Apatinib is a selective VEGFR-2 inhibitor with potent anti-angiogenic activity. In a most recent REALITY phase III trial for RAIR-DTC (n=92) (59), apatinib showed promising efficacy over placebo in median PFS (22.2 months vs. 4.5 months) and ORR (54.3% vs. 2.2%). It is worth noting that apatinib also showed significant clinical benefits in OS (not reached vs. 29.9 months).

Axitinib

Another selective inhibitor of VEGF to block angiogenesis is axitinib. In a phase II trial (n=60) (60), axitinib appears active and well-tolerated in RAIR-DTC of any histology with ORR of 38% and median PFS of 15 months. Another study evaluated the comparative efficacy of axitinib as first-line or second-line treatment options. More favorable efficacy was observed in first-line treatment with an ORR of 53% and a median PFS of 13.6 months, while the counterparts in second-line treatment descended to 16.7% and 10.6 months, which might be ascribed to anti-angiogenic cross-resistance (61). More studies are warranted to explore the mechanism of TKI resistance and schedules of sequential treatment for RAIR-DTC.

MAPK signaling pathway inhibitors

As mentioned above, MKIs do not target specific mutations, which may compromise the safety and durability. Screening molecular abnormalities and practicing genotype-tailored agent selection may boost both anti-tumor efficacy and improve safety profile. Specifically, kinase inhibitors targeted BRAF^{V600E} and MEK have been studied in advanced thyroid cancer (62–66).

Vemurafenib

Vemurafenib is an oncogenic BRAF kinase inhibitor that has been approved for BRAF-positive melanoma. In a phase II study of vemurafenib for advanced thyroid cancer (n=51), the PR rate is 38.5% in the TKI-naive cohort (n=26) and 27.3% in the cohort with previous TKIs (n=25) (62). Vemurafenib also showed the ability to restore RAI avidity in BRAF mutant RAIR-DTC patients with 4 out of 10 patients responding to radioactive iodine (63).

Dabrafenib and trametinib

Dabrafenib is a BRAF inhibitor and trametinib is a MEK inhibitor. In two preliminary trials for advanced thyroid cancer patients harboring BRAF^{V600E} mutation, dabrafenib demonstrated clinical efficacy with PR of 30.1% (n=13) and

the ability of RAI resensitization (6 out of 10 patients) (64, 65). Another landmark phase II trial enrolled 16 BRAF^{V600E}-positive ATC patients receiving the combination of dabrafenib and trametinib. The ORR was 69% and the estimated 12-month OS was 80% (66). Based on this study, the combination of dabrafenib and trametinib was approved by FDA for ATC with BRAF^{V600E} mutation in 2018.

Selumetinib

Selumetinib is another potent selective inhibitor of MEK1/2. In a phase II ‘proof of concept’ trial, selumetinib showed the ability to reverse refractoriness to radioiodine in patients with metastatic thyroid cancer, especially in RAS-mutant disease (67). However, in the phase III ASTRA trial, selumetinib plus adjuvant RAI failed to improve complete remission (CR) rates in patients with DTC at high risk of primary treatment failure versus RAI alone (68).

ALK inhibitor

ALK is a kinase that activates MAPK and PI3K/AKT pathways and is associated with younger age and aggressive behavior in DTC. As reported, ATC patients with ALK rearrangement responded well to ALK inhibitor crizotinib (69, 70). But the experience of the ALK inhibitor in advanced thyroid cancer is still limited and studies are needed to evaluate the efficacy and safety profile of ALK-dependent advanced thyroid cancer.

NTRK inhibitors

Though rarely thyroid cancers can be driven by rearrangements of the NTRK gene, selective inhibitors of TRK kinases larotrectinib or entrectinib provide clinical efficacy in patients with thyroid cancer harboring mutations or rearrangements in the NTRK genes (71–73). In a phase I/II trial, larotrectinib proved to be highly potent with 75% ORR for tumors harboring TPK-fusions including thyroid carcinoma (71). In another phase I/II trial for patients with NTRK fusion-positive solid tumors (n=54), entrectinib resulted in a favorable outcome with an ORR of 57%, including 4 (7%) of CR and 27 (50%) of PR (73). The promising efficacy and safety profile highlight NTRK inhibitors as an optional treatment for selective advanced thyroid cancer though more investigations are warranted.

PI3K/AKT/mTOR signaling pathway inhibitors

Dysregulation of the PI3K pathway has been implicated in oncogenesis and tumor progression, however, buparlisib, a pan-PI3K inhibitor, failed to show the benefit of PFS in RAI FTC and PDTTC (74). As for the inhibitors of downstream mTOR, studies showed that PI3K/mTOR/Akt-mutated dedifferentiated thyroid cancer patients appeared to benefit from mTOR inhibitors, such as everolimus, sirolimus and temsirolimus (75, 76). However, given the relatively low ORR observed, the mTOR

inhibitors have not been clinically used as a single agent in the treatment of advanced thyroid cancer. Notably, given that inhibition of mTORC1 may lead to MAPK pathway activation through a PI3K-dependent feedback loop, the potential of a combined therapeutic approach with mTOR and MAPK inhibitors may be underscored. In a phase II trial, 36 metastatic RAI-DTC received treatment with the combination of sorafenib and temsirolimus. PR was observed in 8 patients (22%), SD in 21 (58%), and PD in 1 (3%); patients who received no prior systemic treatment had a better response rate (77).

RET alteration inhibitors

Multikinase inhibitors with RET inhibitor activity, such as cabozantinib and vandetanib, have been evaluated for tumors with activating RET gene alterations including thyroid cancer, mainly in MTC. However, due to the nonselective nature of multikinase inhibitors, the safety and durability of responses to these agents are at least partially limited by off-target toxic effects. Novel generation of high selective RET alteration inhibitors, pralsetinib and selpercatinib demonstrated promising efficacy and favorable safety profile, and have been approved by FDA for RET-mutant medullary thyroid cancer and RET fusion-positive thyroid cancer (78–80). Though RET mutations occur mainly in medullary thyroid cancers and RET fusions occur rarely in follicular-derived thyroid cancers, novel RET alteration inhibitors may also alter the landscape of RET-dependent advanced thyroid cancers.

HDAC inhibitors

HDAC seems to play a role in regulating the transcription of genes involved in ATC. HDAC inhibitors (HDACIs) can induce tumor growth arrest, differentiation, and apoptosis, and sensitize tumor cells to radiation, increase radioiodine uptake and intratumoral radioiodine accumulation (81). In preclinical models, HDACIs represent anti-tumor activity and the ability to restore RAI-avidity both as monotherapy and in combination with other anticancer agents (82). However, in two clinical trials, valproic acid, a HDAC inhibitor, failed to show anticancer activity in RAI-DTC or ATC (83, 84).

Targeted therapy in ATC

According to heterogeneous mutation and heavy mutant burden, ATC remains intractable to existing treatments. Several novel therapeutic approaches have been proposed in ATC. As mentioned above, dabrafenib and trametinib, BRAF and MEK inhibitors, have been approved by FDA for BRAF^{V600E}-mutated ATC patients (66). The combination of dabrafenib and trametinib is also used as a novel neoadjuvant attempt for

patients with initially unresectable BRAF^{V600E}-mutated ATC (85, 86). As for other MKIs, sorafenib exhibited modest efficacy with a PR rate of 10%, SD rate of 25% and median PFS of 1.9 months in patients with ATC (n=20) (87). Lenvatinib demonstrated clinical activity in ATC patients (n=17) with a median PFS of 7.4 months, median OS of 10.6 months, and ORR of 24% (88). But in a most recent study for ATC (n=34), lenvatinib showed limited efficacy with ORR of 2.9%, PFS of 2.6 months, and OS of 3.2 months (89). Taken together, monotherapy of TKI may be not potent enough for ATC, and more investigations are needed to evaluate TKIs in combination with other novel agents such as anti-PD-1/L1 antibodies for the treatment of ATC (Table 4).

Agents targeted on rarer drivers in ATC may also provide clinical efficacy though further studies are warranted, such as NTRK inhibition with larotrectinib or entrectinib (71, 73), mTOR inhibition with everolimus (90), ALK inhibition with Crizotinib (69, 70) or ceritinib and the RET inhibition with selpercatinib or pralsetinib (78, 79, 91).

Peptide receptor radionuclide therapy

The term theranostics is the combination of diagnosis and therapy. The first and most classic application of this concept is radioactive iodine treatment performed on thyroid cancer patients since 1946. Recently, theranostics using radiolabeled somatostatin analogs have proved to be a milestone in the management of SSTR-expressing tumors. ¹⁷⁷Lu-labeled or ⁹⁰Y-labeled somatostatin analogs that bind somatostatin receptors are the most common PRRT in clinical practice. ¹⁷⁷Lu-DOTATATE demonstrated modest efficacy of biochemical or anatomic response for RAIR-DTC patients (92, 93). In another study of ⁹⁰Y-DOTATOC for RAIR-DTC patients (n=11), disease control was observed in 63.6% (7/11) patients (2 of PR and 5 of SD) with a duration of response of 3.5-11.5 months (94). Despite of heterogeneous response, PRRT may be a potential choice for RAIR-DTC with high expression of SSTRs owing to the efficacy and promising safety profile, and more large-scale studies are needed.

In recent years, FAP-targeted radionuclide therapy with ¹⁷⁷Lu/⁹⁰Y-labeled FAP inhibitors (FAPi) have been reported as novel therapeutic options for refractory cancers, including pancreas, breast, and colorectal cancer. Most recently, a pilot study evaluated the efficacy of ¹⁷⁷Lu-DOTAGA.(SA.FAPi)₂ for RAIR-DTC patients who failed previous sorafenib/lenvatinib with ⁶⁸Ga-DOTA.SA.FAPi uptake in PET/CT(n=15) (95). PR was documented in four (26.7%), and SD in three patients (20%); the serum Tg level significantly decreased after treatment. Another recent study reported a RAIR-DTC patient received SD after 4 circles of treatments of FAP-targeted radionuclide ¹⁷⁷Lu-FAPi-46 (96). The results demonstrated that FAPi-based targeted theranostics might provide a novel treatment option for patients with advanced RAIR-DTC.

Immunotherapy

The relationship between thyroid cancer and the immune system has long been studied owing to the common co-occurrence of papillary thyroid cancer and Hashimoto's thyroiditis. The abnormality of the immune microenvironment and immune response partially contributes to DTC tumorigenesis and progression including the recruitment of immunosuppressive cells such as tumor-associated macrophages (TAMs), the expression of negative immune checkpoints, like programmed death-ligand 1 (PD-L1), cytotoxic T-lymphocyte associated protein (CTLA-4). PD-L1 was positively expressed in 6.1-53.2% of PTCs (97-99). The percentage increased to 61% in pT4 DTC and >70% in advanced-stage (III/IV) PTC, and 75%-80% in the ATC subset (97, 100). PD-L1 positive expression in PTC correlates with a greater risk of recurrence and shortened disease-free/overall survival (97, 101). Based on the above findings, immunotherapeutic strategy including immune checkpoint inhibitors (ICIs) may have a seat to manage advanced thyroid cancer. ICIs have two major classes: those targeting CTLA-4 such as ipilimumab and tremelimumab, and those targeting PD-1 such as nivolumab, pembrolizumab, spartalizumab or its ligand PD-L1 such as avelumab, atezolizumab, and durvalumab. ICIs act to enhance the effector T cells and inhibit the regulatory suppressor cells, and re-establish immune surveillance from which malignant cells are able to evade. Experience with ICIs in the treatment of RAIR-DTC is still limited.

A phase Ib KEYNOTE-028 trial of pembrolizumab enrolled 22 advanced thyroid cancer patients showed a manageable safety profile and clinical efficacy with PR of 9.1%, SD of 59.1%, and PD of 31.8% (102). The FDA approved the pembrolizumab for treatment of previously treated solid tumors with high tumor mutation burden in 2020 based on results of phase II KEYNOTE-158 trial, which included two patients with thyroid cancer (103).

It's worth noting that the identification of immune biomarkers is important for patient selection. PD-L1 might have selective significance as a promising screening indicator for immune therapy (104, 105). A recent phase II single-arm study of spartalizumab, a PD-1 inhibitor, showed a favorable ORR of 29% in PD-L1 (+) vs. 0% in PD-L1 (-) ATC patients (n=42); the highest rate of response was observed in the subset of patients with PD-L1 ≥ 50% (6/17; 35%); median PFS and OS are 1.7 and 5.9 months, respectively; OS also correlated with PD-L1 status, with a median OS of 1.6 months in patients with PD-L1 < 1%, compared with not yet reached in PD-L1(+) patients (106). Notably, the co-existence of thyroid cancer with thyroiditis is common, and PD-L1 expression can also be detected in inflammatory thyroid tissue (107). Therefore, it should be cautious to interpret PD-L1 expression for thyroid cancer combined with thyroiditis and more investigations are needed.

TABLE 4 Clinical trials of ICIs for RAIR-DTC and ATC.

Modality	Combination Type	Targets	Clinical Trials	Population	Phase	Status
Pembrolizumab (2019) (102)	ICI	PD-1	NCT02054806	Advanced solid tumors	I	Completed
Pembrolizumab (2020) (103)	ICI	PD-1	NCT02628067	Advanced solid tumors	II	Recruiting
Pembrolizumab	ICI	PD-1	NCT02688608	ATC, PDTC	II	Completed
Pembrolizumab	ICI	PD-1	NCT03012620	Rare cancers	II	Active, not recruiting
Spartalizumab(2020) (106)	ICI	PD-1	NCT02404441	Advanced solid tumors	I/II	Completed
Durvalumab	ICI	PD-L1	NCT03215095	Recurrent/Metastatic TC	I	Active, not recruiting
Nivolumab, Ipilimumab	ICI+ICI	PD-1, CTLA-4	NCT03246958	RAIR DTC, ATC	II	Active, not recruiting
Nivolumab Ipilimumab	ICI+ICI	PD-1, CTLA-4	NCT02834013	Rare tumors	II	Recruiting
Durvalumab, Tremelimumab	ICI+ICI	PD-L1, CTLA-4	NCT03753919 (DUTHY)	DTC, ATC	II	Recruiting
Pembrolizumab, Lenvatinib	ICI+TKI	PD-1, VEGFR1-3, PDGFR, RET, FGFR I-4, c-KIT	NCT02973997	RAIR DTC	II	Active, not recruiting
Pembrolizumab, Lenvatinib	ICI+TKI	PD-1, VEGFR1-3, PDGFR, RET, FGFR I-4, c-KIT	NCT04171622	ATC	II	Not yet recruiting
Nivolumab, Encorafenib/Binimetinib	ICI+TKI	PD-1	NCT04061980	RAIR BRAF-mutated DTC	II	Recruiting
Atezolizumab, Cabozantinib	ICI+TKI	PD-L1, Tie-2, c-MET, KIT, VEGFR1, VEGFR2, RET	NCT03170960	Locally advanced or metastatic solid tumors	Ib	Active, not recruiting
Atezolizumab, Cabozantinib	ICI+TKI	PD-L1, Tie-2, c-MET, KIT, VEGFR1, VEGFR2, RET	NCT04400474	endocrinal tumors	II	Recruiting
Avelumab, Regorafenib	ICI+TKI	PD-L1, VEGFR 1-3, KIT, PDGFR- α , PDGFR- β , RET	NCT03475953	RAIR DTC	I/II	Recruiting
Cemiplimab, Dabrafenib, Trametinib	ICI+TKI+TKI	PD-1, BRAF ^{V600E} mutation	NCT04238624	ATC (BRAF ^{V600E} +))	II	Recruiting
Pembrolizumab, Dabrafenib, Trametinib (neoadjuvant)	ICI+TKI+TKI	PD-1, BRAF, MEK	NCT04675710	ATC	II	Recruiting
Nivolumab, Ipilimumab, Cabozantinib	ICI+ICI+TKI	PD-1 and CTLA-4, Tie-2, c-MET, KIT, VEGFR1, VEGFR2, RET	NCT03914300	Advanced DTC	II	Active, not recruiting
Pembrolizumab, Docetaxel	ICI+CT	PD-1	NCT03360890	TC and salivary gland tumors	I	Recruiting
Pembrolizumab, Docetaxel, Doxorubicin	ICI+CT	PD-1	NCT03211117	ATC	II	Completed
Atezolizumab, Vemurafenib/ Cobimetinib/Bevacizumab/Paclitaxel	ICI+TKI/anti-angiogenesis agents/CT	PD-L1, BRAF ^{V600E} /MEK/VEGF	NCT03181100	PDTC, ATC Cohort selection depending driver mutation	II	Recruiting
Durvalumab, Tremelimumab, SBRT	ICI+ICI+SBRT	PD-L1 and CTLA-4	NCT03122496	ATC	I	Completed
Pembrolizumab, docetaxel/ doxorubicin, radiation (2019) (115)	ICI+CT+RT	PD-1	NCT03211117	ATC	II	Completed

ICIs, immune checkpoints inhibitors; PD-1, programmed death protein-1; ATC, anaplastic thyroid cancer; CT, chemotherapy; RT, radiation therapy; TKI, tyrosine kinase inhibitors; RAIR, radioactive iodine refractory; DTC, differentiated thyroid cancer; SBRT, stereotactic body radiation therapy; VEGFR, vascular endothelial growth factor receptor; PDGFR, platelet-derived growth factor receptor; EGFR, epidermal growth factor receptor; FGFR, fibroblast growth factor receptor; PD-L1, programmed death-ligand 1; c-kit, mast/stem cell growth factor receptor kit; CTLA-4, cytotoxic T-lymphocyte associated protein.

Treatment combination including immunotherapy

Dual targeting of the immune system in the thyroid tumor microenvironment may, in theory, tone up the clinical benefits. Several clinical trials are ongoing to evaluate dual immunotherapy, such as PD-1 inhibitors (nivolumab) plus CTLA-4 inhibitor (ipilimumab), and PD-L1 inhibitor (durvalumab) plus CTLA-4 inhibitor (tremelimumab) (Table 4).

Immunotherapy combined with TKIs may also augment efficacy in ATC. In the preclinical model, both VEGF-A and BRAF^{V600E} are positively associated with upregulation of checkpoints expression, and the combination of BRAF^{V600E} inhibitor and anti-PD-L1 treatment reduced tumor burden significantly more than either single agent (108–110). Another preclinical study showed that anti-PD-1/PD-L1 therapy augments lenvatinib's efficacy by favorably altering the immune microenvironment of murine ATC (111). Clinically, in a case report, an ATC patient with BRAF and PD-L1 positivity was treated with vemurafenib and nivolumab, the patient continues to be in complete remission for 20 months after initiation of treatment (112). A combination of lenvatinib and pembrolizumab also showed promising efficacy for ATC (n=6) with CR of 66.6%, SD of 16.7%, and PD of 16.6%; the median OS was 18.5 months with three ATC patients being still alive without relapse (40, 27, and 19 months) (113). More phase II studies are currently assessing the effect of combining MKIs with immune therapy, such as pembrolizumab plus lenvatinib, nivolumab plus encorafenib/binimetinib (Table 4).

A preliminary study evaluated RAI and anti-PD-L1 agent durvalumab in recurrent/metastatic thyroid cancer based on the hypothesis that RAI can enhance the presentation of thyroid protein immunogens and the putative neoantigens may amplify the effectiveness of ICIs. In a preliminary trial, eleven recurrent/metastatic thyroid cancer patients were treated with durvalumab and RAI (100 mCi); two patients had PR, 7 had SD, and 2 had PD (114).

Albeit disappointing outcome in a phase II study of pembrolizumab combined with chemoradiotherapy as initial treatment for anaplastic thyroid cancer, other combination strategies, such as ICIs plus SBRT and ICIs plus chemotherapy are ongoing (115) (Table 4).

Challenges and perspectives

Over the past few years, the understanding of the underlying molecular mechanisms involving thyroid dedifferentiation and the identification of key disease-causing driver genes have led to the introduction of several new radionuclide imaging. Some mutations such as EIF1AX, IDH1/IDH2, and other signaling pathways concerning the dedifferentiation process are still not

clear, the importance of which needs to be clarified. Several studies have found that glycosylation, acetylation, methylation, and ubiquitination are closely related to the epigenetics of oncogenesis (116). There are also some studies involving these proteomic analyses in thyroid tumorigenesis (6, 16, 26). But the molecular mechanisms remain unknown, and more studies are needed. Additionally, clinical evaluation of functional imaging of dedifferentiated thyroid cancer has shown the potential of disease diagnosis and treatment, and more studies related to molecular targeted probes are required for the diagnostic and even therapeutical purposes of dedifferentiated thyroid cancer in the future.

The emergence of new targeted therapy has undoubtedly provided us with more treatment options for advanced thyroid cancer. The upcoming results of the phase III trials of anlotinib and donafenib are expected to provide new options for the management of advanced thyroid cancer. But how to properly use these “news weapons” is worthy of attention, whether as a supplement to or complete subversion of the current standard treatment mode. The timing of the initiation with novel agents is of vital significance. Should the intervention be administrated at an early stage or be waited as the last resort of salvage treatment? Moreover, considering the relatively slow rate of disease progression for most RAIR-DTC, how to balance the benefit of PFS/OS and the quality of life of patients? More explorations and investigations are needed to address these issues. In the future, well-designed clinical trials especially head-to-head studies will help understand the comparative efficacy of novel agents. And it's of pivotal significance to identify an appropriate sequential and combined treatment strategy to minimize cross-resistance or exposure to inactive drugs in the long clinical course for advanced thyroid cancer.

Conclusion

The overall prognosis of thyroid cancer is favorable yet the treatment of advanced thyroid cancer patients remains challenging. Thyroid cancer is a heterogeneous disease driven by variable molecular alterations. Over the past decade, advances in the understanding of oncogenic alterations and signaling pathways have helped clinicians diagnose and early recognize potential advanced thyroid cancer patients. The findings of molecular modifications involving DNA methylation, protein post-translational modification such as phosphorylation, acetylation, ubiquitination, and glycosylation also alter the therapeutic strategy for advanced thyroid cancer. Furthermore, the growing number of molecular imaging studies provide more potential for the diagnosis and treatment of advanced thyroid cancer. Targeted therapy, immunotherapy, and theranostic are making robust progress in the personalized management of

advanced thyroid cancer. Further investigations and more real-world clinical outcomes are warranted to develop more effective targeted therapies, and select candidate patients who might benefit and improve the treatment modalities of advanced thyroid cancer.

Author contributions

All authors contributed to the conception and design of the study and to data acquisition and analysis. The first draft of the manuscript was written by JL and YZ. FS contributed to the investigation and resources. LX and XS reviewed and edited the manuscript. All authors contributed to the article and approved the submitted version.

Funding

This work was financially supported by grants from the Shandong Provincial Natural Science Foundation (ZR2021LZL005), the Start-up

fund of Shandong Cancer Hospital (2020PYA04), and the Shandong Provincial Natural Science Foundation (ZR2019PH051).

Conflict of interest

The authors declare that the research was conducted in the absence of any commercial or financial relationships that could be construed as a potential conflict of interest.

The handling editor declared a shared affiliation, though no other collaboration, with the authors at the time of the review.

Publisher's note

All claims expressed in this article are solely those of the authors and do not necessarily represent those of their affiliated organizations, or those of the publisher, the editors and the reviewers. Any product that may be evaluated in this article, or claim that may be made by its manufacturer, is not guaranteed or endorsed by the publisher.

References

- Sung H, Ferlay J, Siegel RL, Laversanne M, Soerjomataram I, Jemal A, et al. Global cancer statistics 2020: GLOBOCAN estimates of incidence and mortality worldwide for 36 cancers in 185 countries. *CA Cancer J Clin* (2021) 71(3):209–49. doi: 10.3322/caac.21660
- Lorusso L, Cappagli V, Valerio L, Giani C, Viola D, Puleo L, et al. Thyroid cancers: From surgery to current and future systemic therapies through their molecular identities. *Int J Mol Sci* (2021) 22(6). doi: 10.3390/ijms22063117
- Tirrò E, Martorana F, Romano C, Vitale SR, Motta G, Di Gregorio S, et al. Molecular alterations in thyroid cancer: From bench to clinical practice. *Genes (Basel)* (2019) 10(9). doi: 10.3390/genes10090709
- Aashiq M, Silverman DA, Na'ara S, Takahashi H, Amit M. Radioiodine-refractory thyroid cancer: Molecular basis of redifferentiation therapies, management, and novel therapies. *Cancers (Basel)* (2019) 11(9). doi: 10.3390/cancers11091382
- Rao SN, Smallridge RC. Anaplastic thyroid cancer: An update. *Best Pract Res Clin Endocrinol Metab* (2022), 101678. doi: 10.1016/j.beem.2022.101678
- Oh JM, Ahn BC. Molecular mechanisms of radioactive iodine refractoriness in differentiated thyroid cancer: Impaired sodium iodide symporter (NIS) expression owing to altered signaling pathway activity and intracellular localization of NIS. *Theranostics* (2021) 11(13):6251–77. doi: 10.7150/thno.57689
- Faugeras L, Pirson AS, Donckier J, Michel L, Lemaire J, Vandervorst S, et al. Refractory thyroid carcinoma: which systemic treatment to use? *Ther Adv Med Oncol* (2018) 10:1758834017752853. doi: 10.1177/1758834017752853
- Karapanou O, Simeakis G, Vlassopoulou B, Alevizaki M, Saltiki K. Advanced RAI-refractory thyroid cancer: an update on treatment perspectives. *Endocr Relat Cancer* (2022) 29(5):R57–r66. doi: 10.1530/erc-22-0006
- Pekova B, Sykorova V, Mastnikova K, Vaclavikova E, Moravcova J, Vlcek P, et al. NTRK fusion genes in thyroid carcinomas: Clinicopathological characteristics and their impacts on prognosis. *Cancers (Basel)* (2021) 13(8). doi: 10.3390/cancers13081932
- Yakushina VD, Lerner LV, Lavrov AV. Gene fusions in thyroid cancer. *Thyroid* (2018) 28(2):158–67. doi: 10.1089/thy.2017.0318
- Wei W, Jiang D, Rosenkrans ZT, Barnhart TE, Engle JW, Luo Q, et al. HER2-targeted multimodal imaging of anaplastic thyroid cancer. *Am J Cancer Res* (2019) 9(11):2413–27.
- Silaghi H, Lozovanu V, Georgescu CE, Pop C, Nasui BA, Cătoi AF, et al. State of the art in the current management and future directions of targeted therapy for differentiated thyroid cancer. *Int J Mol Sci* (2022) 23(7). doi: 10.3390/ijms23073470
- Fallahai P, Ferrari SM, Galdiero MR, Varricchi G, Elia G, Ragusa F, et al. Molecular targets of tyrosine kinase inhibitors in thyroid cancer. *Semin Cancer Biol* (2022) 79:180–96. doi: 10.1016/j.semcancer.2020.11.013
- Pinto N, Ruicci KM, Khan MI, Shaikh MH, Zeng YFP, Yoo J, et al. Introduction and expression of PIK3CA(E545K) in a papillary thyroid cancer BRAF(V600E) cell line leads to a dedifferentiated aggressive phenotype. *J Otolaryngol Head Neck Surg* (2022) 51(1):7. doi: 10.1186/s40463-022-00558-w
- Ratajczak M, Gawel D, Godlewska M. Novel inhibitor-based therapies for thyroid cancer—an update. *Int J Mol Sci* (2021) 22(21). doi: 10.3390/ijms222111829
- Feng F, Yehia L, Ni Y, Chang YS, Jhiang SM, Eng C. A nonpump function of sodium iodide symporter in thyroid cancer via cross-talk with PTEN signaling. *Cancer Res* (2018) 78(21):6121–33. doi: 10.1158/0008-5472.Can-18-1954
- Nikiforova MN, Kimura ET, Gandhi M, Biddinger PW, Knauf JA, Basolo F, et al. BRAF mutations in thyroid tumors are restricted to papillary carcinomas and anaplastic or poorly differentiated carcinomas arising from papillary carcinomas. *J Clin Endocrinol Metab* (2003) 88(11):5399–404. doi: 10.1210/jc.2003-030838
- Chen TY, Lorch JH, Wong KS, Barletta JA. Histological features of BRAF V600E-mutant anaplastic thyroid carcinoma. *Histopathology* (2020) 77(2):314–20. doi: 10.1111/his.14144
- Dong T, Zhang Z, Zhou W, Zhou X, Geng C, Chang LK, et al. WNT10A/ β -catenin pathway in tumorigenesis of papillary thyroid carcinoma. *Oncol Rep* (2017) 38(2):1287–94. doi: 10.3892/or.2017.5777
- Azouzi N, Cailloux J, Cazarin JM, Knauf JA, Cracchiolo J, Al Ghuzlan A, et al. NADPH oxidase NOX4 is a critical mediator of BRAF(V600E)-induced downregulation of the Sodium/Iodide symporter in papillary thyroid carcinomas. *Antioxid Redox Signal* (2017) 26(15):864–77. doi: 10.1089/ars.2015.6616
- Manzella L, Stella S, Pennisi MS, Tirrò E, Massimino M, Romano C, et al. New insights in thyroid cancer and p53 family proteins. *Int J Mol Sci* (2017) 18(6). doi: 10.3390/ijms18061325
- Liu R, Li Y, Chen W, Cong J, Zhang Z, Ma L, et al. Mutations of the TERT promoter are associated with aggressiveness and recurrence/distant metastasis of papillary thyroid carcinoma. *Oncol Lett* (2020) 20(4):50. doi: 10.3892/ol.2020.11904
- Saqcena M, Leandro-Garcia LJ, Maag JLV, Tchekmedyan V, Krishnamoorthy GP, Tamarapu PP, et al. SWI/SNF complex mutations promote thyroid tumor progression and insensitivity to redifferentiation therapies. *Cancer Discovery* (2021) 11(5):1158–75. doi: 10.1158/2159-8290.Cd-20-0735
- Romei C, Elisei R. A narrative review of genetic alterations in primary thyroid epithelial cancer. *Int J Mol Sci* (2021) 22(4). doi: 10.3390/ijms22041726

25. Murugan AK, Qasem E, Al-Hindi H, Alzahrani AS. Analysis of ALK, IDH1, IDH2 and MMP8 somatic mutations in differentiated thyroid cancers. *Mol Clin Oncol* (2021) 15(4):210. doi: 10.3892/mco.2021.2373
26. Spartalis E, Kotrotsios K, Chrysikos D, Spartalis M, Paschou SA, Schizas D, et al. Histone deacetylase inhibitors and papillary thyroid cancer. *Curr Pharm Des* (2021) 27(18):2199–208. doi: 10.2174/1381612826666201211112234
27. Jin Y, Liu B, Younis MH, Huang G, Liu J, Cai W, et al. Next-generation molecular imaging of thyroid cancer. *Cancers (Basel)* (2021) 13(13). doi: 10.3390/cancers1313188
28. Wahl RL, Chareonthaitawee P, Clarke B, Drzezga A, Lindenberg L, Rahmim A, et al. Mars Shot for nuclear medicine, molecular imaging, and molecularly targeted radiopharmaceutical therapy. *J Nucl Med* (2021) 62(1):6–14. doi: 10.2967/jnumed.120.253450
29. Spanu A, Nuvoli S, Marongiu A, Gelo I, Mele L, De Vito A, et al. The diagnostic usefulness of (131)I-SPECT/CT at both radioiodine ablation and during long-term follow-up in patients thyroidectomized for differentiated thyroid carcinoma: Analysis of tissue risk factors ascertained at surgery and correlated with metastasis appearance. *Diagnostics (Basel)* (2021) 11(8). doi: 10.3390/diagnostics11081504
30. Kist JW, de Keizer B, van der Vlies M, Brouwers AH, Huysmans DA, van der Zant FM, et al. 124I PET/CT to predict the outcome of blind 131I treatment in patients with biochemical recurrence of differentiated thyroid cancer: Results of a multicenter diagnostic cohort study (THYROPET). *J Nucl Med* (2016) 57(5):701–7. doi: 10.2967/jnumed.115.168138
31. Samnick S, Al-Momani E, Schmid JS, Mottok A, Buck AK, Lapa C. Initial clinical investigation of [18F]Tetrafluoroborate PET/CT in comparison to [124I] Iodine PET/CT for imaging thyroid cancer. *Clin Nucl Med* (2018) 43(3):162–7. doi: 10.1097/rlu.0000000000001977
32. Dittmann M, Gonzalez Carvalho JM, Rahbar K, Schäfers M, Claesener M, Riemann B, et al. Incremental diagnostic value of [(18)F]tetrafluoroborate PET-CT compared to [(131)I]iodine scintigraphy in recurrent differentiated thyroid cancer. *Eur J Nucl Med Mol Imaging* (2020) 47(11):2639–46. doi: 10.1007/s00259-020-04727-9
33. Lee JW, Lee SM, Lee DH, Kim YJ. Clinical utility of 18F-FDG PET/CT concurrent with 131I therapy in intermediate-to-high-risk patients with differentiated thyroid cancer: dual-center experience with 286 patients. *J Nucl Med* (2013) 54(8):1230–6. doi: 10.2967/jnumed.112.117119
34. Albano D, Tulchinsky M, Dondi F, Mazzeoletti A, Lombardi D, Bertagna F, et al. Thyroglobulin doubling time offers a better threshold than thyroglobulin level for selecting optimal candidates to undergo localizing [(18)F]FDG PET/CT in non-iodine avid differentiated thyroid carcinoma. *Eur J Nucl Med Mol Imaging* (2021) 48(2):461–8. doi: 10.1007/s00259-020-04992-8
35. Liu H, Wang X, Yang R, Zeng W, Peng D, Li J, et al. Recent development of nuclear molecular imaging in thyroid cancer. *BioMed Res Int* (2018) 2018:2149532. doi: 10.1155/2018/2149532
36. Kundu P, Lata S, Sharma P, Singh H, Malhotra A, Bal C. Prospective evaluation of (68)Ga-DOTANOC PET-CT in differentiated thyroid cancer patients with raised thyroglobulin and negative (131)I-whole body scan: comparison with (18)F-FDG PET-CT. *Eur J Nucl Med Mol Imaging* (2014) 41(7):1354–62. doi: 10.1007/s00259-014-2723-9
37. Parihar AS, Mittal BR, Kumar R, Shukla J, Bhattacharya A. (68)Ga-DOTA-RGD (2) positron emission Tomography/Computed tomography in radioiodine refractory thyroid cancer: Prospective comparison of diagnostic accuracy with (18)F-FDG positron emission Tomography/Computed tomography and evaluation toward potential theranostics. *Thyroid* (2020) 30(4):557–67. doi: 10.1089/thy.2019.0450
38. Ciappuccini R, Saguët-Rysanek V, Giffard F, Licaj I, Dorbeau M, Clarisse B, et al. PSMA expression in differentiated thyroid cancer: Association with radioiodine, 18FDG uptake, and patient outcome. *J Clin Endocrinol Metab* (2021) 106(12):3536–45. doi: 10.1210/clinem/dgab563
39. de Vries LH, Lodewijk L, Braat A, Krijger GC, Valk GD, Lam M, et al. (68) Ga-PSMA PET/CT in radioactive iodine-refractory differentiated thyroid cancer and first treatment results with (177)Lu-PSMA-617. *EJNMMI Res* (2020) 10(1):18. doi: 10.1186/s13550-020-0610-x
40. Fu H, Wu J, Huang J, Sun L, Wu H, Guo W, et al. (68)Ga fibroblast activation protein inhibitor PET/CT in the detection of metastatic thyroid cancer: Comparison with (18)F-FDG PET/CT. *Radiology* (2022), 212430. doi: 10.1148/radiol.212430
41. Chen Y, Zheng S, Zhang J, Yao S, Miao W. (68)Ga-DOTA-FAPI-04 PET/CT imaging in radioiodine-refractory differentiated thyroid cancer (RR-DTC) patients. *Ann Nucl Med* (2022). doi: 10.1007/s12149-022-01742-8
42. Li J, Vasilyeva E, Wiseman SM. Beyond immunohistochemistry and immunocytochemistry: a current perspective on galectin-3 and thyroid cancer. *Expert Rev Anticancer Ther* (2019) 19(12):1017–27. doi: 10.1080/14737140.2019.1693270
43. De Rose F, Braeuer M, Braesch-Andersen S, Otto AM, Steiger K, Reder S, et al. Galectin-3 targeting in thyroid orthotopic tumors opens new ways to characterize thyroid cancer. *J Nucl Med* (2019) 60(6):770–6. doi: 10.2967/jnumed.118.219105
44. Gild ML, Tsang VHM, Clifton-Bligh RJ, Robinson BG. Multikinase inhibitors in thyroid cancer: timing of targeted therapy. *Nat Rev Endocrinol* (2021) 17(4):225–34. doi: 10.1038/s41574-020-00465-y
45. Brose MS, Nutting CM, Jarzab B, Elisei R, Siena S, Bastholt L, et al. Sorafenib in radioactive iodine-refractory, locally advanced or metastatic differentiated thyroid cancer: a randomised, double-blind, phase 3 trial. *Lancet* (2014) 384(9940):319–28. doi: 10.1016/s0140-6736(14)60421-9
46. Schlumberger M, Tahara M, Wirth LJ, Robinson B, Brose MS, Elisei R, et al. Lenvatinib versus placebo in radioiodine-refractory thyroid cancer. *N Engl J Med* (2015) 372(7):621–30. doi: 10.1056/NEJMoa1406470
47. Brose MS, Robinson B, Sherman SI, Krajewski J, Lin CC, Vaisman F, et al. Cabozantinib for radioiodine-refractory differentiated thyroid cancer (COSMIC-311): a randomised, double-blind, placebo-controlled, phase 3 trial. *Lancet Oncol* (2021) 22(8):1126–38. doi: 10.1016/s1470-2045(21)00332-6
48. Chi Y, Gao M, Zhang Y, Shi F, Cheng Y, Guo Z, et al. LBA88 anlotinib in locally advanced or metastatic radioiodine-refractory differentiated thyroid carcinoma: A randomized, double-blind, multicenter phase II trial. *Ann Oncol* (2020) 31(S1215). doi: 10.1016/j.annonc.2020.08.2332
49. Lin YS, Yang H, Ding Y, Cheng YZ, Shi F, Tan J, et al. Donafenib in progressive locally advanced or metastatic radioactive iodine-refractory differentiated thyroid cancer: Results of a randomized, multicenter phase II trial. *Thyroid* (2021) 31(4):607–15. doi: 10.1089/thy.2020.0235
50. Chen J, Ji Q, Bai C, Zheng X, Zhang Y, Shi F, et al. Surufatinib in Chinese patients with locally advanced or metastatic differentiated thyroid cancer and medullary thyroid cancer: A multicenter, open-label, phase II trial. *Thyroid* (2020) 30(9):1245–53. doi: 10.1089/thy.2019.0453
51. Ravaud A, de la Fouchardière C, Caron P, Doussau A, Do Cao C, Asselineau J, et al. A multicenter phase II study of sunitinib in patients with locally advanced or metastatic differentiated, anaplastic or medullary thyroid carcinomas: mature data from the THYSU study. *Eur J Cancer* (2017) 76:110–7. doi: 10.1016/j.ejca.2017.01.029
52. Bible KC, Suman VJ, Molina JR, Smallridge RC, Maples WJ, Menefee ME, et al. Efficacy of pazopanib in progressive, radioiodine-refractory, metastatic differentiated thyroid cancers: results of a phase 2 consortium study. *Lancet Oncol* (2010) 11(10):962–72. doi: 10.1016/s1470-2045(10)70203-5
53. Brose MS, Worden FP, Newbold KL, Guo M, Hurria A. Effect of age on the efficacy and safety of lenvatinib in radioiodine-refractory differentiated thyroid cancer in the phase III SELECT trial. *J Clin Oncol* (2017) 35(23):2692–9. doi: 10.1200/jco.2016.71.6472
54. Nava CF, Scheffel RS, Cristo AP, Ferreira CV, Weber S, Zanella AB, et al. Neoadjuvant multikinase inhibitor in patients with locally advanced unresectable thyroid carcinoma. *Front Endocrinol (Lausanne)* (2019) 10:712. doi: 10.3389/fendo.2019.00712
55. Iwasaki H, Toda S, Ito H, Nemoto D, Murayama D, Okubo Y, et al. A case of unresectable papillary thyroid carcinoma treated with lenvatinib as neoadjuvant chemotherapy. *Case Rep Endocrinol* (2020) 2020:6438352. doi: 10.1155/2020/6438352
56. Stewart KE, Strachan MWJ, Srinivasan D, MacNeill M, Wall L, Nixon IJ. Tyrosine kinase inhibitor therapy in locally advanced differentiated thyroid cancer: A case report. *Eur Thyroid J* (2019) 8(2):102–7. doi: 10.1159/000494880
57. Kish JK, Chatterjee D, Wan Y, Yu HT, Liassou D, Feinberg BA. Lenvatinib and subsequent therapy for radioactive iodine-refractory differentiated thyroid cancer: A real-world study of clinical effectiveness in the united states. *Adv Ther* (2020) 37(6):2841–52. doi: 10.1007/s12325-020-01362-6
58. Qin S, Bi F, Gu S, Bai Y, Chen Z, Wang Z, et al. Donafenib versus sorafenib in first-line treatment of unresectable or metastatic hepatocellular carcinoma: A randomized, open-label, parallel-controlled phase II-III trial. *J Clin Oncol* (2021) 39(27):3002–11. doi: 10.1200/jco.21.00163
59. Lin Y, Qin S, Li Z, Yang H, Fu W, Li S, et al. Apatinib vs placebo in patients with locally advanced or metastatic, radioactive iodine-refractory differentiated thyroid cancer: The REALITY randomized clinical trial. *JAMA Oncol* (2022) 8(2):242–50. doi: 10.1001/jamaoncol.2021.6268
60. Cohen EE, Tortorici M, Kim S, Ingrosso A, Pithavala YK, Bycott P. A phase II trial of axitinib in patients with various histologic subtypes of advanced thyroid cancer: long-term outcomes and pharmacokinetic/pharmacodynamic analyses. *Cancer Chemother Pharmacol* (2014) 74(6):1261–70. doi: 10.1007/s00280-014-2604-8
61. Capdevila J, Trigo JM, Aller J, Manzano JL, Adrián SG, Llopiés CZ, et al. Axitinib treatment in advanced RAI-resistant differentiated thyroid cancer (DTC) and refractory medullary thyroid cancer (MTC). *Eur J Endocrinol* (2017) 177(4):309–17. doi: 10.1530/eje-17-0243
62. Brose MS, Cabanillas ME, Cohen EE, Wirth LJ, Riehl T, Yue H, et al. Vemurafenib in patients with BRAF(V600E)-positive metastatic or unresectable

- papillary thyroid cancer refractory to radioactive iodine: a non-randomised, multicentre, open-label, phase 2 trial. *Lancet Oncol* (2016) 17(9):1272–82. doi: 10.1016/s1470-2045(16)30166-8
63. Dunn LA, Sherman EJ, Baxi SS, Tchekmedyan V, Grewal RK, Larson SM, et al. Vemurafenib redifferentiation of BRAF mutant, RAI-refractory thyroid cancers. *J Clin Endocrinol Metab* (2019) 104(5):1417–28. doi: 10.1210/clinem.2018-01478
64. Falchhook GS, Millward M, Hong D, Naing A, Piha-Paul S, Waguespack SG, et al. BRAF inhibitor dabrafenib in patients with metastatic BRAF-mutant thyroid cancer. *Thyroid* (2015) 25(1):71–7. doi: 10.1089/thy.2014.0123
65. Rothenberg SM, McFadden DG, Palmer EL, Daniels GH, Wirth LJ. Redifferentiation of iodine-refractory BRAF V600E-mutant metastatic papillary thyroid cancer with dabrafenib. *Clin Cancer Res* (2015) 21(5):1028–35. doi: 10.1158/1078-0432.Ccr-14-2915
66. Subbiah V, Kreitman RJ, Wainberg ZA, Cho JY, Schellens JHM, Soria JC, et al. Dabrafenib and trametinib treatment in patients with locally advanced or metastatic BRAF V600-mutant anaplastic thyroid cancer. *J Clin Oncol* (2018) 36(1):7–13. doi: 10.1200/jco.2017.73.6785
67. Ho AL, Grewal RK, Leboeuf R, Sherman EJ, Pfister DG, Deandreis D, et al. Selumetinib-enhanced radioiodine uptake in advanced thyroid cancer. *N Engl J Med* (2013) 368(7):623–32. doi: 10.1056/NEJMoa1209288
68. Ho AL, Dedecjus M, Wirth LJ, Tuttle RM, Inabnet WB3rd, Tennvall J, et al. Selumetinib plus adjuvant radioactive iodine in patients with high-risk differentiated thyroid cancer: A phase III, randomized, placebo-controlled trial (ASTRA). *J Clin Oncol* (2022) 40(17):1870–8. doi: 10.1200/jco.21.00714
69. Godbert Y, Henriques de Figueiredo B, Bonichon F, Chibon F, Hostein I, Pérot G, et al. Remarkable response to crizotinib in woman with anaplastic lymphoma kinase-rearranged anaplastic thyroid carcinoma. *J Clin Oncol* (2015) 33(20):e84–7. doi: 10.1200/jco.2013.49.6596
70. Gambacorti-Passerini C, Orlov S, Zhang L, Braiteh F, Huang H, Esaki T, et al. Long-term effects of crizotinib in ALK-positive tumors (excluding NSCLC): A phase 1b open-label study. *Am J Hematol* (2018) 93(5):607–14. doi: 10.1002/ajh.25043
71. Drilon A, Laetsch TW, Kummar S, DuBois SG, Lassen UN, Demetri GD, et al. Efficacy of larotrectinib in TRK fusion-positive cancers in adults and children. *N Engl J Med* (2018) 378(8):731–9. doi: 10.1056/NEJMoa1714448
72. Laetsch TW, DuBois SG, Mascarenhas L, Turpin B, Federman N, Albert CM, et al. Larotrectinib for paediatric solid tumours harbouring NTRK gene fusions: phase 1 results from a multicentre, open-label, phase 1/2 study. *Lancet Oncol* (2018) 19(5):705–14. doi: 10.1016/s1470-2045(18)30119-0
73. Doebele RC, Drilon A, Paz-Ares L, Siena S, Shaw AT, Farago AF, et al. Entrectinib in patients with advanced or metastatic NTRK fusion-positive solid tumours: integrated analysis of three phase 1–2 trials. *Lancet Oncol* (2020) 21(2):271–82. doi: 10.1016/s1470-2045(19)30691-6
74. Borson-Chazot F, Dantony E, Illouz F, Lopez J, Niccoli P, Wassermann J, et al. Effect of buparlisib, a pan-class I PI3K inhibitor, in refractory follicular and poorly differentiated thyroid cancer. *Thyroid* (2018) 28(9):1174–9. doi: 10.1089/thy.2017.0663
75. Hanna GJ, Busaidy NL, Chau NG, Wirth LJ, Barletta JA, Calles A, et al. Genomic correlates of response to everolimus in aggressive radioiodine-refractory thyroid cancer: A phase II study. *Clin Cancer Res* (2018) 24(7):1546–53. doi: 10.1158/1078-0432.Ccr-17-2297
76. Schneider TC, de Wit D, Links TP, van Erp NP, van der Hoeven JJ, Gelderblom H, et al. Everolimus in patients with advanced follicular-derived thyroid cancer: Results of a phase II clinical trial. *J Clin Endocrinol Metab* (2017) 102(2):698–707. doi: 10.1210/clinem.2016-2525
77. Sherman EJ, Dunn LA, Ho AL, Baxi SS, Ghossein RA, Fury MG, et al. Phase 2 study evaluating the combination of sorafenib and temsirolimus in the treatment of radioactive iodine-refractory thyroid cancer. *Cancer* (2017) 123(21):4114–21. doi: 10.1002/cncr.30861
78. Dias-Santagata D, Lennnerz JK, Sadow PM, Frazier RP, Govinda Raju S, Henry D, et al. Response to RET-specific therapy in RET fusion-positive anaplastic thyroid carcinoma. *Thyroid* (2020) 30(9):1384–9. doi: 10.1089/thy.2019.0477
79. Wirth LJ, Sherman E, Robinson B, Solomon B, Kang H, Lorch J, et al. Efficacy of selpercatinib in RET-altered thyroid cancers. *N Engl J Med* (2020) 383(9):825–35. doi: 10.1056/NEJMoa2005651
80. Subbiah V, Hu MI, Wirth LJ, Schuler M, Mansfield AS, Curigliano G, et al. Pralsetinib for patients with advanced or metastatic RET-altered thyroid cancer (ARROW): a multi-cohort, open-label, registration, phase 1/2 study. *Lancet Diabetes Endocrinol* (2021) 9(8):491–501. doi: 10.1016/s2213-8587(21)00120-0
81. Spartalis E, Athanasiadis DI, Chrysikos D, Spartalis M, Boutziog S, Schizas D, et al. Histone deacetylase inhibitors and anaplastic thyroid carcinoma. *Anticancer Res* (2019) 39(3):1119–27. doi: 10.21873/anticancer.13220
82. Hou P, Bojdani E, Xing M. Induction of thyroid gene expression and radioiodine uptake in thyroid cancer cells by targeting major signaling pathways. *J Clin Endocrinol Metab* (2010) 95(2):820–8. doi: 10.1210/jc.2009-1888
83. Nilubol N, Merkel R, Yang L, Patel D, Reynolds JC, Sadowski SM, et al. A phase II trial of valproic acid in patients with advanced, radioiodine-resistant thyroid cancers of follicular cell origin. *Clin Endocrinol (Oxf)* (2017) 86(1):128–33. doi: 10.1111/cen.13154
84. Catalano MG, Pugliese M, Gallo M, Brignardello E, Milla P, Orlandi F, et al. Valproic acid, a histone deacetylase inhibitor, in combination with paclitaxel for anaplastic thyroid cancer: Results of a multicenter randomized controlled phase III/III trial. *Int J Endocrinol* (2016) 2016:2930414. doi: 10.1155/2016/2930414
85. Cabanillas ME, Ferrarotto R, Garden AS, Ahmed S, Busaidy NL, Dadu R, et al. Neoadjuvant BRAF- and immune-directed therapy for anaplastic thyroid carcinoma. *Thyroid* (2018) 28(7):945–51. doi: 10.1089/thy.2018.0060
86. Wang JR, Zafereo ME, Dadu R, Ferrarotto R, Busaidy NL, Lu C, et al. Complete surgical resection following neoadjuvant dabrafenib plus trametinib in BRAF(V600E)-mutated anaplastic thyroid carcinoma. *Thyroid* (2019) 29(8):1036–43. doi: 10.1089/thy.2019.0133
87. Savvides P, Nagaiah G, Lavertu P, Fu P, Wright JJ, Chapman R, et al. Phase II trial of sorafenib in patients with advanced anaplastic carcinoma of the thyroid. *Thyroid* (2013) 23(5):600–4. doi: 10.1089/thy.2012.0103
88. Tahara M, Kiyota N, Yamazaki T, Chayahara N, Nakano K, Inagaki L, et al. Lenvatinib for anaplastic thyroid cancer. *Front Oncol* (2017) 7:25. doi: 10.3389/fonc.2017.00025
89. Wirth LJ, Brose MS, Sherman EJ, Licita L, Schlumberger M, Sherman SI, et al. Open-label, single-arm, multicenter, phase II trial of lenvatinib for the treatment of patients with anaplastic thyroid cancer. *J Clin Oncol* (2021) 39(21):2359–66. doi: 10.1200/jco.20.03093
90. Harris EJ, Hanna GJ, Chau N, Rabinowitz G, Haddad R, Margalit DN, et al. Everolimus in anaplastic thyroid cancer: A case series. *Front Oncol* (2019) 9:106. doi: 10.3389/fonc.2019.00106
91. Gainor JF, Curigliano G, Kim DW, Lee DH, Besse B, Baik CS, et al. Pralsetinib for RET fusion-positive non-small-cell lung cancer (ARROW): a multi-cohort, open-label, phase 1/2 study. *Lancet Oncol* (2021) 22(7):959–69. doi: 10.1016/s1470-2045(21)00247-3
92. Oliván-Sasot P, Falgás-Lacueva M, García-Sánchez J, Vera-Pinto V, Olivás-Arroyo C, Bello-Arques P. Use of (177)Lu-dotatate in the treatment of iodine refractory thyroid carcinomas. *Rev Esp Med Nucl Imagen Mol* (2017) 36(2):116–9. doi: 10.1016/j.remnm.2016.08.001
93. Roll W, Riemann B, Schäfers M, Stegger L, Vrachimis A. 177Lu-DOTATATE therapy in radioiodine-refractory differentiated thyroid cancer: A single center experience. *Clin Nucl Med* (2018) 43(10):e346–e51. doi: 10.1097/rlu.0000000000002219
94. Versari A, Sollini M, Frasoldati A, Fraternali A, Filice A, Froio A, et al. Differentiated thyroid cancer: a new perspective with radiolabeled somatostatin analogues for imaging and treatment of patients. *Thyroid* (2014) 24(4):715–26. doi: 10.1089/thy.2013.0225
95. Ballal S, Yadav MP, Moon ES, Roesch F, Kumari S, Agarwal S, et al. Novel fibroblast activation protein inhibitor-based targeted theranostics for radioiodine-refractory differentiated thyroid cancer patients: A pilot study. *Thyroid* (2022) 32(1):65–77. doi: 10.1089/thy.2021.0412
96. Fu H, Huang J, Sun L, Wu H, Chen H. FAP-targeted radionuclide therapy of advanced radioiodine-refractory differentiated thyroid cancer with multiple cycles of 177Lu-FAPI-46. *Clin Nucl Med* (2022). doi: 10.1097/rlu.0000000000004260
97. Chowdhury S, Veyhl J, Jessa F, Polyakova O, Alenzi A, MacMillan C, et al. Programmed death-ligand 1 overexpression is a prognostic marker for aggressive papillary thyroid cancer and its variants. *Oncotarget* (2016) 7(22):32318–28. doi: 10.18632/oncotarget.8698
98. Ahn S, Kim TH, Kim SW, Ki CS, Jang HW, Kim JS, et al. Comprehensive screening for PD-L1 expression in thyroid cancer. *Endocr Relat Cancer* (2017) 24(2):97–106. doi: 10.1530/erc-16-0421
99. Bai Y, Niu D, Huang X, Jia L, Kang Q, Dou F, et al. PD-L1 and PD-1 expression are correlated with distinctive clinicopathological features in papillary thyroid carcinoma. *Diagn Pathol* (2017) 12(1):72. doi: 10.1186/s13000-017-0662-z
100. Bastman JJ, Serracino HS, Zhu Y, Koenig MR, Mateescu V, Sams SB, et al. Tumor-infiltrating T cells and the PD-1 checkpoint pathway in advanced differentiated and anaplastic thyroid cancer. *J Clin Endocrinol Metab* (2016) 101(7):2863–73. doi: 10.1210/jc.2015-4227
101. Chintakuntlawar AV, Rumilla KM, Smith CY, Jenkins SM, Foote RL, Kasperbauer JL, et al. Expression of PD-1 and PD-L1 in anaplastic thyroid cancer patients treated with multimodal therapy: Results from a retrospective study. *J Clin Endocrinol Metab* (2017) 102(6):1943–50. doi: 10.1210/jc.2016-3756
102. Mehnert JM, Varga A, Brose MS, Aggarwal RR, Lin CC, Prawira A, et al. Safety and antitumor activity of the anti-PD-1 antibody pembrolizumab in patients with advanced, PD-L1-positive papillary or follicular thyroid cancer. *BMC Cancer* (2019) 19(1):196. doi: 10.1186/s12885-019-5380-3
103. Marabelle A, Fakih M, Lopez J, Shah M, Shapira-Frommer R, Nakagawa K, et al. Association of tumour mutational burden with outcomes in patients with

advanced solid tumours treated with pembrolizumab: prospective biomarker analysis of the multicohort, open-label, phase 2 KEYNOTE-158 study. *Lancet Oncol* (2020) 21(10):1353–65. doi: 10.1016/s1470-2045(20)30445-9

104. Gandini S, Massi D, Mandalà M. PD-L1 expression in cancer patients receiving anti PD-1/PD-L1 antibodies: A systematic review and meta-analysis. *Crit Rev Oncol Hematol* (2016) 100:88–98. doi: 10.1016/j.critrevonc.2016.02.001
105. Abdel-Rahman O. Correlation between PD-L1 expression and outcome of NSCLC patients treated with anti-PD-1/PD-L1 agents: A meta-analysis. *Crit Rev Oncol Hematol* (2016) 101:75–85. doi: 10.1016/j.critrevonc.2016.03.007
106. Capdevila J, Wirth LJ, Ernst T, Ponce Aix S, Lin CC, Ramlau R, et al. PD-1 blockade in anaplastic thyroid carcinoma. *J Clin Oncol* (2020) 38(23):2620–7. doi: 10.1200/jco.19.02727
107. Pakkanen E, Kalfert D, Ahtiainen M, Ludvíková M, Kuopio T, Kholová I. PD-L1 and PD-1 expression in thyroid follicular epithelial dysplasia: Hashimoto thyroiditis related atypia and potential papillary carcinoma precursor. *Apmis* (2022) 130(5):276–83. doi: 10.1111/apm.13218
108. Angell TE, Lechner MG, Jang JK, Correa AJ, LoPresti JS, Epstein AL. BRAF V600E in papillary thyroid carcinoma is associated with increased programmed death ligand 1 expression and suppressive immune cell infiltration. *Thyroid* (2014) 24(9):1385–93. doi: 10.1089/thy.2014.0134
109. Brauner E, Gunda V, Vanden Borre P, Zurakowski D, Kim YS, Dennett KV, et al. Combining BRAF inhibitor and anti PD-L1 antibody dramatically improves tumor regression and anti tumor immunity in an immunocompetent murine model of anaplastic thyroid cancer. *Oncotarget* (2016) 7(13):17194–211. doi: 10.18632/oncotarget.7839
110. Gunda V, Gigliotti B, Ndishabandi D, Ashry T, McCarthy M, Zhou Z, et al. Combinations of BRAF inhibitor and anti-PD-1/PD-L1 antibody improve survival and tumour immunity in an immunocompetent model of orthotopic murine anaplastic thyroid cancer. *Br J Cancer* (2018) 119(10):1223–32. doi: 10.1038/s41416-018-0296-2
111. Gunda V, Gigliotti B, Ashry T, Ndishabandi D, McCarthy M, Zhou Z, et al. Anti-PD-1/PD-L1 therapy augments lenvatinib's efficacy by favorably altering the immune microenvironment of murine anaplastic thyroid cancer. *Int J Cancer* (2019) 144(9):2266–78. doi: 10.1002/ijc.32041
112. Kollipara R, Schneider B, Radovich M, Babu S, Kiel PJ. Exceptional response with immunotherapy in a patient with anaplastic thyroid cancer. *Oncologist* (2017) 22(10):1149–51. doi: 10.1634/theoncologist.2017-0096
113. Dierks C, Seufert J, Aumann K, Ruf J, Klein C, Kiefer S, et al. Combination of lenvatinib and pembrolizumab is an effective treatment option for anaplastic and poorly differentiated thyroid carcinoma. *Thyroid* (2021) 31(7):1076–85. doi: 10.1089/thy.2020.0322
114. Bharat B, Eric JS, Anuja K, Loren S, Lara D, James F, et al. Radioiodine (RAI) in combination with durvalumab for recurrent/metastatic thyroid cancers? [abstract]. *J Clin Oncol* (2020) 38(Suppl. 15):6587.
115. Chintakuntlawar AV, Yin J, Foote RL, Kasperbauer JL, Rivera M, Asmus E, et al. A phase 2 study of pembrolizumab combined with chemoradiotherapy as initial treatment for anaplastic thyroid cancer. *Thyroid* (2019) 29(11):1615–22. doi: 10.1089/thy.2019.0086
116. Li J, Zhan X. Mass spectrometry-based proteomics analyses of post-translational modifications and proteoforms in human pituitary adenomas. *Biochim Biophys Acta Proteins Proteom* (2021) 1869(3):140584. doi: 10.1016/j.bbapap.2020.140584



OPEN ACCESS

EDITED BY

Tadashi Nakagawa,
Tohoku University, Japan

REVIEWED BY

Fengchao Lang,
National Institutes of Health (NIH),
United States
Isabel Castro-Piedras,
Texas Tech University Health Sciences
Center, United States

*CORRESPONDENCE

Xianquan Zhan
yjzhan2011@gmail.com

SPECIALTY SECTION

This article was submitted to
Cancer Endocrinology,
a section of the journal
Frontiers in Endocrinology

RECEIVED 18 June 2022

ACCEPTED 23 August 2022

PUBLISHED 12 September 2022

CITATION

Yang J, Song C and Zhan X (2022)
The role of protein acetylation in
carcinogenesis and targeted
drug discovery.
Front. Endocrinol. 13:972312.
doi: 10.3389/fendo.2022.972312

COPYRIGHT

© 2022 Yang, Song and Zhan. This is an
open-access article distributed under
the terms of the [Creative Commons
Attribution License \(CC BY\)](#). The use,
distribution or reproduction in other
forums is permitted, provided the
original author(s) and the copyright
owner(s) are credited and that the
original publication in this journal is
cited, in accordance with accepted
academic practice. No use,
distribution or reproduction is
permitted which does not comply with
these terms.

The role of protein acetylation in carcinogenesis and targeted drug discovery

Jingru Yang^{1,2}, Cong Song² and Xianquan Zhan^{1,2*}

¹Shandong Key Laboratory of Radiation Oncology, Shandong Cancer Hospital and Institute, Shandong First Medical University and Shandong Academy of Medical Sciences, Jinan, China, ²Medical Science and Technology Innovation Center, Shandong First Medical University, Jinan, China

Protein acetylation is a reversible post-translational modification, and is involved in many biological processes in cells, such as transcriptional regulation, DNA damage repair, and energy metabolism, which is an important molecular event and is associated with a wide range of diseases such as cancers. Protein acetylation is dynamically regulated by histone acetyltransferases (HATs) and histone deacetylases (HDACs) in homeostasis. The abnormal acetylation level might lead to the occurrence and deterioration of a cancer, and is closely related to various pathophysiological characteristics of a cancer, such as malignant phenotypes, and promotes cancer cells to adapt to tumor microenvironment. Therapeutic modalities targeting protein acetylation are a potential therapeutic strategy. This article discussed the roles of protein acetylation in tumor pathology and therapeutic drugs targeting protein acetylation, which offers the contributions of protein acetylation in clarification of carcinogenesis, and discovery of therapeutic drugs for cancers, and lays the foundation for precision medicine in oncology.

KEYWORDS

acetylation, HAT, HDAC, post-translational modification, cancer, HDAC inhibitor

Introduction

Cancer is a malignant disease with heterogeneity, and its occurrence and development are affected by a variety of factors (1). It has strong ability to migrate, proliferate, and invade, and can adhere to the surrounding normal tissues. There are many factors to affect cancers, including genetic, epigenetic, and environmental factors, which all enhance tumor malignancy (2).

Epigenetics is the change in the level of gene expression without changes in the gene sequence (3). Abnormal changes in epigenetics may lead to the occurrence and development of various malignant diseases. Epigenetic research mainly includes DNA

covalent modifications such as DNA methylation and poly-methylation, chromatin remodeling, and the regulation of gene expression levels by non-coding RNAs (3). Proteins are the ultimate executors of biological functions. Studies have shown that many abnormal post-translational modifications are closely associated with malignant tumors, such as acetylation, ubiquitination, and phosphorylation (4). Of them, protein acetylation was discovered in the 1960s, but acetylation has not been extensively studied until recent years (5). Acetylation occurs on histones and non-histones, and most of the current research focuses on acetylation on histones (6). Histone is an octamer that constitutes the ribosome, consisting of four core histones (H3\H4\H2A\H2B), which combine with surrounding DNA fragments to form subunits of the ribosome, and the histone tail is easily translated by different post-translational modification to affect chromatin state and gene expression (6). Histones are prone to be acetylated (6). Studies have shown that protein acetylation is closely related to transcriptional regulation (7).

Acetylation modification is the process of covalently binding acyl-CoA compounds to specific amino acid sites of proteins under the action of acetyltransferase, generally binding to lysine residues (8). This process can also be reversed by deacetylases. This process is reversible and plays an important role in chromatin remodeling, gene expression, and regulation of protein function (9). Acetylation processes in different organelles are independent of each other. For example, acetyl-CoA in mitochondria and acetyl-CoA outside mitochondria are independent of each other (8). Acetylation in mitochondria plays an important role in biological processes such as the tricarboxylic acid cycle and fatty acid oxidation (9, 10). Moreover, protein acetylation is involved in the transcriptional regulation of genes, and some transcriptional co-activators have acetylase activity and some transcriptional co-repressors have deacetylase activity (7). Protein acetylation is associated with novel drug targets for a variety of diseases such as cancer (11). Thereby, it emphasizes the important scientific merits of protein acetylation in carcinogenesis and targeted drug discovery.

This article reviews (i) the component and process of protein acetylation system in cancers, including types of acetylation (N-acetylation, O-acetylation, and K-acetylation), regulators of acetylation (writers-acetyltransferases, erasers-deacetylases, acetyl coenzyme A, and readers), (ii) biological role of acetylation in cancer pathophysiology, including apoptosis, autophagy, cellular metabolism, cell cycle, proliferation, migration, and invasion, and (iii) acetylation system-based targeted drugs in cancer, including HAT inhibitors, HAT activators, HDAC inhibitors, and BET inhibitors. Also, we proposed the future perspectives about the roles of protein acetylation in carcinogenesis and targeted drug discovery. In this review, we focus on the classification of acetylation and its impact on pathophysiological processes in tumorigenesis. We

link protein acetylation with epigenetic drugs for tumor treatment to promote the development of cancer precision medicine.

The components and process of acetylation system in cancers

Types of acetylation in cancers

Protein acetylation is the process of covalently binding acyl-CoA class A compound to protein-specific amino acid sites under the action of acetyltransferases. Vincent Allfrey and his colleagues discovered histone lysine acetylation modification in 1964 (7). In subsequent studies, they gradually discovered the mechanism of acetylation modification, the discovery and identification of HAT and HDAC, and the discovery and identification of reader domains, which laid the foundation for protein acetylation. With the development of mass spectrometry and proteomics, non-histone acetylation was discovered and the regulatory process of non-histone acetylation was revealed (7). More and more studies have proved that histone acetylation and non-histone acetylation have the same importance in the regulation of biological processes in organisms (7). After the discovery of non-histone acetylation, histone acetyltransferases were also renamed lysine acetyltransferases and histone deacetylases were renamed lysine deacetylases (7). Histone acetylation occurs in the nucleus and is a type of epigenetic regulation that regulates chromatin structure to regulate transcription and DNA repair. Histone hyperacetylation by histone acetyltransferase is associated with transcriptional activation, while histone deacetylation by histone deacetylase is associated with transcriptional repression. Histone acetylation promotes transcription by remodeling higher-level chromatin structure, attenuating histone-DNA interactions, and providing binding sites for transcription activation complexes (12). Histone deacetylation inhibits transcription, and histone deacetylation and acetylation maintain homeostasis by opposing mechanisms, including the assembly of higher-order chromatin structures and the exclusion of bromo domain-containing transcriptional activation complexes (12). Histone acetylation and tumorigenesis are also closely related, and histone acetylation promotes the expression of certain genes that can lead to tumors (13). For example, P300 is a histone lysine acetyltransferase that catalyzes the attachment of acetyl groups to lysine residues, which leads to the activation of several genes, including several oncogenes. Study finds elevated expression of p300 in breast cancer (13).

Non-histone acetylation is involved in most biological processes in organisms and occurs with very high frequency. Non-histone acetylation is involved in key cellular processes related to organism physiology and tumors, such as gene

transcription, DNA damage repair, cell division, protein folding, autophagy, cell signaling, and metabolism. For example, HDAC6 acts not only on histones, but also on non-histone substrates to maintain the balance of non-histone acetylation (14). α -Tubulin, the first non-histone substrate of HDAC6, reversibly modulates its homeostasis and in turn affects MT stability and function (15). The α -tubulin acetylation affects intracellular trafficking events through the protein encoded by the cylindromatosis gene, thereby participating in mitosis and affecting the development of the cell cycle (14). Non-histone acetylation modifies protein expression through various mechanisms and affects protein function. For example, regulating protein stability, regulating protease activity, affecting subcellular localization, and regulating protein-protein interactions, etc. Protein acetylation can be classified into three types (N-acetylation, O-acetylation, and K-acetylation) according to acetylation site in a protein amino acid sequence.

N-acetylation

N-terminal acetylation in a protein is one of the most common modifications in mammals, which transfers the acetyl group to the N terminus of the protein, the amino group of the first residue in the protein (4). Unlike O-acetylation and K-acetylation, N-acetylation is an irreversible post-translational modification. N-acetylation occurs in 80%-90% of human proteins and is controlled by N-acetyltransferases. The addition of the acetyl group to N-terminus changes the charge carried by the amino acid, neutralizes the positive charge of the amino acid residue itself, changes the molecular weight of amino acid residue, changes the properties of the protein, and then affects the biological function of the protein. Studies have shown that N-acetylation mainly affects protein-membrane binding and protein stability (16). N-acetylation is also one of many factors contributing to tumor progression; for example, slow N-acetylation is a factor in bladder carcinogenesis and muscle invasiveness, and NAT1 is recognized as a biomarker candidate in bladder cancer and a potential target for drug development point (17).

O-acetylation

O-acetylation was detected less frequently than N-acetylation and K-acetylation. O-acetylation occurred mainly on the hydroxyl group at the serine or threonine terminal. O-acetylation was discovered in 2006 by Orth while studying YopJ, a bacterial virulence factor that acts as an acetyltransferase during acetylation (18). Studies have shown that YopJ transfers acetyl groups to the hydroxyl residues of serine or threonine, which inhibits the activation of MAPKK6, thereby inhibits the activation of MAPK and NF- κ B pathways, inhibites

the response of immune responses, and promotes the occurrence and development of malignant diseases (19). The discovery of O-acetylation adds to the complexity of the study of the regulation of gene expression by acetylation. Some studies have found that O-acetylation can compete with phosphorylation at some modification sites (20). Although there are few studies on O-acetylation, it has been found that O-acetylation is closely related to tumorigenesis in recent years (21). GD2 O-acetylation is elevated in neuroblastoma and glioblastoma, which is a potential biomarker of therapeutic target (21). In childhood acute lymphoblastic leukemia, the expression of 9-O-acetylated sialoglycoprotein was enhanced, decreased with the remission of clinical symptoms, and increased again when the disease relapsed (22). These studies indicate that O-acetylation might be a potential biomarker and target for drug-targeted therapy (22).

K-acetylation

Lysine acetylation is currently the most extensive research field of acetylation. Protein deacetylation is very extensive in the human body, with more than 3600 acetylation sites in more than 1750 proteins (23). Lysine acetylation mainly occurs on the histones of ribosomes and is jointly regulated by lysine acetyltransferase and lysine deacetylase to maintain the dynamic balance of lysine acetylation in cells (9). Lysine acetylation also occurs in non-histone proteins in the nucleus, cytoplasm, and mitochondria, and regulates various biological functions of cells (9). For example, DNA repair enzymes can be carried out in the nucleus through acetylation (24). The dynamic balance of lysine acetylation affects multiple functions in the cell, such as gene replication, gene transcription, stability of protein structure, interaction between proteins and proteins, cell cycle, cellular self-regulation, phagocytosis, and cell apoptosis (25). For example, there is a large amount of tubulin in the cytoplasm. Tubulin acts as a cytoskeletal component to maintain the stability of cells. The acetylation of α -tubulin is a significant marker of microtubule stability (26). Studies have shown that the acetylation of cytoskeleton is related to the occurrence of tumors, and tubulin is the target of many anti-tumor drugs. Lysine acetylation is one of the most important post-translational modifications in cell signaling pathways (10). The occurrence and development of many malignant tumors are closely related to lysine acetylation (27). For example, most metabolic enzymes are targets for lysine acetylation, such as ATM, ABL1, CDK9, BTK, CDK1 (25, 28–32), and a large number of acetylated proteins mediated abnormal changes in cell signaling pathways (33). For instance, acetylated phosphoglycerate kinase 1 is involved in glycolysis and amino acid biosynthesis in nonfunctional pituitary neuroendocrine tumors (NF-PitNETs) (34).

Regulators of acetylation in cancers

Acetylation in eukaryotic cells is in a dynamic equilibrium, which is jointly participated by writer-acetyltransferase, eraser-deacetylase, acetyl coenzyme A, and reader (4) (Figure 1).

Writer-acetyltransferases

Protein acetylation is a dynamic process by the joint action of acetyltransferases and deacetylases, including N-acetylation, O-acetylation, and K-acetylation (18). Most of the current studies focus on the acetylation of histones (6). Histone acetylation mainly occurs on lysine residues of histones (K-acetylation) in eukaryotic cells. The group is transferred to the side chain of the lysine residue, which in turn changes the R group of the lysine residue, neutralizes the positive charge on the lysine residue, and then affects the properties of the protein, and affects the structure and regulation of chromatin gene expression. According to structural and sequence similarity, mammalian lysine acetyltransferases are mainly divided into three categories: GCN5-related enzymes, p300-related enzymes, and MYST19-related enzymes (35). These acetyltransferases are present in the nucleus, and there are also acetyltransferases such as ESCO1, ESCO2, and HAT1 present in the nucleus (7). In addition to acetyltransferase in the nucleus, tubulin also contains acetyltransferase TAT1 (36). Acetylation of α -tubulin is a prominent marker of microtubule stability, and p27 promotes microtubule acetylation by binding and stabilizing ATAT-1 in glucose-deficient cells (37). Acetyltransferases have substrate specificity, which can regulate the structure of chromatin and thus regulate gene expression (7). For example, MOZ has a plant homeodomain-linked (PHD) type zinc finger that regulates chromatin by binding to trimethylated lysine 4 of histone 3 Structure (38). Acetyltransferases are also closely associated with

transcriptional activators. For example, loss of Kat2a affects transcription factor binding and reduces transcriptional burst frequency in a subset of gene promoters, thereby enhancing variability at the transcriptional level (39). CBP/p300 blocks the role of estrogen receptor alpha (ER α) in luminal breast cancer by inhibiting enhancer H3K27 acetylation (40). The mechanism of action of acetyltransferase depends on oncogene activation, which is closely related to the occurrence and development of tumors through signal transduction (41). Both Tip60 expression and ABCE1 acetylation were up-regulated in lung cancer cells (42). Downregulation of Tip60 reduced ABCE1 acetylation levels and inhibited cell proliferation, invasion and migration (42). In addition, downregulation of Tip60 activates the apoptotic pathway, thereby achieves its inhibitory effect (42). Naa10 can acetylate and stabilize TSC2, thereby inhibiting mTOR activity and inhibiting cancer development (43). Acetyltransferase can also control the occurrence and development of tumors by regulating kinases in tumor cells. Naa10 inhibits tumor cell migration by inhibiting MYLK kinase activity through acetylation (44). ESCO2 inhibits the nuclear translocation of hnRNPA1 and increases the binding of hnRNPA1 (heterogeneous nuclear ribonucleoprotein A1) to the intron sequence flanking exon 9 (EI9) of PKM RNA, which ultimately inhibits the formation of PKM1 isoforms and induces the formation of PKM2 isoforms to promote glycolysis of tumor cells, and accelerate the metabolism of tumor cells (45).

The abnormal expression of HATs is usually associated with the occurrence and development of several malignant tumors and poor prognosis, which indicates that HATs may be potential tumor therapy targets and potential biomarkers (46). It is still necessary to in-depth study the effect mechanism of HATs on tumors to clarify the applicability and effectiveness of HATs in the clinical treatment of tumors (Table 1).

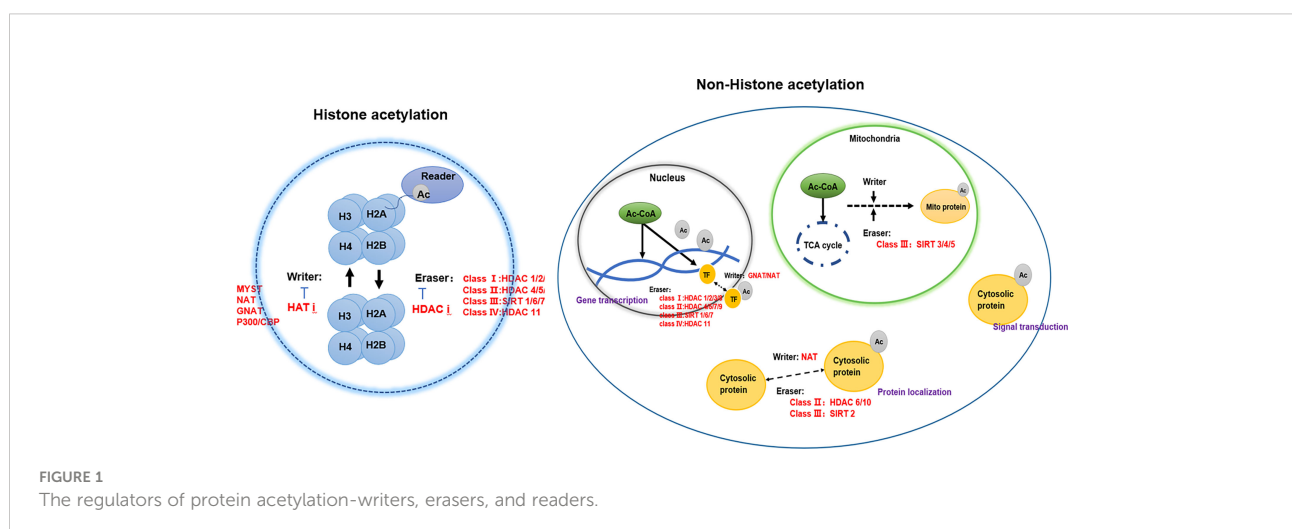


FIGURE 1
The regulators of protein acetylation-writers, erasers, and readers.

TABLE 1 Classification, localization and role of acetylases in cancers.

Family	Name	Location	Effects on cancers	Reference
NAT	Naa10 (NatA)	Nucleus	Represses tumor cell migration	(44)
	Naa20 (NAT5)			
	Naa30 (NAT12)	Cytoplasm		
	Naa40 (NAT11)		Negative regulator of apoptosis	(47)
	Naa50 (NAT5)			
	Naa60 (NAT15)			
	Naa11			
	NAT10			
GNAT	KAT1	Nucleus		
	GCN5 (KAT2A)		Deplete acute myeloid leukemia	(39)
	PCAF (KAT2B)		Modulate protein stability	(48)
	ELP3 (KAT9)		Wnt-driven intestinal tumor initiation	(49)
	ATAT-1			
	AT-1		Regulate apoptosis	(50)
P300/CBP	CBP (KAT3A)		Breast cancer, hematological malignancies	(40, 51)
	P300 (KAT3B)		Breast cancer, hematological malignancies	(36, 52)
MYST	Tip60 (KAT5)		Lung cancer	(42)
	MOZ (KAT6A)		Acute myeloid leukemia	(38)
	MORF (KAT6B)		Leiomyoma	(53)
	HBO1 (KAT7)		Promotes DNA replication licensing	(54)
	MOF (KAT8)		Tumor promoter in GBM	(55)
Others	ESCO1		Promote sister chromatid cohesion	(56)
	ESCO2		Promote LUAD malignant progression	(45)
	HAT1			
	TAT1	Tubulin		

Eraser-deacetylases

Protein deacetylase is called the “eraser” of acetyl group, which reduces the acetyl group attached to the amino acid residue to acetate, affects the R group structure of the amino acid residue, and then reduces the positive charge of the amino acid, and facilitates its binding to negatively charged DNA (52). Protein deacetylases are involved in regulating gene replication, gene transcription, protein structure stability, DNA damage repair, and other cellular functions (7). Mammalian genes encode 18 deacetylases, which act on histone and non-histone proteins in cells to remove their acetyl groups (7). For example, sirtuin enzymes are divided into four classes and localized in different locations of cells (57). Class III belongs to NAD⁺-dependent sirtuin enzymes, which are localized in mitochondria, cytoplasm and nucleus (57). Zn²⁺-dependent HDACs have a highly conserved deacetylase domain, including classes I (HDAC 1, 2, 3, and 8), II (HDAC 4, 5, 7, and 9), and IV (HDAC 11) localized in the nucleus (58). Studies have found that HDAC can not only act on histone deacetylation, but also play other roles on histones, such as decrotonylation, and

desumoylation (9). HDACs have been found to be abnormally expressed or altered in localization in a variety of cancers (59). Studies have shown that the abnormal expression of HDAC in cancer patients is closely related to the dynamic imbalance of acetylation in the human body (60). In addition, the specific domains of individual sirtuins also have their own specific functions, such as maintaining protein stability (52) (Table 2).

Transcription factors are a kind of non-histone proteins, and protein deacetylases regulate gene transcription activity by deacetylating transcription factors (27). For example, HDAC7 regulates the acetylation of H3K27 and the transcriptional activity of super-enhancer-related genes in breast cancer stem cells (80). A common mutation in AML is a chromosome 16 inversion that fuses the core-binding factor beta (CBFB) gene with the smooth muscle myosin heavy chain gene (MYH11) to form the oncogene CBFB-MYH11 (61). The expressed protein CBFBeta-SMMHC forms a heterodimer with the key hematopoietic transcription factor RUNX1, and CBFBeta-SMMHC acts together with RUNX1 to activate the transcription of specific target genes (61). HDAC1 promotes

TABLE 2 Classification, localization and role of deacetylases in cancers.

Family	Name	Location	Cancer	Effects on cancer	Reference
Class I	HDAC 1	Nucleus	Acute myeloid leukemia (AML) glioblastoma	Regulate apoptosis Maintenance of the malignant phenotype	(61–63)
	HDAC 2	Nucleus	Hepatocellular carcinoma (HCC)	Regulate cell cycle, migration, apoptosis, and cell adhesion.	(64, 65)
	HDAC 3	Nucleus	Acute myeloid leukemia (AML), colorectal cancer, lung cancer, melanoma, human maxillary cancer, acute promyelocytic leukemia (APL), multiple myeloma (MM), hepatocellular carcinoma (HCC), breast cancer	Promotes cancer progression	(66–72)
Class II a	HDAC 8	Nucleus	Acute myeloid leukemia	Aberrant expression or deregulated interactions with transcription factors	(73, 74)
	HDAC 4	Nucleus	Breast cancer, Glioblastoma nasopharyngeal carcinoma	Promote proliferation, migration, and invasion in nasopharyngeal carcinoma	(75–77)
	HDAC 5	Nucleus	CAN in HCC	Regulate cell proliferation and invasion, the immune response, and maintenance of stemness	(78, 79)
Class II b	HDAC 7	Nucleus	Breast cancer	Regulates gene expression, cell proliferation, cell differentiation and cell survival	(80, 81)
	HDAC 9	Nucleus	Breast cancers	Anti-estrogen resistance, promotes tissue-specific transcriptional regulation	(82, 83)
	HDAC 6	Cytoplasm	Prostate cancer	Regulate cell proliferation, metastasis, invasion, and mitosis	(14, 84)
Class III	HDAC 10	Cytoplasm	Lung adenocarcinoma		(85)
	SIRT 1	Nucleus	Lung cancer	Involved in gene regulation, genome stability maintenance, apoptosis, autophagy, senescence, proliferation, aging, and tumorigenesis	(86, 87)
	SIRT 2	Cytoplasm	Lung cancer, Glioblastoma melanoma	suppresses NK cell function and proliferation	(76, 86, 88)
	SIRT 3	Mitochondria	Lung cancer, Ovarian cancer	Regulate autophagy	(89, 90)
	SIRT 4		NSCLC, Endometrioid adenocarcinoma		(91) (92)
	SIRT 5		Acute Myeloid Leukemia		(93)
	SIRT 6	Nucleus	Acute Myeloid Leukemia		(94)
Class IV	SIRT 7	Nucleosome	Breast cancer, glioblastoma		(76, 95)
	HDAC11	Nucleus	HCC	High expression in HCC	(96)

transcriptional activation as a cofactor for the leukemic fusion protein CBFbeta-SMMHC (61). HDACs also act directly on proteins involved in tumor migration, metastasis and growth (97). For example, Api5 is a known anti-apoptotic and nuclear protein responsible for inhibiting cell death under conditions of serum starvation (97). The only known post-translational modification of Api5 is the acetylation of lysine 251 (K251) (97). p300 interacts with HDAC1 to regulate cell proliferation by

regulating Api5 acetylation and stability (97). Inactivation of SIRT6 in cancer cells results in the accumulation of nuclear ACLY protein, increasing nuclear acetyl-CoA, which in turn drives site-specific histone acetylation and the expression of cancer cell adhesion and migration genes that promote tumor aggressiveness (98). Novel mechanism by which SIRT6 suppresses aggressive cancer cell phenotypes revealed and acetyl-CoA-responsive cell migration and adhesion genes

identified as downstream targets of SIRT6 (98). Therefore, the regulatory mechanism of HDACs in tumors is difficult to be clearly described.

Class III HDACs are mainly located in mitochondria, which are the center of cellular energy metabolism (57). Acylated mitochondrial proteins are involved in many functions related to cellular metabolism, including TCA cycle, oxidative phosphorylation, nucleotide metabolism, amino acid metabolism, and urea cycle (99). SIRT can regulate energy production by regulating the acetylation and deacetylation of organisms involved in energy metabolism in mitochondria, thereby affecting cellular metabolism (7). For example, sirtuin 3 (Sirt3) is a key player in maintaining mitochondrial function and is involved in ATP production by regulating the acetyl and pyruvate dehydrogenase complex (PDH) (89). The underlying mechanism of SIRT is also related to the metabolic reprogramming of tumors (9). SIRT5 disruption-induced apoptosis is caused by a decrease in oxidative phosphorylation and glutamine utilization and an increase in mitochondrial superoxide, which is attenuated by ectopic superoxide dismutase 2 (93). SIRT5 controls and orchestrates key metabolic pathways in AML, so SIRT5 may be a potential therapeutic target in AML (93).

Class IV HDACs only contain HDAC11, which is highly expressed in HCC and is closely related to disease prognosis (96). Loss of HDAC11 promotes histone acetylation in the LKB1 promoter region, thereby activating the AMPK signaling pathway and inhibiting the glycolysis pathway, thereby increasing the transcription of LKB1, thereby inhibiting tumorigenesis and HCC progression (96). Histone deacetylases are abnormally expressed in clinical tumor patients and are associated with poor prognosis and survival (59). HDAC9 expression is positively associated with up-regulated genes in endocrine therapy-resistant breast cancer, and high HDAC9 levels are associated with poorer prognosis in patients treated with OHTam (82). HDAC10 regulates tumor stem cell properties in KRAS-driven lung adenocarcinoma, and HDAC10 regulates the stem-like properties of kras-expressing tumor cells by targeting SOX9 (85). The expression of SOX9 is significantly increased in HDAC10-depleted tumor cells, TGF β pathway-related genes are enriched in HDAC10 knocked out tumor cells, and activation of TGF β signaling contributes to the induction of SOX9 in HDAC10 knocked out lung adenocarcinoma cells (85). However, HDACs show activating activity in some tumors and inhibitory activity in some tumors, which suggests that their mechanism of action might not be a single one. SIRT1 may exert oncogenic effects by inactivating other tumor suppressors (eg, HIC1) and/or activating tumor-promoting genes (eg, *via* N-Myc stabilization or p53) or other proteins (cortatin) (100–102). There are interactions between HDACs. Studies have shown that inhibition or knockdown of HDAC1 and HDAC3 results in downregulation of HDAC7,

which is associated with reduced histone 3 lysine 27 acetylation (H3K27ac) at transcription start sites (TSS) and super-enhancers (SEs), this is particularly evident in stem-like BrCa cells (80). Inactivation of HDAC7 can lead to suppression of the CSC phenotype, either directly or through the inhibition of HDAC1 and HDAC3, by downregulating multiple se-related oncogenes (80). HDAC7 may be a potential drug target (80).

HDACs inhibitors also have many adverse reactions in clinical application, such as drug resistance and toxic side effects (59). Aberrant expression of HDACs has also been shown to correlate with tumor resistance. HDAC8 increases the expression of p65, a key component of the NF- κ B complex, and promotes the expression of IL-6 and IL-8 (103). This may be because HDAC8 can directly bind to the promoter of p65, increasing its transcription and expression. Thus, HDAC8 promotes DNR resistance in human AML cells by regulating IL-6 and IL-8 (103).

Acetyl coenzyme A

Acetyl Coenzyme A is a key precursor that used to synthesize acetyl. The progression of lysine acetylation can be controlled by regulating the concentration of acetyl-CoA. Acetyl-CoA is an important metabolite in cellular biological processes and is the only donor of acetyl groups during acetylation (104). Acetyl-CoA has different production pathways in different organelles. Acetyl-CoA produced in different organelles can be locally utilized in organelles, produced by decarboxylation of pyruvate in mitochondria, and produced by fatty acid β -oxidation in cytoplasm (105). ACLY, ACS2, PDC can produce acetyl-CoA in organelles to regulate lysine acetylation (106). The interaction between lysine acetylation and acetyl-CoA is influenced by many factors, including the kinds of HATs, the acetyl-CoA/CoA ratio and intracellular pH gradient (107, 108).

Acetyl-CoA is derived from glycolysis and β -oxidation in the mitochondrial matrix, which ultimately leads to the production of cytoplasmic pyruvate, and enters the mitochondria for decarboxylation to form acetyl-CoA (109, 110). Branched-chain amino acids (i.e., valine, leucine, and isoleucine) can also be used to produce acetyl-CoA (111). Most of the acetyl-CoA in the cytoplasm comes from glutamine reductive carboxylation, which generates acetyl-CoA through the TCA cycle (112). Acetyl-CoA also has compartmentalized effects on protein acetylation. Acetyl-CoA exists in mitochondria, nucleus, and cytoplasm (105). Acetyl-CoA in mitochondria has a specific source pathway. Acetyl-CoA can pass through nuclear pores in the nucleus and cytoplasm. During the shuttle, acetyl-CoA has different abundances of acetyl-CoA in the nucleus and cytoplasm, and the occurrence of protein acetylation is also different (105). At the same time, studies have shown that the acetyl-CoA/CoA ratio may be a relevant regulator of HAT enzyme activity, rather than the absolute level of acetyl-CoA (105).

This establishes a link between the nuclear and cytoplasmic abundance of acetyl-CoA and the epigenetic regulation of genes (105). In the process of tumorigenesis, abnormal expression of acetyl-CoA was also found. Acetyl-CoA can affect the proliferation, invasion and migration of tumor cells directly or by affecting protein acetylation (113). Acetyl-CoA induces cell growth and proliferation by promoting acetylation of histones at growth genes (113), and increase the levels of acetyl-CoA and acetylated histones to maintain the accelerated proliferation of cancer cells (105).

Reader

For histone acetylation to exert their biological functions, they also need to be combined with specific recognition proteins. Acetylated lysine in a protein will provide a reading site, recruit proteins with special structural domains, affect biological functions such as gene replication, gene transcription, and repair after DNA damage, and jointly participate in the regulation of gene expression (8). Recognition proteins can contain multiple different recognition domains that cooperate with PTM sites. Studies have shown that lysine-containing acetylation modification sites can be specifically recognized by proteins such as bromodomains, dual-PHD finger domains, and YEATS domains (8).

Four BET proteins have been identified in humans, BRD2, BRD3, BRD4 and the testis-specific protein BRDT (114). BRDT is only present in male germ cells (115). The BET family controls the transcription of various proinflammatory and immunoregulatory genes by recognizing acetylated histones (mainly H3 and H4) and recruiting transcription factors (such as RELA) and transcription elongation complexes (such as P-TEFb) to chromatin, thereby promoting the phosphorylation of RNA polymerase II and subsequent transcription initiation and elongation (116).

Localized in the nucleus, BRD2 can bind to hyperacetylated chromatin and play a role in transcriptional regulation through chromatin remodeling (115). BRD2 can regulate the transcription of the CCND1 gene and play a role in nucleosome assembly (117). Abnormal expression of BRD2 affects the development of various malignant tumors (118). For example, Runx3 forms a complex with BRD2 in a KRas-dependent manner in the early stages of the cell cycle, resulting in the inactivation of Runx3 and promoting the development of lung adenocarcinoma (118). Studies have shown that OCCC cells are susceptible to knockdown of epigenetic gene targets such as bromopseudomin and the extraterminal domain (BET) proteins BRD2 and BRD3, and targeting the BET proteins BRD2 and BRD3 in combination with PI3K-AKT inhibition may as a therapeutic strategy for ovarian clear cell carcinoma (119). The abnormal expression of BRD2 is also closely related to the drug resistance of patients. Studies have shown that BRD2 promotes drug resistance in adult T-LBL through the RasGRP1/Ras/ERK

signaling pathway (120). Targeting BRD2 may be a new strategy to improve treatment efficacy and prolong survival in adults with T-LBL (120).

Localized to the nucleus, BRD3 is a chromatin reader that recognizes and binds hyperacetylated chromatin and plays a role in transcriptional regulation, possibly through chromatin remodeling and interactions with transcription factors (121). BRD3 regulates transcription by promoting the binding of the transcription factor GATA1 to its targets (122). The study found that BRD3 directly interacts with BCL6 and maintains the negative feedback regulatory loop of BCL6 (123). BRD2 and BRD3 preferentially associate with hyperacetylated chromatin throughout the length of transcribed genes *in vivo* (121). BRD2- and BRD3-associated chromatin was significantly enriched in H4K5, H4K12, and H3K14 acetylation reactions, and contained relatively less dimethylated H3K9 (121). Both BRD2 and BRD3 allow RNA polymerase II transcription by nucleosomes in a defined transcription system (121).

Localized in the nucleus, BRD4 is currently the most widely studied chromatin reader protein that recognizes and binds acetylated histones and plays a key role in the transmission of epigenetic memory across cell division and transcriptional regulation (124). Remains associated with acetylated chromatin throughout the cell cycle, and by preserving acetylated chromatin state and maintaining higher-order chromatin structure (125). Studies have shown that BRD4 is a transcriptional repressor of autophagy and lysosomal function (126). BRD4 plays a key role in regulating the transcription of signal-induced genes by binding to the P-TEFb complex and recruiting it to promoters. The P-TEFb complex is also recruited to the distal enhancer, an anti-pause enhancer that cooperates with JMJD6 (125). BRD4 and JMJD6 are required to form the transcriptionally active P-TEFb complex by replacing negative regulators such as HEXIM1 and the 7SK snRNA complex from P-TEFb, thereby converting it to the active form, which can then phosphorylate the C-terminal structure of RNA polymerase II Domain (CTD) (125). MYC regulates its own transcription by restricting its site for BRD4-mediated chromatin remodeling (127). The MYC-stabilizing kinase ERK1 regulates MYC levels directly or indirectly by inhibiting BRD4 kinase activity. These findings suggest that BRD4 negatively regulates MYC levels, which is counteracted by ERK1 activation (127).

BRD4 has three isoforms, BRD4 short isoform and BRD4 long isoform (128). There are two BRD4 short isoforms, which are spliced from other mRNAs. The short isoform of BRD4 promotes tumor metastasis, and the long isoform of BRD4 inhibits tumor metastasis and spread (128). Study shows BRD4 isoforms have opposing functions in breast cancer (128). The role of BRD4 in cancer is largely dependent on the long isoform (BRD4-L), and we demonstrated by isoform-specific knockdown and endogenous protein detection as well as transgene expression that the less abundant short isoform of

BRD4 (BRD4-L) S is oncogenic and BRD4-L has a tumor suppressor role in breast cancer cell proliferation and migration as well as breast tumor formation and metastasis (128). An isoform of BRD4 that acts as a chromatin insulator in DNA damage response pathways (129). Inhibits DNA damage response signaling by recruiting condensin-2 complexes to acetylated histones, leading to remodeling of chromatin structure, shielding this region from DNA by limiting the spread of histone H2AX/H2A.x phosphorylation injury response (129).

Due to the abnormal expression of BRD4 in various tumors, targeting BRD4 has emerged as a potential therapeutic strategy (130). For example, the expression of BRD4 in glioma was significantly higher than that in adjacent normal brain tissue (130). BRD4 inhibitors effectively penetrate the blood-brain barrier and target glioma tumor tissue, but have little effect on normal brain tissue (130). BRD4 is overexpressed in NFPA and GHPA, and the effects of BRD4 inhibitors on PA cells *in vitro* and *in vivo* were evaluated, so BRD4 is a promising therapeutic target for NFPA and GHPA (131).

BRD4 promotes the progression and metastasis of gastric cancer, and the abundance of BRD4 in human gastric cancer tissue is associated with shorter survival in patients with non-metastatic gastric cancer (132). BRD4 recognizes acetylated K146 and K187 on snails in an acetylation-dependent manner to prevent snails from recognition by their E3 ubiquitin ligases FBXL14 and β -Trcp1, thereby inhibiting snail polyubiquitination and proteasome degradation (132).

The mode of action of I-BET151 is due to the repression of transcription of key genes (BCL2, C-MYC and CDK6) by displacing BRD3/4, PAFc and SEC components from chromatin (133). This suggests that replacing BET proteins from chromatin is a potential epigenetic therapy for aggressive leukemia. BRDT (Bromodomain testis-specific protein), localized in the nucleus, exists only in male germ cells, and not often studied in tumors (115).

YEATS family proteins include YAF9, ENL, AF9, TAF14, SAS5 proteins (4). As the “readers” of protein acetylation, YEATS family proteins can combine with proteins to form various chromatin-related complexes with different complex functions, and play a role in chromatin remodeling and gene expression (4). YEATS family proteins are closely related to the occurrence of various malignant tumors. For example, ENL binds to acetylated histone H3, and co-localizes with H3K27ac and H3K9ac on the promoters of actively transcribed genes that are critical for leukemia (134). ENL is a regulator of leukemia. oncogenic transcriptional program (134), and an intact YEATS chromatin-reader domain was essential for ENL-dependent leukemic growth (135). YEATS4 overexpression enhances the malignant features of breast cancer cells, especially inducing epithelial-to-mesenchymal transition, and YEATS4 is associated with poor prognosis in breast cancer (136). YEATS protein

promotes the proliferation of gastric cancer cells and affects tumor development by activating the Wnt/ β -catenin signaling pathway (137). GAS41 is abundantly expressed in non-small cell lung cancer and is closely related to the proliferation of lung cancer cells (138). YEATS2, a target gene of HIF1 α , promotes pancreatic cancer development under hypoxia (139).

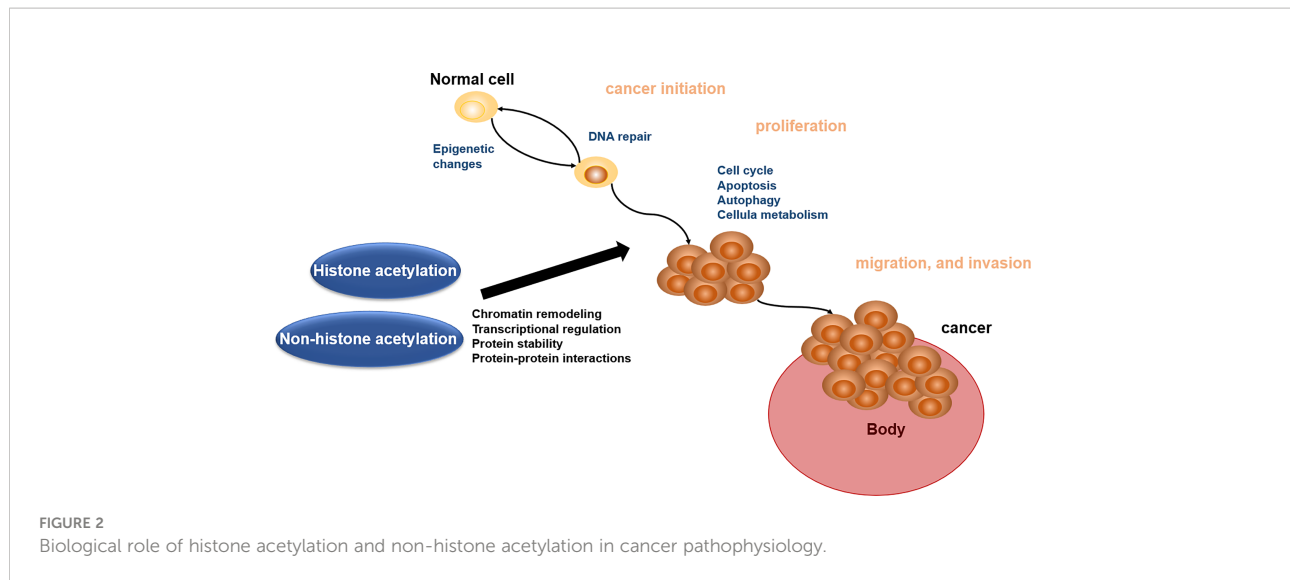
Complex post-translational modifications are affected by many factors, one of which is the way the recognition site binds to the recognition protein. Initial studies believed that a post-translational modification recognition site can only bind to one recognition protein. The researchers found that a PTM recognition site can interact with multiple recognition proteins, eg. At the same time, a single recognition domain can also bind to multiple different protein PTMs, eg. Also, since recognition proteins include multiple distinct domains, synergy is extremely common in recognition proteins.

Biological role of acetylation in cancer pathophysiology

Acetylation of proteins is related to various kinds of cellular processes and human cancer (140). Here, we address the roles of acetylation in cancer cell apoptosis, autophagy, cell metabolism, cell cycle, proliferation, and migration and invasion, which will offer the basis for acetylation enzymes and BETs in reader as the important therapeutic targets (Figure 2).

Role of acetylation in apoptosis

Apoptosis refers to the orderly death of cells controlled by genes, which is a normal programmed death in order to maintain the stability of the internal environment. In the process of cell apoptosis, it can be divided into the initiation stage, which receives apoptosis signals, interacts with apoptosis regulators, and then activates proteolytic enzymes, resulting in apoptosis (141). However, tumors have the characteristics of avoiding apoptosis, and abnormal apoptosis leads to abnormal tumor growth (142). The abnormal expressions of acetyltransferase and deacetylase can affect the normal apoptosis of cells. For example, PDCD5, a protein associated with apoptosis in human cells, binds to Tip60 and enhances the stability of Tip60 protein under stress-free conditions (143). PDCD5 increases Tip60-dependent K120 acetylation of p53 and is involved in p53-dependent expressions of apoptosis-related genes such as Bax (143). The combination of PDCD5 and Tip60 accelerates DNA damage-induced apoptosis, whereas knockdown of PDCD5 or Tip60 inhibits apoptosis-accelerating activity (143). HDAC1 and HDAC2 double knockout cells show significant activation of apoptosis (144). HDAC6 negatively regulates pro-apoptotic acetylation of p53 at K120 in mesenchymal stem cells (MSCs) (145). Studies have



shown that targeting histone acetyltransferases and histone deacetylases can regulate tumor cell apoptosis, thereby affecting tumor growth and development (146). For example, histone deacetylase inhibitors induce apoptosis and autophagy in human neuroblastoma cells (147). Valproic acid induces cell cycle arrest and apoptosis *via* Hsp70 acetylation and inhibits proliferation of HER2-expressing breast cancer cells (148). When rRNA transcription was inhibited, nucleolar RNA content was reduced. The nucleolar protein Myb-binding protein 1A (MYBBP1A) translocates to the nucleoplasm and increases p53 acetylation as the level of nucleolar RNA content decreases (149). Acetylated p53 enhances p21 and BAX expression and induces apoptosis (149). Targeting protein acetylation to regulate tumor apoptotic activity can provide new therapeutic ideas for the clinical treatment of malignant tumors.

Role of acetylation in autophagy

Autophagy is a special substance degradation pathway in cells, which depends on lysosomes for its action (10). The degradation substrates of autophagy include proteins and organelles. The probability of autophagy occurring in normal cells is low, and it mainly occurs in cells under abnormal conditions, such as starvation, hypoxia or organelle damage (150). There are three main types of autophagy. (i) The first type is microautophagy, in which lysosomes wrap a part of the cytoplasm into lysosomes and degrade them. (ii) The second is macroautophagy, which first generates an autophagosome (151). The double-membrane structure of the phagosome, the fruiting body contains the substances that need to be degraded in the cytoplasm, the autophagosome and the lysosome are combined to generate the autophagolysosome, and the acidic substances in the lysosome are used to degrade the autophagosome (151).

Substances are degraded. (iii) The third is chaperone-mediated autophagy. Molecular chaperone-mediated autophagy uses heat shock protein 70 to bind to substrates with specific amino acid sequences and transport the substrates to lysosomes for further development (152). In 2004, Shao et al. found that HDAC inhibitor suberoylanilide hydroxamic acid β -D-glucuronide could induce autophagic death of cancer cells, and researchers gradually began to pay attention to the relationship between protein acetylation and autophagy (153). There is a close relationship between histone acetylation and cell autophagy. Histone acetylation can induce the occurrence of cell autophagy in the face of long-term stress, starvation and other harsh environments (154). The most widely studied is the relationship between H4K16ac and H3K56ac and autophagy. In eukaryotic cells, H4K16ac affects chromatin condensation and promotes gene transcription (155).

There is also a close link between non-histone acetylation and cell autophagy. Non-histone protein associated with autophagy that can be acetylated include transcription factors, autophagy-related proteins, and cytoskeletal proteins (7). The Fox O protein family is a transcriptional activator in eukaryotic cells, and acetylation can affect its biological activity. K on Fox O protein can be acetylated by HAT, and the activity of Fox O protein after acetylation is reduced, inhibiting DNA and its interaction, binding to regulate transcription (156). SIRT1 can also affect autophagy by regulating Fox O activity (157). TFEB protein is also a transcription factor that regulates the transcription of autophagy-related genes, such as LC3, and plays an important role in biological processes such as lysosomal biosynthesis and autophagy activation (158). The biological activity of the TFEB protein family is also affected by acetylation modification, and TFEB deacetylation can significantly enhance the autophagy and lysosomal function of cells (159). The TFEB-specific lysine acetylase is GCN5, which

can acetylate the K276 and K279 sites of TFEB, affect the formation of TFEB dimers, interfere with the binding of TFEB and its targets, and inhibit autophagy happened (160). Acetylations affect subcellular localization, thereby affecting autophagy (161). In general, Bmp300-mediated acetylation sequesters components of the BmAtg8-PE ubiquitin-like system in the nucleus, leading to inhibition of autophagy. Conversely, BmHDAC1-mediated deacetylation leads to nuclear-to-cytoplasmic transfer of components of the BmAtg8-PE ubiquitin-like system, promoting autophagy (161).

Protein acetylation is an important process regulating autophagy and plays an important role in the development of malignant diseases. The phosphorylation of ATG5 (T101) in the lesion tissue of glioblastoma patients is positively regulated by the acetylation modification of the hypoxia-induced autophagy regulator PAK1, which plays an important role in hypoxia-induced autophagy and promotes the occurrence and development of tumors (162). Targeting protein acetylation modification to regulate autophagy activity can provide new therapeutic ideas for clinical treatment of malignant tumors.

Role of acetylation in cell metabolism

A major feature of tumors is uncontrolled proliferation, fueled by corresponding metabolic dysregulation (2). Tumors undergo metabolic reprogramming to promote tumor cell growth, division, invasion and migration. An abnormal response of tumor cell energy metabolism is called the Warburg effect (89). In the presence of oxygen, tumor cells reprogram glucose metabolism by limiting energy metabolism mainly to glycolysis, thereby generating energy for tumor growth (163). Lysine acetylation is a ubiquitous modification in enzymes that catalyze intermediate metabolism. Almost every enzyme in glycolysis, gluconeogenesis, tricarboxylic acid (TCA) cycle, urea cycle, fatty acid metabolism and glycogen metabolism is found to be acetylated in human liver tissue (10). All seven enzymes in the TCA cycle are acetylated (10). Acetylation occurs in most intermediate metabolic enzymes, and acetylation can directly affect the activity or stability of the enzyme (10). The bioenergetic preference of cancer cells promotes tumor acidosis, which in turn results in a marked reduction in glycolysis and glucose-derived acetyl-CoA (164). Protein acetylation affects tumor metabolism by affecting the TCA cycle. CBP acetylates STAT3 to undergo mitochondrial translocation, and STAT3 associates with pyruvate dehydrogenase complex E1, which in turn accelerates the conversion of pyruvate to acetyl-CoA, increases mitochondrial membrane potential and promotes ATP synthesis (165). SIRT5 removes the STAT3 acetyl group, thereby inhibiting its function in mitochondrial pyruvate metabolism (165). The protein also affects lipid metabolism in tumor cells and thus

affects tumor development (166). Dynamic regulation of ME1 phosphorylation and acetylation affects lipid metabolism and colorectal tumorigenesis (166). The manner in which SIRT6 deacetylase antagonizes ACAT1 function involves mutually exclusive ME1 S336 phosphorylation and K337 acetylation (166). ACAT1 acetylates GNPAT at K128, which inhibits TRIM21-mediated GNPAT ubiquitination and degradation (167). GNPAT deacetylation by SIRT4 antagonizes the function of ACAT1. GNPAT inhibits TRIM21-mediated degradation of FASN and promotes lipid metabolism. promote the occurrence of liver cancer (167). Studies have shown that lysine acetylation controls metabolic activity by directly blocking the active site of the enzyme (168).

Role of acetylation in cell cycle

Protein acetylation is closely related to gene transcription. Hyperacetylation promotes gene transcription and expression, while hypoacetylation inhibits gene transcription and expression (12). A large number of proteins involved in chromatin remodeling and cell cycle are acetylated (169). The cell cycle of tumor cells is greatly shortened and disordered. Studies have found that acetylation of tumor cells is also closely related to cell cycle progression (170). Protein acetylation affects tumor cell cycle progression by affecting chromatin remodeling, SIRT2 regulates H4K20me1 deposition through deacetylation of H4K16Ac (acetylation of H4K16), regulates chromatin localization, and affects cell cycle progression (169). Protein acetylation also has effects through the regulation of various factors in the cell cycle. For example, CDC2, a major cyclin-dependent kinase and regulator of S-phase progression and mitosis, is acetylated at residues K6 and K33 in CDC2 (25). SIRT1 interacts with CHK2 and is deacetylated at residue lysine 520, which inhibits CHK2 phosphorylation, dimerization, and thus activation (171). SIRT1 depletion induces CHK2 hyperactivation-mediated cell cycle arrest and subsequent cell death (171). Transcription factor Sp1 is a target of acetylation and is closely associated with cell cycle arrest in colon cancer cell lines (172). Simultaneous regulation of Api5 acetylation and deacetylation is an important factor in cell cycle progression (97).

Role of acetylation in cell proliferation

Cancer cells have unlimited replicative potential with continuous proliferative signals (2). Normal cells and tissues release growth signals in an orderly manner, and these growth signals instruct cells to grow, divide and differentiate in an orderly manner, thereby ensuring the stability of cell numbers and the homeostasis of the internal environment, thereby maintaining normal tissue structure and function (2).

However, tumor cell proliferation signals are abnormal and can continuously obtain proliferation signals from a variety of different pathways. In the abnormal proliferation of tumor cells, protein acetylation plays an important role. For example, acetylation at the K323 site of PGK1 is an important regulatory mechanism that promotes its enzymatic activity and cancer cell metabolism (173).

Acetyltransferase and deacetylase dynamically regulate the balance of acetylation, affecting the apoptosis and autophagy of tumor cells and other death methods, thereby affecting the proliferation of tumor cells. For example, Api5 is a known anti-apoptotic and nuclear protein responsible for inhibiting cell death under serum starvation conditions (97). The only known post-translational modification of Api5 is acetylation at K251. The K251 acetylation in Api5 is responsible for its stability, whereas the deacetylated form of Api5 is unstable (97). Inhibition of acetylation by p300 results in a decrease in Api5 levels, whereas inhibition of deacetylation by HDAC1 results in an increase in Api5 levels (97). Acetylation also affects the proliferation of tumor cells by affecting the activities of various metabolic enzymes in cells. For example, PKM2 K305 acetylation reduces PKM2 enzymatic activity and promotes its lysosome-dependent degradation through chaperone-mediated autophagy (CMA) (174). Degrade and promote tumor growth through chaperone-mediated autophagy (174). Ribonucleotide reductase (RNR) catalyzes the *de novo* synthesis of deoxyribonucleoside diphosphates (dNDPs), which provide dNTP precursors for DNA synthesis (175). Acetylation at residue K95 in RRM2 results in a reduction of the dNTP pool, DNA replication fork arrest, and inhibition of tumor cell growth *in vitro* and *in vivo* (175). P300 acetylates MAT II α at K81 and destabilizes MAT II α by promoting its ubiquitination and subsequent proteasomal degradation, inhibits tumor cell growth, and is reduced in human hepatocellular carcinoma (176). Inactivation of HDAC2 leads to elevated TPD52 acetylation, which impairs the interaction between TPD52 and HSPA8, resulting in impaired CMA function and tumor growth *in vivo* (177). Acetylation-dependent regulation of CMA oncogenic function in PCa by TPD52 suggests the possibility of targeting the TPD52-mediated CMA pathway to control PCa progression (177). p21 depletion converts KLF4 from a cell cycle inhibitor to a promoter of bladder cancer cell proliferation (178). Furthermore, KLF4 is acetylated in a p21-dependent manner to inhibit bladder cancer cell growth as a tumor suppressor (178). Since tumor cell proliferation is affected by acetylation modifications, drugs targeting acetylation can be used to treat abnormal tumor growth. For example, Rg3 extracted from ginsenosides has antiproliferative activity against melanoma by reducing HDAC3 and increasing p53 acetylation *in vitro* and *in vivo* (179). Therefore, Rg3 may serve as a potential therapeutic agent for the treatment of melanoma (179). Therapeutic

modalities targeting acetyltransferases and deacetylases are also a potentially effective tumor treatment modality.

Role of acetylation in migration and invasion

The development of tumor is divided into multiple stages. In the early stage, the primary lesion proliferates indefinitely, and after the formation of an obvious primary lesion, the function of the organ in which it is located is affected (2). Although the primary tumor is extremely malignant, the cause of death in most patients is the abnormal growth of metastatic tumors in sites other than the primary tumor (180). The reasons for these metastases are also unresolved and need to be discovered and solved urgently. Studies have found that protein acetylation is one of the important factors affecting tumor cell metastasis (6). For example, isocitrate dehydrogenase 1 (IDH1) is hyperacetylated in CRC primary tumors and liver metastases (181), sirtuin-2 is the deacetylase of IDH1, and SIRT2 overexpression significantly inhibits CRC cell proliferation, migration and invasion (181). COL6A1 is dysregulated in several human malignancies, and upregulation of H3K27 acetylation-activated COL6A1 promotes cell migration and invasion by inhibiting the STAT1 pathway in OS cells and promotes osteosarcoma lung metastasis (182). ZMYND8 acetylation of P300 at residues K1007 and K1034 is required for HIF activation and breast cancer progression and metastasis (183). TGF- β -activated kinase 1 (TAK1) stimulates phosphorylation by TGF- β and then induces acetylation of tubulin through α TAT1 activation, which subsequently activates AB cell migration and invasion (184). AFP acetylation promotes its oncogenic effects by blocking binding to the phosphatase PTEN and the pro-apoptotic protein caspase-3, thereby increasing signaling of proliferation, migration and invasion and reducing apoptosis (185). In HCC cells, hepatitis B virus X protein (HBx) and palmitic acid (PA) increased the levels of acetylated AFP by disrupting SIRT1-mediated deacetylation (185). AFP acetylation plays an important role in hepatocellular carcinoma progression (185). miR-15a-5p reduces histone H4 acetylation by inhibiting ACSS2 expression, inhibiting acetyl-CoA activity (186). miR-15a-5p inhibits lipid metabolism by inhibiting ACSS2-mediated acetyl-CoA activity and histone acetylation, thereby inhibiting a novel mechanism of lung cancer cell metastasis (186). In addition to histone acetylation affecting tumor cell invasion and migration, non-histone acetylation also affects tumor metastasis. For example, elevated levels of alpha-tubulin acetylation are sufficient reasons for the metastatic potential of breast cancer (187). Metastatic breast cancer cells exhibit high levels of alpha-tubulin acetylation, extending along

microantenna (McTN) protrusions (187). Mutation of acetylation sites on α -tubulin and enzymatic regulation of this post-translational modification had a dramatic effect on McTN frequency and reattachment of suspended tumor cells (187). Reducing alpha-tubulin acetylation significantly inhibited migration but not proliferation (187). Targeting protein acetylation to affect tumor invasion and migration may serve as a potentially effective therapeutic strategy.

Acetylation system-based targeted drugs in cancer

Research on abnormal protein acetylation in cancer mainly focuses on the mechanism of tumorigenesis, identification and prediction of new biomarkers for tumor invasion and migration, and tumor therapy. Since the process of protein acetylation is reversible, treating tumors can restore the acetylation process to normal levels for treatment. Therefore, some inhibitors of protein acetylation have also been approved for clinical treatment (59). For example, HAT inhibitors, HDAC inhibitors, HAT activators, and HDAC activators (59, 188, 189). HDAC activators are currently less studied.

Epigenetic regulation is an extremely promising strategy for the treatment of tumors, so many HAT- and HDAC-related modulatory drugs have been clinically tested (190). A research of NEO2734 in clinical trial revealed that there is an ongoing clinical trial. NEO2734 is a dual BET and CBP/p300 inhibitor targeting patients with advanced solid tumors and is in phase I clinical trials. Curcumin, a natural product-derived epigenetic modulator, the effect of curcumin on HDAC activity is variable and likely cell-line specific (190). Multiple clinical trials of curcumin have been completed, and other clinical trials are ongoing.

HDAC is considered to be a potential next-generation tumor therapy because HDAC inhibitors have been shown to have significant efficacy in a variety of tumor treatments (191, 192). Among them, vorinostat, romidepsin, panobinostat and belinostat have been approved by the US FDA for cancer treatment and are used in peripheral T-cell lymphoma, cutaneous T-cell lymphoma, and multiple myeloma (191, 192).

Vorinostat has been shown to be effective in the treatment of cutaneous T-cell lymphoma and is already in clinical use (192). Romidepsin regulates the expression of the immune checkpoint ligand PD-L1, and suppresses cellular immune function in colon cancer (193). Romidepsin has antitumor effects on several types of solid tumors (193). Romidepsin is used in clinical treatment of T-cell lymphoma (194). The safety and activity of panobinostat in relapsed/refractory Hodgkin lymphoma was also demonstrated in a multicenter phase II trial, and showed a significant reduction in tumor size (195). Belinostat has been found to be effective and well tolerated in patients with

peripheral T-cell lymphoma (PTCL) or cutaneous T-cell lymphoma (CTCL) (196). Abexinostat is an extremely promising new HDAC inhibitor. Clinical trials have been carried out simultaneously in the United States and China. The main indications include hematological tumors (197, 198), metastatic sarcoma (199), breast cancer (200). There are also a number of drugs in clinical trials. Trichostatin A, for example, is in phase I clinical trials and is being tested in the clinic for tolerability in relapsed or refractory hematological malignancies. Ricolinostat is in phase II clinical trials for the treatment of multiple myeloma. The clinical development of HDAC inhibitors illustrates an extremely promising avenue for the treatment of tumors through epigenetic modulation.

HAT inhibitors

HAT is one of the important targets of tumor therapy. HAT inhibitors are inhibitors of protein acetyltransferase, which can inhibit its activity and reduce the level of protein acetylation. Three types of HAT inhibitors have been reported, dual substrate inhibitors, natural compounds and synthetic compounds (201). HAT inhibitors are widely used in tumor treatment. Currently, the main researches are drug inhibitors targeting CBP/P300 and small molecule inhibitors of HAT domain (201) (Table 3).

Anacardiic acid, a natural compound extracted from natural plants, is a p300/CBP histone acetyltransferase inhibitor, significantly reduces the viability of PTEN^{-/-} cells not in PTEN^{+/+} cells by inducing apoptosis (209). Delphinoside induces p53-mediated apoptosis in human prostate cancer LNCaP cells by inhibiting HDAC activity and activating p53 acetylation (211). Therefore, delphinidin may have a role in the prevention of prostate cancer (211). There are also synthetic compounds acting on HAT, targeting HAT as inhibitors to regulate intracellular acetylation homeostasis (210). A-485 competes with acetyl-CoA. A-485 selectively inhibits proliferation of lineage-specific tumor types, including several hematological malignancies and androgen receptor-positive prostate cancer (202). WM-3835 is a potent and highly specific HBO1 (KAT7 or MYST2) inhibitor that directly binds to the acetyl-CoA binding site of HBO1 33 WM-3835 activates apoptosis while inhibiting osteosarcoma (OS) cells proliferation, migration and invasion (216). WM-3835 has antitumor activity and potently inhibits the growth of osteosarcoma xenografts in mice (216). TH1834 dihydrochloride is a specific Tip60 (KAT5) histone acetyltransferase inhibitor (215). TH1834 dihydrochloride induces apoptosis and increases DNA damage in breast cancer cells. TH1834 dihydrochloride does not affect the activity of the related histone acetyltransferase MOF. Anticancer activity (215). Combination therapy of CK1 inhibitor SR3029 and Tip60 inhibitor MG149 had stronger

TABLE 3 Classification and targets of HAT inhibitors in cancers.

Class	Drug	Targets	Cancer	references
dual substrate inhibitor	A-485	P300/CBP	Prostate cancer, Growth hormone pituitary adenoma, Human melanoma	(202–204)
	PU139	GCN5 P300 PCAF CBP	Neuroblastoma	(205)
	NEO2734	P300/CBP	Prostate cancer, Acute myeloid leukemia, Multiple myeloma	(206–208)
Natural compounds	Anacardic acid	P300 PCAF	Breast cancer	(209)
	Garcinol	PCAF	Colon cancer, Breast cancer, Prostate cancer, Head and neck cancer, Hepatocellular carcinoma	(210)
	Curcumin	P300/CBP		
	Delphinidin	P300/CBP	prostate cancer	(211)
synthetic compounds	C646	P300	Pancreatic cancer	(212)
	Acetaminophen	NAT2		
	WM-1119	KAT6A	Lymphoma	(213)
	Remodelin hydrobromide	NAT10		
	MG 149	Tip60	Colon cancer	(214)
	TH1834 dihydrochloride	Tip60	Breast cancer	(215)
	PF-9363	KAT6A/KAT6B		
	WM-3835	KAT7/MYST2	Osteosarcoma	(216)

inhibitory effects on β -catenin acetylation, transcription of Wnt target genes, and viability and proliferation of colon cancer cells (214). Transcriptional activity of β -catenin can be regulated through the CK1 δ /e- β -catenin-Tip60 axis, which may be a potential therapeutic target for colon cancer (214).

HAT activators

HAT activators are activators that act on protein acetyltransferases and can activate acetyltransferases to increase the level of protein acetylation. For example, CTB can induce acetylation of P53 protein by increasing the expression of P300, thereby inducing significant cell death in MCF-7, but it may be well tolerated in MRC-5 (217). Therefore, CTB can be applied in cancer treatment (217). The research on HAT activators is not very extensive, and most of them are activators targeting the CBP/P300 complex (217) (Table 4).

HDAC inhibitor

HDACs are found to be abnormally expressed in malignant tumors (219). The expression of HDACs is closely related to

clinical treatment prognosis and tumor occurrence and development. In liver cancer, inhibition of HDAC2 expression can promote histone acetylation in the promoter region of MIR22HG, thereby upregulating the expression of MIR22HG, promoting the production of miR-22-5p, and ultimately increasing the sensitivity to radiotherapy (64). In acute B lymphocytic leukemia, inhibits the activity of HDAC3, which enhances the sensitivity of acute B lymphocytic leukemia cells to drugs by inhibiting the JAK/signal transducer and activator of transcription 3 signaling pathway (220). Inhibition of HDAC8 activity causes cytotoxic effects, cell cycle arrest in human monocytic leukemia followed by apoptosis, and cytostatic effects in p53-deficient human myelocytic leukemia cells (73). SIRT1/2 inhibition results in HSPA5 acetylation and dissociation from EIF2AK3, leading to endoplasmic reticulum stress response, which in turn upregulates ATF4 and dit4, triggering autophagy (86). Sirtuins have become a promising target for a novel class of anti-cancer drugs. HDAC inhibitor can reverse this phenomenon and reactivate the expression of tumor suppressors, and HDAC inhibitor can act on histone acetylation and non-histone acetylation to inhibit tumor growth, invasion and metastasis, and has become a clinically effective anti-tumor drug (221) (Table 5).

TABLE 4 Targets of HAT activators and associated cancers.

Drug	Targets	Cancer	References
CTB	P300	Breast cancer	(217)
TTK21	CBP/P300		
CTPB	P300		
I-CBP112	CBP/p300	Leukemia	(218)
YF-2	CBP PCAF GCN5		

Studies have shown that HDAC inhibitor has a significant inhibitory effect on P53, HSP90, NF- κ B factors and multiple dephosphorylation enzymes, and a variety of HDAC inhibitors have been developed (59). The FDA has developed and approved several HDAC inhibitors for clinical cancer treatment. HDAC inhibitors are mainly divided into five categories according to different structures, including short-chain fatty acids, amides, hydroxamic acids, cyclic peptides, and chemical substances extracted from plants (265). Among histone deacetylase inhibitors, fatty acids are one of the less commonly used inhibitors. Valproic acid is an anticonvulsant drug that has been used clinically in bipolar disorder (266). The study found that valproic acid can also inhibit histone deacetylase 9, affect Notch cell signaling, and inhibit the activity of human neuroblastoma cells (267). The HDAC inhibitor of the benzamide class is the first inhibitor that selectively targets class I HDACs. There are also a large number of benzamide drugs in clinical trials for tumor treatment (59). The enzyme kinetics study of aminobenzamide-based HDAC inhibitors shows that the aminobenzamide motif has a tight binding mechanism (slow start/slow shutdown) unlike the classical fast-on/fast-off kinetics of hydroxamic acid-based HDAC inhibitors (268).

Hydroxamic acid HDAC inhibitors are the first class of HDAC inhibitors to be developed (59). Vorinostat is the first HDAC inhibitor on the market. At appropriate concentrations, vorinostat can inhibit HDAC1, 2, 3, 6, inhibit the activity of HDAC, and lead to significant hyperacetylation of H4 at residues lysine 5, 8, 12, 1, and 6 (269). These hyperacetylation are closely related to transcriptional changes, and vorinostat can simultaneously increase or decrease the transcription of specific genes in tumor cells, suggesting that HDAC inhibitor can have completely opposite effects throughout the genome (265). Vorinostat is currently approved for the treatment of cutaneous T-cell lymphoma (CTCL). Studies have shown that vorinostat has activity in the treatment of recurrent glioblastoma multiforme (270). Clinically, it can be used in combination with other drugs to treat tumors (270). Vorinostat is clinically used in combination with gefitinib in the treatment of lung cancer to enhance the induction of apoptosis of lung cancer cells (271). Panobinostat is involved in many biological processes, including

DNA replication and repair, chromatin remodeling, gene transcription, cell cycle progression, protein degradation and cytoskeleton reorganization (226). For example, in prostate cancer, Panobinostat reverses HepaCAM gene expression and inhibits proliferation by increasing histone acetylation (226). Panobinostat can also be used in combination with other drugs to improve treatment efficiency, such as in acute myeloid leukemia, studies have shown that the combination of panobinostat differentiation and arsenic trioxide apoptosis can significantly improve survival (272). Another HDAC inhibitor is SIRT inhibitor, inhibition of SIRT1 and SIRT2 induces cancer cell apoptosis and plays multiple roles in regulating autophagy (86). Salermide in NSCLC cells, inhibiting SIRT1 and 2 by acetylating HSPA5, and then activating ATF4 and dit4 to inhibit the mTOR signaling pathway, thereby inducing pro-survival autophagy (86). Ginsenoside Rg1 inhibits cell proliferation and induces cellular senescence in acute myeloid leukemia cells CD34+CD38- leukemia stem cells by activating Sirtuin 1 (SIRT1)/tuberous sclerosis complex 2 (TSC2) signaling pathway (273). Capsaicin attenuates cell migration by enhancing corticosteroid and -catenin acetylation in bladder cancer cells through SIRT1 targeting and inhibition (274). Capsaicin-reduced cell migration is associated with downregulation of sirtuin 1 (SIRT1) deacetylase, possibly through proteasome-mediated protein degradation (274). Combination therapy of SIRT1/2 inhibitor and drug autophagy inhibitor is an effective therapeutic strategy (86). Some studies have found that synthetic HDAC inhibitors may have toxic side effects such as atrial fibrillation, researchers turned their attention to natural inhibitors extracted from plants (59). Plant-derived inhibitors also showed good activity in inhibiting tumors. For example, hawthorn polyphenol extract (HPE) can significantly reduce ROS levels, apoptosis and inflammation-related factor expression in cells, and also inhibit AMPK/SIRT1/NF- κ B and miR-34a/SIRT1/p53 pathways by regulating acetylation (275). Pathway is involved in hyperglycemia-induced inflammation and apoptosis of human retinal epithelial cells (275). These inhibitors can significantly inhibit tumor proliferation, migration and invasion, and can induce apoptosis and induce autophagy (59). However, the application of these inhibitor drugs in clinical practice requires more in-depth research.

TABLE 5 Classification and targets of sirtuins in cancers.

Class	Drug	Targets	Cancer	Reference	
Hydroxamates	Vorinostat	HDACs 1, 2, 3, 6	CTCL, BCR-ABL-negative myeloproliferative neoplasms, Triple-negative breast cancer, Melanoma	(222–225)	
	Panobinostat	HDACs	Multiple myeloma, Prostate cancer, Acute myelogenous leukemia	(226, 227)	
	Trichostatin A (TSA)	HDACs 7, 8	Esophageal squamous, Cholangiocarcinoma, Cholangiocarcinoma, Osteosarcoma	(228–231)	
	Belinostat	HDACs	PTCL, Pancreatic cancer, Lung squamous cell carcinoma, Breast cancer	(232–235)	
	Dacinostat (LAQ824)		Medulloblastoma, Malignant Melanoma	(236, 237)	
	Givinostat	HDACs	Chronic myeloproliferative neoplasms, Hematological malignancies	(238, 239)	
	Resminostat	HDACs	Hodgkin’s lymphoma, Hepatocellular carcinoma, Lymphoma	(240, 241)	
	Abexinostat	HDAC 1	Lymphoma, Leukemia, Lymphocytic	(198)	
	Quisinostat	HDACs	Lymphoma, Neoplasms, Myelodysplastic syndromes, Hepatocellular carcinoma, Neuroblastoma, Tongue squamous cell carcinoma	(242–244)	
	CUDC-101	HDACs	Lymphoma, Pancreatic cancer, Liver cancer, Breast cancer, Gastric cancer	(245, 246)	
	CUDC-907	HDACs	Lymphoma, Solid tumors, Breast cancer, Multiple myeloma, NUT midline carcinoma	(247, 248)	
	Short-chain fatty acids	MPT0E028	HDACS 1, 2, 6		
		CHR-3996	HDACs		
LMK235		HDACs 4, 5			
Valproic acid (VPA)		HDACs 2, 9	Acute myeloid leukemia Cholangiocarcinoma	(229, 249)	
Phenylbutyrate		HDACs 1-11	Oral squamous cell carcinoma	(250, 251)	
Pivanex (AN-9)		HDACs	Lung cancer, Liver cancer	(252)	
AR-42		HDACs	Acoustic neuroma, Testicular lymphoma, Intraocular lymphoma, Esophageal squamous cell carcinoma, Adult T-cell leukemia, Lymphoma osteolytic bone tumors, Vestibular schwannoma	(253, 254)	
Cyclic tetrapeptide	Romidepsin (Depsipeptide/FK228)	HDACs 1, 2, 4, 6	CTCL	(255)	

(Continued)

TABLE 5 Continued

Class	Drug	Targets	Cancer	Reference
Benzamides	Mocetinostat (MGCD0103)	HDACs 1, 2, 3	Lymphoma, Urothelial carcinoma, Relapsed and refractory, Myelodysplastic syndrome, Metastatic leiomyosarcoma	(256)
	Entinostat (MS-275)	HDACs	Breast cancer, NCSLC, Osteosarcoma, Ovarian cancer, Hematologic malignancies, Oral squamous cell carcinoma	(257–262)
	Tacedinaline (CI-994)		Lung cancer, Multiple myeloma	
	Chidamide	HDAC 1, 2, 3, 10	T-cell lymphoma	(263)
	Ricolinostat (ACY-1215)	HDAC 6	Multiple myeloma	(264)

BET inhibitor

As a scaffold protein, BET can read epigenetic code, recognize histone acetylation or non-histone acetylation, and regulate gene expression, and play an important role in cell function (115). However, abnormal expression of BET leads to abnormal gene expression, resulting in abnormal cell function, which is related to the development of many malignant diseases. The study found that the abnormal expression of BRD4 is related to glioma, and the expression in glioma is significantly higher than that in normal tissue (130); BRD4 inhibitors effectively penetrated the blood-brain barrier and targeted glioma tumor tissue, but had little effect on normal brain tissue (130). Therefore, BRD4 is a target for the treatment of glioma (130). Targeting BET protein therapy is a very promising tumor treatment strategy. The BET-bromodomain-specific inhibitors JQ1, I-BET and I-BET151 represent initial successes in the development of BET inhibitors (276). The small molecule BET inhibitor drug, JQ1, is a potent growth inhibitor for many cancers and holds promise for cancer therapy (276). However, studies have found that JQ1 can activate other oncogenic pathways and may affect epithelial-to-mesenchymal transition (EMT) (276). That is to say, JQ1 has an unexpected role in promoting prostate cancer invasion (276). In the application of tumor treatment, attention should be paid to the possible toxic and side effects of JQ1. BET inhibitor treatment in HCC cell lines reduces cell migration by downregulating SMARCA4 (277). GS-5829 inhibits CLL cell proliferation and induces leukemia cell apoptosis by deregulating key signaling pathways such as BLK, AKT, ERK1/2, and MYC (278). BRD2 supports borderline activity and raises the possibility that pharmacological BET inhibitors may partially affect gene expression by interfering with regional borderline function (279). Disruption of negative autoregulation by BET inhibitor (BETi) leads to a marked increase in BCL6 transcription, which further activates the

mTOR signaling pathway by inhibiting tumor suppressor death-associated protein kinase 2 (123).

The effectiveness of BET-specific targeted inhibitors is often affected by tumor drug resistance (280). There is also an urgent need to address the issue of BET inhibitor resistance. Prostate cancer-associated SPOP mutations confer resistance to BET inhibitors by stabilizing BRD4 (281). Tumor-suppressive effects of SPOP in prostate cancer, where it acts as a negative regulator of BET protein stability, and also provides a molecular mechanism for resistance to BET inhibitors in individuals with prostate cancer carrying SPOP mutations (281). Prostate cancer-associated SPOP mutants display impaired binding to BET proteins, leading to reduced proteasomal degradation and accumulation of the protein in prostate cancer cell lines and patient specimens, and causing resistance to BET inhibitors (282). Transcriptomic and BRD4 enzymatic analysis revealed enhanced expression of GTPase RAC1 and cholesterol biosynthesis-related genes, and activation of AKT-mTORC1 signaling due to BRD4 stabilization (282). Resistance to BET inhibitors in SPOP-mutant prostate cancer can be overcome by combination with AKT inhibitors and further supports the evaluation of SPOP mutations as biomarkers to guide BET inhibitor-directed therapy in prostate cancer patients (282).

Although research on BET inhibitors is still a research focus, the combination use of BET inhibitors with other drugs is also being explored. BET inhibitors can be used in combination with other types of inhibitors in order to promote the therapeutic effect or reduce adverse reactions (283). For example, the combination of BET inhibitor I-BET762 and PARP inhibitor Talazoparib Synergy is used in the treatment of SCLC and has a synergistic effect (283). At the same time, a strategy of combined application of HDAC inhibitor and JQ1 inhibitor has shown good efficacy in the treatment of AML (284). Based on the combination drug strategy, dual-target inhibitors of HDAC and BET are also being developed, and have shown more significant

efficacy than single-target inhibitors in the treatment of pancreatic cancer (285). This multi-targeted drug can ensure the efficacy and durability of the anti-cancer effect, and this combination approach also reduces the possibility of tumor resistance (285). This provides a new scope of research for BET inhibitors in the treatment of tumors. BET and HDAC inhibitors are synergistic at reduced doses, suggesting a potential approach to avoid overlapping toxicities of the two drug classes (280). The combination of CPI-0610 with a PRAP inhibitor has been found to better address PRAP inhibitor resistance in ovarian cancer patients (286). It also proposes new therapeutic strategies to address PARP inhibitor resistance using drugs already approved or in clinical development that have the potential to rapidly transform and benefit a broad range of ovarian cancer patients (286) (Table 6).

Future perspectives

Tumor is currently the most troublesome problem in human life and seriously affects human health. The development of tumors is affected by many factors, including genetic factors and epigenetic factors (6). The development of tumor is the result of the joint

influence of many factors (6). Protein acetylation is at the junction of genetics, epigenetics and tumor microenvironment (9). Protein acetylation is affected by many aspects to promote the occurrence and development of tumors (9). For example, protein acetylation writer, eraser, and reader may be abnormally expressed (7). Regulatory factor or regulatory factors aberrantly promote tumorigenesis and are associated with multiple malignant phenotypes of tumors. The study of protein acetylation provides a deeper understanding of tumor-related mechanisms, facilitates the discovery of potentially effective biomarkers and therapeutic targets, and facilitates the discovery and application of therapeutic drugs (11). At the same time, it is beneficial to solve the drug resistance and recurrence of tumors. At the same time, we also emphasize the strengthening of these studies on protein acetylation in different cancers, combined with PPPM in clinical practice for the treatment of malignant tumors (301).

Conclusions

This review summarized current studies about the role of protein acetylation in tumors and related targeted therapy drugs, including the classification of protein acetylation, related regulators of protein acetylation, the pathological role of protein acetylation in tumors, and targeted proteins acetylated drugs. Protein acetylation affects various physiological functions of tumors and is therefore associated with tumor development and progression. Protein acetylation plays an important role in the link between cancer pathology and post-translational modifications. Therefore, protein acetylation plays an important role in tumor therapy. Drugs about protein acetylation have been extensively studied. Drugs targeting protein acetylation have promising applications in tumor therapy, and combined use with other pathway drugs is a potential therapeutic strategy.

Author contributions

JY collected and analyzed literature, and wrote the manuscript. CS participated in partial literature analysis. XZ conceived the concept, designed the manuscript, coordinated and critically revised manuscript, and was responsible for its financial supports and the corresponding works. All authors contributed to the article and approved the submitted version.

Acknowledgments

The authors acknowledge the financial supports from the Shandong First Medical University Talent Introduction Funds (to XZ), Shandong First Medical University High-level Scientific Research Achievement Cultivation Funding Program (to XZ), the Shandong Provincial Natural Science Foundation (ZR202103020356/

TABLE 6 Targets of BET inhibitors and related cancers.

Name	Targets	Cancer	References
Molibresib	BRD2, BRD3, BRD4	Hematological malignancies	(287)
ARV-771			
HJB97			
Birabresib	BRD2, BRD3, BRD4	Solid tumor	(288)
MS436	BRD4		
BRD4 D1-IN-2	BRD4		
AGB1			
JQ1		Prostate cancer, Retinoblastoma, Ovarian cancer	(276, 289, 290)
I-BET762		SCLC, Pancreatic ductal adenocarcinoma, Hepatocellular carcinoma	(283, 291, 292)
I-BET151	BRD4	Ovarian cancer, Multiple myeloma, MLL-fusion leukemia,	(133, 293, 294)
CPI-0610		Multiple myeloma, Ovarian cancer	(286, 295)
PFI-1		Prostate cancer	(296)
I-BET726		Human skin squamous cell carcinoma, Neuroblastoma	(297, 298)
ABBV-744		Acute myeloid leukemia, Prostate cancer	(299, 300)

ZR2021MH156 to XZ), and the Academic Promotion Program of Shandong First Medical University (2019ZL002).

Conflict of interest

The authors declare that the research was conducted in the absence of any commercial or financial relationships that could be construed as a potential conflict of interest.

References

- Gerlinger M, Rowan AJ, Horswell S, Math M, Larkin J, Endesfelder D, et al. Intratumor heterogeneity and branched evolution revealed by multiregion sequencing. *N Engl J Med* (2012) 366(10):883–92. doi: 10.1056/NEJMoa1113205
- Hanahan D. Hallmarks of cancer: New dimensions. *Cancer Discovery* (2022) 12(1):31–46. doi: 10.1158/2159-8290.CD-21-1059
- Dawson MA, Kouzarides T. Cancer epigenetics: from mechanism to therapy. *Cell* (2012) 150(1):12–27. doi: 10.1016/j.cell.2012.06.013
- Verdin E, Ott M. 50 years of protein acetylation: from gene regulation to epigenetics, metabolism and beyond. *Nat Rev Mol Cell Biol* (2015) 16(4):258–64. doi: 10.1038/nrm3931
- Phillips DM. The presence of acetyl groups of histones. *Biochem J* (1963) 87:258–63. doi: 10.1042/bj0870258
- Audia JE, Campbell RM. Histone modifications and cancer. *Cold Spring Harb Perspect Biol* (2016) 8(4):a019521. doi: 10.1101/cshperspect.a019521
- Narita T, Weinert BT, Choudhary C. Functions and mechanisms of non-histone protein acetylation. *Nat Rev Mol Cell Biol* (2019) 20(3):156–74. doi: 10.1038/s41580-018-0081-3
- Hu M, He F, Thompson EW, Ostrikov KK, Dai X. Lysine acetylation, cancer hallmarks and emerging onco-therapeutic opportunities. *Cancers (Basel)* (2022) 14(2):346. doi: 10.3390/cancers14020346
- Harachi M, Masui K, Cavenee WK, Mischel PS, Shibata N. Protein acetylation at the interface of genetics, epigenetics and environment in cancer. *Metabolites* (2021) 11(4):216. doi: 10.3390/metabo11040216
- Zhao S, Xu W, Jiang W, Yu W, Lin Y, Zhang T, et al. Regulation of cellular metabolism by protein lysine acetylation. *Science* (2010) 327(5968):1000–4. doi: 10.1126/science.1179689
- Wen S, Li J, Yang J, Li B, Li N, Zhan X. Quantitative acetyloomics revealed acetylation-mediated molecular pathway network changes in human nonfunctional pituitary neuroendocrine tumors. *Front Endocrinol (Lausanne)* (2021) 12:753606. doi: 10.3389/fendo.2021.753606
- Albaugh BN, Arnold KM, Denu JM. KAT(ching) metabolism by the tail: insight into the links between lysine acetyltransferases and metabolism. *Inchibiochem Eur J Chem Biol* (2011) 12(2):290–8. doi: 10.1002/cbic.201000438
- Yang H, Pinello CE, Luo J, Li D, Wang Y, Zhao LY, et al. Small-molecule inhibitors of acetyltransferase p300 identified by high-throughput screening are potent anticancer agents. *Mol Cancer Ther* (2013) 12(5):610–20. doi: 10.1158/1535-7163.MCT-12-0930
- Li T, Zhang C, Hassan S, Liu X, Song F, Chen K, et al. Histone deacetylase 6 in cancer. *J Hematol Oncol* (2018) 11(1):111. doi: 10.1186/s13045-018-0654-9
- Deakin NO, Turner CE. Paxillin inhibits HDAC6 to regulate microtubule acetylation, golgi structure, and polarized migration. *J Cell Biol* (2014) 206(3):395–413. doi: 10.1083/jcb.201403039
- Starheim KK, Gevaert K, Arnesen T. Protein n-terminal acetyltransferases: when the start matters. *Trends Biochem Sci* (2012) 37(4):152–61. doi: 10.1016/j.tibs.2012.02.003
- El Kawak M, Dhaini HR, Jabbour ME, Moussa MA, El Asmar K, Aoun M. Slow n-acetylation as a possible contributor to bladder carcinogenesis. *Mol Carcinog* (2020) 59(9):1017–27. doi: 10.1002/mc.23232
- Diallo I, Seve M, Cunin V, Minassian F, Poisson JF, Michelland S, et al. Current trends in protein acetylation analysis. *Expert Rev Proteomics* (2019) 16(2):139–59. doi: 10.1080/14789450.2019.1559061
- Mittal R, Peak-Chew SY, McMahon HT. Acetylation of MEK2 and I kappa b kinase (IKK) activation loop residues by YopJ inhibits signaling. *Proc Natl Acad Sci U.S.A.* (2006) 103(49):18574–9. doi: 10.1073/pnas.0608995103

Publisher's note

All claims expressed in this article are solely those of the authors and do not necessarily represent those of their affiliated organizations, or those of the publisher, the editors and the reviewers. Any product that may be evaluated in this article, or claim that may be made by its manufacturer, is not guaranteed or endorsed by the publisher.

- Kouzarides T. Acetylation: a regulatory modification to rival phosphorylation? *EMBO J* (2000) 19(6):1176–9. doi: 10.1093/emboj/19.6.1176
- Cavdarli S, Schroter L, Albers M, Baumann AM, Vicogne D, Le Doussal JM, et al. Role of sialyl-O-Acetyltransferase CASD1 on GD2 ganglioside O-acetylation in breast cancer cells. *Cells* (2021) 10(6):1468. doi: 10.3390/cells10061468
- Chowdhury S, Chandra S, Mandal C. 9-o-acetylated sialic acids differentiating normal haematopoietic precursors from leukemic stem cells with high aldehyde dehydrogenase activity in children with acute lymphoblastic leukaemia. *Glycoconj J* (2014) 31(6-7):523–35. doi: 10.1007/s10719-014-9550-x
- Choudhary J, Grant SG. Proteomics in postgenomic neuroscience: the end of the beginning. *Nat Neurosci* (2004) 7(5):440–5. doi: 10.1038/nn1240
- Li S, Shi B, Liu X, An HX. Acetylation and deacetylation of DNA repair proteins in cancers. *Front Oncol* (2020) 10:573502. doi: 10.3389/fonc.2020.573502
- Choudhary C, Kumar C, Gnad F, Nielsen ML, Rehman M, Walther TC, et al. Lysine acetylation targets protein complexes and co-regulates major cellular functions. *Science* (2009) 325(5942):834–40. doi: 10.1126/science.1175371
- Eshun-Wilson L, Zhang R, Portran D, Nachury MV, Toso DB, Lohr T, et al. Effects of α -tubulin acetylation on microtubule structure and stability. *Proc Natl Acad Sci USA* (2019) 116(21):10366–71. doi: 10.1073/pnas.1900441116
- Gil J, Ramirez-Torres A, Encarnacion-Guevara S. Lysine acetylation and cancer: a proteomics perspective. *J Proteomics* (2017) 150:297–309. doi: 10.1016/j.jprot.2016.10.003
- Lin H, Su X, He B. Protein lysine acylation and cysteine succinylation by intermediates of energy metabolism. *ACS Chem Biol* (2012) 7(6):947–60. doi: 10.1021/cb3001793
- Sun Y, Jiang X, Chen S, Fernandes N, Price BD. A role for the Tip60 histone acetyltransferase in the acetylation and activation of ATM. *Proc Natl Acad Sci U.S.A.* (2005) 102(37):13182–7. doi: 10.1073/pnas.0504211102
- di Bari MG, Ciuffini L, Mingardi M, Testi R, Soddu S, Barila D. C-abl acetylation by histone acetyltransferases regulates its nuclear-cytoplasmic localization. *EMBO Rep* (2006) 7(7):727–33. doi: 10.1038/sj.embor.7400700
- Fu J, Yoon HG, Qin J, Wong J. Regulation of p-TEFb elongation complex activity by CDK9 acetylation. *Mol Cell Biol* (2007) 27(13):4641–51. doi: 10.1128/MCB.00857-06
- Liu Z, Mai A, Sun J. Lysine acetylation regulates bruton's tyrosine kinase in b cell activation. *J Immunol* (2010) 184(1):244–54. doi: 10.4049/jimmunol.0902324
- Valiuleni G, Vitkeviciene A, Navakauskienė R. The epigenetic treatment remodel genome-wide histone H4 hyper-acetylation patterns and affect signaling pathways in acute promyelocytic leukemia cells. *Eur J Pharmacol* (2020) 889:173641. doi: 10.1016/j.ejphar.2020.173641
- Zhan X, Desiderio DM. Mass spectrometric identification of *in vivo* nitrotyrosine sites in the human pituitary tumor proteome. *Methods Mol Biol* (2009) 566:137–63. doi: 10.1007/978-1-59745-562-6_10
- Sheikh BN, Akhtar A. The many lives of KATs - detectors, integrators and modulators of the cellular environment. *Nat Rev Genet* (2019) 20(1):7–23. doi: 10.1038/s41576-018-0072-4
- Li G, Chen S, Zhang Y, Xu H, Xu D, Wei Z, et al. Matrix stiffness regulates alpha-TAT1-mediated acetylation of alpha-tubulin and promotes silica-induced epithelial-mesenchymal transition via DNA damage. *J Cell Sci* (2021) 134(2):jcs243394. doi: 10.1242/jcs.243394
- Nowosad A, Creff J, Jeannot P, Culerrier R, Codogno P, Manenti S, et al. p27 controls autophagic vesicle trafficking in glucose-deprived cells via the regulation of ATAT1-mediated microtubule acetylation. *Cell Death Dis* (2021) 12(5):481. doi: 10.1038/s41419-021-03759-9

38. Zhou C, Liu W, Duan Y. MOZ/KAT6A: a promising target for acute myeloid leukemia therapy. *Future Med Chem* (2020) 12(9):759–61. doi: 10.4155/fmc-2020-0047
39. Domingues AF, Kulkarni R, Giotopoulos G, Gupta S, Vinnenberg L, Arede L, et al. Loss of Kat2a enhances transcriptional noise and depletes acute myeloid leukemia stem-like cells. *Elife* (2020) 9:e51754. doi: 10.7554/eLife.51754
40. Waddell A, Mahmud I, Ding H, Huo Z, Liao D. Pharmacological inhibition of CBP/p300 blocks estrogen receptor alpha (ERalpha) function through suppressing enhancer H3K27 acetylation in luminal breast cancer. *Cancers (Basel)* (2021) 13(11):2799. doi: 10.3390/cancers13112799
41. Butler JS, Koutelou E, Schibler AC, Dent SY. Histone-modifying enzymes: regulators of developmental decisions and drivers of human disease. *Epigenomics* (2012) 4(2):163–77. doi: 10.2217/epi.12.3
42. Liang Z, Yu Q, Ji H, Tian D. Tip60-siRNA regulates ABCE1 acetylation to suppress lung cancer growth via activation of the apoptotic signaling pathway. *Exp Ther Med* (2019) 17(4):3195–202. doi: 10.3892/etm.2019.7302
43. Kuo HP, Lee DF, Chen CT, Liu M, Chou CK, Lee HJ, et al. ARD1 stabilization of TSC2 suppresses tumorigenesis through the mTOR signaling pathway. *Sci Signal* (2010) 3(108):ra9. doi: 10.1126/scisignal.2000590
44. Shin DH, Chun YS, Lee KH, Shin HW, Park JW. Arrest defective-1 controls tumor cell behavior by acetylating myosin light chain kinase. *PLoS One* (2009) 4(10):e7451. doi: 10.1371/journal.pone.0007451
45. Zhu HE, Li T, Shi S, Chen DX, Chen W, Chen H. ESCO2 promotes lung adenocarcinoma progression by regulating hnRNP1 acetylation. *J Exp Clin Cancer Res* (2021) 40(1):64. doi: 10.1186/s13046-021-01858-1
46. Di Martile M, Del Bufalo D, Trisciuglio D. The multifaceted role of lysine acetylation in cancer: prognostic biomarker and therapeutic target. *Oncotarget* (2016) 7(34):55789–810. doi: 10.18632/oncotarget.10048
47. Pavlou D, Kirmizis A. Depletion of histone n-terminal-acetyltransferase Naa40 induces p53-independent apoptosis in colorectal cancer cells via the mitochondrial pathway. *Apoptosis* (2016) 21(3):298–311. doi: 10.1007/s10495-015-1207-0
48. Dang F, Jiang C, Zhang T, Inuzuka H, Wei W. PCAF and SIRT1 modulate betaTrCP1 protein stability in an acetylation-dependent manner. *J Genet Genomics* (2021) 48(7):652–5. doi: 10.1016/j.jgg.2021.07.004
49. Ladang A, Rapino F, Heukamp LC, Tharun L, Shostak K, Hermand D, et al. Eip3 drives wnt-dependent tumor initiation and regeneration in the intestine. *J Exp Med* (2015) 212(12):2057–75. doi: 10.1084/jem.20142288
50. Mak AB, Pehar M, Nixon AM, Williams RA, Utrecht AC, Puglielli L, et al. Post-translational regulation of CD133 by ATase1/ATase2-mediated lysine acetylation. *J Mol Biol* (2014) 426(11):2175–82. doi: 10.1016/j.jmb.2014.02.012
51. Hogg SJ, Motorna O, Cluse LA, Johanson TM, Coughlan HD, Raviram R, et al. Targeting histone acetylation dynamics and oncogenic transcription by catalytic P300/CBP inhibition. *Mol Cell* (2021) 81(10):2183–200.e13. doi: 10.1016/j.molcel.2021.04.015
52. Seto E, Yoshida M. Erasers of histone acetylation: the histone deacetylase enzymes. *Cold Spring Harb Perspect Biol* (2014) 6(4):a018713. doi: 10.1101/cshperspect.a018713
53. Moore SD, Herrick SR, Ince TA, Kleinman MS, Dal Cin P, Morton CC, et al. Uterine leiomyomata with t(10;17) disrupt the histone acetyltransferase MORF. *Cancer Res* (2004) 64(16):5570–7. doi: 10.1158/0008-5472.CAN-04-0050
54. Lan R, Wang Q. Deciphering structure, function and mechanism of lysine acetyltransferase HBO1 in protein acetylation, transcription regulation, DNA replication and its oncogenic properties in cancer. *Cell Mol Life Sci* (2020) 77(4):637–49. doi: 10.1007/s00018-019-03296-x
55. Dong Z, Zou J, Li J, Pang Y, Liu Y, Deng C, et al. MYST1/KAT8 contributes to tumor progression by activating EGFR signaling in glioblastoma cells. *Cancer Med* (2019) 8(18):7793–808. doi: 10.1002/cam4.2639
56. Kawasumi R, Abe T, Arakawa H, Garre M, Hirota K, Branzei D. ESCO1/2's roles in chromosome structure and interphase chromatin organization. *Genes Dev* (2017) 31(21):2136–50. doi: 10.1101/gad.306084.117
57. Houtkooper RH, Pirinen E, Auwerx J. Sirtuins as regulators of metabolism and healthspan. *Nat Rev Mol Cell Biol* (2012) 13(4):225–38. doi: 10.1038/nrm3293
58. Wang P, Wang Z, Liu J. Role of HDACs in normal and malignant hematopoiesis. *Mol Cancer* (2020) 19(1):5. doi: 10.1186/s12943-019-1127-7
59. McClure JJ, Li X, Chou CJ. Advances and challenges of HDAC inhibitors in cancer therapeutics. *Adv Cancer Res* (2018) 138:183–211. doi: 10.1016/bs.acr.2018.02.006
60. Falkenberg KJ, Johnstone RW. Histone deacetylases and their inhibitors in cancer, neurological diseases and immune disorders. *Nat Rev Drug Discov* (2014) 13(9):673–91. doi: 10.1038/nrd4360
61. Richter LE, Wang Y, Becker ME, Coburn RA, Williams JT, Amador C, et al. HDAC1 is a required cofactor of CBFbeta-SMMHC and a potential therapeutic target in inversion 16 acute myeloid leukemia. *Mol Cancer Res* (2019) 17(6):1241–52. doi: 10.1158/1541-7786.MCR-18-0922
62. Bandyopadhyay D, Mishra A, Medrano EE. Overexpression of histone deacetylase 1 confers resistance to sodium butyrate-mediated apoptosis in melanoma cells through a p53-mediated pathway. *Cancer Res* (2004) 64(21):7706–10. doi: 10.1158/0008-5472.CAN-03-3897
63. Song Y, Jiang Y, Tao D, Wang Z, Wang R, Wang M, et al. NFAT2-HDAC1 signaling contributes to the malignant phenotype of glioblastoma. *Neuro Oncol* (2020) 22(1):46–57. doi: 10.1093/neuonc/noz136
64. Jin Q, Hu H, Yan S, Jin L, Pan Y, Li X, et al. lncRNA MIR22HG-derived miR-22-5p enhances the radiosensitivity of hepatocellular carcinoma by increasing histone acetylation through the inhibition of HDAC2 activity. *Front Oncol* (2021) 11:572585. doi: 10.3389/fonc.2021.572585
65. Gediya P, Parikh PK, Vyas VK, Ghate MD. Histone deacetylase 2: A potential therapeutic target for cancer and neurodegenerative disorders. *Eur J Medicinal Chem* (2021) 216:113332. doi: 10.1016/j.ejmech.2021.113332
66. Chen Z, Huo D, Li L, Liu Z, Li Z, Xu S, et al. Nuclear DEK preserves hematopoietic stem cells potential via NCoR1/HDAC3-Akt1/2-mTOR axis. *J Exp Med* (2021) 218(5):e20201974. doi: 10.1084/jem.20201974
67. Adhikari N, Amin SA, Trivedi P, Jha T, Ghosh B. HDAC3 is a potential validated target for cancer: An overview on the benzamide-based selective HDAC3 inhibitors through comparative SAR/QSAR/QAAR approaches. *Eur J Medicinal Chem* (2018) 157:1127–42. doi: 10.1016/j.ejmech.2018.08.081
68. Zhang L, Chen Y, Jiang Q, Song W, Zhang L. Therapeutic potential of selective histone deacetylase 3 inhibition. *Eur J Medicinal Chem* (2019) 162:534–42. doi: 10.1016/j.ejmech.2018.10.072
69. Sarkar R, Banerjee S, Amin SA, Adhikari N, Jha T. Histone deacetylase 3 (HDAC3) inhibitors as anticancer agents: A review. *Eur J Medicinal Chem* (2020) 192:112171. doi: 10.1016/j.ejmech.2020.112171
70. Tong L, Liang H, Zhuang H, Liu C, Zhang Z. The relationship between HDAC3 and malignant tumors: A mini review. *Crit Rev Eukaryot Gene Expr* (2020) 30(3):279–84. doi: 10.1615/CritRevEukaryotGeneExpr.2020034380
71. Adhikari N, Jha T, Ghosh B. Dissecting histone deacetylase 3 in multiple disease conditions: Selective inhibition as a promising therapeutic strategy. *J Medicinal Chem* (2021) 64(13):8827–69. doi: 10.1021/acs.jmedchem.0c01676
72. Ma L, Qi L, Li S, Yin Q, Liu J, Wang J, et al. Aberrant HDAC3 expression correlates with brain metastasis in breast cancer patients. *Thorac Cancer* (2020) 11(9):2493–505. doi: 10.1111/1759-7714.13561
73. Spreafico M, Gruszka AM, Valli D, Mazzola M, Deflorian G, Quinte A, et al. HDAC8: A promising therapeutic target for acute myeloid leukemia. *Front Cell Dev Biol* (2020) 8:844. doi: 10.3389/fcell.2020.00844
74. Chakrabarti A, Melesina J, Kolbinger FR, Oehme I, Senger J, Witt O, et al. Targeting histone deacetylase 8 as a therapeutic approach to cancer and neurodegenerative diseases. *Future Medicinal Chem* (2016) 8(13):1609–34. doi: 10.4155/fmc-2016-0117
75. Sjoblom T, Jones S, Wood LD, Parsons DW, Lin J, Barber TD, et al. The consensus coding sequences of human breast and colorectal cancers. *Science* (2006) 314(5797):268–74. doi: 10.1126/science.1133427
76. Kunadis E, Lakiotaki E, Korkolopoulou P, Piperi C. Targeting post-translational histone modifying enzymes in glioblastoma. *Pharmacol Ther* (2021) 220:107721. doi: 10.1016/j.pharmthera.2020.107721
77. Cheng C, Yang J, Li S-W, Huang G, Li C, Min W-P, et al. HDAC4 promotes nasopharyngeal carcinoma progression and serves as a therapeutic target. *Cell Death Dis* (2021) 12(2):137. doi: 10.1038/s41419-021-03417-0
78. Lachenmayer A, Toffanin S, Cabellos L, Alsinet C, Hoshida Y, Villanueva A, et al. Combination therapy for hepatocellular carcinoma: additive preclinical efficacy of the HDAC inhibitor panobinostat with sorafenib. *J Hepatol* (2012) 56(6):1343–50. doi: 10.1016/j.jhep.2012.01.009
79. Yang J, Gong C, Ke Q, Fang Z, Chen X, Ye M, et al. Insights into the function and clinical application of HDAC5 in cancer management. *Front In Oncol* (2021) 11:661620. doi: 10.3389/fonc.2021.661620
80. Caslini C, Hong S, Ban YJ, Chen XS, Ince TA. HDAC7 regulates histone 3 lysine 27 acetylation and transcriptional activity at super-enhancer-associated genes in breast cancer stem cells. *Oncogene* (2019) 38(39):6599–614. doi: 10.1038/s41388-019-0897-0
81. Wang Y, Abrol R, Mak JYW, Das Gupta K, Ramnath D, Karunakaran D, et al. Histone deacetylase 7: a signalling hub controlling development, inflammation, metabolism and disease. *FEBS J* (2022). doi: 10.1111/febs.16437
82. Linares A, Assou S, Lapierre M, Thouennon E, Duraffourd C, Fromaget C, et al. Increased expression of the HDAC9 gene is associated with antiestrogen resistance of breast cancers. *Mol Oncol* (2019) 13(7):1534–47. doi: 10.1002/1878-0261.12505
83. Yang C, Croteau S, Hardy P. Histone deacetylase (HDAC) 9: versatile biological functions and emerging roles in human cancer. *Cell Oncol (Dordrecht)* (2021) 44(5):997–1017. doi: 10.1007/s13402-021-00626-9

84. Ai J, Wang Y, Dar JA, Liu J, Liu L, Nelson JB, et al. HDAC6 regulates androgen receptor hypersensitivity and nuclear localization via modulating Hsp90 acetylation in castration-resistant prostate cancer. *Mol Endocrinol* (2009) 23(12):1963–72. doi: 10.1210/me.2009-0188
85. Li Y, Zhang X, Zhu S, Dejene EA, Peng W, Sepulveda A, et al. HDAC10 regulates cancer stem-like cell properties in KRAS-driven lung adenocarcinoma. *Cancer Res* (2020) 80(16):3265–78. doi: 10.1158/0008-5472.CAN-19-3613
86. Mu N, Lei Y, Wang Y, Wang Y, Duan Q, Ma G, et al. Inhibition of SIRT1/2 upregulates HSPA5 acetylation and induces pro-survival autophagy via ATF4-DDIT4-mTORC1 axis in human lung cancer cells. *Apoptosis* (2019) 24(9-10):798–811. doi: 10.1007/s10495-019-01559-3
87. Alves-Fernandes DK, Jasiulionis MG. The role of SIRT1 on DNA damage response and epigenetic alterations in cancer. *Int J Mol Sci* (2019) 20(13):3153. doi: 10.3390/ijms20133153
88. Zhang M, Acklin S, Gillenwater J, Du W, Patra M, Yu H, et al. SIRT2 promotes murine melanoma progression through natural killer cell inhibition. *Sci Rep* (2021) 11(1):12988. doi: 10.1038/s41598-021-92445-z
89. Chen X, Hao B, Li D, Reiter RJ, Bai Y, Abay B, et al. Melatonin inhibits lung cancer development by reversing the warburg effect via stimulating the SIRT3/PDH axis. *J Pineal Res* (2021) 71(2):e12755. doi: 10.1111/jpi.12755
90. Shi Y, He R, Yang Y, He Y, Zhan L, Wei B. Potential relationship between Sirt3 and autophagy in ovarian cancer. *Oncol Lett* (2020) 20(5):162. doi: 10.3892/ol.2020.12023
91. Fu L, Dong Q, He J, Wang X, Xing J, Wang E, et al. SIRT4 inhibits malignancy progression of NSCLCs, through mitochondrial dynamics mediated by the ERK-Drp1 pathway. *Oncogene* (2017) 36(19):2724–36. doi: 10.1038/onc.2016.425
92. Chen X, Lai X, Wu C, Tian Q, Lei T, Pan J, et al. Decreased SIRT4 protein levels in endometrioid adenocarcinoma tissues are associated with advanced AJCC stage. *Cancer Biomark* (2017) 19(4):419–24. doi: 10.3233/CBM-160419
93. Yan D, Franzini A, Pomietter AD, Halverson BJ, Antelope O, Mason CC, et al. Sirt5 is a druggable metabolic vulnerability in acute myeloid leukemia. *Blood Cancer Discov* (2021) 2(3):266–87. doi: 10.1158/2643-3230.bcd-20-0168
94. Zhang Y, Huang Z, Sheng F, Yin Z. MYC upregulated LINC00319 promotes human acute myeloid leukemia (AML) cells growth through stabilizing SIRT6. *Biochem Biophys Res Commun* (2019) 509(1):314–21. doi: 10.1016/j.bbrc.2018.12.133
95. Tang X, Shi L, Xie N, Liu Z, Qian M, Meng F, et al. SIRT7 antagonizes TGF-beta signaling and inhibits breast cancer metastasis. *Nat Commun* (2017) 8(1):318. doi: 10.1038/s41467-017-00396-9
96. Bi L, Ren Y, Feng M, Meng P, Wang Q, Chen W, et al. HDAC11 regulates glycolysis through the LKB1/AMPK signaling pathway to maintain hepatocellular carcinoma stemness. *Cancer Res* (2021) 81(8):2015–28. doi: 10.1158/0008-5472.CAN-20-3044
97. Sharma VK, Lahiri M. Interplay between p300 and HDAC1 regulate acetylation and stability of Api5 to regulate cell proliferation. *Sci Rep* (2021) 11(1):16427. doi: 10.1038/s41598-021-95941-4
98. Zheng W, Tasselli L, Li TM, Chua KF. Mammalian SIRT6 represses invasive cancer cell phenotypes through ATP citrate lyase (ACLY)-dependent histone acetylation. *Genes (Basel)* (2021) 12(9):1460. doi: 10.3390/genes12091460
99. Williams AS, Kovacs TR, Davidson MT, Crown SB, Fisher-Wellman KH, Torres MJ, et al. Disruption of acetyl-lysine turnover in muscle mitochondria promotes insulin resistance and redox stress without overt respiratory dysfunction. *Cell Metab* (2020) 31(1):131–47. doi: 10.1016/j.cmet.2019.11.003
100. Yao J, Yang J, Yang Z, Wang X-P, Yang T, Ji B, et al. FBXW11 contributes to stem-cell-like features and liver metastasis through regulating HIC1-mediated SIRT1 transcription in colorectal cancer. *Cell Death Dis* (2021) 12(10):930. doi: 10.1038/s41419-021-04185-7
101. Ong ALC, Ramasamy TS. Role of Sirtuin1-p53 regulatory axis in aging, cancer and cellular reprogramming. *Ageing Res Rev* (2018) 43:64–80. doi: 10.1016/j.arr.2018.02.004
102. Chang H-C, Guarente L. SIRT1 and other sirtuins in metabolism. *Trends Endocrinol Metab* (2014) 25(3):138–45. doi: 10.1016/j.tem.2013.12.001
103. Wu J, Zhang L, Feng Y, Khadka B, Fang Z, Liu J. HDAC8 promotes daunorubicin resistance of human acute myeloid leukemia cells via regulation of IL-6 and IL-8. *Biol Chem* (2021) 402(4):461–8. doi: 10.1515/hsz-2020-0196
104. Choudhary C, Weinert BT, Nishida Y, Verdin E, Mann M. The growing landscape of lysine acetylation links metabolism and cell signalling. *Nat Rev Mol Cell Biol* (2014) 15(8):536–50. doi: 10.1038/nrm3841
105. Pietrocola F, Galluzzi L, Bravo-San Pedro JM, Madeo F, Kroemer G. Acetyl coenzyme a: a central metabolite and second messenger. *Cell Metab* (2015) 21(6):805–21. doi: 10.1016/j.cmet.2015.05.014
106. Taverna SD, Li H, Ruthenburg AJ, Allis CD, Patel DJ. How chromatin-binding modules interpret histone modifications: lessons from professional pocket pickers. *Nat Struct Mol Biol* (2007) 14(11):1025–40. doi: 10.1038/nsmb1338
107. Wagner GR, Payne RM. Widespread and enzyme-independent ne-acetylation and ne-succinylation of proteins in the chemical conditions of the mitochondrial matrix. *J Biol Chem* (2013) 288(40):29036–45. doi: 10.1074/jbc.M113.486753
108. Denisov IG, Sligar SG. A novel type of allosteric regulation: functional cooperativity in monomeric proteins. *Arch Biochem Biophys* (2012) 519(2):91–102. doi: 10.1016/j.abb.2011.12.017
109. Rufer AC, Thoma R, Hennig M. Structural insight into function and regulation of carnitine palmitoyltransferase. *Cell Mol Life Sci CMLS* (2009) 66(15):2489–501. doi: 10.1007/s00018-009-0035-1
110. Herzog S, Raemy E, Montessuit S, Veuthey J-L, Zamboni N, Westermann B, et al. Identification and functional expression of the mitochondrial pyruvate carrier. *Sci (New York NY)* (2012) 337(6090):93–6. doi: 10.1126/science.1218530
111. Harris RA, Joshi M, Jeoung NH, Obayashi M. Overview of the molecular and biochemical basis of branched-chain amino acid catabolism. *J Nutr* (2005) 135(6 Suppl):1527S–30S. doi: 10.1093/jn/135.6.1527S
112. Zaidi N, Swinnen JV, Smans K. ATP-citrate lyase: a key player in cancer metabolism. *Cancer Res* (2012) 72(15):3709–14. doi: 10.1158/0008-5472.CAN-11-4112
113. Cai L, Sutter BM, Li B, Tu BP. Acetyl-CoA induces cell growth and proliferation by promoting the acetylation of histones at growth genes. *Mol Cell* (2011) 42(4):426–37. doi: 10.1016/j.molcel.2011.05.004
114. Shi J, Vakoc CR. The mechanisms behind the therapeutic activity of BET bromodomain inhibition. *Mol Cell* (2014) 54(5):728–36. doi: 10.1016/j.molcel.2014.05.016
115. Taniguchi Y. The bromodomain and extra-terminal domain (BET) family: Functional anatomy of BET paralogous proteins. *Int J Mol Sci* (2016) 17(11):1849. doi: 10.3390/ijms17111849
116. Wang N, Wu R, Tang D, Kang R. The BET family in immunity and disease. *Signal Transduction Targeted Ther* (2021) 6(1):23. doi: 10.1038/s41392-020-00384-4
117. Li X, Li S, Li B, Li Y, Aman S, Xia K, et al. Acetylation of ELF5 suppresses breast cancer progression by promoting its degradation and targeting CCND1. *NPJ Precis Oncol* (2021) 5(1):20. doi: 10.1038/s41698-021-00158-3
118. Lee Y-S, Lee J-W, Jang J-W, Chi X-Z, Kim J-H, Li Y-H, et al. Runx3 inactivation is a crucial early event in the development of lung adenocarcinoma. *Cancer Cell* (2013) 24(5):603–16. doi: 10.1016/j.ccr.2013.10.003
119. Shigeta S, Lui GYL, Shaw R, Moser R, Gurley KE, Durenberger G, et al. Targeting BET proteins BRD2 and BRD3 in combination with PI3K-AKT inhibition as a therapeutic strategy for ovarian clear cell carcinoma. *Mol Cancer Ther* (2021) 20(4):691–703. doi: 10.1158/1535-7163.MCT-20-0809
120. Tian X-P, Cai J, Ma S-Y, Fang Y, Huang H-Q, Lin T-Y, et al. BRD2 induces drug resistance through activation of the RasGRP1/Ras/ERK signaling pathway in adult T-cell lymphoblastic lymphoma. *Cancer Commun (London England)* (2020) 40(6):245–59. doi: 10.1002/cac2.12039
121. LeRoy G, Rickards B, Flint SJ. The double bromodomain proteins Brd2 and Brd3 couple histone acetylation to transcription. *Mol Cell* (2008) 30(1):51–60. doi: 10.1016/j.molcel.2008.01.018
122. Lamonica JM, Deng W, Kadauke S, Campbell AE, Gamsjaeger R, Wang H, et al. Bromodomain protein Brd3 associates with acetylated GATA1 to promote its chromatin occupancy at erythroid target genes. *Proc Natl Acad Sci USA* (2011) 108(22):E159–E68. doi: 10.1073/pnas.1102140108
123. Guo J, Liu Y, Lv J, Zou B, Chen Z, Li K, et al. BCL6 confers KRAS-mutant non-small-cell lung cancer resistance to BET inhibitors. *J Clin Invest* (2021) 131(1):e133090. doi: 10.1172/JCI133090
124. Slaughter MJ, Shanle EK, Khan A, Chua KF, Hong T, Boxer LD, et al. HDAC inhibition results in widespread alteration of the histone acetylation landscape and BRD4 targeting to gene bodies. *Cell Rep* (2021) 34(3):108638. doi: 10.1016/j.celrep.2020.108638
125. Patel MC, Debrosse M, Smith M, Dey A, Huynh W, Sarai N, et al. BRD4 coordinates recruitment of pause release factor p-TEFb and the pausing complex NELF/DSIF to regulate transcription elongation of interferon-stimulated genes. *Mol Cell Biol* (2013) 33(12):2497–507. doi: 10.1128/MCB.01180-12
126. Sakamaki J-I, Wilkinson S, Hahn M, Tasdemir N, O'Prey J, Clark W, et al. Bromodomain protein BRD4 is a transcriptional repressor of autophagy and lysosomal function. *Mol Cell* (2017) 66(4):517–32. doi: 10.1016/j.molcel.2017.04.027
127. Devaiah BN, Mu J, Akman B, Uppal S, Weissman JD, Cheng D, et al. MYC protein stability is negatively regulated by BRD4. *Proc Natl Acad Sci USA* (2020) 117(24):13457–67. doi: 10.1073/pnas.1919507117
128. Wu S-Y, Lee C-F, Lai H-T, Yu C-T, Lee J-E, Zuo H, et al. Opposing functions of BRD4 isoforms in breast cancer. *Mol Cell* (2020) 78(6):1114–32. doi: 10.1016/j.molcel.2020.04.034
129. Floyd SR, Pacold ME, Huang Q, Clarke SM, Lam FC, Cannell IG, et al. The bromodomain protein Brd4 insulates chromatin from DNA damage signalling. *Nature* (2013) 498(7453):246–50. doi: 10.1038/nature12147

130. Yang H, Wei L, Xun Y, Yang A, You H. BRD4: An emerging prospective therapeutic target in glioma. *Mol Ther Oncolytics* (2021) 21:1–14. doi: 10.1016/j.omto.2021.03.005
131. Shi C, Ye Z, Han J, Ye X, Lu W, Ji C, et al. BRD4 as a therapeutic target for nonfunctioning and growth hormone pituitary adenoma. *Neuro Oncol* (2020) 22(8):1114–25. doi: 10.1093/neuonc/noaa084
132. Qin Z-Y, Wang T, Su S, Shen L-T, Zhu G-X, Liu Q, et al. BRD4 promotes gastric cancer progression and metastasis through acetylation-dependent stabilization of snail. *Cancer Res* (2019) 79(19):4869–81. doi: 10.1158/0008-5472.CAN-19-0442
133. Dawson MA, Prinjha RK, Dittmann A, Giotopoulos G, Bantscheff M, Chan W-I, et al. Inhibition of BET recruitment to chromatin as an effective treatment for MLL-fusion leukaemia. *Nature* (2011) 478(7370):529–33. doi: 10.1038/nature10509
134. Wan L, Wen H, Li Y, Lyu J, Xi Y, Hoshii T, et al. ENL links histone acetylation to oncogenic gene expression in acute myeloid leukaemia. *Nature* (2017) 543(7644):265–9. doi: 10.1038/nature21687
135. Erb MA, Scott TG, Li BE, Xie H, Paulk J, Seo H-S, et al. Transcription control by the ENL YEATS domain in acute leukaemia. *Nature* (2017) 543(7644):270–4. doi: 10.1038/nature21688
136. Li Y, Li L, Wu J, Qin J, Dai X, Jin T, et al. YEATS4 is associated with poor prognosis and promotes epithelial-to-mesenchymal transition and metastasis by regulating ZEB1 expression in breast cancer. *Am J Cancer Res* (2021) 11(2):416–40.
137. Ji S, Zhang Y, Yang B. YEATS domain containing 4 promotes gastric cancer cell proliferation and mediates tumor progression via activating the wnt/ β -catenin signaling pathway. *Oncol Res* (2017) 25(9):1633–41. doi: 10.3727/096504017X14878528144150
138. Hsu C-C, Shi J, Yuan C, Zhao D, Jiang S, Lyu J, et al. Recognition of histone acetylation by the GAS41 YEATS domain promotes H2A.Z deposition in non-small cell lung cancer. *Gene Dev* (2018) 32(1):58–69. doi: 10.1101/gad.303784.117
139. Zeng Z, Lei S, He Z, Chen T, Jiang J. YEATS2 is a target of HIF1 α and promotes pancreatic cancer cell proliferation and migration. *J Cell Physiol* (2021) 236(3):2087–98. doi: 10.1002/jcp.29995
140. Zaib S, Rana N, Khan I. Histone modifications and their role in epigenetics of cancer. *Curr Med Chem* (2021) 29(14):2399–411. doi: 10.2174/092986732866621108105214
141. Wyllie AH. "Where, O death, is thy sting?" a brief review of apoptosis biology. *Mol Neurobiol* (2010) 42(1):4–9. doi: 10.1007/s12035-010-8125-5
142. Wong RSY. Apoptosis in cancer: from pathogenesis to treatment. *J Exp Clin Cancer Res CR* (2011) 30:87. doi: 10.1186/1756-9966-30-87
143. Xu L, Chen Y, Song Q, Xu D, Wang Y, Ma D. PDCD5 interacts with Tip60 and functions as a cooperator in acetyltransferase activity and DNA damage-induced apoptosis. *Neoplasia (New York NY)* (2009) 11(4):345–54. doi: 10.1593/neo.81524
144. Lin C-L, Tsai M-L, Lin C-Y, Hsu K-W, Hsieh W-S, Chi W-M, et al. HDAC1 and HDAC2 double knockout triggers cell apoptosis in advanced thyroid cancer. *Int J Mol Sci* (2019) 20(2):454. doi: 10.3390/ijms20020454
145. Park S-Y, Phorl S, Jung S, Sovannarith K, Lee S-I, Noh S, et al. HDAC6 deficiency induces apoptosis in mesenchymal stem cells through p53 K120 acetylation. *Biochem Biophys Res Commun* (2017) 494(1-2):51–6. doi: 10.1016/j.bbrc.2017.10.087
146. Bao L, Diao H, Dong N, Su X, Wang B, Mo Q, et al. Histone deacetylase inhibitor induces cell apoptosis and cycle arrest in lung cancer cells via mitochondrial injury and p53 up-acetylation. *Cell Biol Toxicol* (2016) 32(6):469–82. doi: 10.1007/s10565-016-9347-8
147. Francisco R, Pérez-Perarnau A, Cortés C, Gil J, Tauler A, Ambrosio S. Histone deacetylase inhibition induces apoptosis and autophagy in human neuroblastoma cells. *Cancer Lett* (2012) 318(1):42–52. doi: 10.1016/j.canlet.2011.11.036
148. Mawatari T, Ninomiya I, Inokuchi M, Harada S, Hayashi H, Oyama K, et al. Valproic acid inhibits proliferation of HER2-expressing breast cancer cells by inducing cell cycle arrest and apoptosis through Hsp70 acetylation. *Int J Oncol* (2015) 47(6):2073–81. doi: 10.3892/ijo.2015.3213
149. Kumazawa T, Nishimura K, Katagiri N, Hashimoto S, Hayashi Y, Kimura K. Gradual reduction in rRNA transcription triggers p53 acetylation and apoptosis via MYBBP1A. *Sci Rep* (2015) 5:10854. doi: 10.1038/srep10854
150. Yorimitsu T, Klionsky DJ. Autophagy: molecular machinery for self-eating. *Cell Death Differentiation* (2005) 12 Suppl 2:1542–52. doi: 10.1038/sj.cdd.4401765
151. Feng Y, He D, Yao Z, Klionsky DJ. The machinery of macroautophagy. *Cell Res* (2014) 24(1):24–41. doi: 10.1038/cr.2013.168
152. Kaushik S, Cuervo AM. The coming of age of chaperone-mediated autophagy. *Nat Rev Mol Cell Biol* (2018) 19(6):365–81. doi: 10.1038/s41580-018-0001-6
153. Shao Y, Gao Z, Marks PA, Jiang X. Apoptotic and autophagic cell death induced by histone deacetylase inhibitors. *Proc Natl Acad Sci USA* (2004) 101(52):18030–5. doi: 10.1073/pnas.0408345102
154. Bánréti A, Sass M, Graba Y. The emerging role of acetylation in the regulation of autophagy. *Autophagy* (2013) 9(6):819–29. doi: 10.4161/auto.23908
155. Füllgrabe J, Klionsky DJ, Joseph B. The return of the nucleus: transcriptional and epigenetic control of autophagy. *Nat Rev Mol Cell Biol* (2014) 15(1):65–74. doi: 10.1038/nrm3716
156. Brown AK, Webb AE. Regulation of FOXO factors in mammalian cells. *Curr Top Dev Biol* (2018) 127:165–92. doi: 10.1016/bs.ctdb.2017.10.006
157. Mammucari C, Milan G, Romanello V, Masiero E, Rudolf R, Del Piccolo P, et al. FoxO3 controls autophagy in skeletal muscle. *in vivo. Cell Metab* (2007) 6(6):458–71. doi: 10.1016/j.cmet.2007.11.001
158. Settembre C, Di Malta C, Polito VA, Garcia Arencibia M, Vetri F, Erdin S, et al. TFEB links autophagy to lysosomal biogenesis. *Sci (New York NY)* (2011) 332(6036):1429–33. doi: 10.1126/science.1204592
159. Bao J, Zheng L, Zhang Q, Li X, Zhang X, Li Z, et al. Deacetylation of TFEB promotes fibrillar $\alpha\beta$ degradation by upregulating lysosomal biogenesis in microglia. *Protein Cell* (2016) 7(6):417–33. doi: 10.1007/s13238-016-0269-2
160. Wang Y, Huang Y, Liu J, Zhang J, Xu M, You Z, et al. Acetyltransferase GCN5 regulates autophagy and lysosome biogenesis by targeting TFEB. *EMBO Rep* (2020) 21(1):e48335. doi: 10.15252/embr.201948335
161. Wu W, Li K, Guo S, Xu J, Ma Q, Li S, et al. P300/HDAC1 regulates the acetylation/deacetylation and autophagic activities of LC3/Atg8-PE ubiquitin-like system. *Cell Death Discov* (2021) 7(1):128. doi: 10.1038/s41420-021-00513-0
162. Feng X, Zhang H, Meng L, Song H, Zhou Q, Qu C, et al. Hypoxia-induced acetylation of PAK1 enhances autophagy and promotes brain tumorigenesis via phosphorylating ATG5. *Autophagy* (2021) 17(3):723–42. doi: 10.1080/15548627.2020.1731266
163. Li N, Li H, Wang Y, Cao L, Zhan X. Quantitative proteomics revealed energy metabolism pathway alterations in human epithelial ovarian carcinoma and their regulation by the antiparasite drug ivermectin: data interpretation in the context of 3P medicine. *EPMA J* (2020) 11(4):661–94. doi: 10.1007/s13167-020-00224-z
164. Corbet C, Pinto A, Martherus R, Santiago de Jesus JP, Polet F, Feron O. Acidosis drives the reprogramming of fatty acid metabolism in cancer cells through changes in mitochondrial and histone acetylation. *Cell Metab* (2016) 24(2):311–23. doi: 10.1016/j.cmet.2016.07.003
165. Xu YS, Liang JJ, Wang Y, Zhao X-ZJ, Xu L, Xu Y-Y, et al. STAT3 undergoes acetylation-dependent mitochondrial translocation to regulate pyruvate metabolism. *Sci Rep* (2016) 6:39517. doi: 10.1038/srep39517
166. Zhu Y, Gu L, Lin X, Liu C, Lu B, Cui K, et al. Dynamic regulation of ME1 phosphorylation and acetylation affects lipid metabolism and colorectal tumorigenesis. *Mol Cell* (2020) 77(1):138–49. doi: 10.1016/j.molcel.2019.10.015
167. Gu L, Zhu Y, Lin X, Tan X, Lu B, Li Y. Stabilization of FASN by ACAT1-mediated GNPAT acetylation promotes lipid metabolism and hepatocarcinogenesis. *Oncogene* (2020) 39(11):2437–49. doi: 10.1038/s41388-020-1156-0
168. Nakayasu ES, Burnet MC, Walukiewicz HE, Wilkins CS, Shukla AK, Brooks S, et al. Ancient regulatory role of lysine acetylation in central metabolism. *mBio* (2017) 8(6):e01894–17. doi: 10.1128/mBio.01894-17
169. Serrano L, Martínez-Redondo P, Marazuela-Duque A, Vazquez BN, Dooley SJ, Voigt P, et al. The tumor suppressor SirT2 regulates cell cycle progression and genome stability by modulating the mitotic deposition of H4K20 methylation. *Gene Dev* (2013) 27(6):639–53. doi: 10.1101/gad.211342.112
170. Wang C, Fu M, Mani S, Wadler S, Senderowicz AM, Pestell RG. Histone acetylation and the cell-cycle in cancer. *Front Biosci* (2001) 6:D610–D29. doi: 10.2741/1wang1
171. Zhang W, Feng Y, Guo Q, Guo W, Xu H, Li X, et al. SIRT1 modulates cell cycle progression by regulating CHK2 acetylation-phosphorylation. *Cell Death Differentiation* (2020) 27(2):482–96. doi: 10.1038/s41418-019-0369-7
172. Waby JS, Chirakkal H, Yu C, Griffiths GJ, Benson RSP, Bingle CD, et al. Sp1 acetylation is associated with loss of DNA binding at promoters associated with cell cycle arrest and cell death in a colon cell line. *Mol Cancer* (2010) 9:275. doi: 10.1186/1476-4598-9-275
173. Hu H, Zhu W, Qin J, Chen M, Gong L, Li L, et al. Acetylation of PGK1 promotes liver cancer cell proliferation and tumorigenesis. *Hepatol (Baltimore Md)* (2017) 65(2):515–28. doi: 10.1002/hep.28887
174. Lv L, Li D, Zhao D, Lin R, Chu Y, Zhang H, et al. Acetylation targets the M2 isoform of pyruvate kinase for degradation through chaperone-mediated autophagy and promotes tumor growth. *Mol Cell* (2011) 42(6):719–30. doi: 10.1016/j.molcel.2011.04.025

175. Chen G, Luo Y, Warncke K, Sun Y, Yu DS, Fu H, et al. Acetylation regulates ribonucleotide reductase activity and cancer cell growth. *Nat Commun* (2019) 10(1):3213. doi: 10.1038/s41467-019-11214-9
176. Yang H-B, Xu Y-Y, Zhao X-N, Zou S-W, Zhang Y, Zhang M, et al. Acetylation of MAT 1 α represses tumour cell growth and is decreased in human hepatocellular cancer. *Nat Commun* (2015) 6:6973. doi: 10.1038/ncomms7973
177. Fan Y, Hou T, Gao Y, Dan W, Liu T, Liu B, et al. Acetylation-dependent regulation of TPD52 isoform 1 modulates chaperone-mediated autophagy in prostate cancer. *Autophagy* (2021) 17(12):4386–400. doi: 10.1080/15548627.2021.1917130
178. Jia Z-M, Ai X, Teng J-F, Wang Y-P, Wang B-J, Zhang X. p21 and CK2 interaction-mediated HDAC2 phosphorylation modulates KLF4 acetylation to regulate bladder cancer cell proliferation. *Tumour Biol J Int Soc For Oncodevelopmental Biol Med* (2016) 37(6):8293–304. doi: 10.1007/s13277-015-4618-1
179. Shan X, Fu Y-S, Aziz F, Wang X-Q, Yan Q, Liu J-W. Ginsenoside Rg3 inhibits melanoma cell proliferation through down-regulation of histone deacetylase 3 (HDAC3) and increase of p53 acetylation. *PLoS One* (2014) 9(12):e115401. doi: 10.1371/journal.pone.0115401
180. Ganesh K, Massagué J. Targeting metastatic cancer. *Nat Med* (2021) 27(1):34–44. doi: 10.1038/s41591-020-01195-4
181. Wang B, Ye Y, Yang X, Liu B, Wang Z, Chen S, et al. SIRT2-dependent IDH1 deacetylation inhibits colorectal cancer and liver metastases. *EMBO Rep* (2020) 21(4):e48183. doi: 10.15252/embr.201948183
182. Zhang Y, Liu Z, Yang X, Lu W, Chen Y, Lin Y, et al. H3K27 acetylation activated-COL6A1 promotes osteosarcoma lung metastasis by repressing STAT1 and activating pulmonary cancer-associated fibroblasts. *Theranostics* (2021) 11(3):1473–92. doi: 10.7150/thno.51245
183. Chen Y, Zhang B, Bao L, Jin L, Yang M, Peng Y, et al. ZMYND8 acetylation mediates HIF-dependent breast cancer progression and metastasis. *J Clin Invest* (2018) 128(5):1937–55. doi: 10.1172/JCI95089
184. Yoshimoto S, Morita H, Okamura K, Hiraki A, Hashimoto S. α TAT1-induced tubulin acetylation promotes ameloblastoma migration and invasion. *Lab Investigation; J Tech Methods Pathol* (2022) 102(1):80–9. doi: 10.1038/s41374-021-00671-w
185. Xue J, Cao Z, Cheng Y, Wang J, Liu Y, Yang R, et al. Acetylation of alpha-fetoprotein promotes hepatocellular carcinoma progression. *Cancer Lett* (2020) 471:12–26. doi: 10.1016/j.canlet.2019.11.043
186. Ni Y, Yang Y, Ran J, Zhang L, Yao M, Liu Z, et al. miR-15a-5p inhibits metastasis and lipid metabolism by suppressing histone acetylation in lung cancer. *Free Radical Biol Med* (2020) 161:150–62. doi: 10.1016/j.freeradbiomed.2020.10.009
187. Boggs AE, Vitolo MI, Whipple RA, Charpentier MS, Goloubeva OG, Ioffe OB, et al. α -tubulin acetylation elevated in metastatic and basal-like breast cancer cells promotes microtubule formation, adhesion, and invasive migration. *Cancer Res* (2015) 75(1):203–15. doi: 10.1158/0008-5472.CAN-13-3563
188. Feng L, Wang G, Chen Y, He G, Liu B, Liu J, et al. Dual-target inhibitors of bromodomain and extra-terminal proteins in cancer: A review from medicinal chemistry perspectives. *Med Res Rev* (2022) 42(2):710–43. doi: 10.1002/med.21859
189. Oike T, Komachi M, Ogiwara H, Amornwichee N, Saitoh Y, Torikai K, et al. C646, a selective small molecule inhibitor of histone acetyltransferase p300, radiosensitizes lung cancer cells by enhancing mitotic catastrophe. *Radiother Oncol* (2014) 111(2):222–7. doi: 10.1016/j.radonc.2014.03.015
190. Meja KK, Rajendrasozhan S, Adenuga D, Biswas SK, Sundar IK, Spooner G, et al. Curcumin restores corticosteroid function in monocytes exposed to oxidants by maintaining HDAC2. *Am J Respir Cell Mol Biol* (2008) 39(3):312–23. doi: 10.1165/rcmb.2008-0012OC
191. Fan W, Zhang L, Jiang Q, Song W, Yan F, Zhang L. Histone deacetylase inhibitor based prodrugs. *Eur J Medicinal Chem* (2020) 203:112628. doi: 10.1016/j.ejmech.2020.112628
192. Siegel D, Hussein M, Belani C, Robert F, Galanis E, Richon VM, et al. Vorinostat in solid and hematologic malignancies. *J Hematol Oncol* (2009) 2:31. doi: 10.1186/1756-8722-2-31
193. Shi Y, Fu Y, Zhang X, Zhao G, Yao Y, Guo Y, et al. Romidepsin (FK228) regulates the expression of the immune checkpoint ligand PD-L1 and suppresses cellular immune functions in colon cancer. *Cancer Immunol Immunother CII* (2021) 70(1):61–73. doi: 10.1007/s00262-020-02653-1
194. Smolewski P, Robak T. The discovery and development of romidepsin for the treatment of T-cell lymphoma. *Expert Opin On Drug Discov* (2017) 12(8):859–73. doi: 10.1080/17460441.2017.1341487
195. Younes A, Sureddi A, Ben-Yehuda D, Zinzani PL, Ong T-C, Prince HM, et al. Panobinostat in patients with relapsed/refractory hodgkin's lymphoma after autologous stem-cell transplantation: results of a phase II study. *J Clin Oncol Off J Am Soc Clin Oncol* (2012) 30(18):2197–203. doi: 10.1200/JCO.2011.38.1350
196. Foss F, Advani R, Duvic M, Hymes KB, Intragumtornchai T, Lekhakula A, et al. A phase II trial of belinostat (PXD101) in patients with relapsed or refractory peripheral or cutaneous T-cell lymphoma. *Br J Haematology* (2015) 168(6):811–9. doi: 10.1111/bjh.13222
197. Vey N, Prebet T, Thalamas C, Charbonnier A, Rey J, Kloos I, et al. Phase I dose-escalation study of oral abexinostat for the treatment of patients with relapsed/refractory higher-risk myelodysplastic syndromes, acute myeloid leukemia, or acute lymphoblastic leukemia. *Leukemia Lymphoma* (2017) 58(8):1880–6. doi: 10.1080/10428194.2016.1263843
198. Ribrag V, Kim WS, Bouabdallah R, Lim ST, Coiffier B, Illes A, et al. Safety and efficacy of abexinostat, a pan-histone deacetylase inhibitor, in non-Hodgkin lymphoma and chronic lymphocytic leukemia: results of a phase II study. *Haematologica* (2017) 102(5):903–9. doi: 10.3324/haematol.2016.154377
199. Choy E, Flamand Y, Balasubramanian S, Butrynski JE, Harmon DC, George S, et al. Phase I study of oral abexinostat, a histone deacetylase inhibitor, in combination with doxorubicin in patients with metastatic sarcoma. *Cancer* (2015) 121(8):1223–30. doi: 10.1002/cncr.29175
200. Salvador MA, Wicinski J, Cabaud O, Toiron Y, Finetti P, Josselin E, et al. The histone deacetylase inhibitor abexinostat induces cancer stem cells differentiation in breast cancer with low xist expression. *Clin Cancer Res an Off J Am Assoc For Cancer Res* (2013) 19(23):6520–31. doi: 10.1158/1078-0432.CCR-13-0877
201. Huang MY, Huang JK, Zheng YC, Sun Q. Histone acetyltransferase inhibitors: An overview in synthesis, structure-activity relationship and molecular mechanism. *Eur J Medicinal Chem* (2019) 178:259–86. doi: 10.1016/j.ejmech.2019.05.078
202. Lasko LM, Jakob CG, Edalji RP, Qiu W, Montgomery D, Digiammarino EL, et al. Discovery of a selective catalytic p300/CBP inhibitor that targets lineage specific tumours. *Nature* (2018) 558(7710):E1–E. doi: 10.1038/s41586-018-0111-5. (vol 550, pg 128, 2017).
203. Ji C, Xu W, Ding H, Chen Z, Shi C, Han J, et al. The p300 inhibitor a-485 exerts antitumor activity in growth hormone pituitary adenoma. *J Clin Endocrinol Metab* (2022) 107(6):e2291–e300. doi: 10.1210/clinem/dgac128
204. Wang R, He Y, Robinson V, Yang Z, Hessler P, Lasko LM, et al. Targeting lineage-specific MITF pathway in human melanoma cell lines by a-485, the selective small-molecule inhibitor of p300/CBP. *Mol Cancer Ther* (2018) 17(12):2543–50. doi: 10.1158/1535-7163.MCT-18-0511
205. Gajer JM, Furdas SD, Grunder A, Gothwal M, Heinicke U, Keller K, et al. Histone acetyltransferase inhibitors block neuroblastoma cell growth. *vivo. Oncogenesis* (2015) 4:e137. doi: 10.1038/oncso.2014.51
206. Spriano F, Gaudio E, Cascione L, Tarantelli C, Melle F, Motta G, et al. Antitumor activity of the dual BET and CBP/EP300 inhibitor NEO2734. *Blood Adv* (2020) 4(17):4124–35. doi: 10.1182/bloodadvances.2020001879
207. van Gils N, Martiánez Canales T, Vermue E, Rutten A, Denkers F, van der Deure T, et al. The novel oral BET-CBP/p300 dual inhibitor NEO2734 is highly effective in eradicating acute myeloid leukemia blasts and Stem/Progenitor cells. *HemaSphere* (2021) 5(8):e610. doi: 10.1097/HS9.0000000000000610
208. Ryan KR, Giles F, Morgan GJ. Targeting both BET and CBP/EP300 proteins with the novel dual inhibitors NEO2734 and NEO1132 leads to anti-tumor activity in multiple myeloma. *Eur J Haematology* (2021) 106(1):90–9. doi: 10.1111/ejh.13525
209. Liu WJ, Cui Y, Ren W, Irudayaraj J. Epigenetic biomarker screening by FLIM-FRET for combination therapy in ER plus breast cancer. *Clin Epigenet* (2019) 11:1–9. doi: 10.1186/s13148-019-0620-6
210. Kopytko P, Piotrowska K, Janisiak J, Tarnowski M. Garcinol-a natural histone acetyltransferase inhibitor and new anti-cancer epigenetic drug. *Int J Mol Sci* (2021) 22(6):2828. doi: 10.3390/ijms22062828
211. Jeong M-H, Ko H, Jeon H, Sung G-J, Park S-Y, Jun WJ, et al. Delphinidin induces apoptosis via cleaved HDAC3-mediated p53 acetylation and oligomerization in prostate cancer cells. *Oncotarget* (2016) 7(35):56767–80. doi: 10.18632/oncotarget.10790
212. Ono H, Kato T, Murase Y, Nakamura Y, Ishikawa Y, Watanabe S, et al. C646 inhibits G2/M cell cycle-related proteins and potentiates anti-tumor effects in pancreatic cancer. *Sci Rep* (2021) 11(1):10078. doi: 10.1038/s41598-021-89530-8
213. Baell JB, Leaver DJ, Hermans SJ, Kelly GL, Brennan MS, Downer NL, et al. Inhibitors of histone acetyltransferases KAT6A/B induce senescence and arrest tumour growth. *Nature* (2018) 560(7717):253–7. doi: 10.1038/s41586-018-0387-5
214. Ning J, Sun Q, Su Z, Tan L, Tang Y, Sayed S, et al. The CK1 δ/ϵ -Tip60 axis enhances wnt/ β -catenin signaling regulating β -catenin acetylation in colon cancer. *Front In Oncol* (2022) 12:844477. doi: 10.3389/fonc.2022.844477
215. Idrissou M, Judes G, Daures M, Sanchez A, El Ouardi D, Besse S, et al. TIP60 inhibitor TH1834 reduces breast cancer progression in xenografts in mice. *OMICS* (2019) 23(9):457–9. doi: 10.1089/omi.2019.0126
216. Gao Y-Y, Ling Z-Y, Zhu Y-R, Shi C, Wang Y, Zhang X-Y, et al. The histone acetyltransferase HBO1 functions as a novel oncogenic gene in osteosarcoma. *Theranostics* (2021) 11(10):4599–615. doi: 10.7150/thno.55655

217. Dastjerdi MN, Salahshoor MR, Mardani M, Hashemibeni B, Roshankhah S. The effect of CTB on P53 protein acetylation and consequence apoptosis on MCF-7 and MRC-5 cell lines. *Adv BioMed Res* (2013) 2:24. doi: 10.4103/2277-9175.108005
218. Picaud S, Fedorov O, Thanasopoulou A, Leonards K, Jones K, Meier J, et al. Generation of a selective small molecule inhibitor of the CBP/p300 bromodomain for leukemia therapy. *Cancer Res* (2015) 75(23):5106–19. doi: 10.1158/0008-5472.CAN-15-0236
219. Ishihama K, Yamakawa M, Semba S, Takeda H, Kawata S, Kimura S, et al. Expression of HDAC1 and CBP/p300 in human colorectal carcinomas. *J Clin Pathol* (2007) 60(11):1205–10. doi: 10.1136/jcp.2005.029165
220. Guo Y, Li X, He Z, Ma D, Zhang Z, Wang W, et al. HDAC3 silencing enhances acute b lymphoblastic leukaemia cells sensitivity to MG-132 by inhibiting the JAK/Signal transducer and activator of transcription 3 signaling pathway. *Chemotherapy* (2020) 65(3-4):85–100. doi: 10.1159/000500713
221. Yang T, Wang P, Yin X, Zhang J, Huo M, Gao J, et al. The histone deacetylase inhibitor PCI-24781 impairs calcium influx and inhibits proliferation and metastasis in breast cancer. *Theranostics* (2021) 11(5):2058–76. doi: 10.7150/thno.48314
222. Tiffon C, Adams J, van der Fits L, Wen S, Townsend P, Ganesan A, et al. The histone deacetylase inhibitors vorinostat and romidepsin downmodulate IL-10 expression in cutaneous T-cell lymphoma cells. *Br J Pharmacol* (2011) 162(7):1590–602. doi: 10.1111/j.1476-5381.2010.01188.x
223. Cardoso BA, Ramos TL, Belo H, Vilas-Boas F, Real C, Almeida AM. Vorinostat synergizes with antioxidant therapy to target myeloproliferative neoplasms. *Exp Hematol* (2019) 72:60–71. doi: 10.1016/j.exphem.2019.02.002
224. Palczewski MB, Kuschman HP, Bovee R, Hickok JR, Thomas DD. Vorinostat exhibits anticancer effects in triple-negative breast cancer cells by preventing nitric oxide-driven histone deacetylation. *Biol Chem* (2021) 402(4):501–12. doi: 10.1515/hsz-2020-0323
225. Wang L, Leite de Oliveira R, Huijberts S, Bosdriesz E, Pencheva N, Brunen D, et al. An acquired vulnerability of drug-resistant melanoma with therapeutic potential. *Cell* (2018) 173(6):1413–25. doi: 10.1016/j.cell.2018.04.012
226. Chen E, Liu N, Zhao Y, Tang M, Ou L, Wu X, et al. Panobinostat reverses HepaCAM gene expression and suppresses proliferation by increasing histone acetylation in prostate cancer. *Gene* (2022) 808:145977. doi: 10.1016/j.gene.2021.145977
227. Morabito F, Voso MT, Hohaus S, Gentile M, Vigna E, Recchia AG, et al. Panobinostat for the treatment of acute myelogenous leukemia. *Expert Opin On Investigational Drugs* (2016) 25(9):1117–31. doi: 10.1080/13543784.2016.1216971
228. Ma J, Guo X, Zhang S, Liu H, Lu J, Dong Z, et al. A histone deacetylase inhibitor, suppresses proliferation and promotes apoptosis of esophageal squamous cell lines. *Mol Med Rep* (2015) 11(6):4525–31. doi: 10.3892/mmr.2015.3268
229. Wang JH, Lee EJ, Ji M, Park SM. HDAC inhibitors, trichostatin A and valproic acid, increase e-cadherin and vimentin expression but inhibit migration and invasion of cholangiocarcinoma cells. *Oncol Rep* (2018) 40(1):346–54. doi: 10.3892/or.2018.6441
230. Geng Y, Liu J, Xie Y, Jiang H, Zuo K, Li T, et al. Trichostatin A promotes GLI1 degradation and P21 expression in multiple myeloma cells. *Cancer Manage Res* (2018) 10:2905–14. doi: 10.2147/CMAR.S167330
231. Bai Y, Chen Y, Chen X, Jiang J, Wang X, Wang L, et al. Trichostatin A activates FOXO1 and induces autophagy in osteosarcoma. *Arch Med Sci AMS* (2019) 15(1):204–13. doi: 10.5114/aoms.2018.73860
232. Lee H-Z, Kwitkowski VE, Del Valle PL, Ricci MS, Saber H, Habtemariam BA, et al. FDA Approval: Belinostat for the treatment of patients with relapsed or refractory peripheral T-cell lymphoma. *Clin Cancer Res an Off J Am Assoc For Cancer Res* (2015) 21(12):2666–70. doi: 10.1158/1078-0432.CCR-14-3119
233. Wang B, Wang X-b, Chen L-y, Huang L, Dong R-z. Belinostat-induced apoptosis and growth inhibition in pancreatic cancer cells involve activation of TAK1-AMPK signaling axis. *Biochem Biophys Res Commun* (2013) 437(1):1–6. doi: 10.1016/j.bbrc.2013.05.090
234. Kong LR, Tan TZ, Ong WR, Bi C, Huynh H, Lee SC, et al. Belinostat exerts antitumor cytotoxicity through the ubiquitin-proteasome pathway in lung squamous cell carcinoma. *Mol Oncol* (2017) 11(8):965–80. doi: 10.1002/1878-0261.12064
235. Zuo Y, Xu H, Chen Z, Xiong F, Zhang B, Chen K, et al. 17-AAG synergizes with belinostat to exhibit a negative effect on the proliferation and invasion of MDA-MB-231 breast cancer cells. *Oncol Rep* (2020) 43(6):1928–44. doi: 10.3892/or.2020.7563
236. Zhang S, Gong Z, Oladimeji PO, Currier DG, Deng Q, Liu M, et al. A high-throughput screening identifies histone deacetylase inhibitors as therapeutic agents against medulloblastoma. *Exp Hematol Oncol* (2019) 8:30. doi: 10.1186/s40164-019-0153-x
237. Garmpis N, Damaskos C, Garmpi A, Dimitroulis D, Spartalis E, Margonis G-A, et al. Targeting histone deacetylases in malignant melanoma: A future therapeutic agent or just great expectations? *Anticancer Res* (2017) 37(10):5355–62. doi: 10.21873/anticancer.11961
238. Ganai SA. Histone deacetylase inhibitor givinostat: the small-molecule with promising activity against therapeutically challenging haematological malignancies. *J Chemother (Florence Italy)* (2016) 28(4):247–54. doi: 10.1080/1120009X.2016.1145375
239. Amaru Calzada A, Pedrini O, Finazzi G, Leoni F, Mascagni P, Introna M, et al. Givinostat and hydroxyurea synergize in vitro to induce apoptosis of cells from JAK2(V617F) myeloproliferative neoplasm patients. *Exp Hematol* (2013) 41(3):253–60. doi: 10.1016/j.exphem.2012.10.013
240. Bitzer M, Horger M, Giannini EG, Ganten TM, Wörms MA, Siveke JT, et al. Resminostat plus sorafenib as second-line therapy of advanced hepatocellular carcinoma - the SHELTER study. *J Hepatol* (2016) 65(2):280–8. doi: 10.1016/j.jhep.2016.02.043
241. Streubel G, Schrepfer S, Kallus H, Parnitzke U, Wulff T, Hermann F, et al. Histone deacetylase inhibitor resminostat in combination with sorafenib counteracts platelet-mediated pro-tumoral effects in hepatocellular carcinoma. *Sci Rep* (2021) 11(1):9587. doi: 10.1038/s41598-021-88983-1
242. Wang X, Liu K, Gong H, Li D, Chu W, Zhao D, et al. Death by histone deacetylase inhibitor quisinostat in tongue squamous cell carcinoma via apoptosis, pyroptosis, and ferroptosis. *Toxicol Appl Pharmacol* (2021) 410:115363. doi: 10.1016/j.taap.2020.115363
243. Kommalapati VK, Kumar D, Tangutur AD. Quisinostat mediated autophagy is associated with differentiation in neuroblastoma SK-N-SH cells. *Mol Biol Rep* (2021) 48(5):4973–9. doi: 10.1007/s11033-021-06481-z
244. He B, Dai L, Zhang X, Chen D, Wu J, Feng X, et al. The HDAC inhibitor quisinostat (JNJ-26481585) suppresses hepatocellular carcinoma alone and synergistically in combination with sorafenib by G0/G1 phase arrest and apoptosis induction. *Int J Biol Sci* (2018) 14(13):1845–58. doi: 10.7150/ijbs.27661
245. Li H, Cui R, Ji M, Jin S-Y. CUDC-101 enhances the chemosensitivity of gemcitabine-treated lymphoma cells. *Leukemia Res* (2021) 106:106575. doi: 10.1016/j.leukres.2021.106575
246. Ji M, Li Z, Lin Z, Chen L. Antitumor activity of the novel HDAC inhibitor CUDC-101 combined with gemcitabine in pancreatic cancer. *Am J Cancer Res* (2018) 8(12):2402–18.
247. Li X, Su Y, Hege K, Madlambayan G, Edwards H, Knight T, et al. The HDAC and PI3K dual inhibitor CUDC-907 synergistically enhances the antileukemic activity of venetoclax in preclinical models of acute myeloid leukemia. *Haematologica* (2021) 106(5):1262–77. doi: 10.3324/haematol.2019.233445
248. Li Z-J, Hou Y-J, Hao G-P, Pan X-X, Fei H-R, Wang F-Z. CUDC-907 enhances TRAIL-induced apoptosis through upregulation of DR5 in breast cancer cells. *J Cell Commun Signal* (2020) 14(4):377–87. doi: 10.1007/s12079-020-00558-3
249. Rucker FG, Lang KM, Futterer M, Komarica V, Schmid M, Dohner H, et al. Molecular dissection of valproic acid effects in acute myeloid leukemia identifies predictive networks. *Epigenetics* (2016) 11(7):517–25. doi: 10.1080/15592294.2016.1187350
250. Al-Keilani MS, Al-Sawalha NA. Potential of phenylbutyrate as adjuvant chemotherapy: An overview of cellular and molecular anticancer mechanisms. *Chem Res Toxicol* (2017) 30(10):1767–77. doi: 10.1021/acs.chemrestox.7b00149
251. Qian K, Sun L, Zhou G, Ge H, Meng Y, Li J, et al. Sodium phenylbutyrate inhibits tumor growth and the epithelial-mesenchymal transition of oral squamous cell carcinoma *In vitro* and *In vivo*. *Cancer Biotherapy Radiopharmaceuticals* (2018) 33(4):139–45. doi: 10.1089/cbr.2017.2418
252. Gridelli C, Rossi A, Maione P. The potential role of histone deacetylase inhibitors in the treatment of non-small-cell lung cancer. *Crit Rev In Oncol/hematol* (2008) 68(1):29–36. doi: 10.1016/j.critrevonc.2008.03.002
253. Zhu Y, Yuan T, Zhang Y, Shi J, Bai L, Duan X, et al. AR-42: A pan-HDAC inhibitor with antitumor and antiangiogenic activities in esophageal squamous cell carcinoma. *Drug Design Dev Ther* (2019) 13:4321–30. doi: 10.2147/DDDT.S211665
254. Elshafae SM, Kohart NA, Breitbach JT, Hildreth BE, Rosol TJ. The effect of a histone deacetylase inhibitor (AR-42) and zoledronic acid on adult T-cell Leukemia/Lymphoma osteolytic bone tumors. *Cancers* (2021) 13(20):16. doi: 10.3390/cancers13205066
255. Pojani E, Barlocco D. Romidepsin (FK228), a histone deacetylase inhibitor and its analogues in cancer chemotherapy. *Curr Med Chem* (2021) 28(7):1290–303. doi: 10.2174/0929867327666200203113926
256. Bounber Y, Younes A, Garcia-Manero G. Mocetinostat (MGCD0103): a review of an isotype-specific histone deacetylase inhibitor. *Expert Opin Investig Drugs* (2011) 20(6):823–9. doi: 10.1517/13543784.2011.577737
257. Ruiz R, Raez LE, Rolfo C. Entinostat (SNDX-275) for the treatment of non-small cell lung cancer. *Expert Opin Investig Drugs* (2015) 24(8):1101–9. doi: 10.1517/13543784.2015.1056779
258. Trapani D, Esposito A, Criscitello C, Mazzarella L, Locatelli M, Minchella I, et al. Entinostat for the treatment of breast cancer. *Expert Opin Investig Drugs* (2017) 26(8):965–71. doi: 10.1080/13543784.2017.1353077

259. Kiany S, Harrison D, Gordon N. The histone deacetylase inhibitor Entinostat/Syndax 275 in osteosarcoma. *Adv In Exp Med Biol* (2020) 1257:75–83. doi: 10.1007/978-3-030-43032-0_7
260. Gupta VG, Hirst J, Petersen S, Roby KF, Kusch M, Zhou H, et al. Entinostat, a selective HDAC1/2 inhibitor, potentiates the effects of olaparib in homologous recombination proficient ovarian cancer. *Gynecol Oncol* (2021) 162(1):163–72. doi: 10.1016/j.ygyno.2021.04.015
261. Knipstein J, Gore L. Entinostat for treatment of solid tumors and hematologic malignancies. *Expert Opin On Investigational Drugs* (2011) 20(10):1455–67. doi: 10.1517/13543784.2011.613822
262. Marques AEM, do Nascimento Filho CHV, Marinho Bezerra TM, Guerra ENS, Castilho RM, Squarize CH. Entinostat is a novel therapeutic agent to treat oral squamous cell carcinoma. *J Oral Pathol Med Off Publ Int Assoc Oral Pathol Am Acad Oral Pathol* (2020) 49(8):771–9. doi: 10.1111/jop.13039
263. Sun Y, Xu Z, Jiang J, Xu T, Xu J, Liu P. High expression of succinate dehydrogenase subunit a which is regulated by histone acetylation, acts as a good prognostic factor of multiple myeloma patients. *Front Oncol* (2020) 10:563666. doi: 10.3389/fonc.2020.563666
264. Richardson PG, Moreau P, Laubach JP, Maglio ME, Lonial S, San-Miguel J. Deacetylase inhibitors as a novel modality in the treatment of multiple myeloma. *Pharmacol Res* (2017) 117:185–91. doi: 10.1016/j.phrs.2016.11.020
265. Zhao C, Dong H, Xu Q, Zhang Y. Histone deacetylase (HDAC) inhibitors in cancer: a patent review (2017-present). *Expert Opin Ther Pat* (2020) 30(4):263–74. doi: 10.1080/13543776.2020.1725470
266. Romoli M, Mazzocchetti P, D'Alonzo R, Siliquini S, Rinaldi VE, Verrotti A, et al. Valproic acid and epilepsy: From molecular mechanisms to clinical evidences. *Curr Neuropharmacol* (2019) 17(10):926–46. doi: 10.2174/1570159X17666181227165722
267. Stockhausen MT, Sjolund J, Manetopoulos C, Axelson H. Effects of the histone deacetylase inhibitor valproic acid on notch signalling in human neuroblastoma cells. *Br J Cancer* (2005) 92(4):751–9. doi: 10.1038/sj.bjc.6602309
268. Chou CJ, Herman D, Gottesfeld JM. Pimelic diphenylamide 106 is a slow, tight-binding inhibitor of class I histone deacetylases. *J Biol Chem* (2008) 283(51):35402–9. doi: 10.1074/jbc.M807045200
269. Bantscheff M, Hopf C, Savitski MM, Dittmann A, Grandi P, Michon A-M, et al. Chemoproteomics profiling of HDAC inhibitors reveals selective targeting of HDAC complexes. *Nat Biotechnol* (2011) 29(3):255–65. doi: 10.1038/nbt.1759
270. Bezecny P. Histone deacetylase inhibitors in glioblastoma: pre-clinical and clinical experience. *Med Oncol (Northwood London England)* (2014) 31(6):985. doi: 10.1007/s12032-014-0985-5
271. Park SE, Kim DE, Kim MJ, Lee JS, Rho JK, Jeong S-Y, et al. Vorinostat enhances gefitinib-induced cell death through reactive oxygen species-dependent cleavage of HSP90 and its clients in non-small cell lung cancer with the EGFR mutation. *Oncol Rep* (2019) 41(1):525–33. doi: 10.3892/or.2018.6814
272. Salmon JM, Bots M, Vidacs E, Stanley KL, Atadja P, Zuber J, et al. Correction to: Combining the differentiating effect of panobinostat with the apoptotic effect of arsenic trioxide leads to significant survival benefit in a model of t (8,21) acute myeloid leukemia. *Clin Epigenet* (2020) 12(1):178. doi: 10.1186/s13148-020-00964-9
273. Tang YL, Zhang CG, Liu H, Zhou Y, Wang YP, Li Y, et al. Ginsenoside Rg1 inhibits cell proliferation and induces markers of cell senescence in CD34+CD38-leukemia stem cells derived from KG1alpha acute myeloid leukemia cells by activating the sirtuin 1 (SIRT1)/Tuberosin sclerosis complex 2 (TSC2) signaling pathway. *Med Sci Monit* (2020) 26:e918207. doi: 10.12659/MSM.918207
274. Islam A, Yang YT, Wu WH, Chueh PJ, Lin MH. Capsaicin attenuates cell migration via SIRT1 targeting and inhibition to enhance cortactin and beta-catenin acetylation in bladder cancer cells. *Am J Cancer Res* (2019) 9(6):1172–82.
275. Liu S, Fang Y, Yu J, Chang X. Hawthorn polyphenols reduce high glucose-induced inflammation and apoptosis in ARPE-19 cells by regulating miR-34a/SIRT1 to reduce acetylation. *J Food Biochem* (2021) 45(2):e13623. doi: 10.1111/jfbc.13623
276. Wang L, Xu M, Kao C-Y, Tsai SY, Tsai M-J. Small molecule JQ1 promotes prostate cancer invasion via BET-independent inactivation of FOXA1. *J Clin Invest* (2020) 130(4):1782–92. doi: 10.1172/JCI126327
277. Choi HI, An GY, Baek M, Yoo E, Chai JC, Lee YS, et al. BET inhibitor suppresses migration of human hepatocellular carcinoma by inhibiting SMARCA4. *Sci Rep* (2021) 11(1):11799. doi: 10.1038/s41598-021-91284-2
278. Kim E, Ten Hacken E, Sivina M, Clarke A, Thompson PA, Jain N, et al. The BET inhibitor GS-5829 targets chronic lymphocytic leukemia cells and their supportive microenvironment. *Leukemia* (2020) 34(6):1588–98. doi: 10.1038/s41375-019-0682-7
279. Hsu SC, Gilgenast TG, Bartman CR, Edwards CR, Stonestrom AJ, Huang P, et al. The BET protein BRD2 cooperates with CTCF to enforce transcriptional and architectural boundaries. *Mol Cell* (2017) 66(1):102–16. doi: 10.1016/j.molcel.2017.02.027
280. Doroshow DB, Eder JP, LoRusso PM. BET inhibitors: a novel epigenetic approach. *Ann Oncol Off J Eur Soc For Med Oncol* (2017) 28(8):1776–87. doi: 10.1093/annonc/mdx157
281. Dai X, Gan W, Li X, Wang S, Zhang W, Huang L, et al. Prostate cancer-associated SPOP mutations confer resistance to BET inhibitors through stabilization of BRD4. *Nat Med* (2017) 23(9):1063–71. doi: 10.1038/nm.4378
282. Zhang P, Wang D, Zhao Y, Ren S, Gao K, Ye Z, et al. Intrinsic BET inhibitor resistance in SPOP-mutated prostate cancer is mediated by BET protein stabilization and AKT-mTORC1 activation. *Nat Med* (2017) 23(9):1055–62. doi: 10.1038/nm.4379
283. Fiorentino FP, Marchesi I, Schröder C, Schmidt R, Yokota J, Bagella L. BET-inhibitor I-BET762 and PARP-inhibitor talazoparib synergy in small cell lung cancer cells. *Int J Mol Sci* (2020) 21(24):9595. doi: 10.3390/ijms21249595
284. Braun T, Gardin C. Investigational BET bromodomain protein inhibitors in early stage clinical trials for acute myelogenous leukemia (AML). *Expert Opin On Investigational Drugs* (2017) 26(7):803–11. doi: 10.1080/13543784.2017.1335711
285. He S, Dong G, Li Y, Wu S, Wang W, Sheng C. Potent dual BET/HDAC inhibitors for efficient treatment of pancreatic cancer. *Angewandte Chemie (International Ed In English)* (2020) 59(8):3028–32. doi: 10.1002/anie.201915896
286. Lui GYL, Shaw R, Schaub FX, Stork IN, Gurley KE, Bridgwater C, et al. BET, SRC, and BCL2 family inhibitors are synergistic drug combinations with PARP inhibitors in ovarian cancer. *EBioMedicine* (2020) 60:102988. doi: 10.1016/j.ebiom.2020.102988
287. Sun Y, Han J, Wang Z, Li X, Sun Y, Hu Z. Safety and efficacy of bromodomain and extra-terminal inhibitors for the treatment of hematological malignancies and solid tumors: A systematic study of clinical trials. *Front In Pharmacol* (2020) 11:621093. doi: 10.3389/fphar.2020.621093
288. Lewin J, Soria J-C, Stathis A, Delord J-P, Peters S, Awada A, et al. Phase Ib trial with birabresib, a small-molecule inhibitor of bromodomain and extraterminal proteins, in patients with selected advanced solid tumors. *J Clin Oncol Off J Am Soc Clin Oncol* (2018) 36(30):3007–14. doi: 10.1200/JCO.2018.78.2292
289. Zhang Y, Duan S, Jang A, Mao L, Liu X, Huang G. JQ1, a selective inhibitor of BRD4, suppresses retinoblastoma cell growth by inducing cell cycle arrest and apoptosis. *Exp Eye Res* (2021) 202:108304. doi: 10.1016/j.exer.2020.108304
290. Bagratuni T, Mavrianou N, Gavalas NG, Tzannis K, Arapinis C, Lontos M, et al. JQ1 inhibits tumour growth in combination with cisplatin and suppresses JAK/STAT signalling pathway in ovarian cancer. *Eur J Cancer (Oxford Engl 1990)* (2020) 126:125–35. doi: 10.1016/j.ejca.2019.11.017
291. Xie F, Huang M, Lin X, Liu C, Liu Z, Meng F, et al. The BET inhibitor I-BET762 inhibits pancreatic ductal adenocarcinoma cell proliferation and enhances the therapeutic effect of gemcitabine. *Sci Rep* (2018) 8(1):8102. doi: 10.1038/s41598-018-26496-0
292. Liu M, Zhou J, Liu X, Feng Y, Yang W, Wu F, et al. Targeting monocyte-intrinsic enhancer reprogramming improves immunotherapy efficacy in hepatocellular carcinoma. *Gut* (2020) 69(2):365–79. doi: 10.1136/gutjnl-2018-317257
293. Liu A, Fan D, Wang Y. The BET bromodomain inhibitor i-BET151 impairs ovarian cancer metastasis and improves antitumor immunity. *Cell Tissue Res* (2018) 374(3):577–85. doi: 10.1007/s00441-018-2906-y
294. Guo N-H, Zheng J-F, Zi F-M, Cheng J. I-BET151 suppresses osteoclast formation and inflammatory cytokines secretion by targeting BRD4 in multiple myeloma. *Bioscience Rep* (2019) 39(5):12. doi: 10.1042/BSR20181245
295. Siu KT, Ramachandran J, Yee AJ, Eda H, Santo L, Panaroni C, et al. Preclinical activity of CPI-0610, a novel small-molecule bromodomain and extra-terminal protein inhibitor in the therapy of multiple myeloma. *Leukemia* (2017) 31(8):1760–9. doi: 10.1038/leu.2016.355
296. Hupe MC, Hoda MR, Zengerling F, Perner S, Merseburger AS, Cronauer MV. The BET-inhibitor PFI-1 diminishes AR/AR-V7 signaling in prostate cancer cells. *World J Urol* (2019) 37(2):343–9. doi: 10.1007/s00345-018-2382-8
297. Liu Z, Li P, Yang Y-Q, Cai S, Lin X, Chen M-B, et al. I-BET726 suppresses human skin squamous cell carcinoma cell growth *in vitro* and *in vivo*. *Cell Death Dis* (2020) 11(5):318. doi: 10.1038/s41419-020-2515-z
298. Healy JR, Hart LS, Shazad AL, Gagliardi ME, Tsang M, Elias J, et al. Limited antitumor activity of combined BET and MEK inhibition in neuroblastoma. *Pediatr Blood Cancer* (2020) 67(6):e28267. doi: 10.1002/pbc.28267
299. Zhang L, Cai T, Lin X, Huang X, Bui MH, Plotnik JP, et al. Selective inhibition of the second bromodomain of BET family proteins results in robust antitumor activity in preclinical models of acute myeloid leukemia. *Mol Cancer Ther* (2021) 20(10):1809–19. doi: 10.1158/1535-7163.MCT-21-0029
300. Faivre EJ, McDaniel KF, Albert DH, Mantena SR, Plotnik JP, Wilcox D, et al. Selective inhibition of the BD2 bromodomain of BET proteins in prostate cancer. *Nature* (2020) 578(7794):306–10. doi: 10.1038/s41586-020-1930-8
301. Wen S, Li C, Zhan X. Multi-omics integration analysis revealed molecular network alterations in human nonfunctional pituitary neuroendocrine tumors in the framework of 3P medicine. *EPMA J* (2022) 13(1):9–37. doi: 10.1007/s13167-022-00274-5

Glossary

ACLY	ATP- citrate lyase
ACSS2	Acyl- CoA synthetase short- chain family member 2
Api5	Apoptosis inhibitor 5
ATAT-1	Alpha-tubulin N-acetyltransferase 1
BET	Bromodomain and extra-terminal
BET1	Bromodomain and extra-terminal inhibitor
BRD2	Bromodomain 2
BRD3	Bromodomain 3
BRD4	Bromodomain 4
BRDT	Bromodomain testis-specific protein
CBFB	Core-binding factor beta
CBP	CREB- binding protein
CMA	Chaperone-mediated autophagy
CTCL	Cutaneous T-cell lymphoma
CTD	C-terminal structure of RNA polymerase II Domain
EMT	Epithelial-to-mesenchymal transition
ERalpha	Estrogen receptor alpha
ESCO1	Establishment of sister chromatid cohesion N-acetyltransferase 1
ESCO2	Establishment of sister chromatid cohesion N-acetyltransferase 2
Fox O	Forkhead box-containing protein
O subfamily	
GCN5	General control of amino acid synthesis protein 5
H3	Histone 3
H3K14	Histone H3 lysine 14
H3K27	Histone H3 lysine 27
H3K27ac	Histone H3 lysine 27 acetylation
H3K56ac	Histone H3 lysine 56 acetylation
H3K9	Histone H3 lysine 9
H3K9ac	Histone H3 lysine 9 acetylation
H4	Histone 4
H4K12	Histone H4 lysine 12
H4K16ac	Histone H4 lysine 16 acetylation
H4K20me1	Histone H4 lysine 20 mono-methylation
H4K5	Histone H4 lysine 5
HAT	Histone acetyltransferase
HAT1	Histone acetyltransferase 1
HBO1	Histone acetyltransferase binding to ORC1
HBx	Hepatitis B virus X protein
HCC	Hepatocellular carcinoma
HDAC	Histone deacetylase
hnRNPA1	Heterogeneous nuclear ribonucleoprotein A1
HPE	Hawthorn polyphenol extract
Hsp70	Heat shock protein 70
HSPA5	Heat shock protein family A (Hsp70) member 5
HSPA8	Heat shock protein family A (Hsp70) member 8
IDH1	Isocitrate dehydrogenase 1
IL-6	Interleukin- 6
IL-8	Interleukin- 8

Continued

McTN	Microantenna
MOF	Males absent on the first
MOZ	Monocytic leukemia zinc finger protein
MSCs	Mesenchymal stem cells
mTOR	Mechanistic target of rapamycin kinase
Naa10	N-alpha-acetyltransferase 10
NAT1	Arylamine N-acetyltransferase 1
NF-PitNETs	Nonfunctional pituitary neuroendocrine tumors
NF-kB	Nuclear factor k-B
NSCLC	Non-small cell lung cancer
OCCC	Ovarian clear cell carcinoma
OS	Osteosarcoma
PA	Palmitic acid
PDH	Pyruvate dehydrogenase complex
PHD	Plant homeodomain-linked
PKM	Pyruvate kinase
PKM2	Pyruvate kinase M1/2
PRAP	Proline-rich acidic protein
PTM	Post-translational modification
RNR	Ribonucleotide reductase
SCLC	Small Cell Lung Cancer
Ses	Super-enhancers
SIRT1	Sirtuin 1
SIRT2	Sirtuin 2
SIRT3	Sirtuin 3
SIRT4	Sirtuin 4
SIRT5	Sirtuin 5
SIRT6	Sirtuin 6
snRNA	Small nuclearRNA
TAK1	TGF-β-activated kinase 1
TAT1	α-tubulin N- acetyltransferase 1
TCA	Tricarboxylic acid
Tip60	60 kDa Tat- interactive protein
TSC2	Tuberous sclerosis complex 2
TSC2	Tuberous sclerosis complex 2
TSS	Transcription start sites
YEATS2	YEATS domain containing 2
YEATS4	YEATS domain containing 4
YopJ	Serine/threonine-protein acetyltransferase YopJ.

(Continued)



OPEN ACCESS

EDITED BY

Tadashi Nakagawa,
Tohoku University, Japan

REVIEWED BY

Yanfen Liu,
ShanghaiTech University, China
Fuminori Tokunaga,
Osaka Metropolitan University, Japan

*CORRESPONDENCE

Xianquan Zhan
yjzhan2011@gmail.com

SPECIALTY SECTION

This article was submitted to
Cancer Endocrinology,
a section of the journal
Frontiers in Endocrinology

RECEIVED 16 June 2022

ACCEPTED 25 August 2022

PUBLISHED 15 September 2022

CITATION

Zhan X, Lu M, Yang L, Yang J, Zhan X,
Zheng S, Guo Y, Li B, Wen S, Li J and
Li N (2022) Ubiquitination-mediated
molecular pathway alterations in
human lung squamous cell
carcinomas identified by quantitative
ubiquitinomics.
Front. Endocrinol. 13:970843.
doi: 10.3389/fendo.2022.970843

COPYRIGHT

© 2022 Zhan, Lu, Yang, Yang, Zhan,
Zheng, Guo, Li, Wen, Li and Li. This is an
open-access article distributed under
the terms of the [Creative Commons
Attribution License \(CC BY\)](https://creativecommons.org/licenses/by/4.0/). The use,
distribution or reproduction in other
forums is permitted, provided the
original author(s) and the copyright
owner(s) are credited and that the
original publication in this journal is
cited, in accordance with accepted
academic practice. No use,
distribution or reproduction is
permitted which does not comply with
these terms.

Ubiquitination-mediated molecular pathway alterations in human lung squamous cell carcinomas identified by quantitative ubiquitinomics

Xianquan Zhan^{1,2*}, Miaolong Lu^{2,3}, Lamei Yang², Jingru Yang²,
Xiaohan Zhan^{2,3}, Shu Zheng², Yuna Guo², Biao Li^{2,3},
Siqi Wen^{2,3}, Jiajia Li^{2,3} and Na Li^{1,2}

¹Shandong Key Laboratory of Radiation Oncology, Shandong Cancer Hospital and Institute, Shandong First Medical University and Shandong Academy of Medical Sciences, Jinan, China, ²Medical Science and Technology Innovation Center, Shandong First Medical University, Jinan, China, ³Key Laboratory of Cancer Proteomics of Chinese Ministry of Health, Xiangya Hospital, Central South University, Changsha, China

Abnormal ubiquitination is extensively associated with cancers. To investigate human lung cancer ubiquitination and its potential functions, quantitative ubiquitinomics was carried out between human lung squamous cell carcinoma (LSCC) and control tissues, which characterized a total of 627 ubiquitin-modified proteins (UPs) and 1209 ubiquitinated lysine sites. Those UPs were mainly involved in cell adhesion, signal transduction, and regulations of ribosome complex and proteasome complex. Thirty three UPs whose genes were also found in TCGA database were significantly related to overall survival of LSCC. Six significant networks and 234 hub molecules were obtained from the protein-protein interaction (PPI) analysis of those 627 UPs. KEGG pathway analysis of those UPs revealed 47 statistically significant pathways, and most of which were tumor-associated pathways such as mTOR, HIF-1, PI3K-Akt, and Ras signaling pathways, and intracellular protein turnover-related pathways such as ribosome complex, ubiquitin-mediated proteolysis, ER protein processing, and proteasome complex pathways. Further, the relationship analysis of ubiquitination and differentially expressed proteins shows that ubiquitination regulates two aspects of protein turnover - synthesis and degradation. This study provided the first profile of UPs and molecular networks in LSCC tissue, which is the important resource to insight into new mechanisms, and to identify new biomarkers and therapeutic targets/drugs to treat LSCC.

KEYWORDS

lung squamous cell carcinoma, ubiquitination, ubiquitinated protein, signaling pathway, ubiquitin-proteasome system, biomarker

Introduction

Lung squamous cell carcinoma (LSCC) is closely related to smoking (1), which is 25%-30% of non-small cell lung cancer (NSCLC), and >70% LSCC patients were diagnosed in late stage (2, 3), with high mortality (~0.4 million/year) in the world (4). Although the incidence has decreased due to tobacco control and changes in lifestyle in recent decades, LSCC still brings huge burdens to society (5). In terms of treatment, radical thoracic surgery is preferred for early-stage cases of LSCC; however, unfortunately the proportion of this type of patients is very small. Besides, chemotherapy and radiotherapy are also indispensable treatments, especially in advanced (or metastatic) LSCC subpopulation (6). Recent years, although some encouraging targeted drugs such as anaplastic lymphoma kinase inhibitors and epithelial growth factor receptor (EGFR) tyrosine kinase inhibitors have been used to significantly improve the therapy of late-stage lung adenocarcinoma (4), there is still lack of FDA-approved targeted therapy for advanced LSCC patients. For most patients with advanced LSCC, first-line standard chemotherapy is a 4-6-cycle platinum-based third-generation cytotoxic drug with an effective rate of 20%-30%. The median survival time (MST) is 8-10 months, the time to progression (TTP) is 3-5 months (7). In addition, LSCC still lacks universally accepted biomarkers for early diagnosis and prognostic evaluation. Obviously, the current predictive, preventive, and personalized medicine (PPPM) of LSCC is still unmet; therefore, it is necessary to clarify molecular mechanism and discover new biomarkers and therapeutic targets/drugs to manage LSCC.

Protein ubiquitination is an important molecular event, which covalently link the C-terminus of ubiquitin (8.5 kDa, 76

amino acids, coded by four genes RPS27A, UBA52, UBC, and UBB) to the ϵ -amino group at lysine residue in a protein (8, 9). Ubiquitination is a multi-step reaction process, which is catalyzed by enzymes E1, E2, and E3 (8). Protein ubiquitinations are classified into monoubiquitination that means one ubiquitin in one protein, multiubiquitination that means several ubiquitination sites in a protein and each ubiquitination site links one ubiquitin, and polyubiquitination that means a polyubiquitin chain to be added to lysine residues or N-terminus of the previous ubiquitin (10); and different types of ubiquitinations have different biological functions (11). Also, there are seven lysine residues in an ubiquitin, which make polyubiquitin chain more complicated. Moreover, ubiquitination process can be reversed, which is catalyzed by more than 100 deubiquitination enzymes (12). The reversible ubiquitination reaction regulates multiple biological processes including protein degradation (13), and associated with a wide range of diseases including cancers, and inflammatory diseases (14). Ubiquitin-proteasome system (UPS) is the important protein degradation pathway, which has important roles in tumorigenesis. Targeting the UPS system is the promising anti-tumor strategies. Thereby, several effective anti-tumor drugs targeting UPS have been approved by FDA, including bortezomib (15), carfilzomib (16), thalidomide, pomalidomide, and lenalidomide (17), for different cancer treatment. At present, LSCC still lacks specific early diagnostic biomarkers, and in addition to surgery, radiotherapy, and chemotherapy, there is lack of effective molecular therapeutic drugs. Therefore, the study of ubiquitinome might have important scientific merits for discovery of effective biomarkers and novel therapeutic targets/drugs for LSCC.

Liquid chromatography in combination with tandem mass spectrometry (LC-MS/MS) is an effective method to identify ubiquitination sites and quantify the abundance of ubiquitination (18). However, endogenous ubiquitination is low abundant event, it is necessary to enrich the ubiquitinated tryptic peptides prior to MS/MS analysis. The commercial anti-K ϵ -GG antibodies is able to effectively enrich ubiquitinated tryptic peptides (19). For antibody-based enrichment of ubiquitinated tryptic peptides, it is the best to avoid any salt, acid, and basic factors to negatively impact this enrichment. Compared to the isotope-labeling quantitative proteomics such as iTRAQ (isobaric tags for relative and absolute quantification) and TMT (tandem mass tags) that introduce above interfered factors to negatively impact antibody-antigen reaction, label-free quantitative proteomics is a preferred approach to identify and quantify endogenous ubiquitination, which does not label the analyzed protein component in a proteome (20) but quantify the protein with area under the curve (AUC) and signal intensity in the MS spectrum, and spectral counting based on MS/MS analysis (21). Thus, anti-ubiquitin antibody in combination with label-free LC-MS/MS is an effective quantitative ubiquitinomics, which has identified up to 10,000

Abbreviations: ALK, anaplastic lymphoma kinase; AUC, area under the curve; BP, biological processes; CC, cellular components; CS, core subunit; DTT, dithiothreitol; E1, ubiquitin-activating enzyme; E2, ubiquitin-conjugating enzyme; E3, ubiquitin ligase; EPC, edge percolated component; ER, endoplasmic reticulum; GO, gene ontology; IAP, immunoaffinity purification; ICAT, isotope-coded affinity tags; iTRAQ, isobaric tags for relative and absolute quantification; KEGG, Kyoto Encyclopedia of Genes and Genomes; LC, liquid chromatography; LSCC, lung squamous cell cancer; MCC, maximal clique centrality; MCODE, molecular complex detection; MF, molecular functions; MNC, maximum neighborhood component; MS/MS, tandem mass spectrometry; NSCLC, non-small-cell lung cancer; PMSF, phenylmethyl-sulfonyl fluoride; PPI, protein-protein interaction; PPPM, predictive, preventive and personalized medicine; PTM, post-translational modification; RACs, RS assembly chaperones; RQC, ribosome-associated quality control; RS, regulatory subunit; SILAC, isotope labels with amino acids in cell culture; TAC, tumor-adjacent control; TFA, Trifluoroacetic acid; TKI, tyrosine kinase inhibitors; TTP, time to progression; UPS, ubiquitinated proteins; 2D-DIGE, 2D fluorescence difference in-gel electrophoresis; 2D-PAGE, two-dimensional polyacrylamide gel electrophoresis.

ubiquitination sites in an experiment (22). For lung cancer analysis, currently researchers mainly focused on the study on ubiquitinome of lung cancer cells (23, 24), and these studies were not based strictly on LSCC cell lines.

This study used anti-ubiquitin antibody coupled with label-free LC-MS/MS to detect, identify, and quantify ubiquitinated proteins (UPs) and ubiquitination sites in fresh human LSCC tissues compare to controls. Gene ontology (GO) enrichment analysis was used to determine the functional characteristics of UPs, and Kyoto Encyclopedia of Genes and Genomes (KEGG) enrichment analysis was used to mine the ubiquitination-involved pathway networks. This study provides the holistic profile of ubiquitination in LSCC tissue, and underscores ubiquitination may promote the occurrence and development of LSCC by affecting the intracellular protein turnover, and paving the way for further research on specific ubiquitination regulatory mechanisms.

Materials and methods

Tissue samples and protein preparation

Human LSCC tissues (n = 5) and tumor-adjacent control (TAC) tissues (n = 5) (Supplementary Table 1; these samples were at early stage of LSCC) were removed by thoracic surgery, and stored in -80°C , for protein extraction. A total of 750 mg LSCC tissues (n = 5; 150 mg per patient) and 750 mg TAC tissues (n = 5; 150 mg per patient) derived from 5 patients were homogenized, after removal of blood contamination, in solution that included 2 M thiourea, 7 M urea, 1 mM phenylmethyl-sulfonyl fluoride (PMSF), and 100 mM dithiothreitol (DTT); followed by sonication (80 W, 10 s, and interval 15 s; 10 x), and centrifugation at 4°C (15,000xg, and 20 min). The supernatant was the extracted proteins, whose protein content was determined with Bradford assay.

Preparation of tryptic peptides and enrichment of ubiquitinated tryptic peptides

The protein sample (LSCC; TAC) was reduced with final concentration of 10 mM DTT (37°C , 1.5 h), and alkylated with final concentration of 50 mM iodoacetamide (30 min, dark). The mixture was diluted to 2 M uranyl acetate with 50 mM Tris-HCl (pH 8.0), followed by addition of trypsin (1:50 for the ratio of trypsin to protein), and incubation (15–18 h; 37°C) to digest the proteins. Then, the digestion reaction was stopped with addition of trifluoroacetic acid (TFA) to adjust $\text{pH} \leq 3$. The tryptic peptide mixture was desalted, and lyophilized. The lyophilized

tryptic peptides were redissolved in 1.4 mL solution that contained 50 mM NaCl, 10 mM Na_2HPO_4 , and 50 mM MOPS/NaOH pH 7.2, followed by addition of anti-K- ϵ -GG antibody beads [PTMScan ubiquitin remnant motif (K- ϵ -GG) kit, Cell Signal Technology], incubation (1.5 h, 4°C), and centrifugation (30 s, 2,000xg). The beads with antibody-binding ubiquitinated peptides were washed for 3 times with 1 mL solution that contained 50 mM NaCl, 10 mM Na_2HPO_4 , and 50 mM MOPS/NaOH pH 7.2, followed by washing with water for 3 times. The ubiquitinated tryptic peptides were eluted with 40 μL 0.15% TFA, followed by centrifugation (30 s, 2,000xg), and desalting with C18 STAGE Tips.

LC-MS/MS analysis of enriched ubiquitinated peptides

The prepared ubiquitinated tryptic peptides were treated with a reverse-phase trap column (nanoViper C18, 2 cm x 100 μm), and then were separated in a reverse-phase analytical column (C18, 10 cm length x 75 μm i.d., and 3 μm resin) with buffers A (0.1% formic acid) and B (0.1% formic acid + 84% acetonitrile) for 2 h (flow-rate = 300 nl/min) on the Q Exactive mass spectrometer (Thermo Scientific) to obtain MS/MS raw data. MaxQuant software (version 1.5.3.17) was used to search MS/MS data against human protein database uniprot_human_156639_20170105.fasta, with database search parameters (4 missed cleavages, trypsin, 6 ppm for MS, 20 ppm for MS/MS, GlyGly at Lys, acetylation at protein N-term, oxidation at Met, and carbamidomethyl at Cys). The peptide was determined by MS/MS data with false discovery rate (FDR) ≤ 0.01 , ubiquitination site with FDR ≤ 0.01 , and protein with FDR ≤ 0.01 . The abundance of ubiquitination was determined with MaxQuant label-free calculation based on peptide intensity and peptide counting.

Bioinformatics and statistical analysis

The functional characteristics of the identified UPs, including biological processes (BPs), molecular functions (MFs), and cellular components (CCs) were analyzed with DAVID software (version 6.8, <https://david.ncifcrf.gov/>) (25). Ubiquitination-mediated signaling pathways were analyzed with the KEGG tool KOBAS (<http://kobas.cbi.pku.cn>) (26). The protein-protein interaction (PPI) networks that UPs are involved in were analyzed with STRING software (<https://string-db.org/>; version 10.0) (27), with statistical significance of a combined score > 0.4 , in the Cytoscape program (version 3.6.0) (28). Also, molecular complex detection (MCODE) in the Cytoscape program was used to identify significant modules in

the PPI networks with cutoff values (max depth=100, node score=0.2, degree=2, k-score=2, and MCODE score>5) (29). The hub nodes of PPI network were determined with cytoHubba (version 0.1) in Cytoscape package through 6 different topological algorithms (30), including Maximal Clique Centrality (MCC; cutoff score=100 with this node that had at least 5 molecules linked), Maximum Neighborhood Component (MNC; cutoff score=10 with this node that had at least 5 molecules linked), Degree (cutoff score=10 with this node that had at least 5 molecules linked), Edge Percolated Component (EPC; cutoff score=10 with this node that had at least 5 molecules linked), Closeness (cutoff=150 with this node that had at least 5 molecules linked), and Riality (cutoff score=5 with this node that had at least 5 molecules linked). The final hub nodes were identified with overlapped analysis of six sets of hub nodes that were derived from 6 topological algorithms. The transcriptomic data (level 2 count data) and corresponding clinical survival data of LSCC patients were obtained from TCGA database with R-languages “RTCGA.mRNA” (version 1.12.0) and “RTCGA.clinical” (version 20151101.14.0), respectively. The survival analysis was performed with R-languages “survival” (version 2.44-1.1) and “survminer” (version 0.4.6).

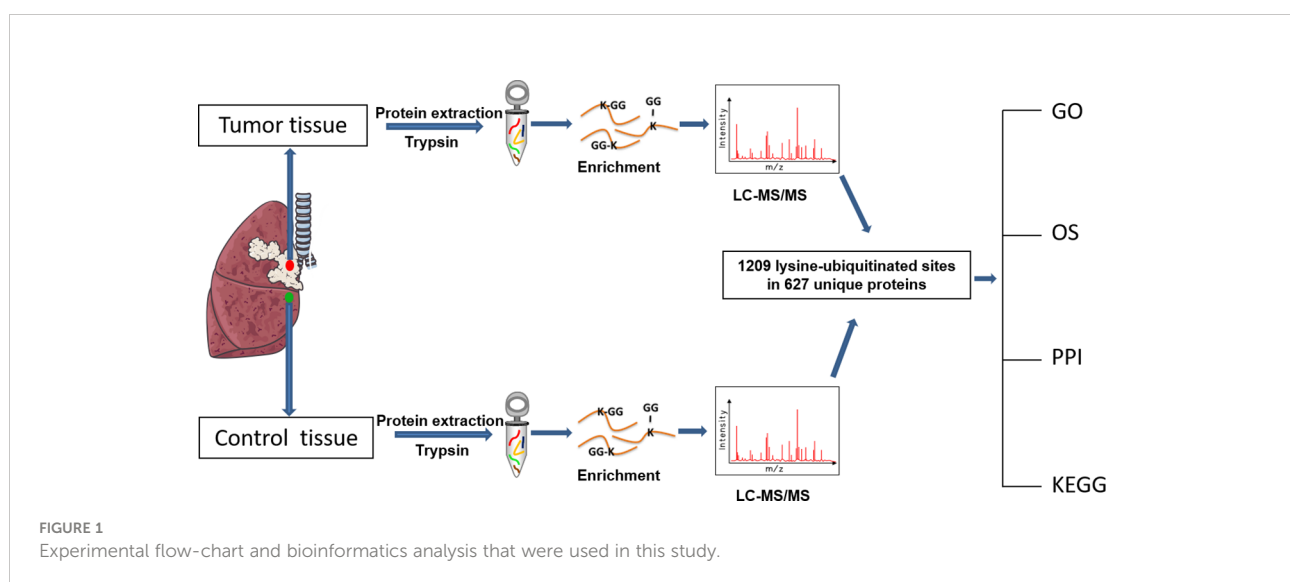
The overall flow-chart to identify and analyze the ubiquitination profile and the corresponding functional characteristics in LSCC was summarized (Figure 1).

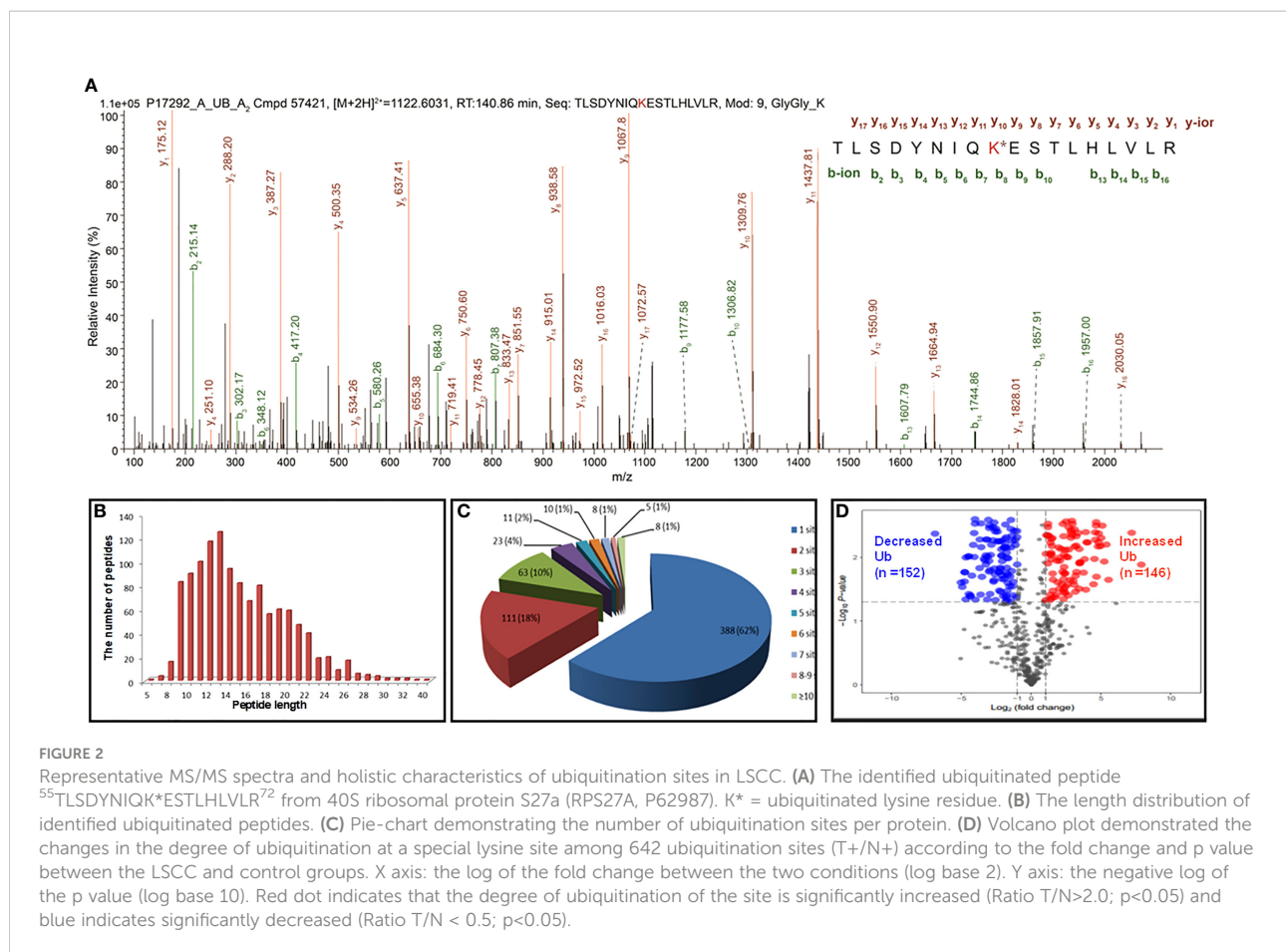
Results

Ubiquitination profile in human LSCC

In total, 627 UPs and 1209 ubiquitination sites were identified with MS/MS data, which referred to 1086 ubiquitinated tryptic

peptides, in human LSCC tissues (Supplementary Table 2). For example, the MS/MS spectrum of tryptic peptide ⁵⁵TLSDYNIQK*ESTLHLVLR⁷² ([M+2H]²⁺ m/z =1122.6031, RT = 140.86 min) was derived from 40S ribosomal protein S27a (RPS27A; P62987) (Figure 2A), with high S/N (signal to noise) ratio, excellent γ -ion (γ_1 - γ_{17}) and b-ion (b_2 - b_{10} , b_{13} - b_{16}) series, localization of ubiquitination site at residue K₆₃, and a decreased ubiquitination level at residue K63 (Ratio T/N = 0.425; P=0.0529) in LSCCs compared to TAC controls (Supplementary Table 2). In addition, another six ubiquitination sites were also identified in this RPS27A (P62987) in LSCC tissues compare to TAC tissues, including ubiquitinations at residues K6 (Ratio T/N = 0.271; P=5.07E-03), K11 (Ratio T/N=0.496; P=1.28E-02), K27 (Ratio T/N=3.812; P=4.53E-05), K29 (Ratio T/N=0.933; P=8.55E-01), K33 (Ratio T/N=2.903; P=3.75E-04), and K48 (Ratio T/N=0.839; P=5.47E-01) (Supplementary Table 2). It clearly demonstrated that 7 ubiquitination sites were identified in this RPS27A, with decreased ubiquitination levels at residues K6, K11, K29, K48, and K63 (of them, significantly decreased level at residues K6 and K11), and significantly increased ubiquitination levels at residues K27 and K33. This is an interesting result, because, in the same protein, the ubiquitination level at some Lys sites were decreased (K6, K11, K29, K48, and K63), and whereas the ubiquitination levels at some Lys sites were increased (K27 and K33). This phenomenon might be easily explained from the angle of proteoforms encoded by the same gene RPS27A. Another reason might be due to the kinetics change of ubiquitin linkages in LSCC because there are four ubiquitin-encoding genes, including UBB, UBC, UBA52 (which encodes RPL40), and UBA80 (also known as RPS27A; RPS27A encodes a fusion protein consisting of ubiquitin at the N terminus and ribosomal protein S27a at the C terminus), and all of which produce the identical ubiquitin protein; if S27a protein does not change, but the ubiquitin chain linking pattern increases or decreases, it is not due to the RPS27A gene alone; thereby thus





results in the alteration of ubiquitin ligation dynamics mediated by ubiquitin ligases in LSCC.

For 1086 ubiquitinated tryptic peptides, their lengths were in the range of 5–40 amino acids (Figure 2B). Analysis of the number of ubiquitination sites in human LSCC UPs found that the number of putative ubiquitination sites per protein was arranged from 1 to 15. A total of 388 ($388/627 = 62\%$) UPs had only one ubiquitination site, 18% (111/627) UPs had two sites, 10% (63/627) UPs had three sites, 4% (23/627) UPs had four sites, and 7% (42/627) UPs had five sites (Figure 2C). A total of 1133 ($1133/1209 = 93.7\%$) ubiquitination sites had quantitative information, including 642 ($642/1133 = 56.7\%$) sites with T+/N+, 395 ($395/1133 = 34.9\%$) with T+/N-, and 96 ($96/1133 = 8.4\%$) with T-/N+; and among these 1133 sites, 699 (61.7%) sites had increased ubiquitination levels and 434 (38.3%) sites had decreased ubiquitination levels in LSCC compared to TAC tissues. Another 76 ($76/1209 = 6.3\%$) sites did not have quantitative information between LSCC and TAC tissues. Here showed the distribution of intensity changes of these 642 ubiquitination sites (T+/N+), including 146 sites had significantly increased ubiquitination levels (Ratio T/N > 2; $p < 0.05$), and 152 sites had significantly decreased ubiquitination levels (Ratio T/N < 0.5; $p < 0.05$) (Figure 2D), the corresponding detailed information was listed in Supplementary Table 2.

Functional characteristics of identified UPs in LSCC

The functional characteristics of 627 UPs were enriched with GO analysis, including BPs, MFs, and CCs. For BP analysis, UPs were mainly enriched in cellular process (258 UPs), metabolic process (147 UPs), biological regulation (100 UPs), and localization (85 UPs) (Figure 3A). For MF analysis, UPs were mainly enriched in binding activity (222 UPs), catalytic activity (180 UPs), transporter activity (44 UPs), structural molecule activity (38 UPs), molecular function regulator (26 UPs), and transcription regulator activity (16 UPs) (Figure 3B). For CC analysis, UPs were mainly enriched in cell (258 UPs), organelle (134 UPs), protein-containing complex (50 UPs), membrane (38 UPs), extracellular region (17 UPs), and cell junction (13 UPs) (Figure 3C).

These BPs, MFs, and CCs were further grouped into 7 functional clusters (Supplementary Table 3), including cell adhesion, multiple signaling pathways that were closely related to tumorigenesis, such as Wnt signaling, tumor necrosis factor-mediated signaling, NF-kappa B signaling, assembly and functional regulation of proteasome, assembly and functional

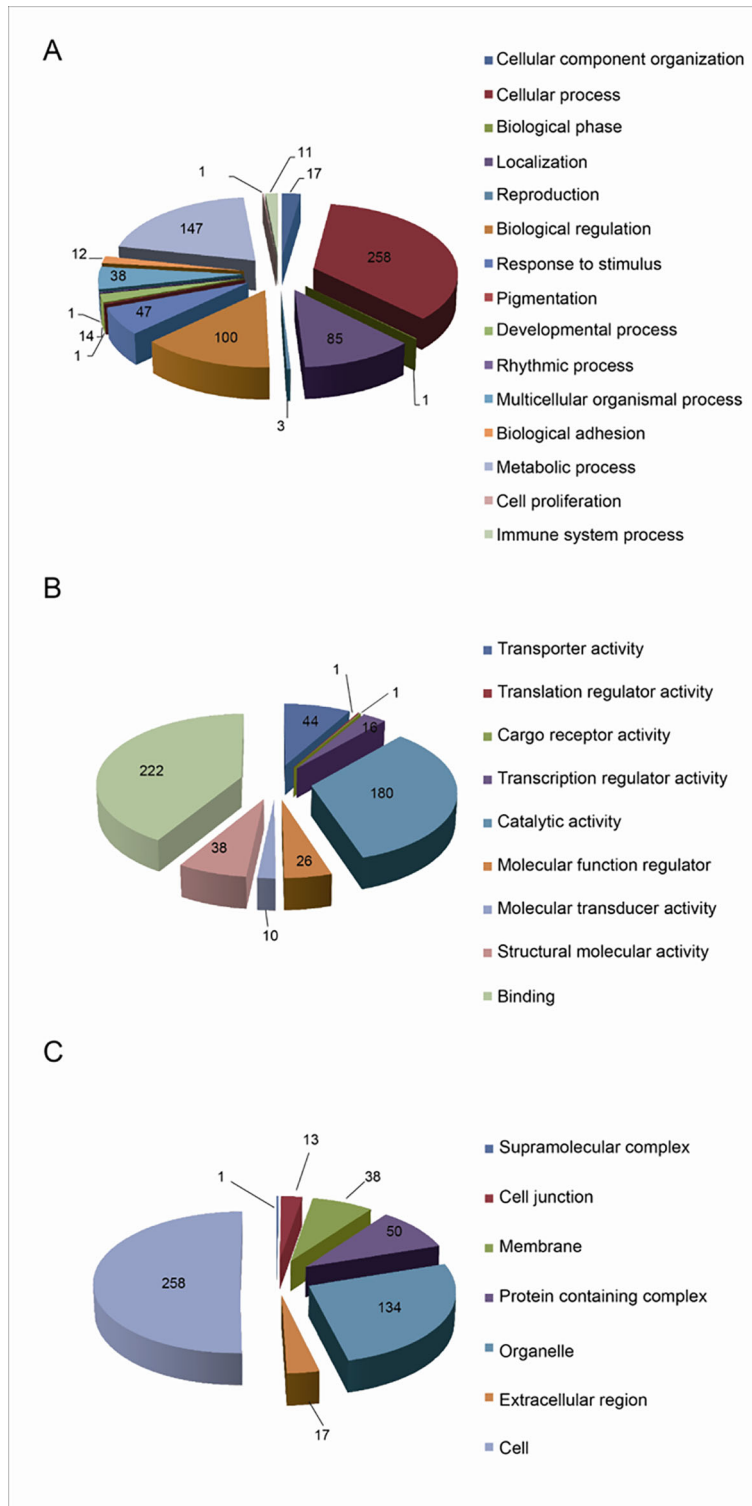


FIGURE 3 Functional characteristics of 627 Ups identified with GO enrichment analysis. (A) The BP profile of Ups. (B) The MF profile of Ups. (C) The CC profile of Ups.

regulation of ribosome, haptoglobin hemoglobin complex, DNA damage recognition, and hemoglobin complex.

Survival-related UPs in LSCC

A total of 1030 overall survival-related genes were obtained from LSCC data in TCGA database (Supplementary Tables 4-6). A total of 33 overlapped molecules (UPs; survival-related genes) were obtained when overlapping analysis was performed between the identified 627 UPs and 1030 overall survival-related genes (Figure 4A), which showed that those 33 overlapped molecules were survival-related UPs. GO enrichment analysis of these 33 survival-related UPs showed that these UPs were significantly involved in different BPs, and were closely related to tumorigenesis, including cell growth, blood vessel development, and regulation of intracellular signal transduction (Figure 4B). Among them, the higher expressions of 11 overlapped molecules (UPs; survival-related genes), including SPG20, PFN2, SET, CBX1, HISTIH1B, DSC3, ENO1, NONO, HISTIH4H, ACTA2 and PGK showed a better prognosis, which suggested their protective effects; while the higher expressions of 22 overlapped molecules (UPs; survival-related genes), including PRKCKBP, DDX5, ATP11A, EPB2, RPS2, ITGB1, TANK, GPRC5A, TRIM47, MVP, RNF213, SAP18, HM13, ICAM1, SLC16A4, LRSAM1, TM9SF3, CALD1, SYNPO, CLTB, CA1 and GJA5 demonstrated a worse

prognosis, which suggested their tumor-promoting effects. Here showed the overall survival curve of RPS2 (Figure 4C), and RPS2 was further identified as a hub molecule.

Ubiquitination-mediated molecular networks and network-based hub molecules derived from 627 UPs in LSCCs

To deeper understand cellular processes regulated by ubiquitination in LSCC, 627 UPs were input into STRING online software, 457/627 UPs were legible for PPI network analysis, which identified 6 significantly molecular networks (Figures 5A-F and Supplementary Table 7). The functional analyses of genes within each network were carried out with DAVID, which found that network 1 (31 nodes and MCODE score=27.55) was mainly involved in multiple proteasome and ribosomal subunits to regulate UPS and ribosome large subunits assembly, translation, protein processing, and intracellular signaling pathway; network 2 (27 nodes and MCODE score=8.08) was mainly involved in intranuclear regulation of gene expression; network 3 (40 nodes and MCODE score=7.44) was mainly referred to cell movement; network 4 (43 nodes and MCODE score=5.24) mainly participated in cell adhesion and membrane organization; network 5 (16 nodes and MCODE score=5.20) did not have significant biological processes; and

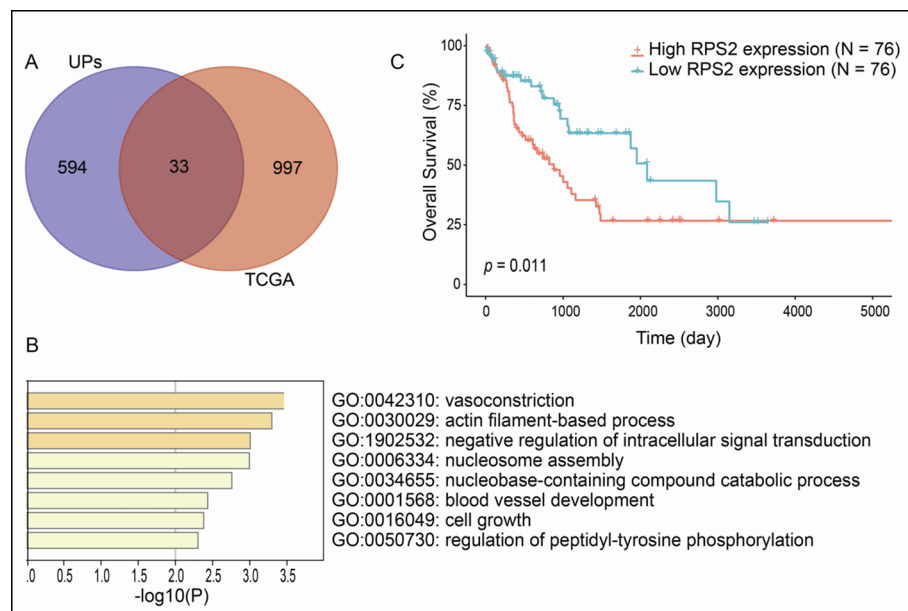


FIGURE 4

Overall survival-related UPs identified with overlapping analysis between 627 UPs and survival-related genes derived from TCGA database. (A) Venn diagram showed 33 molecules were associated with prognosis. (B) The biological processes involved in these prognostic related molecules. (C) Overall survival curve of RPS2.

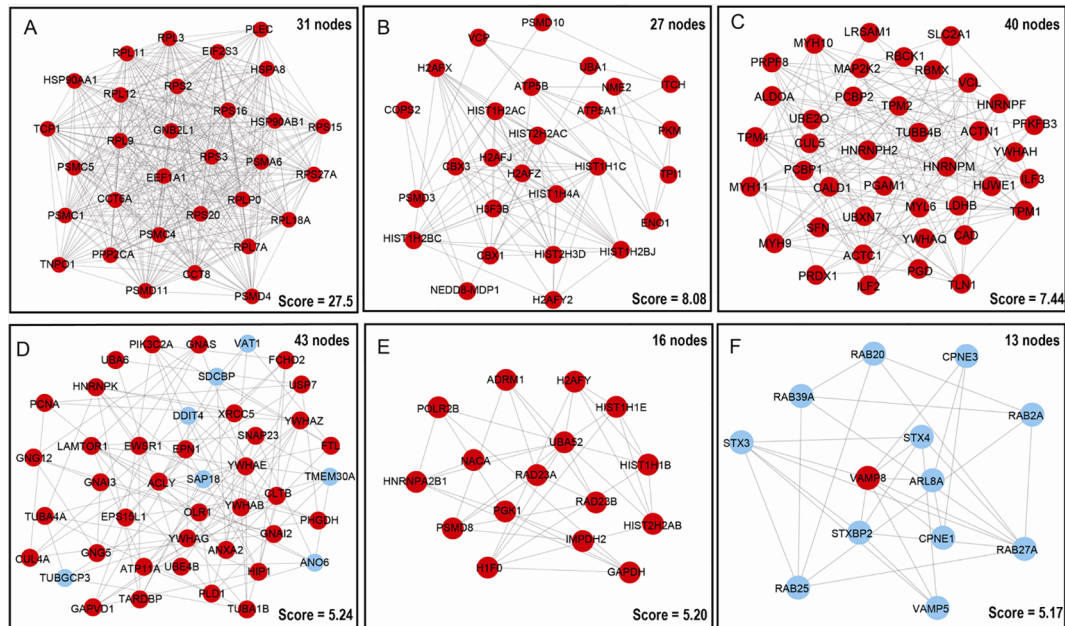


FIGURE 5

Molecular interaction modules and hub nodes based on PPI molecular networks of 627 UPs. (A–F) Six molecular interaction modules that meet screening criteria derived from the entire UPs PPI network. Red nodes represented the hub molecules. Blue node means it was not recognized as hub molecule due to low score.

network 6 (13 nodes and MCODE score=5.17) played important roles in protein transport and small GTPase-mediated signal transduction (Supplementary Table 8).

Moreover, 627 UPs were input into cytoHubba to determine hub molecules with 6 different topological algorithms, respectively; which identified 263 hub molecules with MCC, 232 with MNC, 268 with Degree, 278 with EPC, 347 with Closeness, and 334 with Raliality (Supplementary Table 9). Overlapped analysis of these six sets of hub molecules finally obtained 234 hub molecules (Supplementary Table 9). These finally determined 234 hub molecules were clustered into 5 functional categories, including cell-cell adhesion, ribosome-related biological process, proteasome-related biological process, cellular signaling pathways, and cellular energy metabolism (Supplementary Table 10). Interestingly, these results were also consistent with those results of GO enrichment analysis of 627 UPs (Supplementary Table 3).

Ubiquitination-mediated signaling pathways in LSCC

To reveal ubiquitination-mediated signaling pathway changes in LSCCs, 47 statistically significant pathways were revealed with KEGG pathway analysis of 627 UPs (Figure 6 and Supplementary Table 11). Multiple signaling pathways were

cancer-related pathways, including (i) ubiquitin-mediated proteolysis (10 UPs, and FDR =0.0184), ribosome complex (14 UPs, and FDR<0.01), ER-mediated protein processing (13 UPs, and FDR<0.01), proteasome complex (12 UPs, and FDR<0.01), and biosynthesis of amino acids (10UPs, and FDR<0.01), which was intracellular protein turnover-related pathways, and might disturb the synthesis-degradation balance of protein in tumorigenesis; (ii) PI3K-Akt signaling pathway (25 UPs, and FDR < 0.01), Ras signaling pathway (15 UPs, and FDR < 0.01), mTOR signaling pathway (10 UPs, and FDR = 0.03), HIF-1 signaling pathway (10 UPs, and FDR < 0.01), cell cycle (9 UPs, and FDR = 0.03), and apoptosis pathway (10 UPs, and FDR = 0.02), which might function in tumorigenesis; (iii) glycolysis/ gluconeogenesis (10 UPs, and FDR<0.01), carbon metabolism (12 UPs, and FDR<0.01), central carbon metabolism in cancer (9 UPs, and FDR<0.01), Fructose and mannose metabolism (5 UPs, and FDR=0.019), metabolomic pathways (46 UPs, and FDR=0.031), drug metabolism-other enzymes (5 UPs, and FDR=0.0457), and sphingolipid signaling pathway (11 UPs, and FDR<0.01), which were obviously metabolism-related pathways; (iv) Tight junction (16 UPs, and FDR<0.01), adherens junction (8 UPs, and FDR=0.0126), gap junction (8 UPs, and FDR<0.01), and non-homologous end-joining (3 UPs, and FDR<0.0356), which were involved in cell adherens and junction; (v) endocytosis (18 UPs, and FDR<0.01), and SNARE interactions in vesicular transport (5 UPs, and FDR=0.0118).

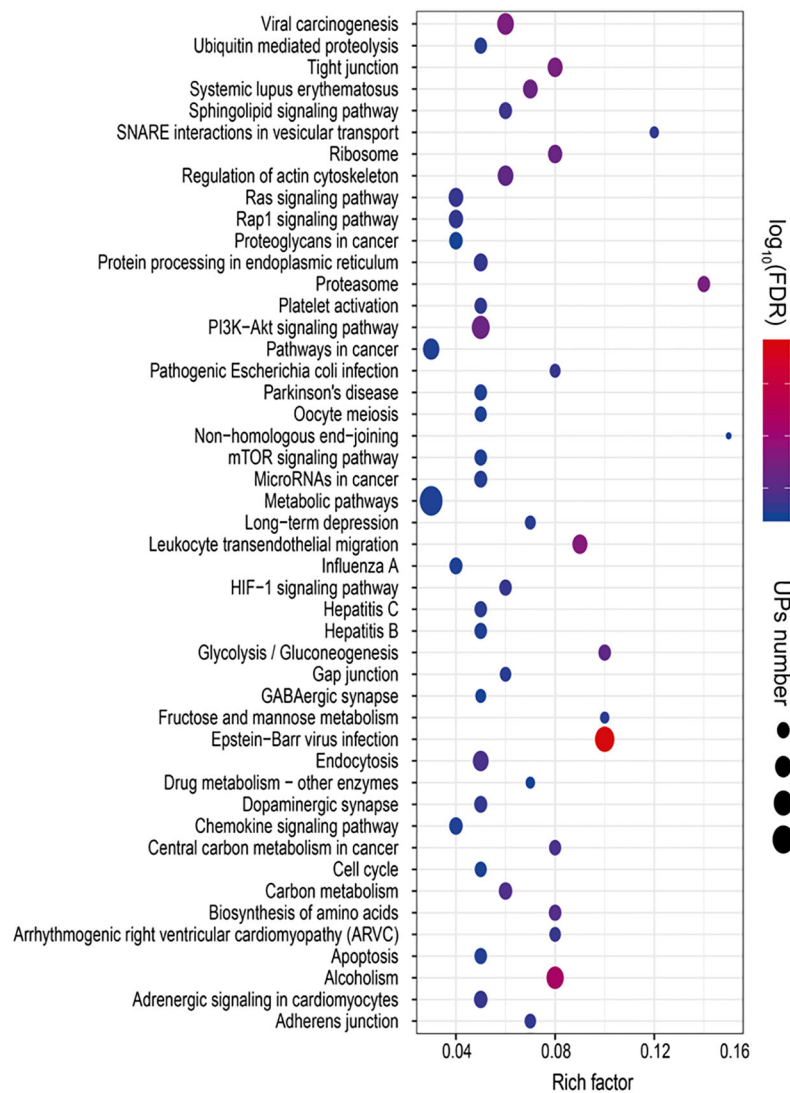


FIGURE 6

Statistically significant signaling pathways identified with KEGG pathway analysis of 627 UPs. A total of 47 KEGG pathways was significantly enriched from those UPs ($p < 0.05$; $\text{FDR} < 0.05$).

which might be substance transport-related pathways; (vi) dopaminergic synapse (11 UPs, and $\text{FDR}=0.0115$), and GABAergic synapse (7 UPs, and $\text{FDR}=0.0415$), which function in synapse pathway; and (vii) others pathways such as chemokine signaling pathway (12 UPs, and $\text{FDR}=0.0287$), Rap1 signaling pathway (14 UPs, and $\text{FDR}=0.0124$), proteoglycans in cancer (12 UPs, and $\text{FDR}=0.0466$), pathways in cancer (20 UPs, and $\text{FDR}=0.0287$), microRNAs in cancer (11 UPs, and $\text{FDR}=0.0208$), leukocyte transendothelial migration (16 UPs, and $\text{FDR}<0.01$), regulation of actin cytoskeleton (18 UPs, and $\text{FDR}<0.01$), and platelet activation (10 UPs, and $\text{FDR}=0.0129$). These ubiquitination-mediated cancer-related signaling pathways clearly demonstrated that ubiquitination

played important roles in LSCC pathophysiological processes, and that ubiquitination was not only involved in the synthesis-degradation process of protein, but also in other multiple cancer-related signaling pathways.

As described in Table 1, multiple proteins are decreased or increased in LSCC tissues relative to control tissues, which might be due to the alteration of ubiquitination-mediated protein synthesis-degradation system. (i) Ribosome, the central site for protein synthesis or translation, is a dense ribonucleoprotein particle that includes two subunits (large and small), and each subunit contains one rRNA and many different protein molecules. The small subunit is responsible for sequence-specific recognition of the template mRNA, such as the

TABLE 1 Differentially expressed proteins with significantly ubiquitination alterations in LSCC tissues compared to controls.

Accession No.	Gene name	Protein name	Ubiquitinated peptides	Ubiquitinated positions	Differentially ubiquitinated Sites Ratio (T/N)	Differentially expressed protein Ratio (T/N)
A0A024R1N1	MYH9	Myosin, heavy polypeptide 9, non-muscle, isoform CRA_a	DYVQK*AQTK	403	6.391	1.66
			VK*PLLQVSR	835	8.094	
			VAAYDKLEK*TK	1413	T+/N-	
			K*AGKLDPHLVLDQLR	679	T+/N-	
A0A024R3E3	APOA1	Apolipoprotein A-I, isoform CRA_a	DYVSQFEGSALGK*QLNLK	64	0.039	4.80
			VSFLSALEEYTK*K*	263	T-/N+	
			VSFLSALEEYTK*K	262	T-/N+	
			VQPYLDDDFQKK*	131	T-/N+	
A0A024RAY2	KRT18	Keratin 18, isoform CRA_a	NLK*ASLENSLR	317	9.286	0.52
A0A087WUZ3		Spectrin, beta, erythrocytic (Includes spherocytosis, clinical type I) variant (Fragment)	IHCLENVDK*ALQFLK	118	T-/N+	0.68
A0A0D9SGC1	MYO6	Unconventional myosin-VI	SLDSYPVTSK*NDGTRPK	1045	T-/N+	0.24
A0A0G2JW1	HSPA1B	Heat shock 70 kDa protein 1B	LIGDAAK*NQVALNPQNTVFDAK	57	2.302	0.62
			AMTK*DNNLLGR	452	3.120	
			MVQEAEK*YKADEVQR	525	3.486	
			YK*AEDEVQR	527	3.554	
			RK*ELEQVCNPIISGLYQGAGGPGGGFGAQQGPK*	598	8.518	
			QATK*DAGVIAGLNVLR	160	10.868	
			ANK*TTITNDK	501	14.562	
			K*FGDPVVQSDMK	78	T+/N-	
			VLDK*CQEVISWLDANTLAEKDEFEHK	574	T+/N-	
A0A0S2Z3S6	CYBB	Cytochrome b-245 beta polypeptide isoform 1 (Fragment)	VVITK*VVTHPFK	299	T+/N-	1.64
A8K287	SNAP23	Synaptosomal-associated protein	TITMLDEQK*EQLNR	49	T+/N-	0.60
B2R5T5	PRKAR1A	Protein kinase, cAMP-dependent, regulatory, type I, alpha (Tissue specific extingisher 1), isoform CRA_a	VSILESLDK*WER	261	0.086	0.43
B2R6J2	EZR	Ezrin	FGDYNK*EVHK	139	0.151	0.33
D9YZU5	HBD	Delta globin	K*VLGAFSDGLAHLNLIK	67	0.032	1.42
			VHLTPEEK*SAVTALWGK	9	0.052	
			FFESFGDLSTPDAVMGNPKVK*	62	0.056	
			GTFATLSELHCDK*LHVDPENFR	96	0.096	

(Continued)

TABLE 1 Continued

Accession No.	Gene name	Protein name	Ubiquitinated peptides	Ubiquitinated positions	Differentially ubiquitinated Sites Ratio (T/N)	Differentially expressed protein Ratio (T/N)
G3V1N2	HBA2	HCG1745306, isoform CRA_a	VVAGVANALAHK*YH	145	0.165	0.64
			VLGAFSDGLAHLNLK*GTFATLSELHCDK	83	T-/N+	
			FFESFGDLSTPDAVMGNPK*VK	60	T-/N+	
			TYFPHFDLSHGSAQVK*GHGK	25	0.045	
O95864	FADS2	Fatty acid desaturase 2	MFLSFPTTK*TYFPHFDLSHGSAQVK	9	0.142	0.65
			EVSVPFTFSWEEIQK*HNLR	28	28.124	
P00915	CA1	Carbonic anhydrase 1	HDTSLK*PISVSYNPATAK	46	0.078	7.70
			TSETK*HDTSLKPISVSYNPATAK	40	T-/N+	
			ASPDWGYDDK*NGPEQWSK	11	T-/N+	
P04075	ALDOC	Fructose-bisphosphate aldolase	YASICQQNGIVPIVEPEILPDGDHDLK*R	200	3.801	1.60
P04075	ALDOA	Fructose-bisphosphate aldolase A	VDK*GVVPLAGTNGETTTQGLDGLSER	111	3.837	0.63
P04083	ANXA1	Annexin A1	AAMK*GLGTDEDLIEILASR	128	0.388	1.58
			CATSK*PAFFAEK	274	6.312	
			DLAK*DITSDTSGDFR	166	T+/N-	
P04406	GAPDH	Glyceraldehyde-3-phosphate dehydrogenase	TVDGPGSK*LWR	194	2.669	6.10
			GALQNIIPASTGAAK*AVGK	215	3.215	
			VVK*QASEGPLK	263	3.450	
			VIHDNFGIVEGLMTTVHAIATQK*TVDGPGSK	186	25.358	
			AGAHLQGGAK*R	117	T+/N-	
P04792	HSPB1	Heat shock protein beta-1	DGVVEITGK*HEER	123	30.905	5.80
			AQLGGPEAAK*SDETAAK	198	T+/N-	
P04899	GNAS	Guanine nucleotide-binding protein G(s) subunit alpha isoforms Xlas	LLLLGAGESGK*STIVK	46	T+/N-	9.50
P06454	PTMA	Prothymosin alpha	SDAAVDTSSIEITK*DLK	15	T+/N-	5.60
P06576	ATP5B	ATP synthase subunit beta, mitochondrial	VLDSGAPIK*IPVGPETLGR	133	T+/N-	2.68
P06702	S100A9	Protein S100-A9	TCK*MSQLER	4	0.172	3.18
			LGHPTLNQGEFK*ELVR	38	T+/N-	
P08069	IGF1R	Insulin-like growth factor 1 receptor	VAIK*TVNEAASMR	1033	T+/N-	5.50
P08670	VIM	Vimentin	QYVESVAAK*NLQEAEEWYK	282	0.129	2.40
			K*VESLQEEIAFLK	223	0.169	
			SK*FADLSEAANR	294	0.204	
			RQVDQLTNDK*AR	168	0.210	
			TLLIK*TVETR	445	0.258	
			FLEQQNK*ILLAELEQLKGQGK	129	0.293	
			ETNLDSLPLVDTHSK*R	439	0.361	

(Continued)

TABLE 1 Continued

Accession No.	Gene name	Protein name	Ubiquitinated peptides	Ubiquitinated positions	Differentially ubiquitinated Sites Ratio (T/N)	Differentially expressed protein Ratio (T/N)
P08670	DES	Mutant desmin	RQVQSLTCEVDALK*GTNESLER	334	0.363	
			LREK*LQEEMLQR	188	0.406	
			ILLAELEQLK*GQGK	139	0.491	
P09936	UCHL1	Ubiquitin carboxyl-terminal hydrolase isozyme L1	K*LLEGEESR	402	0.264	0.50
P14735	IDE	Insulin-degrading enzyme	MQLK*PMEINPEMLNK	4	16.321	0.58
			CFEK*NEAIQAAHDAVAQEGQCR	135	T+/N-	
			EVNAVDSEHEK*NVMNDAWR	192	0.039	1.86
P16070	CD44	CD44 antigen	SQEMVHLVNK*ESSETPDQFMTADETR	715	4.018	6.80
P16152	CBR1	Carbonyl reductase [NADPH] 1	ALK*SCSPELQK	148	T+/N-	5.80
P20700	LMNB1	Lamin-B1	K*QLADETLLK	182	T+/N-	0.47
			IESLSSQLSNLQK*ESR	312	T+/N-	
P27708	CAD	CAD protein	NK*SELLPTVR	1325	7.916	1.73
			DDQLK*VIECNVR	1211	T+/N-	
			LSSFVTK*GYR	1411	T+/N-	
			LGPVK*GEVRPELGSR	1657	T+/N-	
P29353	SHC1	SHC-transforming protein 1	DLFDMK*PFEDALR	462	T+/N-	1.79
P31946	YWHAB	14-3-3 protein beta/alpha	VISSIEQK*TER	70	0.045	0.60
P46734	MAP2K3	Dual specificity mitogen-activated protein kinase kinase 3	ATVNSQEYK*R	105	T+/N-	0.74
P48507	GCLM	Glutamate-cysteine ligase regulatory subunit	EFPDVLECTVSHAVEK*INPDER	80	T+/N-	2.61
P62249	RPS16	40S ribosomal protein S16	LLEPVLLGK*ER	60	T+/N-	0.47
P63218	GNG5	Guanine nucleotide-binding protein G (I)/G(S)/G(O) subunit gamma-5	SGSSSVAAMKK*	12	T-/N+	4.70
P67936	TPM4	Tropomyosin alpha-4 chain	AGLNSLEAVK*R	11	T+/N-	3.00
P68104	EEF1A1	Elongation factor 1-alpha 1	AAGAGK*VTK	450	26.878	0.61
			QTVAVGVK*AVDKK	439	108.563	
			QLIVGVNK*MDSTEPPYSQK	154	T+/N-	
			FEK*EAAEMGK	44	T+/N-	
			VETGVLK*PGMVVTFAPVNVTTVEK	273	T+/N-	
			KLEDGPK*FLK	392	T+/N-	
P98172	EFNB1	Ephrin-B1	AAALSSTLASPK*GGSGTAGTEPSDIIIPLR	289	T+/N-	2.38
Q12965	MYO1E	Unconventional myosin-1e	DIILQSNPLLEAFGNAK*TVR	160	T+/N-	0.61
Q4W4Y1	DRIP4	Dopamine receptor interacting protein 4	MK*QSNNEANLR	640	2.767	1.49

(Continued)

TABLE 1 Continued

Accession No.	Gene name	Protein name	Ubiquitinated peptides	Ubiquitinated positions	Differentially ubiquitinated Sites Ratio (T/N)	Differentially expressed protein Ratio (T/N)
Q6IA69	NADSYN1	Glutamine-dependent NAD(+) synthetase	HK*MTTLTPAYHAENYSPEDNR	649	T+/N-	4.20
Q6IBN1	HNRPK	HNRPK protein	IILDLISESPIK*GR HESGASIK*IDEPLEGSER ILLQSK*NAGAVIGK LLHQSLAGGIIGVK*GAK	219 422 52 163	T-/N+ T+/N- T+/N-	4.70

The symbol * means K* = ubiquitinated lysine residue. T+/N- means that ubiquitination occurred in tumors but not in controls. T-/N+ means that ubiquitination occurred in controls but not in tumors.

recognition of the initial part, the interaction of codon with anti-codon, and the binding site of mRNA is also on this subunit. The large subunit is responsible for carrying amino acids and tRNAs, including peptide bond formation, and peptidyl-RAN binding. In this study, 7 UPs [ribosomal proteins L3e (P39023), L11e (P62913), L9e (P32969), L7Ae (P62424), L40e (P62987), L18Ae (Q02543), and L12e (A0A024RBS2)] were identified in large subunit with significantly increased ubiquitination level in ribosomal proteins L11e, L12e, L18Ae, and L40e in LSCC tissues relative to controls, and 6 UPs [ribosomal proteins S20e (P60866), S3e (P23396), S2e (P15880), S16e (P62249),

S27Ae (B2RDW1), and S9e (A0A024R4M0)] in small subunit with significantly increased ubiquitination level in ribosomal proteins S3e, S9e, S16e, and S27e in LSCC tissues relative to controls (Figure 7). (ii) Endoplasmic reticulum (ER) is the cellular organelle, and is responsible for the assembly of multi-subunit proteins, formation of proper conformation of protein, protein secretion, lipid biosynthesis, and calcium homeostasis. The correctly folded proteins are transited into the Golgi complex. ER stress occurs under normal or pathophysiological conditions, which can lead to accumulation of misfolded proteins in the ER lumen to restore the correct fold. Proteins

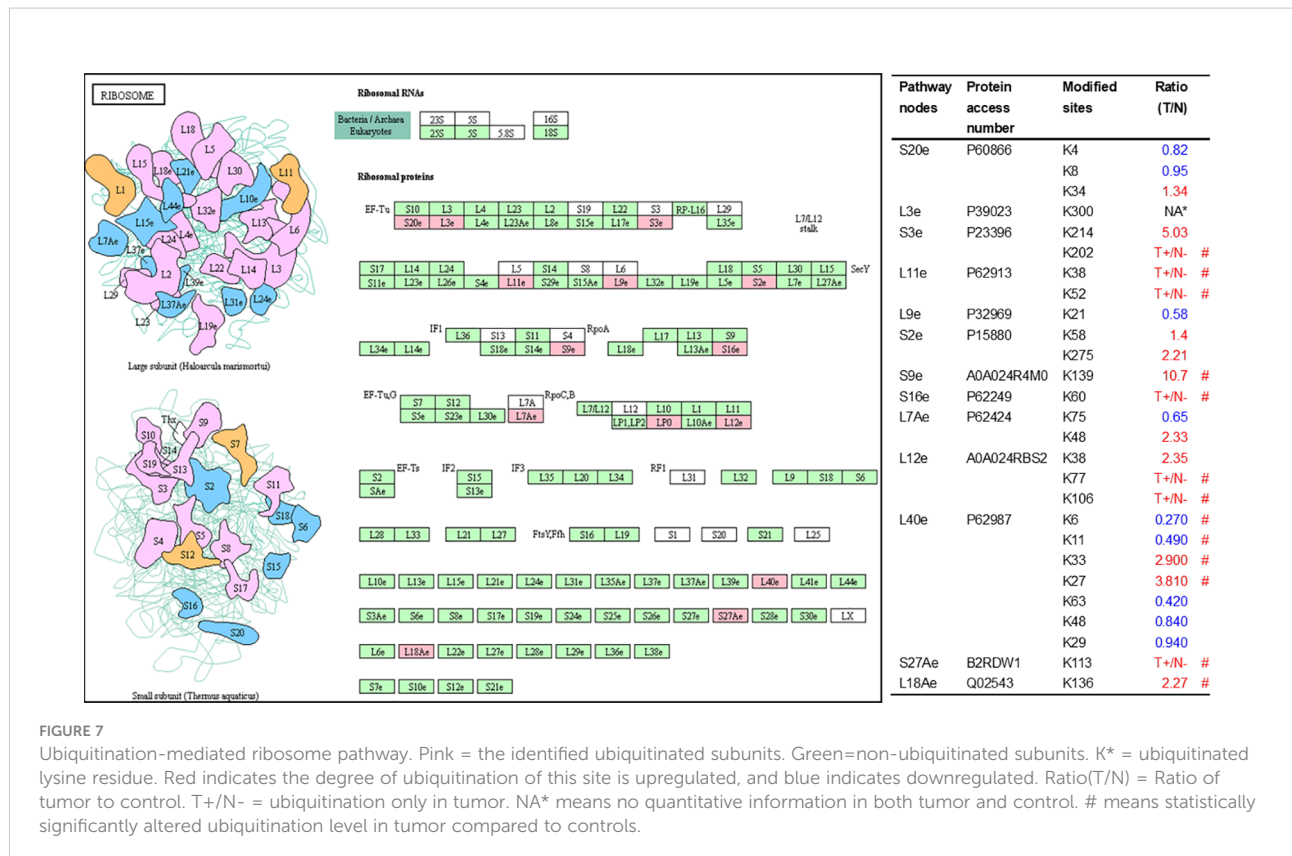


FIGURE 7

Ubiquitination-mediated ribosome pathway. Pink = the identified ubiquitinated subunits. Green = non-ubiquitinated subunits. K* = ubiquitinated lysine residue. Red indicates the degree of ubiquitination of this site is upregulated, and blue indicates downregulated. Ratio(T/N) = Ratio of tumor to control. T+/N- = ubiquitination only in tumor. NA* means no quantitative information in both tumor and control. # means statistically significantly altered ubiquitination level in tumor compared to controls.

that ultimately failed to recover to normal folding were transported to the proteasome for ubiquitination-mediated degradation, which is named as ER-associated degradation (ERAD) (31). Accumulation of misfolded proteins can also lead to ER stress and ultimately lead to the activation of a range of signaling pathways, which was called UPR (unfolded protein response). In the case of severely damaged cells, UPR is insufficient to restore the function of ER, when the cells undergo apoptosis. In this study, 13 UPs [EIF2AK2 (P19525), CAPN1 (P07384), BCAP31 (P51572), EL52 (K9JA46), YOD1 (Q5VVQ6), UBE4B (O95155), RAD23B (P54727), NGLY1 (Q96IV0), VCP (P55072), HSPA8 (P11142), DNAJB1 (P25685), HSP90AB1 (A0A024RD80), and RAD23A (A0A024R7G8)] with 39 ubiquitination sites were identified in protein ER processing pathway, with significantly decreased ubiquitination levels in proteins YOD1, and VCP (K8, K18, K109, K389, K651, K658, and K668), and with significantly increased ubiquitination levels in proteins BCAP31, EL52, RAD23B, VCP(K217, and K614), HSPA8, and DNAJB1

(Figure 8). (iii) Ubiquitination was multiple enzymatic reaction process that requires enzymes E1, E2, and E3. In this study, 9 Ups, including six E3s [UBE4B (O95155), CUL5 (Q93034), ITCH (Q96J02), CUL4A (Q13619), PML (P29590), and HUWE1 (A0A024R9W5)], two E2s [UBE2O (Q9C0C9), and UBE2N (P61088)], and one E1 [UBE1 (A0A024RDB0)], were identified, with significantly decreased ubiquitination levels in E2 UBE2N, and with significantly increased ubiquitination levels at E3s ITCH, HUWE1, and CUL4A, in LSCC tissues relative to controls (Figure 9). For these six E3s, HUWE1 and ITCH were HECT type E3, UBE4B were U-box type E3, PML was single RING-finger type E3, and CUL5 and CUL4A were multi subunit RING-finger type E3. (iv) Proteasome is the crucial machine to response for ubiquitin-mediated proteolysis, which includes one 20S core, one 19S regulatory lid (PA700), and one 19S regulatory base (PA700) in the 26S proteasome complex. The 20S core particle provides an enclosed cavity where proteins are degraded. This present study identified 7 UPs (Rpn13, and Rpt 1-6) in PA700 (Base) with significantly increased ubiquitination levels

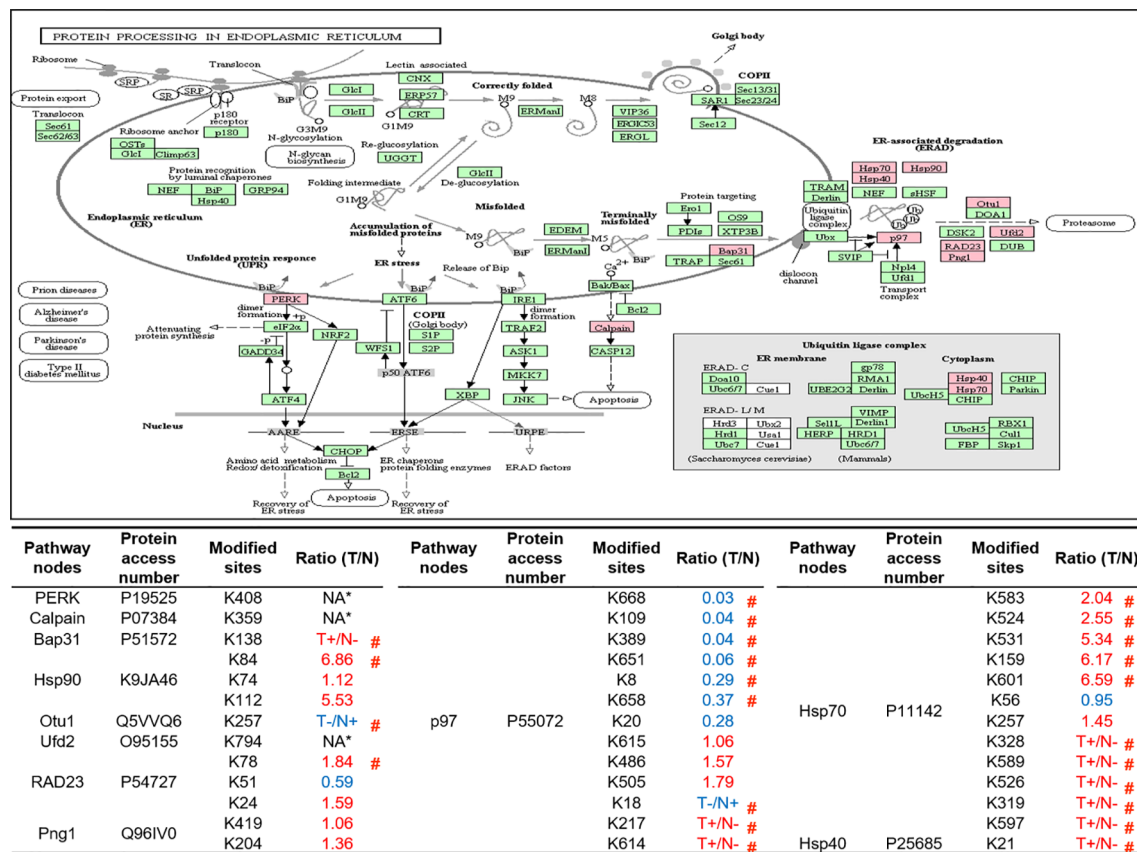


FIGURE 8

Ubiquitination-mediated endoplasmic reticulum protein processing pathway. Pink = the identified ubiquitinated subunits. Green = non-ubiquitinated subunits. K* = ubiquitinated lysine residue. Red indicates the degree of ubiquitination of this site is upregulated, and blue indicates downregulated. Ratio(T/N) = Ratio of tumor to control. T+/N- = ubiquitination only in tumor. T-/N+ = ubiquitination only in control. NA* means no quantitative information in both tumor and control. # means statistically significantly altered ubiquitination level in tumor compared to controls.

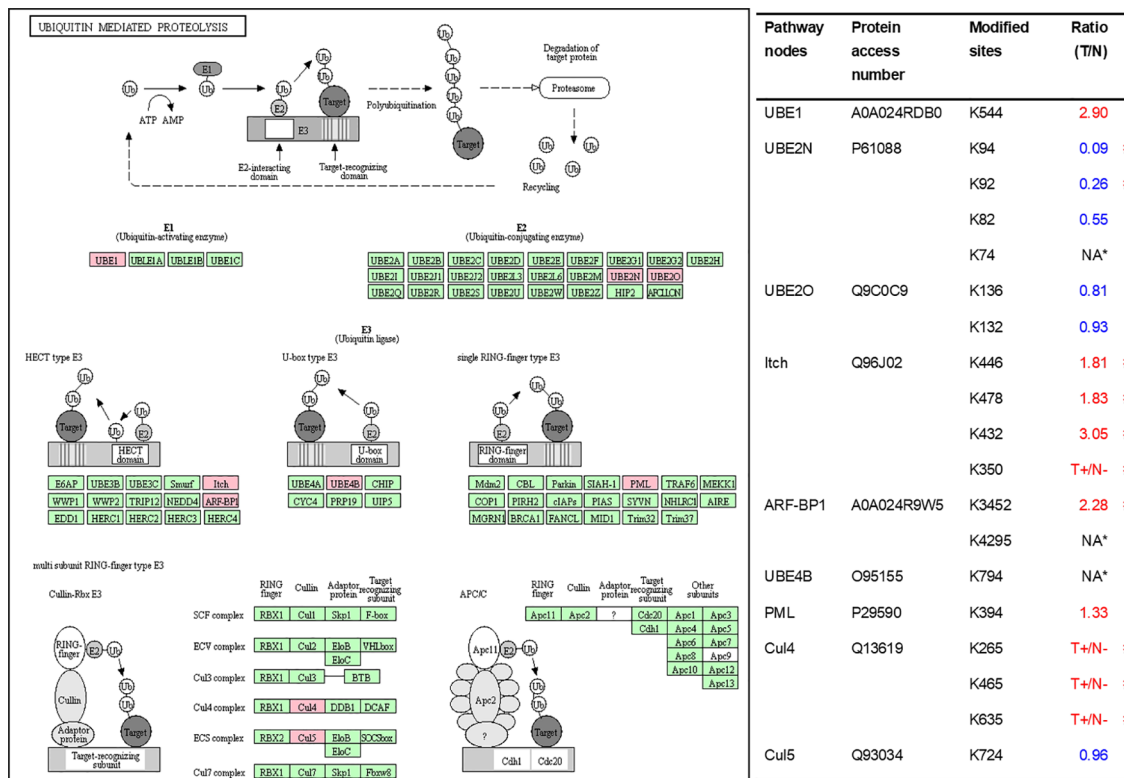


FIGURE 9

Ubiquitination-mediated UPS-related enzymes. Pink = the identified ubiquitinated subunits. Green = non-ubiquitinated subunits. K* = ubiquitinated lysine residue. Red indicates the degree of ubiquitination of this site is upregulated, and blue indicates downregulated. Ratio(T/N) = Ratio of tumor to control. T+/N- = ubiquitination only in tumor. NA* means no quantitative information in both tumor and control. # means statistically significantly altered ubiquitination level in tumor compared to controls.

in proteins Rpn13, Rpt1, Rpt3, Rpt4, Rpt5 (K276 and K372), and Rpt6, and significantly decreased ubiquitination level in protein Rpt 5 (K53); and 5 UPs (Rpn 3, 5, 6, 10, and 12) in PA700 (Lid) with significantly increased ubiquitination level, in human LSCC tissues relative to controls (Figure 10), but no any ubiquitination was found in the 20S core.

Overlapping analysis of differentially ubiquitinated proteins and differentially expressed proteins in LSCC

One of the consequences of ubiquitination is to degrade proteins. Those DEPs with differentially ubiquitinated modifications might have more relevance to tumorigenesis. A set of 265 DEP data in LSCC tissues compared to controls extracting from the published data (32–36) (Supplementary Table 12) were compared to this set of 464 DUP data with 789 differentially ubiquitinated sites in LSCC tissues compared to controls (Supplementary Table 13). A total of 45 DEPs in LSCC

were found to have significantly differentially ubiquitinated modifications (Table 1). When one analyzed the relationship between DUP and DEP in LSCC, those 45 DEPs were grouped into 5 categories (Table 2): (i) When the ubiquitination level was decreased, the protein expression level was increased, including APOA1, HBD, CA1, VIM, IDE, and GNG5; (ii) When the ubiquitination level was increased, the protein expression level was decreased, including KRT18, HSPA1B, SNAP23, FADS2, ALDOA, UCHL1, LMNB1, MAP2K3, RPS16, EEF1A1, and MYO1E; (iii) When the ubiquitination level was decreased, the protein expression level was decreased, including MYO6, PRKAR1A, EZR, HBA2, DES, YWHAB, and erythrocytic spectrin beta; (iv) When the ubiquitination level was increased, the protein expression level was increased, including MYH9, CYBB, ALDOC, GAPDH, HSPB1, GNAS, PTMA, ATP5B, IGF1R, CD44, CBRI, CAD, SHC1, GCLM, TMP4, EFN1B, DRIP4, and NADSYN1; and (v) when a protein existed both increased and decreased ubiquitination sites, the protein expression level was increased, including ANXA1, S100A9, and HNRPK.

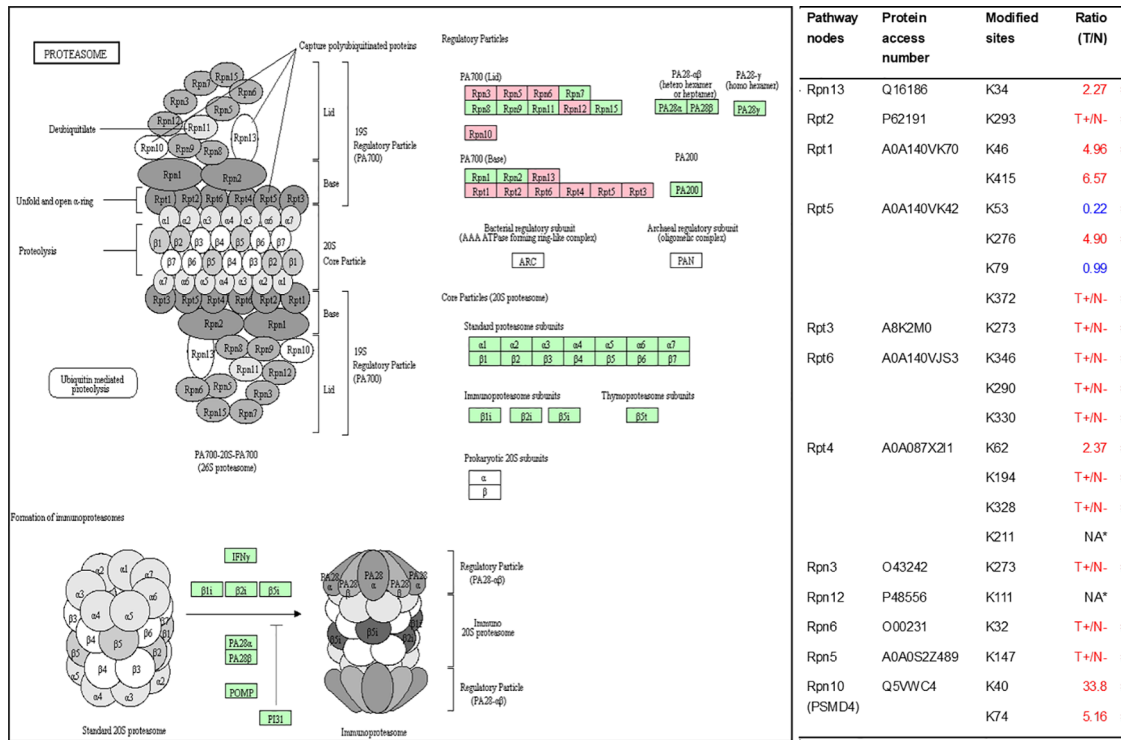


FIGURE 10

Ubiquitination-mediated proteasome pathway. Pink=the identified ubiquitinated subunits. Green = non-ubiquitinated subunits. K* = ubiquitinated lysine residue. Red indicates the degree of ubiquitination of this site is upregulated, and blue indicates downregulated. Ratio(T/N) = Ratio of tumor to control. T+/N- = ubiquitination only in tumor. NA* means no quantitative information in both tumor and control. # means statistically significantly altered ubiquitination level in tumor compared to controls.

Discussion

Protein ubiquitination profile and ubiquitination-mediated signaling pathways in LSCC

To investigate ubiquitination profile and its potential functions in LSCC, and to promote PPPM of LSCC, label-free quantitative proteomics was used to investigate ubiquitination in LSCC tissues. This present study provided the first comprehensive, quantitative ubiquitination profile in LSCC tissues. A total of 627 UPs with 1209

ubiquitination sites were identified, and 93.7% of identified ubiquitination sites had quantitative intensity. These UPs were involved in multiple functional categories, cellular biological processes, and signaling pathways in LSCC. In total, 47 statistically significant pathways were identified to involve UPs in LSCC, and most of these signaling pathways were cancer-related pathways, including ubiquitin-mediated proteolysis, ribosome complex, ER-mediated protein processing, proteasome complex, biosynthesis of amino acids, PI3K-Akt signaling pathway, Ras signaling pathway, mTOR signaling pathway, HIF-1 signaling pathway, cell cycle, apoptosis pathway, glycolysis/gluconeogenesis,

TABLE 2 The relationship between DUP and DEP in LSCC tissues compared to controls.

DUP	DEP	Proteins
-	+	APOA1, HBD, CA1, VIM, IDE, GNG5
+	-	KRT18, HSPA1B, SNAP23, FADS2, ALDOA, UCHL1, LMNB1, MAP2K3, RPS16, EEF1A1, MYO1E
-	-	MYO6, PRKARIA, EZR, HBA2, DES, YWHAB, Erythrocytic spectrin beta
+	+	MYH9, CYBB, ALDOC, GAPDH, HSPB1, GNAS, PTMA, ATP5B, IGF1R, CD44, CBR1, CAD, SHC1, GCLM, TMP4, EFN1, DRIP4, NADSYN1
+/-	+	ANXA1, S100A9, HNRPK

For DUP, - means the significantly decreased ubiquitination level; + means the significantly increased ubiquitination level; and +/- means that the significantly increased and decreased ubiquitination sites existed in a protein. For DEP, + means upregulation; and - means downregulation.

carbon metabolism, central carbon metabolism in cancer, fructose and mannose metabolism, metabolomic pathways, drug metabolism-other enzymes, sphingolipid signaling pathway, tight junction, adherens junction, gap junction, non-homologous end-joining, endocytosis, SNARE interactions in vesicular transport, dopaminergic synapse, GABAergic synapse, chemokine signaling pathway, Rap1 signaling pathway, proteoglycans in cancer, pathways in cancer, microRNAs in cancer, leukocyte transendothelial migration, regulation of actin cytoskeleton, and platelet activation. These ubiquitination-mediated signaling pathways provide the functional profiles of ubiquitination in LSCC.

Ubiquitination-mediated tumor protein turnover in LSCC

It is well-known that one of main functions of ubiquitination is involved in protein degradation, and participates in protein turnover in tumor pathophysiological processes. Interestingly, this study found that ubiquitination was significantly involved in four protein turnover-associated pathways, including ribosome complex, ubiquitin-mediated proteolysis, ER-mediated protein processing, and proteasome complex pathways, which are discussed in detailed here.

Proteins are vital parts of living organisms, and are in dynamic balance between generation and degradation. Protein turnover is the protein synthesis-degradation balance, which gives cells the flexibility to adjust the abundance and function of the protein in response to various intracellular or extracellular stimuli (37). Protein synthesis is determined by both transcription and translation. The mRNA transcribed into the cytoplasm and binds to the ribosome to begin the process of protein synthesis. The overall activity of ribosome and the rate of translation initiation and elongation have an important effect on the rate of protein synthesis. The newly synthesized protein does not have a spatial structure and corresponding functions, which needs to be folded and assembled in ER. The processing time of different proteins in ER is also different. The UPS and autophagy are the main pathways for protein degradation (38, 39). The former selectively degrades the misfolded proteins and short half-life proteins that have been labeled with ubiquitin in the proteasome, while the latter transports denatured long-lived proteins and damaged or excess organelles to the lysosome for degradation. The ability to adjust protein abundances in a timely and precise manner based on external environmental stimuli is critical to maintain the normal function of cells. Protein turnover abnormalities are associated with the development of multiple diseases, including neurodegenerative diseases (40, 41) and tumors (42, 43). Targeting altered protein turnover provides new opportunities and challenges to develop anti-tumor drugs (44).

Studies demonstrate that multiple ribosomal subunits have been ubiquitinated in eukaryotes (45–47). This study also found 13 ubiquitinated ribosome subunits in LSCC, which demonstrates the important regulatory roles of ubiquitination in ribosomal complex. Ubiquitination affects protein turnover by affecting the function of ribosomes in several ways.

First, ubiquitination regulates multiple steps of ribosome biogenesis (48), which involves the production and correct assembly of rRNAs and ribosomal proteins. Abnormal ribosome biogenesis inevitably affects the turnover of intracellular proteins. However, this study did not find the ribosome biogenesis pathway in KEGG enrichment analysis, which suggests that ubiquitination might not affect protein turnover by participating in regulating ribosome biogenesis in LSCC. Moreover, ubiquitination of ribosomal proteins regulates ribosome-associated quality control (RQC) (49, 50). Ribosomes are not only responsible for protein synthesis, but also execute RQC to minimize production of aberrant proteins. Many factors cause abnormal protein synthesis in ribosomes. RQC is a biologically evolved surveillance mechanism that timely terminates the protein synthesis of ribosomes, and initiates corresponding pathways to degrade nascent polypeptides when there exist interrupted translation (51). Obviously, dysfunction of RQC results in accumulating abnormal proteins in cells, which eventually affects the protein turnover. Study showed that the poly (A) tails of mature mRNA stalled ribosomes, repressed downstream translation, and initiated RQC; this is a process known as ribosome stall resolution (49). One study showed that in the initiation of this process, it is essential for ubiquitin ligase ZNF598 to catalyze ubiquitination at residue K₈ in RPS20 (P60866) and at residues K₁₃₈ and K₁₃₉ in RPS10, and the ubiquitination failure of RPS20 or RPS10 would lead to defective resolution of stalled ribosomes (50). Another study also found that ZNF598 primarily mono-ubiquitinated two lysine residues K₄ and K₈ in RPS20, which was required to stall ribosomes during poly (A) translation (49). In the yeast model, study found that ubiquitination at residue K₈ in 40S ribosomal protein uS10 (corresponding to RPS20 in human) catalyzed by E3 ubiquitin ligase Hel2 switched on RQC (52). Those studies showed that ubiquitination at residue K₈ in RPS20 was species conservation, and played a pivotal role in RQC pathways. Besides RPS20, recent study demonstrated that the balance between mono-ubiquitination at residue K₂₁₄ in RPS3 (P23396) catalyzed by RNF123 E3 ligase and deubiquitination by USP10, also participated in the regulation of RQC (53). This study found ubiquitination level was decreased at residue K₈ (T/N ratio=0.95, *P* value = 0.78) in RPS20 and increased at residue K₂₁₄ (T/N ratio=5.03, *P* value = 0.32) in RPS3, which means that the impaired RQC in LSCC tissue may contribute to the abnormal protein turnover. Further, ribosome ubiquitination participated in reprogramming of ribosomal protein translation

that was induced by unfolded protein reaction (UPR). UPR not only induced ER stress and disturbed protein homeostasis, but also reprogrammed translation; and persistent UPR might lead to cell death. Reprogramming of ribosomal protein translation is an intracellular response to protein homeostasis, and it can also affect the turnover of intracellular proteins. One study demonstrated that ubiquitination at residues K₅₈ or K₂₇₅ in RPS2 (P15880) and at residue K₈ in RPS20 participate in UPR-induced ribosomal translation reprogram, and these two proteins without ubiquitination at these residues promoted UPR-induced cell death (54). This study identified ubiquitination at residues K₅₈ (T/N = 1.4; *P* value = 0.06) and K₂₇₅ (T/N = 2.21; *P* value = 0.21) in RPS2 increased in LSCC. Therefore, ubiquitination in proteins RPS3, RPS20, and RPS2 in 40S subunits play an important role in ribosome-related protein turnover regulation.

Both ribosome and ER are indispensable organelles for intracellular protein homeostasis and protein turnover, and this study demonstrates that ubiquitination also has regulatory effects on ER. Among the various biological processes of ER, UPR and ERAD are essential for maintaining protein homeostasis and turnover. The former regulates the expression of multiple downstream genes through at least three pathways to recover UPR-induced ER stress (55). The latter relieves ER stress through the process of retro-translocation (terminally misfolded proteins were translocated from the ER lumen into the cytoplasm through the translocation pore in the ER membrane) and ultimately degraded by proteasome (56). Our results showed that UPs mainly concentrated in the above two biological processes. For example, study demonstrated that EIF2AK2 (P19525) was responsible for starting a branch of the UPR. When ER stress was activated, EIF2AK2 itself was oligomerized and phosphorylated, and also ubiquitously translational initiation factor eIF2a was indirectly inactivated to inhibit translation of mRNA. Thus, EIF2AK2 inhibits the flux of protein to enter ER to alleviate ER stress and restore protein homeostasis (55). This study qualitatively identified the ubiquitination at residue K₄₀₈ in EIF2AK2. Currently, the exact effect of ubiquitination on the function of EIF2AK2 is not clear, but study reported that the residues K₆₉ and K₁₅₉ have been ISGylated, one type of ubiquitin-like modification, that down-regulated protein translation (57). During ERAD, studies showed that molecular chaperones not only assist in folding of the protein in ER, but also play a variety of important functions to ensure ERAD (58). These molecular chaperones assist degradation through substrate recognition and preventing substrate aggregation (59). This study identified the ubiquitination of three molecular chaperones (HSPA8, DNAJB1 and K9JA46) indicating that ubiquitination can affect

the function of molecular chaperones, which in turn affects ERAD and protein turnover.

The UPS is another determinant of intracellular protein turnover, because the degradation of many proteins is carried out by UPS in mammalian cells (60). Under physiological conditions, the activity of UPS is dynamically regulated by different signaling pathways in response to various stimuli (60). As mentioned above, UPS contains a large number of components, so dysfunction of any one component can lead to abnormal protein degradation, which eventually affects protein turnover. In this study, it was found that 11 proteasome subunits (all belong to the 19S regulatory subunit) and 9 UPS-related enzymes were ubiquitinated, which revealed that ubiquitination can regulate protein turnover by regulating proteasome activity and UPS-related enzymes.

The 26S proteasome is a core component of UPS, and proteins labeled with K48-linked polyubiquitin chains are recognized by its 19S regulatory subunit (RS) and degraded by its 20S core subunit (CS) (61, 62). A variety of factors affect proteasome activity, such as proteasome biogenesis and PTMs (63). For example, the RS has two subunits (lid and base), among which the base assembly is associated with 4 RS assembly chaperones (RACs): Rpn14 (PAAF1), S5b (PSMD5), p28 (PSMD10), and p27 (PSMD9) (64). Loss of these chaperones leads to base subcomplex of RS assembly defect (65). This study identified ubiquitination at residues K₂₃ (no quantitative information) and K₃₀ (T+/N-) in PSMD10 (O75832) in LSCC for the first time. We hypothesize that ubiquitination may affect the intracellular abundance or function of PSMD10, which finally affects proteasome biogenesis and the activity of proteasome. The specific regulatory mechanism needs further research. PTMs of various proteasome subunits make the regulation of proteasome function more complicated. Ubiquitination is one of the 11 PTMs of proteasome subunits that have been identified so far (66). At present, phosphorylation has been deeply studied in the regulation mechanism of proteasome activity, and researches had revealed that a variety of kinases and phosphatases regulate proteasome (67). The functional consequences of other PTMs (including ubiquitination) in regulation of proteasome are presently lacking. In our study, all ubiquitinated proteasome subunits belong to the RS, which suggests that ubiquitination may affect the activity of the proteasome by regulating the function of the RS not the CS in LSCC. Under normal circumstances, Rpn13 and Rpn10/S5a are responsible for identification of the ubiquitin chains on the protein committed to degradation, after that protein is translocated through the ATPase ring into the CS (68). However, when the proteasome is impaired under various circumstances (such as proteotoxic stresses and treated with bortezomib), Ube3c ubiquitinates residues K₂₁ and K₃₄ in

Rpn13 and inhibits the binding of 26S particles to ubiquitin conjugates (69). Our study found the increased ubiquitination level at residue K₃₄ (T/N=2.27; $p = 0.01$) in Rpn13, which can be seen as a sign of impaired proteasome function in LSCC. More importantly, if we can confirm the above results in LSCC, the degree of ubiquitination of Rpn13 can be used as a biomarker to predict the severity of impaired proteasome function, and the biological effects produced by proteasome activity inhibitors *in vivo*. In addition to the ubiquitination of Rpn13, monoubiquitination of Rpn10 induced by Rsp5, a member of NEDD4 ubiquitin protein ligase family, significantly inhibits the interaction of Rpn10 with substrates to decrease the activities of proteasome complex (70). Different from the previous yeast-based research that discovered four ubiquitination sites (K₇₁, K₈₄, K₉₉, and K₂₆₈), this study identified significantly increased ubiquitination levels at residues K₄₀ (N/T = 33.8; $p < 0.01$) and K₇₄ (N/T = 5.2, $p = 0.01$) in Rpn10 in LSCC tissue. Both K₄₀ and K₇₄ in Rpn10 are located in the VWFA domain that has been implicated to be responsible for stabilizing the lid-base association of RS. In LSCC, monoubiquitination of K₄₀ and K₇₄ in Rpn10 may participate in the regulation of proteasome activity.

In addition to proteasome biogenesis and PTMs, the amount of some proteasome subunits can also affect the activity of proteasome. For example, the activity of the proteasome is positively correlated with the expression level of PSMD11, and overexpression of PSMD11 increases the activity of the proteasome in stem cells (71). Specially, the dysregulated proteasomal activities were showed in the muscles of PSMC4-knockout animals (72). The ubiquitination of both PSMD11 and PSMC4 have been identified in this study. If these proteins are degraded by UPS, which means ubiquitination of these proteins will affect the activity of proteasome. So it is especially important to clarify the specific ubiquitination regulatory mechanisms of these proteins. As mentioned above, few studies are involved in the impact of ubiquitination on proteasome subunits, ubiquitination proteomics can be used as a powerful screening tool to provide direction for further studies.

Above description discussed the effect of ubiquitination on proteasome activity. Further, we discuss the ubiquitination regulation on the UPS-related enzymes. Our study found 9 UPS-related enzymes including E1, E2 and E3, which indicate that enzymes in the process of protein ubiquitination are also regulated by ubiquitination. Currently, studies have focused on the roles of ubiquitin in these enzymes; however, just relatively few studies were focused on the roles of the ubiquitination in these 9 enzymes. For instance, PML (P29590) was ubiquitinated by several E3s to result in the degradation of proteasome complex (73, 74). ITCH (Q96J02) can be ubiquitinated by itself *via* lysine-63 linkages to control the cytoplasmic-nuclear shuffling of ITCH (75). Of course, ubiquitination and even other PTMs might extensively affect these enzyme activities, currently known ubiquitination are only the tip of the iceberg.

The relationship between ubiquitination and protein expression level in LSCC

One of main functions of ubiquitination is to degrade proteins. A total of 265 DEP data in LSCC tissues was obtained from the published data (32–36) (Supplementary Table 12). This study identified 464 DUP data with 789 differentially ubiquitinated sites in LSCC tissues compared to controls (Supplementary Table 13). Overlapping analysis of the DUP data and DEP data found 45 DEPs with significantly altered ubiquitination level (Table 1). Five types of relationships between DUP and DEP were found in LSCC (Table 2), including: (i) the protein expression level was increased with the decrease of ubiquitination level, which might be due to the constant synthesis velocity and the decreased degradation velocity; (ii) the protein expression level was decreased with the increase of ubiquitination level, which might be due to the constant synthesis velocity and the increased degradation velocity; (iii) the protein expression level was decreased with decreased of the ubiquitination level, which might be because the protein degradation velocity was faster than its synthesis velocity; (iv) the protein expression level was increased with the increase of the ubiquitination level, which might be because protein degradation velocity was slower its synthesis velocity; (v) the protein expression level was increased with both increase and decrease of ubiquitination sites in a protein, this type of reseason was complex. These results clearly demonstrate the complexity of protein synthesis-degradation system. Further experiment studies would be needed to confirm the real status. Moreover, one should note that only 265 DEPs are obtained due to a limited list of DEPs in the published literature, an expanded quantitative proteomics would be needed to identify more DEPs in LSCC tissues compared to controls, which will reveal more DEPs with significant ubiquitination alteration.

Conclusions

This study provides the first quantitative ubiquitination proteomics analysis of LSCC tissue, and shows that ubiquitination can affect the occurrence and development of LSCC in multiple biological functions and pathways. Here focuses on the regulation mechanism of ubiquitination on intracellular protein turnover-related pathways. The results showed that ubiquitination affected UPS functions by regulating proteasome activity and UPS-related enzymes. In addition, ubiquitination also affected protein turnover by regulating ribosome assembly, ribosome-associated quality control (RQC), ER stress response, and ER-associated degradation (ERAD). Although ubiquitination studies in tumors have made significant progress, many anti-tumor drugs have been clinically applied and have achieved excellent therapeutic effects, yet considering that ubiquitination has extensive regulatory networks

and the complexity of ubiquitination itself, so there is still a lot of unknown things waiting for ones to explore. This study paved the way for further exploration of the specific regulatory mechanisms of ubiquitination in LSCC.

Data availability statement

The datasets presented in this study can be found in online repositories. The names of the repository/repositories and accession number(s) can be found in the article/[Supplementary Material](#).

Ethics statement

The studies involving human participants were reviewed and approved by Xiangya Hospital Medical Ethics Committee of Central South University, China. The patients/participants provided their written informed consent to participate in this study.

Author contributions

XHZ conceived the concept, designed experiments and manuscript, instructed experiments and data analysis, supervised results, coordinated, wrote and critically revised manuscript, and was responsible for its financial supports and the corresponding works. ML collected tissue samples, analyzed ubiquitinomic data, prepared figures and tables, and wrote the manuscript. XZ and LY analyzed the relationship between ubiquitination and protein differential expression. JY, XHZ, SZ, YG, BL, SW, JL, and NL participated in partial experiments. All authors approved the final manuscript.

References

- Gandara DR, Hammerman PS, Sos ML, Lara PN, Hirsch FR. Squamous cell lung cancer: from tumor genomics to cancer therapeutics. *Clin Cancer Res* (2015) 21(10):2236–43. doi: 10.1158/1078-0432.CCR-14-3039
- Socinski MA, Obasaju C, Gandara D, Hirsch FR, Bonomi P, Bunn PA Jr., et al. Current and emergent therapy options for advanced squamous cell lung cancer. *J Thorac Oncol* (2018) 13:165–83. doi: 10.1016/j.jtho.2017.11.111
- Zhang X-C, Wang J, Shao G-G, Wang Q, Qu X, Wang B, et al. Comprehensive genomic and immunological characterization of Chinese non-small cell lung cancer patients. *Nat Commun* (2019) 10:1772. doi: 10.1038/s41467-019-09762-1
- Network CGAR. Comprehensive genomic characterization of squamous cell lung cancers. *Nature*. (2012) 489:519. doi: 10.1038/nature11404
- Janssen-Heijnen ML, Coebergh J-WW. The changing epidemiology of lung cancer in Europe. *Lung cancer*. (2003) 41:245–58. doi: 10.1016/S0169-5002(03)00230-7
- Perez-Moreno P, Brambilla E, Thomas R, Soria J-C. Squamous cell carcinoma of the lung: molecular subtypes and therapeutic opportunities. *Clin Cancer Res* (2012) 18:2443–51. doi: 10.1158/1078-0432.CCR-11-2370
- Zhang T, Shan L, Zhang D. Advances of molecular targeted drugs used in maintenance therapy of non-small cell lung cancer. *Zhongguo fei ai za zhi= Chin J Lung cancer*. (2010) 13:1070–3. doi: 10.3779/j.issn.1009-3419.2010.11.14
- Ciechanover A. The ubiquitin-proteasome proteolytic pathway. *Cell*. (1994) 79:13–21. doi: 10.1016/0092-8674(94)90396-4
- Kimura Y, Tanaka K. Regulatory mechanisms involved in the control of ubiquitin homeostasis. *J Biochem* (2010) 147:793–8. doi: 10.1093/jb/mvq044
- Swatek KN, Komander D. Ubiquitin modifications. *Cell Res* (2016) 26:399. doi: 10.1038/cr.2016.39

Funding

This work was supported by the Shandong First Medical University Talent Introduction Funds (to XZ), Shandong First Medical University High-level Scientific Research Achievement Cultivation Funding Program (to XZ), the Shandong Provincial Natural Science Foundation (ZR202103020356 or ZR2021MH156 to XZ), and the Academic Promotion Program of Shandong First Medical University (2019ZL002).

Conflict of interest

The authors declare that the research was conducted in the absence of any commercial or financial relationships that could be construed as a potential conflict of interest.

Publisher's note

All claims expressed in this article are solely those of the authors and do not necessarily represent those of their affiliated organizations, or those of the publisher, the editors and the reviewers. Any product that may be evaluated in this article, or claim that may be made by its manufacturer, is not guaranteed or endorsed by the publisher.

Supplementary material

The Supplementary Material for this article can be found online at: <https://www.frontiersin.org/articles/10.3389/fendo.2022.970843/full#supplementary-material>

11. Pickart CM, Fushman D. Polyubiquitin chains: polymeric protein signals. *Curr Opin Chem Biol* (2004) 8:610–6. doi: 10.1016/j.cbpa.2004.09.009
12. Wilkinson KD. Ubiquitination and deubiquitination: targeting of proteins for degradation by the proteasome. *Semin Cell Dev Biol* (2000) 11 (3):141–8. doi: 10.1006/scdb.2000.0164
13. Komander D, Rape M. The ubiquitin code. *Annu Rev Biochem* (2012) 81:203–29. doi: 10.1146/annurev-biochem-060310-170328
14. Kessler BM. Ubiquitin–omics reveals novel networks and associations with human disease. *Curr Opin Chem Biol* (2013) 17:59–65. doi: 10.1016/j.cbpa.2012.12.024
15. Adams J, Kauffman M. Development of the proteasome inhibitor Velcade™ (Bortezomib). *Cancer Invest* (2004) 22:304–11. doi: 10.1081/CNV-120030218
16. Vij R, Siegel DS, Jagannath S, Jakubowiak AJ, Stewart AK, McDonagh K, et al. An open-label, single-arm, phase 2 study of single-agent carfilzomib in patients with relapsed and/or refractory multiple myeloma who have been previously treated with bortezomib. *Br J haematology*. (2012) 158:739–48. doi: 10.1111/j.1365-2141.2012.09232.x
17. Morrow JK, Lin H-K, Sun S-C, Zhang S. Targeting ubiquitination for cancer therapies. *Future medicinal Chem* (2015) 7:2333–50. doi: 10.4155/fmc.15.148
18. Danielsen JM, Sylvestersen KB, Bekker-Jensen S, Szklarczyk D, Poulsen JW, Horn H, et al. Mass spectrometric analysis of lysine ubiquitylation reveals promiscuity at site level. *Mol Cell Proteomics*. (2011) 10:M110.003590. doi: 10.1074/mcp.M110.003590
19. Udeshi ND, Mertins P, Svinkina T, Carr SA. Large-Scale identification of ubiquitination sites by mass spectrometry. *Nat Protoc* (2013) 8:1950. doi: 10.1038/nprot.2013.120
20. Zhu W, Smith JW, Huang C-M. Mass spectrometry-based label-free quantitative proteomics. *J BioMed Biotechnol* (2010) 2010:840518. doi: 10.1155/2010/840518
21. Neilson KA, Ali NA, Muralidharan S, Mirzaei M, Mariani M, Assadourian G, et al. Less label, more free: approaches in label-free quantitative mass spectrometry. *Proteomics*. (2011) 11:535–53. doi: 10.1002/pmic.201000553
22. Low TY, Magliozzi R, Guardavaccaro D, Heck AJ. Unraveling the ubiquitin-regulated signaling networks by mass spectrometry-based proteomics. *Proteomics*. (2013) 13:526–37. doi: 10.1002/pmic.201200244
23. Wu Q, Cheng Z, Zhu J, Xu W, Peng X, Chen C, et al. Suberoylanilide hydroxamic acid treatment reveals crosstalks among proteome, ubiquitylome and acetylome in non-small cell lung cancer A549 cell line. *Sci Rep* (2015) 5:9520. doi: 10.1038/srep09520
24. Qin X, Chen S, Qiu Z, Zhang Y, Qiu F. Proteomic analysis of ubiquitination-associated proteins in a cisplatin-resistant human lung adenocarcinoma cell line. *Int J Mol Med* (2012) 29:791–800. doi: 10.3892/ijmm.2012.912
25. Wei Huang D, Sherman BT, Tan Q, Collins JR, Alvord WG, Roayaei J, et al. The DAVID gene functional classification tool: a novel biological module-centric algorithm to functionally analyze large gene lists. *Genome Biol* (2007) 8:1–16. doi: 10.1186/gb-2007-8-9-r183
26. Wu J, Mao X, Cai T, Luo J, Wei L. KOBAS server: a web-based platform for automated annotation and pathway identification. *Nucleic Acids Res* (2006) 34: W720–W4. doi: 10.1093/nar/gkl167
27. Franceschini A, Szklarczyk D, Frankild S, Kuhn M, Simonovic M, Roth A, et al. STRING v9.1: protein-protein interaction networks, with increased coverage and integration. *Nucleic Acids Res* (2012) 41:D808–D15. doi: 10.1093/nar/gks1094
28. Smoot ME, Ono K, Ruscheinski J, Wang P-L, Ideker T. Cytoscape 2.8: new features for data integration and network visualization. *Bioinformatics* (2010) 27:431–2. doi: 10.1093/bioinformatics/btq675
29. Bader GD, Hogue CW. An automated method for finding molecular complexes in large protein interaction networks. *BMC Bioinf* (2003) 4:2. doi: 10.1186/1471-2105-4-2
30. Chin C-H, Chen S-H, Wu H-H, Ho C-W, Ko M-T, Lin C-Y. cytoHubba: identifying hub objects and sub-networks from complex interactome. *BMC Syst Biol* (2014) 8:S11. doi: 10.1186/1752-0509-8-S4-S11
31. McCracken AA, Brodsky JL. Assembly of ER-associated protein degradation *in vitro*: dependence on cytosol, calnexin, and ATP. *J Cell Biol* (1996) 132:291–8. doi: 10.1083/jcb.132.3.291
32. Zeng GQ, Zhang PF, Li C, Peng F, Li MY, Xu Y, et al. Comparative proteome analysis of human lung squamous carcinoma using two different methods: two-dimensional gel electrophoresis and iTRAQ analysis. *Technol Cancer Res Treat* (2012) 11(4):395–408. doi: 10.7785/tcrt.2012.500287
33. Li B, Chang J, Chu Y, Kang H, Yang J, Jiang J, et al. Membrane proteomic analysis comparing squamous cell lung cancer tissue and tumour-adjacent normal tissue. *Cancer Lett* (2012) 319(1):118–24. doi: 10.1016/j.canlet.2011.12.037
34. Xu Y, Cao LQ, Jin LY, Chen Z, Zeng G, Tang CE, et al. Quantitative proteomic study of human lung squamous carcinoma and normal bronchial epithelial acquired by laser capture microdissection. *J BioMed Biotechnol* (2012) 2012:510418. doi: 10.1155/2012/510418
35. Poschmann G, Sitek B, Sipos B, Ulrich A, Wiese S, Stephan C, et al. Identification of proteomic differences between squamous cell carcinoma of the lung and bronchial epithelium. *Mol Cell Proteomics*. (2009) 8(5):1105–16. doi: 10.1074/mcp.M800422-MCP200
36. Dowling P, O'Driscoll L, Meleady P, Henry M, Roy S, Ballot J, et al. 2-d difference gel electrophoresis of the lung squamous cell carcinoma versus normal sera demonstrates consistent alterations in the levels of ten specific proteins. *Electrophoresis*. (2007) 28(23):4302–10. doi: 10.1002/elps.200700246
37. Waterlow JC, Garlick PJ, MILL W. *Protein turnover in mammalian tissues and in the whole body*. 335 Jan van Galenstraat, PO Box 211: Elsevier/North-Holland Biomedical Press (1978).
38. Ciechanover A. Proteolysis: from the lysosome to ubiquitin and the proteasome. *Nat Rev Mol Cell Biol* (2005) 6:79. doi: 10.1038/nrm1552
39. Klionsky DJ. Autophagy: from phenomenology to molecular understanding in less than a decade. *Nat Rev Mol Cell Biol* (2007) 8:931. doi: 10.1038/nrm2245
40. Riederer IM, Schiffrin M, Kövari E, Bouras C, Riederer BM. Ubiquitination and cysteine nitrosylation during aging and alzheimer's disease. *Brain Res bulletin*. (2009) 80:233–41. doi: 10.1016/j.brainresbull.2009.04.018
41. Lim K-L. Ubiquitin–proteasome system dysfunction in parkinson's disease: current evidence and controversies. *Expert Rev proteomics*. (2007) 4:769–81. doi: 10.1586/14789450.4.6.769
42. Deng S, Zhou H, Xiong R, Lu Y, Yan D, Xing T, et al. Over-expression of genes and proteins of ubiquitin specific peptidases (USPs) and proteasome subunits (PSs) in breast cancer tissue observed by the methods of RFDD-PCR and proteomics. *Breast Cancer Res Treat* (2007) 104:21–30. doi: 10.1007/s10549-006-9393-7
43. Kammerl IE, Caniard A, Merl-Pham J, Ben-Nissan G, Mayr CH, Mossina A, et al. Dissecting the molecular effects of cigarette smoke on proteasome function. *J proteomics*. (2019) 193:1–9. doi: 10.1016/j.jpro.2018.12.015
44. Demarchi F, Brancolini C. Altering protein turnover in tumor cells: new opportunities for anti-cancer therapies. *Drug resistance updates*. (2005) 8:359–68. doi: 10.1016/j.drug.2005.12.001
45. Xu G, Paige JS, Jaffrey SR. Global analysis of lysine ubiquitination by ubiquitin remnant immunofluorescence profiling. *Nat Biotechnol* (2010) 28:868. doi: 10.1038/nbt.1654
46. Kim W, Bennett EJ, Huttlin EL, Guo A, Li J, Possemato A, et al. Systematic and quantitative assessment of the ubiquitin-modified proteome. *Mol Cell* (2011) 44:325–40. doi: 10.1016/j.molcel.2011.08.025
47. Matsumoto M, Hatakeyama S, Oyama K, Oda Y, Nishimura T, Nakayama KI. Large-Scale analysis of the human ubiquitin-related proteome. *Proteomics*. (2005) 5:4145–51. doi: 10.1002/pmic.200401280
48. Stavreva DA, Kawasaki M, Dundr M, Koberna K, Müller WG, Tsujimura-Takahashi T, et al. Potential roles for ubiquitin and the proteasome during ribosome biogenesis. *Mol Cell Biol* (2006) 26:5131–45. doi: 10.1128/MCB.02227-05
49. Juszkievicz S, Hegde RS. Initiation of quality control during poly (A) translation requires site-specific ribosome ubiquitination. *Mol Cell* (2017) 65:743–50.e4. doi: 10.1016/j.molcel.2016.11.039
50. Sundaramoorthy E, Leonard M, Mak R, Liao J, Fulzele A, Bennett EJ. ZNF598 and RACK1 regulate mammalian ribosome-associated quality control function by mediating regulatory 40S ribosomal ubiquitylation. *Mol Cell* (2017) 65:751–60.e4. doi: 10.1016/j.molcel.2016.12.026
51. Brandman O, Hegde RS. Ribosome-associated protein quality control. *Nat Struct Mol Biol* (2016) 23:7. doi: 10.1038/nsmb.3147
52. Matsuo Y, Ikeuchi K, Saeki Y, Iwasaki S, Schmidt C, Udagawa T, et al. Ubiquitination of stalled ribosome triggers ribosome-associated quality control. *Nat Commun* (2017) 8:159. doi: 10.1038/s41467-017-00188-1
53. Jung Y, Kim HD, Yang HW, Kim HJ, Jang C-Y, Kim J. Modulating cellular balance of Rps3 mono-ubiquitination by both Hel2 E3 ligase and Ubp3 deubiquitinase regulates protein quality control. *Exp Mol Med* (2017) 49:e390. doi: 10.1038/emmm.2017.128
54. Higgins R, Gendron JM, Rising L, Mak R, Webb K, Kaiser SE, et al. The unfolded protein response triggers site-specific regulatory ubiquitylation of 40S ribosomal proteins. *Mol Cell* (2015) 59:35–49. doi: 10.1016/j.molcel.2015.04.026
55. Walter P, Ron D. The unfolded protein response: from stress pathway to homeostatic regulation. *Science*. (2011) 334:1081–6. doi: 10.1126/science.1209038
56. Christianson JC, Ye Y. Cleaning up in the endoplasmic reticulum: ubiquitin in charge. *Nat Struct Mol Biol* (2014) 21:325. doi: 10.1038/nsmb.2793
57. Okumura F, Okumura AJ, Uematsu K, Hatakeyama S, Zhang D-E, Kamura T. Activation of double-stranded RNA-activated protein kinase (PKR) by interferon-stimulated gene 15 (ISG15) modification down-regulates protein translation. *J Biol Chem* (2013) 288:2839–47. doi: 10.1074/jbc.M112.401851

58. Bukau B, Weissman J, Horwich A. Molecular chaperones and protein quality control. *Cell*. (2006) 125:443–51. doi: 10.1016/j.cell.2006.04.014
59. Nishikawa S-I, Brodsky JL, Nakatsukasa K. Roles of molecular chaperones in endoplasmic reticulum (ER) quality control and ER-associated degradation (ERAD). *J Biochem* (2005) 137:551–5. doi: 10.1093/jb/mvi068
60. Huang X, Dixit VM. Drugging the undruggables: exploring the ubiquitin system for drug development. *Cell Res* (2016) 26:484. doi: 10.1038/cr.2016.31
61. Yu H, Matouschek A. Recognition of client proteins by the proteasome. *Annu Rev biophys.* (2017) 46:149–73. doi: 10.1146/annurev-biophys-070816-033719
62. Finley D. Recognition and processing of ubiquitin-protein conjugates by the proteasome. *Annu Rev Biochem* (2009) 78:477–513. doi: 10.1146/annurev.biochem.78.081507.101607
63. Livneh I, Cohen-Kaplan V, Cohen-Rosenzweig C, Avni N, Ciechanover A. The life cycle of the 26S proteasome: from birth, through regulation and function, and onto its death. *Cell Res* (2016) 26:869. doi: 10.1038/cr.2016.86
64. Rousseau A, Bertolotti A. An evolutionarily conserved pathway controls proteasome homeostasis. *Nature*. (2016) 536:184. doi: 10.1038/nature18943
65. Le Tallec B, Barrault M-B, Guérois R, Carré T, Peyroche A. Hsm3/S5b participates in the assembly pathway of the 19S regulatory particle of the proteasome. *Mol Cell* (2009) 33:389–99. doi: 10.1016/j.molcel.2009.01.010
66. Kikuchi J, Iwafune Y, Akiyama T, Okayama A, Nakamura H, Arakawa N, et al. Co-And post-translational modifications of the 26S proteasome in yeast. *Proteomics*. (2010) 10:2769–79. doi: 10.1002/pmic.200900283
67. Guo X, Huang X, Chen MJ. Reversible phosphorylation of the 26S proteasome. *Protein Cell* (2017) 8:255–72. doi: 10.1007/s13238-017-0382-x
68. Peth A, Kukushkin N, Bossé M, Goldberg AL. Ubiquitinated proteins activate the proteasomal ATPases by binding to Usp14 or Uch37 homologs. *J Biol Chem* (2013) 288:7781–90. doi: 10.1074/jbc.M112.441907
69. Besche HC, Sha Z, Kukushkin NV, Peth A, Hock EM, Kim W, et al. Autoubiquitination of the 26S proteasome on Rpn13 regulates breakdown of ubiquitin conjugates. *EMBO J* (2014) 33:1159–76. doi: 10.1002/embj.201386906
70. Isasa M, Katz EJ, Kim W, Yugo V, González S, Kirkpatrick DS, et al. Monoubiquitination of RPN10 regulates substrate recruitment to the proteasome. *Mol Cell* (2010) 38:733–45. doi: 10.1016/j.molcel.2010.05.001
71. Vilchez D, Boyer L, Morante I, Lutz M, Merkwirth C, Joyce D, et al. Increased proteasome activity in human embryonic stem cells is regulated by PSMD11. *Nature*. (2012) 489:304. doi: 10.1038/nature11468
72. Kitajima Y, Tashiro Y, Suzuki N, Warita H, Kato M, Tateyama M, et al. Proteasome dysfunction induces muscle growth defects and protein aggregation. *J Cell Sci* (2014) 127:5204–17. doi: 10.1242/jcs.150961
73. Yuan W-C, Lee Y-R, Huang S-F, Lin Y-M, Chen T-Y, Chung H-C, et al. A Cullin3-KLHL20 ubiquitin ligase-dependent pathway targets PML to potentiate HIF-1 signaling and prostate cancer progression. *Cancer Cell* (2011) 20:214–28. doi: 10.1016/j.ccr.2011.07.008
74. Lim JH, Liu Y, Reineke E, Kao H-Y. Mitogen-activated protein kinase extracellular signal-regulated kinase 2 phosphorylates and promotes Pin1 protein-dependent promyelocytic leukemia protein turnover. *J Biol Chem* (2011) 286:44403–11. doi: 10.1074/jbc.M111.289512
75. Scialpi F, Malatesta M, Peschiaroli A, Rossi M, Melino G, Bernassola F. Itch self-polyubiquitylation occurs through lysine-63 linkages. *Biochem Pharmacol* (2008) 76:1515–21. doi: 10.1016/j.bcp.2008.07.028



OPEN ACCESS

EDITED BY

Xianquan Zhan,
Shandong First Medical University,
China

REVIEWED BY

Na Li,
Shandong Cancer Hospital, China
Olga Golubnitschaja,
University of Bonn, Germany

*CORRESPONDENCE

Godfrey Grech
godfrey.grech@um.edu.mt

SPECIALTY SECTION

This article was submitted to
Cancer Endocrinology,
a section of the journal
Frontiers in Endocrinology

RECEIVED 02 August 2022

ACCEPTED 28 September 2022

PUBLISHED 18 October 2022

CITATION

Scerri J, Scerri C, Schäfer-Ruoff F,
Fink S, Templin M and Grech G (2022)
PKC-mediated phosphorylation
and activation of the MEK/ERK
pathway as a mechanism of
acquired trastuzumab resistance in
HER2-positive breast cancer.
Front. Endocrinol. 13:1010092.
doi: 10.3389/fendo.2022.1010092

COPYRIGHT

© 2022 Scerri, Scerri, Schäfer-Ruoff,
Fink, Templin and Grech. This is an
open-access article distributed under
the terms of the [Creative Commons
Attribution License \(CC BY\)](https://creativecommons.org/licenses/by/4.0/). The use,
distribution or reproduction in other
forums is permitted, provided the
original author(s) and the copyright
owner(s) are credited and that the
original publication in this journal is
cited, in accordance with accepted
academic practice. No use,
distribution or reproduction is
permitted which does not comply with
these terms.

PKC-mediated phosphorylation and activation of the MEK/ERK pathway as a mechanism of acquired trastuzumab resistance in HER2-positive breast cancer

Jeanesse Scerri¹, Christian Scerri¹, Felix Schäfer-Ruoff²,
Simon Fink², Markus Templin² and Godfrey Grech^{3*}

¹Department of Physiology & Biochemistry, University of Malta, Msida, Malta, ²NMI Natural and Medical Sciences Institute, University of Tübingen, Reutlingen, Germany, ³Department of Pathology, University of Malta, Msida, Malta

Protein expression, activation and stability are regulated through inter-connected signal transduction pathways resulting in specific cellular states. This study sought to differentiate between the complex mechanisms of intrinsic and acquired trastuzumab resistance, by quantifying changes in expression and activity of proteins (phospho-protein profile) in key signal transduction pathways, in breast cancer cellular models of trastuzumab resistance. To this effect, we utilized a multiplex, bead-based protein assay, DigiWest[®], to measure around 100 proteins and protein modifications using specific antibodies. The main advantage of this methodology is the quantification of multiple analytes in one sample, utilising input volumes of a normal western blot. The intrinsically trastuzumab-resistant cell line JIMT-1 showed the largest number of concurrent resistance mechanisms, including PI3K/Akt and RAS/RAF/MEK/ERK activation, β catenin stabilization by inhibitory phosphorylation of GSK3 β , cell cycle progression by Rb suppression, and CREB-mediated cell survival. MAPK (ERK) pathway activation was common to both intrinsic and acquired resistance cellular models. The overexpression of upstream RAS/RAF, however, was confined to JIMT 1; meanwhile, in a cellular model of acquired trastuzumab resistance generated in this study (T15), entry into the ERK pathway seemed to be mostly mediated by PKC α activation. This is a novel observation and merits further investigation that can lead to new therapeutic combinations in HER2-positive breast cancer with acquired therapeutic resistance.

KEYWORDS

acquired resistance, breast cancer, phospho-profile, PKC/MEK/ERK, signalosome, HER2 positive, patient stratification

Introduction

HER2 and trastuzumab

The human epidermal growth factor receptor 2 (HER2) protein is overexpressed in approximately 15% of breast cancers (1). Having no known ligands, it forms heterodimers with other members of the HER family of receptor tyrosine kinases (HER1/EGFR, HER3, HER4 (2)). HER2 activation results in the phosphorylation and activation of multiple downstream signaling proteins, including phospholipase C γ 1 (PLC γ 1), phosphatidylinositol 3-kinase (PI3K) regulatory and catalytic subunits, RasGAP, and heat shock protein 90 (3). The ensuing signaling cascade, mostly represented by the PI3K/AKT and RAS/RAF/ERK pathways, leads to uncontrolled cellular proliferation and invasion. Protein phosphatase 2A (PP2A), a ubiquitous serine/threonine phosphatase, is also a central regulatory component of PI3K/Akt pathway; its inactivation through phosphorylation at its tyrosine residue p.tyr307 has been found to be increased in HER2-positive tumor samples and correlated to tumor progression (4). Of interest, HER2 signaling increases c-myc phosphorylation at Ser62 and is maintained through attenuation of the phosphatase, PP2A (5). In fact, PP2A activators promote c-myc protein degradation (6). Clinically, high nuclear myc staining is positively associated with lymph-node positive disease in HER2 amplified breast cancer tumors (7). Hence, the HER2-MYC-PP2A axis is of clinical relevance and provides potential therapeutic targeting of breast cancers with co-amplification of HER2 and MYC. In a murine model of HER2 knock-in mammary tumors, overexpression of HER2 significantly upregulated β -catenin and its transcriptional targets Cyclin D1, SOX9 and c-Myc. High cytoplasmic β -catenin, expression of basal markers and loss of membranous E-cadherin are associated with poor prognosis in human HER2+ invasive ductal carcinomas (8).

Trastuzumab (Herceptin[®]), an immunoglobulin G1 (IgG1) antibody consisting of two mouse-derived antigen binding sites specific to the HER2 receptor extracellular domain (ED) and a humanized Fc portion (9), has been hailed as one of the successes of personalized medicine for the treatment of HER2-positive breast cancer. Its mode of action, though not yet fully understood, involves both direct and indirect pathways of inhibition. The former is brought about by the binding of the antibody to the ED of Her2, inhibiting its cleavage (10), and resulting in downstream signaling inhibition (mainly the PI3K/Akt pathway (11), through internalization and degradation of the HER2 receptor (12). The inhibition of heterodimer formation with other HER family members leads to reduced VEGF-mediated angiogenesis (13). The most important indirect pathway of inhibition is the activation of antibody-dependent cellular toxicity by the recruitment of Fc-competent immune effector cells (14). Trastuzumab is always administered

adjuvantly to chemotherapeutic agents, where it also inhibits the repair of chemotherapy-induced DNA damage (15).

Trastuzumab resistance mechanisms

Nonetheless, intrinsic resistance to the drug in some cases, and tumour recurrence due to acquired resistance in others, are important caveats of the targeted therapy (16). Mechanisms of trastuzumab-HER2 binding inhibition are associated with intrinsic resistance. Steric hindrance by cell surface proteins such as mucin-4 (MUC4) inhibits this binding (17); sensitivity to trastuzumab was enhanced upon knockdown of MUC4 expression in a JIMT-1 cell model (18), suggesting that MUC4 occupies the trastuzumab-binding sites of HER2. Overexpression of stem cell marker CD44 and its ligand, hyaluronan, also mask the trastuzumab binding domain on the HER2 ED and provide an independent prognostic factor for poor disease-free survival in HER2 positive patients treated with adjuvant trastuzumab (19). Proteolytic cleavage of the HER2 receptor generates a constitutively activated, truncated HER2 receptor lacking the ED, p95-HER2, which is associated with lymph node involvement (20) and trastuzumab resistance (21), attributed to the absence of the trastuzumab-binding domain.

Deregulation of signalling pathways downstream to HER2, and the activation of alternative cellular proliferation pathways, are alternative trastuzumab resistance mechanisms. Suppressed PTEN phosphatase activity prevents trastuzumab-induced growth arrest through sustained PI3K/AKT phosphorylation and signal transduction (22). A combination of low PTEN expression and PIK3CA oncogenic mutations predict trastuzumab response in HER2-positive breast cancer patients (23). In addition, trastuzumab-induced growth arrest of HER2-positive tumour cells is counteracted by an increase in insulin-like growth factor-1 receptor (IGF-IR) signalling (24). IGF-IR mediated trastuzumab-resistance is attributed to enhanced degradation of p27 and hence release from cell cycle arrest induced by trastuzumab treatment (25). Resistance to trastuzumab was also associated with increased expression of c-Met (26), and CAV-1 involved in caveolae-mediated endocytosis (27).

Immune escape is another mechanism of trastuzumab resistance. Genomic polymorphisms in Fc γ RIIIa that significantly suppress the affinity of IgG1 antibodies to the immune cell Fc γ receptor will impair ADCC activation (28). Furthermore, exosomes may transfer transforming growth factor beta 1 (TGF β 1), an immunosuppressive cytokine, and programmed death-ligand-1 (PD-L1), a lymphocyte activation inhibitor, to tumour cells. The presence of these exosomes was correlated with resistance to ADCC, suggesting a role of exosomes in suppressed immune-mediated response to trastuzumab (29). Exosomes generated by SKBR3 cell lines are

also positive for the receptor, and may act as decoy by binding to trastuzumab, reducing its availability to target tumour cells (30).

High-throughput biomarker detection

In addition to diagnostic biomarkers, the discovery of predictive markers of treatment resistance is a key aspect of personalized medicine. In the era of network medicine and high-throughput “omics”, it is important to study the interplay of the different complex mechanisms leading to drug resistance. The classification of breast cancer into molecular subtypes with prognostic and predictive implications, based on high-throughput gene expression data, has led to the development of gene panels such as the Oncotype DX (31) or the MammaPrint™ (32) assays. For Her2-positive breast cancer, however, there is no FDA-approved gene panel to date for the clinical prediction of response to trastuzumab-containing treatment regimes. The use of bead-based, multiplex RNA (33) and protein (34) assays has shown effectiveness in medium- to high-throughput cancer biomarker discovery and detection.

This study sought to differentiate between the complex mechanisms of intrinsic and acquired trastuzumab resistance, by quantifying changes in expression and activity of proteins in key signal transduction pathways, in cellular models of resistance. We utilized JIMT-1 as a cellular model of intrinsic resistance, and generated an acquired trastuzumab resistance model (T15) to study differential signaling signatures.

Materials and methods

Generation of trastuzumab-resistant cell line

SKBR3 cells with acquired trastuzumab resistance were obtained by conditioning with the drug as described by Zazo et al. (35). Briefly, the cell line (ATCC® HTB-30™), grown in Dulbecco's Modified Eagle Medium (DMEM, Sigma-Aldrich, St. Louis, MO) supplemented with 10% foetal bovine serum (FBS) and 1% GlutaMAX™ (Thermo Fisher Scientific, Waltham, MA), was acclimatised for 30 days in 10µg/mL trastuzumab followed by long-term culturing in medium containing 15µg/mL of the drug. Resistance to trastuzumab was confirmed by cell viability assay (MTT), which showed a maintenance of ≥80% viability after 72 hours incubation with 25-100µg/mL trastuzumab concentration (compared to the parent cells which showed reduced viability at these drug concentrations). The resulting cell line will be henceforth referred to as T15. The JIMT-1 cell line (DSMZ ACC-589), kindly donated by M. Barok at the University of Helsinki, Finland, was cultured in DMEM supplemented with 10% heat-inactivated FBS.

Bead-based, multiplex phosphoprotein profiling

High-throughput multiplex phosphoprotein profiling was subsequently carried out by the DigiWest® technique, as described by Treindl et al. (36), on the parental and conditioned cell lines. Briefly, cell pellets containing 5x10⁵ cells or more were lysed, and gel electrophoresis and blotting onto PVDF membranes was performed using the NuPAGE system as recommended by the manufacturer (Life Technologies, Carlsbad, CA, USA). The membranes were washed in PBST, then incubated in NHS-PEG12-Biotin (50µM) in PBST for 1 hour to biotinylate the blotted proteins, followed by another wash in PBST and drying. Individual sample lanes were cut into 96 molecular weight fractions (0.5mm each), with the separated proteins in each fraction eluted in 96-well plates using 10µL elution buffer (8M urea, 1% Triton-X100 in 100mM Tris-HCl pH 9.5) per well. The eluted proteins from each molecular weight fraction were then coupled with neutravidin-coated Luminex beads (MagPlex, Luminex, Austin, TX, USA) of a specific bead identity (red-infrared spectral wavelength), yielding 96 size-specific bead identities per sample. 384 Luminex bead sets were employed and the protein-loaded beads from 4 different sample lanes were pooled into a bead-mix having a concentration of 40 beads/µL in carboxy block storage buffer (CBS), which was sufficient for over 100 antibody incubations. Antibodies specific proteins and phosphoproteins with roles in HER2 downstream signaling pathways and other aforementioned mechanisms of interest were utilized (Table 1).

For each target protein or phosphoprotein to be quantified, an aliquot of the DigiWest bead-mixes was added to a well of a 96-well plate containing 50µL assay buffer (Blocking Reagent for ELISA supplemented with 0.2% milk powder, 0.05% Tween-20, and 0.02% sodium azide, Roche). Following a brief incubation in assay buffer, the buffer was discarded by keeping the 96-well plate on a magnet. The beads were then incubated with 30µL of a specific primary antibody diluted in assay buffer per well. After overnight incubation at 15°C on a shaker, the bead-mixes were washed twice with PBST and PE-labelled (Phycoerythrin) secondary antibodies (Dianova) specific to the primary antibody species were added and incubated for 1 hour at 23°C. Beads were washed twice and resuspended in PBST prior to the readout on a Luminex® FlexMAP 3D®.

For the quantification of the antibody specific signals, the DigiWest® analysis tool (version 3.8.6.1, Excel-based) was employed. This tool uses the 96 values for each initial lane obtained from the Luminex® measurements on the 96 molecular weight fractions, identifies the peaks at the appropriate molecular weight, calculates a baseline using the local background, and integrates the peaks. The obtained values are based on relative fluorescence (AFI, accumulated fluorescence intensity). For analysis, the data was normalized to the total

TABLE 1 Selected antibodies, fluorescence intensities and Log₂ FC in protein & phosphoprotein quantities in T15 and JIMT-1 relative to SKBR3.

Pathway	Analyte	Supplier	Cat. No.	Species + Clonality	Fluorescence Intensity			LOG ₂ FC rel. to SKBR3	
					JIMT1	SKBR3	T15	JIMT1	T15
PI3K/mTOR	4E-BP1	Epitomics	1557-1	Rb mAb	2490	240	283	3.37	0.24
PI3K/mTOR	4E-BP1 - phosphoThr70	Cell Signaling	9455	Rb pAb	754	119	164	2.66	0.46
PI3K	Akt	Cell Signaling	4685	Rb mAb	3567	2125	2901	0.75	0.45
PI3K	Akt1	Cell Signaling	2938	Rb mAb	1105	1443	2341	-0.39	0.70
PI3K	Akt1 - phosphoSer129	Cell Signaling	13461	Rb mAb	1	1	328	0.00	8.36
mTOR	AMPK alpha	Cell Signaling	2532	Rb pAb	657	418	544	0.65	0.38
mTOR	AMPK alpha - phosphoThr172	Cell Signaling	2535	Rb mAb	1217	135	300	3.17	1.15
MEK/ERK	A-Raf	Cell Signaling	4432	Rb pAb	2952	1177	1051	1.33	-0.16
MEK/ERK	A-Raf - phosphoTyr301/Tyr302_58kDa	Biorbyt	orb5910	Rb pAb	28345	31881	29893	-0.17	-0.09
MEK/ERK	A-Raf - phosphoTyr301/Tyr302_68kDa	Biorbyt	orb5910	Rb pAb	21540	22850	19923	-0.09	-0.20
MEK/ERK	A-Raf - phosphoTyr301/Tyr302_Total	Biorbyt	orb5910	Rb pAb	49885	54729	49815	-0.13	-0.14
PI3K/WNT	beta-Catenin	Cell Signaling	8480	Rb mAb	24084	188	382	7.00	1.02
PI3K/WNT	beta-Catenin - phosphoSer552	Cell Signaling	9566	Rb pAb	449	1	1	8.81	0.00
PI3K/WNT	beta-Catenin (non-pospho Ser33/37/Thr41; active)	Cell Signaling	8814	Rb mAb	3541	1	1	11.79	0.00
MEK/ERK	b-Raf - phosphoSer445	Cell Signaling	2696	Rb pAb	208	143	160	0.54	0.16
Cell cycle	CDK4	Cell Signaling	12790	Rb mAb	32451	3328	2931	3.29	-0.18
PI3K	c-myc_57kDa	Cell Signaling	9402	Rb pAb	207	205	241	0.01	0.23
PI3K	c-myc_70kDa	Cell Signaling	9402	Rb pAb	549	520	337	0.08	-0.63
PI3K	c-myc_Total	Cell Signaling	9402	Rb pAb	756	724	577	0.06	-0.33
MEK/ERK	c-Raf	Cell Signaling	9422	Rb pAb	632	161	135	1.97	-0.25
MEK/ERK	c-Raf - phosphoSer259	Cell Signaling	9421	Rb pAb	2423	873	874	1.47	0.00
MEK/ERK	c-Raf - phosphoSer289/296/301	Cell Signaling	9431	Rb pAb	374	186	168	1.01	-0.15
PI3K	CREB - phosphoSer133	Cell Signaling	9198	Rb mAb	177	1	56	7.47	5.80
PI3K	eIF4E	Cell Signaling	2067	Rb mAb	13776	16186	17424	-0.23	0.11
PI3K	eIF4E - phosphoSer209	Cell Signaling	9741	Rb pAb	348	927	1193	-1.41	0.36
MEK/ERK	Elk-1	Cell Signaling	9182	Rb pAb	653	656	813	-0.01	0.31
MEK/ERK	Elk-1 - phosphoSer383	Cell Signaling	9186	ms mab	644	1580	1651	-1.29	0.06
MEK/ERK	Erk1/2 (MAPK p44/42)_p42	Cell Signaling	4695	Rb mAb	17917	30972	41263	-0.79	0.41
MEK/ERK	Erk1/2 (MAPK p44/42)_p44	Cell Signaling	4695	Rb mAb	3100	1702	1774	0.87	0.06
MEK/ERK	Erk1/2 (MAPK p44/42)_Total	Cell Signaling	4695	Rb mAb	21016	32673	43036	-0.64	0.40
MEK/ERK	Erk1/2 (MAPK p44/42) - phosphoThr202/Tyr204_p42	Cell Signaling	4370	Rb mAb	4211	788	1190	2.42	0.60
MEK/ERK	Erk1/2 (MAPK p44/42) - phosphoThr202/Tyr204_p44	Cell Signaling	4370	Rb mAb	1656	93	294	4.16	1.67
MEK/ERK	Erk1/2 (MAPK p44/42) - phosphoThr202/Tyr204_Total	Cell Signaling	4370	Rb mAb	5866	880	1482	2.74	0.75
MEK/ERK	ERK1/2 (MAPK) - phosphoThr202/Tyr204_p42	Cell Signaling	9101	Rb pAb	4653	257	480	4.18	0.90
MEK/ERK	ERK1/2 (MAPK) - phosphoThr202/Tyr204_p44	Cell Signaling	9102	Rb pAb	1340	113	143	3.57	0.34
MEK/ERK	ERK1/2 (MAPK) - phosphoThr202/Tyr204_Total	Cell Signaling	9103	Rb pAb	5993	368	621	4.02	0.75
MEK/ERK	Erk2 (MAPK p42)	Cell Signaling	9108	Rb pAb	2649	6720	10792	-1.34	0.68
WNT	GSK-3 alpha	Cell Signaling	4337	Rb mAb	4395	4403	4928	0.00	0.16
WNT	GSK3 alpha - phosphoSer21_51kDa	Cell Signaling	9331	Rb pAb	229	443	409	-0.95	-0.11
PI3K/WNT	GSK3 alpha/beta - phosphoSer21/Ser9_Total	Cell Signaling	9331	Rb pAb	548	443	409	0.31	-0.11

(Continued)

TABLE 1 Continued

Pathway	Analyte	Supplier	Cat. No.	Species + Clonality	Fluorescence Intensity			LOG2 FC rel. to SKBR3	
					JIMT1	SKBR3	T15	JIMT1	T15
PI3K	GSK3 beta - phosphoTyr216_47kDa	Abcam	ab68476	Rb mAb	129	232	281	-0.85	0.28
PI3K	GSK3 alpha - phosphoTyr279_51kDa	Abcam	ab68476	Rb mAb	706	125	148	2.50	0.25
PI3K	GSK3 alpha/beta - phosphoTyr279/Tyr216_Total	Abcam	ab68476	Rb mAb	834	355	429	1.23	0.27
PI3K	GSK3 beta - phosphoSer9	Cell Signaling	9336	Rb pAb	511	1	1	9.00	0.00
PI3K	GSK3 beta	Cell Signaling	9315	Rb mAb	11035	3642	2050	1.60	-0.83
HER2	Her2	DAKO	A0485	Rb pAb	3595	5008	8862	-0.48	0.82
Multiple	HSP 90	Abcam	ab59459	Ms mAb	150805	456009	861935	-1.60	0.92
IGF1	IGF1 receptor beta (Insulin receptor beta, CD221)	Cell Signaling	3018	Rb mAb	308	153	166	1.02	0.12
MEK/ERK	MAPKAPK-2	Cell Signaling	12155	Rb mAb	392	556	453	-0.50	-0.29
MEK/ERK	MEK 1	Cell Signaling	9124	Rb pAb	1128	610	644	0.89	0.08
MEK/ERK	MEK1 - phosphoSer298	Cell Signaling	98195	Rb mAb	896	1	1	9.81	0.00
MEK/ERK	MEK1 - phosphoThr292	Cell Signaling	26975	Rb mAb	1036	1	1	10.02	0.00
MEK/ERK	MEK1/2 - phosphoSer217/Ser221	Cell Signaling	9154	Rb mAb	3200	135	416	4.56	1.62
MEK/ERK	MEK2	Cell Signaling	9125	Rb pAb	953	171	131	2.48	-0.38
MEK/ERK	Mnk1	Cell Signaling	2195	Rb mAb	239	161	164	0.57	0.03
MEK/ERK	MSK1 - phosphoSer376	Millipore	04-384	Rb mAb	2302	2436	9259	-0.08	1.93
PI3K/ mTOR	mTOR (FRAP)	Cell Signaling	2983	Rb mAb	3077	1394	2232	1.14	0.68
PI3K/ mTOR	mTor - phosphoSer2448	Cell Signaling	5536	Rb mAb	1211	521	997	1.22	0.94
MEK/ERK	p38 MAPK	Cell Signaling	9212	Rb pAb	572	258	273	1.15	0.08
Cell cycle	p53	R&D	af1355	Gt pAb	9935	1601	2117	2.63	0.40
PI3K/ mTOR	p70 S6 kinase	Cell Signaling	2708	Rb mAb	5905	2365	3004	1.32	0.34
PI3K/ mTOR	p70 S6 kinase - phosphoThr421/Ser424	Cell Signaling	9204	Rb pAb	632	93	177	2.76	0.92
PI3K	PDK1	Cell Signaling	3062	Rb pAb	1398	808	1294	0.79	0.68
PI3K	PDK1 - phosphoSer241	Cell Signaling	3061	Rb pAb	142	73	193	0.96	1.39
PI3K	PI3-kinase p110 delta_110kDa	Santa cruz	sc-7176	Rb pAb	734	220	238	1.74	0.11
PI3K	PI3-kinase delta_60kDa	Santa cruz	sc-7176	Rb pAb	11463	12042	11384	-0.07	-0.08
PI3K	PI3-kinase delta_Total	Santa cruz	sc-7176	Rb pAb	12196	12262	11620	-0.01	-0.08
PI3K	PI3-kinase p110 alpha	Cell Signaling	4255	Rb pAb	31	253	266	-3.05	0.07
PI3K	PI3-kinase p110 beta_110kDa	Millipore	04-400	Rb mAb	2897	916	995	1.66	0.12
PI3K	PI3-kinase p110 beta_60kDa	Millipore	04-400	Rb mAb	1514	1835	1665	-0.28	-0.14
PI3K	PI3-kinase p110 beta_Total	Millipore	04-400	Rb mAb	4409	2750	2659	0.68	-0.05
PI3K	PI3-kinase p85 alpha	Epitomics	1675-1	Rb mAb	363	87	118	2.06	0.44
PI3K	PI3-kinase p85	Cell Signaling	4292	Rb pAb	437	129	157	1.76	0.28
PI3K	PI3-kinase p85/p55 - phosphoTyr458/Tyr199_55kDa only	Cell Signaling	4228	Rb pAb	336	3158	3154	-3.23	0.00
PI3K	PKC (pan) - phosphoSer660	Cell Signaling	9371	Rb pAb	1073	1180	4669	-0.14	1.98
PI3K	PKC (pan) gamma - phosphoThr514_80kDa	Cell Signaling	38938	Rb mAb	1102	1141	2533	-0.05	1.15
PI3K	PKC (pan) gamma - phosphoThr514_85kDa	Cell Signaling	38938	Rb mAb	2613	3150	5891	-0.27	0.90
PI3K	PKC (pan) gamma - phosphoThr514_Total	Cell Signaling	38938	Rb mAb	3715	4290	8423	-0.21	0.97
PI3K	PKC alpha - phosphoSer657	Abcam	AB180848	Rb mAb	1769	1122	4227	0.66	1.91
PI3K	PKC alpha - phosphoThr497	Abcam	AB76016	Rb mAb	1526	1948	2841	-0.35	0.54

(Continued)

TABLE 1 Continued

Pathway	Analyte	Supplier	Cat. No.	Species + Clonality	Fluorescence Intensity			LOG2 FC rel. to SKBR3	
					JIMT1	SKBR3	T15	JIMT1	T15
PI3K	PKC alpha	BD Biosciences	610107	Ms mAb	1	77	80	-6.27	0.05
PI3K	PKC alpha/beta II - phosphoThr638/Thr641	Cell Signaling	9375	Rb pAb	980	1570	1473	-0.68	-0.09
PI3K	PP2A C	Cell Signaling	2259	Rb mAb	5653	3171	2571	0.83	-0.30
PI3K	PP2A C - phosphoTyr307	R&D	AF3989	Rb pAb	4986	20990	10084	-2.07	-1.06
PI3K	PTEN	Cell Signaling	9552	Rb pAb	228	203	304	0.16	0.58
MEK/ERK	Ras	Cell Signaling	8955	Rb mAb	2280	742	1103	1.62	0.57
Cell cycle	Rb	Cell Signaling	9309	Ms mAb	405	131	119	1.62	-0.15
Cell cycle	Rb - phosphoSer795	Cell Signaling	9301	Rb pAb	149	53	1	1.49	-5.73
Cell cycle	Rb - phosphoSer807/Ser811	Epitomics	2004-1	Rb mAb	1618	342	347	2.24	0.02
Multiple	RSK 1 (p90RSK)	Cell Signaling	9344	Rb pAb	1038	306	334	1.76	0.13
Multiple	RSK 1 (p90RSK) - phosphoSer380	Cell Signaling	9341	Rb pAb	317	228	853	0.48	1.90
Multiple	RSK 1 (p90RSK) - phosphoThr573	Abcam	ab62324	Rb mAb	556	115	303	2.27	1.40
Multiple	RSK 1/2/3	Cell Signaling	9347	Rb pAb	1059	438	453	1.27	0.05
Multiple	RSK 3	Epitomics	2012-1	Rb mAb	1005	409	648	1.30	0.67
Multiple	RSK 3 - phosphoThr356/Ser360	Cell Signaling	9348	Rb pAb	87	1	104	6.45	6.70
PI3K/ mTOR	S6 ribosomal protein	Cell Signaling	2317	Ms mAb	6810	14092	11270	-1.05	-0.32
PI3K/ mTOR	S6 ribosomal protein - phosphoSer235/Ser236	Cell Signaling	2211	Rb pAb	11823	31835	20663	-1.43	-0.62
PI3K/ mTOR	S6 ribosomal protein - phosphoSer240/Ser244	Cell Signaling	2215	Rb pAb	9573	38584	21969	-2.01	-0.81
PI3K/ mTOR	TSC2 (Tuberin)	Cell Signaling	4308	Rb mAb	2138	489	1073	2.13	1.13
PI3K/ mTOR	Tuberin/TSC2 - phosphoSer1387	Cell Signaling	23402	Rb mAb	1369	233	564	2.55	1.27

Antibodies were organized into the main canonical pathways of signal transduction and cellular proliferation. Antibody species: Rb: rabbit, Ms: mouse, Gt: goat; antibody clonality: mAb: monoclonal, pAb: polyclonal. Fluorescence intensity values less than 100 are deemed inaccurate and should be interpreted with caution. Fold changes ≥ 1 are denoted in light orange and fold changes ≤ -1 are denoted in light green.

protein amount corresponding to the sample, and the relative quantification of each protein and phosphoprotein was expressed as \log_2 fold-change (FC) in T15 and JIMT-1 as compared to SKBR3. Differentially expressed targets were organized into established signal transduction pathways and phosphosite \log_2 FC were used to predict whether each protein was under- or over-activated.

Results and discussion

MEK/ERK pathway is a central mechanism of acquired trastuzumab resistance

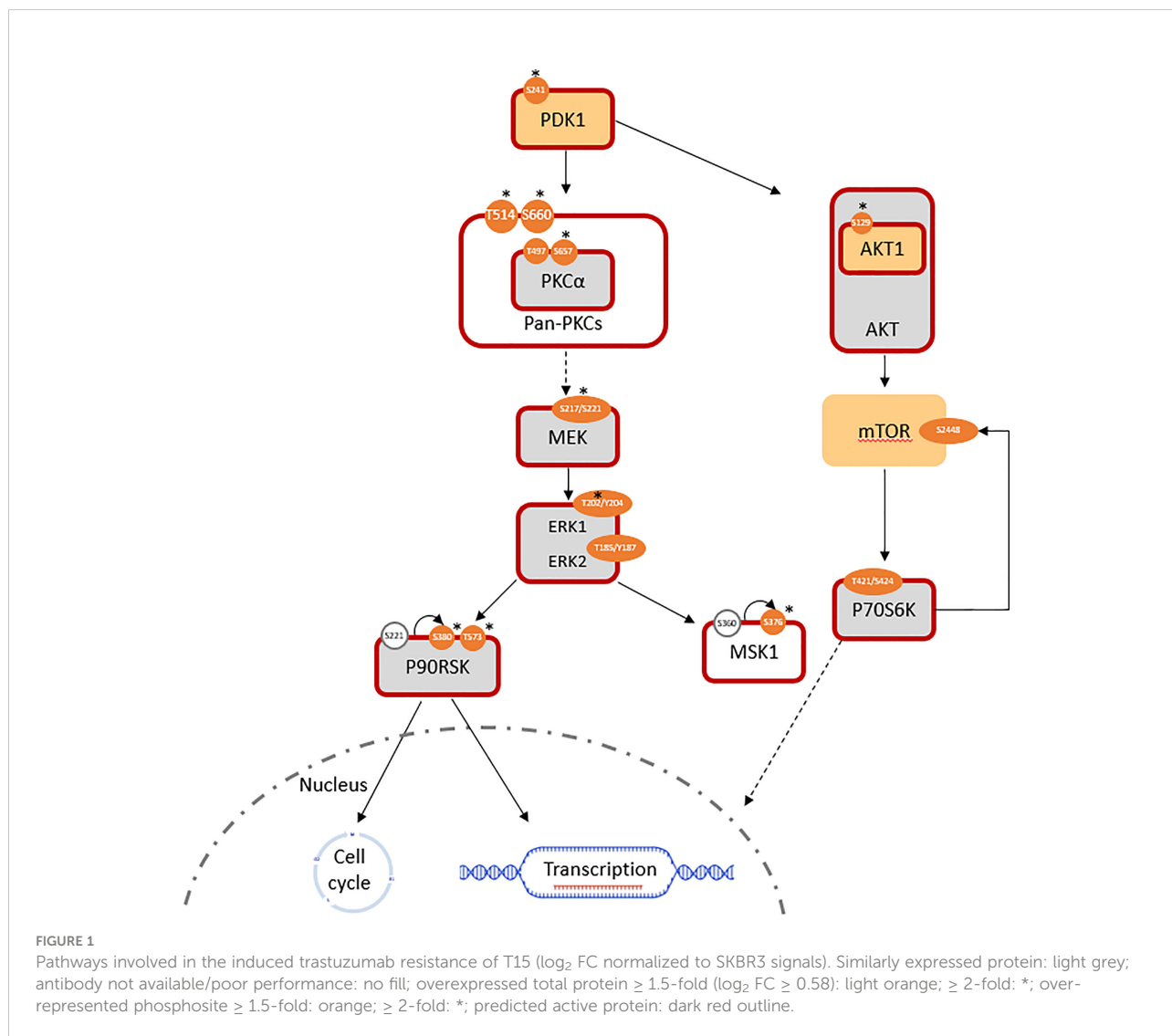
Phosphoinositide-dependent kinase-1 (PDK1) activity was significantly increased (\log_2 FC(PDK1) = +0.7; \log_2 FC

(pPDK1^{ser241} = +1.4) in T15. A lack of significant change in RAF expression was expected to be consistent with a lack of alteration in downstream MEK1/2 signaling; however, the MEK/ERK pathway was still found to be overall activated. The expression of total MEK1 was equivalent, while that of MEK2 was slightly downregulated (\log_2 FC = -0.36) in T15 when compared to SKBR3. Meanwhile, activated pMEK1^{ser217/221}/pMEK2^{ser222/226} (antibody does not distinguish between the two isoforms) was significantly upregulated in T15 (\log_2 FC = +1.6). ERK (MAPK) activity reflected the changes observed in its upstream activator, MEK: despite minimal changes in total protein expression (\log_2 FC(ERK1) = +0.06, \log_2 FC(ERK2) = +0.41), phosphorylated (active) forms of ERK1 and ERK2 were over-represented, thus resulting in a higher ratio of phosphorylated to total ERK1/2 (\log_2 FC(pERK1^{thr202/tyr204} = +1.7; \log_2 FC(pERK2^{thr185/tyr187} = +0.6). The results were confirmed with two different antibody clones (Cell

Signaling product ID 4370 and 9101; log₂ fold changes reported here obtained with the former), both of which bind to ERK1 and ERK2 and give two specific peaks of 44 and 42 kDa, respectively (Figure 1; Table 1). T15 also showed hyper-activation of the ribosomal protein S6 kinase α-5 protein, MSK1 (log₂ FC (pMSK1^{ser376}) = +1.9; Figure 1). MSK1 is directly phosphorylated by MAPKs at serine 360, threonine 581, and threonine 700, and subsequently autophosphorylates at serine 376 for protein activation (37). Seemingly conflicting roles for MSK1 in breast cancer have been described: it shows tumor suppressor functions by acting as a transcriptional coactivator of P53 and mediating phosphorylation of histone H3 in the transcriptional activation of *p21* (37), but has also been associated with epithelial-mesenchymal transition (EMT) and subsequent skeletal metastasis by histone H3 acetylation and phosphorylation of Snail, which downregulates E-cadherin to promote cellular migration and invasion (38).

Activation of the MEK/ERK pathway is through PKCα activation in acquired resistance

In the absence of RAF overexpression, entry into the MEK/ERK pathway can be mediated by the protein kinase C (PKC) family, via PDK1. PKCα and PKCγ are both members of the diacylglycerol (DAG) sensitive, Ca²⁺ responsive conventional PKC (cPKC) isoform subgroup. Activation downstream to receptor tyrosine kinases, such as ErbB receptors, involves the Ca²⁺ sensitive recruitment of phosphatidylinositol (4, 5)-bisphosphate [PtdIns (4, 5)P₂]-specific phospholipases Cγ1/2 (PtdIns-PLCγ1/2) through their SH2 domains; PDK1-dependent activation loop phosphorylation, together with C-terminal phosphorylation events, catalyze PKC activity by maintaining the active conformation of the kinase domains (39). While PKCγ is more specific to the brain, PKCα is



detected in all normal and most tumor tissue types (40). The presence of activated pan-PKC and specifically PKC α was determined by the over-representation of phospho-proteins in T15 (\log_2 FC(PKCA) = +0.05; \log_2 FC(pPKCA^{thr497}) = +0.54; \log_2 FC(pPKCA^{ser657}) = +1.91), as well as the overexpression of PDK-1 p-ser241, an autophosphorylation site essential for PDK1 activity (Figure 1). Increased levels of this phosphoprotein are a frequent event in breast cancer metastasis, and have been proposed as a candidate for chemosensitisation in innate and acquired resistance (41).

PKC- α , like other protein kinases, plays a role in the regulation of various cellular functions, ranging from cell proliferation and differentiation to control of apoptosis. Requiring HSP90 (\log_2 FC in T15 = 0.92) and mTORC2 complex to prime phosphorylation, it is sequentially phosphorylated at Thr497 in the kinase domain by PDK1 and at Thr638 and Ser657 autophosphorylation sites. While in the cytoplasm, the phosphorylated PKC- α is still inactive, until it is recruited to the plasma membrane, where it exerts its functions (42). Its importance in cellular proliferation renders its abnormal expression a transformative event: initial recognition of the role of PKC- α in tumorigenesis was reported by Ways and colleagues (43), where ectopic expression of the isoform in MCF7 cells led to a more aggressive phenotype characterized by increased cell proliferation, anchorage-independent growth, loss of epithelial morphology, and enhanced tumorigenicity in nude mice. Using the same cell line, Gupta et al. (44) attributed the increase in cellular proliferation to ERK activation by PKC- α .

PKC family members were also identified as kinases involved in HER2 endocytosis by Bailey and colleagues (45), by using tanespimycin to inactivate HSP90 (and thus promote receptor internalization for degradation), followed by a kinase inhibitor screen to identify kinases whose inhibition correlated with reduced cell surface clearance of HER2. The activation of PKC by phorbol myristate acetate (PMA), and the specific ectopic expression of constitutively active PKC- α , promoted its colocalization with HER2 into a juxtannuclear compartment without subsequent degradation. Conversely, knockdown of PKC- α by siRNA impaired HER2 trafficking to the ERC. In a previous study, PKC- α was implicated in the positive regulation of cell surface HER2 receptor levels, as assessed by flow cytometry, in breast cancer cell lines classified as HER2 2+ on immunohistochemistry without gene amplification as determined by fluorescence *in situ* hybridization (FISH) (46).

Multiple PKC-independent pathways are activated in intrinsic resistance model, JIMT-1

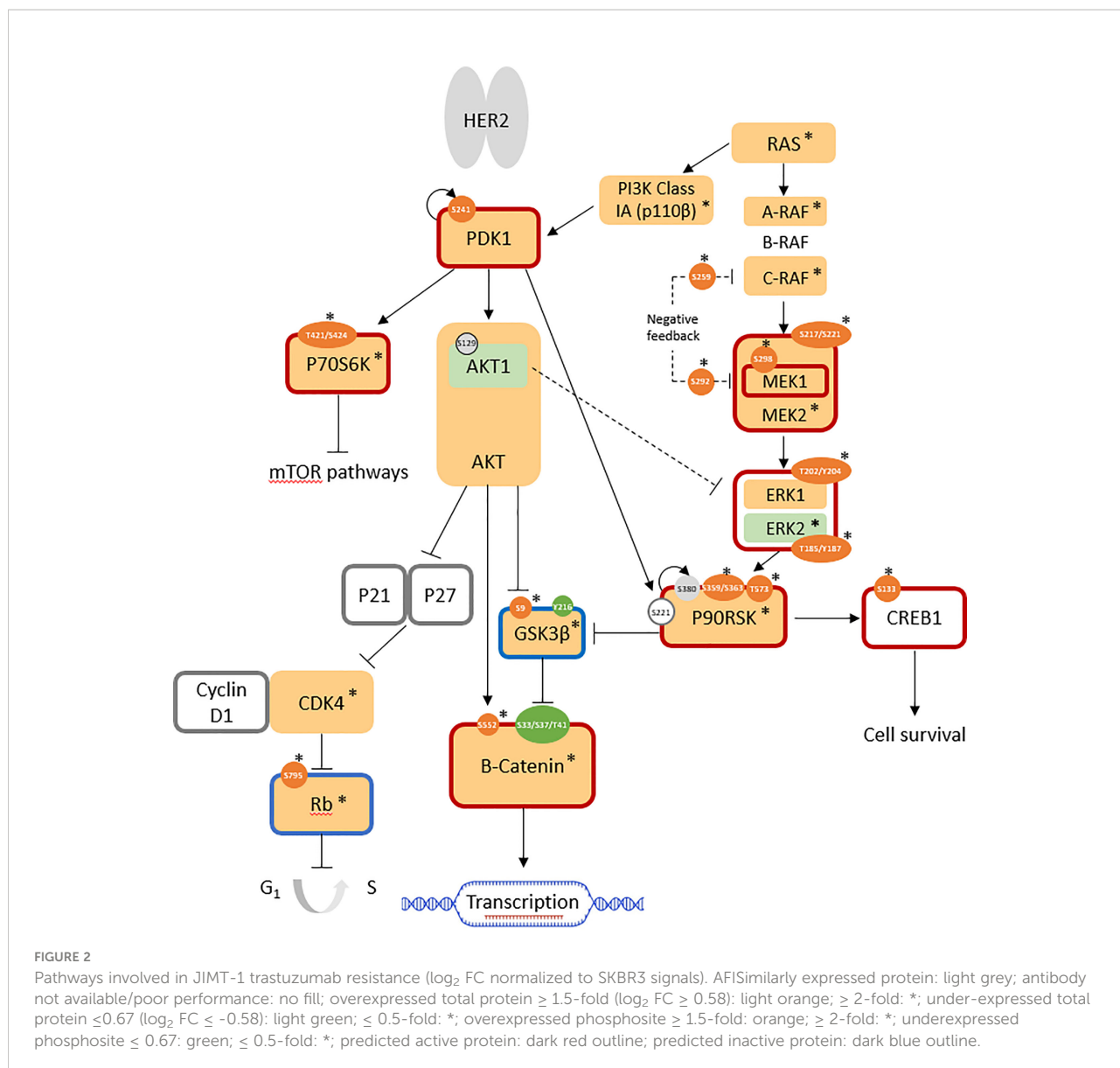
Upon phosphoprotein profiling of JIMT-1 as a HER2-positive breast cancer cell line with intrinsic trastuzumab resistance, it was immediately evident that multiple cell

survival and proliferation pathways were simultaneously upregulated in comparison with SKBR3, but these did not involve PKC proteins (Figure 2). Specifically, the RAS/RAF/MEK/ERK pathway was highly activated, together with the overexpression of the highly important kinases, PI3K class Ia (p110 β isoform; \log_2 FC = +1.7) and PDK1 (\log_2 FC = +0.8). Upregulated cell cycle progression was indicated by the highly over-expressed CDK4 (\log_2 FC: +3.3) and the overall downregulation of the retinoblastoma-associated protein (Rb) tumor suppressor (\log_2 FC(Rb) = +1.6; \log_2 FC(pRb^{ser807/811}) = +2.2; normalized AFI(pRb^{ser795}) = 189 (not detected in SKBR3)). GSK3 β activity was suppressed (\log_2 FC(GSK3 β) = +1.6; AFI (pGSK3 β ^{ser9}) = 511 (not detected in SKBR3)), leading to increased expression (\log_2 FC: +7.0) and activity (non-phospho-ser33/37/thr41: AFI = 3541; not detected in SKBR3) of β -catenin, which is associated with an increase in transcriptional activation. Enhanced cell survival was indicated by the overall activation of the cAMP-response-element-binding protein (CREB); despite total protein expression being below the cutoff in all cell lines, the active phosphosite at ser133 was not expressed in SKBR3 but expressed (normalized AFI = 177) in JIMT-1 (Figure 2; Table 1).

Control of these complex signal transduction cascades by feedback loop mechanisms makes the interpretation of some phospho-proteomic results more challenging. Specifically, both activators of the S6 ribosomal protein (RPS6), the p70S6 kinase (p70S6K/S6K1) and the ribosomal S6 kinase (p90RSK/RSK1), were activated in both models of resistance (i.e. T15 and JIMT-1), while RPS6 itself was downregulated in both cell lines. Activation of p70S6K was confirmed by the over-representation of its phosphorylation target on mTOR at serine 2448 (47), while activation of RSK1 was confirmed by the over-representation of different activating phosphosites, in both models (Figures 1, 2; Table 1). Also of interest, deregulation of PP2A and the HER2-MYC-PP2A axis were not apparently involved in the intrinsic resistance of JIMT-1 to trastuzumab or the resistance acquired by T15. The PP2A C regulatory subunit was overexpressed at a \log_2 FC of 0.83 in JIMT-1 and was not significantly differentially expressed in T15, while its inactivating phosphosite p.tyr307 was significantly underexpressed in both cell lines. Meanwhile, no change in expression of c-myc was observed in the two cell lines in relation to SKBR3 (Table 1).

Clinical perspectives

In this study, we focused on the differential protein expression and phosphorylation events in a cellular model of intrinsic resistance (JIMT-1) and one with generated trastuzumab-induced acquired resistance (T15). PKC-mediated MEK/ERK pathway activation was observed in the acquired model (T15) only. Apart from its above-mentioned functions, PKC- α expression maintains the invasiveness of triple-negative



breast cancer (TNBC) and endocrine resistant cell lines through upregulation of FOXC2, a transcriptional repressor of p120-catenin (CTNND1); a high FOXC2:CTNND1ratio was also associated with shorter disease free survival in TNBC patients in The Cancer Genome Atlas (TCGA) dataset (48). FOXC2 is an epithelial-mesenchymal transition (EMT) marker, a process known to be significantly associated with HER2-positive, metastatic breast cancer in the clinical setting (49). Cells undergoing EMT commonly show upregulation of metalloproteinases (50, 51), which promote HER2 cleavage/shedding and thus a high ratio of p95:p185 HER2, associated with trastuzumab resistance and poor disease-free survival in HER2+ breast cancer (52). Assessment of the p95:p185 HER2 ratio in plasma exosomes derived from HER2-positive breast cancer patients (30) is a potential tool for the detection of early

metastatic disease and monitoring of response to trastuzumab therapy.

Using the DigiWest[®] methodology, we interrogated major signal transduction pathways to understand the complex interplay of these pathways and changes following resistance to therapy. Bead-based, multiplex (phospho)protein assays are a very efficient means of studying these pathways, whereby the supporting data from many members of the same pathway, rather than a few candidates (as is permitted by traditional Western blotting techniques) lends robustness to the overall observations. The use of this methodology to characterise exosomes for HER2 receptor ratios, FOXC2 and other EMT markers, metalloproteases, TGFβ; and PD-L1, and other markers of therapeutic resistance can accompany the other developments in liquid biopsy, such as circulating tumour cells

(CTCs) (53) and patterns of cell-free nucleic acids in plasma (54), as well as protein biomarkers in other biofluids such as tears (55), to predict disease development and progression. The potential use of DigiWest[®] to quantitate proteins from various sources provides a multiplex method that can be translated to the clinic, since ultra-high throughput proteomics by mass spectroscopy remain challenging to use in the clinical setting. Understanding treatment resistance mechanisms and incorporating multiplex assays in personalised medicine allows the prediction of early therapeutic resistance and prevents the use of non-beneficial therapies.

Conclusion

MAPK (ERK) pathway activation was common to both intrinsic and acquired resistance cellular models. PKC-mediated MEK/ERK pathway activation in the cellular model of acquired trastuzumab resistance generated in this study (T15) was not observed in the intrinsic model, JIMT-1, which is in turn characterized by the PKC-independent activation of various pathways, including PI3K/Akt and RAS/RAF/MEK/ERK activation, β catenin stabilization by inhibitory phosphorylation of GSK3 β , cell cycle progression by Rb suppression, and CREB-mediated cell survival. This is a novel observation which merits further investigation that can lead to new therapeutic combinations in HER2-positive breast cancer with acquired therapeutic resistance to trastuzumab.

Data availability statement

The original contributions presented in the study are included in the article/supplementary material. Further inquiries can be directed to the corresponding author.

Author contributions

JS carried out the experiments and data analysis and contributed to the draft of the manuscript. FS-R and SF

supervised JS during DigiWest analysis that was performed at the NMI institute under the approval of MT. The data analysis was performed using tools provided by MT. CS and GG conceived the study, designed and coordinated the project. GG contributed to the writing of the manuscript. All authors contributed to the article and approved the submitted version.

Funding

This study was funded by the ALIVE Charity Foundation through the Research Innovation and Development Trust (RIDT), providing a scholarship to JS and bench fees. This work received financial support from the State Ministry of Baden-Wuerttemberg for Economic Affairs, Labour and Tourism.

Acknowledgments

We would like to acknowledge the Institute of Molecular Medicine & Biobanking and the Faculty of Medicine & Surgery for the support in the use of the facilities at the University of Malta.

Conflict of interest

The authors declare that the research was conducted in the absence of any commercial or financial relationships that could be construed as a potential conflict of interest.

Publisher's note

All claims expressed in this article are solely those of the authors and do not necessarily represent those of their affiliated organizations, or those of the publisher, the editors and the reviewers. Any product that may be evaluated in this article, or claim that may be made by its manufacturer, is not guaranteed or endorsed by the publisher.

References

- Patani N, Martin LA, Dowsett M. Biomarkers for the clinical management of breast cancer: International perspective. *Int J Cancer* (2013) 133:1–13. doi: 10.1002/ijc.27997
- Graus-Porta D, Beerli RR, Daly JM, Hynes NE. ErbB-2, the preferred heterodimerization partner of all ErbB receptors, is a mediator of lateral signaling. *EMBO J* (1997) 16:1647–55. doi: 10.1093/emboj/16.7.1647
- Bose R, Molina H, Patterson AS, Bitok JK, Periaswamy B, Bader JS, et al. Phosphoproteomic analysis of Her2/neu signaling and inhibition. *Proc Natl Acad Sci U.S.A.* (2006) 103:9773–8. doi: 10.1073/pnas.0603948103
- Wong LL, Chang CF, Koay ES, Zhang D. Tyrosine phosphorylation of PP2A is regulated by HER-2 signalling and correlates with breast cancer progression. *Int J Oncol* (2009) 34:1291–301. doi: 10.3892/ijo_00000256
- Janghorban M, Farrell AS, Allen-Petersen BL, Pelz C, Daniel CJ, Oddo J, et al. Targeting c-MYC by antagonizing PP2A inhibitors in breast cancer. *Proc Natl Acad Sci U.S.A.* (2014) 111:9157–62. doi: 10.1073/pnas.1317630111
- Risom T, Wang X, Liang J, Zhang X, Pelz C, Campbell LG, et al. Deregulating MYC in a model of HER2+ breast cancer mimics human intertumoral heterogeneity. *J Clin Invest* (2020) 130:231–46. doi: 10.1172/JCI126390

7. Dueck AC, Reinholz MM, Geiger XJ, Tenner K, Ballman K, Jenkins RB, et al. Impact of c-MYC protein expression on outcome of patients with early-stage HER2+ breast cancer treated with adjuvant trastuzumab NCCTG (Alliance) N9831. *Clin Cancer Res* (2013) 19:5798–807. doi: 10.1158/1078-0432.CCR-13-0558
8. Schade B, Lesurf R, Sanguin-Gendreau V, Bui T, Deblois G, O'Toole SA, et al. β -catenin signaling is a critical event in ErbB2-mediated mammary tumor progression. *Cancer Res* (2013) 73:4474–87. doi: 10.1158/0008-5472.CAN-12-3925
9. Hudis CA. Trastuzumab – mechanism of action and use in clinical practice. *N Engl J Med* (2007) 357:39–51. doi: 10.1056/NEJMra043186
10. Molina MA, Codony-Servat J, Albanell J, Rojo F, Arribas J, Baselga J. Trastuzumab (herceptin), a humanized anti-Her2 receptor monoclonal antibody, inhibits basal and activated Her2 ectodomain cleavage in breast cancer cells. *Cancer Res* (2001) 61:4744–9.
11. Yakes FM, Chinratanalab W, Ritter CA, King W, Seelig S, Arteaga CL. Herceptin-induced inhibition of phosphatidylinositol-3 kinase and akt is required for antibody-mediated effects on p27, cyclin D1, and antitumor action. *Cancer Res* (2002) 62:4132–41.
12. Klapper LN, Waterman H, Sela M, Yarden Y. Tumor-inhibitory antibodies to HER-2/ErbB-2 may act by recruiting c-cbl and enhancing ubiquitination of HER-2. *Cancer Res* (2000) 60:3384–8.
13. Yen L, You XL, Al Moustafa AE, Batist G, Hynes NE, Mader S, et al. Heregulin selectively upregulates vascular endothelial growth factor secretion in cancer cells and stimulates angiogenesis. *Oncogene* (2000) 19:3460–9. doi: 10.1038/sj.onc.1203685
14. Clynes RA, Towers TL, Presta LG, Ravetch JV. Inhibitory fc receptors modulate *in vivo* cytotoxicity against tumor targets. *Nat Med* (2000) 6:443–6. doi: 10.1038/74704
15. Pietras RJ, Fendly BM, Chazin VR, Pegram MD, Howell SB, Slamon DJ. Antibody to HER-2/neu receptor blocks DNA repair after cisplatin in human breast and ovarian cancer cells. *Oncogene* (1994) 9:1829–38.
16. Nahta R, Yu D, Hung MC, Hortobagyi GN, Esteva FJ. Mechanisms of disease: understanding resistance to HER2-targeted therapy in human breast cancer. *Nat Clin Pract Oncol* (2006) 3:269–80. doi: 10.1038/ncononc0509
17. Price-Schiavi SA, Jepson S, Li P, Arango M, Rudland PS, Yee L, et al. Rat Muc4 (sialomucin complex) reduces binding of anti-ErbB2 antibodies to tumor cell surfaces, a potential mechanism for herceptin resistance. *Int J Cancer* (2002) 99:783–91. doi: 10.1002/ijc.10410
18. Nagy P, Friedländer E, Tanner M, Kapanen AI, Carraway KL, Isola J, et al. Decreased accessibility and lack of activation of ErbB2 in JIMT-1, a herceptin-resistant, MUC4-expressing breast cancer cell line. *Cancer Res* (2005) 65:473–82. doi: 10.1158/0008-5472.473.65.2
19. Seo AN, Lee HJ, Kim EJ, Jang MH, Kim YJ, Kim JH, et al. Expression of breast cancer stem cell markers as predictors of prognosis and response to trastuzumab in HER2-positive breast cancer. *Br J Cancer* (2016) 114:1109–16. doi: 10.1038/bjc.2016.101
20. Molina MA, Sáez R, Ramsey EE, Garcia-Barchino MJ, Rojo F, Evans AJ, et al. NH(2)-terminal truncated HER-2 protein but not full-length receptor is associated with nodal metastasis in human breast cancer. *Clin Cancer Res* (2002) 8:347–53.
21. Ozkavruk Eliyatkin N, Aktas S, Ozgur H, Ercetin P, Kupelioglu A. The role of p95HER2 in trastuzumab resistance in breast cancer. *J BUON* (2016) 21:382–9.
22. Nagata Y, Lan KH, Zhou X, Tan M, Esteva FJ, Sahin AA, et al. PTEN activation contributes to tumor inhibition by trastuzumab, and loss of PTEN predicts trastuzumab resistance in patients. *Cancer Cell* (2004) 6:117–27. doi: 10.1016/j.ccr.2004.06.022
23. Berns K, Horlings HM, Hennessy BT, Madiredjo M, Hijmans EM, Beelen K, et al. A functional genetic approach identifies the PI3K pathway as a major determinant of trastuzumab resistance in breast cancer. *Cancer Cell* (2007) 12:395–402. doi: 10.1016/j.ccr.2007.08.030
24. Lu Y, Zi X, Zhao Y, Mascarenhas D, Pollak M. Insulin-like growth factor-I receptor signaling and resistance to trastuzumab (Herceptin). *J Natl Cancer Inst* (2001) 93:1852–7. doi: 10.1093/jnci/93.24.1852
25. Lu Y, Zi X, Pollak M. Molecular mechanisms underlying IGF-I-induced attenuation of the growth-inhibitory activity of trastuzumab (Herceptin) on SKBR3 breast cancer cells. *Int J Cancer* (2004) 108:334–41. doi: 10.1002/ijc.11445
26. Shattuck DL, Miller JK, Carraway KL, Sweeney C. Met receptor contributes to trastuzumab resistance of Her2-overexpressing breast cancer cells. *Cancer Res* (2008) 68:1471–7. doi: 10.1158/0008-5472.CAN-07-5962
27. Chung YC, Chang CM, Wei WC, Chang TW, Chang KJ, Chao WT. Metformin-induced caveolin-1 expression promotes T-DM1 drug efficacy in breast cancer cells. *Sci Rep* (2018) 8:1–9. doi: 10.1038/s41598-018-22250-8
28. Pandey JP, Nambodiri AM. Genetic variants of IgG1 antibodies and Fc γ RIIIa receptors influence the magnitude of antibody-dependent cell-mediated cytotoxicity against prostate cancer cells. *Oncoimmunology* (2014) 3:e27317. doi: 10.4161/onci.27317
29. Martinez VG, O'Neill S, Salimu J, Breslin S, Clayton A, Crown J, et al. Resistance to HER2-targeted anti-cancer drugs is associated with immune evasion in cancer cells and their derived extracellular vesicles. *Oncoimmunology* (2017) 6:e1362530. doi: 10.1080/2162402X.2017.1362530
30. Ciravolo V, Huber V, Ghedini GC, Venturelli E, Bianchi F, Campiglio M, et al. Potential role of HER2-overexpressing exosomes in countering trastuzumab-based therapy. *J Cell Physiol* (2012) 227:658–67. doi: 10.1002/jcp.22773
31. Paik S, Tang G, Shak S, Kim C, Baker J, Kim W, et al. Gene expression and benefit of chemotherapy in women with node-negative, estrogen receptor–positive breast cancer. *J Clin Oncol* (2006) 24:3726–34. doi: 10.1200/JCO.2005.04.7985
32. van 't Veer LJ, Dai H, van de Vijver MJ, He YD, Hart AAM, Mao M, et al. Gene expression profiling predicts clinical outcome of breast cancer. *Nature* (2002) 415:530–6. doi: 10.1038/415530a
33. Scerri J, Baldacchino S, Saliba C, Scerri C, Grech G. Bead-based RNA multiplex panels for biomarker detection in oncology samples. *Methods* (2019) 158:86–91. doi: 10.1016/j.ymeth.2018.10.008
34. Kim BK, Lee JW, Park PJ, Shin YS, Lee WY, Lee KA, et al. The multiplex bead array approach to identifying serum biomarkers associated with breast cancer. *Breast Cancer Res* (2009) 11:R22. doi: 10.1186/bcr2247
35. Zazo S, González-Alonso P, Martín-Aparicio E, Chamizo C, Cristóbal I, Arpi O, et al. Generation, characterization, and maintenance of trastuzumab-resistant HER2+ breast cancer cell lines. *Am J Cancer Res* (2016) 6:2661–78.
36. Treindl F, Ruprecht B, Beiter Y, Schultz S, Döttinger A, Staebler A, et al. A bead-based western for high-throughput cellular signal transduction analyses. *Nat Commun* (2016) 7:12852. doi: 10.1038/ncomms12852
37. Ahn J, Lee JG, Chin C, In S, Yang A, Park HS, et al. MSK1 functions as a transcriptional coactivator of p53 in the regulation of p21 gene expression. *Exp Mol Med* (2018) 50:1–12. doi: 10.1038/s12276-018-0160-8
38. Hsu YL, Hou MF, Kuo PL, Huang YF, Tsai EM. Breast tumor-associated osteoblast-derived CXCL5 increases cancer progression by ERK/MSK1/Elk-1/Snail signaling pathway. *Oncogene* (2013) 32:4436–47. doi: 10.1038/onc.2012.444
39. Parker P, Murray-Rust J. PKC at a glance. *J Cell Sci* (2004) 117:131–2. doi: 10.1242/jcs.00982
40. Uhlén M, Fagerberg L, Hallström BM, Lindskog C, Oksvold P, Mardinoglu A, et al. Proteomics. tissue-based map of the human proteome. *Science* (2015) 347:1260419. doi: 10.1126/science
41. Emmanouilidi A, Falasca M. Targeting PDK1 for chemosensitization of cancer cells. *Cancers (Basel)* (2017) 9:140. doi: 10.3390/cancers9100140
42. Singh RK, Kumar S, Gautam PK, Tomar MS, Verma PK, Singh SP, et al. Protein kinase c- α and the regulation of diverse cell responses. *Biomol Concepts* (2017) 8:143–53. doi: 10.1515/bmc-2017-0005
43. Ways DK, Kukoly CA, deVente J, Hooker JL, Bryant WO, Posekany KJ, et al. MCF-7 breast cancer cells transfected with protein kinase c-alpha exhibit altered expression of other protein kinase c isoforms and display a more aggressive neoplastic phenotype. *J Clin Invest* (1995) 95:1906–15. doi: 10.1172/JCI117872
44. Gupta AK, Galoforo SS, Berns CM, Martinez AA, Corry PM, Guan KL, et al. Elevated levels of ERK2 in human breast carcinoma MCF-7 cells transfected with protein kinase c alpha. *Cell Prolif* (1996) 29:655–63. doi: 10.1111/j.1365-2184.1996.tb00979.x
45. Bailey TA, Luan H, Tom E, Bielecki TA, Mohapatra B, Ahmad G, et al. A kinase inhibitor screen reveals protein kinase c-dependent endocytic recycling of ErbB2 in breast cancer cells. *J Biol Chem* (2014) 289:30443–58. doi: 10.1074/jbc.M114.608992
46. Magnifico A, Albano L, Campaner S, Campiglio M, Pilotti S, Ménard S, et al. Protein kinase c alpha determines HER2 fate in breast carcinoma cells with HER2 protein overexpression without gene amplification. *Cancer Res* (2007) 67:5308–17. doi: 10.1158/0008-5472.CAN-06-3936
47. Chiang GG, Abraham RT. Phosphorylation of mammalian target of rapamycin (mTOR) at ser-2448 is mediated by p70S6 kinase. *J Biol Chem* (2005) 280:25485–90. doi: 10.1074/jbc.M501707200
48. Pham TND, Perez White BE, Zhao H, Mortazavi F, Tonetti DA. Protein kinase c α enhances migration of breast cancer cells through FOXC2-mediated repression of p120-catenin. *BMC Cancer* (2017) 17:832. doi: 10.1186/s12885-017-3827-y
49. Giordano A, Gao H, Anfossi S, Cohen E, Mego M, Lee BN, et al. Epithelial-mesenchymal transition and stem cell markers in patients with HER2-positive metastatic breast cancer. *Mol Cancer Ther* (2012) 11:2526–34. doi: 10.1158/1535-7163.MCT-12-0460
50. Duhachek-Muggy S, Qi Y, Wise R, Alyahya L, Li H, Hodge J, et al. Metalloprotease-disintegrin ADAM12 actively promotes the stem cell-like phenotype in claudin-low breast cancer. *Mol Cancer* (2017) 16:32. doi: 10.1186/s12943-017-0599-6
51. Nami B, Wang Z. HER2 in breast cancer stemness: A negative feedback loop towards trastuzumab resistance. *Cancers (Basel)* (2017) 9:40. doi: 10.3390/cancers9050040

52. Feldinger K, Generali D, Kramer-Marek G, Gijzen M, Ng TB, Wong JH, et al. ADAM10 mediates trastuzumab resistance and is correlated with survival in HER2 positive breast cancer. *Oncotarget* (2014) 5:6633–46. doi: 10.18632/oncotarget.1955

53. Ignatiadis M, Rothé F, Chaboteaux C, Durbecq V, Rouas G, Criscitiello C, et al. HER2-positive circulating tumor cells in breast cancer. *PloS One* (2011) 6: e15624. doi: 10.1371/journal.pone.0015624

54. Crigna AT, Samec M, Koklesova L, Liskova A, Giordano FA, Kubatka P, et al. Cell-free nucleic acid patterns in disease prediction and monitoring - hype or hope? *EPMA J* (2020) 11:603–27. doi: 10.1007/s13167-020-00226-x

55. Zhan X, Li J, Guo Y, Golubnitschaja O. Mass spectrometry analysis of human tear fluid biomarkers specific for ocular and systemic diseases in the context of 3P medicine. *EPMA J* (2021) 12:449–75. doi: 10.1007/s13167-021-00265-y



OPEN ACCESS

EDITED BY

Naoyuki Kataoka,
The University of Tokyo, Japan

REVIEWED BY

Jinhui Liu,
Nanjing Medical University, China
Giovanni Nigita,
The Ohio State University,
United States

*CORRESPONDENCE

Xianquan Zhan
yjzhan2011@gmail.com
Na Li
qianshoulina@163.com

SPECIALTY SECTION

This article was submitted to
Cancer Endocrinology,
a section of the journal
Frontiers in Endocrinology

RECEIVED 18 June 2022

ACCEPTED 18 November 2022

PUBLISHED 05 December 2022

CITATION

Zheng P, Li N and Zhan X (2022)
Ovarian cancer subtypes based on
the regulatory genes of RNA
modifications: Novel prediction
model of prognosis.
Front. Endocrinol. 13:972341.
doi: 10.3389/fendo.2022.972341

COPYRIGHT

© 2022 Zheng, Li and Zhan. This is an
open-access article distributed under
the terms of the [Creative Commons
Attribution License \(CC BY\)](https://creativecommons.org/licenses/by/4.0/). The use,
distribution or reproduction in other
forums is permitted, provided the
original author(s) and the copyright
owner(s) are credited and that the
original publication in this journal is
cited, in accordance with accepted
academic practice. No use,
distribution or reproduction is
permitted which does not comply
with these terms.

Ovarian cancer subtypes based on the regulatory genes of RNA modifications: Novel prediction model of prognosis

Peixian Zheng^{1,2}, Na Li^{1,2*} and Xianquan Zhan^{1,2*}

¹Shandong Key Laboratory of Radiation Oncology, Shandong Cancer Hospital and Institute, Shandong First Medical University, Jinan, Shandong, China, ²Medical Science and Technology Innovation Center, Shandong First Medical University, Jinan, Shandong, China

Background: Ovarian cancer (OC) is a female reproductive system tumor. RNA modifications play key roles in gene expression regulation. The growing evidence demonstrates that RNA methylation is critical for various biological functions, and that its dysregulation is related to the progression of cancer in human.

Method: OC samples were classified into different subtypes (Clusters 1 and 2) based on various RNA-modification regulatory genes (RRGs) in the process of RNA modifications (m1A, m6A, m6Am, m5C, m7G, ac4C, m3C, and Ψ) by nonnegative matrix factorization method (NMF). Based on differently expressed RRGs (DERRGs) between clusters, a pathologically specific RNA-modification regulatory gene signature was constructed with Lasso regression. Kaplan-Meier analysis and receiver operating characteristic (ROC) curves were used to evaluate the prognostic ability of the identified model. The correlations of clinicopathological features, immune subtypes, immune scores, immune cells, and tumor mutation burden (TMB) were also estimated between different NMF clusters and riskscore groups.

Results: In this study, 59 RRGs in the process of RNA modifications (m1A, m6A, m6Am, m5C, m7G, ac4C, m3C, and Ψ) were obtained from TCGA database. These RRGs were interactional, and sample clusters based on these regulators were significantly correlated with survival rate, clinical characteristics (involving survival status and pathologic stage), drug sensibility, and immune microenvironment. Furthermore, Lasso regression based on these 21 DERRGs between clusters 1 and 2 constructed a four-DERRG signature (ALYREF, ZC3H13, WTAP, and METTL1). Based on this signature, 307 OC patients were classified into high- and low-risk groups based on median value of riskscores from lasso regression. This identified signature was significantly associated with overall survival, radiation therapy, age, clinical stage, cancer status, and immune cells (involving CD4+ memory resting T cells, plasma cells, and Macrophages M1) of ovarian cancer patients. Further, GSEA revealed that multiple biological behaviors were significantly enriched in different groups.

Conclusions: OC patients were classified into two subtypes per these RRGs. This study identified four-DERRG signature (ALYREF, ZC3H13, WTAP, and METTL1) in OC, which was an independent prognostic model for patient stratification, prognostic evaluation, and prediction of response to immunotherapy in ovarian cancer by classifying OC patients into high- and low-risk groups.

KEYWORDS

ovarian cancer, RNA-modification regulatory gene (RRG), differentially expressed RRG (DERRG), RNA modification-related model, tumor immune microenvironment, risk score

Introduction

Ovarian cancer (OC) is a malignant gynecological disease in female reproductive system, which evolves as the eighth most frequent type of cancer and also the eighth most conventional death cause in women, accounting for 3.4% and 4.4%, respectively (1). OCs could be classified into epithelial and non-epithelial subtypes. According to histological characteristics of tumor cells, epithelial ovarian cancers are classified into mucinous, serous, endometrioid, or clear cell (2, 3). Different subtypes of OCs significantly influence its prognosis and should be treated in diverse therapy strategies (4). It is reported that 5-year relative survival is below 45% (5), which means there is a poor prognosis in OCs. Currently, surgical cytoreduction remains the main treatment of OCs, followed by neoadjuvant chemotherapy; targeted treatments such as poly ADP-ribose polymerase inhibitors and bevacizumab gradually become the maintenance treatment in the first line of clinical practice (6). Immunotherapy in OCs is getting increasing attention, and the predictiveness of response to immunotherapy may be improved by evaluating sensitive and resistant targeted therapy subpopulations on the basis of tumor biomarkers (7).

RNA modification is an addition of a chemical group on RNA nucleotide chains to regulate the functions of RNA biological behaviors with reference to post-transcriptional regulation (8, 9), which is also called epitranscriptome (10). Up to 170 types of chemical modifications have been discovered in RNAs (11), among which N1-methyladenosine (m1A), N6-methyladenosine (m6A), 2-O-dimethyladenosine (m6Am), 5-methylcytosine (m5C), N7-methyladenosine (m7G), N4-acetylcytidine (ac4C), 3-methylcytidine (m3C), and pseudouridine (Ψ) were especially critical. The process of RNA modification was regulated by three distinct clusters of specific proteins called writers, readers, and erasers (9, 12). Writers catalyze the formation of a specific chemical modification on RNAs; erasers catalyze the elimination of a specific chemical modification from the modified RNAs; and

readers are RNA-binding proteins that could recognize and bind the modified RNAs (10). Previous studies identified different varieties of writers, erasers and readers of m1A, m6A, m6Am, m5C, m7G, ac4C, m3C, and Ψ . For m6A, its writer genes have KIAA1429, ZC3H13, METTL3, METTL14, WTAP, RBM15, and RBM15B, which catalyzed m6A methylation; Erasers included FTO and ALKBH5, which could reverse m6A modification through demethylation change; and readers contained YTHDC1, YTHDC2, YTHDF1, YTHDF2, HNRNPC, IGF2BP1, IGF2BP2, YTHDF3, IGF2BP3, HNRNPA2B1, and RBMX, which could recognize and bind the modified RNAs (13, 14). For m5C, writers (m5C methyltransferases) included TRDMT1, DNMT1, DNMT3A, DNMT3B, NSUN1, NSUN2, NSUN3, NSUN4, NSUN5, NSUN6, and NSUN7; erasers encompassed TET1, TET2, and TET3; and readers included YBX1 and ALYREF (15). For m1A, writers involved TRMT6, TRMT61A, TRMT61B, TRMT10C, and RRP8; erasers included ALKBH1 and ALKBH3; and readers included YTHDF1, YTHDF2, YTHDF3, and YTHDC1 (9, 16, 17). For ac4C, writers included NAT10 and THUMP1; and erasers and readers remain unknown (18, 19). For m3C, only one writer METTL8 was discovered, and erasers and readers were still undetected (20). For m6Am, writers included PCIF1, METTL3, and METTL4; eraser involved FTO; and no readers were discovered (21–24). For m7G, writers included RNMT, METTL1, and WDR4; the only detected eraser was NUDT16, and readers were still unknown (25, 26). For Ψ , only writers were known, including PUS1, PUS3, PUS4, PUS7, PUS9, TRUB1, and TRUB2 (9, 10).

With the gradual in-depth studies of RNA modifications, an increasing number of RNA-modification regulatory genes (RRGs) were proved to play crucial roles in the occurrence and development of OCs. For instance, ALKBH3 affected the prognosis of OCs through inducing m1A demethylation to increase the CSF-1 stability (27). m6A demethylase ALKBH5 accelerated the process of ovarian carcinogenesis through NF- κ B pathway in a simulated tumor microenvironment (28).

DNMT3A/3B interacted with microRNA-29b in a double-negative feedback way to result in OC progression (29). FTO played a role in the acceleration of cell proliferation, inhibition of apoptosis, and autophagy activation in OC cells (30). The upregulation of HNRNPA2B1 in OC tissue promotes the proliferation of OC cells, which suggests that the upregulation of HNRNPA2B1 was associated with poor prognosis of OCs (31). IGF2BP1 enhanced the invasion of OC cells through inhibiting miRNA impairment gene expression (32). Elevated levels of IGF2BP3 and RNA-binding protein Lin28B were related to platinum chemoresistance as well as poor prognosis of OCs (33). From these studies, it is obvious that different varieties of RRGs significantly influenced the tumorigenesis, tumor progression, tumor aggressiveness, tumor cell proliferation, and drug resistance.

To search for novel cancer treatment strategies, tumor immune microenvironment (TIM) and immunotherapy became a new research hotspot. A study found that EZH2-mediated H3K27me3 along with DNMT1-mediated DNA methylation inhibited generation of Th1 chemokines, including CXCL9 and CXCL10, which helped effector T cells migrate to microenvironment in tumor. In that study, epigenetic modulators were used to eliminate the inhibition in tumor-bearing mice, increasing tumor infiltration of T cells, retarding progression of tumor, and promoting response to PD-L1 checkpoint blockade along with adoptive T cell transfusion. Further, EZH2 in combination with DNMT1 had a negative correlation with CD8+ T cells tumor infiltration and prognosis of OC patients (34). Another study certified the strong physical relationship between RNA-binding ubiquitin ligase MEX3A and IGF2BP2, PABPC1, LAMTOR2, and KHDRBS2, indicating the intense correlation of MEX3A expression level and infiltration of neutrophils, macrophages, dendritic cells, B cells, and CD8+ T cells. Activation of immune cells and immune modulators was related to decrease of mortality rate in OC patients. Additionally, the relevance of MEX3A and lymphocytes (neutrophils, macrophages, dendritic cells, B cells, and CD8+ T cells), immune stimulators, immune inhibitors, and MHC molecules was detected (35). Thereby, RRGs could affect TIM and play crucial roles in prediction of immunotherapy outcomes of OC treatment.

Our study classified 307 OC patients into 2 subtypes based on the expressions of 59 RRGs and identified 21 differentially expressed RRGs (DERRGs) between 2 subtypes. In previous studies, OC subtypes were clustered based on different types of genes using non-negative matrix factorization (NMF) method. According to 426 immune lncRNA pair data, OC samples could be classified into 2 molecular subtypes (36). Similarly, based on the expression profiles of 177 metabolism-related genes after a filtration of prognostic association, 3 different molecular subtypes of OC were obtained (37). Based on the immune cell infiltration in OC tumor microenvironment (TME), all OC samples were

defined into 4 TME clusters, after which 2 genomic OC subtypes were identified according to differential expression genes among TME clusters (38). Another study reported that no more than 3 molecular subtypes should be classified for high-grade serous OC based on cross-population analysis (39). All these obtained subtype classifications were well effective, validated by their clinical feature correlation. Compared to them, this present study classified OC samples into 2 subtypes based on 59 RRGs expression profile, and also got a good consistency with clinical features. Then, lasso regression was used to construct a four-DERRG signature (ALYREF, ZC3H13, WTAP, and METTL1) model, which found the most valuable and critical regulators in m1A, m6A, m6Am, m5C, m7G, ac4C, m3C, and Ψ RNA modification processes. We conducted a comprehensive study of different types of RNA-modification regulators rather than only one specific RNA modification, which was more generally applicable to the evaluation of OC patients. The four-DERRG signature acted as an independent risk factor, which could be used in patient stratification, prediction, prevention, and immunotherapy targets of OCs. The research flow chart was presented for this study (Figure 1).

Methods

Data processing

In total, 307 OC patients were enrolled in this study, which contains both complete clinical information and expression data. The corresponding clinical features, including survival status, survival time, and progression-free-survival (PFS) time, were also downloaded from The Cancer Genome Atlas (TCGA) website (Supplementary Table 1). The mRNA expression level of 59 RRGs for different RNA modifications (m1A, m6A, m6Am, m5C, m7G, ac4C, m3C, and Ψ) was obtained from TCGA website (<https://portal.gdc.cancer.gov/>) (Supplementary Table 2), and those data were transformed with FPKM. The 59 RRGs included m6A regulators (KIAA1429, ZC3H13, METTL3, METTL14, WTAP, RBM15, RBM15B, FTO, ALKBH5, YTHDC1, YTHDC2, YTHDF1, YTHDF2, HNRNPC, IGF2BP1, IGF2BP2, YTHDF3, IGF2BP3, HNRNPA2B1, and RBMX), m5C regulators (TRDMT1, DNMT1, DNMT3A, DNMT3B, NSUN1, NSUN2, NSUN3, NSUN4, NSUN5, NSUN6, NSUN7, TET1, TET2, TET3, YBX1, and ALYREF), m1A regulators (TRMT6, TRMT61A, TRMT61B, TRMT10C, RRP8, ALKBH1, ALKBH3, YTHDF1, YTHDF2, YTHDF3, and YTHDC1), ac4C regulators (NAT10, and THUMPD1), m3C regulator METTL8, m6Am regulators (PCIF1, FTO, METTL3, and METTL4), m7G regulators (RNMT, METTL1, WDR4, and NUDT16), and Ψ regulators (PUS1, PUS3, PUS4, PUS7, PUS9, TRUB1, and TRUB2).

The protein-protein interaction network and drug sensibility of RRGs

In order to evaluate the interactive associations of 59 RRGs for eight types of RNA modifications (m1A, m6A, m6Am, m5C, m7G, ac4C, m3C, and Ψ), their protein-protein interaction (PPI) network was mapped in the STRING database (<https://string-db.org/>) with combined score >0.9 (Supplementary Table 3).

The CellMiner (<https://discover.nci.nih.gov/cellminer/>) was used to evaluate the association between RRG expressions and drug sensibility. CellMiner is a genomic and drug analysis tool for exploring transcripts and drug paradigms of NCI-60 cell line set. NCI-60 cell line set, explored by National Cancer Institute’s (NCI) Developmental Therapeutics Program (DTP) in US, was used for anti-cancer drug screening and efficacy evaluation. Their correlation was validated in Corrplot R package with Spearman method ($p < 0.05$, and $|\text{Cor}| > 0.4$) on the basis of the relevant data obtained from CellMiner in OCs (Supplementary Table 4).

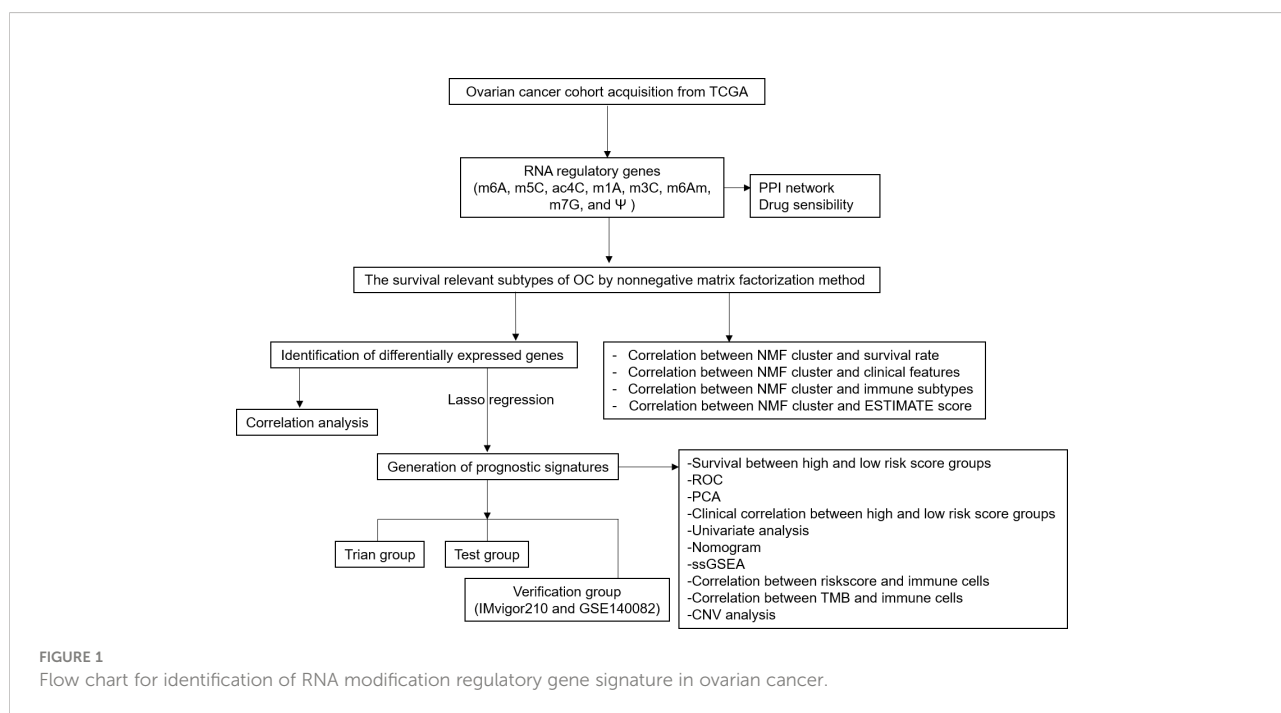
Identification of OC subclasses

Based on these 59 RRGs, non-negative matrix factorization (NMF) clustering was analyzed subsequently. NMF clustering method was generally used to identify cancer molecular subtypes. Extracting biological correlation coefficient of data in gene expression matrix, NMF clustering could capture internal structural features to cluster cancer samples by organizing genes and samples. Target dataset was obtained *via* merging gene data

and expression matrix after reading in them. During NMF clustering operation, different numbers of NMF subtypes were obtained. According to cophenetic value, the optimum clustering number was determined, based on which final grouping situation was settled. A filtration process was performed prior to NMF to exclude candidate genes whose median absolute deviation (MAD) values were low ($\text{MAD} \leq 0.5$) in OC patients. The NMF R package (<https://www.rdocumentation.org/packages/NMF/versions/0.23.0>) was used to perform unsupervised NMF clustering (R version 4.1.1) on the metadata set, and the optimal cluster number 2 was selected as the coexistence correlation coefficient K value (Supplementary Table 5). Based on Kaplan–Meier method, the overall survival (OS) and PFS curves of OC subgroups were obtained using “survival” package in R (R version 4.1.1) software (<https://www.bioconductor.org/packages/devel/bioc/vignettes/survtype/inst/doc/survtype.html>).

The correlation of clinical features in OC subclasses

The corresponding clinical features, including survival time, survival status, age at initial pathologic diagnosis, clinical stage, anatomic subdivision, radiation therapy, primary therapy outcome, histologic grade, lymphatic invasion, cancer status, and tumor residual disease, were also downloaded from TCGA website (Supplementary Table 1). Chi-square test (χ^2) was used to analyze the correlation of clinical characteristics between NMF clusters 1 and 2, with statistical significance level of p



<0.05. The clinical heatmap of 59 RRGs was performed with “pheatmap” R package (<https://cran.r-project.org/web/packages/pheatmap/index.html>) between different OC subclasses.

The different immune subtype, and immune score between different NMF subtypes in OCs

OC samples were classified into four clusters, involving wound healing (Immune C1), IFN-gamma dominant (Immune C2), inflammatory (Immune C3), and lymphocyte depleted (Immune C4) based on immune model subtypes (Supplementary Table 1). Different immune subtype distribution between NFM clusters was analyzed with ggalluvial R package (<https://www.rdocumentation.org/packages/ggalluvial/versions/0.12.3/topics/ggalluvial-package>).

Based on expression data, stromal cells and immune cells in tissues of malignant tumor were estimated using an ESTIMATE algorithm. Based on specific biomarkers associated with stromal and immune cells infiltration in tumor samples, immune scores were estimated with ESTIMATE algorithm, which was derived from the public source website (<https://sourceforge.net/projects/estimateproject/>). The immune scores were calculated for each sample (Supplementary Table 6), and compared between different NFM subtypes in OCs. The violin-plots of ESTIMATE algorithm between different NFM subtypes were drawn with ggpubr R package (<https://www.rdocumentation.org/packages/ggpubr/versions/0.4.0>) with statistical significance level of $p < 0.05$.

Determination of DERRGs between different clusters in OCs

Unpaired student *t*-tests were used to calculate DERRGs of 59 RRGs between the NMF clusters 1 and 2 in OC patients, whose difference was statistically significant with adjusted *p*-value <0.05. Subsequently, Spearman method was used to perform the association between DERRGs by means of Corrplot R package (<https://www.rdocumentation.org/packages/corrplot/versions/0.92>) ($p < 0.05$).

Establishment of DERRG signature in OCs with lasso regression

Lasso regression was a data processing tool, with the help of which prediction accuracy and rationality of the statistical model were enhanced *via* selection and regularization of variates. To obtain better performance parameters, variates were selectively put into the constructed model. Further, overfitting could be avoided *via* regularization of model complexity. The

regularization degree of lasso regression was controlled by parameter lambda, and the penalty intensity of linear model with more variates was positively correlated with the value of lambda, based on which a model with fewer variates could be obtained. The prognostic model was constructed through identifying the relationship between the optimal selection of subset and lasso coefficient estimation. Lasso regression was performed based on DERRGs to identify the DERRG signature related to high risk of OCs, which was validated with the glmnet R package (<https://www.rdocumentation.org/packages/glmnet/versions/4.1-4>). The DERRG signature model identified by lasso regression calculated a riskscore associated with pathologically related clinical features for each OC tissue sample. Accordingly, 307 OC patients were randomly assigned to training and test groups, with each group assigned to high-risk and low-risk groups based on the median value of all riskscores (Supplementary Table 7). Further, measurements of riskscore-based classification were tested with receiver operating characteristic (ROC) curve and principal component analysis (PCA). The validity of the prognostic model was evaluated with Kaplan–Meier method in training and test groups.

To eliminate the over-fitting effect, the prognostic value of the DERRG signature was verified with two independent external validation cohorts, including cohorts imvigor210 (Supplementary Tables 8, 9) and GSE140082 (Supplementary Table 10). Imvigor210 study is a phase II clinical study using PD-L1 monoclonal antibody atezolizumab in one arm of locally progressive or metastatic tumor after platinum chemotherapy failure. Objective response rate (ORR) is primary end point, whereas PFS and OS are secondary end points. The response to immunotherapy based on imvigor210 cohort involved stable disease (SD), progressive disease (PD), complete response (CR), and partial response (PR) (Supplementary Table 9). GSE140082 cohort included 380 OC samples and corresponding integrated clinical follow-up information. The validity of the prognostic model in imvigor210 validation cohort and GSE140082 validation cohort was evaluated with Kaplan–Meier method.

Moreover, Cox regression was used to analyze clinical features related to OS in OC patients with univariate model. The clinical relevance of high-risk and low-risk groups was detected with pheatmap R package (<http://bioconductor.org/packages/3.8/bioc/html/heatmaps.html>). This riskscore evaluation nomogram was performed to assess the prognosis of OC patients including 1-, 3-, and 5-year survival rates, and then verified with decision-making tree method.

Gene-set enrichment analysis (GSEA) is a gratis software for analyzing genomic microarray data containing various functional gene sets. A total of 307 patients were classified into high-risk and low-risk groups based on OC riskscores. GSEA analysis was performed on TCGA data of the two groups to search for the significantly enriched gene sets in high-risk and low-risk groups (Supplementary Table 11).

The correlations between riskscore or TMB or CNV and immune cells

CIBERSORT algorithm and LM22 gene signature were used to determine the proportions of different immune cells in OCs, which allow for identifying 22 types of human immune cell phenotypes with high sensitivity and specificity. Preparation of gene expression profiles was performed with standard annotation files, and corresponding data were submitted to the CIBERSORT website (<http://cibersort.stanford.edu/>), in which LM22 signature and 1,000 permutations were used to run the algorithm (Supplementary Table 12). Corrrplot R package was used to analyze the correlation between immune cells and riskscore (<https://www.rdocumentation.org/packages/corrplot/versions/0.92>) with Spearman method ($p < 0.05$), encompassing monocytes, macrophages M1, macrophages M2, macrophages M0, eosinophils, neutrophils, mast cells activated, mast cells resting, dendritic cells activated, dendritic cells resting, NK cells activated, NK cells resting, T cells regulatory (Tregs), T cells follicular helper, T cells gamma delta, B cells naïve, plasma cells, B cells memory, T cells CD4 naïve, T cells CD4 memory activated, T cells CD4 memory resting, and T cells CD8.

Apart from this, the Level 3 RNA-seq data of immune checkpoints were selected from TCGA database (<https://portal.gdc.cancer.gov/>). Different levels of immune checkpoints were analyzed between different methylation subtypes in OCs with unpaired student *t*-tests, including VTCN1, PDCD1, CTLA4, CD276, CD80, CD274, PDCD1LG2, and CD86.

TMB scores were generated with Maftools R package (Supplementary Table 13). The relevance of TMB and immune cells was validated with Corrrplot R package (<https://www.rdocumentation.org/packages/corrplot/versions/0.92>) with Spearman method ($p < 0.05$).

Copy number variant (CNV) data were based on UCSC Xena datasets (<https://xenabrowser.net/datapages/>) in Supplementary Table 14. The correlation between identified gene expression in LASSO model and CNV was calculated with Kruskal test ($p < 0.05$), and boxplots were plotted with barplot R package (<https://www.rdocumentation.org/packages/graphics/versions/3.6.2/topics/barplot>).

Statistical analysis

For variables following a normal distribution, unpaired student *t*-test was used to calculate the *p* value, and $p < 0.05$ was set as the level of statistical significance. Survival curves were generated with the Kaplan-Meier method, and statistical significance of differences was evaluated through the Log-rank (Mantel-Cox) test, in which $p < 0.05$ represented differences were statistically significant. The hazard ratio of univariate Cox proportional hazard regression model was established with statistical significance of $p < 0.05$. We also shared the code that

was used for this study in a public repository-GitHub (<https://github.com/peixianzheng/OCmodel.git>).

Results

Ovarian cancer subtypes based on RRGs with NMF

In total, 59 RRGs for RNA modifications (m1A, m6A, m6Am, m5C, m7G, ac4C, m3C, and Ψ) were obtained from TCGA website (Supplementary Table 2), including m6A regulators (KIAA1429, ZC3H13, METTL3, METTL14, WTAP, RBM15, RBM15B, FTO, ALKBH5, YTHDC1, YTHDC2, YTHDF1, YTHDF2, HNRNPC, IGF2BP1, IGF2BP2, YTHDF3, IGF2BP3, HNRNPA2B1, and RBMX), m5C regulators (TRDMT1, DNMT1, DNMT3A, DNMT3B, NSUN1, NSUN2, NSUN3, NSUN4, NSUN5, NSUN6, NSUN7, TET1, TET2, TET3, YBX1, and ALYREF), m1A regulators (TRMT6, TRMT61A, TRMT61B, TRMT10C, RRP8, ALKBH1, ALKBH3, YTHDF1, YTHDF2, YTHDF3, and YTHDC1), ac4C regulators (NAT10, and THUMP1), m3C regulator METTL8, m6Am regulators (PCIF1, FTO, METTL3, and METTL4), m7G regulators (RNMT, METTL1, WDR4, and NUDT16), and Ψ regulators (PUS1, PUS3, PUS4, PUS7, PUS9, TRUB1, and TRUB2).

NMF method is an efficient tool for dimensionality reduction of cancer subtype identification. In this study, the best value of clusters number (*K*) was obtained using factoextra package. When *K* was equal to 2, the OC samples ($n=307$) were classified into two distinct subtypes (Cluster 1: $n=110$; Cluster 2: $n=197$) by NMF method (Figure 2A; Supplementary Table 5), showing a favourable match between OC samples and their identified subtypes. It is worth noting that OC patients in Cluster 1 showed fine OS status, whereas Cluster 2 patients displayed poor prognosis (Figure 2B). Meanwhile, OC patients in Cluster 1 showed good PFS rate, whereas Cluster 2 had poor prognosis (Figure 2C; Supplementary Table 1).

The significant PPI network of RRGs and the drug sensibility

Protein-protein interaction analysis was performed on 59 RRGs with STRING. The spectrum of nodes combined scores was from 0.900 to 0.999 (Figure 2D; Supplementary Table 3). Some protein-protein interactions showed high combined scores (>0.999), such as ZC3H13 and KIAA1429, WTAP and KIAA1429, METTL14 and KIAA1429, KIAA1429 and METTL3, METTL1 and WDR4, KIAA1429 and METTL14, METTL14 and METTL3, WTAP and METTL14, METTL3 and KIAA1429, WTAP and METTL3, METTL3 and METTL14, RBM15 and WTAP, TRMT6 and TRMT61A, TRMT61A and TRMT6, WDR4 and METTL1, ZC3H13 and WTAP, KIAA1429 and

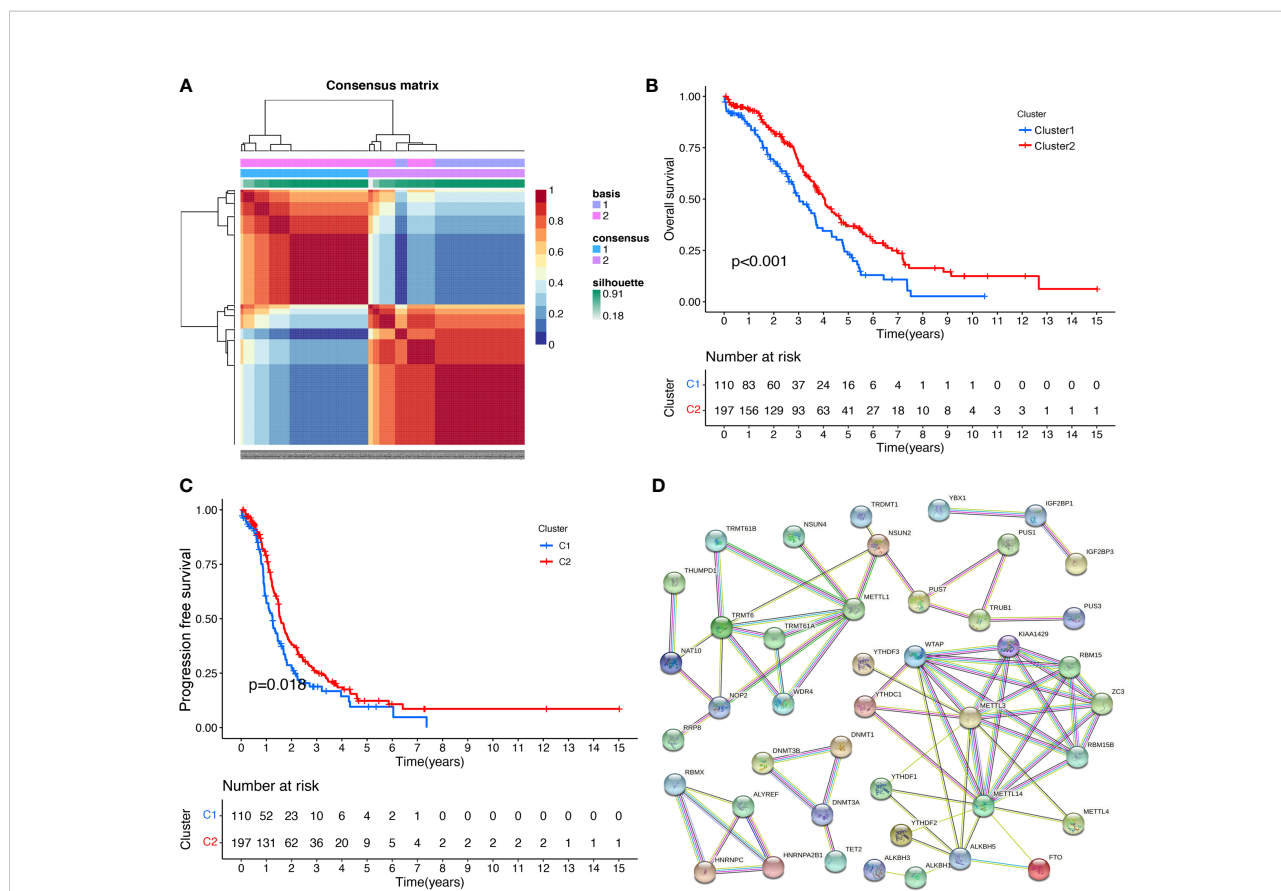


FIGURE 2
The RNA modification subtypes based on NMF analysis. **(A)** Clustering heat map of samples at consensus $k = 2$. Different colors reflect different cluster numbers; the color gradient is from white to blue, indicating the consensus of progression. **(B)** The OS analysis between two RNA-modification subtypes in ovarian cancer. **(C)** The PFS analysis between two RNA modification subtypes in ovarian cancer. **(D)** The PPI network of RNA-modification regulatory genes.

WTAP, WTAP and METTL3, WTAP and RBM15, METTL14 and WTAP, KIAA1429 and ZC3H13, and ZC3H13 and WTAP.

Some RRGs showed significant associations with drug sensibility, with $|\text{correlation coefficient}| > 0.5$ and $p < 0.05$ (Supplementary Table 4), such as PUS1 and triethylenemelamine, PUS1 and thiotepa, ZC3H13 and dabrafenib, PUS1 and 5-fluoro deoxy uridine 10mer, NSUN5 and vorinostat, YTHDC2 and nelarabine, ZC3H13 and selumetinib, ALYREF and floxuridine, RBMX and nelarabine, PUS1 and cytarabine, PUS1 and cladribine, TRUB2 and vorinostat, NSUN6 and nelarabine, RBMX and chelerythrine, ALYREF and 5-fluoro deoxy uridine 10mer, DNMT3A and nelarabine, IGF2BP2 and dexrazoxane, IGF2BP2 and SR16157. Some of them were plotted (Figure 3A).

DERRGs between clusters 1 and 2 of OCs

The DERRGs of 59 RRGs were calculated with adjusted p -value < 0.05 , from which 21 DERRGs were identified, including

PUS9, ALYREF, TRDMT1, ZC3H13, YTHDF2, YBX1, WTAP, TRUB2, TET2, RNMT, RBM15B, PUS7, NSUN5, NSUN2, METTL3, METTL4, METTL14, METTL1, IGF2BP3, HNRNPC, and FTO (Figure 3B). Subsequently, the association between DERRGs was evaluated using Corrplot with Spearman method ($p < 0.05$). Some of them showed high correlation coefficient, including METTL14 and TET2, METTL1 and TET2, HNRNPC and METTL1, HNRNPC and METTL3, HNRNPC and ALYREF, ALYREF and TRUB2, METTL4 and RNMT (Figure 3C).

Correlation between OC subtypes and clinical characteristics or immune

Clinical information was obtained from TCGA database, including age (from 30 to 84 years), survival status (alive and dead), anatomic subdivision (left, bilateral and right), follow-up outcome (complete remission/response, partial remission/response, stable disease, and progressive disease), pathologic

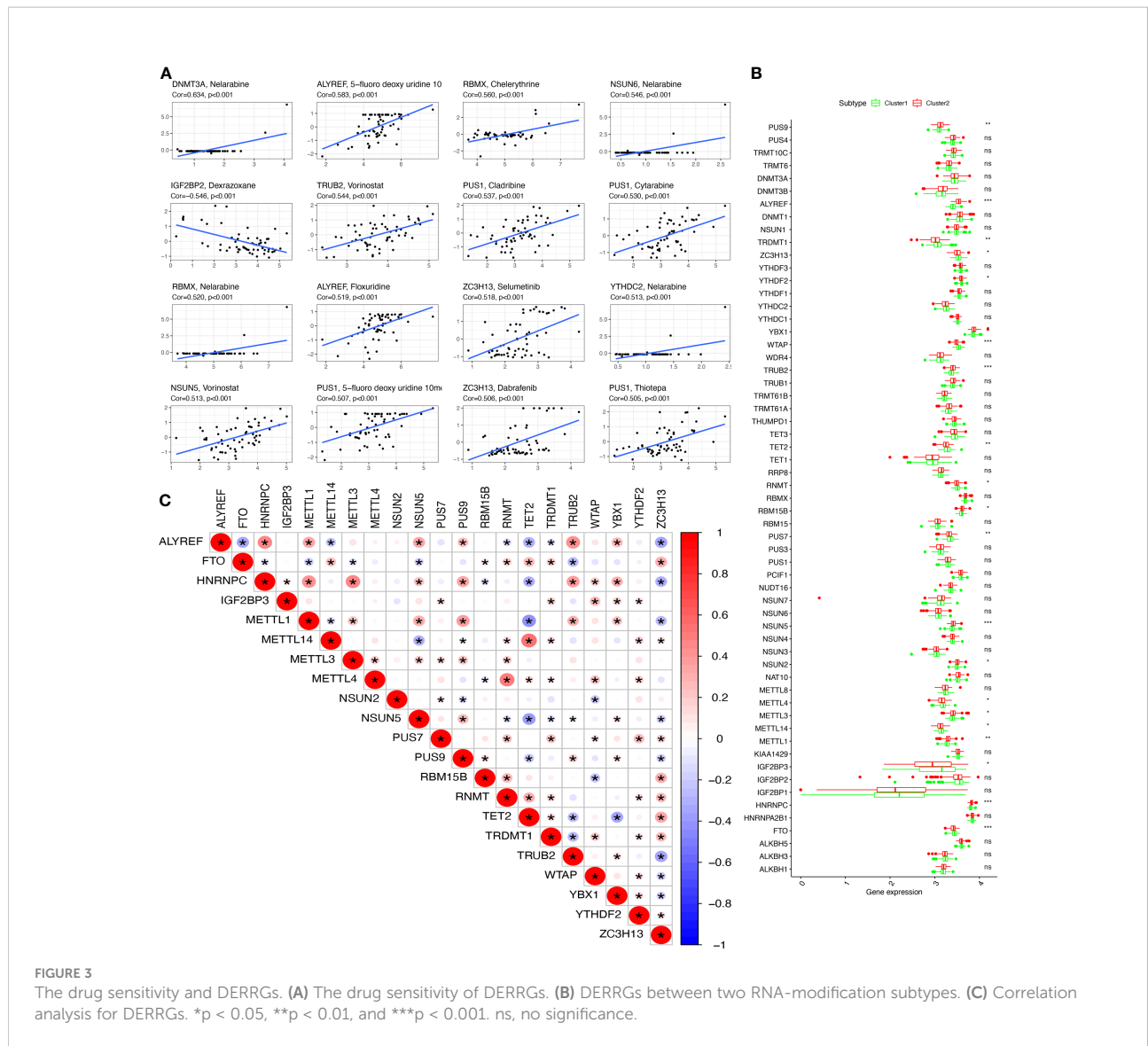


FIGURE 3 The drug sensitivity and DERRGs. **(A)** The drug sensitivity of DERRGs. **(B)** DERRGs between two RNA-modification subtypes. **(C)** Correlation analysis for DERRGs. *p < 0.05, **p < 0.01, and ***p < 0.001. ns, no significance.

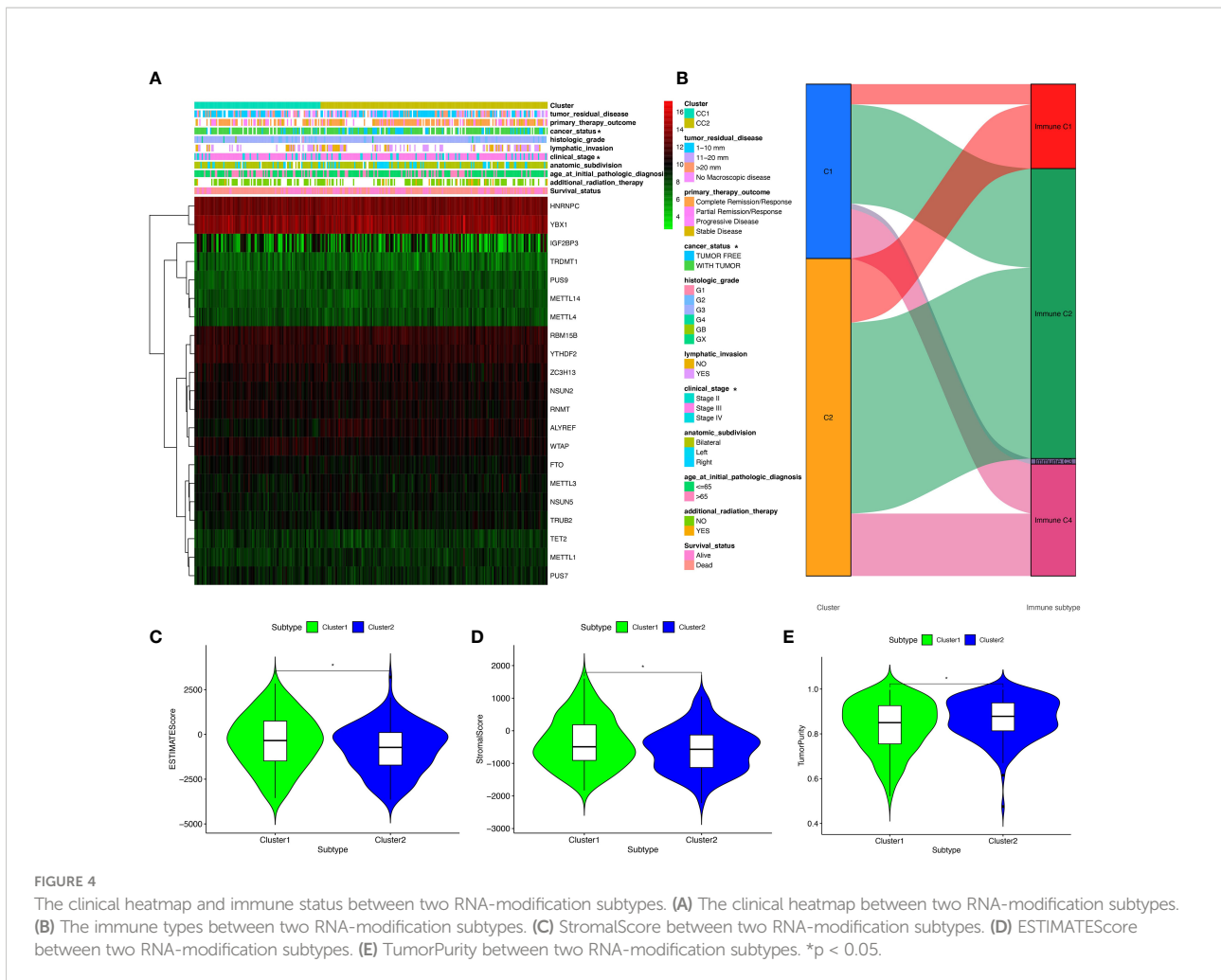
stage (stages I, II, III, and IV), cancer status (with tumor or tumor-free), lymph node metastasis (yes/no), radiation therapy (yes/no), histologic grade (G1-G3), and tumor residual disease (No macroscopic disease, 1-10 mm, 11-20 mm, and >20 mm) (Supplementary Table 1). Further, the correlation between clinical characteristics and OC subtypes was explored. Some clinical characteristics, such as pathologic stage and cancer status, were significantly associated with OC subtypes (Figure 4A).

Additionally, the correlation between OC subtypes and immune was also analyzed, including immune type (Supplementary Table 1) and immune-related scores (Supplementary Table 6). Immune type correlation analysis showed that, in Cluster 1, 11 samples were enriched in immune type C1, 52 samples in immune type C2, 3 samples in immune type C3, and 27 samples in immune type C4; whereas, in Cluster 2, 35 samples were enriched in immune type C1, 104 samples in

immune type C2, and 34 samples in immune type C4. Clusters 1 and 2 showed significant different distribution among different immune types (Figure 4B). In terms of immune-related scores, Cluster 1 showed higher StromalScore and ESTIMATEScore, and lower TumorPurity compared to Cluster 2 (Figures 4C-E).

Construction of riskscore model based on four DERRGs

The OC samples were randomly divided into training (n=155) and test groups (n=152). Training and test groups were divided into high-risk and low-risk score groups according to the riskscores based on 21 DERRGs (Supplementary Table 7). A set of four DERRGs (ALYREF, ZC3H13, WTAP, and METTL1) were found to increase the

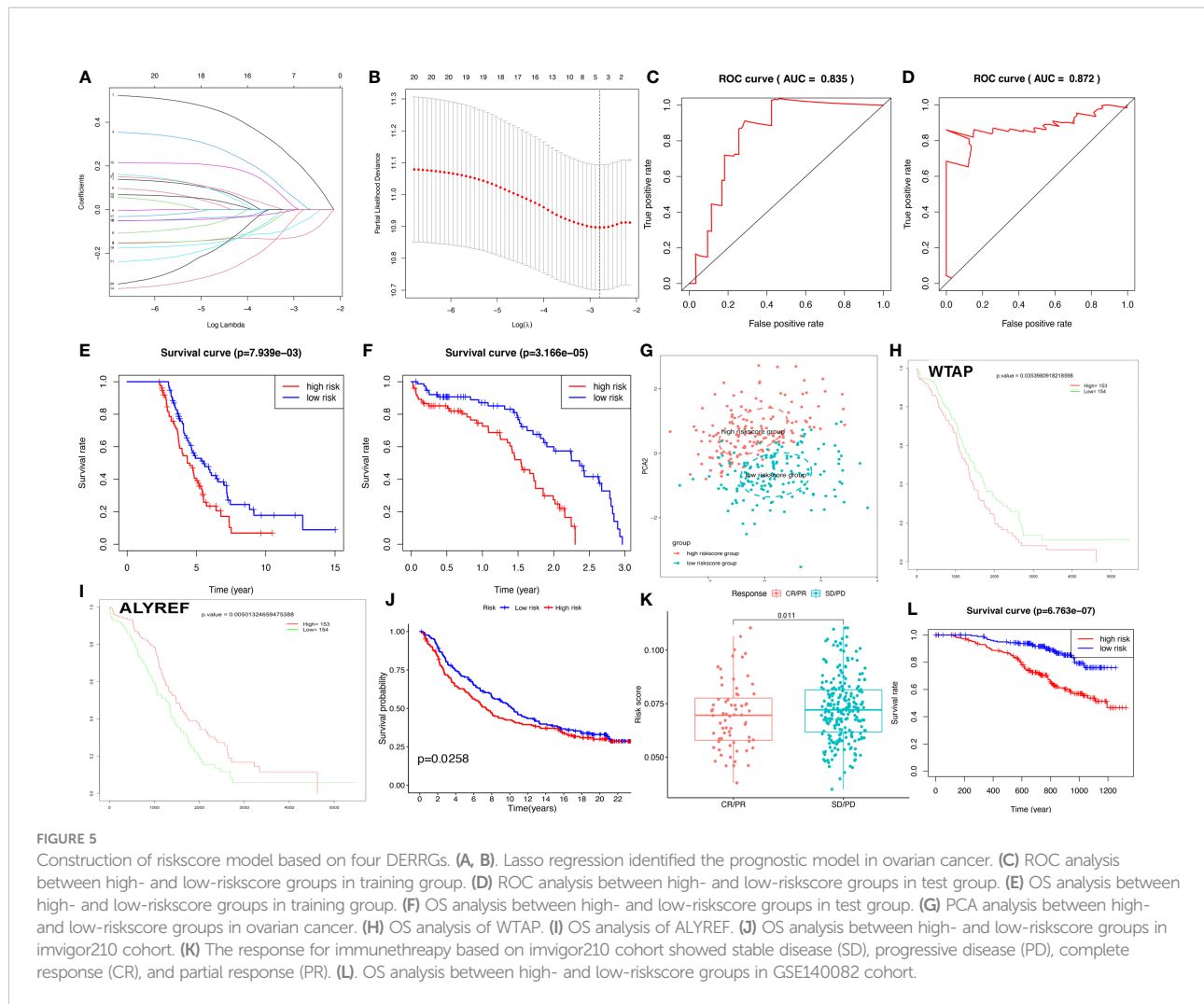


risk of poor prognosis in OCs based on Lasso regression analysis (Figures 5A, B; Supplementary Table 7), when log (lambda) was set between -2 and -3. Thus, the obtained risk scoring formula was as follows: risk score = -0.116404020427426*ALYREF + 0.0203573242796506*ZC3H13 + 0.186320163255671*WTAP + -0.0528745603956501*METTL1. Per the ROC curve, area under the curve (AUC) was equal to 0.835 in training group, and ROC curve showed AUC= 0.872 in test group (Figures 5C, D). OS analysis was performed with Kaplan–Meier method between high-risk and low-risk score groups in the training and test clusters, respectively. Overall survival rate was significantly different (Figures 5E, F). Validated by PCA, it is observed that the whole OC samples were well classified into high-risk and low-risk groups based on riskscores (Figure 5G). Among the identified DERRGs in prognosis model, ALYREF and WTAP individually was significantly related to OS (Figures 5H, I). The constructed riskscore model based on 4 DERRGs was also verified by two independent external validation cohorts (Supplementary Tables 8–10). The invigor210 cohort showed that the prognosis of high-riskscore group was poorer than that

of low-riskscore group (Figure 5J). The response to immunotherapy based on invigor210 cohort showed that PD and SD had high riskscores, whereas PR and CR had low riskscores (Figure 5K). Additionally, the GSE140082 cohort showed that the prognosis of high-riskscore group was poorer than that of low-riskscore group too (Figure 5L).

The heatmap illustrated that the riskscore group had a significant connection with clinical characteristics, including age at initial diagnosis, cancer status, pathologic stage, and radiation therapy (Figure 6A). The univariate Cox regression analysis found that OS was significantly correlated with age at initial pathologic diagnosis, cancer status, anatomic subdivision, tumor residual disease, primary therapy outcome, and riskscore (Figure 6B). Furthermore, the nomogram was drawn to predict the survival rate (1, 3, 5 year) of OC patients based on basic clinical features and riskscore (Figure 6C). The decision-making tree plot verified that nomogram could provide good effect (Figure 6D).

The ssGSEA was executed between high- and low-riskscore groups to show the different gene sets. A total of 44 significant gene sets have been enriched (Supplementary Table 11). The gene sets



were significantly enriched in WELCSH BRCA1 TARGETS DN, PENG GLUTAMINE DEPRIVATION DN, REACTOME PROCESSING OF CAPPED INTRONLESS PRE MRNA, BONOME OVARIAN CANCER POOR SURVIVAL DN, WONG EMBRYONIC STEM CELL CORE, KEGG OXIDATIVE PHOSPHORYLATION, LU EZH2 TARGETS UP, etc, between high and low risk score groups (Figure 6E, F; Supplementary Table 11).

The four-DERRG signature-based risk scores were significantly correlated with immune and TMB and CNV

The four-DERRG signature-based risk scores were positively correlated with CD4+ memory resting T cells, and negatively correlated with macrophages M1 and plasma cells (Figure 7A, Supplementary Table 12). Additionally, immune checkpoints also showed significant differences between these high- and low-risk score subtypes (Figure 7B), such as CD276. The TMB was

positively correlated with Macrophages M1, T cells gamma delta, B cells memory, and showed negative correlation with NK cells activated, and B cells naïve (Figure 7C; Supplementary Table 13).

CNV was the repeated sections of the genome that varied between individuals. Whether the CNV affected the expression of identified genes in LASSO model (ALYREF, ZC3H13, WTAP, and METTL1), the expression perturbations of identified genes were therefore explored (Supplementary Table 14). The CNV alteration frequencies of those genes were widespread positively correlated with the expressions of those genes (Figures 7D–G).

Discussion

Role of RNA modification and its regulation in OCs

More than 170 diverse types of post-transcriptional modifications were detected to be emerged in RNAs. All these

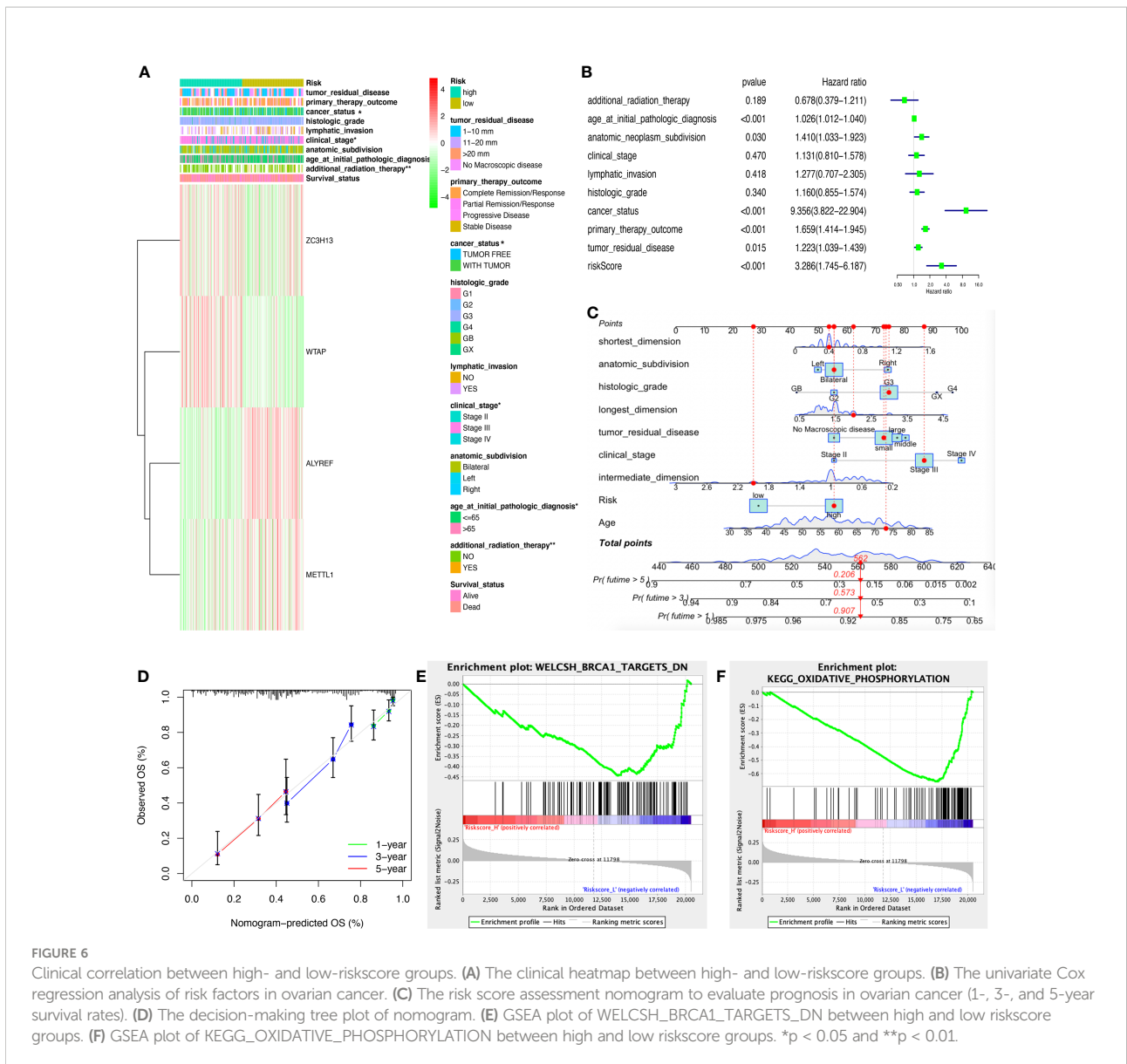


FIGURE 6

Clinical correlation between high- and low-risk score groups. (A) The clinical heatmap between high- and low-risk score groups. (B) The univariate Cox regression analysis of risk factors in ovarian cancer. (C) The risk score assessment nomogram to evaluate prognosis in ovarian cancer (1-, 3-, and 5-year survival rates). (D) The decision-making tree plot of nomogram. (E) GSEA plot of WELCSH_BRCA1_TARGETS_DN between high and low risk score groups. (F) GSEA plot of KEGG_OXIDATIVE_PHOSPHORYLATION between high and low risk score groups. *p < 0.05 and **p < 0.01.

modifications could occur in ribose and four RNA bases, and all RNA species could be modified, especially transfer RNAs (tRNAs) and ribosomal RNAs (rRNAs) (40). Much evidence suggested that dysregulation of the RNA epigenetic pathways played a crucial role in pathogenesis of many human cancers (9). It is known that RNA modification process was dynamic, which helped cells promptly adapt to changes in the microenvironment (41). The capability of adapting the changes of microenvironment played a crucial role in survival of tumor cells, suggesting that RNA modification was vital in cancer (10). Cancer was defined as a disease featured by the progressive accumulation of genetic and epigenetic changes in diverse oncogenes as well as tumor suppressor genes. Meanwhile, a growing number of studies have showed that epitranscriptomics played an important part in the pathological process. RNA

modifications have been proved to be crucial regulators of cancer (9). Abnormal expressions of RNA modification regulators were functionally associated with cell proliferation, cell differentiation, cell self-renewal, invasion, stress adaptation, treatment resistance, and survival; and all of them were important features in cancer (10). For instance, in liver cancer, YTHDF2 promoted the phenotype of cancer stem cell and cancer metastasis through regulation in m6A methylation of pluripotency factor OCT4 mRNA (42). In bladder cancer, ALYREF was proved to strengthen the stability of PKM2 mRNA and bind to m5C sites of specific regions. ALYREF high expression increased cancer cell proliferation *via* glycolysis reaction mediated by PKM2 (43). Also in bladder cancer, ac4C modification mediated by NAT-10 has been certified to increase bladder cancer progression (44). Additionally, in lung cancer,

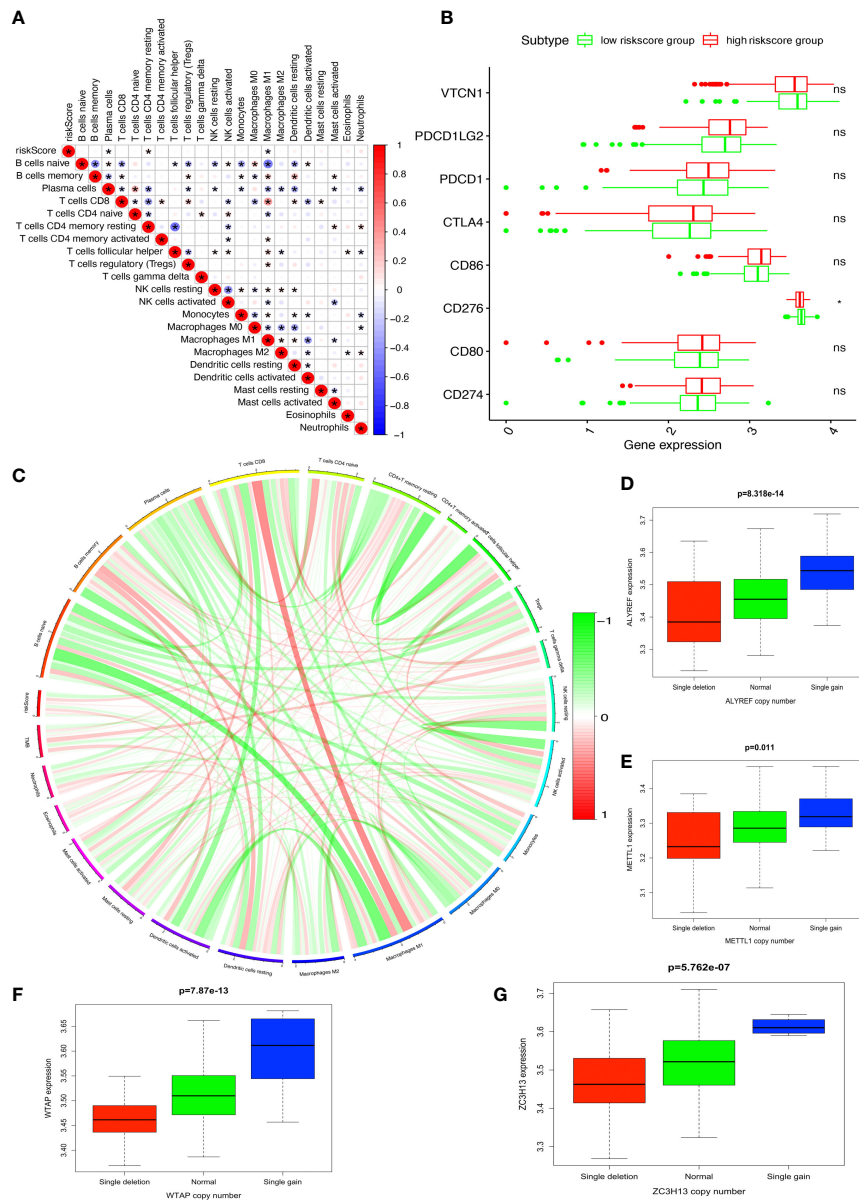


FIGURE 7
 Immune and TMB between high- and low-riskscore groups. **(A)** The correlation between riskscore and immune cells. **(B)** The correlation between riskscore and immune checkpoints. **(C)** The correlation between TMB and immune cells. **(D)** The cor-relations between mRNA expression and CNV alteration frequency of ALYREF in ovarian cancer. **(E)** The cor-relations between mRNA expression and CNV alteration frequency of ZC3H13 in ovarian cancer. **(F)** The cor-relations between mRNA expression and CNV alteration frequency of WTAP in ovarian cancer. **(G)** The cor-relations between mRNA expression and CNV alteration frequency of METTL1 in ovarian cancer. * $p < 0.05$, ** $p < 0.01$, and *** $p < 0.001$. ns, no significance.

m7G tRNA modifications mediated by METTL1/WDR4 were found to play a crucial role in regulation of mRNA translation process and cancer progression (45). In OCs, m6A modifications mediated by FTO restrained cancer stem cells self-renewing process through inhibition of cAMP signaling (46). This present study further demonstrated the significance of RNA modification along with its regulation in cancers involving OCs.

Role of RNA modification and its regulation in immune microenvironment and immunotherapy of OCs

RNA modifications and its regulation were closely associated with immune microenvironment in OCs and other types of tumors, including immune molecules, immune cells, and

immune pathways. Recent studies revealed that RNA modifications regulated activation of immune cells and their infiltration in tumor microenvironment, and afterwards influenced the immunotherapy outcomes. In consequence, RNA modifications had great value as tumor immunotherapy targets (47). A study found that ALKBH5, an important m6A demethylase, regulated PD-L1 expression in intrahepatic cholangiocarcinoma. ALKBH5 suppressed enlargement and cytotoxicity of T cells through preserving PD-L1 expression. Moreover, ALKBH5 played a complex part in tumor immune microenvironment, mainly manifested in overexpression of PD-L1 on mononuclear macrophage and reduced infiltration of myeloid-derived suppressor-like cells (48). Another study revealed positive correlation between m6A writer METTL3 expressions and effector molecules in natural killer (NK) cells. The homeostasis of NK cells was changed with loss of METTL3 in NK cells, and infiltration and function of NK cells were inhibited in tumor microenvironment, which resulted in increasing rate of tumor growth and reduced survival time in mice. The protein expression level of SHP-2 modified by m6A regulators was decreased in METTL3-deficient NK cells. IL-15 response was decreased with reduced SHP-2 activity in METTL3-deficient NK cells, which was related to inhibition of activating AKT and MAPK signaling pathways (49). In addition, a study reported overexpression of circIGF2BP3 was negatively correlated with CD8+ T cells infiltration in non-small cell lung cancer, which functionally compromised antitumor immunity in immunodeficient mice. METTL3 mediated circIGF2BP3 m6A modification and promoted its circulation *via* YTHDC1. CircIGF2BP3 disrupted cancer immune response through upregulating PKP3 expression *via* miR-328-3p and miR-3173-5p. Further, PKP3 strengthened the stability of OTUB1 mRNA through binding to the RNA-binding protein FXR1, which increased PD-L1 enrichment through promoting deubiquitination. The deletion of PD-L1 in tumor entirely interrupted the effect of circIGF2BP3/PKP3 axis on response to CD8+ T cells. CircIGF2BP3/PKP3 inhibition increased the efficacy of anti-PD-1 treatment in lung cancer mouse model (50). In terms of ovarian OCs, a study demonstrated m1A modifications played critical roles in tumor immune microenvironment formation and prognosis of OC patients (51). Identically, m6A modification was proved to play an essential part in tumor microenvironment cell infiltration in OCs (52). This present study further analyzed the relationship of OC subtypes and immune types. The results showed obviously different distribution of immune types in different clusters, indicating immune molecules, immune cells, or immune pathways involved in different OC subtypes may be different. Additionally, we constructed four-DERRG signature model to calculate riskscores of OC patients and found it was positively correlated with CD4+ memory resting T cells, and negatively correlated with plasma cells and macrophages M1, which suggested ones to pay more attention to these three types of

immune cells and their potential target functions in OC immunotherapy.

Role of identified RNA regulator genes and significance of related drug sensibility in OCs

In total, 59 RRGs were identified in this study, most of which were proved to be associated with OC pathogenesis in previous studies. DNMT1 was a key RRG in chemotherapy resistance of OCs, and the feedback regulation between DNMT1 and miR-30a/c-5p played an important part in epithelial-mesenchymal transition and cisplatin-resistance (53). Similarly, overexpression of miR-185 or miR-152 inhibited cell proliferation and promoted apoptosis to increase drug sensibility to cisplatin through suppressing DNMT1 directly in OCs (54). Another study reported that ubiquitin-conjugating enzyme E2 N regulated paclitaxel sensibility of OC cells *via* DNMT1-CHFR-Aurora A pathway (55). A transcriptome m6A methylation analysis towards endometrioid ovarian cancer showed the influence of METTL3 on endometrioid ovarian cancer, and revealed the knockout of METTL3 resulted in distinct decrease of proliferation, increasing apoptosis, and G0/G1 blocking of cell cycle (56). Other studies proved that METTL3 increased OC progression and promoted invasion *via* epithelial-mesenchymal transition and AXL translation (57), and accelerated tumorigenesis and metastasis through suppressing CCNG2 expression targeting miR-1246 in OC (58). Furthermore, another study illustrated the important role of METTL3 in mediating miR-126-5p maturation and promoting OC progression *via* PI3K/Akt/mTOR pathway (59). A meta-analysis suggested that METTL3 upregulation was significantly associated with poor prognosis of OC patients (60). TBX1 was a prognostic marker of multidrug resistance and cancer progression. Nuclear YBX1 expression level might be an independent factor of poor prognosis in OCs (61), and YBX1 nuclear translocation was regulated by Akt activation, influencing drug resistance genes expression in OC cells (62). YBX1 inhibition might contribute to reduction of cancer progression, antagonism of treatment resistance, and decrease of OC patient mortality (63). IGF2BP1 strengthened aggressiveness of OC cells through antagonizing miRNA-impaired gene expression (32), and enhanced invasive growth of OC cells driven by SRC/MAPK (64). DNMT3A promoted Warburg effect *via* miR-145 in OC cells (65). Double negative feedback of miR-29b and DNMT3A/3B promoted OC progression (29). Feedback between DNMT3A and miR-143 was a critical epigenetic regulator of cisplatin resistance in OCs (66). WTAP acting as an oncogenic factor promoted OC progression *via* WTAP-HBS1L/FAM76A axis (67). WTAP was highly expressed in high-grade serous OCs. WTAP overexpression was significantly related to lymphatic

metastasis, whereas down regulation of WTAP contributed to weakness of cell proliferation as well as migration, and increased apoptosis in OC cell lines (68). ALKBH5 suppressed autophagy and enhanced proliferation and invasion *via* BCL-2 and miR-7 in epithelial ovarian cancer (69). Tumor growth and resistance to cisplatin were promoted *via* ALKBH5-HOXA10 loop through mediating JAK2/STAT3 signaling pathway in epithelial ovarian cancer (70). A multi-omics analysis of OCs showed that YTHDF1 promoted translation of EIF3C through combining with EIF3C mRNA modified by m6A and simultaneously promoted the whole output of translation to accelerate the OC tumorigenesis and metastasis (71). Knockdown of YTHDF1 suppressed cancer stem cell-like characteristics in OC cells resistant to cisplatin (72). TET1 inhibited Wnt/ β -catenin signaling pathway through demethylating and upregulating SFRP2 and DKK1, two upstream antagonists in this pathway, to suppress cell metastasis and epithelial-mesenchymal transition in OCs (73). TET1 expression was related to not only low survival rate of terminal epithelial ovarian carcinoma, but migration, growth, stemness, and tumorigenicity of OC cells (74). TET1 expression also resulted in cisplatin resistance targeting vimentin in OCs (75). A study found that TET2 was significantly correlated with tumor-related fibroblast infiltration in OCs (76). IGF2BP2 increased aggressiveness and stemness by upregulating circ_0000745 *via* a miR-3187-3p/ERBB4/PI3K/AKT axis in OC cells (77). HNRNPC and nuclear factor I X were targeted by miR-744-5p in inducing apoptosis of OC cells (78). HNRNPA2B1 promoted OC malignant phenotype by upregulating expression of Lin28B (31). YTHDF2 distinctly accelerated cell proliferation and metastasis in epithelial ovarian cancer cell lines, and its overexpression reversed the decrease of cell proliferation and migration of epithelial ovarian cancer mediated by miR-145 (79). YTHDC2 was verified to play a key part in controlling meiosis in human, within which pathogenic variants were related to primary ovarian insufficiency (80). NAT10 was involved in tubulin processing, associated with cell growth in epithelial ovarian cancer (81). METTL14 overexpression inhibited cell proliferation of OC through suppressing expression of TROAP based on m6A RNA methylation (82). IGF2BP3 overexpression inhibited cancer cell apoptosis. The volume of tumors decreased and cancer metastasis indicator proteins were downregulated after treated with IGF2BP3 siRNA in ovarian clear cell carcinoma (83). Knockdown of IGF2BP3 reduced cell proliferation, invasion and migration, and enhanced platinum sensibility through increasing hCTR1 expression in OC cells, a copper transporter taking part in platinum uptake (33). FTO inhibited self-renewing of stem cells in OC and tumorigenesis *via* cAMP signaling pathway (46). Overexpression of FTO significantly promoted viability and autophagy, but reduced apoptosis in OCs (30). A bioinformatics analysis suggested that PUS7 was a potential marker for diagnosis and target for OC treatment (84). TET3 blocked epithelial-mesenchymal transition induced by

TGF- β 1 through demethylating miR-30d precursor gene promoter to suppress OCs (85). TRDMT1 overexpression decreased cisplatin sensibility and TRDMT1 inhibitor could reverse this change (86). TRMT10C silencing inhibited cell proliferation, migration and clone formation in OCs (87). These research results demonstrated that RRGs played crucial roles in OC biological behaviors and clinical characteristics. Further, RRGs were potential therapeutic targets in OC treatment strategies.

In previous study, many RRGs were certified to associate with drug sensibility or drug resistance in OCs, such as DNMT1 and cisplatin (53, 54), DNMT1 and paclitaxel (55), DNMT3A and cisplatin (66), ALKBH5 and cisplatin (70), TET1 and cisplatin (75), IGF2BP3 and platinum (33), and TRDMT1 and cisplatin (86). Similarly, this present study also found some RRGs were significantly associated with different types of drug sensibility in OCs, such as PUS1 and triethylenemelamine, PUS1 and thiotepa, ZC3H13 and dabrafenib, PUS1 and 5-fluoro deoxy uridine 10mer, NSUN5 and vorinostat, YTHDC2 and nelarabine, ZC3H13 and selumetinib, ALYREF and floxuridine, RBMX and nelarabine, PUS1 and cytarabine, PUS1 and cladribine, TRUB2 and vorinostat, NSUN6 and nelarabine, RBMX and chelerythrine, ALYREF and 5-fluoro deoxy uridine 10mer, DNMT3A and nelarabine, IGF2BP2 and dexrazoxane, and IGF2BP2 and SR16157. Vorinostat, one kind of histone deacetylase inhibitor, has been validated to play a role in multiple tumor treatments, such as melanoma (88), malignant glioma (89), and glioblastoma (90), in a RNA modification regulation manner. Chelerythrine, extracted from four plants of families Rutaceae and Papaveraceae, was one type of plant active ingredient with diverse functions involving anti-inflammation, analgesia, anti-bacteria and anticancer (91). Cladribine, a chlorodeoxyadenosine, acted as the first line treatment of hairy cell leukemia, and it could also be used in the drug therapies of adult systemic mastocytosis and multiple sclerosis (92–94). Cytarabine was one of the most crucial chemotherapy drugs in acute myeloid leukemia, which was usually combined with daunorubicin (95). Dabrafenib was an inhibitor of BRAF kinase, which could be used solely to treat unresectable or metastatic melanoma with BRAF V600E mutation, and to treat BRAF V600E or V600K mutated melanoma combined with trametinib (96). Similarly, for anaplastic thyroid cancer with BRAF V600E mutation, dabrafenib was also recommended together with trametinib (97). Dexrazoxane was an antidote for anthracycline chemotherapy extravasation approved by Food and Drug Administration (FDA), with a prominent cardioprotectant role in anthracycline-induced cardiotoxicity when treating cancers such as breast cancer (98–100). Floxuridine was a pyrimidine analogue routinely applied in colorectal cancer liver metastases management, progressively evolving as the superior drug for hepatic arterial infusional chemotherapy (101). Nelarabine, a synthetic antineoplastic compound targeted to T cell lymphoblastic leukemia and lymphoma, was an effective drug to

treat pediatric and adult T cell acute lymphoblastic leukemia and lymphoma (102). Selumetinib, a highly specific inhibitor of mitogen activated protein kinase 1 and 2, was mainly used in treatments of neurofibromas related to neurofibromatosis type 1, pediatric low-grade gliomas, non-small cell lung cancer, and melanoma (103). SR16157 was a steroid sulfatase inhibitor and also a selective estrogen receptor α modulator, which has been used in clinical trials of breast cancer (104). Triethylenemelamine, owning a nitrogen mustardlike effect, was a crucial chemotherapy agent useful in the management of diverse neoplastic diseases, such as Hodgkin's disease, malignant lymphoma, and chronic lymphocytic leukemia (105). Thiotepea was an alkylating agent used in the treatment of breast cancer, ovarian cancer, and bladder cancer currently (106–108). This finding gave ones a deep insight to understand the relationship between RRGs and drug sensibility. Meanwhile, it provided clues to explore the mechanism of drug sensibility change that is regulated at the RNA modification level, and opened up various novel possibilities in OC treatment strategies.

Significance of four-DERRG signature model and differential signaling pathway

Among 21 DERRGs, four DERRGs (ALYREF, ZC3H13, WTAP, and METTL1) that were significantly associated with poor prognosis in OCs were selected to construct a four-DERRG signature model with Lasso regression analysis. Based on the established risk scoring formula, one could calculate riskscore of every OC sample with high accuracy, and then all OC patients were classified into high-risk and low-risk groups according to the mean values of their riskscores. This study found that overall survival rate was connected with subgroups both in training and test groups, indicating that overall survival rate of OC patients could be forecasted based on this riskscore model. External validation cohort results were also consistent with internal ones, and further suggested this riskscore model can be applicable for assessment of immunotherapy response and prognosis in OC patients. Additionally, a significant correlation between clinical features and risk groups was discovered, including age at initial diagnosis, clinical stage, cancer status, and radiation therapy, which suggested that potential initial diagnostic time, clinicopathological typing of tumors, tumorigenesis, and effectiveness of treatment strategies in OCs could be estimated based on this risk model. Moreover, riskscore was found to act as an independent hazard factor for overall survival rate of OC patients. Thus, this present study provided a succinct and clear method to estimate the patient survival rate of one-, three- and five-year, in which shortest dimension, longest dimension, intermediate dimension, anatomic subdivision, histologic grade, tumor residual disease, clinical stage, age, and riskscore were involved. It provided ones

a novel pattern to score the prognosis of OC patients, which would contribute to patient stage grading and clinical treatment.

Among four-DERRGs (ALYREF, ZC3H13, WTAP, and METTL1) in the prognosis model, WTAP has been widely studied in OCs. WTAP acting as an oncogenic factor was related to cell proliferation, migration, cancer progression, and lymphatic metastasis of OCs (67, 68). According to the riskscore formula, the value of calculated riskscore showed positive correlation with WTAP expression level, which was consistent with previous study. Furthermore, the value of riskscore was also positively correlated with ZC3H13, whereas it was negatively correlated with ALYREF and METTL1. Although no specific clinical researches explore the association between OC prognosis and expression levels of ZC3H13, ALYREF, and METTL1, this present study emphasized their important roles in OC pathological features and prognosis.

Differentially enriched pathways were found between high-risk and low-risk groups. In high-risk group, significantly enriched pathways included calcium signaling pathway, focal adhesion, arrhythmogenic right ventricular cardiomyopathy (arvc), complement and coagulation cascades, vascular smooth muscle contraction, dilated cardiomyopathy, hypertrophic cardiomyopathy (hcm), and neuroactive ligand receptor interaction. Among them, focal adhesion was an important signaling pathway in cell migration (109), and calcium signaling pathway controlled multiple cell processes, such as cell proliferation and metabolism (110), which were consistent with features of OC cells. Other pathways like arrhythmogenic right ventricular cardiomyopathy (arvc), dilated cardiomyopathy, complement and coagulation cascades, vascular smooth muscle contraction, and hypertrophic cardiomyopathy (hcm), were all key pathways in disease of cardiovascular system, which indicated that drugs targeting these signaling pathways for cardiovascular diseases might have potential roles in reduction of OC risk and treatment. The discovery of differential enriched pathways provided ones with novel medication regimens to lower the risk of OCs through blocking these signaling pathways.

Relationship between RNA methylation and identified differential immune cells/immune checkpoints/TMB and role in OCs

This present study found that the prognostic model-based riskscore was positively correlated with CD4+ memory resting T cells, and negatively correlated with plasma cells and macrophages M1, which demonstrated that high-risk group was dominated by high-level infiltration of CD4+ memory resting T cells. Both high-level of CD4+ memory resting T cells infiltration and low-level of plasma cells and

macrophages M1 infiltration might imply poor prognosis of OC patients. CD4+ memory resting T cells were differentiated from naïve CD4+ T cells experiencing an antigen so that molecular alterations inevitably emerged in CD4+ memory resting T cells after exposure. A multi-omic comparative analysis showed that methylation levels of promoter regions in kinases LYN, SGK1, and transmethylese METTL7A, and hydrolase DDAH2 were elevated, and concurrently gene expression levels decreased (111). Plasma cells as antibody-secreting cells had tremendous speed of immunoglobulin-coding genes in transcription, translation, assembly and secretion. Plasma cells were differentiated from B cells with the help of IRF4 and Blimp-1. Blimp-1 and XBP1 were critical upstream regulatory factors of the unfolded protein response in plasma cells (112). Macrophages M1 were induced by IFN- γ with the function of intense bactericidal and anti-inflammatory effects. m6A writer METTL3 actuated macrophages M1 polarization through methylating STAT1 mRNA (113).

Immune checkpoint therapy was a novel and attention-getting tumor treatment, which could strengthen anti-tumor immune response of T cells with broad application prospects. CD276, also known as B7-H3, was a member of B7 family. A review summarized the role of CD276 in cancers, regulation mechanism and its potential therapeutic value (114). CD276 took part in the regulation of cell cycle, cell differentiation, proliferation, invasion, apoptosis, and epithelial-mesenchymal transition, and also participated in tumor metastasis. Moreover, in aspect of immune regulation, CD276 had synergistic effects with CTLA4, PD-1, PD-L1, and PD-L2 in inhibition of T cells proliferation and activation, and IFN- γ , TNF- α , and other cytokines secretion (114). This present study found that CD276 was a differential immune checkpoint molecule between high- and low-risk groups, which indicated its crucial function in OC progression and suggested that CD276 immune checkpoint inhibitors might have a considerable effect on OC immune therapy.

Tumor mutation burden (TMB) was an emerging potential biomarker for immune checkpoint blockade selection in diverse cancers. Mutation-derived neoantigens in tumor DNA could be identified and targeted by human immune system. After transcription and translation, peptides containing mutation-derived neoantigens could be processed and transferred to MHC molecules, and appear on the surface of cells. It is certain that the more mutations a tumor had, the more neoantigens it formed, and the more likely immune treatments would work (115). TMB has become an important predictor of immune checkpoint blockade outcomes and an available biomarker to identify patients who would benefit from immune therapy (115). A study found that high TMB was significantly correlated with better PFS and OS in OCs (116). This present study found that TMB was positively correlated with macrophages M1, T cells gamma delta, B cells memory, and negatively correlated with NK cells activated, and B cells naïve,

which demonstrated that TMB could be estimated *via* immune cell infiltration and further contributed to immune therapy strategies of OCs. Although the experimental validation of LASSO model in clinical samples is able to strengthen a computational study, it is generally not required for a computational study; the use of extra database to validate it is also acceptable. Also, it is so difficult to collect enough samples to verify the LASSO model. Thus, we used extra database to verify our LASSO model, which provides us the preliminary work for the deep validation in real clinical samples in future.

Conclusion

RNA modification and its regulation played a crucial role in tumorigenesis, progression, and prognosis of OC patients. The constructed four-DERRG signature (ALYREF, ZC3H13, WTAP, and METTL1) model might be an independent prognostic model to divide OC patients into high- and low-risk groups, which was of great significance for prognostic assessment, patient stratification, and predictive evaluation of immunotherapy outcomes in OCs.

Data availability statement

The datasets presented in this study can be found in online repositories. The names of the repository/repositories and accession number(s) can be found in the article/[Supplementary Material](#).

Ethics statement

Written informed consent was not obtained from the individual(s) for the publication of any potentially identifiable images or data included in this article.

Author contributions

PZ analyzed data and wrote the manuscript draft. NL conceived the concept, analyzed data, and wrote the manuscript. XZ conceived the concept, coordinated, critically revised manuscript, and was responsible for the corresponding works. All authors contributed to the article and approved the submitted version.

Funding

This work was supported by the Shandong Cancer Hospital Qihang Plan (to NL), the Shandong First Medical University

Talent Introduction Funds (to XZ), Shandong First Medical University High-level Scientific Research Achievement Cultivation Funding Program (to XZ), the Shandong Provincial Natural Science Foundation (ZR2021MH156 to XZ; and ZR2022QH112 to NL), Shandong Provincial Taishan Scholar Engineering Project Special Funds (to XZ), National Nature Scientific Funds (82203592 to NL; and the Academic Promotion Program of Shandong First Medical University (2019ZL002).

Conflict of interest

The authors declare that the research was conducted in the absence of any commercial or financial relationships that could be construed as a potential conflict of interest.

References

- Bray F, Ferlay J, Soerjomataram I, Siegel RL, Torre LA, Jemal A. Global cancer statistics 2018: GLOBOCAN estimates of incidence and mortality worldwide for 36 cancers in 185 countries. *CA Cancer J Clin* (2018) 68(6):394–424. doi: 10.3322/caac.21492
- Gaona-Luviano P, Medina-Gaona LA, Magaña-Pérez K. Epidemiology of ovarian cancer. *Chin Clin Oncol* (2020) 9(4):47. doi: 10.21037/cco-20-34
- Torre LA, Trabert B, DeSantis CE, Miller KD, Samimi G, Runowicz CD, et al. Ovarian cancer statistics, 2018. *CA Cancer J Clin* (2018) 68(4):284–96. doi: 10.3322/caac.21456
- Köbel M, Kalloger SE, Boyd N, McKinney S, Mehl E, Palmer C, et al. Ovarian carcinoma subtypes are different diseases: implications for biomarker studies. *PloS Med* (2008) 5(12):e232. doi: 10.1371/journal.pmed.0050232
- Webb PM, Jordan SJ. Epidemiology of epithelial ovarian cancer. *Best Pract Res Clin Obstet Gynaecol* (2017) 41:3–14. doi: 10.1016/j.bpobgyn.2016.08.006
- Kuroki L, Guntupalli SR. Treatment of epithelial ovarian cancer. *Bmj* (2020) 371:m3773. doi: 10.1136/bmj.m3773
- Morand S, Devanaboyina M, Staats H, Stanbery L, Nemunaitis J. Ovarian cancer immunotherapy and personalized medicine. *Int J Mol Sci* (2021) 22(12):6532. doi: 10.3390/ijms22126532
- Wang X, Han Y, Li J, Hong D, Xue Z, Huang H, et al. Multi-omics analysis of copy number variations of RNA regulatory genes in soft tissue sarcoma. *Life Sci* (2021) 265:118734. doi: 10.1016/j.lfs.2020.118734
- Barbieri I, Kouzarides T. Role of RNA modifications in cancer. *Nat Rev Cancer* (2020) 20(6):303–22. doi: 10.1038/s41568-020-0253-2
- Nombela P, Miguel-Lopez B, Blanco S. The role of m(6)A, m(5)C and psi RNA modifications in cancer: Novel therapeutic opportunities. *Mol Cancer* (2021) 20(1):18. doi: 10.1186/s12943-020-01263-w
- Boccaletto P, Machnicka MA, Purta E, Piatkowski P, Baginski B, Wirecki TK, et al. MODOMICS: a database of RNA modification pathways. 2017 update. *Nucleic Acids Res* (2018) 46(D1):D303–d7. doi: 10.1093/nar/gkx1030
- Dor Y, Cedar H. Principles of DNA methylation and their implications for biology and medicine. *Lancet* (2018) 392(10149):777–86. doi: 10.1016/S0140-6736(18)31268-6
- Deng LJ, Deng WQ, Fan SR, Chen MF, Qi M, Lyu WY, et al. m6A modification: recent advances, anticancer targeted drug discovery and beyond. *Mol Cancer* (2022) 21(1):52. doi: 10.1186/s12943-022-01510-2
- Wiener D, Schwartz S. The epitranscriptome beyond m(6)A. *Nat Rev Genet* (2021) 22(2):119–31. doi: 10.1038/s41576-020-00295-8
- Chen YS, Yang WL, Zhao YL, Yang YG. Dynamic transcriptomic m(5) c and its regulatory role in RNA processing. *Wiley Interdiscip Rev RNA* (2021) 12(4):e1639. doi: 10.1002/wrna.1639
- Zheng Q, Yu X, Zhang Q, He Y, Guo W. Genetic characteristics and prognostic implications of m1A regulators in pancreatic cancer. *Biosci Rep* (2021) 41(4):BSR20210337. doi: 10.1042/BSR20210337
- Safra M, Sas-Chen A, Nir R, Winkler R, Nachshon A, Bar-Yaacov D, et al. The m1A landscape on cytosolic and mitochondrial mRNA at single-base resolution. *Nature* (2017) 551(7679):251–5. doi: 10.1038/nature24456
- Arango D, Sturgill D, Alhusaini N, Dillman AA, Sweet TJ, Hanson G, et al. Acetylation of cytidine in mRNA promotes translation efficiency. *Cell* (2018) 175(7):1872–86.e24. doi: 10.1016/j.cell.2018.10.030
- Sas-Chen A, Thomas JM, Matzov D, Taoka M, Nance KD, Nir R, et al. Dynamic RNA acetylation revealed by quantitative cross-evolutionary mapping. *Nature* (2020) 583(7817):638–43. doi: 10.1038/s41586-020-2418-2
- Huang MH, Peng GX, Mao XL, Wang JT, Zhou JB, Zhang JH, et al. Molecular basis for human mitochondrial tRNA m3C modification by alternatively spliced METTL8. *Nucleic Acids Res* (2022) 50(7):4012–28. doi: 10.1093/nar/gkac184
- Goh YT, Koh CWQ, Sim DY, Roca X, Goh WSS. METTL4 catalyzes m6Am methylation in U2 snRNA to regulate pre-mRNA splicing. *Nucleic Acids Res* (2020) 48(16):9250–61. doi: 10.1093/nar/gkaa684
- Sendinc E, Valle-Garcia D, Dhall A, Chen H, Henriques T, Navarrete-Perea J, et al. PCIF1 catalyzes m6Am mRNA methylation to regulate gene expression. *Mol Cell* (2019) 75(3):620–30.e9. doi: 10.1016/j.molcel.2019.05.030
- Mauer J, Luo X, Blanjoie A, Jiao X, Grozhik AV, Patil DP, et al. Reversible methylation of m(6)A(m) in the 5' cap controls mRNA stability. *Nature* (2017) 541(7637):371–5. doi: 10.1038/nature21022
- Engel M, Eggert C, Kaplick PM, Eder M, Röh S, Tietze L, et al. The role of m(6)A/m-RNA methylation in stress response regulation. *Neuron* (2018) 99(2):389–403.e9. doi: 10.1016/j.neuron.2018.07.009
- Kiledjian M, Zhou M, Jiao X. Normal and aberrantly capped mRNA decapping. *Enzymes* (2012) 31:165–80. doi: 10.1016/B978-0-12-404740-2.00008-2
- Luo Y, Yao Y, Wu P, Zi X, Sun N, He J. The potential role of N(7)-methylguanosine (m7G) in cancer. *J Hematol Oncol* (2022) 15(1):63. doi: 10.1186/s13045-022-01285-5
- Woo HH, Chambers SK. Human ALKBH3-induced m(1)A demethylation increases the CSF-1 mRNA stability in breast and ovarian cancer cells. *Biochim Biophys Acta Gene Regul Mech* (2019) 1862(1):35–46. doi: 10.1016/j.bbaggm.2018.10.008
- Jiang Y, Wan Y, Gong M, Zhou S, Qiu J, Cheng W. RNA Demethylase ALKBH5 promotes ovarian carcinogenesis in a simulated tumour microenvironment through stimulating NF-κB pathway. *J Cell Mol Med* (2020) 24(11):6137–48. doi: 10.1111/jcmm.15228
- Teng Y, Zuo X, Hou M, Zhang Y, Li C, Luo W, et al. A double-negative feedback interaction between MicroRNA-29b and DNMT3A/3B contributes to ovarian cancer progression. *Cell Physiol Biochem* (2016) 39(6):2341–52. doi: 10.1159/000447926
- Zhao L, Kong X, Zhong W, Wang Y, Li P. FTO accelerates ovarian cancer cell growth by promoting proliferation, inhibiting apoptosis, and activating autophagy. *Pathol Res Pract* (2020) 216(9):153042. doi: 10.1016/j.prp.2020.153042

Publisher's note

All claims expressed in this article are solely those of the authors and do not necessarily represent those of their affiliated organizations, or those of the publisher, the editors and the reviewers. Any product that may be evaluated in this article, or claim that may be made by its manufacturer, is not guaranteed or endorsed by the publisher.

Supplementary material

The Supplementary Material for this article can be found online at: <https://www.frontiersin.org/articles/10.3389/fendo.2022.972341/full#supplementary-material>

31. Yang Y, Wei Q, Tang Y, Yuanyuan W, Luo Q, Zhao H, et al. Loss of hnRNP2B1 inhibits malignant capability and promotes apoptosis via down-regulating Lin28B expression in ovarian cancer. *Cancer Lett* (2020) 475:43–52. doi: 10.1016/j.canlet.2020.01.029
32. Müller S, Bley N, Glaß M, Busch B, Rousseau V, Misiak D, et al. IGF2BP1 enhances an aggressive tumor cell phenotype by impairing miRNA-directed downregulation of oncogenic factors. *Nucleic Acids Res* (2018) 46(12):6285–303. doi: 10.1093/nar/gky229
33. Hsu KF, Shen MR, Huang YF, Cheng YM, Lin SH, Chow NH, et al. Overexpression of the RNA-binding proteins Lin28B and IGF2BP3 (IMP3) is associated with chemoresistance and poor disease outcome in ovarian cancer. *Br J Cancer*. (2015) 113(3):414–24. doi: 10.1038/bjc.2015.254
34. Peng D, Kryczek I, Nagarsheth N, Zhao L, Wei S, Wang W, et al. Epigenetic silencing of TH1-type chemokines shapes tumour immunity and immunotherapy. *Nature* (2015) 527(7577):249–53. doi: 10.1038/nature15520
35. Zhang P, Su T, Zhang S. Comprehensive analysis of prognostic value of MEX3A and its relationship with immune infiltrates in ovarian cancer. *J Immunol Res* (2021) 2021:5574176. doi: 10.1155/2021/5574176
36. Wang X, Wang J, Yu M. Immune subtype profiling and establishment of prognostic immune-related lncRNA pairs in human ovarian cancer. *Comput Math Methods Med* (2022) 2022:8338137. doi: 10.1155/2022/8338137
37. Chen Z, Jiang W, Li Z, Zong Y, Deng G. Immune-and metabolism-associated molecular classification of ovarian cancer. *Front Oncol* (2022) 12:877369. doi: 10.3389/fonc.2022.877369
38. Huo X, Yang M, Zhang X, Wang S, Sun H. Identification of tumor microenvironment scoring scheme based on bioinformatics analysis of immune cell infiltration pattern of ovarian cancer. *J Oncol* (2022) 2022:7745675. doi: 10.1155/2022/7745675
39. Way GP, Rudd J, Wang C, Hamidi H, Fridley BL, Konecny GE, et al. Comprehensive cross-population analysis of high-grade serous ovarian cancer supports no more than three subtypes. *G3 (Bethesda)*. (2016) 6(12):4097–103. doi: 10.1534/g3.116.033514
40. Li S, Mason CE. The pivotal regulatory landscape of RNA modifications. *Annu Rev Genomics Hum Genet* (2014) 15:127–50. doi: 10.1146/annurev-genom-090413-025405
41. Chan CT, Dyavaiah M, DeMott MS, Taghizadeh K, Dedon PC, Begley TJ. A quantitative systems approach reveals dynamic control of tRNA modifications during cellular stress. *PLoS Genet* (2010) 6(12):e1001247. doi: 10.1371/journal.pgen.1001247
42. Zhang C, Huang S, Zhuang H, Ruan S, Zhou Z, Huang K, et al. YTHDF2 promotes the liver cancer stem cell phenotype and cancer metastasis by regulating OCT4 expression via m6A RNA methylation. *Oncogene* (2020) 39(23):4507–18. doi: 10.1038/s41388-020-1303-7
43. Wang JZ, Zhu W, Han J, Yang X, Zhou R, Lu HC, et al. The role of the HIF-1 α /ALYREF/PKM2 axis in glycolysis and tumorigenesis of bladder cancer. *Cancer Commun (Lond)*. (2021) 41(7):560–75. doi: 10.1002/cac2.12158
44. Wang G, Zhang M, Zhang Y, Xie Y, Zou J, Zhong J, et al. NAT10-mediated mRNA N4-acetylcytidine modification promotes bladder cancer progression. *Clin Transl Med* (2022) 12(5):e738. doi: 10.1002/ctm2.738
45. Ma J, Han H, Huang Y, Yang C, Zheng S, Cai T, et al. METTL1/WDR4-mediated m(7)G tRNA modifications and m(7)G codon usage promote mRNA translation and lung cancer progression. *Mol Ther* (2021) 29(12):3422–35. doi: 10.1016/j.yjth.2021.08.005
46. Huang H, Wang Y, Kandpal M, Zhao G, Cardenas H, Ji Y, et al. FTO-dependent N(6)-methyladenosine modifications inhibit ovarian cancer stem cell self-renewal by blocking cAMP signaling. *Cancer Res* (2020) 80(16):3200–14. doi: 10.1158/0008-5472.CAN-19-4044
47. Li X, Ma S, Deng Y, Yi P, Yu J. Targeting the RNA m(6)A modification for cancer immunotherapy. *Mol Cancer*. (2022) 21(1):76. doi: 10.1186/s12943-022-01558-0
48. Qiu X, Yang S, Wang S, Wu J, Zheng B, Wang K, et al. M(6)A demethylase ALKBH5 regulates PD-L1 expression and tumor immunoenvironment in intrahepatic cholangiocarcinoma. *Cancer Res* (2021) 81(18):4778–93. doi: 10.1158/0008-5472.CAN-21-0468
49. Song H, Song J, Cheng M, Zheng M, Wang T, Tian S, et al. METTL3-mediated m(6)A RNA methylation promotes the anti-tumour immunity of natural killer cells. *Nat Commun* (2021) 12(1):5522. doi: 10.1038/s41467-021-25803-0
50. Liu Z, Wang T, She Y, Wu K, Gu S, Li L, et al. N(6)-methyladenosine-modified circIGF2BP3 inhibits CD8(+) T-cell responses to facilitate tumor immune evasion by promoting the deubiquitination of PD-L1 in non-small cell lung cancer. *Mol Cancer*. (2021) 20(1):105. doi: 10.1186/s12943-021-01398-4
51. Liu J, Chen C, Wang Y, Qian C, Wei J, Xing Y, et al. Comprehensive of N1-methyladenosine modifications patterns and immunological characteristics in ovarian cancer. *Front Immunol* (2021) 12:746647. doi: 10.3389/fimmu.2021.746647
52. Luo Y, Sun X, Xiong J. Characterization of m6A regulator-mediated methylation modification patterns and tumor microenvironment infiltration in ovarian cancer. *Front Cell Dev Biol* (2021) 9:794801. doi: 10.3389/fcell.2021.794801
53. Han X, Zhen S, Ye Z, Lu J, Wang L, Li P, et al. A feedback loop between miR-30a/c-5p and DNMT1 mediates cisplatin resistance in ovarian cancer cells. *Cell Physiol Biochem* (2017) 41(3):973–86. doi: 10.1159/000460618
54. Xiang Y, Ma N, Wang D, Zhang Y, Zhou J, Wu G, et al. MiR-152 and miR-185 co-contribute to ovarian cancer cells cisplatin sensitivity by targeting DNMT1 directly: a novel epigenetic therapy independent of decitabine. *Oncogene* (2014) 33(3):378–86. doi: 10.1038/ncr.2012.575
55. Zhang X, Feng Y, Wang XY, Zhang YN, Yuan CN, Zhang SF, et al. The inhibition of UBC13 expression and blockage of the DNMT1-CHFR-Aurora a pathway contribute to paclitaxel resistance in ovarian cancer. *Cell Death Dis* (2018) 9(2):93. doi: 10.1038/s41419-017-0137-x
56. Yang L, Chen X, Qian X, Zhang J, Wu M, Yu A. Comprehensive analysis of the transcriptome-wide m6A methylome in endometrioid ovarian cancer. *Front Oncol* (2022) 12:844613. doi: 10.3389/fonc.2022.844613
57. Hua W, Zhao Y, Jin X, Yu D, He J, Xie D, et al. METTL3 promotes ovarian carcinoma growth and invasion through the regulation of AXL translation and epithelial to mesenchymal transition. *Gynecol Oncol* (2018) 151(2):356–65. doi: 10.1016/j.ygyno.2018.09.015
58. Bi X, Lv X, Liu D, Guo H, Yao G, Wang L, et al. METTL3 promotes the initiation and metastasis of ovarian cancer by inhibiting CCGNG2 expression via promoting the maturation of pri-microRNA-1246. *Cell Death Discovery* (2021) 7(1):237. doi: 10.1038/s41420-021-00600-2
59. Bi X, Lv X, Liu D, Guo H, Yao G, Wang L, et al. METTL3-mediated maturation of miR-126-5p promotes ovarian cancer progression via PTEN-mediated PI3K/Akt/mTOR pathway. *Cancer Gene Ther* (2021) 28(3-4):335–49. doi: 10.1038/s41417-020-00222-3
60. Liu K, Gao Y, Gan K, Wu Y, Xu B, Zhang L, et al. Prognostic roles of N6-methyladenosine METTL3 in different cancers: A system review and meta-analysis. *Cancer Control*. (2021) 28:1073274821997455. doi: 10.1177/1073274821997455
61. Oda Y, Ohishi Y, Basaki Y, Kobayashi H, Hirakawa T, Wake N, et al. Prognostic implications of the nuclear localization of γ -box-binding protein-1 and CXCR4 expression in ovarian cancer: their correlation with activated akt, LRP/MVP and p-glycoprotein expression. *Cancer Sci* (2007) 98(7):1020–6. doi: 10.1111/j.1349-7006.2007.00492.x
62. Basaki Y, Hosoi F, Oda Y, Fotovati A, Maruyama Y, Oie S, et al. Akt-dependent nuclear localization of γ -box-binding protein 1 in acquisition of malignant characteristics by human ovarian cancer cells. *Oncogene* (2007) 26(19):2736–46. doi: 10.1038/sj.onc.1210084
63. Tailor D, Resendez A, Garcia-Marques FJ, Pandrala M, Going CC, Bermudez A, et al. γ box binding protein 1 inhibition as a targeted therapy for ovarian cancer. *Cell Chem Biol* (2021) 28(8):1206–20.e6. doi: 10.1016/j.chembiol.2021.02.014
64. Bley N, Schott A, Müller S, Misiak D, Lederer M, Fuchs T, et al. IGF2BP1 is a targetable SRC/MAPK-dependent driver of invasive growth in ovarian cancer. *RNA Biol* (2021) 18(3):391–403. doi: 10.1080/15476286.2020.1812894
65. Zhang S, Pei M, Li Z, Li H, Liu Y, Li J. Double-negative feedback interaction between DNA methyltransferase 3A and microRNA-145 in the warburg effect of ovarian cancer cells. *Cancer Sci* (2018) 109(9):2734–45. doi: 10.1111/cas.13734
66. Han X, Liu D, Zhou Y, Wang L, Hou H, Chen H, et al. The negative feedback between miR-143 and DNMT3A regulates cisplatin resistance in ovarian cancer. *Cell Biol Int* (2021) 45(1):227–37. doi: 10.1002/cbin.11486
67. Wang J, Xu J, Li K, Huang Y, Dai Y, Xu C, et al. Identification of WTAP-related genes by weighted gene co-expression network analysis in ovarian cancer. *J Ovarian Res* (2020) 13(1):119. doi: 10.1186/s13048-020-00710-y
68. Yu HL, Ma XD, Tong JF, Li JQ, Guan XJ, Yang JH. WTAP is a prognostic marker of high-grade serous ovarian cancer and regulates the progression of ovarian cancer cells. *Onco Targets Ther* (2019) 12:6191–201. doi: 10.2147/OTT.S205730
69. Zhu H, Gan X, Jiang X, Diao S, Wu H, Hu J. ALKBH5 inhibited autophagy of epithelial ovarian cancer through miR-7 and BCL-2. *J Exp Clin Cancer Res* (2019) 38(1):163. doi: 10.1186/s13046-019-1159-2
70. Nie S, Zhang L, Liu J, Wan Y, Jiang Y, Yang J, et al. ALKBH5-HOXA10 loop-mediated JAK2 m6A demethylation and cisplatin resistance in epithelial ovarian cancer. *J Exp Clin Cancer Res* (2021) 40(1):284. doi: 10.1186/s13046-021-02088-1
71. Liu T, Wei Q, Jin J, Luo Q, Liu Y, Yang Y, et al. The m6A reader YTHDF1 promotes ovarian cancer progression via augmenting EIF3C translation. *Nucleic Acids Res* (2020) 48(7):3816–31. doi: 10.1093/nar/gkaa048
72. Hao L, Wang JM, Liu BQ, Yan J, Li C, Jiang JY, et al. m6A-YTHDF1-mediated TRIM29 upregulation facilitates the stem cell-like phenotype of cisplatin-resistant ovarian cancer cells. *Biochim Biophys Acta Mol Cell Res* (2021) 1868(1):118878. doi: 10.1016/j.bbamcr.2020.118878

73. Duan H, Yan Z, Chen W, Wu Y, Han J, Guo H, et al. TET1 inhibits EMT of ovarian cancer cells through activating wnt/ β -catenin signaling inhibitors DKK1 and SFRP2. *Gynecol Oncol* (2017) 147(2):408–17. doi: 10.1016/j.ygyno.2017.08.010
74. Chen LY, Huang RL, Chan MW, Yan PS, Huang TS, Wu RC, et al. TET1 reprograms the epithelial ovarian cancer epigenome and reveals casein kinase 2 α as a therapeutic target. *J Pathol* (2019) 248(3):363–76. doi: 10.1002/path.5266
75. Han X, Zhou Y, You Y, Lu J, Wang L, Hou H, et al. TET1 promotes cisplatin-resistance via demethylating the vimentin promoter in ovarian cancer. *Cell Biol Int* (2017) 41(4):405–14. doi: 10.1002/cbin.10734
76. Wan F, Chen F, Fan Y, Chen D. Clinical significance of TET2 in female cancers. *Front Bioeng Biotechnol* (2022) 10:790605. doi: 10.3389/fbioe.2022.790605
77. Wang S, Li Z, Zhu G, Hong L, Hu C, Wang K, et al. RNA-Binding protein IGF2BP2 enhances circ_0000745 abundance and promotes aggressiveness and stemness of ovarian cancer cells via the microRNA-3187-3p/ERBB4/PI3K/AKT axis. *J Ovarian Res* (2021) 14(1):154. doi: 10.1186/s13048-021-00917-7
78. Kleemann M, Schneider H, Unger K, Sander P, Schneider EM, Fischer-Posovszky P, et al. miR-744-5p inducing cell death by directly targeting HNRNPC and NFIX in ovarian cancer cells. *Sci Rep* (2018) 8(1):9020. doi: 10.1038/s41598-018-27438-6
79. Li J, Wu L, Pei M, Zhang Y. YTHDF2, a protein repressed by miR-145, regulates proliferation, apoptosis, and migration in ovarian cancer cells. *J Ovarian Res* (2020) 13(1):111. doi: 10.1186/s13048-020-00717-5
80. McGlacken-Byrne SM, Del Valle I, Quesne Stabej PL, Bellutti L, Garcia-Alonso L, Ocala LA, et al. Pathogenic variants in the human m6A reader YTHDC2 are associated with primary ovarian insufficiency. *JCI Insight* (2022) 7(5):e154671. doi: 10.1172/jci.insight.154671
81. Tan TZ, Miow QH, Huang RY, Wong MK, Ye J, Lau JA, et al. Functional genomics identifies five distinct molecular subtypes with clinical relevance and pathways for growth control in epithelial ovarian cancer. *EMBO Mol Med* (2013) 5(7):1051–66. doi: 10.1002/emmm.201201823
82. Li Y, Peng H, Jiang P, Zhang J, Zhao Y, Feng X, et al. Downregulation of methyltransferase-like 14 promotes ovarian cancer cell proliferation through stabilizing TROAP mRNA. *Front Oncol* (2022) 12:824258. doi: 10.3389/fonc.2022.824258
83. Liu H, Zeng Z, Afsharpar M, Lin C, Wang S, Yang H, et al. Overexpression of IGF2BP3 as a potential oncogene in ovarian clear cell carcinoma. *Front Oncol* (2019) 9:1570. doi: 10.3389/fonc.2019.01570
84. Li H, Chen L, Han Y, Zhang F, Wang Y, Han Y, et al. The identification of RNA modification gene PUS7 as a potential biomarker of ovarian cancer. *Biol (Basel)* (2021) 10(11):1130. doi: 10.3390/biology10111130
85. Ye Z, Li J, Han X, Hou H, Chen H, Zheng X, et al. TET3 inhibits TGF- β 1-induced epithelial-mesenchymal transition by demethylating miR-30d precursor gene in ovarian cancer cells. *J Exp Clin Cancer Res* (2016) 35:72. doi: 10.1186/s13046-016-0350-y
86. Zhu X, Wang X, Yan W, Yang H, Xiang Y, Lv F, et al. Ubiquitination-mediated degradation of TRDMT1 regulates homologous recombination and therapeutic response. *NAR Cancer* (2021) 3(1):zcab010. doi: 10.1093/narcan/zcab010
87. Wang Q, Zhang Q, Huang Y, Zhang J. m(1)A regulator TRMT10C predicts poorer survival and contributes to malignant behavior in gynecological cancers. *DNA Cell Biol* (2020) 39(10):1767–78. doi: 10.1089/dna.2020.5624
88. Fiziev P, Akdemir KC, Miller JP, Keung EZ, Samant NS, Sharma S, et al. Systematic epigenomic analysis reveals chromatin states associated with melanoma progression. *Cell Rep* (2017) 19(4):875–89. doi: 10.1016/j.celrep.2017.03.078
89. Xu J, Sampath D, Lang FF, Prabhu S, Rao G, Fuller GN, et al. Vorinostat modulates cell cycle regulatory proteins in glioma cells and human glioma slice cultures. *J Neurooncol*. (2011) 105(2):241–51. doi: 10.1007/s11060-011-0604-7
90. Singh MM, Manton CA, Bhat KP, Tsai WW, Aldape K, Barton MC, et al. Inhibition of LSD1 sensitizes glioblastoma cells to histone deacetylase inhibitors. *Neuro Oncol* (2011) 13(8):894–903. doi: 10.1093/neuonc/nor049
91. Chen N, Qi Y, Ma X, Xiao X, Liu Q, Xia T, et al. Rediscovery of traditional plant medicine: An underestimated anticancer drug of chelerythrine. *Front Pharmacol* (2022) 13:906301. doi: 10.3389/fphar.2022.906301
92. Maitre E, Cornet E, Troussard X. Hairy cell leukemia: 2020 update on diagnosis, risk stratification, and treatment. *Am J Hematol* (2019) 94(12):1413–22. doi: 10.1002/ajh.25653
93. Pardanani A. Systemic mastocytosis in adults: 2021 update on diagnosis, risk stratification and management. *Am J Hematol* (2021) 96(4):508–25. doi: 10.1002/ajh.26118
94. Piehl F. Current and emerging disease-modulatory therapies and treatment targets for multiple sclerosis. *J Intern Med* (2021) 289(6):771–91. doi: 10.1111/joim.13215
95. Ishii H, Yano S. New therapeutic strategies for adult acute myeloid leukemia. *Cancers (Basel)*. (2022) 14(11):2806. doi: 10.3390/cancers14112806
96. Dean L. Dabrafenib therapy and BRAF and G6PD genotype. In: Pratt VM, Scott SA, Pirmohamed M, Esquivel B, Kane MS, Kattman BL, et al, editors. *Medical genetics summaries*. Bethesda (MD: National Center for Biotechnology Information (US) (2012).
97. Saini S, Tulla K, Maker AV, Burman KD, Prabhakar BS. Therapeutic advances in anaplastic thyroid cancer: a current perspective. *Mol Cancer*. (2018) 17(1):154. doi: 10.1186/s12943-018-0903-0
98. Blum RH. Clinical status and optimal use of the cardioprotectant, dexrazoxane. *Oncol (Williston Park)*. (1997) 11(11):1669–77.
99. Kreidieh FY, Moukadem HA, El Saghir NS. Overview, prevention and management of chemotherapy extravasation. *World J Clin Oncol* (2016) 7(1):87–97. doi: 10.5306/wjco.v7.i1.87
100. Padeigimas A, Clasen S, Ky B. Cardioprotective strategies to prevent breast cancer therapy-induced cardiotoxicity. *Trends Cardiovasc Med* (2020) 30(1):22–8. doi: 10.1016/j.tcm.2019.01.006
101. Doussot A, Kemeny NE, D'Angelica MI. Hepatic arterial infusional chemotherapy in the management of colorectal cancer liver metastases. *Hepat Oncol* (2015) 2(3):275–90. doi: 10.2217/hep.15.9
102. Kadia TM, Gandhi V. Nelarabine in the treatment of pediatric and adult patients with T-cell acute lymphoblastic leukemia and lymphoma. *Expert Rev Hematol* (2017) 10(1):1–8. doi: 10.1080/17474086.2017.1262757
103. Campagne O, Yeo KK, Fangusaro J, Stewart CF. Clinical pharmacokinetics and pharmacodynamics of selumetinib. *Clin Pharmacokinet* (2021) 60(3):283–303. doi: 10.1007/s40262-020-00967-y
104. Rasmussen LM, Zaveri NT, Stenvang J, Peters RH, Lykkesfeldt AE. A novel dual-target steroid sulfatase inhibitor and antiestrogen: SR 16157, a promising agent for the therapy of breast cancer. *Breast Cancer Res Treat* (2007) 106(2):191–203. doi: 10.1007/s10549-007-9494-y
105. Rundles RW, Barton WB. Triethylene melamine in the treatment of neoplastic disease. *Blood* (1952) 7(5):483–507. doi: 10.1182/blood.V7.5.483.483
106. Stoll BA. Thiotepe and breast cancer. *Br Med J* (1963) 1(5322):54–5. doi: 10.1136/bmj.1.5322.54-a
107. Englander O, Sarangi A. Effect of thio-TEPA on advanced malignant ovarian tumours. *Br J Cancer*. (1960) 14(1):28–44. doi: 10.1038/bjc.1960.4
108. Fallah F, Fallah M, Sajadi Nia RS. Thiotepe versus bacille calmette-guérin in non-muscle invasive bladder cancer. *Curr Urol*. (2013) 6(3):160–4. doi: 10.1159/000343532
109. Paluch EK, Aspalter IM, Sixt M. Focal adhesion-independent cell migration. *Annu Rev Cell Dev Biol* (2016) 32:469–90. doi: 10.1146/annurev-cellbio-111315-125341
110. Berridge MJ. The inositol Trisphosphate/Calcium signaling pathway in health and disease. *Physiol Rev* (2016) 96(4):1261–96. doi: 10.1152/physrev.00006.2016
111. Mitchell CJ, Getnet D, Kim MS, Manda SS, Kumar P, Huang TC, et al. A multi-omic analysis of human naive CD4⁺ T cells. *BMC Syst Biol* (2015) 9:75. doi: 10.1186/s12918-015-0225-4
112. Teller J, Nutt SL. Plasma cells: The programming of an antibody-secreting machine. *Eur J Immunol* (2019) 49(1):30–7. doi: 10.1002/eji.201847517
113. Liu Y, Liu Z, Tang H, Shen Y, Gong Z, Xie N, et al. The N(6)-methyladenosine (m(6)A)-forming enzyme METTL3 facilitates M1 macrophage polarization through the methylation of STAT1 mRNA. *Am J Physiol Cell Physiol* (2019) 317(4):C762–c75. doi: 10.1152/ajpcell.00212.2019
114. Liu S, Liang J, Liu Z, Zhang C, Wang Y, Watson AH, et al. The role of CD276 in cancers. *Front Oncol* (2021) 11:654684. doi: 10.3389/fonc.2021.654684
115. Chan TA, Yarchoan M, Jaffee E, Swanton C, Quezada SA, Stenzinger A, et al. Development of tumor mutation burden as an immunotherapy biomarker: utility for the oncology clinic. *Ann Oncol* (2019) 30(1):44–56. doi: 10.1093/annonc/mdy495
116. Fan S, Gao X, Qin Q, Li H, Yuan Z, Zhao S. Association between tumor mutation burden and immune infiltration in ovarian cancer. *Int Immunopharmacol*. (2020) 89(Pt A):107126. doi: 10.1016/j.intimp.2020.107126

Glossary

ac4C	N4-acetylcytidine
ADP	adenosine diphosphate
AUC	area under curve
BCL-2	B cell lymphoma-2
cAMP	cyclic adenosine monophosphate
CCNG2	cyclin G2
CR	complete response
CSF-1	colony stimulating factor-1
CTLA4	cytotoxic T lymphocyte-associated protein 4;
CXCL	chemokine C-X-C motif ligand
DDAH2	dimethylarginine dimethylaminohydrolase 2
DERRG	differently expressed RNAmodification regulatory gene
DKK1	dickkopf-1
DTP	Developmental Therapeutics Program
EIF3C	eukaryotic initiation factor 3c
EZH2	enhancer of zeste homolog 2
FXR1	fragile X autosomal homolog 1
GSEA	gene-set enrichment analysis
hCTR1	human copper transporter 1;
H3K27me3	trimethylation of lys-27 in histone 3
Ψ	pseudouridine
IFN	interferon
IL	interleukin
IRF4	interferon regulatory factor 4
LYN	lck/yesrelated protein tyrosine kinase
m1A	N1-methyladenosine
m3C	3-methylcytidine
m5C	5-methylcytosine
m6A	N6-methyladenosine;
m6Am	2-O-dimethyladenosine
m7G	N7-methyladenosine
MAD	median absolute deviation
MEX3A	Mex-3 RNA Binding Family Member A
MHC	major histocompatibility complex
NCI	National Cancer Institute
NF-κB	nuclear factor kappa beta
NK	natural killer cell
NMF	nonnegative matrix factorization
OC	ovarian cancer
OCT4	octamer-binding transcription factor 4
ORR	objective response rate
OS	overall survival
OTUB1	OUT domain-containing ubiquitin aldehyde-binding protein 1
PABPC1	poly A binding protein 1
PCA	principal component analysis
PD	progressive disease
PD-1	programmed cell death protein-1

Continued

PD-L1	programmed cell death ligand-1
PD-L2	programmed cell death ligand-2
PFS	progressionfree- survival
PKM2	pyruvate kinase M2
PKP3	plakophilin 3
PPI	protein-protein interaction
PR	partial response
ROC	receiver operating characteristic
RRG	RNA-modification regulatory gene
rRNA	ribosomal RNA
SD	stable disease
SFRP2	secreted frizzled-related protein 2
SGK1	serum and glucocorticoid-induced protein kinase 1
SHP-2	SH2 domaincontaining protein tyrosine phosphatase-2
STAT1	signal transducer and activator of transcription 1
TCGA	The Cancer Genome Atlas
TGF	transforming growth factor
Th1	T-helper 1
TIM	tumor immune microenvironment
TMB	tumor mutation burden
TNF	tumor necrosis factor
Tregs	T cells regulatory
tRNA	transfer RNA
TROAP	trophininassociated protein
WDR4	WD repeat domain 4
XBP1	X-box binding protein 1

(Continued)

Frontiers in Endocrinology

Explores the endocrine system to find new therapies for key health issues

The second most-cited endocrinology and metabolism journal, which advances our understanding of the endocrine system. It uncovers new therapies for prevalent health issues such as obesity, diabetes, reproduction, and aging.

Discover the latest Research Topics

[See more →](#)

Frontiers

Avenue du Tribunal-Fédéral 34
1005 Lausanne, Switzerland
frontiersin.org

Contact us

+41 (0)21 510 17 00
frontiersin.org/about/contact

